

# **Defining the role and mechanisms of miRNAs in cartilage ageing and disease**

Thesis submitted in accordance with the requirements of the  
University of Liverpool for the degree of Doctor in Philosophy

by

**Panagiotis Balaskas**

**March 2021**

# Table of contents

Acknowledgements.....	i
Abbreviations.....	ii
Abstract.....	vii
Chapter 1: General Introduction.....	1
1.1 General information about articular cartilage.....	3
1.2 Components of articular cartilage .....	5
1.2.1 Chondrocyte.....	5
1.2.2 The extracellular matrix (ECM) .....	5
1.3 Chondrogenesis and cartilage formation.....	10
1.4 Ageing and articular cartilage .....	15
1.4.1 Ageing-related changes in the ECM of articular cartilage .....	15
1.4.2 Age-related chondrocyte senescence, inflammation and oxidative stress .....	17
1.4.3 Age-related chondrocyte autophagy and apoptosis.....	19
1.5 Osteoarthritis .....	22
1.5.1 Definition, epidemiology and management of osteoarthritis .....	22
1.5.2 Risk factors for osteoarthritis development .....	26
1.5.3 Macroscopic changes in knee osteoarthritic cartilage .....	29
1.5.4 Microscopic/histological changes in knee osteoarthritic cartilage.....	31
1.5.5 Molecular changes in osteoarthritic cartilage .....	36
1.6 MicroRNAs .....	39
1.6.1 MicroRNA general remarks and biogenesis.....	39
1.6.2 MicroRNA and mRNA pairing: microRNA function .....	42
1.6.3. MicroRNA databases, nomenclature and target prediction tools.....	47
1.6.4 miRNAs in cartilage development and homeostasis .....	49
1.6.5 miRNAs in cartilage ageing.....	51
1.6.6 miRNAs in OA cartilage .....	52
Chapter 2: General Materials and Methods .....	58
2.1 Collection of human knee cartilage .....	62
2.2 Collection of intact/healthy knee cartilage from non-OA donors .....	63
2.3 Macroscopic scoring of human knee osteoarthritic cartilage .....	65
2.4 Paraffin embedding of human knee OA cartilage.....	65
2.5 Sectioning of human knee cartilage.....	65
2.6 Haematoxylin and eosin staining .....	66
2.7 Safranin-O and fast-green staining .....	67

2.8 Histological scoring of human knee OA cartilage .....	68
2.9 Isolation of human primary chondrocytes from articular cartilage.....	70
2.10 Isolation of healthy equine primary chondrocytes from cartilage tissue.....	71
2.11 Human and equine chondrocyte culture and passaging .....	72
2.12 Homogenisation of human knee cartilage tissue .....	72
2.13 Total RNA extraction from human knee cartilage tissue and human/equine chondrocytes ...	73
2.13.1 Total RNA extraction from human knee articular cartilage tissue using the mirVana™ miRNA Isolation Kit with phenol.....	73
2.13.2 Total RNA extraction from equine primary chondrocytes using the miRNeasy Mini Kit ..	75
2.13.3 Total RNA extraction from human knee articular cartilage and human primary chondrocytes using the guanidinium thiocyanate-phenol-chloroform method (TRIzol) .....	76
2.14 Microarray analysis for detection of differentially expressed miRNAs .....	78
2.15 Small RNA-Seq analysis for detection of differentially expressed miRNAs .....	80
2.16 Poly(A) cDNA synthesis for miRNA quantification .....	83
2.17 cDNA synthesis for mRNA quantification .....	85
2.18 qPCR for miRNA quantification.....	85
2.19 qPCR for mRNA quantification.....	86
2.20 Primer efficiency calculation.....	87
2.21 List of sncRNA and mRNA primers.....	88
2.22 Treatment of human primary chondrocytes with IL-1 $\beta$ .....	91
2.23 Overexpression and knockdown of miRNAs in IL-1 $\beta$ induced human primary chondrocytes .	92
2.24 Collection and lysis of human primary chondrocytes for LC-MS/MS analysis.....	94
2.25 Pierce™ 660nm Protein Assay for protein quantification.....	95
2.26 SDS-PAGE for protein quality assessment .....	96
2.27 Silver staining of polyacrylamide gels .....	97
2.28 Protein sample preparation for LC-MS/MS .....	98
2.29 Coomassie Brilliant Blue staining of polyacrylamide gels.....	99
2.30 LC-MS/MS workflow .....	100
2.31 Bioinformatic analysis of microarray experiment.....	101
2.32 Bioinformatic analysis of small RNA-Seq experiment.....	101
2.33 Bioinformatic analysis of LC-MS/MS experiment .....	103
2.34 Primer design .....	104
2.35 miRNA target prediction tools .....	104
2.36 Ingenuity Pathway Analysis of miRNA-gene interactions.....	105
2.37 Enrichr analysis of predicted target genes.....	106

2.38 ToppGene Suite, REVIGO and Cytoscape analysis for gene network generation and visualisation .....	107
2.39 STRING analysis for identification of protein-protein interactions .....	107
2.40 Selection of reference genes for qPCR data normalisation .....	107
2.41. Principal Component Analysis using MetaboAnalyst .....	108
2.42 Statistical Analysis .....	108
Chapter 3: MicroRNA profiling in young intact, old OA intact and old OA lesioned human knee cartilage using microarray analysis .....	109
3.1 Introduction .....	110
3.2 Study aim and rationale .....	111
3.3 Experimental design.....	111
3.3.1 Human knee cartilage specimens .....	112
3.3.2 Kellgren-Lawrence grading of human knee OA cartilage samples .....	112
3.3.3 Macroscopic assessment of human knee OA cartilage samples .....	113
3.3.4 Histologic assessment of human knee OA cartilage samples .....	113
3.3.5 RNA extraction from human cartilage samples for microarray analysis .....	114
3.3.6 Microarray analysis between young intact, old OA intact and old OA lesioned human knee cartilage samples .....	114
3.3.7 Target gene prediction and identification of miRNA/mRNA-related biological pathways	114
3.4 Results.....	115
3.4.1 Kellgren-Lawrence grading of human knee OA femoral condyles.....	115
3.4.2 Outerbridge grading of human knee OA femoral condyles.....	117
3.4.3 Histological scoring of old OA intact and lesioned human knee cartilage.....	120
3.4.4 Microarray analysis overview .....	125
3.4.5 Differentially expressed miRNAs in young intact, old OA intact and old OA lesioned human cartilage.....	132
3.5 Discussion.....	143
3.6 Conclusion.....	149
Chapter 4: Validation of miRNA profiling in young intact, old OA intact and old OA lesioned human cartilage and investigation of selected miRNAs in an in vitro OA inflammatory model .....	150
4.1 Introduction .....	151
4.2 Study aim and rationale .....	152
4.3 Experimental design.....	152
4.3.1 Selection of specific DE miRNAs for follow up studies following microarray analysis .....	152
4.3.2 Human knee cartilage specimens used for qPCR validation of microarray results .....	153
4.3.3 Young healthy and old healthy human knee cartilage specimens for the investigation of ageing in selected miRNAs.....	154

4.3.4 Histologic assessment of young healthy and old healthy cartilage samples .....	155
4.3.5 Treatment of human primary chondrocytes with human recombinant IL-1 $\beta$ .....	155
4.3.6 Total RNA extraction from human cartilage samples and primary chondrocytes for qPCR validation .....	156
4.3.7 Poly(A) cDNA synthesis for miRNA quantification .....	156
4.3.8 cDNA synthesis for mRNA quantification .....	157
4.3.9 qPCR for miRNA and mRNA quantification .....	157
4.3.10 Selection of endogenous reference genes for qPCR data normalisation .....	157
4.4 Results .....	158
4.4.1 Selection of specific DE miRNAs from microarray analysis.....	158
4.4.2 Selection of reference genes for qPCR data normalisation .....	160
4.4.3 qPCR validation of microarray findings in the dependent cohort .....	163
4.4.4 qPCR validation of microarray findings in the independent cohort .....	166
4.4.5 Investigation of selected miRNAs in cartilage ageing .....	171
4.4.6 Investigation of selected miRNAs in an OA <i>in vitro</i> inflammatory model .....	176
4.5 Discussion.....	187
4.5.1 Validation of microarray results.....	187
4.5.2 Investigation of selected miRNAs in cartilage ageing .....	189
4.5.3 Investigation of selected miRNAs in an <i>in vitro</i> OA inflammatory model .....	190
4.6 Conclusion .....	195
Chapter 5: Modulation of expression of selected miRNAs in human primary OA chondrocytes and investigation of selected target gene expression.....	197
5.1 Introduction .....	198
5.2 Study aim and rationale .....	199
5.3 Experimental design.....	199
5.3.1 Selection of predicted target genes .....	199
5.3.2 Treatment of human OA chondrocytes with miRNA mimics and inhibitors .....	200
5.3.3 Total RNA extraction from human primary OA chondrocytes for qPCR validation of selected target genes.....	203
5.3.4 cDNA synthesis for miRNA and mRNA quantification .....	203
5.3.5 qPCR for miRNA and mRNA quantification .....	203
5.3.6 Selection of endogenous reference genes for qPCR data normalisation .....	203
5.3.7 Collection, lysis and preparation of human primary chondrocytes for LC-MS/MS analysis .....	204
5.3.8 STRING analysis for identification of protein interactions.....	204
5.3.9 IPA analysis for identification of miR-143-3p relevant biological pathways following LC-MS/MS analysis .....	205

5.4 Results.....	206
5.4.1 Selection of predicted targets for miR-361-5p, -379-5p and -107.....	206
5.4.2 Expression of selected target genes in human primary OA chondrocytes treated with miR-361-5p mimics and inhibitors in an <i>in vitro</i> OA inflammatory model.....	207
5.4.3 Expression of selected target genes in human primary OA chondrocytes treated with miR-379-5p mimics and inhibitors in an <i>in vitro</i> OA inflammatory model.....	211
5.4.4 Expression of selected target genes in human primary OA chondrocytes treated with miR-107 mimics and inhibitors in an <i>in vitro</i> OA inflammatory model.....	216
5.4.5 Investigation of miRNA predicted target genes in human articular cartilage tissue .....	219
5.4.6 Proteomic investigation of human primary OA chondrocytes treated with miR-143-3p mimic and inhibitor.....	224
5.5 Discussion.....	238
5.5.1 Justification of target gene selection .....	238
5.5.2 Evaluation of predicted targets of miR-361-6p, -379-5p and -107.....	239
5.5.3 Investigation of miR-143-3p in cartilage and OA.....	243
5.6 Conclusion.....	245
Chapter 6: Investigation of miRNA expression in equine ageing chondrocytes using small RNA Sequencing.....	247
6.1 Introduction .....	248
6.2 Study aim and rationale.....	249
6.3 Experimental design.....	249
6.3.1 Isolation of young and old healthy equine chondrocytes.....	250
6.3.2 Equine chondrocyte culture, passaging and total RNA extraction .....	250
6.3.3 Small RNASeq analysis for detection of differentially expressed miRNAs in young and old healthy equine chondrocytes .....	250
6.3.4 Pathway analysis of DE miRNAs between young and old equine chondrocytes .....	251
6.3.5 cDNA synthesis and qPCR for miRNA quantification .....	251
6.4 Results.....	252
6.4.1 Differential Expression Analysis of Small RNA-Seq Data .....	252
6.4.2 IPA analysis of DE miRNAs in equine chondrocyte ageing.....	254
6.4.3 Validation of DE miRNAs in young and old equine chondrocytes using qPCR .....	259
6.5 Discussion.....	261
6.6 Conclusion.....	264
Chapter 7: General Discussion and Future Directions .....	265
7.1 General Discussion.....	266
7.2 Future Directions .....	274
7.3 Conclusion.....	275

References .....	276
Appendix to Chapter 3 .....	293
Appendix to Chapter 5 .....	329
Appendix to Chapter 6 .....	351
Small Non-Coding RNAome of Ageing Chondrocytes .....	362
List of publications during PhD .....	384

## Acknowledgements

The present work was carried out at the Department of Musculoskeletal Biology, at the Institute of Life Course and Medical Sciences, University of Liverpool. I would like to take this opportunity to acknowledge and express my gratitude to everyone who has supported me throughout my PhD.

First and foremost, I would like to thank and express my sincerest gratitude to my primary supervisor, Professor Mandy Peffers. Without her expertise on omics technologies and cartilage biology, her encouragement, continuous support and guidance throughout these 4 years, this work would never have been accomplished, and I am honoured to have been her student. I am also grateful to my co-supervisors, Dr Kasia Goljanek-Whysall for her expertise and guidance in the field of miRNA biology, Professor Peter Clegg for his expertise in cartilage biology and for supporting my research and my project, and Professor David Young for providing guidance and advice.

In addition, I would like to thank the Medical Research Council DiMeN Doctoral Training Partnership and the Institute of Life Course and Medical Sciences at the University of Liverpool for their generous funding and support throughout my PhD project. Moreover, I would like to thank the Liverpool Musculoskeletal Biobank, the Clatterbridge Hospital at Wirral and all the donors for providing human cartilage samples to support my PhD. Also, I would like to thank the laboratory of Professor Tim Welting, Maastricht UMC+, the Netherlands, for providing samples of cartilage tissue/chondrocytes for microarray analysis and validation and the Wellcome Trust for funding the microarray experiment.

Special thanks to all the people in Liverpool and Greece, in and outside of the lab, who have been here on this journey with me, physically or mentally, from the beginning to the end, and with whom I share many happy memories from the last 4 years.

Finally, I would like to thank my family for their love and support they have given me while I was in the UK, away from them, studying for my PhD. My dad Michalis, my mom Spyridoula and my two sisters, Theodora and Angeliki.

## Abbreviations

<b>43S PIC</b>	43S Preinitiation Complex
<b>4E-T</b>	EIF4E-Transporter
<b>ACAN</b>	Aggrecan
<b>ACL</b>	Anterior Cruciate Ligament
<b>ADAMTS</b>	A Disintegrin and Metalloproteinase with Thrombospondin Motifs
<b>Ago</b>	Argonaute
<b>AKT</b>	Protein Kinase B
<b>AmBic</b>	Ammonium Bicarbonate
<b>AMPK</b>	5' AMP-Activated Protein Kinase
<b>ASPN</b>	Asporin
<b>ATG5</b>	Autophagy Related 5
<b>ATP5F1A</b>	ATP Synthase F1 Subunit Alpha
<b>BCL-2</b>	B Cell Lymphoma 2
<b>BMI</b>	Body Mass Index
<b>BMP</b>	Bone Morphogenetic Protein
<b>BSA</b>	Bovine Serum Albumin
<b>C/Ebp<math>\beta</math></b>	CCAAT Enhancer Binding Protein Beta
<b>CALM</b>	Calmodulin
<b>CASP1</b>	Caspase 1
<b>CCR4-NOT</b>	Carbon Catabolite Repression-Negative On TATA-Less
<b>CEBPA</b>	CCAAT Enhancer Binding Protein Alpha
<b>CGR</b>	Centre for Genomic Research
<b>COL10A1</b>	Collagen Type X Alpha 1 Chain
<b>COL2A1</b>	Collagen Type II Alpha 1 Chain
<b>COL9A2</b>	Collagen Type IX Alpha 2 Chain
<b>COMP</b>	Cartilage Oligomeric Matrix Protein
<b>COX-2</b>	Cyclooxygenase 2
<b>CPR</b>	Centre for Proteome Research

<b>DDX6</b>	DEAD-Box Helicase 6
<b>DE</b>	Differentially Expressed
<b>DGCR8</b>	DiGeorge Critical Region 8
<b>DIO2</b>	Iodothyronine Deiodinase 2
<b>DMEM</b>	Dulbecco's Modified Eagle Medium
<b>DNPEP</b>	Aspartyl Aminopeptidase
<b>DPBS</b>	Dulbecco's Phosphate Buffered Saline
<b>DTT</b>	Dithiothreitol
<b>ECM</b>	Extracellular Matrix
<b>EDTA</b>	Ethylenediaminetetraacetic Acid
<b>eIF</b>	Eukaryotic Translation Initiation Factor
<b>F/Z</b>	Amphotericin B/Fungizone
<b>FBS</b>	Foetal Bovine Serum
<b>FDR</b>	False Discovery Rate
<b>FGF</b>	Fibroblast Growth Factor
<b>FOXO3A</b>	Forkhead Box O3 A
<b>FST</b>	Follistatin
<b>GAGs</b>	Glycosaminoglycans
<b>GAPDH</b>	Glyceraldehyde-3-Phosphate Dehydrogenase
<b>GDF5</b>	Growth/Differentiation Factor 5
<b>GO</b>	Gene Ontology
<b>H&amp;E</b>	Haematoxylin and Eosin
<b>HDAC</b>	Histone Deacetylase
<b>HHGS</b>	Histological-Histochemical Grading System
<b>HIF</b>	Hypoxia-Inducible Factor
<b>HMGB2</b>	High Mobility Group Box 2
<b>IAA</b>	Iodoacetamide
<b>IGF-1</b>	Insulin Growth Factor 1
<b>IGFBP</b>	Insulin-Like Growth Factor Binding Protein

<b>IHH</b>	Indian Hedgehog
<b>IL-1<math>\beta</math></b>	Interleukin 1 Beta
<b>IL-6</b>	Interleukin 6
<b>iNOS</b>	Nitric Oxide Synthase 2 Inducible
<b>IPA</b>	Ingenuity Pathway Analysis
<b>IRF</b>	Interferon Regulatory Factor
<b>KL</b>	Kellgren-Lawrence
<b>LARP1</b>	La Ribonucleoprotein 1 Translational Regulator
<b>LC3</b>	Microtubule-Associated Protein 1 Light Chain 3
<b>LC-MS/MS</b>	Liquid Chromatography-Tandem Mass Spectrometry
<b>lncRNAs</b>	Long Coding RNAs
<b>LogFC</b>	Log2 Fold Change
<b>LPS</b>	Lipopolysaccharides
<b>m/z</b>	Mass-To-Charge Ratio
<b>MAPK</b>	Mitogen-Activated Protein Kinase
<b>miRNA/miR</b>	microRNA
<b>MLXIPL</b>	MLX Interacting Protein Like
<b>MMP</b>	Matrix Metallopeptidase
<b>MRI</b>	Magnetic Resonance Imaging
<b>mRNA</b>	Messenger RNA
<b>MSCs</b>	Mesenchymal Stem Cells
<b>mTOR</b>	Mechanistic Target of Rapamycin Kinase
<b>NCAM</b>	Neural Cell Adhesion Molecule
<b>NF-<math>\kappa</math>B</b>	Nuclear Factor Kappa-Light-Chain-Enhancer of Activated B Cells
<b>NO</b>	Nitric Oxide
<b>NSAIDs</b>	Non-Steroidal Anti-Inflammatory Drugs
<b>nt</b>	Nucleotides
<b>OA</b>	Osteoarthritis
<b>OARSI</b>	Osteoarthritis Research Society International

<b>P/S</b>	Penicillin-Streptomycin
<b>PABP</b>	Poly(A) Binding Protein
<b>PAN</b>	Poly(A)-Binding Protein-Dependent Poly(A) Ribonuclease
<b>PCA</b>	Principal Component Analysis
<b>PDGFR<math>\alpha</math></b>	Platelet Derived Growth Factor Receptor Alpha
<b>PE</b>	Phycoerythrin
<b>PGE2</b>	Prostaglandin 2
<b>PI3K</b>	Phosphoinositide 3-Kinase
<b>piRNAs</b>	Piwi-Interacting RNAs
<b>PKA</b>	Protein Kinase A
<b>pre-miRNA</b>	Precursor-miRNA
<b>pri-miRNA</b>	Primary miRNA
<b>PTEN</b>	Phosphatase and Tensin Homolog
<b>PTHrP</b>	Parathyroid Hormone-Related Protein
<b>PTOA</b>	Post-Traumatic OA
<b>qPCR</b>	Quantitative Polymerase Chain Reaction
<b>RALA</b>	RAS Like Proto-Oncogene A
<b>RANKL</b>	Receptor Activator of Nuclear Factor Kappa-B Ligand
<b>RHOA</b>	Ras Homolog Family Member A
<b>RISC</b>	RNA-Induced Silencing Complex
<b>RMA</b>	Robust Microarray Data Analysis
<b>RNA-Seq</b>	RNA Sequencing
<b>ROCK</b>	Rho Associated Coiled-Coil Containing Protein Kinase
<b>ROS</b>	Reactive Oxygen Species
<b>RPL13A</b>	Ribosomal Protein L13a
<b>RPL3</b>	Ribosomal Protein L3
<b>RPL4</b>	Ribosomal Protein L4
<b>RPLP0</b>	Ribosomal Protein Lateral Stalk Subunit P0
<b>rpm</b>	Rounds Per Minute

<b>RUNX2</b>	RUNX Family Transcription Factor 2
<b>SASP</b>	Senescence-Associated Secretory Phenotype
<b>SD</b>	Standard Deviation
<b>SDS-PAGE</b>	Sodium Dodecyl Sulphate–Polyacrylamide Gel Electrophoresis
<b>SIRT1</b>	Sirtuin-1
<b>SMAD</b>	Small Mothers Against Decapentaplegic
<b>sncRNAs</b>	Small Non-Coding RNAs
<b>snoRNAs</b>	Small Nucleolar RNAs
<b>snRNAs</b>	Small Nuclear RNAs
<b>S-O/FG</b>	Safranin O/Fast Green
<b>SOD2</b>	Superoxide Dismutase 2
<b>SOX</b>	Sex Determining Region Y-Box Transcription Factor
<b>SP1</b>	Sp1 Transcription Factor
<b>TFA</b>	Trifluoroacetic Acid
<b>TGFBR</b>	Transforming Growth Factor Beta Receptor
<b>TGF-β</b>	Transforming Growth Factor Beta
<b>TKA</b>	Total Knee Arthroplasty
<b>TNFSF11</b>	TNF Ligand Superfamily Member 11
<b>TNF-α</b>	Tumour Necrosis Factor Alpha
<b>TNRC6</b>	Trinucleotide Repeat Containing Adaptor 6
<b>TRAF</b>	TNF Receptor-Associated Factor
<b>tRNAs</b>	Transfer RNAs
<b>TUT</b>	Terminal Uridylyl Transferase
<b>ULK1</b>	Unc-51-Like Kinase 1
<b>UTR</b>	Untranslated Region
<b>VEGFA</b>	Vascular Endothelial Growth Factor A
<b>WNT</b>	Wingless-Related Integration Site
<b>YWHAE</b>	Tyrosine 3-Monooxygenase/Tryptophan 5-Monooxygenase Activation Protein Epsilon

## **Abstract**

Articular cartilage is susceptible to age-related diseases, such as osteoarthritis (OA). OA is the most common degenerative joint disorder and it affects millions. It presents with degradation of articular cartilage which leads to loss of joint mobility and function, accompanied by chronic pain. The molecular landscape underlying OA pathogenesis is complex and includes several genetic and epigenetic mechanisms. It is hypothesised that there are distinct molecular mechanisms that drive cartilage ageing and disease. MicroRNAs (miRNAs or miRs) are gene expression regulators that act post-transcriptionally and control tissue homeostasis in response to environmental and intracellular changes. This thesis established differentially expressed (DE) miRNAs between cartilage from young [age ± standard deviation (SD)=23.8±3.8] patients undergoing anterior cruciate ligament (ACL) surgery and OA intact and lesioned cartilage from old (age±SD=62.6±7.3) patients undergoing total knee replacement (TKA) by using microarray analysis. Differential expression of selected miRNAs was further assessed in an extended cohort of human young ACL and old OA cartilage samples by quantitative Polymerase Chain Reaction (qPCR), and the response of these miRNAs was characterised in an *in vitro* OA inflammatory cell model by treating chondrocytes with human recombinant interleukin-1 beta (IL-1 $\beta$ ) for different time points (6h, 24h and 5 days). Potential mRNA targets of specific miRNAs were selected by utilising online target prediction tools and miRNA-mRNA interactions were experimentally investigated by undertaking gain and loss of function approaches in human primary OA chondrocytes, coupled with transcriptomic and proteomic detection methods, such as qPCR and Liquid Chromatography-Tandem Mass Spectrometry (LC-MS/MS). Moreover, this thesis investigated the effect of ageing without OA involvement on miRNA expression by using small RNA Sequencing (RNA-Seq) between young (age mean±SD=4±1 years) and old (age mean±SD=17.4±1.9 years) healthy equine chondrocytes.

miRNAs have attracted a lot of scientific interest in the last few years. In this thesis, the use of microarray analysis allowed the identification of several DE miRNAs between young ACL cartilage and old OA human cartilage. Bioinformatics analysis indicated the involvement of DE miRNAs in ageing and OA-related mechanisms and revealed a distinct set of molecular

pathways involved in disease progression, including inflammation and mechanical stress. qPCR validation of selected miRNAs, such as miR-361-5p, -379-5p, -107 and -143-3p in an extended cohort of human cartilage samples confirmed microarray findings. Furthermore, investigation of these miRNAs in an *in vitro* inflammatory environment revealed a time-dependent catabolic effect of inflammation on the expression of the selected miRNAs, which differed per timepoint, level of dysregulation and miRNA species. While no differences were observed in miRNA expression between IL-1 $\beta$ -treated and control chondrocytes at the 6h timepoint, miR-361-5p and miR-107 showed decreased expression in IL-1 $\beta$ -treated cells after 24h, which further decreased after 5 days of treatment. miR-379-5p showed no difference at the 24h timepoint but had the largest decrease in IL-1 $\beta$ -treated cells after 5 days of treatment. Interestingly, miR-143-3p showed increased expression in IL-1 $\beta$ -treated cells at the 24h timepoint, but its expression was decreased after 5 days of IL-1 $\beta$  treatment.

Gain and loss of function approaches supported a role for miR-107 and miR-143-3p in important pathways relevant to OA. qPCR analysis suggested the involvement of miR-107 in the Wingless-Related Integration Site (WNT) and Indian Hedgehog (IHH) signalling pathways, through the targeting of *WNT4* and *IHH*, respectively, in human primary OA chondrocytes treated with miR-107 mimics and inhibitors and in human ACL and OA cartilage tissues. LC-MS/MS in human primary chondrocytes treated with miR-143-3p mimics and inhibitors indicated a role for miR-143-3p in stress response and suggested a link between miR-143-3p and Eukaryotic Translation Initiation Factor (EIF) 2 signalling. In addition, results suggested the targeting of Transforming Growth Factor Beta Receptor (*TGFBR*) 1 by miR-379-5p in human OA chondrocytes, however this interaction was not validated in human cartilage tissues. Also, there were no specific interactions identified between miR-361-5p and the target genes that were selected for validation. Finally, small RNA-Seq in young and old healthy equine chondrocytes identified a well-defined profile of DE miRNAs in chondrocyte ageing, including miR-143-3p.

This thesis identified a large set of DE miRNAs involved in cartilage biology and OA and supported the implication of specific miRNAs in important cellular mechanisms that regulate chondrocyte proliferation, hypertrophy and protein translation. In addition, it has set the ground for future research on the role of miRNAs in cartilage and chondrocyte homeostasis and their connection to disease.

# **Chapter 1: General Introduction**

Articular cartilage is a specialised type of connective tissue found in diarthrodial joints and covers the end of bones, protecting them from friction and load bearing. It is devoid of blood vessels and nerves and has a limited intrinsic healing capacity. Alteration in articular cartilage begin to accumulate with age, predisposing the tissue to age-related diseases such as osteoarthritis (OA). OA is the most common musculoskeletal disorder and a major cause of disability in older individuals. According to the World Health Organisation, 10-15% of people over 60 years have some degree of OA and this percentage is expected to increase as the ageing population increases (Wittenauer et al., 2013). It is estimated that by 2050, 130 million people will suffer from OA worldwide, of which 40 million will be severely affected (Wittenauer et al., 2013). In the UK this is also reflected on the economic burden, as musculoskeletal diseases have the highest rate of medical consultation (Wittenauer et al., 2013).

OA commonly affects the knee and hip joints, and primarily presents with articular cartilage degeneration that leads to impaired joint movement and increased frailty. Other symptoms include subchondral bone remodelling, osteophyte formation and joint inflammation (Martel-Pelletier et al., 2016). Many risk factors have been identified, such as genetics and obesity, however age is the most common (Loeser et al., 2016). Although OA is not the direct result of ageing, it is believed that age-related changes in the joint make articular cartilage susceptible to OA (Loeser et al., 2016). Moreover, there is an imbalance between anabolic and catabolic processes in OA, but the molecular mechanisms that drive disease pathogenesis still remain elusive.

MicroRNAs (miRNAs/miRs) are a class of short [~22 nucleotides (nt)], endogenous, non-coding RNA molecules which act at the post-transcriptional level to regulate gene expression (Li et al., 2015). They function by targeting complementary sequences in messenger RNAs (mRNAs) which leads to translational repression and/or mRNA degradation (Iwakawa et al., 2015). It is estimated that miRNAs bind 1/3 of human genes and are involved in many different physiological processes, including cartilage ageing and metabolism (Li et al., 2015, Ukai et al., 2012). Indeed, miRNAs play an important role in maintaining normal cartilage physiology (Li et al., 2015, Miyaki et al., 2010), but have also been implicated in the pathogenesis of OA (Miyaki et al., 2012, Nugent, 2016, Yu et al., 2015). Many studies have reported differentially expressed (DE) miRNAs in cartilage from OA patients compared to normal cartilage (Akhtar et

al., 2010, Chen et al., 2016a, Wu et al., 2017, Zhang et al., 2017), highlighting their potential value as therapeutic targets and disease biomarkers.

This thesis hypothesises that alterations in miRNA expression in ageing cartilage result in gene expression dysregulation and hence altered chondrocyte phenotype contributing to OA. To test this, I set the following objectives:

1. Establish DE miRNAs between young intact and old OA human knee cartilage using microarrays to investigate miRNAs that change with ageing and OA.
2. Investigate selected miRNAs in an *in vitro* OA inflammatory model.
3. Characterise selected target genes of a set of DE miRNAs based on their predicted function in cartilage homeostasis and investigate the role of physiologically relevant miRNA:target interactions through miRNA gain- and loss-of-function approaches, quantitative polymerase chain reaction (qPCR) and liquid chromatography-tandem mass spectrometry (LC-MS/MS).
4. Establish DE miRNAs between young healthy and old healthy equine chondrocytes using small RNA sequencing (RNA-Seq).

## **1.1 General information about articular cartilage**

Cartilage is a highly specialised connective tissue found in different anatomical positions within the human body. It consists of chondrocytes, the only cell type present in the tissue, and the extracellular matrix (ECM). Dependent on ECM composition, three different types of cartilage exist: hyaline, elastic and fibrous cartilage (Krishnan et al., 2018). Hyaline cartilage is the most common type in humans and it is found in the ribs, nose, trachea as well as in the articulating surfaces of diarthrodial joints, in which case it is called articular cartilage (Krishnan et al., 2018).

Articular cartilage is a type of tissue that does not contain blood vessels and nerves and receives nutrients via synovial fluid and to a lesser degree via subchondral bone (Wang et al., 2013). The main function of articular cartilage is to support joint movement by providing a smooth gliding surface between bones, to facilitate load bearing and load transferring through the joint, as well as act as shock absorber (Camarero-Espinosa et al., 2016).

Three distinct zones make up the full thickness of articular cartilage; the superficial or tangential zone, the middle or transitional zone and the deep zone, all of which have different chondrocyte and ECM organisation (Sophia Fox et al., 2009) (**Figure 1.1**). The superficial zone is the thinnest of the three zones and makes up approximately 10-20% of articular cartilage thickness. This zone protects the deeper layers and is responsible for the tensile and stretching-resistant properties of articular cartilage. The middle zone makes up 40-60% of cartilage thickness and provides the first line of resistance to compressive forces. Finally, the deep zone makes up around 30% of tissue thickness and shows the greatest resistance to compressive forces (Sophia Fox et al., 2009). A layer of calcified cartilage is found beneath the deep zone and acts as a bridge between articular cartilage and subchondral bone.

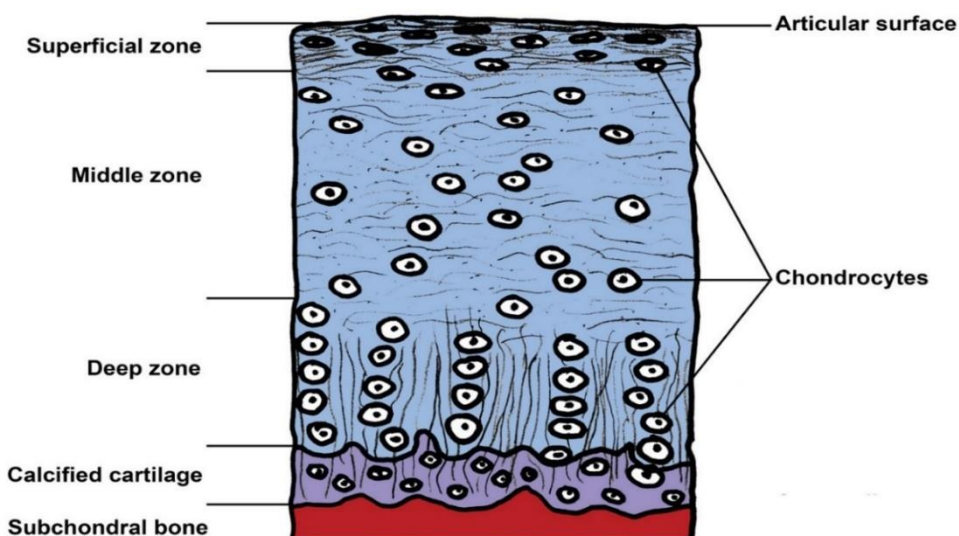


**Figure 1.1: Zonal organisation of articular cartilage.** The three main zones of articular cartilage: superficial, middle and deep zone, are characterised by different chondrocyte organisation and ECM composition and are responsible for the tensile and force-resistant abilities of the tissue. A layer of calcified cartilage acts as an anchor between articular cartilage and subchondral bone. Figure adapted from (Bohaček et al., 2015) with permission from the journal (the contents of PERIODICUM BIOLOGORUM may be reproduced without permission provided that credit is given to the journal).

## **1.2 Components of articular cartilage**

### **1.2.1 Chondrocyte**

Chondrocytes are the only cell type present in articular cartilage and make up approximately 5% of cartilage total volume (Rahmati et al., 2017). Their number, shape and size differ dependent on which of the three main zones the cells are located in. Chondrocytes in the superficial zone are flatter and smaller, in the middle zone are rounder with a random orientation, whereas in the deep zone are larger and organised in columns perpendicular to the articular surface (Sophia Fox et al., 2009, Goldring, 2012). Chondrocytes are sparsely distributed in cartilage and they do not form cell to cell interactions. Mature chondrocytes in adults show very little proliferative capacity and remain in a steady phase which resembles the resting chondrocytes of the growth plate during development (Correa et al., 2017). This results to the very limited healing capacity of articular cartilage (Sophia Fox et al., 2009).

Mature chondrocytes are quiescent, fully differentiated cells that are responsible for maintaining the synthesis of ECM components such as collagens, proteoglycans, glycoproteins and other non-collagenous molecules (Singh et al., 2018). These molecules have a low turnover and chondrocytes are responsible for maintaining the balance between anabolic and catabolic processes, thus maintaining the integrity of the tissue.

### **1.2.2 The extracellular matrix (ECM)**

The ECM makes up approximately the remaining 95% of articular cartilage volume and consists of 80% water and 20% solid components (Camarero-Espinosa et al., 2016). The solid component of the ECM consists of different types of proteins, such as collagens, proteoglycans and other non-collagenous proteins (Camarero-Espinosa et al., 2016). The composition of the ECM varies between the different zones of articular cartilage (Armiento et al., 2018). In addition to the differences observed between zones, the ECM shows a radial/regional organisation as well. Single or grouped chondrocytes are surrounded by a microenvironment called the pericellular matrix and this structure together with the

surrounded cell constitutes a chondron. Chondrons are surrounded by the territorial matrix and the region between chondrons is called the interterritorial matrix (Armiento et al., 2018, Camarero-Espinosa et al., 2016) (**Figure 1.2**).

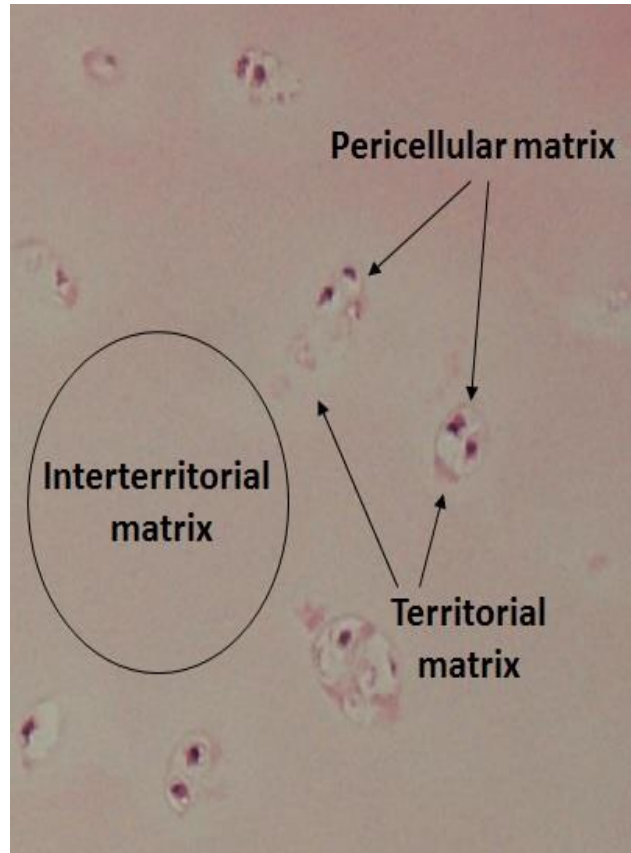


**Figure 1.2: The regional organization of the ECM of articular cartilage.** Three different regions have been described in the ECM: the pericellular matrix, the territorial matrix and the interterritorial matrix. Original figure, courtesy of the author.

### 1.2.2.1 Collagen

Collagens are the main proteins that make up the solid component of the ECM in articular cartilage (approximately 50-75% of the solid component) (Camarero-Espinosa et al., 2016). Chondrocytes secrete premature forms of collagens called procollagens. Procollagens are further processed by enzymes in the ECM and they form the mature collagen fibrils that are

found throughout articular cartilage (Camarero-Espinosa et al., 2016). These collagen fibrils are linked in a specific way and form an extensive meshwork which is responsible for many of the load-bearing and tensile properties of the tissue (Eyre, 2002). There are different types of ECM collagen, such as collagen type II, III, VI, IX, X and XI (Eyre, 2002). The abundance and localisation of each type is different (**Table 1.1**).

**Table 1.1: Distribution of different types of collagen in articular cartilage and their percentage of total collagen content.** Table compiled with information from (Camarero-Espinosa et al., 2016, Eyre et al., 2006, Luo et al., 2017, Wu et al., 2010).

<b>Collagen type</b>	<b>% of total collagen content</b>	<b>Distribution</b>
Collagen II	90-95	Throughout the tissue
Collagen IX	1	Throughout the tissue, associated with type II (cross-linking)
Collagen XI	3	Throughout the tissue, associated with type II (cross-linking)
Collagen VI	<1	Concentrated in the pericellular matrix
Collagen X	1	Deep and calcified zones

Collagen III	0.5-10	Throughout the tissue, associated with type II
--------------	--------	---

Collagen type II is the most abundant type of collagen in articular cartilage and accounts for approximately 90-95% of the total collagen content in the adult tissue (Camarero-Espinosa et al., 2016, Eyre et al., 2006). Transmission electron microscopy reveals a specific pattern in the three cartilage zones (Eyre et al., 2006). In the superficial zone, collagen fibrils tend to be thinner and aligned parallel to cartilage surface. In the middle zone, collagen fibrils are thicker and more randomly distributed, whereas in the deep zone fibrils seem to obtain an orthogonal orientation perpendicular to cartilage surface (Eyre, 2002, Eyre et al., 2006). A similar pattern is seen within the regional organisation of the ECM, with thinner collagen fibrils closer to the pericellular matrix and thicker fibrils closer to the interterritorial matrix (Eyre, 2004, Eyre et al., 2006).

Collagen type IX and XI are two other collagen types important for the assembly of the collagen meshwork in articular cartilage. Even though they account for a small percentage of the total collagen content in the adult tissue (about 1% and 3%, respectively) (Camarero-Espinosa et al., 2016), they form a heteropolymer along with collagen type II which is essential for the formation of the basic cartilage structure (Eyre et al., 2006). Specifically, collagen type IX cross-links with collagen type II and other collagen type IX fibrils forming the heteromeric fibrils observed in articular cartilage (Eyre et al., 2006, Luo et al., 2017). Collagen type XI fibrils cross-link mainly to each other but also to collagen type II fibrils and they regulate cartilage formation by constraining the lateral growth of collagen type II network (Eyre, 2002, Luo et al., 2017).

### 1.2.2.2 Proteoglycans

Proteoglycans account for about 10% to 15% of cartilage dry weight (Camarero-Espinosa et al., 2016, Vynios, 2014). As their name suggests, proteoglycans consist of a core protein and

one or more polysaccharide branches which are called glycosaminoglycans (GAGs). GAGs are linear polysaccharides, with the most common being chondroitin sulphate, keratan sulphate, dermatan sulphate and hyaluronan (Camarero-Espinosa et al., 2016). GAGs, except for hyaluronan, have a negative charge and are responsible for the osmotic pressure generated within cartilage and contribute significantly to the compressive and load bearing ability of the tissue (Knudson et al., 2001, Sophia Fox et al., 2009). Based on their GAG content, composition and properties, proteoglycans are divided into several families (Vynios, 2014). Each contains different members but the most important and well-studied proteoglycans are aggrecan, decorin and biglycan (Vynios, 2014).

Aggrecan is the largest and most abundant proteoglycan in articular cartilage (Sophia Fox et al., 2009). Its core protein consists of three globular domains (G1, G2 and G3) and three interglobular domains. Chondroitin sulphate and keratan sulphate are the two types of GAGs found on aggrecan, and they bind the core protein on the interglobular domain between G2 and G3 (Knudson et al., 2001). Aggrecan strongly binds hyaluronan through a link protein. More than 100 aggrecan molecules bind a single string of hyaluronan to form aggregates (Dudhia, 2005) which contribute significantly to the load-bearing function of articular cartilage.

Decorin and biglycan belong to the family of small leucine-rich proteoglycans. The family derives its name from the leucine-rich motif found in adjacent domains in the protein (Roughley, 2006). Decorin has one chain of dermatan sulphate, whereas biglycan has two (Roughley, 2006, Sophia Fox et al., 2009). In contrast to aggrecan, decorin and biglycan do not form aggregates. Instead, they are linked to the collagen meshwork by achieving a ‘horse-shoe’ confirmation which interacts with individual collagen fibrils (Roughley, 2006). This helps fibril formation, development and interaction in the ECM. Moreover, decorin, biglycan, and other proteoglycans from this family, can bind to proteins which are produced intracellularly but are secreted in the ECM. These include fibronectin, elastin, growth factors such as transforming growth factor beta (TGF- $\beta$ ), as well as cytokines such as tumour necrosis factor alpha (TNF- $\alpha$ ). In this way, these proteoglycans sequester proteins that play an important role in cartilage metabolism and make these secreted signalling factors available to chondrocytes (Roughley, 2006). A schematic representation of the ECM of articular cartilage can be seen in

**Figure 1.3.**

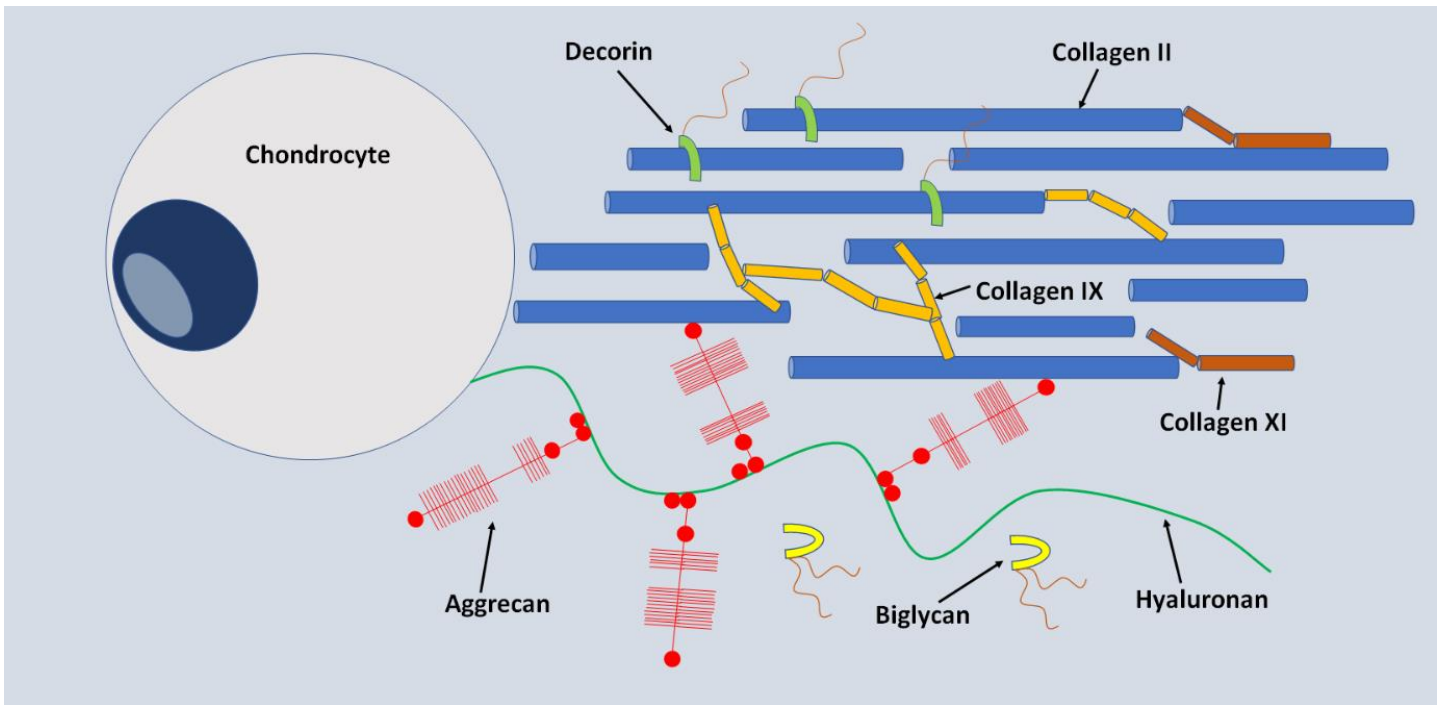


**Figure 1.3: Schematic representation of the ECM of articular cartilage.** Chondrocytes in articular cartilage are embedded in a thick ECM, made up mainly by different types of collagens and proteoglycans. The organisation of the matrix is responsible for many properties of the tissue. Original diagram compiled with information from (Eyre et al., 2006, Knudson et al., 2001).

### 1.3 Chondrogenesis and cartilage formation

Chondrogenesis is an important process during skeletal development which results in the formation of cartilage intermediate (or cartilage anlagen) and long bone through endochondral ossification (Goldring et al., 2006). During the first weeks of gestation, mesenchymal stem cells (MSCs) from the mesoderm start forming the limb buds by undergoing mitosis and forming cell condensates (Camarero-Espinosa et al., 2016). Cell condensation is the result of cell to cell and cell-matrix interactions. TGF- $\beta$  is one of the first signalling pathways activated in MSC condensates and leads to the expression of fibronectin which, then, regulates the expression of neural cell adhesion molecule (NCAM), a protein which is important for cell adhesion and MSC condensation (Goldring et al., 2006). MSCs in

condensates undergo differentiation into chondroprogenitor cells which form the cartilage anlagen. During this process, cells lose their elongated MSC-like appearance and become rounder, resembling chondrocytes (Burden et al., 2009). These chondroprogenitor cells switch off expression of condensation markers and start expressing early cartilage-related proteins, such as collagen type II, IX and XI (Goldring, 2012).

A transcription factor essential for chondrogenesis is sex determining region Y-box transcription factor (SOX) 9. SOX9 is a master regulator of chondrogenesis, expressed not only during embryogenesis but also in adult articular cartilage (Song et al., 2020). During embryogenesis it is expressed as early as MSC condensate formation and differentiation into chondroprogenitor cells (Hallett et al., 2019, Song et al., 2020). Its expression is regulated through the bone morphogenetic protein (BMP) signalling pathway and it interacts with two other SOX members, SOX5 and SOX6, to form the so-called ‘SOX trio’. SOX trio activates the expression of collagen type II, XI and aggrecan in the differentiated chondroprogenitor cells (Hallett et al., 2019).

At the centre of the cartilage anlagen the growth plate is formed which consists of four different chondrocyte layers (Lefebvre et al., 2005). In the outer layer, there are resting chondrocytes which produce large amounts of ECM components (Camarero-Espinosa et al., 2016). The next layer is the proliferating zone which undergoes hypertrophy, adding to the third layer of the growth plate, the transformation zone (Burden et al., 2009, Lefebvre et al., 2005). The final layer is the degeneration zone where the terminally differentiated hypertrophic chondrocytes undergo apoptosis accompanied by cartilage matrix calcification, blood cell invasion (angiogenesis) and, finally, ossification (Goldring et al., 2006) (**Figure 1.4**).

The molecular pathways associated with growth plate formation and bone development are complex. One of the key transcription factors essential for chondrocyte maturation, endochondral ossification and bone formation is RUNX family transcription factor 2 (RUNX2). RUNX2 is expressed in resting and proliferative chondrocytes at low levels, but its expression is increased in prehypertrophic chondrocytes (Komori, 2018, Nishimura et al., 2018). RUNX2 induces the expression of Indian hedgehog (IHH) in prehypertrophic chondrocytes. IHH has an array of roles in cartilage and bone development (Nishimura et al., 2018), such as inducing the expression of parathyroid hormone-related protein (PTHrP) in the zone of resting and proliferating chondrocytes which promotes chondrocyte proliferation and keeps

chondrocytes in the proliferating stage (Melrose et al., 2016). However, IHH can also act in a PTHrP-independent manner and studies have shown that, in addition, it can promote chondrocyte maturation and matrix calcification (Amano et al., 2008, Nishimura et al., 2018).

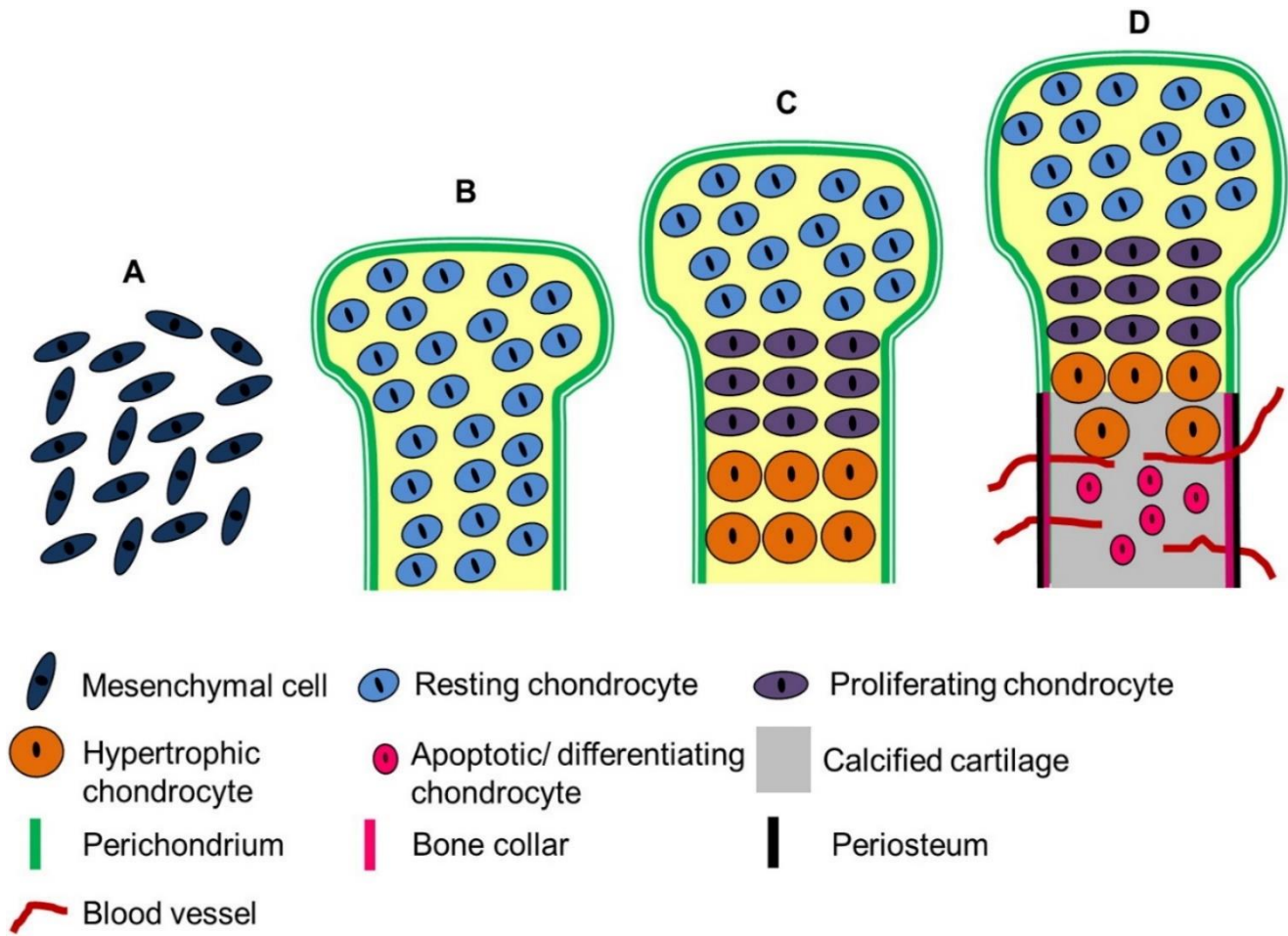


**Figure 1.4: Chondrocyte differentiation and growth plate formation during embryonic development of long bones.** A schematic representation of the sequential stages of chondrocyte differentiation during long bone development is depicted here. The cartilage anlagen is surrounded by a chondrogenic structure called the perichondrium. Following blood vessel invasion, osteoblasts arrive at the site to form new bone (bone collar and periosteum). Figure copied with permission from (Melrose et al., 2016) (License Number: 4987800547939).

In addition to IHH, RUNX2 regulates the expression of other target proteins, including collagen type X in hypertrophic chondrocytes and matrix metallopeptidase (MMP) 13 and vascular endothelial growth factor A (VEGFA) in terminally differentiated chondrocytes (Komori, 2020). Collagen type X is a well-recognised marker of chondrocyte hypertrophy and it is believed that the matrix formed by collagen type X provides support during cartilage degradation and is easily replaced by bone (Shen, 2005). Moreover, collagen type X binds to specific matrix vesicles which rapidly uptake  $\text{Ca}^{2+}$ , suggesting that this type of collagen plays a role in calcification and matrix mineralisation during endochondral ossification (Shen, 2005). Furthermore, MMP13 is responsible for the breakdown of the ECM by cleaving collagen type II in the layer of terminally differentiated chondrocytes (Malemud, 2006). VEGFA drives blood vessel invasion and vascularisation of the forming bone (Vadalà et al., 2018). **Figure 1.5** summarises the basic molecular signalling pathways during growth plate development.

Articular cartilage forms at the end of long bones, however the events that lead to its formation, maturation and permanent status are less clear. It is believed that articular cartilage is formed from flat, densely packed MSCs which appear at each site of joint formation in the cartilage anlagen. These MSCs are called the ‘interzone’ and they are dedifferentiated chondrocytes from the chondrocyte anlagen (Decker et al., 2015). Postnatally, articular cartilage undergoes growth and re-modeling to form mature cartilage. Again, the events responsible for the maturation of the tissue and its zonal organisation are not clear. Studies have shown the presence of i) slow-proliferating, stem-like cells within the superficial zone, and ii) rapidly-dividing cells in the middle and upper layers of the deep zone (Hayes et al., 2001, Hunziker et al., 2007). The stem cells in the superficial zone have a dual role; by dividing they contribute to the lateral growth of articular cartilage, and also provide daughter cells to the rapidly-dividing middle and deep zone which, in turn, are responsible for the vertical growth of the tissue (Hunziker et al., 2007).

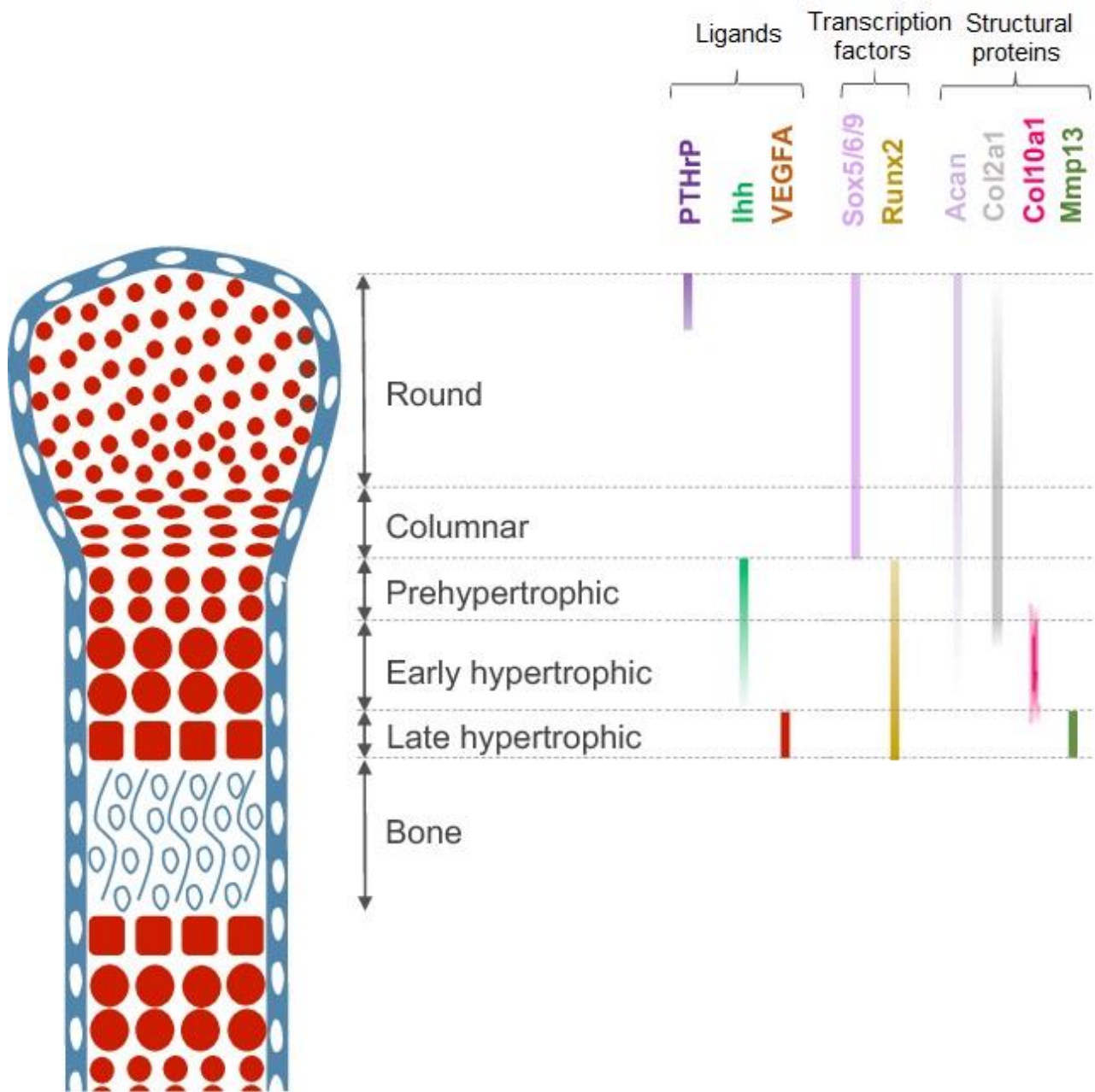


**Figure 1.5: Simplified overview of the molecular signalling pathways in the growth plate during endochondral ossification.** During embryonic development, a growth plate is formed in each side of the long bones and consists of different layers of chondrocytes, each with its own organisation and specific molecular signals involved. A complex network of proteins, including ligands, transcription factors and structural proteins, acts in each layer to regulate growth plate elongation and bone formation. Growth plate development is a highly specialised process and the signalling pathways involved need to be tightly regulated in each layer. Figure modified from (Kozhemyakina et al., 2015).

## **1.4 Ageing and articular cartilage**

Ageing can be defined as the accumulation of changes in the biological, psychological and social aspect of an organism and is a life-long process (Kalache, 1999). Biological ageing refers to the accumulation of damage at the molecular and cellular level that impacts the well-being of an organism. Ageing can influence the function of all organs in an organism and, therefore, it can have an adverse effect on proper articular cartilage and joint function and, in turn, can predispose individuals to an increased risk for developing joint diseases and pathologies (Rahmati et al., 2017). This is evident from that fact that ageing is the leading risk factor for developing OA (Loeser et al., 2016). Changes with ageing in articular cartilage have been observed at the molecular, cellular and extracellular level and these are discussed below.

### **1.4.1 Ageing-related changes in the ECM of articular cartilage**

Articular cartilage has a limited healing capacity and a very slow turnover. Aged cartilage exhibits reduced synthesis of anabolic markers and ECM components (Mobasher et al., 2015), but also the quality of the ECM itself decreases. Collagen type II has a half-life of more than 100 years (Loeser et al., 2016). However, non-enzymatic cross-linking of collagen type II is observed with increasing age (Loeser et al., 2016). Collagen cross-linking results in the accumulation of advanced glycation end-products which occur as the result of non-enzymatic glycation of proteins, and specifically when reducing sugars, such as glycose and fructose, react with lysine or arginine (Loeser, 2010). This extensive cross-linking impacts the mechanical properties of the tissue, making articular cartilage stiffer and more brittle, and leads to focal defects which accumulate with age (Loeser, 2010). Moreover, these advanced glycation end-products result in bigger collagen fibres which reduces collagen elasticity, making the tissue more susceptible to damage (Rahmati et al., 2017). A Magnetic Resonance Imaging (MRI) study between young (20-30 years) and old (50-78 years) individuals with no OA or other knee-related defects, showed thinning of knee femoral articular cartilage in the old group compared to young (Hudelmaier et al., 2001). Moreover, this study reported less

deformation of cartilage in the old group, which supports that the tissue becomes more brittle with increasing age (Hudelmaier et al., 2001).

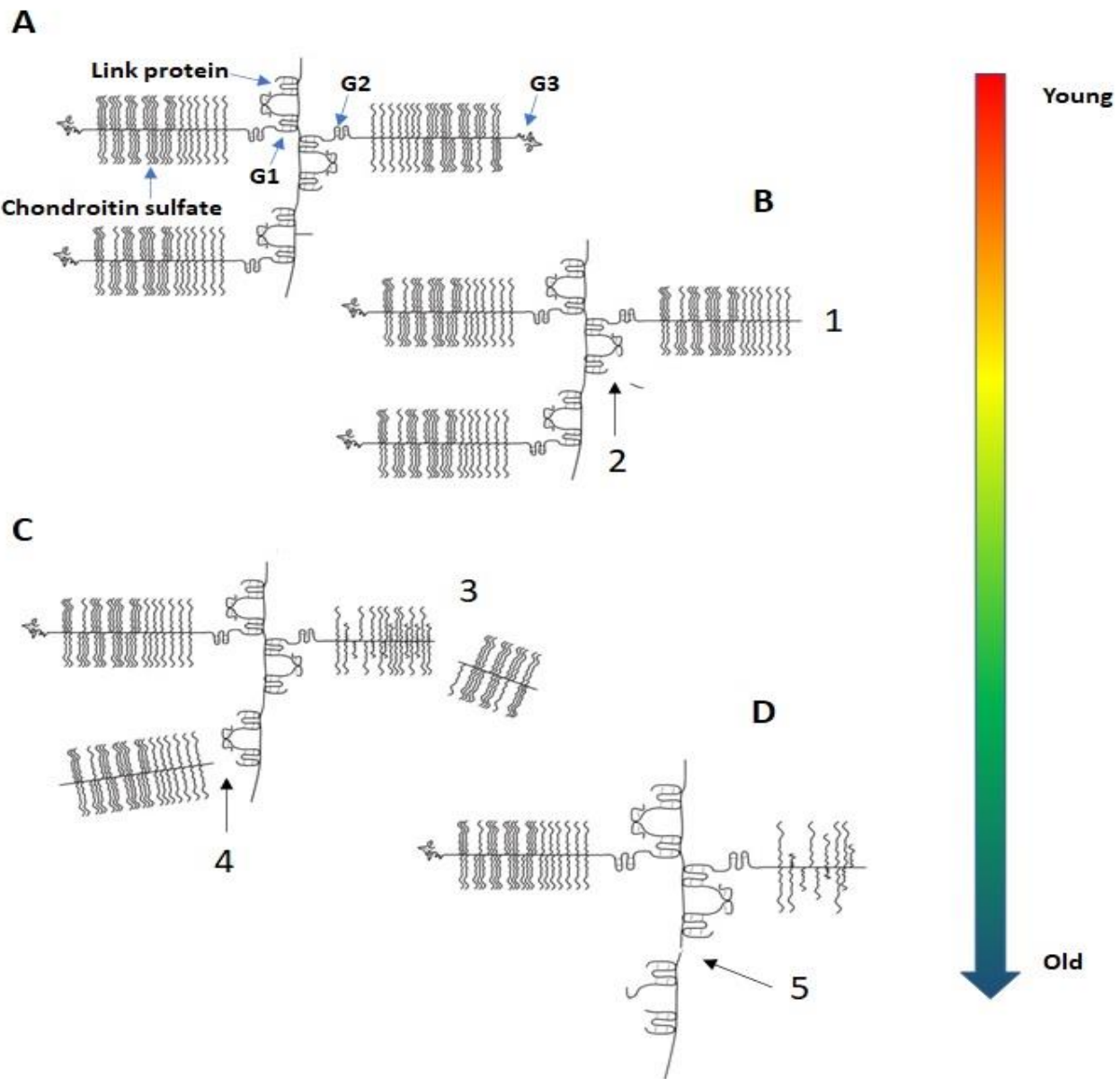


**Figure 1.6: Increasing proteolytic cleavage of aggrecan with ageing.** Aggrecan molecules within ECM undergo increasing trimming with ageing. (A) One hyaluronan filament can be bound by many aggrecan molecules. (B) The first events of proteolytic cleavage take place at the G3 domain (1) and the link protein (2). (C) With increasing ageing, aggrecan is further trimmed at the chondroitin sulphate chain, which results in aggrecan molecules with different lengths of chondroitin sulphate chains (3, 4). (D) Final cleavage events lead to free G1 and link protein domains which remain in the ECM or are diffused in synovial fluid (5). Figure modified with permission from (Dudhia, 2005) (License Number: 4987820394205).

Ageing also impacts the proteoglycan content in articular cartilage. The size of the aggregates formed by aggrecan decreases with ageing, caused by changes in the length of keratan and chondroitin sulphates (Rahmati et al., 2017). Studies have shown that there is an increase in the length of keratan sulphate chains and a decrease in the length of chondroitin sulphates with age (Dudhia, 2005). This results in changes in the structure and sulphate-content of the aggregates, thus limiting the functional properties of the tissue (Loeser, 2010). In addition, proteolytic cleavage from both ends of the aggrecan molecules have been observed with ageing (Dudhia, 2005) (**Figure 1.6**). The trimming usually starts at the C-terminal of the G3 domain and the N-terminal of the link protein and they are the first events of proteolytic cleavage of aggrecan. Then, with increasing age, the trimming continues to the chondroitin sulphate region which can result in a heterogeneous mixture of aggrecan molecules of different length. Following from this, the interglobular domain is cleaved and the chondroitin sulphate chains are diffused in the synovial fluid and, finally, as the trimming continues, there are just G1 domains left attached in hyaluronan filaments or free G1 domains in the ECM (Dudhia, 2005). This is supported by studies that have shown that the free G1 molecules are more abundant in aged normal cartilage compared to link protein molecules which seem to be cleaved early in life (Wells et al., 2003). These events change the composition of the aggregates and interfere with the ability of the tissue to maintain its functionality. The thinner appearance of aged human cartilage compared to young cartilage can also be explained by the limited amount of water held within the aggregates of the ECM due to the structural and functional changes in aggrecan (Loeser, 2010).

#### **1.4.2 Age-related chondrocyte senescence, inflammation and oxidative stress**

A cell is characterised as senescent when it stops proliferating and enters a growth arrest phase with altered metabolism (Rahmati et al., 2017). Senescence is considered a hallmark of ageing, and aged or diseased chondrocytes may display features of senescence, termed chondrosenescence (Mobasheri et al., 2015). One of the mechanisms which can lead to senescence is telomere shortening through repetitive cell proliferation, referred to as replicative senescence (Rahmati et al., 2017). However, chondrocytes are long-lived cells that have a very slow proliferating rate, therefore telomere shortening alone is unlikely to be an

explanatory mechanism of chondrosenescence in articular cartilage (Loeser, 2010). Instead, chondrosenescence can also be caused by other events, such as trauma, DNA damage and oxidative stress (Rahmati et al., 2017). DNA damage accumulates with ageing especially in chondrocytes which divide very slowly, leading to changes in gene expression and predisposing them to disease (Loeser et al., 2016, Rose et al., 2012).

Oxidative stress is another major contributor of age-related cell damage that could lead to senescence in chondrocytes. Oxidative stress is caused by the accumulation of free reactive oxygen species (ROS) which are produced during mitochondrial respiration and can damage DNA and proteins, resulting in altered cellular function (Sacitharan et al., 2016). ROS production is linked to mitochondrial function which worsens with ageing, causing an imbalance between the production of these damaging agents and the antioxidant mechanisms of the cell (Loeser et al., 2016). Increased levels of different ROS groups have been identified in aged articular chondrocytes of different species, including superoxide derivatives in rat (Jallali et al., 2005) and nitrotyrosine in human and monkey (Loeser et al., 2002). In addition, decreased levels of antioxidants have been found in aged cartilage/chondrocytes. Specifically, the activity of superoxide dismutase 2 (SOD2), a protein which metabolises ROS, was decreased in cartilage from old rats compared to young (Fu et al., 2016), and *Sod2* knockout mice exhibited cartilage degeneration and increased superoxide production compared to control (Koike et al., 2015). ROS also acts by oxidising antioxidant proteins in chondrocytes, interfering with their antioxidant activity, such as in the hyperoxidation of the peroxiredoxin enzyme family, which was increased in chondrocytes from older humans compared to young (Collins et al., 2016).

Once senescence is established in a cell, this results in more phenotypic changes that could have a detrimental effect on cell homeostasis. A characteristic of ageing linked to senescence is the systemic low-grade inflammation, termed inflammageing (Franceschi et al., 2000). Production of pro-inflammatory cytokines, such as IL-1 $\beta$  and interleukin 6 (IL-6), increase with ageing and are linked to age-related diseases of the musculoskeletal system such as OA (Loeser, 2010). Inflammation is considered a feature of aged senescent chondrocytes which seem to acquire the so-called ‘senescence-associated secretory phenotype’ (SASP). SASP is characterised by increased production of pro-inflammatory mediators and matrix degrading

enzymes, such as MMP13, and therefore aged senescent chondrocytes with SASP may contribute to the development of disease (Li et al., 2017, Loeser, 2010, Loeser et al., 2016).

Moreover, aged senescent chondrocytes are characterised by altered responses to growth factors and other stimuli. Studies have shown that chondrocytes isolated from old healthy human cartilage have a reduced response when treated with insulin growth factor 1 (IGF-1) and BMP-7 (also known as osteogenic protein-1) compared to chondrocytes isolated from young donors (Loeser et al., 2014). Both IGF-1 and BMP-7 exert an anabolic effect on cartilage, resulting in proteoglycan synthesis. Old chondrocytes had reduced proteoglycan synthesis due to reduced sensitivity to these two growth factors. In the same study, oxidative stress-induced chondrocytes showed less proteoglycan synthesis due to the inhibition of IGF-1 signalling, providing further evidence on the link between age, senescence and altered cellular signalling (Loeser et al., 2014).

#### **1.4.3 Age-related chondrocyte autophagy and apoptosis**

Autophagy is an essential mechanism which acts to maintain cell homeostasis during nutrient supply shortage and energy/metabolism stress by removing and recycling defective or unnecessary organelles or proteins of the cell, thus promoting cell survival (Li et al., 2017, Rahmati et al., 2017). Increased autophagy is associated with longevity, and several studies have reported a decreased autophagic activity and autophagy-promoting proteins in aged chondrocytes and cartilage. Caramés *et al* (2015) reported reduced autophagic vesicles in the knee joints of old mice compared to young, and concluded that the expression of key autophagic proteins, such as autophagy related 5 (ATG5) and microtubule-associated protein 1 light chain 3 (LC3), was decreased with age (Caramés et al., 2015). In an earlier study, the same group demonstrated decreased levels of three key proteins that drive autophagy, Unc-51-like kinase 1 (ULK1), Beclin1 and LC3, in cartilage and chondrocytes from old human donors compared to young (Caramés et al., 2010). In another study, Petursson *et al* (2013) demonstrated that the expression of another autophagy-related protein, 5' AMP-activated protein kinase (AMPK), was decreased in the joints of old mice compared to young (Petursson et al., 2013). A study by Ulgherait *et al* (2014), demonstrated that overexpression of AMPK in

*Drosophila melanogaster* led to increased autophagy and longevity (Ulgherait et al., 2014), thus providing further evidence on the link between autophagy and age.

In addition, an important mechanism associated with ageing and autophagy is the mechanistic target of rapamycin kinase (mTOR) signalling pathway. mTOR regulates cellular growth and metabolism in response to nutrient intake reduction. Inhibition or deletion of the gene that codes for mTOR leads to increased lifespan in many organisms, including mammals (Johnson et al., 2013). Autophagy is a target of mTOR signalling, supported by the fact that autophagy declines with ageing while mTOR signalling increases. AMPK promotes autophagy by activating ULK1 directly and mTOR disrupts the interaction between these two proteins (Kim et al., 2011). Deletion of the *mTOR* gene in cartilage resulted in i) increased expression of the autophagy markers ATG5, ULK1, LC3 and AMPK, ii) increased expression of collagen type II and aggrecan, iii) decreased expression of catabolic markers, such as MMP13 and iv) protection of mouse joints from induced OA (Zhang et al., 2015b).

Apoptosis, also called programmed cell death, is the regulated process of cell death during embryonic development (Mobasher et al., 2015). However, it is now clear that apoptosis is a characteristic of various age-related diseases, including OA. The link between apoptosis and cartilage ageing is unclear. There seems to be a reduction in the number of chondrocytes with ageing, however the effect of ageing on chondrocyte number and density is still debatable. An older study from Vignon et al (1976) reported a 40% decrease in total chondrocyte number and cell density in the femoral head of donors ranging from 20 up to 90 years old, with the superficial zone showing the most profound decrease among the ECM zones (Vignon et al., 1976). However, another study in human knee cartilage, did not detect significant apoptosis in aged cartilage samples (Aigner et al., 2001). This does not seem to be the case for other species, as there was significant apoptosis detected in the joints of old mice and rats compared to young controls (Adams et al., 1998), highlighting potential species differences. Although the level of apoptosis in aged cartilage is unclear, a potential mechanism through which age could promote apoptosis in chondrocytes is through the high mobility group box 2 (*HMGB2*). *HMGB2* is expressed only in the superficial zone and its expression decreases with ageing in humans and mice (Taniguchi et al., 2009). Mice lacking *Hmgb2* had decreased cellularity and increased apoptosis in the superficial zone, suggesting *Hmgb2* plays an important role in the survival of chondrocytes located in the superficial zone (Taniguchi et al.,

2009). An age-related decrease in the levels of *HMGB2* could contribute to increased apoptosis in the superficial zone justifying, in part, the chondrocyte loss and fibrillation observed in the superficial zone of old healthy donors with no history of OA. Nonetheless, further research is needed to elucidate the effect of ageing on chondrocyte apoptosis. **Table 1.2** summarises the age-related changes observed in articular cartilage and the ways these changes contribute to OA.

**Table 1.2. Summary of age-related changes in articular cartilage and their contribution to OA.** Table compiled with information from (Loeser, 2010).

Changes with ageing	Contribution to OA
Formation of end glycation products	Non-enzymatic collagen cross linking resulting in stiffer and more brittle ECM
Trimming of aggrecan molecules	Loss of water content and decreased ECM resiliency and tensile strength
Chondrosenescence with cells exhibiting the senescent secretory phenotype	Increased cytokine and MMP production that stimulates matrix degradation
Oxidative stress/damage	Increased susceptibility to cell death and reduced matrix synthesis
Decreased growth factor responsiveness	Reduced matrix synthesis and repair
Decreased chondrocyte autophagy	Reduced cell survival and energy stress response
Increased apoptosis	Reduced cell density and increased ECM degradation

## 1.5 Osteoarthritis

### 1.5.1 Definition, epidemiology and management of osteoarthritis

Osteoarthritis (OA) is the most common joint disease and type of arthritis. It can affect any joint but the most commonly affected are the knee, the hip, the hand, the foot and the spine. The information given in this section will primarily focus on knee OA, which is the main joint discussed in this thesis. OA is one of the leading causes of disability and millions are affected worldwide; approximately 250 million people are suffering from knee OA alone (O'Neill et al., 2018). Even though the major clinical feature is cartilage loss, it is now accepted that OA is a disease of the whole joint and several joint tissues, such as bone, synovium, ligaments and muscles, are also affected (Martel-Pelletier et al., 2016).

OA is usually diagnosed based on radiographic findings. The radiographic criteria commonly used to diagnose OA are based on the Kellgren-Lawrence (KL) grading system (Kellgren et al., 1957). According to this, there are five grades of OA severity based on x-ray findings: grade 0 (normal), grade 1 (doubtful), grade 2 (minimal), grade 3 (moderate) and grade 4 (severe). This grading system is based on the presence or absence of various morphological features in a joint, such as formation of osteophytes (small bony projections), narrowing of the joint space, sclerosis of subchondral bone and altered shape of the bone ends (Kellgren et al., 1957) (**Figure 1.7**).

Moreover, OA can be divided into different subclasses based on the underlying cause (primary and secondary OA), and whether there are symptoms present or not (symptomatic and asymptomatic OA). It is called primary (or idiopathic) OA when there is not an identifiable underlying cause but instead it develops as the result of several risk factors. In contrast, it is characterised as secondary when it develops as the result of a specific underlying cause, such as joint trauma, joint defect during birth, joint surgery and others (Martel-Pelletier et al., 2016). Symptomatic OA is characterised by radiographic findings and the presence of symptoms, such as pain, joint stiffness, loss of joint function and movement, which have a significant impact on the quality of life for patients. However, up to 50% of OA cases show radiographic findings with no symptoms present, in which case it is referred to as

asymptomatic or structural or radiographic OA (Hannan et al., 2000, Martel-Pelletier et al., 2016).

## Kellgren and Lawrence (KL) Grading System



### Grade 0

No radiographic features of OA

### Grade 1

Possible osteophytic lipping  
Doubtful joint space narrowing

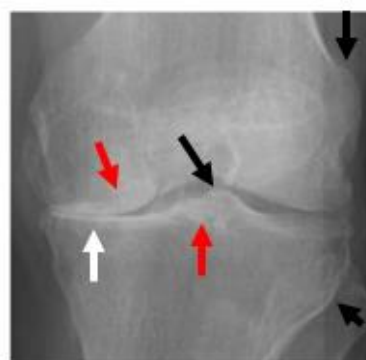
### Grade 2

Definite osteophytes  
Possible joint space narrowing



### Grade 3

Multiple osteophytes  
Definite joint space narrowing  
Sclerosis



### Grade 4

Large osteophytes  
Marked joint space narrowing  
Severe sclerosis

**Figure 1.7: Kellgren and Lawrence (KL) grading system.** The KL scoring system assesses OA severity based on radiographic findings. According to it, there are five different grades of OA severity and each grade is characterised by a set of radiographic findings based on changes in the morphology and shape of the joint, such as osteophytes (black arrows), joint space narrowing (white arrows) and sclerosis (red arrows). Figure modified with permission from (Chen et al., 2019) (License Number: 4987821189921).

The prevalence of OA differs among different populations. However, for both asymptomatic and symptomatic OA, the prevalence increases with age, and especially in women (**Figure 1.8**). It is clear that management and treatment for OA are a significant economic burden, and the costs in developed countries are estimated to be between 1% and 2.5% of the gross domestic product (Hiligsmann et al., 2013).

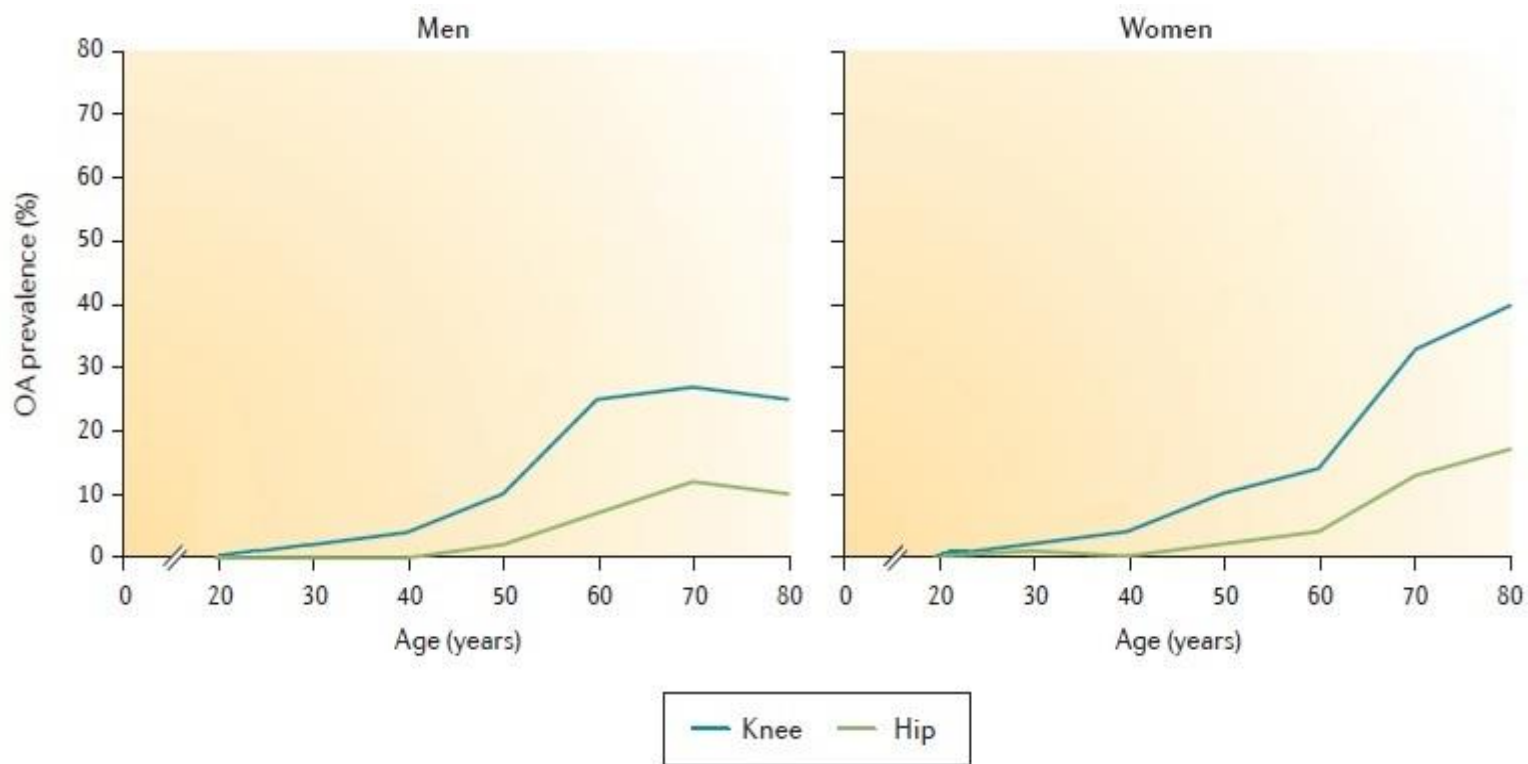


**Figure 1.8: Percentage of knee and hip OA prevalence according to age and sex.** Knee and hip OA prevalence increases with ageing for both sexes and especially for women. A steep increase is observed after the age of 40 for both sexes and especially for women. Data comes from a Dutch population sample. Data was reported by (Oliveria et al., 1995). Figure modified with permission from (Martel-Pelletier et al., 2016) (License Number: 4987830303042).

Early management of knee OA usually begins by educating patients and proposing lifestyle modifications. These may include weight loss, the use of knee braces or walking assisting devices and muscle strengthening (Gress et al., 2020). If symptoms persist, patients can be administered drugs, such as non-steroidal anti-inflammatory drugs (NSAIDs), to relieve pain. In cases where patients are not responding to NSAIDs treatment, they can be treated with injectable corticosteroids to alleviate symptoms (Gress et al., 2020). Corticosteroids act by suppressing inflammation, thus decreasing swelling of the joint. However, due to side effects, injections should not be administered too often and other treatment options should be considered.

Surgical intervention for end-stage OA patients who are unresponsive to drug treatment and experience advanced symptoms is another option. There are different surgical treatments for OA and the correct type of surgery depends on patient and disease characteristics (Gress et al., 2020). So far, the most successful model of surgery for treating end-stage knee OA is TKA, also known as total knee/joint replacement. The procedure involves the dissection and exposure of the knee joint, removal of femoral condyles and tibial plateau and finally fitting and cementing of the prosthetic part (Gress et al., 2020). A study that compared OA patients who received TKA to patients receiving non-surgical treatment (physiotherapy, weight-management, exercise and pain medication), found that TKA significantly reduced pain and improved quality of life for patients, but was associated with more adverse events compared to the non-surgical group (Skou et al., 2015). As with most surgeries, patient selection is critical to achieve maximum patient satisfaction and the best possible outcome. Predictive factors include number of affected joints and presence of comorbidities, as patients with more than one troublesome joints and comorbidities are more likely to have a less satisfactory TKA outcome (Hawker et al., 2013). In a previous study, approximately 10% to 34% of patients who had a knee TKA still reported long-term pain (Beswick et al., 2012). In fact, a percentage of patients who undergo TKA will need a second operation as they need adjustments and revisions to their initial arthroplasty (Gress et al., 2020).

TKA is an invasive operation and a heavy economic burden for the health system, despite being the best option for end-stage OA at the moment. In the last few years, research has focused on alternative surgical interventions for OA. One of them is autologous chondrocyte implantation which involves the insertion of healthy chondrocytes in local cartilage defects in

the joint, in order to delay OA progression and potentially reverse the disease (Gress et al., 2020). Unfortunately, the results so far have been discouraging as studies have not demonstrated significant improvement in the groups that underwent chondrocyte implantation and several of the patients required TKA to manage the disease progression (Knutsen et al., 2016).

### **1.5.2 Risk factors for osteoarthritis development**

There are many risk factors associated with the initiation and progression of OA. Usually these can be divided into two categories: systemic or person-level and mechanical or joint-level (Martel-Pelletier et al., 2016, O'Neill et al., 2018). Systemic risk factors are age, genetics, sex, ethnicity, whereas mechanical risk factors include joint structure, occupation, joint trauma and physical activity. However, it is not always possible to categorise risk factors as certain of them, such as body mass index (BMI), could fall in both categories. Some of these risk factors are analysed further below, except for ageing which has already been discussed extensively.

The role of genetics in the development of OA is still not completely understood. Studies have shown that the contribution of genetics in OA is approximately 50%, but this contribution is polygenic (O'Neill et al., 2018). This means that there is not a single genetic locus responsible for OA, but, instead, there are multiple genetic loci, each contributing minorly to the development of the disease. Genome-wide association studies have identified several such loci, which include variants associated with genes and pathways important for cartilage biology, such as TGF- $\beta$  and (Wingless-related integration site) WNT signalling pathway, mitogen-activated protein kinase (MAPK) signalling pathway, growth/differentiation factor 5 (*GDF5*), iodothyronine deiodinase 2 (*DIO2*), asporin (*ASPN*) genes and others (Martel-Pelletier et al., 2016, Valdes et al., 2011, Zengini et al., 2018). Even though the contribution of each locus in OA development is only small/moderate, they still provide useful information regarding the involvement of specific genes in OA susceptibility and biomarker discovery.

BMI/obesity is another strong risk factor for OA development, especially in the knee. Overweight (BMI >25 kg/m<sup>2</sup>) and obese (BMI >30kg/m<sup>2</sup>) patients have an increased likelihood for developing knee OA compared to non-obese (BMI <25 kg/m<sup>2</sup>) (Silverwood et al., 2015).

Similarly, loss of weight results in decreased likelihood for developing knee OA (Felson et al., 1992). This is partially due to the excessive strain put on the knee joint from increased weight.

Altered biomechanics is a significant risk factor for developing OA and an abnormal joint structure can increase the risk significantly. Abnormal alignment in the knee joint increases the risk for both OA initiation and progression (Sharma et al., 2010). In fact, based on the type of deformity, the medial or the lateral knee condyle can be affected (Sharma et al., 2010).

The relationship between mechanical loading and OA is of great importance. Physical activity is crucial for healthy cartilage and joint development in children, and there seems to be an excessive cartilage volume loss in adults who remain immobilised for a long time due to injury (Martel-Pelletier et al., 2016). Normal mechanical loading is also crucial for chondrocyte homeostasis and development, as it promotes growth factor stimulation and matrix synthesis (Sanchez-Adams et al., 2014). However, the effect of mechanical load on chondrocytes and the ECM depends on different factors such as degree of strain, frequency and duration, among others. There is a range within which mechanical load is beneficial to cartilage and too little or too much stress could jeopardise joint function and lead to decreased matrix synthesis and catabolic responses (Sanchez-Adams et al., 2014) (**Figure 1.9**). This is also evident from studies regarding the effect of physical activity on knee OA risk. In a related study, light and moderate exercise did not increase the risk for knee OA, whereas heavy exercise (>4h per day) increased the risk for knee radiographic OA significantly (McAlindon et al., 1999). In addition, the underlying health of the joint plays a role. In subjects with established knee OA, physical exercise increased the risk for joint replacement surgery (Wang et al., 2011), whereas physical activity had a beneficial effect on healthy subjects with no history of knee disease (Racunica et al., 2007).

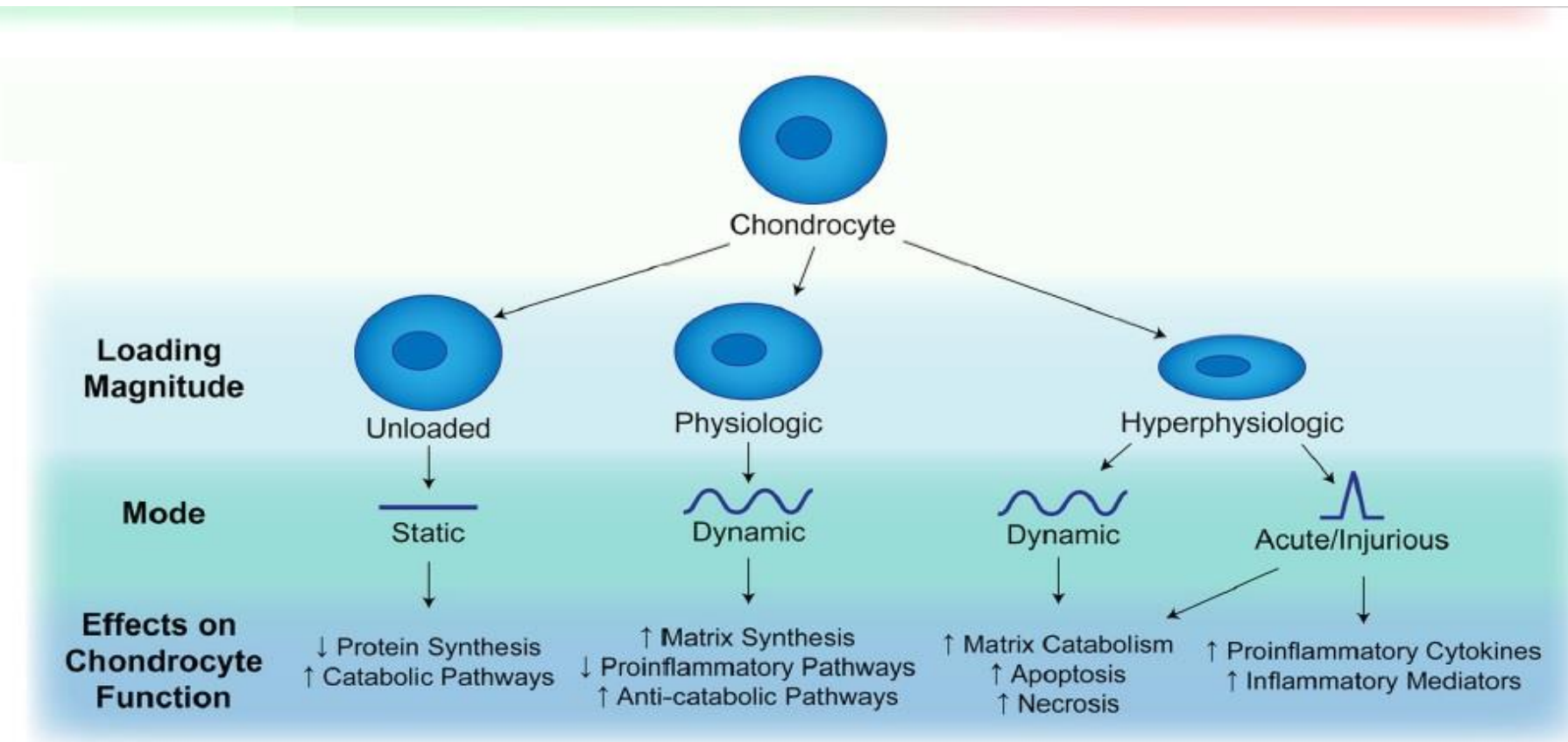


**Figure 1.9: Effect of mechanical loading on chondrocyte function and ECM physiology.** The effect of mechanical loading on cartilage depends on the degree of strain, duration, frequency and loading history. Chondrocytes need physiologic loading in a dynamic manner which stimulates growth factor production and synthesis of matrix components. Too little loading in a static manner, or too much loading in a frequent manner will lead to an inflammatory response, cell death and catabolism. An acute mechanical load beyond the bearing capacity of cartilage will lead to trauma. Figure copied with permission from (Sanchez-Adams et al., 2014) (License Number: 4987830706852).

Trauma to the joint is another risk factor associated with OA, which, in this case, is called post-traumatic OA (PTOA). PTOA is a distinctive type of OA which usually differs from age-related OA and it accounts for approximately 12% of symptomatic OA cases (O'Neill et al., 2018). The mechanism behind PTOA is usually excessive loading and strain on the joint during injury and/or changes in the structure of the joint tissues (O'Neill et al., 2018). An example of joint trauma is ACL rupture. ACL rupture usually occurs in younger individuals who participate in high-activity sports. Patients with ACL rupture have a higher chance of developing PTOA in the long term, even after ACL reconstruction surgery (Ajuied et al., 2014). In an ACL patient cohort, about 34% of patients showed K&L grade I radiological changes 10 years after injury, and 31.5% had grade II radiological changes. Only 14% did not have any radiographical changes (grade 0) 10 years after ACL injury (Ajuied et al., 2014).

### **1.5.3 Macroscopic changes in knee osteoarthritic cartilage**

OA is a disease of the whole joint. However, articular cartilage is one of the main joint tissues affected. At an early stage of the disease, there is swelling of the ECM caused by increased water content in the articular cartilage of the femoral condyles and tibia plateau. This results in superficial fibrillation of the articular surface and the presence of small cracks in the superficial zone (Goldring et al., 2016). Typically, as the disease progresses, there is increased loss of cartilage from the surface towards the deeper zones which leads to the formation of lesions and fissures that extend in the deeper layers (Goldring et al., 2016). In end-stage OA, there is complete loss of cartilage and exposure of the underlying subchondral bone, either from the whole condyle/plateau or parts of these (Goldring et al., 2016).

In 1961, Outerbridge published a classification scoring system to macroscopically describe cartilage lesions (Outerbridge, 1961). Even though this scoring system was initially used to describe lesions in chondromalacia patellae, it has since been used to describe and classify macroscopic/gross changes in knee cartilage or other joints too (Curl et al., 1997). This classification is based on direct visualisation of articular cartilage through an open joint or arthroscopy and is mainly used among clinicians to classify group patients for research, guide treatment or as a prognostic marker (Slattery et al., 2018).

The Outerbridge scoring system is described in **Table 1.3** and examples of different-grade knee cartilage according to the Outerbridge system are seen in **Figure 1.10**.

**Table 1.3: The Outerbridge scoring system for describing macroscopic cartilage lesions.**

Grade	Pathology
I	Softening and swelling of articular cartilage
II	Fragmentation and fissuring of articular cartilage affecting an area of less than 0.5 inches
III	Fragmentation and fissuring of articular cartilage affecting an area of greater than 0.5 inches
IV	Cartilage erosion to bone

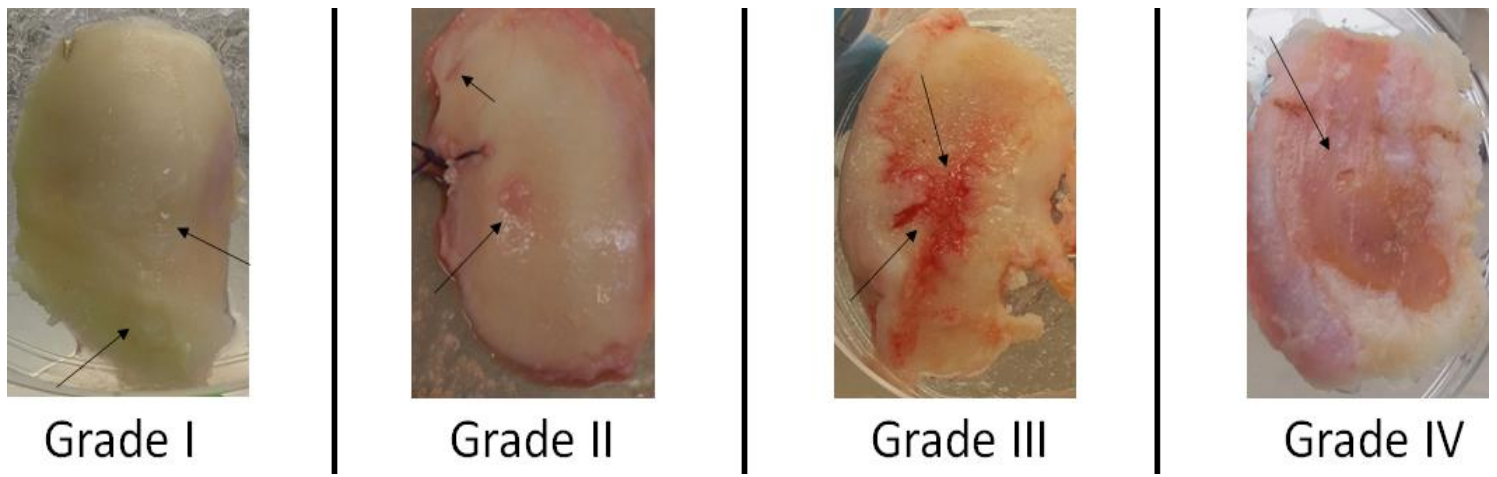
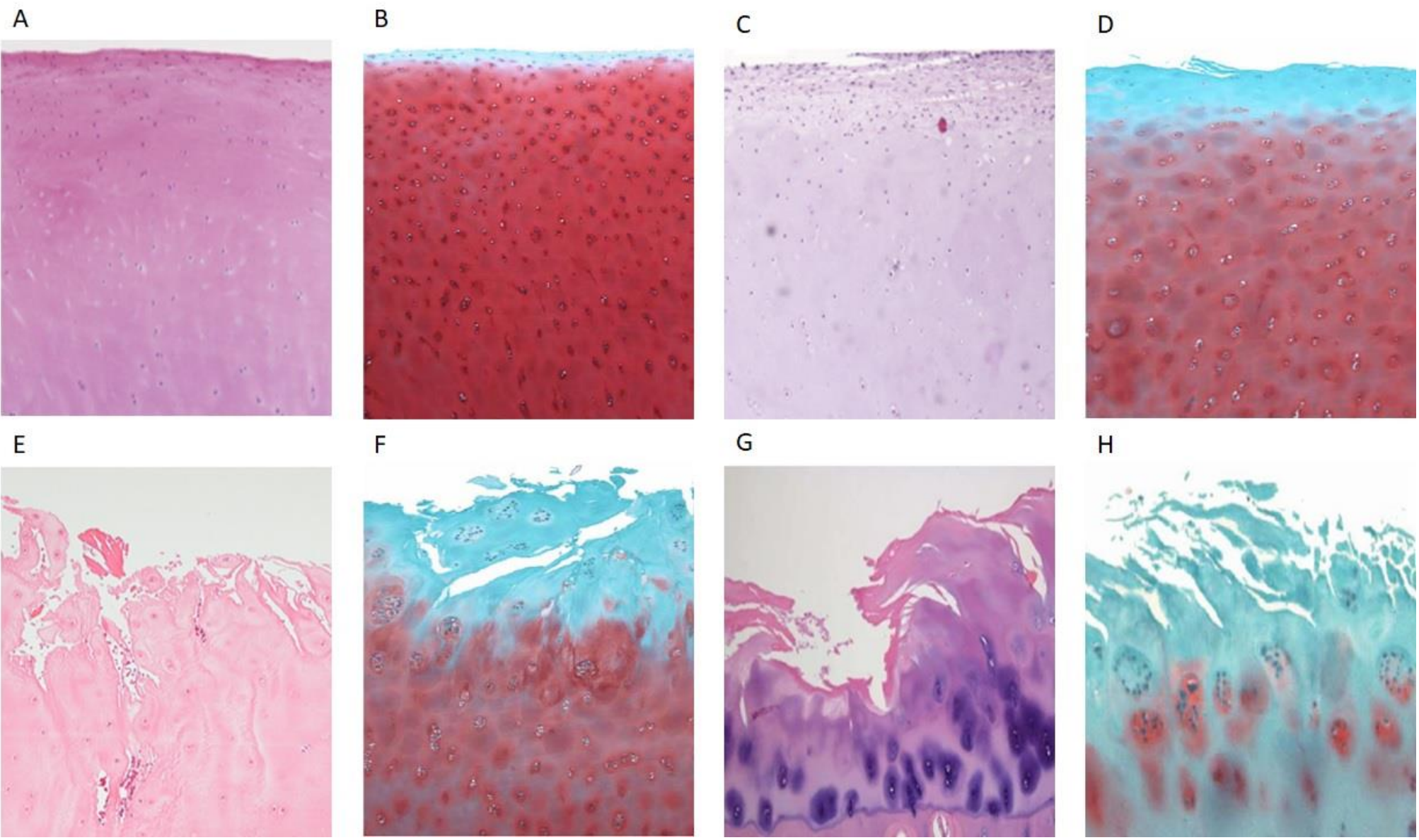


**Figure 1.10: Different grades of gross damage in knee cartilage according to the Outerbridge scoring system.** The Outerbridge scoring system consists of four different grades, based on gross changes in articular cartilage. Knee femoral cartilage is depicted here and the changes are marked with black arrows. Grade I is characterised by swelling of the tissue. Grade II and III by fragmentation, fissuring and lesions of different sizes. Grade IV represents full erosion of cartilage down to the subchondral bone. Original figure, courtesy of the author.

#### **1.5.4 Microscopic/histological changes in knee osteoarthritic cartilage**

Histology is one of the main tools used to visualise microscopic changes in the ECM and chondrocytes of OA cartilage. Simple staining techniques, such as haematoxylin and eosin (H&E) or safranin O/fast green (S-O/FG), are widely used in cartilage research to assess OA lesions. H&E stains the chondrocyte nuclei blue-purple and the ECM pink, whereas S-O/FG stains the proteoglycan and GAG content red and in the absence of these, the tissue is stained light blue (Schmitz et al., 2010). H&E staining of healthy knee cartilage shows the zonal organisation of the tissue and chondrocyte distribution. The surface of the tissue, along the superficial zone, is a smooth line that does not contain cracks (**Figure 1.11A**). Normal cartilage stained with S-O/FG appears red due to the high proteoglycan content (**Figure 1.11B**). In early OA there is fibrillation of the superficial zone, small cracks start to appear on the surface and chondrocytes begin to proliferate as a response to cartilage breakdown (Goldring et al., 2016, Pritzker et al., 2006) (**Figure 1.11C**). There is also small loss of proteoglycans and GAGs (**Figure 1.11D**). As OA progresses, there is extended cartilage breakdown and cracks extend vertically into the deeper zones to form fissures (Pritzker et al., 2006). Chondrocytes shift into a hypertrophic phenotype and are mostly organised into clusters. (Goldring et al., 2016) (**Figure 1.11E**). There is increased chondrocyte apoptosis observed at this stage and most of the proteoglycan content is missing from the superficial and middle zones (**Figure 1.11F**). End-stage OA is characterised by erosion of cartilage to the bone, as a significant percentage of the ECM has been degraded by this point. Only the deep zone remains focally, and in some areas, there is exposure of the underlying bone (**Figure 1.11G**). S-O/FG staining reveals almost complete loss of proteoglycan and GAG content (**Figure 1.11H**).

**Figure 1.11: Histological assessment of OA cartilage stages.** A, C, E and G: H&E staining of normal, early, moderate and end-stage OA cartilage. B, D, F and H: S-O/FG staining of normal, early, moderate and end-stage OA cartilage. Main changes include loss of ECM and proteoglycan content, fissure formation, chondrocyte clustering and apoptosis. Figures 1.11A, B, C, D, F, G and H modified with permission from (Pritzker et al., 2006, Shen et al., 2016, Sulzbacher, 2013) (License Number: 4987840685333, 4987841293921 and 4987850237765). Figure 1.11E is an original figure, courtesy of the author.



Histological evaluation of OA cartilage provides useful information on disease stage. It is widely used in research to stratify patients and, as with macroscopic classification, there are different scoring systems for assessing cartilage changes at microscopic level. Two of the most widely used are the Mankin histological-histochemical grading system (HHGS) (Mankin et al., 1971) and the Osteoarthritis Research Society International (OARSI) histopathology scoring system (Pritzker et al., 2006).

The Mankin HHGS was developed by Mankin *et al* in 1971 for scoring hip OA but has since been applied to other joints too. This system assesses features such as structure of cartilage, relative number of cells, S-O/FG staining or loss of it, as well as tidemark integrity (**Table 1.4**). Each feature is assigned a grade based on severity and the final score is calculated. Minimum score is 0 and denotes normal cartilage and maximum score is 14 and denotes end-stage OA cartilage. This system is still widely used but has received criticism over its capability to distinguish between mild and moderate OA stages (Ostergaard et al., 1999).

**Table 1.4: Mankin's histological-histochemical grading system.** Pannus refers to the invasion of fibrous granulated tissue in hyaline articular cartilage, a common finding in OA patients (Shibakawa et al., 2003). Table copied with permission from (Pearson et al., 2011). (License Number: 4987850693987).

	<b>Grade</b>
<b>I. Structure</b>	
a. Normal	0
b. Surface irregularities	1
c. Pannus and surface irregularities	2
d. Clefts to middle zone	3
e. Clefts to deep zone	4
f. Clefts to calcified zone	5
g. Complete disorganisation	6
<b>II. Cells</b>	
a. Normal	0
b. Diffuse hypercellularity	1
c. Cloning	2
d. Hypocellularity	3
<b>III. Safranin-O staining</b>	
a. Normal	0
b. Slight reduction	1

c. Moderate reduction	2
d. Severe reduction	3
e. No dye noted	4
<b>IV. Tidemark integrity</b>	
a. Intact	0
b. Crossed by blood vessels	1

The OARSI histopathology scoring system is a more recent grading system that was developed in 2006. This system utilises grades and stages in order to provide a more comprehensive and standard manner for scoring articular cartilage lesions. In this system, there are six grades which represent depth of the lesion (**Table 1.5**) and four stages which represent the percentage of articular surface that is affected (**Table 1.6**). Multiplying grade score by stage score gives the final score, which ranges between 0 and 24 (Pritzker et al., 2006). The OARSI scoring system provides more detailed information about histopathology of OA cartilage compared to previous scoring systems and it is fairly easy to use. However, as with every scoring system, there are limitations. As it has been noted by others, it is quite difficult to generate sections from the whole articular cartilage surface for stage assessment (Moskowitz, 2006). This holds true for human samples especially, where usually a small block of tissue is collected.

**Table 1.5: The OARSI histopathology scoring system: the grade assessment (depth progression of cartilage lesion).** Table copied with permission from (Pritzker et al., 2006) (License Number: 4987840685333).

<b>Grade (key feature)</b>	<b>Associated criteria (tissue reaction)</b>
<b>Grade 0: surface intact, cartilage morphology intact</b>	Matrix: normal architecture  Cells: intact, appropriate orientation

<b>Grade 1: surface intact</b>	Matrix: superficial zone intact, oedema and/or superficial fibrillation (abrasion), focal superficial matrix condensation.  Cells: death, proliferation (clusters), hypertrophy, superficial zone. Reaction must be more than superficial fibrillation only
<b>Grade 2: surface discontinuity</b>	As above  +Matrix discontinuity at superficial zone (deep fibrillation)  ±Cationic stain matrix depletion (Safranin O or Toluidine Blue) upper 1/3 of cartilage.  ±Focal perichondronal increased stain (mid zone).  ±Disorientation of chondron columns.  Cells: death, proliferation (clusters), hypertrophy
<b>Grade 3: vertical fissures (clefts)</b>	As above  Matrix vertical fissures into mid zone, branched fissures.  ±Cationic stain depletion (Safranin O or Toluidine Blue) into lower 2/3 of cartilage (deep zone)  ±New collagen formation (polarized light microscopy, Picro Sirius Red stain)  Cells: death, regeneration (clusters), hypertrophy, cartilage domains adjacent to fissures
<b>Grade 4: erosion</b>	Cartilage matrix loss: delamination of superficial layer, mid layer cyst formation. Excavation: matrix loss superficial layer and mid zone
<b>Grade 5: denudation</b>	Surface: sclerotic bone or reparative tissue including fibrocartilage within denuded surface. Microfracture with repair limited to bone surface

<b>Grade 6: deformation</b>	Bone remodelling (more than osteophyte formation only). Includes: microfracture with fibrocartilaginous and osseous repair extending above the previous surface.
-----------------------------	---

**Table 1.6: The OARSI histopathology scoring system: the stage assessment (percentage of articular cartilage surface affected).** Table copied with permission from (Pritzker et al., 2006) (License Number: 4987840685333).

<b>Stage</b>	<b>% Involvement (surface, area, volume)</b>
<b>Stage 0</b>	No OA activity seen
<b>Stage 1</b>	<10%
<b>Stage 2</b>	10-25%
<b>Stage 3</b>	25-50%
<b>Stage 4</b>	>50%

### 1.5.5 Molecular changes in osteoarthritic cartilage

In healthy articular cartilage there is a balance between anabolism and catabolism, as the action of matrix-synthesising factors counteracts that of matrix-degrading enzymes. In early OA there is an increase in catabolic factors which leads to ECM degradation. The tissue reacts by synthesising increased amounts of ECM components in an attempt to repair tissue damage. However, the tissue is unable to cope with the extended damage and the balance soon shifts in favour of catabolism leading to further cartilage destruction (Goldring et al., 2016). The molecular landscape of OA is very complex and still not completely understood. Years of research have highlighted the implication of several molecular pathways in the pathogenesis of OA; the TGF- $\beta$  pathway, the WNT/beta-Catenin pathway, the phosphoinositide 3-kinase (PI3K)/protein kinase B (AKT)/mTOR pathway, the Notch pathway

and the Sirtuin-1 (SIRT1) and AMPK pathway (He et al., 2020). The interplay of these pathways is extremely complex and beyond the scope of this review. Instead, focus will be given to the role of inflammation and the function of specific transcription factors which are of specific interest in cartilage and OA.

Inflammation of the joint is an important component of OA pathogenesis. Both ageing and mechanical stress on the joint are characterised by low-grade inflammation and the release of proinflammatory cytokines such as IL-1 $\beta$ , IL-6 and TNF- $\alpha$ , which predispose cartilage to OA (He et al., 2020). These are produced by chondrocytes and other cell types in the joint, such as synoviocytes, osteoblasts and mononuclear cells, and they have a numerous of downstream effects in cell signalling and gene expression by eliciting an inflammatory response and contributing to the catabolic effects observed in OA cartilage (Chow et al., 2020).

IL-1 $\beta$  is the most researched cytokine in OA and cartilage degradation. It plays a role in various cellular functions, including cell proliferation and apoptosis, and it is elevated in cartilage, synovium and synovial fluid from OA patients (Chow et al., 2020). Its significance in OA is realised by the plethora of its downstream effects in chondrocytes (**Figure 1.12**). IL-1 $\beta$  reduces the synthesis of ECM components, such as collagen type II and aggrecan (Chow et al., 2020). Moreover, it induces the expression of other proinflammatory cytokines, such as IL-6 and TNF- $\alpha$  (Chow et al., 2020, Wojdasiewicz et al., 2014). This leads to activation of the nuclear factor kappa-light-chain-enhancer of activated B cells (NF- $\kappa$ B), which promotes the expression of matrix-degrading enzymes, such as MMP3 and MMP13, contributing further to cartilage degradation (Chow et al., 2020, Wojdasiewicz et al., 2014). It stimulates the expression of A Disintegrin and Metalloproteinase with Thrombospondin motifs (ADAMTS) 4 protein, also known as aggrecanase for its ability to cleave aggrecan (Wojdasiewicz et al., 2014). IL-1 $\beta$  also promotes the production of ROS, such as nitric oxide (NO), contributing to the senescence and DNA damage evident in OA chondrocytes (Rose et al., 2012). In addition, IL-1 $\beta$  induces the expression of cyclooxygenase 2 (COX-2), which, in turn, enhances the expression of prostaglandin 2 (PGE2) leading to decreased synthesis of ECM components and loss of chondrocyte proliferative capacity (Chow et al., 2020). Such is the effect of IL-1 $\beta$  in chondrocytes, that it is routinely used in chondrocyte cultures to mimic an *in vitro* OA inflammatory system in these cells (Chow et al., 2020).

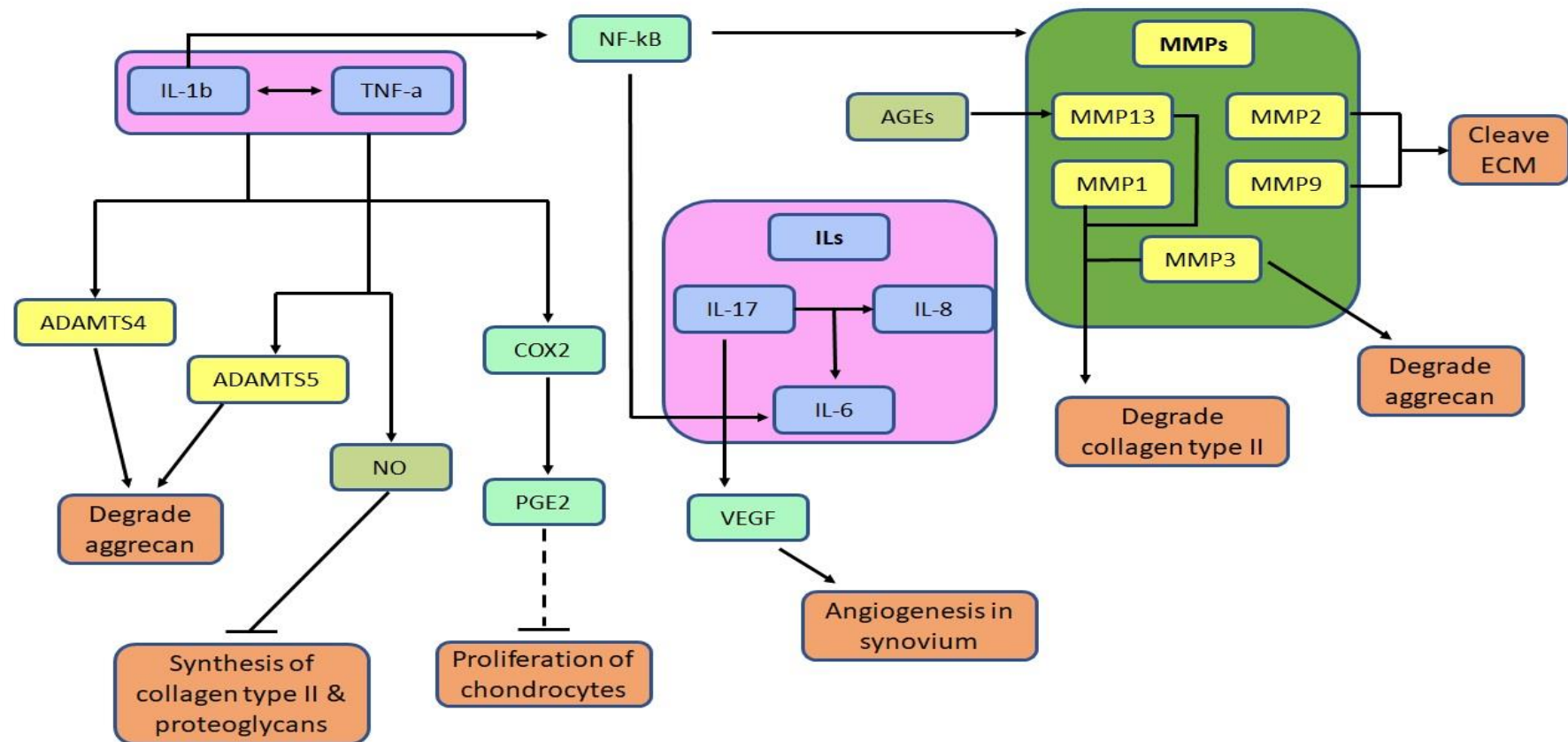


**Figure 1.12: Functions of IL-1 $\beta$  in OA cartilage.** IL-1 $\beta$  is one of the main proinflammatory cytokines with several different functions in OA cartilage. It has an inhibitory effect on anabolic factors and ECM synthesis, while it promotes cartilage degradation via increased synthesis of matrix-degrading enzymes. It functions alongside other proinflammatory cytokines of the IL and TNF family to exert their catabolic effect on OA chondrocytes. Figure redrawn with modifications from (Chow et al., 2020).

Transcription factors play significant roles in cartilage development and chondrogenesis and they are also implicated in OA pathogenesis. SOX9, which is the master regulator in cartilage development, is upregulated in early OA which leads to increased synthesis of ECM components such as collagen type II and aggrecan (Zhang et al., 2015a). This increased expression is probably an attempt of the tissue to compensate for the cartilage loss during the early disease stages. As OA develops further, expression of SOX9 decreases along with collagen type II and aggrecan (Zhang et al., 2015a). Moreover, a usual feature of OA cartilage is hypertrophy of chondrocytes and apoptosis which closely resembles the process of endochondral ossification during long bone development. RUNX2 is a pivotal transcription factor during this process and it has also been linked to molecular changes seen in OA. RUNX2 expression is increased in OA cartilage and it was shown that this increased expression was positively correlated with OA grading (Zhong et al., 2016). RUNX2 can induce the expression of matrix-degrading enzymes and collagen type X contributing to chondrocyte hypertrophy and osteophyte formation (Neefjes et al., 2020, Nishimura et al., 2020). CCAAT enhancer binding protein beta (C/EBP $\beta$ ), a transcriptional partner of RUNX2, is also implicated in OA and it is believed to act along RUNX2 to bind the *MMP13* gene to induce its expression (Nishimura et al., 2020). Hypoxia-inducible factor (HIF) 2 $\alpha$  is another transcription factor that can bind elements on the *MMP3*, *MMP13*, collagen type X alpha 1 chain (*COL10A1*) and *VEGFA* gene promoters and induce their expression in OA (Goldring et al., 2016). In addition, HIF2 $\alpha$  can also act as an upstream regulator of C/EBP $\beta$  and contribute to cartilage degradation (Nishimura et al., 2020).

## 1.6 MicroRNAs

### 1.6.1 MicroRNA general remarks and biogenesis

Cellular function is highly determined by the information that lies within the genome of an organism. From the simplest life forms to the most complex organisms, genes play the most crucial role in development. Some genes are transcribed into RNA, and RNA is translated into protein. Proteins are the molecules responsible for carrying out cellular function and are

involved in all stages of life cycle. However, for some genes, the process of gene expression stops at the RNA level and the end-product is RNA and not protein. These RNA molecules are called non-coding RNAs because they do not code for proteins. Instead, they have other regulatory or structural roles in the cell. Dependent on their sequence length, non-coding RNAs are divided into long coding RNAs (lncRNAs), which are longer than 200nt, and small non-coding RNAs (sncRNAs), which are shorter than 200nt. There are different types of sncRNAs, including miRNAs, small nuclear RNAs (snRNAs), small nucleolar RNAs (snoRNAs), transfer RNAs (tRNAs), piwi-interacting RNAs (piRNAs) and others. Among these, miRNAs are the most researched sncRNAs in development and disease.

miRNAs are short in length, between 17 and 25nt long, with an average length of 22nt. They are epigenetic, post-transcriptional regulators of gene expression and they function by targeting complementary sequences in mRNA targets leading to translational repression and/or mRNA decay (Matsuyama et al., 2019). The first miRNA was discovered in *Caenorhabditis elegans* and was transcribed by gene *lin-4* (Lee et al., 1993). Since then, multiple miRNAs have been discovered in plants and animals, and some miRNAs have been found in protists and viruses (Ha et al., 2014). Specifically, in humans, there is an estimate of 2300 true miRNAs (Alles et al., 2019).

miRNA genes are located throughout the genome. In humans, most of the miRNAs are transcribed by genes located within regions of other non-coding genes or within introns of coding genes. However, some miRNAs are located within exons of other genes (Ha et al., 2014). Moreover, miRNA genes can be organised individually in a locus (monocistronic), or in clusters (polycistronic) (Matsuyama et al., 2019). Biogenesis of canonical miRNAs involves several steps (**Figure 1.13**). miRNAs are transcribed into long primary miRNA (pri-miRNA) transcripts, by RNA polymerase II. Pri-miRNAs are approximately 33bp double-strand stems with hairpin structures which undergo cleavage by the microprocessor complex in the nucleus (Matsuyama et al., 2019). The microprocessor complex consists of two proteins, DROSHA, an RNase III endoribonucleolytic enzyme, and DiGeorge critical region 8 (DGCR8), which is a double-strand RNA-binding protein. DGCR8 positions the pri-miRNAs in such way, so that DROSHA cleaves the molecule at a specific site, 11bp away from the base of the hairpin structure (Yates et al., 2013). This gives rise to the precursor-miRNA (pre-miRNA), which is a

~70nt stem-loop that has a 3' overhang. Pre-miRNAs exit the nucleus and are exported to the cytoplasm via exportin-5.

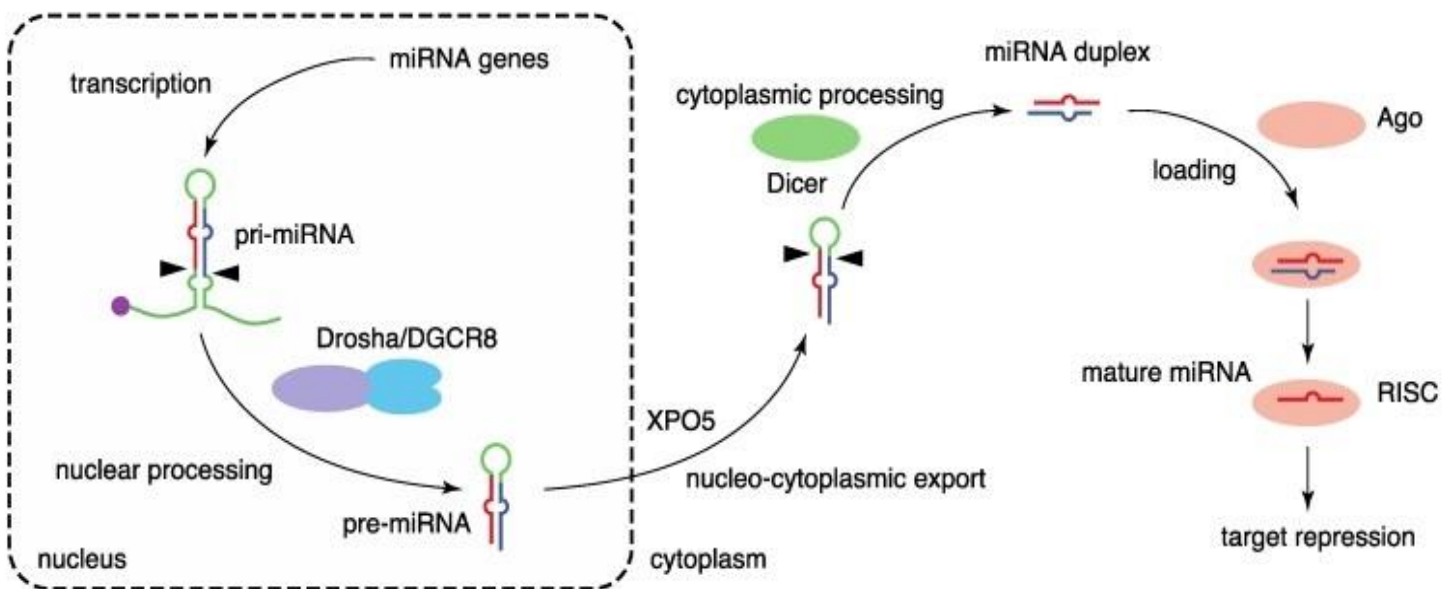


**Figure 1.13. miRNA biogenesis.** miRNA biogenesis is a multi-step process where the initial long miRNA transcript is cleaved sequentially to form the mature miRNA. The process begins in the nucleus and is finalised in the cytoplasm and includes several different proteins. The mature miRNA is incorporated into the RISC complex to exert its function on the mRNA target. Figure copied with permission from (Matsuyama et al., 2019) (No special permission is required to reuse all or part of article published by MDPI, including figures and tables).

In the cytoplasm, pre-miRNAs are cleaved further by another endoribonucleolytic enzyme with RNase III activity, DICER (Yates et al., 2013). After cleavage, there is a ~22nt RNA duplex left with 3' overhangs at both ends. This RNA duplex is loaded into an Argonaute (Ago) protein to form the RNA-induced silencing complex (RISC). From the two strands of the RNA duplex, the one complementary to the mRNA target (called the guide strand) is selected, whereas the other strand (called the passenger strand) is quickly discarded and degraded (Matsuyama et al., 2019, Yates et al., 2013). The guide RNA strand that remains, is the mature miRNA. Depending on the mRNA target, both strands of the RNA duplex within the RISC complex have the potential to be selected and become the mature miRNA. The mature miRNA that arises

from the 5' arm of the RNA duplex is annotated with the suffix -5p, whereas the one that arises from the 3' arm is annotated with the suffix -3p (Matsuyama et al., 2019).

### 1.6.2 MicroRNA and mRNA pairing: microRNA function

miRNAs have emerged as potent gene regulators. They act at the post-transcriptional level by binding their mRNA targets at the 3' untranslated region (UTR). Complementarity between the mature miRNA and mRNA differs and is based on miRNA/mRNA sequence and species. In plants the mature miRNA usually has perfect complementarity to the mRNA target sequence. In contrast to plants, in animals there is usually partial pairing between the miRNA and the mRNA target (Dexheimer et al., 2020). Nucleotides 2 to 7 or 2 to 8 relative to 5' end of the mature miRNA are called the 'seed' region and are the most important for miRNA/mRNA pairing. Even though in animals there may not be perfect complementarity between the entire miRNA sequence and the mRNA target, the seed sequence is usually perfectly complementary to the mRNA sequence. If there is a mismatch between the seed region and the mRNA target, then this is compensated by near-perfect complementarity between the 3' end of the miRNA and the mRNA sequence (Huang et al., 2010) (**Figure 1.14**). Because miRNA-mRNA pairing is primarily dependent on the 7 or 8 nucleotides of the seed region, this means that a single miRNA can bind different mRNA targets, given the short length of the seed region. Moreover, the 3' UTR of a single mRNA can be bound by many different miRNAs at the same time, highlighting the complexity of gene expression regulation.

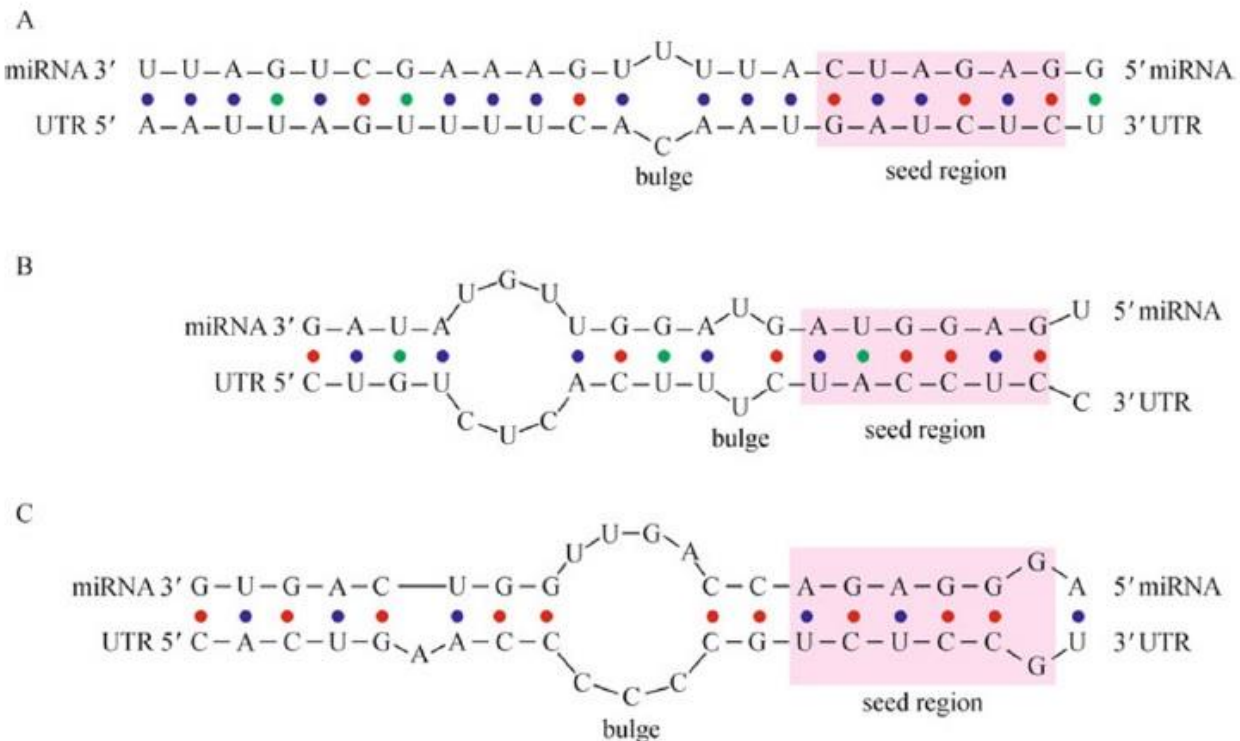


**Figure 1.14: The three main types of miRNA and mRNA pairing in animals.** **A.** The 5' dominant canonical type: There is perfect or near perfect complementarity between the miRNA/mRNA duplex with a mismatch (bulge) in the middle of the duplex. **B.** The 5' dominant seed only type: There is perfect complementarity between the seed region of the miRNA and the mRNA but several mismatches closer to 3' end. **C.** The 3' compensatory type: There is a mismatch between the seed region of the miRNA and the mRNA target which is compensated by perfect complementarity at the 3' end of the miRNA. Figure copied with permission from (Huang et al., 2010) (License Number: 4987860749835).

Perfect or near perfect complementarity between the miRNA and the mRNA in plants leads to mRNA cleavage by Ago of the RISC complex due to its 5' to 3' exonuclease activity (Iwakawa et al., 2015). However, in animals, due to only partial complementarity the mode of action is different. There are two proposed modes of miRNA-induced silencing of gene expression in animals: translational repression and mRNA decay (Dexheimer et al., 2020). The relative contribution of each mechanism is still unclear. At first, it was believed that silencing was achieved by translational repression without any effect on the mRNA level. However, this could not account for the extensive transcriptomic changes seen in some studies when miRNA expression was modulated. Moreover, some researchers proposed a slightly different model

where a miRNA could induce moderate silencing of its targets by affecting protein levels through translational repression and only the targets that were highly repressed showed reduction at mRNA level too. In addition, polysome analysis concluded that changes at the protein level were only modest and that mRNA level changes were more profound. However, these studies did not take into account different transcript isoforms and their contribution to gene expression and protein synthesis. When accounted for these isoforms, changes at protein levels became more apparent. Thus, it is clear that neither the mechanism of translational repression nor that of mRNA decay alone can explain all the available data (Cloonan, 2015). It is generally accepted that these two mechanisms work together to induce gene silencing and they are closely linked. Current data suggests that translational repression precedes mRNA decay and occurs in a rapid manner but has a modest effect, followed by mRNA decay which comes later and has a more substantial role in gene silencing (Dexheimer et al., 2020, Iwakawa et al., 2015). However, this also depends on the cell type, developmental stage, miRNA-RISC context, as well as position and number of miRNA binding sites (Dexheimer et al., 2020, Iwakawa et al., 2015).

The mechanisms through which miRNAs induce gene silencing through translational repression and mRNA decay are also under investigation. In both proposed models, a protein called Gawky or GW182 in *Drosophila melanogaster*, and its human ortholog, trinucleotide repeat containing adaptor 6 (TNRC6), is a key protein in miRNA-induced gene silencing (Iwakawa et al., 2015). In mRNA decay, GW182 acts as a recruiter protein by recruiting two deadenylase complexes to the mRNA target, the Carbon Catabolite Repression-Negative On TATA-less (CCR4-NOT) complex and the Poly(A)-binding protein-dependent poly(A) ribonuclease (PAN)2-PAN3 complex (Iwakawa et al., 2015). These two complexes function by inducing shortening of the poly(A) tail resulting in mRNA destabilisation. Destabilised mRNAs are subjected to oligouridylation by terminal uridylyl transferase (TUT) 4/7 and are targeted for degradation (Iwakawa et al., 2015). mRNA decay is further promoted by decapping of the 5' end of the mRNA target by decapping activators, such as DEAD-box helicase 6 (DDX6), which are recruited onto the CCR4-NOT complex (Iwakawa et al., 2015).

Translational repression probably occurs at the initiation step and three mechanisms have been proposed as to how this is accomplished: i) GW182-mediated poly(A) binding protein (PABP) displacement, ii) recruitment of translational repressors through GW182 and iii)

dissociation of eukaryotic translation initiation factor (eIF) 4A from the cap-binding complex eIF4F (Iwakawa et al., 2015). GW182 directly interacts with PABP and promotes its dissociation from the poly(A) tail, thus disrupting mRNA translation (Iwakawa et al., 2015). Moreover, GW182 can recruit translational repressors to the mRNA target, such as eIF4E-Transporter (4E-T), which is recruited to the CCR4-NOT complex through DDX6 and represses translation. This highlights how closely linked mRNA decay and translational repression are, since both modes of silencing share common mechanisms. The last mechanism through which translational repression is achieved, is through dissociation of eIF4A from the eIF4F cap-binding complex. EIF4A functions by recruiting the ribosome to the mRNA target and dissociation of eIF4A promotes translational repression of the mRNA target.

**Figure 1.15** illustrates the two proposed models of mRNA decay and translational repression for miRNA-induced gene silencing.

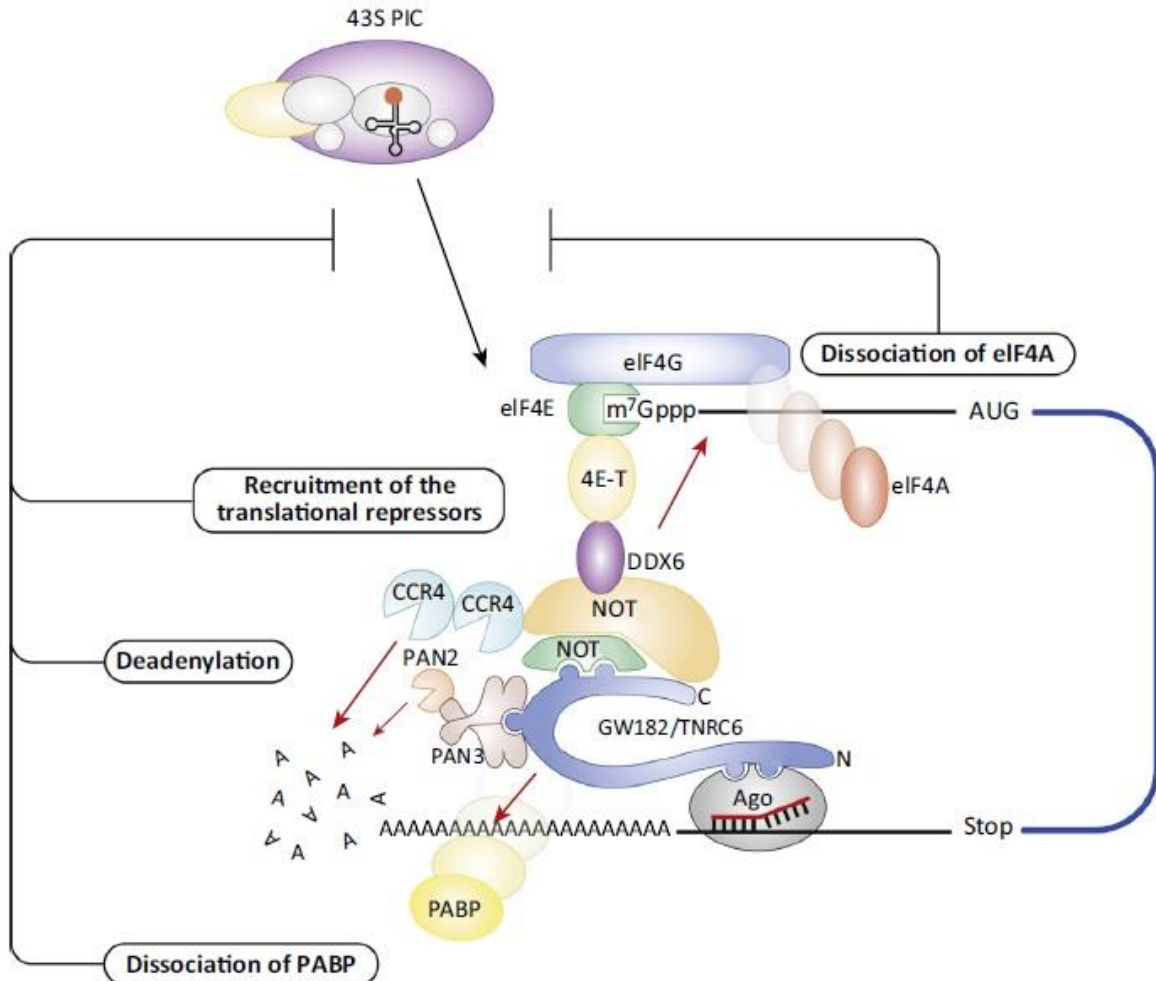


**Figure 1.15: miRNA-induced gene silencing is mediated through mRNA decay and translational repression.** mRNA decay is mediated through deadenylation of the mRNA target through GW182 protein in *Drosophila*, and TNRC6 in humans, which recruits the CCR4-NOT and PAN2-PAN3 complexes for poly(A) tail removal. Translational repression occurs through three mechanisms: dissociation of PABP, recruitment of translational repressors such as 4E-T and DDX6 (which is also a de-capping activator promoting mRNA decay) and dissociation of eIF4A, a factor which assists in ribosomal recruitment (43S preinitiation complex (43S PIC)). The first two mechanisms of translational repression are also mediated via GW182/TNRC6, whereas the last one via an independent manner. Both mRNA decay and translational repression work together to achieve miRNA-induced gene silencing. Figure modified with permission from (Iwakawa et al., 2015) (License Number: 4987861098678).

### **1.6.3. MicroRNA databases, nomenclature and target prediction tools**

miRNAs have attracted a lot of attention since their discovery in *Caenorhabditis elegans* in 1993 (Lee et al., 1993). It is estimated that approximately 60% of protein-coding transcripts in human are subjected to miRNA regulation, which highlights their biological significance (Dexheimer et al., 2020). Moreover, miRNAs seem to be quite conserved among different taxa of organisms (Dexheimer et al., 2020). This holds true, especially for the seed region which is the most conserved site in the miRNA sequence. Apart from the seed region, some miRNAs show conservation in their entire sequence across a large evolutionary distance. For example, miRNA let-7 is exactly the same from worms to humans, which highlights the significance of not just the seed sequence, but of the entire let-7 sequence across evolution (Pasquinelli et al., 2000). Therefore, it comes as no surprise that research on miRNAs has increased substantially in the last few years due to their role in gene expression regulation. Subsequently, the number of annotated miRNAs in different species has also increased. To account for the growing number of novel miRNAs and the need of researchers to have a common point of reference for miRNA-related information, the miRBase database was created (Griffiths-Jones et al., 2006, Kozomara et al., 2019). miRBase contains information on miRNA annotation, sequence and genomic location of pre-miRNAs and mature miRNAs from hundreds of organisms. The user has access to both mature miRNA forms (5p and 3p) that arise from the same stem-loop hairpin sequence. Furthermore, the data can be downloaded and the database provides links to open-access research papers that are relevant to the miRNA of interest. The newest released version is miRBase 22.1 (up until the writing of this section) and contains information for 271 organisms, 38589 pre-miRNAs and 48860 mature miRNAs (Kozomara et al., 2019, Shaker et al., 2020).

Moreover, miRBase offers information on miRNA nomenclature. Mature miRNAs are named by using the prefix ‘miR’, followed by a hyphen (-) and the number of the miRNA, followed by a hyphen and ‘5p’ or ‘3p’ (if known), depending on whether the mature miRNA comes from the 5p or the 3p arm of the pre-miRNA. A three-letter code at the beginning of the mature miRNA name can be used to denote the species. For example, hsa-miR-221-5p, is the *Homo sapiens* mature miRNA 221 that arises from the 5p arm of the pre-miRNA 221. The pre-miRNA/stem-loop sequence uses the prefix ‘mir’ and in the above example it is hsa-mir-221

(Ambros et al., 2003). miRNAs that have the same seed region but differ in other parts of the miRNA sequence constitute a miRNA family (Dexheimer et al., 2020). These miRNAs arise from gene duplication events and the members are usually named by using the same number. A letter after the number is used to distinguish between members of a miRNA family, for example, hsa-miR-30a-5p and hsa-miR-30b-5p. An exception to the above nomenclature rules is miRNA family let-7. miRNA let-7 was first discovered in *Caenorhabditis elegans* and retains the same name in other species too, without prefix ‘miR’.

miRNAs target mRNAs based primarily on complementarity. Elucidating the role of miRNAs requires extensive knowledge of their mRNA targets via which they exert their function. The first step is understanding which mRNAs are targeted by miRNAs. To this direction, several online target prediction tools have been developed. These include: TargetScan (Agarwal et al., 2015), miRWalk (Dweep et al., 2015), miRmap (Vejnar et al., 2012), miRDB (Chen et al., 2020), miRTar (Hsu et al., 2011) and several others (Huang et al., 2010, Shaker et al., 2020). These tools use a specific set of criteria to make predictions. The main criteria for predicting miRNA-mRNA interactions are usually three: i) miRNA-mRNA sequence complementarity, ii) amount of free energy of miRNA-mRNA duplex and iii) how conserved the miRNA-mRNA interaction is (Huang et al., 2010). The first criterion has been discussed above. On the free energy criterion, the lower the free energy an RNA-RNA duplex has, the more stable it is, and this is taken into account when predicting miRNA targets. In addition, the more conserved the binding interaction is, the higher the possibility it represents a true interaction (Huang et al., 2010). Each tool has a different interface, gives the user different options to choose from and presents results in its own characteristic way. Therefore, each tool comes with its own advantages and disadvantages and, even though they have contributed significantly to miRNA target validation, it is worth noting that they also produce many false positives, at a rate that ranges between 20 and 50% (Cloonan, 2015). This constitutes experimental validation of a predicted miRNA target a necessity in miRNA research (Shaker et al., 2020).

In addition to the online predicting tools, there are also online databases which list experimentally validated targets of miRNAs, such as DIANA-TarBase (Karagkouni et al., 2018) and miRTarBase (Chou et al., 2018). These databases also list the experimental approach via which the miRNA-mRNA interaction was validated, related gene networks and diseases, gene

ontology and others. Finally, databases on miRNA expression, function, networks and disease pathways have also been developed in the last few years (Shaker et al., 2020).

#### **1.6.4 miRNAs in cartilage development and homeostasis**

miRNA research has shown that these molecules play important roles in organism development and disease. Their expression and function are regulated in a temporal and spatial manner by several different ways and dysregulation of their normal function can disrupt homeostasis and contribute to disease (Ha et al., 2014, Matsuyama et al., 2019). miRNAs play an important role in the skeletal system and specifically cartilage and bone development. Chondrocyte-specific deletion of DICER in the growth plate of mice reduced the number of proliferating chondrocytes, increased hypertrophic chondrocytes and led to severe skeletal defects and premature death (Kobayashi et al., 2008). DICER is a key protein for miRNA biogenesis, thus ablation of the gene that encodes for it leads to dysfunctional miRNA biogenesis. In the previous study, DICER-deficient chondrocytes demonstrated very low levels of miRNA expression compared to control (Kobayashi et al., 2008).

One of the most important miRNAs in cartilage is miR-140, as it has multiple roles in maintaining chondrocyte homeostasis. miR-140 expression is regulated by SOX9, the master transcription regulator of chondrogenesis (Miyaki et al., 2010), but it was reported that miR-140 can also regulate SOX9 expression, indicating a reciprocal regulation between miR-140 and SOX9. Decreased miR-140 expression correlated with decreased SOX9 and aggrecan levels and it was found that this was mediated through targeting of RAS like proto-oncogene A (RALA) (Karlsen et al., 2014). Moreover, miR-140 inhibited chondrocyte hypertrophy and promoted chondrocyte proliferation through inhibiting histone deacetylase (HDAC) 4 in mouse embryos, providing further evidence on the role of miR-140 in cartilage development. This was also supported by a study in which mice that overexpressed miR-140 displayed resistance to antigen-induced arthritis (Miyaki et al., 2010). In the same study, mice lacking miR-140 expression showed mild skeletal abnormalities and were more prone to spontaneous OA (Miyaki et al., 2010). These results were attributed to miR-140 targeting ADAMTS5, a major aggrecanase in cartilage and OA.

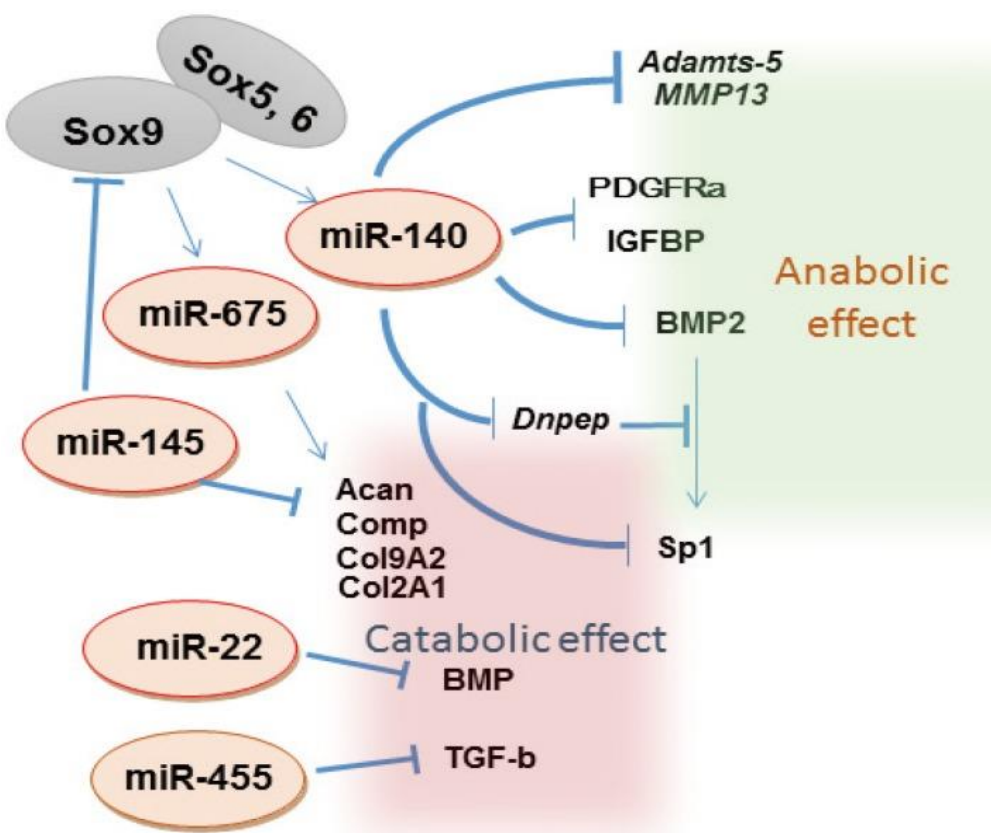


**Figure 1.16. Example of miRNA regulation in chondrogenesis.** Chondrogenesis and chondrocyte homeostasis are regulated by several miRNAs. Some of these promote chondrocyte proliferation and cartilage formation exerting an anabolic effect, whereas others exert a catabolic effect when needed. Many miRNAs have been reported to have a role in this process by targeting genes and pathways important for chondrocyte proliferation and apoptosis. Abbreviations: Platelet derived growth factor receptor alpha (*PDGFRa*), Insulin-like growth factor binding protein (*IGFBP*), Aspartyl aminopeptidase (*DNPEP*), Sp1 transcription factor (*SP1*), Cartilage oligomeric matrix protein (*COMP*), Collagen type II alpha 1 chain (*COL2A1*), Collagen type IX alpha 2 chain (*COL9A2*), Aggrecan (*ACAN*). Figure copied with permission from (Asahara, 2016) (This is an Open Access article distributed under the terms of the Creative Commons Attribution Non-Commercial License which permits unrestricted non-commercial use, distribution, and reproduction in any medium, provided the original work is properly cited).

miR-140 is not the only miRNA that has a role in cartilage development. miR-23b was shown to promote differentiation of human MSCs into chondrocytes and, thus, promote chondrogenesis, by targeting protein kinase A (PKA) (Ham et al., 2012). miR-488 and miR-21 were also reported to be positive regulators of chondrogenesis by targeting different genes (Liu et al., 2018, Song et al., 2013). Other *in vitro* studies have also revealed the positive regulation of chondrogenesis by more miRNAs, such as miR-199a, miR-130b, miR-152, miR-28, miR-26b, miR-455 (Asahara, 2016). However, as discussed earlier, chondrogenesis and endochondral ossification is a tightly regulated process, with stages of chondrocyte proliferation and chondrocyte hypertrophy and apoptosis. Therefore, miRNAs can also have a negative effect on cartilage development. miR-145 reduced levels of collagen type II and aggrecan and increased levels of RUNX2 and MMP13 in human articular chondrocytes by directly targeting SOX9 (Martinez-Sanchez et al., 2012). In addition, miR-29a had a negative effect on differentiation of human MSCs into chondrocytes by targeting forkhead box O3 A (*FOXO3A*) and repressing the expression of cartilage-specific markers (Guérat et al., 2014). It is, therefore, inferred that chondrogenesis is under the control of both transcriptional and epigenetic regulation through various transcription factors and signalling pathways, but also via the numerous miRNAs that regulate such pathways, suggesting an even more complex landscape in cartilage development (**Figure 1.16**).

### 1.6.5 miRNAs in cartilage ageing

Ageing is the main risk factor for OA. Several cellular pathways are altered with ageing predisposing to disease. miRNA expression is also altered with ageing in many tissues including the musculoskeletal system (Weilner et al., 2015). While there are numerous published articles on miRNAs and OA, there are very few studies on miRNAs and ageing cartilage or chondrocytes without the effect of OA. Ukai *et al* (2012), by using microarrays, compared miRNA expression between chondrocytes isolated from the fingers of infants diagnosed with polydactylysm (average age: 13 months) and normal, non-load bearing articular cartilage from young patients undergoing ACL reconstruction (average age: 22.3 years) (Ukai et al., 2012). They reported increased expression of miR-199a-3p and miR-193b,

and decreased expression of miR-320c in the ACL group compared to the infant group. By overexpressing miR-199a-3p and miR-193b in chondrocytes, they detected reduced expression of *COL2A1*, *ACAN* and *SOX9* compared to control, whereas the opposite occurred when inhibiting the expression of these two miRNAs in chondrocytes. Furthermore, when they overexpressed miR-320c, the group reported reduced expression of *ADAMTS5*, whereas the opposite was shown when they inhibited miR-320c (Ukai et al., 2012). The group concluded that miR-199a-3p and miR-193b are potentially involved in chondrocyte senescence, and miR-320c in chondrogenesis.

In addition, Peffers *et al* (2013) by using RNA-Seq between young (4 years) and old (>15 years) normal cartilage samples from the metacarpophalangeal joints of horses, detected significantly higher expression of miR-21 in the old group, proposing that this miRNA could potentially be involved in cartilage ageing (Peffers et al., 2013).

### **1.6.6 miRNAs in OA cartilage**

In many tissues, miRNAs play important roles in maintaining homeostasis. Therefore, dysfunctional miRNA network could contribute to disease and, vice versa, disease could lead to dysfunctional miRNA network. There is a significant amount of research on the role of miRNAs in OA (Jeffries, 2019, Reynard et al., 2020). Dozens of miRNAs have been implicated in OA, either having a protective or a destructive role in cartilage (**Table 1.7**), and usually linked to important cellular processes, such as inflammation, autophagy and senescence (Endisha et al., 2018). Genome and proteome-wide analyses, such as RNASeq/small RNASeq, microarrays and LC-MS/MS, have made it possible to analyse for thousands of miRNAs and target genes at the same time, contributing to the exponentially increasing evidence in this field. miR-92a-3p was reported to be downregulated in human OA cartilage and in cells treated with IL-1 $\beta$ , leading to increased expression of its target genes: *ADAMTS4*, *ADAMTS5* and *HDAC2* (Endisha et al., 2018). Moreover, miR-502-5p, which protects cartilage by targeting TNF receptor-associated factor (*TRAF*) 2 and inhibiting NF- $\kappa$ B signalling, is also downregulated in human OA cartilage, leading to increase NF- $\kappa$ B signalling and expression of matrix-degrading enzymes (Zhang et al., 2016). miR-98 and miR-34a promoted apoptosis and cartilage degradation by regulating B cell lymphoma 2 (*BCL-2*) and nitric oxide synthase 2

inducible (*iNOS*), respectively (Endisha et al., 2018). However, in some cases, studies have reported controversial results regarding specific miRNAs. In one study, miR-145 was downregulated in human OA cartilage and TNF- $\alpha$ -treated rat chondrocytes (Hu et al., 2017b), whereas in another study, the same miRNA was upregulated in human OA cartilage and IL-1 $\beta$ -treated chondrocytes (Yang et al., 2014). These differences could be due to study designs, experimental approach and donor variability.

**Table 1.7: List of miRNAs implicated in OA.** Table compiled with information from (Endisha et al., 2018).

miRNA	Role
miR-320a	
miR-441	
miR-27b	
miR-148a	
miR-127-5p	
miR-140	
miR-30a	
miR-125b	
miR-15a	
miR-92a-3p	
miR-502-5p	
miR-130a	
miR-193b	
miR-149	

**Cartilage protective**

miR-146	
miR-142-3p	
miR-370	
miR-373	
miR-210	
miR-26a-5p	
miR-26b	
miR-33	
miR-602	
miR-608	
miR-488	
miR-558	
miR-199a-3p	
miR-24	
miR-105	
miR-221-3p	
miR-222	
miR-19a	
miR-17-5p	
miR-381	
miR-100	<b>Cartilage destructive</b>
miR-139	

miR-15a-5p	
miR-181b	
miR-34a	
miR-30b	
miR-302b	
miR-181a-5p	
miR-4454	
miR-23a-5p	
miR-216b	
miR-138-5p	
miR-101	
miR-16-5p	
miR-4262	
miR-449	
miR-21	
miR-146a	
miR-223	
miR-155	
miR-483-5p	
miR-365	<b>Cartilage protective and destructive</b>
miR-9	
miR-98	

The clinical value of miRNAs in OA lies within their use as prognostic or disease-monitoring biomarkers and their potential use as therapeutic agents. miRNAs are stable, sensitive to disease changes and easy to detect in body fluids, thus making them suitable candidates for disease biomarkers by using non interventional approaches (Bottani et al., 2020). Indeed, there is great need to discover miRNAs that could be used to discriminate between healthy subjects and OA patients, but also between different stages of OA, as symptoms are usually diagnosed after cartilage has been affected beyond repair (Endisha et al., 2018). Several studies have tested the potential use of circulating cell-free miRNAs as biomarkers in synovial fluid and serum/plasma. By using microarrays, a study found that seven miRNAs (miR-23a-3p, 24-3p, 27a-3p, 27b-3p, 29c-3p, 34a-5p and 186-5p) were DE in synovial fluid from patients with early-stage OA (KL score I/II) compared to late-stage OA (KL score III/IV) (Li et al., 2016). In the same study, miR-378-5p was detected in late-stage OA samples only, providing evidence of a potential miRNA biomarker in differentiating OA stages and disease progression. Moreover, miRNAs can be packed in extracellular vesicles, called exosomes, which are produced by one cell type and can travel to target cells to elicit a specific response. Withrow *et al* (2016) found that the miRNA content of synovial fluid exosomes was different in patients with OA compared to age-matched normal controls and some miRNAs were DE between the two groups (Withrow et al., 2016). Interestingly, some miRNAs may be possible to distinguish between different diseases that affect the musculoskeletal system. For example, miR-16, miR-146a, miR-155 and miR-223 were significantly higher in synovial fluid from rheumatoid arthritis patients compared to OA patients (Murata et al., 2010).

Studies in serum/plasma have also shed light on the potential use of circulating miRNAs as biomarkers. Ntoumou *et al* (2017) used a microarray platform to assess circulating miRNAs in the serum of OA patients and controls and identified 279 DE miRNAs. Among these, miR-140 was identified as significantly downregulated in OA patients in accordance with previous reports from cartilage tissue (Ntoumou et al., 2017). In a similar study between OA patients and healthy controls, 12 circulating miRNAs were DE in plasma from OA patients. These

miRNAs were predicted to target genes important for cartilage metabolism (Borgonio Cuadra et al., 2014). Furthermore, miRNAs could be used for monitoring disease severity. In another microarray study by Kong *et al* (2017), plasma circulating miRNAs miR-19b-3p, miR-122-5p and miR-486-5p were independent risk factors for OA and miR-19b-3p and miR-486-5p were positively correlated to disease severity (Kong et al., 2017). However, no common circulating miRNAs were discovered between all the above studies. Five miRNAs (miR-122, miR-885, miR-140, miR-93 and miR-663a) were common in two of the studies, which might offer some direction on future experiments regarding the use of circulating miRNAs as OA biomarkers (Swingler et al., 2019).

Finally, miRNAs could be used in OA therapeutics, either by using overexpression or inhibiting agents, dependent on the action of the miRNA. These can be delivered directly into the joint via intra-articular injections or via lentiviral vectors (Swingler et al., 2019). One potential problem is the uptake of the construct by cartilage. Even though there have been successful trials of delivery in mouse and rat joints, it is still doubtful whether these can be applied to man (Swingler et al., 2019). An alternative way is the use of exosomes for miRNA delivery. Indeed, they have been successful studies in which exosomes produced by MSCs treated with overexpressing or inhibiting miRNA agents were delivered and taken up by chondrocytes in mouse and rat models (Mao et al., 2018, Tao et al., 2017). Yet, it is still a long way before these experimental approaches can be applied in man.

# **Chapter 2: General Materials and Methods**

<b>Chemicals/Reagents</b>	<b>Manufacturer</b>
2-Mercaptoethanol	Sigma-Aldrich, Dorset, UK
Acetic acid	Fisher Scientific, Loughborough, UK
Acid alcohol	Leica Biosystems, Milton Keynes, UK
Acid-phenol:chloroform	Sigma-Aldrich, Dorset, UK
Affymetrix FlashTag™ Biotin HSR RNA Labeling Kit	ThermoFisher Scientific, Paisley, UK
Alcoholic eosin	Leica Biosystems, Milton Keynes, UK
Ammonium Bicarbonate	Sigma-Aldrich, Dorset, UK
Amphotericin B/fungizone	Gibco/ThermoFisher Scientific, Paisley, UK
Benzonase nuclease	Biocompare, San Francisco, USA
Cap-Clip Acid Pyrophosphatase	Cellscript, Madison, USA
Chloroform	Sigma-Aldrich, Dorset, UK
Collagenase type 2 Worthington	Biochemicals, Danehill, UK
cOComplete™ ULTRA, EDTA-free, tablet of protease inhibitor cocktail	Roche Life Science, Penzberg, Germany
Coomassie Brilliant Blue R-250 Destaining Solution	Bio-Rad, Watford, UK
Coomassie Brilliant Blue R-250 Staining Solution	Bio-Rad, Watford, UK
Dithiothreitol	Sigma-Aldrich, Dorset, UK
DNase I	Qiagen, Manchester, UK
Dulbecco's phosphate buffered saline	Sigma-Aldrich, Dorset, UK
Dulbecco's Modified Eagle Medium	ThermoFisher Scientific, Paisley, UK
Ethanol	Fisher Scientific, Loughborough, UK
Ethanol-molecular biology grade	Fisher Scientific, Loughborough, UK
Fast-green solution	Sigma-Aldrich, Dorset, UK
Foetal bovine serum	Gibco/ThermoFisher Scientific, Paisley, UK
GlycoBlue™ Coprecipitant	Invitrogen by ThermoFisher Scientific, Paisley, UK
Harris haematoxylin	Leica Biosystems, Milton Keynes, UK

HiPerFect Transfection Reagent	Qiagen, Manchester, UK
Recombinant Human IL-1 beta	R&D Systems, Abingdon, UK
Iodoacetamide	Sigma-Aldrich, Dorset, UK
Isopropanol	Sigma-Aldrich, Dorset, UK
Kapa Library Quantification Kit	Roche Life Science, Penzberg, Germany UK
L-glutamine	Gibco/ThermoFisher Scientific, Paisley, UK
miRNeasy Mini Kit	Qiagen, Manchester, UK
mirVana™ miRNA Isolation Kit with phenol	Ambion by Life Technologies, Paisley, UK
miScript II RT Kit	Qiagen, Manchester, UK
miScript SYBR® Green PCR Kit	Qiagen, Manchester, UK
M-MLV reverse transcriptase	Promega, Southampton, UK
M-MLV 5X Reaction Buffer	Promega, Southampton, UK
NEBNext® Small RNA Library Prep Set for Illumina®/Multiplex Compatible	New England Biolabs, Herts, UK
Novex™ Sharp Pre-stained Protein Standard ladder	ThermoFisher Scientific, Paisley, UK
Novex™ Tris-Glycine SDS Sample Buffer	ThermoFisher Scientific, Paisley, UK
NuPAGE® MES Running Buffer	ThermoFisher Scientific, Paisley, UK
NuPAGE™ 4% to 12% (w/v), Bis-Tris gel	ThermoFisher Scientific, Paisley, UK
PBS containing 0.1% (w/v) Bovine Serum Albumin	R&D Systems, Abingdon, UK
PCR Nucleotide Mix	Promega, Southampton, UK
Penicillin-streptomycin	Gibco/ThermoFisher Scientific, Paisley, UK
Pierce Silver Stain Kit	ThermoFisher Scientific, Paisley, UK
Pierce™ 660nm Protein Assay	ThermoFisher Scientific, Paisley, UK
Pierce™ Water, LC-MS Grade	ThermoFisher Scientific, Paisley, UK
Pre-diluted BSA protein assay standards	ThermoFisher Scientific, Paisley, UK
QIAquick PCR Purification Kit	Qiagen, Manchester, UK
Qubit® dsDNA HS Assay Kit	ThermoFisher Scientific, Paisley, UK
RapiGest SF Surfactant	Waters, Herts, UK

Random Primers	Promega, Southampton, UK
RNaseZAP	Sigma-Aldrich, Dorset, UK
RNasin(R) Plus RNase Inhibitor	Promega, Southampton, UK
Safranin-O	Sigma-Aldrich, Dorset, UK
Trifluoroacetic acid	Sigma-Aldrich, Dorset, UK
TRIzol reagent	Ambion by Life Technologies, Paisley, UK
Trypsin/Lys-C Mix, Mass Spec Grade	Promega, Southampton, UK
Trypsin-Ethylenediaminetetraacetic acid	Sigma-Aldrich, Dorset, UK
Xylene	Fisher Scientific, Loughborough, UK

Instrument/Consumables	Manufacturer
96-well PCR plate	StarLab, Milton Keynes, UK
Affymetrix GeneChip scanner 3000 7G	ThermoFisher Scientific, Paisley, UK
Affymetrix GeneChip® miRNA 4.0 Arrays	ThermoFisher Scientific, Paisley, UK
Affymetrix hybridisation oven 645	ThermoFisher Scientific, Paisley, UK
Agilent 2100 Bioanalyser RNA Pico chips	Agilent, Stockport, UK
Cell strainer	Fisher Scientific, Loughborough, UK
ChemiDoc XRS+ Gel Imaging System	Bio-Rad, Watford, UK
DNA high sensitivity Bioanalyzer chip	Agilent, Stockport, UK
FLUOstar Omega Microplate Reader	BMG LABTECH, Aylesbury, UK
GeneChip Fluidics station 450	ThermoFisher Scientific, Paisley, UK
Haemocytometer	Hawksley, Sussex, UK
Illumina MiSeq platform	Illumina, Cambridge, UK
Leica CV5030 Fully Automated Glass Coverslipper	Leica Biosystems, Milton Keynes
Leica ST5020 Multistainer	Leica Biosystems, Milton Keynes, UK
LightCycler® 480 Instrument II	Roche Life Science, Penzberg, Germany
LightCycler® 96 Instrument	Roche Life Science, Penzberg, Germany
Microscope slides	ThermoFisher Scientific, Paisley, UK

Mikro-dismembrator S	Sartorius, Melsungen, Germany
Nanodrop 2000 Spectrophotometer	ThermoFisher Scientific, Paisley, UK
Pippin Prep instrument	Sage Science, Beverly, USA
Soniprep 150 ultrasonic disintegrator	MSE, East Sussex, UK
T75/T175 flask	Greiner Bio-One, Stonehouse, UK

## 2.1 Collection of human knee cartilage

Human knee OA cartilage was collected from the femoral condyles of patients undergoing TKA and processed the same day. Human OA cartilage for microarray analysis in Chapter 3 and subsequent validation with qPCR in Chapter 4, was collected by Tim Welting's laboratory group at Maastricht University, Netherlands following ethical approval (Maastricht University Medical Centre approval IDs: MEC 08-4-028 and 14-4-038). Two cartilage samples were collected per patient: one sample from an intact area of femoral cartilage, and one sample from a lesioned area of femoral cartilage (**Figure 2.1**). Specifically, the medial and lateral femoral condyles were placed in saline and kept on ice until transferred in the laboratory. Then femoral condyles were placed in a class II laminar flow hood and transferred to petri dishes. Scalpels, cleaned with RNaseZAP (Sigma-Aldrich, Dorset, UK) to inactivate RNases, were used to collect cartilage from an intact area and a lesioned area. Excised cartilage tissue was snap frozen in liquid nitrogen and stored at -80°C.

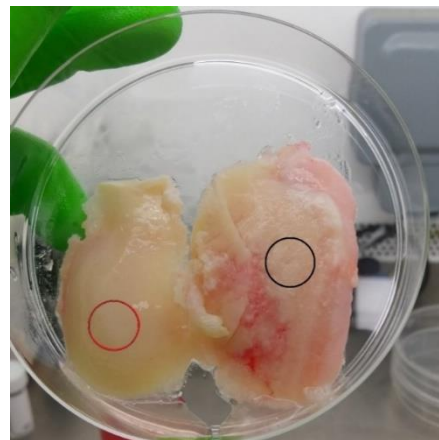


**Figure 2.1: Example of intact and lesioned human knee OA cartilage.** Cartilage biopsies were collected from intact (red circle) and lesioned areas (black circle) of knee femoral condyles from end-stage OA patients, after surgery. Full thickness cartilage was collected (for lesioned cartilage, full thickness was collected when possible). Original figure, courtesy of the author.

## 2.2 Collection of intact/healthy knee cartilage from non-OA donors

In the current thesis, three groups of human intact/healthy knee cartilage were collected:

- i) Young cartilage from patients undergoing ACL reconstruction, to include in microarray analysis in Chapter 3. Cartilage was collected from the area of the intercondylar notch (**Figure 2.2**) as a by-product of the procedure. Tissue was collected, snap-frozen and stored at -80°C by Tim Welting's laboratory group at Maastricht University, Netherlands, following ethical approval (Maastricht University Medical Centre approval IDs: MEC 08-4-028 and 14-4-038). Samples were shipped to the Institute of Life Course and Medical Sciences, University of Liverpool, UK and further processed by the author. This group will be referred to throughout the thesis as Young intact cartilage.
- ii) Young cartilage from cadavers with no history of OA or knee disease. Samples were purchased from Proteogenex, USA and were collected from the lateral and medial femoral condyles of young non-OA cadavers with an unrelated cause of death. Therefore, ethical approval was not needed. This group was used for qPCR analysis

in Chapter 4 and will be referred to throughout the thesis as Young healthy cartilage.

- iii) Old cartilage from cadavers with no history of OA or knee disease. Samples were purchased from Proteogenex, USA and were collected from the lateral and medial femoral condyles of old non-OA cadavers with an unrelated cause of death. Therefore, ethical approval was not needed. This group was used for qPCR analysis in Chapter 4 and will be referred to throughout the thesis as Old healthy cartilage.

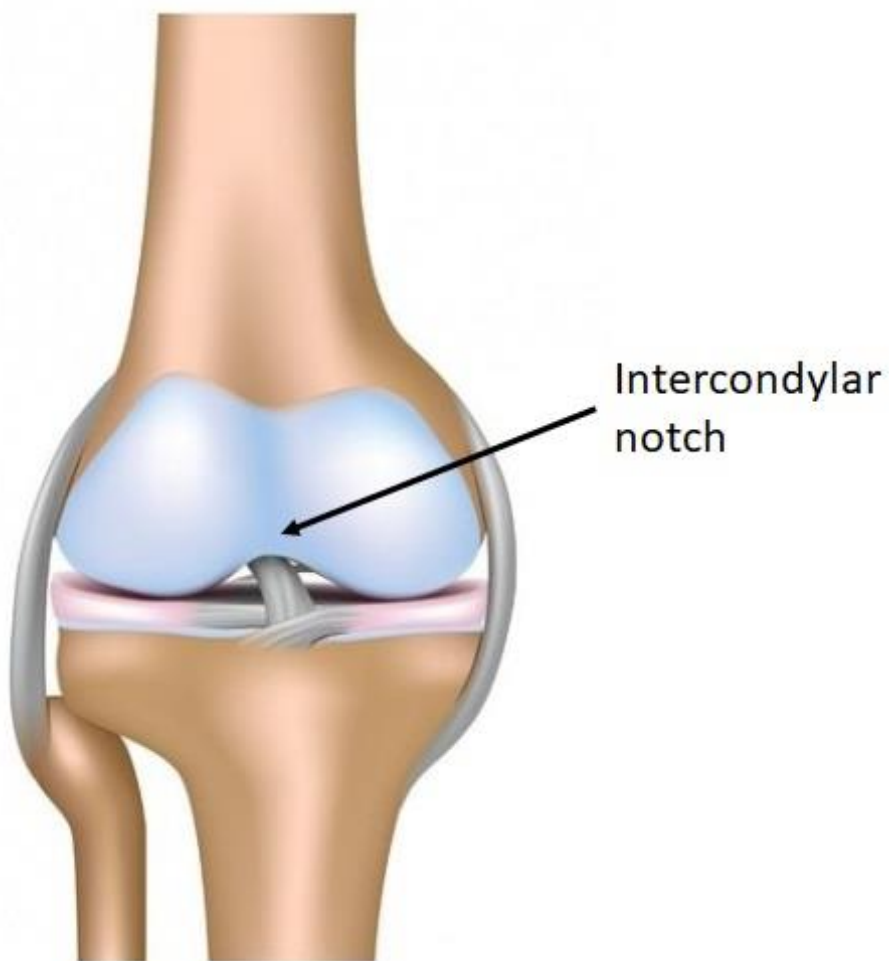


**Figure 2.2: The intercondylar notch.** The intercondylar notch in the human knee joint is located between the two femoral condyles, and above the ACL. Figure modified from (Ruane, 2016).

## **2.3 Macroscopic scoring of human knee osteoarthritic cartilage**

Medial and lateral femoral condyles from human knee OA joints were scored macroscopically using the Outerbridge scoring system (**Table 2.1**) (Outerbridge, 1961). Samples were scored by two independent scorers at two different time points. Scorer agreement was calculated using Cohen's weighted kappa coefficient (Cohen, 1960), available here: (StatsToDo, 2020).

**Table 2.1: The Outerbridge scoring system.**

<b>Grade</b>	<b>Pathology</b>
<b>0</b>	Normal
<b>I</b>	Softening and swelling of articular cartilage
<b>II</b>	Fragmentation and fissuring of articular cartilage affecting an area of less than 0.5 inches
<b>III</b>	Fragmentation and fissuring of articular cartilage affecting an area of greater than 0.5 inches
<b>IV</b>	Cartilage erosion to bone

## **2.4 Paraffin embedding of human knee OA cartilage**

Paraffin embedding of human, intact and lesioned, knee OA cartilage was performed by Tim Welting's laboratory group at Maastricht University, Netherlands. Paraffin blocks were shipped to the Institute of Life Course and Medical Sciences, University of Liverpool, UK and further processed by the author.

## **2.5 Sectioning of human knee cartilage**

Sectioning of human knee cartilage (OA and healthy) was undertaken as follows:

- A) For histological analysis of knee OA cartilage, paraffin-embedded human knee OA cartilage, blocks were cooled at 4°C for 30min. Blocks were sectioned at 4µm using a Leica RM 2235 microtome (Leica Biosystems, Milton Keynes, UK). Sections were left to float on a water-bath for 2-3min to smooth out any wrinkles and then placed on microscope slides (ThermoFisher Scientific, Paisley, UK). Sections were left to dry on a warm surface for 15min and then at 37°C overnight. Once dried, sections were kept at room temperature.
- B) For histological analysis of young and old healthy human knee cartilage from cadavers, samples were cryosectioned using a Leica CM1520 cryostat (Leica Biosystems, Milton Keynes, UK). Temperature inside the cryostat was set to -20°C and tissue samples were kept frozen on dry-ice. Tissue was mounted on a cryostat chuck using tissue freezing medium (Leica Biosystems, Milton Keynes, UK). Tissue was sectioned at 10µm and sections were placed on microscope slides. Slides were either stained immediately or kept at -80°C for a short amount of time until staining.

## **2.6 Haematoxylin and eosin staining**

Paraffin embedded sections of human knee OA cartilage were stained with H&E using the Leica ST5020 Multistainer (Leica Biosystems, Milton Keynes, UK) in conjunction with the Leica CV5030 Fully Automated Glass Coverslipper (Leica Biosystems, Milton Keynes, UK). Specifically, sections were placed at 37°C for 30min prior to staining to warm the wax around the section. Then, sections were placed in the following solutions for dewaxing:

- 5min in xylene (x2) (Fisher Scientific, Loughborough, UK)
- 5min in 100% (v/v) ethanol (Fisher Scientific, Loughborough, UK)
- 5min in 90% (v/v) ethanol
- 5min in 70% (v/v) ethanol

After dewaxing, sections were washed with water for 10sec and then placed in Harris haematoxylin (Leica Biosystems, Milton Keynes, UK) for 7min. Excess of haematoxylin was washed away by placing the sections in water for 10sec and then in 1% (v/v) acid alcohol (Leica Biosystems, Milton Keynes, UK) for another 10sec. Sections were washed further by

water for 5min and counter stained with alcoholic eosin (Leica Biosystems, Milton Keynes, UK) for 10min. Excess eosin was washed away with water for 10min and then sections were dehydrated by placing them in the following solutions:

- 1min in 96% (v/v) ethanol (x2)
- 1min in 100% (v/v) ethanol (x2)
- 1min in xylene (v/v) (x2)

Sections were covered with coverslips and left to dry in the fume hood overnight.

Cryosections of young and old healthy knee cartilage from cadavers were stained with H&E following the same process, except for the dewaxing steps. Cryosections were placed straight in ethanol instead of xylene. Aibek Smagul, PhD Student, University of Liverpool, sectioned and stained young healthy cartilage samples.

## **2.7 Safranin-O and fast-green staining**

Paraffin embedded sections of human knee OA cartilage were stained with Saf-O/FG using the Leica ST5020 Multistainer (Leica Biosystems, Milton Keynes, UK) in conjunction with the Leica CV5030 Fully Automated Glass Coverslipper (Leica Biosystems, Milton Keynes, UK). As with H&E staining, sections were placed at 37°C for 30min prior to staining to warm the wax around the section. Then, sections were placed in the following solutions for dewaxing:

- 10min in xylene (x2)
- 2min in 100% (v/v) ethanol
- 2min in 90% (v/v) ethanol
- 2min in 70% (v/v) ethanol

After dewaxing, sections were placed in Harris haematoxylin for 30sec and then washed with water for 5min. Sections were stained with 0.2% (w/v) fast-green solution (Sigma-Aldrich, Dorset, UK) for 10min and then placed in 1% (v/v) acetic acid (Fisher Scientific, Loughborough, UK) for 20sec (x2). Sections were washed shortly with water for 10sec and then stained with 0.5% (w/v) safranin-O solution (Sigma-Aldrich, Dorset, UK) for 2min. Sections were dehydrated by placing them in the following solutions:

- 20 sec in 70% (v/v) ethanol
- 2 min in 90% (v/v) ethanol
- 2 min in 100% (v/v) ethanol
- 3 min in xylene

Sections were covered with coverslips and left to dry in the fume hood overnight.

## 2.8 Histological scoring of human knee OA cartilage

Human knee OA cartilage sections from intact and lesioned areas, stained with H&E and Safranin-O/FG, were scored using two scoring systems for comparison: the Mankin HHGS (Mankin et al., 1971) (**Table 2.2**) and the OARSI scoring system (Pearson et al., 2011) (**Table 2.3**). Sections were viewed using a Nikon Eclipse 80i microscope (Nikon, UK).

**Table 2.2: The Mankin HHGS was used to score human knee OA cartilage sections.** Adapted from (Mankin et al., 1971).

	Grade
<b>I. Structure</b>	
h. Normal	0
i. Surface irregularities	1
j. Pannus and surface irregularities	2
k. Clefts to middle zone	3
l. Clefts to deep zone	4
<b>II. Cells</b>	
e. Normal	0
f. Diffuse hypercellularity	1
g. Cloning	2
h. Hypocellularity	3
<b>III. Safranin-O staining</b>	
f. Normal	0
g. Slight reduction	1
h. Moderate reduction	2
i. Severe reduction	3
j. No dye noted	4

**Table 2.3: The OARSI scoring system that was used to score stained human knee OA cartilage sections.** Adapted from (Pearson et al., 2011).

Grade (key feature)	Associated criteria (tissue reaction)
<b>Grade 0: surface intact, cartilage morphology intact</b>	<p>Matrix: normal architecture</p> <p>Cells: intact, appropriate orientation</p>
<b>Grade 1: surface intact</b>	<p>Matrix: superficial zone intact, oedema and/or superficial fibrillation (abrasion), focal superficial matrix condensation.</p> <p>Cells: death, proliferation (clusters), hypertrophy, superficial zone. Reaction must be more than superficial fibrillation only.</p>
<b>Grade 2: surface discontinuity</b>	<p>As above</p> <p>+Matrix discontinuity at superficial zone (deep fibrillation)</p> <p>±Cationic stain matrix depletion (Safranin-O) upper 1/3 of cartilage.</p> <p>±Focal perichondronal increased stain (mid zone).</p> <p>±Disorientation of chondron columns.</p> <p>Cells: death, proliferation (clusters), hypertrophy.</p>
<b>Grade 3: vertical fissures (clefts)</b>	<p>As above</p> <p>Matrix vertical fissures into mid zone, branched fissures.</p> <p>±Cationic stain depletion (Safranin-O) into lower 2/3 of cartilage (deep zone).</p> <p>Cells: death, regeneration (clusters), hypertrophy, cartilage domains adjacent to fissures.</p>

<b>Grade 4: erosion</b>	Cartilage matrix loss: delamination of superficial layer, mid layer cyst formation. Excavation: matrix loss superficial layer and mid zone.
-------------------------	---

Cartilage samples collected as in Section 2.1 did not include the calcified zone or subchondral bone. Therefore, the Mankin HHGS scoring system used here did not include parameters 'I.f', 'I.g', 'IV.a' and 'IV.b' as described in Table 1.4 of Chapter 1. Maximum score was 11. Similarly, the OARSI scoring system used here did not include grade 5 and 6, as described in Table 1.5 of Chapter 1, since these refer to changes in the subchondral bone. Moreover, the OARSI scoring system used here did not include stage assessment, as this would require stained sections from the whole articular surface of femoral condyles which was not possible. Therefore, maximum score was 4. Sections were scored by two independent scorers, in two different time points. Scorer agreement was calculated using Cohen's weighted kappa coefficient (Cohen, 1960), available here: (StatsToDo, 2020)

## 2.9 Isolation of human primary chondrocytes from articular cartilage

For isolation of human primary OA chondrocytes, human OA cartilage was collected by the Liverpool Musculoskeletal Biobank, following Sponsorship Approval (Sponsor Ref: UoL001398) and Clatterbridge Hospital, Wirral following ethical approval (IRAS ID 242434; Main Investigator: Dr Simon Tew, Senior Lecturer, University of Liverpool). Isolation of human primary chondrocytes from cartilage tissue was carried out under sterile conditions in a class II laminar flow hood and all items were sprayed with 70% (v/v) ethanol prior to use to maintain sterility. Once tissue was transferred to the laboratory, it was placed in a sterile hood. A sterile scalpel was used to excise pieces of cartilage from the femoral condyles and remove the subchondral bone. To remove debris and blood, excised cartilage tissue was washed twice with sterile complete media consisting of Dulbecco's Modified Eagle Medium (DMEM) (ThermoFisher Scientific, Paisley, UK), with the following composition:

- low glucose (1g/L)
- pyruvate (110.0mg/L)

- 1% (v/v) L-glutamine
- phenol-red (15mg/L)

and supplemented with:

- 10% (v/v) foetal bovine serum (FBS) (Gibco/ThermoFisher Scientific, Paisley, UK)
- 1% (v/v) penicillin-streptomycin (P/S) (Gibco/ThermoFisher Scientific, Paisley, UK)
- 0.2% (v/v) amphotericin B/fungizone (F/Z) (Gibco/ThermoFisher Scientific, Paisley, UK)

Cartilage was cut into 2-3mm pieces and transferred in a 50mL falcon of complete media supplemented with 0.08% (w/v) collagenase type 2 (Worthington Biochemicals, Danehill, UK). The falcon was placed in a shaking incubator at 37°C overnight for tissue digestion and chondrocyte extraction from the ECM. Next day, the solution was passed through a 70µm sterile cell strainer (Fisher Scientific, Loughborough, UK) to remove undigested cartilage pieces. The solution was centrifuged at 1400 rounds per minute (rpm), at room temperature for 4min. Isolated chondrocytes were pelleted and supernatant removed. Chondrocytes were resuspended and washed in 5mL complete media and spun down as before. Supernatant was removed and chondrocytes were resuspended in 12mL complete media and transferred to a T75 flask (Greiner Bio-One, Stonehouse, UK) to attach. Flask was placed in a tissue culture incubator at 37°C, supplied with 20% (v/v) O<sub>2</sub> and 5% (v/v) CO<sub>2</sub>.

## **2.10 Isolation of healthy equine primary chondrocytes from cartilage tissue**

Healthy primary chondrocytes were isolated from the metacarpophalangeal joints of non-Thoroughbred horses. The Animal (Scientific procedures) Act 1986, Schedule 2, does not define collection from these sources as scientific procedures. Ethical approval was therefore not required. Horses euthanised for other reasons were collected from the abattoir. Horse legs were cleaned and sprayed with 70% (v/v) ethanol. An incision was made across the leg using a scalpel to remove the skin around the joint. Then, the metacarpophalangeal joint cavity was opened using a sterile scalpel and the joint was inspected macroscopically for lesions and signs of cartilage degradation. Only healthy joints were selected and full thickness cartilage was excised and transferred to a laminar flow hood. Chondrocytes were isolated from the tissue using the same methodology as with human chondrocytes in Section 2.9.

Chondrocytes in T175 flasks were placed in a tissue culture incubator at 37°C, supplied with 20% (v/v) O<sub>2</sub> and 5% (v/v) CO<sub>2</sub>.

## **2.11 Human and equine chondrocyte culture and passaging**

After chondrocyte isolation, human and equine chondrocytes were placed in T75/T175 flasks to proliferate. Complete media was changed twice a week until chondrocytes reached 90% confluence. To collect or passage chondrocytes, media was removed and cells were washed twice with 5mL 1x Dulbecco's phosphate buffered saline (DPBS) (Sigma-Aldrich, Dorset, UK). DPBS was removed and 5mL of 1x trypsin-Ethylenediaminetetraacetic acid (EDTA) (Sigma-Aldrich, Dorset, UK) was added to the cells. Cells were placed at 37°C for 3min to detach from plastic and trypsin-EDTA was deactivated by adding 5mL of complete media. Cells were collected and centrifuged at 1400rpm for 4min. Supernatant was removed and cell pellet was resuspended in 5mL of complete media. Cells were counted with a haemocytometer (Hawksley, Sussex, UK) and cell number was calculated by using the formula below:

**total cell number:** *number of cells counted in four corner squares / 4 x 10<sup>3</sup> x initial volume*

Cells were either collected and lysed or seeded in well plates in appropriate density according to the experimental procedure downstream. Chondrocytes up to passage 1 were used for all experiments.

## **2.12 Homogenisation of human knee cartilage tissue**

Due to its extensive ECM, human knee cartilage tissue needs to be ground before isolation of nucleic acids and especially RNA. Disruption and grinding of cartilage tissue were carried out using a mikro-dismembrator S (Sartorius, Melsungen, Germany). Approximately 100mg of tissue were used per sample. Prior to the procedure, the metallic flasks and grinding balls of the dismembrator were cleaned with RNaseZAP and autoclaved. On the day of the procedure, samples were cut into 2-3mm small pieces and kept in 1.5mL tubes and snap frozen in liquid nitrogen. Metallic flasks and grinding balls were also snap frozen in liquid nitrogen to maintain low temperature during grinding. By working fast, one sample at a time was placed in a clean set of metallic flasks along with a grinding ball. The flasks were then placed in the

dismembrator and cartilage tissue was grinded into powder at 2000rpm for 1min. Appropriate lysis buffer was added in the cartilage powder and transferred in a 1.5mL tube and kept on ice if RNA extraction was carried out on the same day, or stored at -80°C.

## **2.13 Total RNA extraction from human knee cartilage tissue and human/equine chondrocytes**

For this thesis, total RNA, containing sncRNAs, was extracted in three different ways dependent on the downstream application. The mirVana™ miRNA Isolation Kit with phenol (Ambion by Life Technologies, Paisley, UK) was used for extracting total RNA from human knee articular cartilage for microarray analysis and subsequent qPCR validation in Chapter 3. The miRNeasy Mini Kit (Qiagen, Manchester, UK) was used for extraction of total RNA from equine primary chondrocytes for small RNA-Seq and subsequent qPCR validation in Chapter 6. Finally, extraction of total RNA from samples that would be used for standard analysis, such as qPCR analysis in human articular cartilage and human primary chondrocytes in Chapter 4 and 5, was carried out with the commonly used acid guanidinium thiocyanate-phenol-chloroform method (Chomczynski et al., 1987), using TRIzol reagent (Ambion by Life Technologies, Paisley, UK) for cell lysis. DNase treatment was not performed except for RNA extraction from equine primary chondrocytes as it was required for the downstream small RNA-Seq experiment. In our experience, genomic DNA carry over is minimal and does not interfere with downstream analysis. Moreover, total RNA extraction from cartilage tissue does not produce high concentrations of RNA and during DNase treatment some amount of RNA is lost. Therefore, DNase treatment was omitted from all other RNA extraction methods as it could compromise the amount of total RNA isolated. Each method is analysed further below.

### **2.13.1 Total RNA extraction from human knee articular cartilage tissue using the mirVana™ miRNA Isolation Kit with phenol**

Total RNA, intended for microarray analysis, was extracted from human knee articular cartilage using the mirVana™ miRNA Isolation Kit with phenol according to the manufacturer's

protocol (Ambion, 2011), with minor modifications. Prior to RNA extraction, solutions ‘Wash solution 1’ and ‘Wash solution 2/3’ were prepared by adding 21mL and 40mL of 100% (v/v) molecular biology-grade ethanol (Fisher Scientific, Loughborough, UK). Human knee articular cartilage was ground into powder as described in Section 2.12. Then:

- 1mL of Lysis/Binding Buffer was added to the powder and collected in 1.5mL tubes. Lysate was vortexed for 5min to aid tissue disruption.
- 100µL of miRNA Homogenate Additive was added to the lysate and left at room temperature for 10min. Lysate was then vortexed and centrifuged at 13,000rpm at room temperature for 10min. Supernatant was collected in a fresh tube and cartilage powder at the bottom of the tube was discarded to avoid contamination of the supernatant.
- An equal volume of acid-phenol:chloroform (Sigma-Aldrich, Dorset, UK) was added to the supernatant and sample was vortexed for 1min and centrifuged at 13,000rpm at room temperature for 5min to separate the aqueous and organic phases. The aqueous phase was transferred to a fresh tube without disturbing the organic phase.
- 1.25x volumes of 100% (v/v) molecular biology-grade ethanol (room temperature) was added to the aqueous phase. Up to 700µL of sample was then transferred onto a filter cartridge placed in a collection tube and centrifuged at room temperature at 10,000rpm for 15sec. Total RNA was captured on the filter cartridge and the flow-through was discarded.
- 700µL of Wash solution 1 was applied to the filter cartridge and centrifuged at 10,000rpm for 10sec. Flow-through was discarded and 500µL of wash solution 2/3 was added and spun down at 10,000rpm for 10sec. This step was repeated with extra 500µL of wash solution 2/3. Flow through was discarded.
- Filter cartridge in the collection tube was centrifuged at 10,000rpm for 1min to remove any fluid left. Then, the filter cartridge was placed in a new collection tube.
- 70µL of nuclease-free water, pre-heated at 95°C, was added onto the filter cartridge and sample was centrifuged at 13,000rpm for 1min to elute total RNA. Eluate with total RNA was kept on ice and the filter cartridge was placed in a new collection tube (Note: Elution buffer provided with the kit was avoided as it could potentially interfere with downstream microarray analysis).

- An extra 70µL of pre-heated nuclease-free water was added onto the filter cartridge and centrifuged as before to collect a second elution, for maximum total RNA recovery.
- RNA concentration and purity were measured using a Nanodrop 2000 Spectrophotometer (ThermoFisher Scientific, Paisley, UK). RNA was stored at -80°C.

### **2.13.2 Total RNA extraction from equine primary chondrocytes using the miRNeasy Mini Kit**

Total RNA, intended for small RNA-Seq analysis, was extracted from equine primary chondrocytes using the miRNeasy Mini Kit, according to the manufacturer's protocol (Qiagen, 2020). Equine cells growing in T175 flasks were trypsinised and collected in complete media as described in Section 2.11. Cells were centrifuged at 1,400rpm at room temperature for 4min and media was removed. 5mL of 1x DPBS was added to wash and resuspend the pellet and then cells were pelleted again as above. DPBS was removed and total RNA was extracted using the miRNeasy Mini Kit, including a DNase I (Qiagen, Manchester, UK) digestion step. Specifically, before starting the procedure, 2x and 4x volumes of 100% (v/v) molecular biology-grade ethanol was added to buffer RWT and buffer RPE, respectively. Lyophilised DNase I was dissolved in 550µL of RNase-free water and mixed gently by flicking the vial. Then:

- 1mL of Qiazol Lysis Reagent was added to the cells. Sample was vortexed for 2min to lyse the cells. Lysate was placed at room temperature for 5min.
- 200µL of chloroform (Sigma-Aldrich, Dorset, UK), was added to the lysate. Lysate was shaken vigorously for 15sec to achieve thorough mixing. Sample was left at room temperature for 2-3min until an aqueous phase appeared on top.
- The sample was centrifuged at 13,000rpm at 4°C for 20min for complete phase separation. The upper/aqueous phase was transferred with caution to a new tube to avoid transferring any of the interphase.
- 1.5x volumes of 100% (v/v) molecular biology-grade ethanol was added to the aqueous phase and pipetted up and down to mix thoroughly.
- An RNeasy Mini spin column was placed in a 2mL collection tube and up to 700µL of sample was loaded on the column. The sample was centrifuged at 13,000rpm at room

temperature for 15sec and flow-through was discarded. This step was repeated for the remaining of the sample.

- 350µL of buffer RWT was pipetted onto the RNeasy Mini spin column and centrifuged at 13,000rpm at room temperature for 15sec to wash the RNA on the filter of the column. Flow-through was discarded.
- 10µL of DNase I was added to 70µL of buffer RDD and mixed gently by flicking the tube. The 80µL of this mix was pipetted directly on the centre of the column and the sample was placed at room temperature for 15min for DNA digestion.
- 350µL of buffer RWT was pipetted onto the column and centrifuged at 13,000rpm at room temperature for 15sec. Flow-through was discarded.
- 500µL of buffer RPE was added onto the RNeasy Mini spin column and the sample was centrifuged at 13,000rpm at room temperature for 15sec. Flow-through was discarded. This step was repeated with an extra of 500µL of buffer RPE and the sample was spun at 13,000rpm at room temperature for 2min. Flow-through was discarded.
- The RNeasy Mini spin column was placed in another collection tube and spun at 13,000rpm at room temperature for 1min to dry the filter and remove any remaining liquid.
- The RNeasy Mini spin column was placed in a 1.5mL tube and 30µL of RNase-free water was added directly onto the column. The column was centrifuged at 13,000rpm at room temperature for 1min to elute the RNA.
- The RNeasy Mini spin column was placed in a second 1.5mL tube. Additional 30µL of RNase-free water was added directly onto the column and the column was centrifuged as above to elute the remaining of the RNA.
- RNA concentration and purity were measured using a Nanodrop 2000 Spectrophotometer. RNA was stored at -80°C.

### **2.13.3 Total RNA extraction from human knee articular cartilage and human primary chondrocytes using the guanidinium thiocyanate-phenol-chloroform method (TRIzol)**

Total RNA, intended for qPCR analysis, was isolated from human knee articular cartilage and human primary chondrocytes using the TRIzol protocol with minor modifications. Human

cartilage tissue was homogenised as described in Section 2.12. For chondrocytes growing in well-plates, media was removed and cells washed twice with 1x DPBS. DPBS was then discarded and cells lysed. Specifically, for tissue and cells:

- 1mL of TRIzol was added to 100mg of homogenised human cartilage tissue (powder). For human chondrocytes, the amount of TRIzol dependent on the number of cells. Chondrocytes growing in 12-well and 24-well plates were lysed in 700µL and 500µL of TRIzol, respectively.
- The sample was lysed by vortexing for 2min. Specifically for tissue, after vortexing, the sample was placed on a rotator and rotated at medium speed at room temperature for 10min to aid lysis. Then, the sample was centrifuged at 13,000rpm at 4°C for 5min to pellet any non-lysed powder. Supernatant was transferred to a new 1.5mL tube and passed ten times through a 21-gauge needle to aid lysis and breakdown of proteoglycans.
- 200µL of chloroform (or less, dependent on amount of TRIzol added, TRIZol:chloroform 5:1) was added to the lysate and shaken vigorously to mix. The sample was left at room temperature for 2-3min until the aqueous phase appeared on top.
- The sample was then centrifuged at 13,000rpm at 4°C for 20min for phase separation. The aqueous phase was transferred to a new 1.5mL tube.
- 2µL of GlycoBlue™ Coprecipitant (Invitrogen by ThermoFisher Scientific, Paisley, UK) was added to the aqueous phase and mixed.
- An equal amount of isopropanol (Sigma-Aldrich, Dorset, UK) was added and the tube was inverted ten times to mix. The sample was left on ice for 30min to precipitate total RNA.
- The sample was centrifuged at 13,000rpm at 4°C for 20min to pellet RNA. Supernatant was discarded.
- The pelleted RNA was washed with 1mL of 75% (v/v) ice-cold molecular biology-grade ethanol. The sample was centrifuged at 13,000rpm at 4°C for 5min. Most of the ethanol was discarded by decanting. To remove any ethanol left, the sample was pulse spun and the excess of ethanol was pipetted out of the tube. The sample was left on the bench to air dry (approximately for 10min).

- The RNA pellet was dissolved in 15µL of nuclease-free water.
- RNA concentration and purity were measured using a Nanodrop 2000 Spectrophotometer. RNA was stored at -80°C.

## **2.14 Microarray analysis for detection of differentially expressed miRNAs**

Differential miRNA expression analysis in cartilage samples was undertaken by appropriate personnel at the Centre for Genomic Research (CGR) at the University of Liverpool, using the Affymetrix GeneChip® miRNA 4.0 Arrays (ThermoFisher Scientific, Paisley, UK). Arrays assayed for all mature miRNAs in miRBase Release 20 and contained probes for 2578 human mature miRNAs and 2025 human precursor miRNAs (Affymetrix, 2016). Quantity and quality of RNA submitted to CGR was assessed using the Agilent 2100 Bioanalyser RNA Pico chips (Agilent, Stockport, UK). 500ng of total RNA was used as the initial input and speed-vac was undertaken to reduce the volume to 8µL per sample. Then, the Affymetrix FlashTag™ Biotin HSR RNA Labeling Kit (ThermoFisher Scientific, Paisley, UK) was used to prepare samples for hybridisation according to manufacturer's instructions (Affymetrix, 2012). Specifically, small RNAs, including miRNAs, were polyadenylated and then ligated to biotin-labelled 3DNA® dendrimers for robust signal detection (**Figure 2.3**). Each labelled sample was mixed with the hybridisation cocktail and then injected into an Affymetrix GeneChip miRNA 4.0 array. Arrays were placed in the Affymetrix hybridisation oven 645 (ThermoFisher Scientific, Paisley, UK) and incubated at 48°C at 60rpm for 17.5h. After hybridisation, the hybridisation cocktail was extracted from each array and the arrays were washed using the Affymetrix Hybridisation wash and stain kit on the GeneChip Fluidics station 450 (ThermoFisher Scientific, Paisley, UK) using fluidics script FS450\_0002, and scanned using the Affymetrix GeneChip scanner 3000 7G (ThermoFisher Scientific, Paisley, UK).

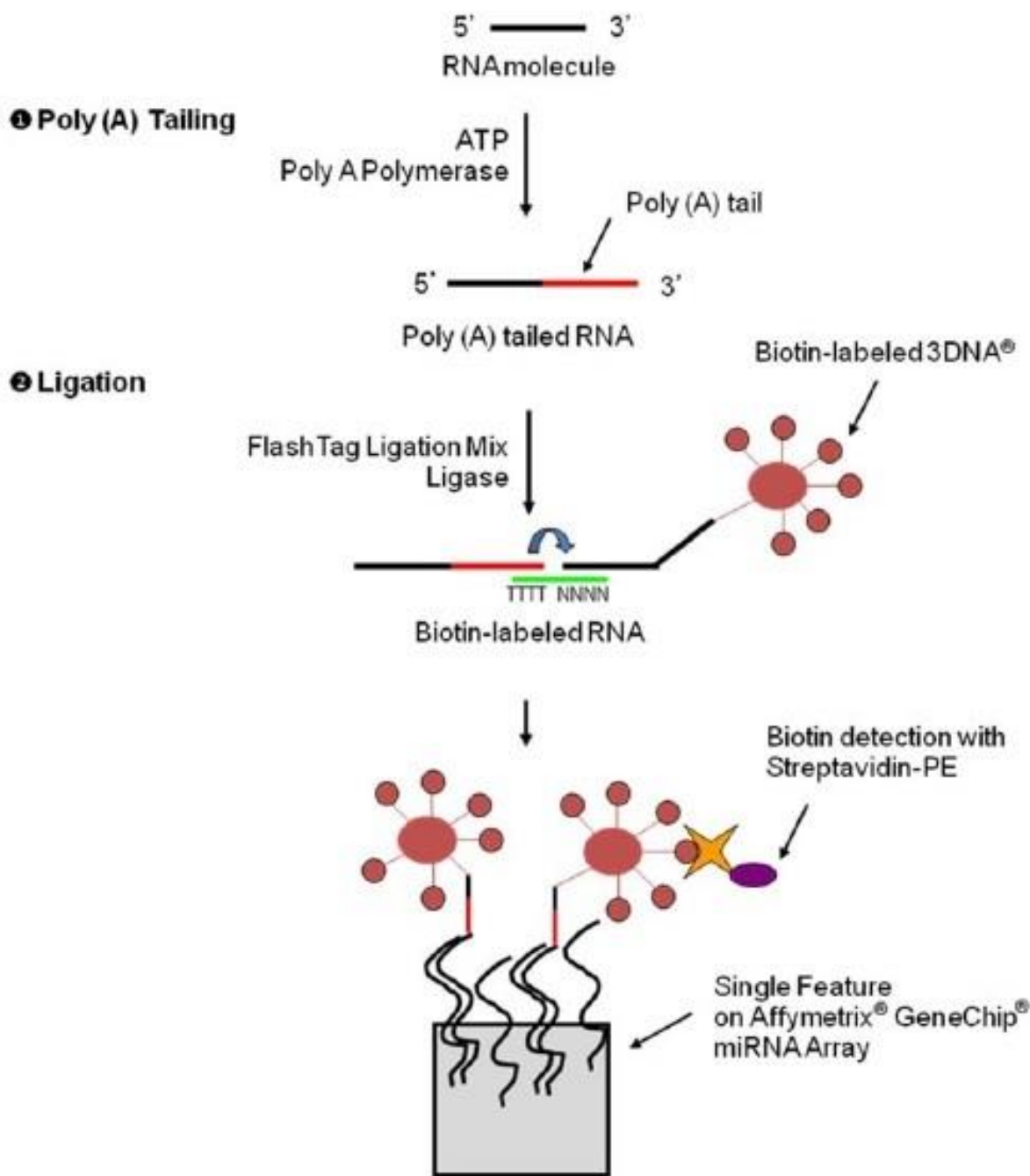


**Figure 2.3: The Affymetrix FlashTag™ Biotin HSR RNA Labeling protocol.** miRNAs were polyadenylated by poly(A) polymerase. Then, biotin-labelled 3DNA® dendrimers were ligated to the polyadenylated miRNAs by T4 DNA Ligase through a bridge oligonucleotide. Labelled polyadenylated miRNAs were hybridised onto the Affymetrix GeneChip miRNA 4.0 arrays and signal detection was achieved through the Streptavidin-PE system. Abbreviations: Phycoerythrin (PE). Figure modified from (Affymetrix, 2012).

## 2.15 Small RNA-Seq analysis for detection of differentially expressed miRNAs

Differential expression analysis in equine chondrocytes was undertaken by appropriate personnel at CGR using the Illumina MiSeq platform (Illumina, Cambridge, UK). Prior to sequencing, cDNA library preparation was carried out using the NEBNext® Small RNA Library Prep Set for Illumina®/Multiplex Compatible (New England Biolabs, Herts, UK) according to the manufacturer's protocol (NewEngland-Biolabs, 2020) (**Figure 2.4**). In short, total RNA was ligated to a 3' SR Adaptor and then subjected to Cap-Clip Acid Pyrophosphatase treatment (Cellscript, Madison, USA) to remove some 5' cap structures found on some snRNAs. Then, total RNA was ligated to a 5' SR Adaptor and cDNA synthesis through a reverse transcription primer was performed, followed by PCR Amplification and the addition of barcodes to the amplicons. PCR products were purified using the QIAquick PCR Purification Kit (Qiagen, Manchester, UK) and quantity of the recovered cDNA was checked with the Qubit® dsDNA HS Assay Kit (ThermoFisher Scientific, Paisley, UK). Quality check of the libraries was undertaken on a DNA high sensitivity Bioanalyzer chip (Agilent, Stockport, UK) and size selection for small RNAs (0-280bp) was undertaken with the Pippin Prep instrument using the 3% (w/v) agarose, dye-free gel with internal standards (Sage Science, Beverly, USA). The quantity and quality of the final pool was assessed by Qubit and Bioanalyzer as before, and subsequently by qPCR using the Kapa Library Quantification Kit (Roche Life Science, Penzberg, Germany), run on a LightCycler® 480 Instrument II (Roche Life Science, Penzberg, Germany). Briefly, a 20µL qPCR reaction (performed in triplicate for each pooled library) was prepared on ice with 12µL SYBR Green I Master Mix and 4µL of diluted pooled cDNA (dilutions: 1:1000 to 1:100,000 depending on the initial concentration determined by the Qubit® dsDNA HS Assay Kit). Following calculation using the qPCR data, 5µL of the final pool was denatured for 5min at room temperature using 5µL of freshly diluted 0.1N NaOH and the reaction was subsequently terminated by the addition of the HT1 Hybridization Buffer. The final loading concentration of 10.5pM was reached by adding the required HT1 buffer volume. The libraries were sequenced on an Illumina MiSeq platform to generate 2x150bp paired-end reads.

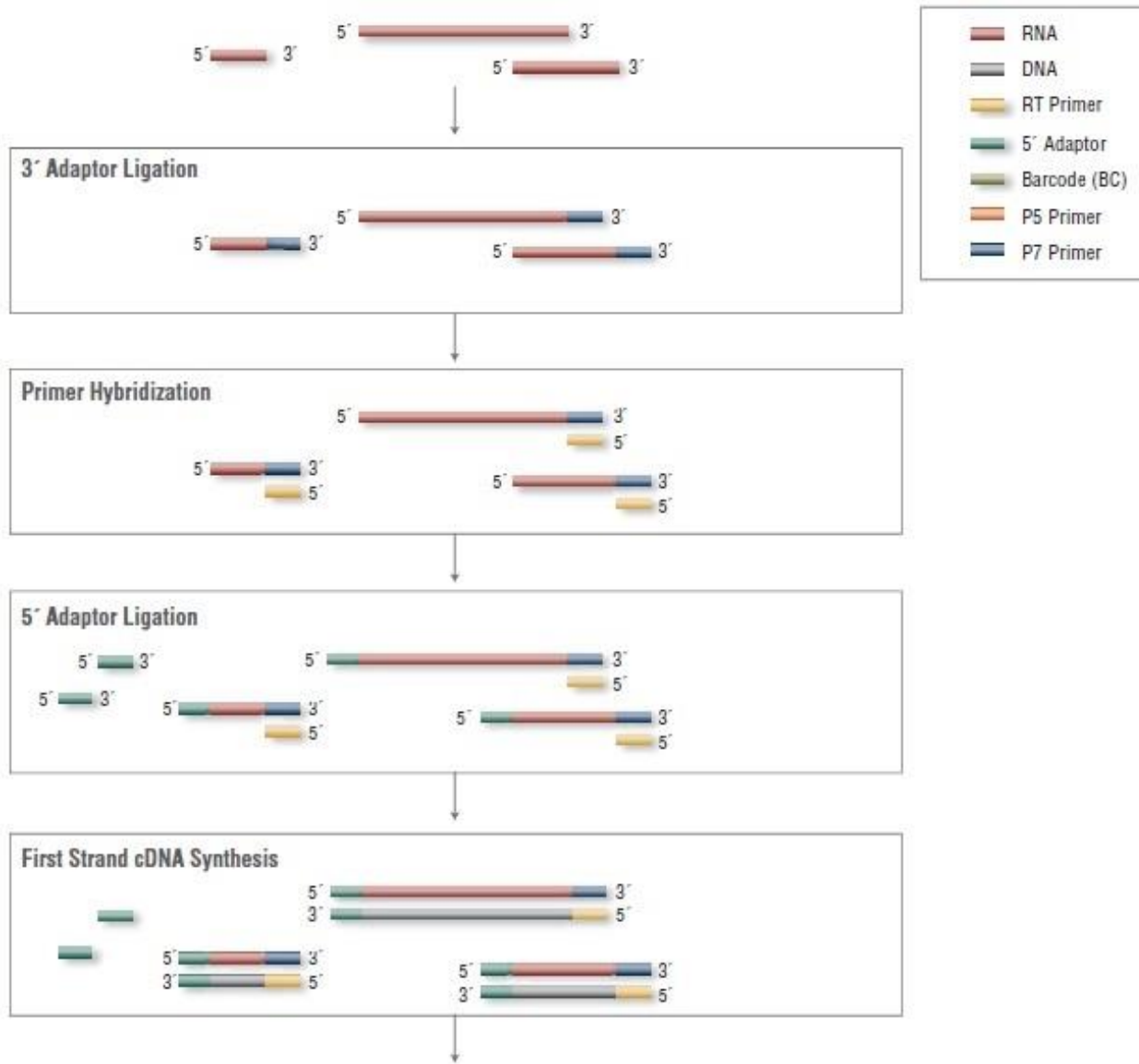


(Figure continues on next page)

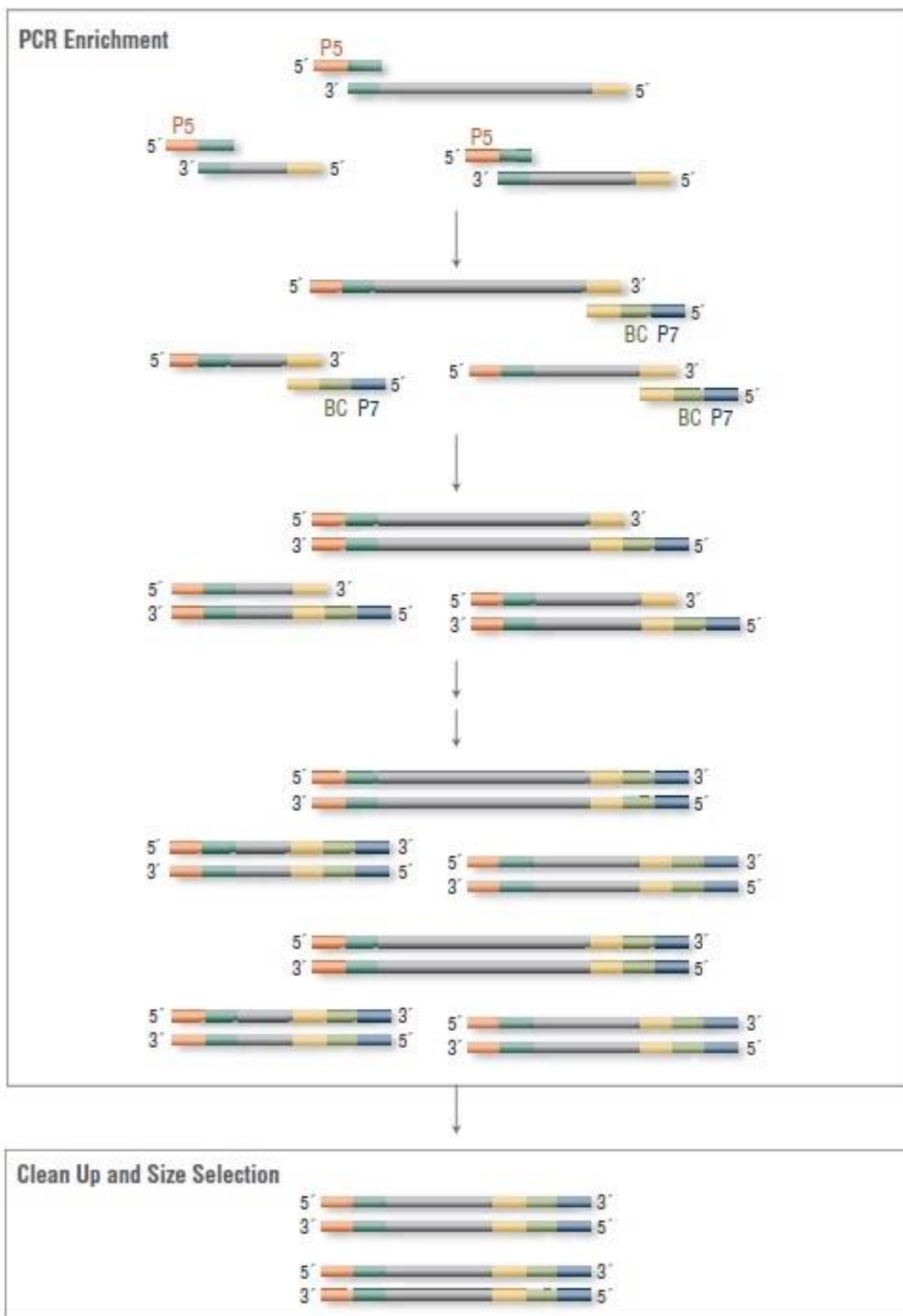


**Figure 2.4: The Multiplex Small RNA Library Prep Workflow for Illumina.** Figure copied with modifications from (NewEngland-Biolabs, 2020).

## **2.16 Poly(A) cDNA synthesis for miRNA quantification**

Using total RNA as the starting material, miRNAs and specific snRNAs and snoRNAs were converted into poly(A) cDNA for miRNA quantification using the miScript II RT Kit (Qiagen, Manchester, UK) (Qiagen, 2011b). SncRNAs lack a poly(A) tail and the miScript system facilitates both the addition of poly(A) tails and reverse transcription into cDNA (**Figure 2.5**). This system uses an oligo-dT primer that binds the poly(A) tail. A universal tag attached to the oligo-dT primer enabled the use of a universal reverse primer for miRNA qualification, irrespective of the miRNA sequence.

Per sample, 200ng of total RNA was converted into poly(A) cDNA. This was mixed with 4 $\mu$ L of 5x miScript HiSpec Buffer, 2 $\mu$ L of 10x Nucleics Mix and 1 $\mu$ L of miScript Reverse Transcriptase Mix. The reaction was brought to a final volume of 20 $\mu$ L with the addition of nuclease-free water. The tube was mixed gently and pulse spun. The mixture was incubated at 37°C for 60min for poly(A) cDNA synthesis and then at 95°C for 5min for reverse transcriptase inactivation. Samples were stored at -20°C.

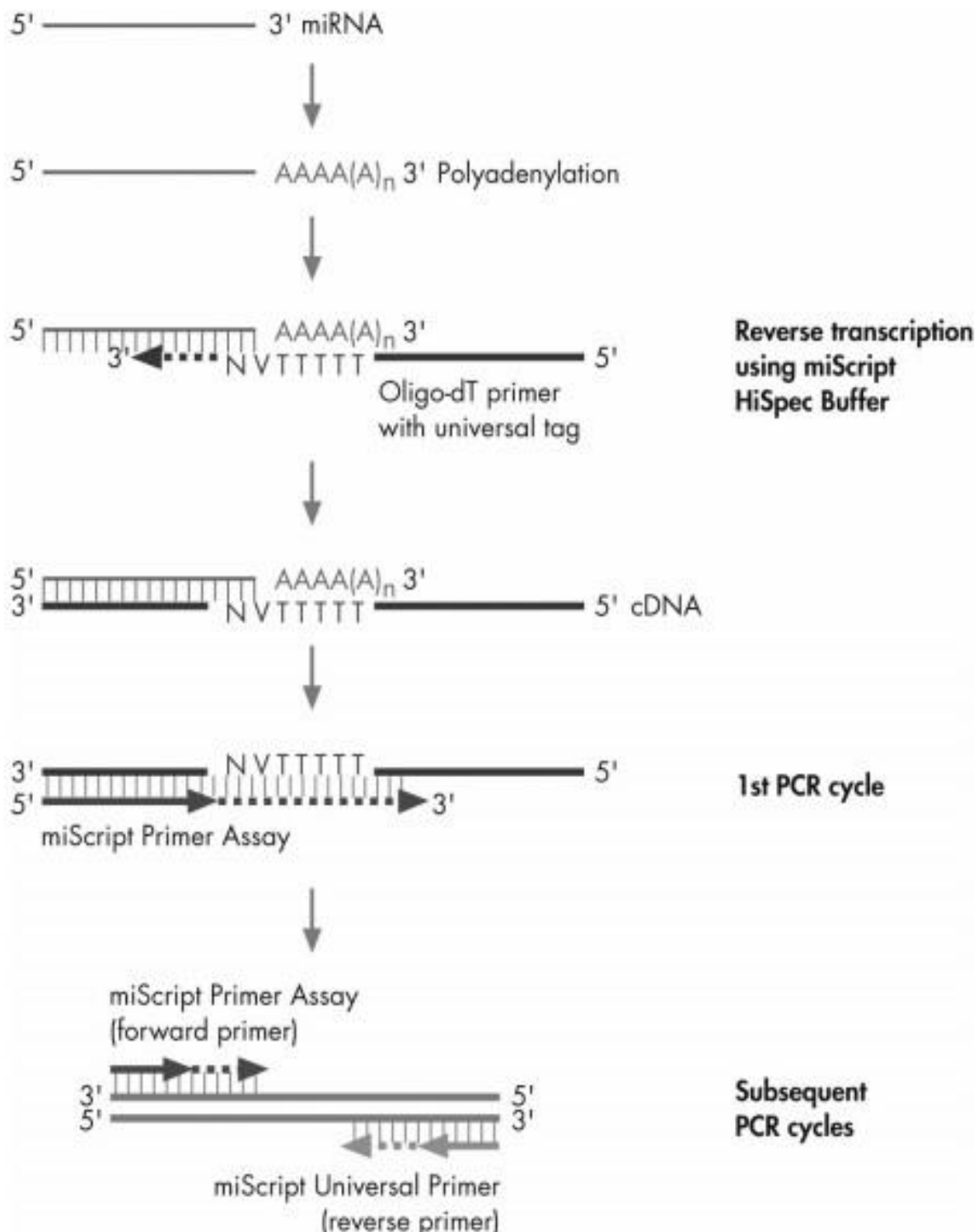


**Figure 2.5: Overview of the miScript system for poly(A) cDNA synthesis and miRNA quantification.** Figure copied from (Qiagen, 2011b).

## **2.17 cDNA synthesis for mRNA quantification**

Total RNA was reverse transcribed into cDNA for mRNA quantification using the M-MLV reverse transcriptase (Promega, Southampton, UK) (Promega, 2016). 500ng of total RNA was converted into cDNA. This was mixed with 0.5µL of random primers (Promega, Southampton, UK) and with nuclease-free water up to final volume of 18.3µL. This was incubated at 70°C for 5min to dissociate secondary RNA structures. Then, the mixture was mixed with 5µL of M-MLV 5X Reaction Buffer (Promega, Southampton, UK), 0.6µL of 25mM PCR Nucleotide Mix (Promega, Southampton, UK), 0.6µL of RNasin(R) Plus RNase Inhibitor (Promega, Southampton, UK) and 0.5µL M-MLV Reverse Transcriptase, up to final volume of 25µL. The final mixture was mixed well and incubated at 37°C for 60min for reverse transcription. Reverse transcriptase was inactivated at 93°C for 5min and cDNA stored at -20°C.

## **2.18 qPCR for miRNA quantification**

miRNA amplification by qPCR was carried out using the miScript SYBR® Green PCR Kit (Qiagen, Manchester, UK) (Qiagen, 2011a). This system offers the use of a miRNA-specific forward primer, whereas the reverse primer is a universal primer that can be used for quantification of any miRNA, using poly(A) cDNA prepared with the miScript II RT Kit as starting material. Poly(A) cDNA was diluted with nuclease-free water to a working concentration of 1ng/µL. Then, in a 96-Well Semi-Skirted PCR Plate (StarLab, Milton Keynes, UK), the following were added per well: 5µL of diluted poly(A) cDNA (5ng per reaction), 7.5µL of QuantiTect SYBR Green PCR Master Mix, 1µL of miRNA-specific forward primer (final concentration in reaction: 330nM), 1µL of miScript Universal Reverse Primer (final concentration in reaction: 330nM) and 0.5µL of nuclease-free water. Final volume was 15µL per reaction. Each reaction was run in duplicate or triplicate. miRNA amplification was undertaken by a LightCycler® 96 Instrument (Roche Life Science, Penzberg, Germany) under the following cycling conditions:

- 1 cycle of: 95°C for 15min, for HotStarTaq DNA Polymerase activation
- 45 cycles of:
  - 94°C for 15sec, for double strand dissociation
  - 55°C for 30sec, for primer annealing
  - 70°C for 30sec, for strand elongation

- Melting curve: 95°C for 10sec  
65°C for 60sec  
97°C for 1sec (acquisition mode: continuous)

miRNA expression was calculated using the  $2^{-\Delta CT}$  method (Livak et al., 2001), relative to appropriate reference genes.

## 2.19 qPCR for mRNA quantification

mRNA amplification by qPCR was carried out using the QuantiTect SYBR Green PCR Master Mix (Qiagen, Manchester, UK). Primers were either designed by the author or OriGene (OriGene, Herford, Germany) and synthesised by Eurogentec (Seraing, Belgium), or designed and synthesised by Primerdesign (Chandler's Ford, UK). When possible, primers were designed to be exon spanning (**Table 2.6**).

cDNA was diluted with nuclease-free water at a working concentration of 2.5ng/ $\mu$ L. Eurogentec forward and reverse primers were mixed and diluted at a working concentration of 20 $\mu$ M per primer. Primerdesign primers were resuspended as a primer mix at a working concentration of 6 $\mu$ M. In a 96-Well Semi-Skirted PCR Plate, the following were added per well: 4 $\mu$ L of diluted cDNA (10ng per reaction), 5 $\mu$ L of QuantiTect SYBR Green PCR Master Mix, 0.2 $\mu$ L of Eurogentec primer mix (final concentration in reaction: 400nM) or 0.67 $\mu$ L of Primerdesign primer mix (final concentration in reaction: 400nM). Nuclease-free water was added up to 10 $\mu$ L final volume per reaction. Each reaction was set up in duplicate or triplicate. mRNA amplification was carried out by a LightCycler® 96 Instrument under the following cycling conditions:

- 1 cycle of: 95°C for 15min, for HotStarTaq DNA Polymerase activation
- 45 cycles of: 94°C for 15sec, for double strand dissociation  
55°C for 30sec, for primer annealing  
70°C for 30sec, for strand elongation
- Melting curve: 95°C for 10sec  
65°C for 60sec  
97°C for 1sec (acquisition mode: continuous)

mRNA expression was calculated using the  $2^{-\Delta CT}$  method (Livak et al., 2001), relative to the appropriate reference genes.

## 2.20 Primer efficiency calculation

Primer efficiency for protein-coding genes was calculated by qPCR by using serial dilutions of cDNA from human primary chondrocytes. The following serial dilutions of template cDNA were used (**Table 2.4**):

**Table 2.4: Serial dilutions of cDNA used for primer efficiency calculation.**

Template cDNA amount (ng)	Dilution to starting cDNA amount	Log10(template cDNA amount)
40	1:1	1.602059991 [ $\log_{10}(40)$ ]
20	1:2	1.301029996 [ $\log_{10}(20)$ ]
10	1:4	1 [ $\log_{10}(10)$ ]
5	1:8	0.698970004 [ $\log_{10}(5)$ ]
2.5	1:16	0.397940009 [ $\log_{10}(2.5)$ ]
1.25	1:32	0.096910013 [ $\log_{10}(1.25)$ ]
0.625	1:64	-0.204119983 [ $\log_{10}(0.625)$ ]
0.3125	1:128	-0.505149978 [ $\log_{10}(0.3125)$ ]

For each primer pair, qPCR reactions were set up in triplicate per dilution and carried out as described in Section 2.19. Primer concentration was kept at 400nM in all dilutions. The average of  $C_T$  values for each dilution was plotted against  $\log_{10}(\text{template cDNA amount})$  in Excel (Microsoft, Reading, UK) and the slope of the graph was calculated. Primer efficiency was calculated using the formula (Ginzinger, 2002):

$$\text{Primer efficiency} = [10^{(-1/\text{Slope})-1}] * 100$$

## 2.21 List of sncRNA and mRNA primers

**Table 2.5: Primers used for sncRNA quantification**

Type	Name	Sequence/Qiagen ID	Species
snoRNA	SNORD68	Proprietary to Qiagen/MS00033712	Human
miRNA	miR-6786-5p	Proprietary to Qiagen/MS00046928	Human
miRNA	miR-107	Proprietary to Qiagen/MS00031255	Human
miRNA	miR-143-3p	Proprietary to Qiagen/MS00003514	Human/Equine
miRNA	miR-379-5p	Proprietary to Qiagen/MS00009653	Human
miRNA	miR-361-5p	Proprietary to Qiagen/MS00004032	Human
miRNA	miR-20a-5p	Proprietary to Qiagen/MS00003199	Human
miRNA	miR-6087	Proprietary to Qiagen/MS00045402	Human
miRNA	miR-1915-3p	Proprietary to Qiagen/MS00044604	Human
miRNA	miR-140-5p	Proprietary to Qiagen/MS00003500	Human
miRNA	miR-155-5p	Proprietary to Qiagen/MS00031486	Human
miRNA	miR-132-3p	Proprietary to Qiagen/MS00003458	Human
miRNA	miR-122	Proprietary to Qiagen/MS00003416	Human/Equine
miRNA	miR-145	Proprietary to Qiagen/MS00003528	Human/Equine
miRNA	miR-148a	Proprietary to Qiagen/MS00003556	Human/Equine
miRNA	miR-181b	Proprietary to Qiagen/MS00006699	Human/Equine
snRNA	U6	Proprietary to Qiagen/MS00033740	Human/Equine
N/A	Universal Reverse primer	Proprietary to Qiagen	N/A

**Table 2.6: Primers used for mRNA quantification.** Abbreviations: Glyceraldehyde-3-phosphate dehydrogenase (*GAPDH*), Ribosomal protein L13a (*RPL13A*), Ribosomal protein lateral stalk subunit P0 (*RPLP0*), Ribosomal protein L3 (*RPL3*), Ribosomal protein L4 (*RPL4*), ATP synthase F1 subunit alpha (*ATP5F1A*), Tyrosine 3-monooxygenase/tryptophan 5-monooxygenase activation protein epsilon (*YWHAE*), Ras homolog family member A (*RHOA*), Transforming growth factor beta receptor (*TGFBR*) 1, Fibroblast growth factor (*FGF*) 2, Interferon regulatory factor (*IRF*) 1, Calmodulin (*CALM*) 3, Small mothers against decapentaplegic (*SMAD*) 9. N/A: primer efficiency not calculated.

Name	Sequence/Qiagen ID	Species	Efficiency	Exon Spanning	Ordered from
<b>GAPDH</b>	F: TCGGAGTCAACGGATTGGT	Human	100%	Yes	Eurogentec
	R: TGAAGGGGTCTTGATGGCA				
<b>COL2A1</b>	F: CCAGATTGAGAGCATCCGC	Human	99%	Yes	Eurogentec
	R: CCAGTAGTCTCCACTCTTCCAC				
<b>ACAN</b>	F: ACCGTCAGATACCCCATTGTG	Human	104%	Yes	Eurogentec
	R: CATCGTAGGTCTCTGTTGATGGG				
<b>MMP13</b>	F: GGAATTAAAGGAGCATGGCGACT	Human	92%	Yes	Eurogentec
	R: TCATCAAAATGGGCATCTCCTCC				
<b>ADAMTS4</b>	F: GGCTATGGCACTGTCTCTTA	Human	99%	Yes	Eurogentec
	R: AGCATCATAGTCCTGCCAGG				
<b>COL10A1</b>	F: CCAGCACGCAGAACATCCATC	Human	100%	Yes	Eurogentec
	R: CCTGTGGGCATTGGTATCG				
<b>SOX9</b>	F: GCTCTGGAGACTTCTGAACGA	Human	95%	Yes	Eurogentec
	R: CCGTTCTCACCGACTTCCT				

RUNX2	F: GAGTGGACGAGGCAGAGATT	Human	N/A	Yes	Eurogentec
	R: GTTCCCGAGGTCCATCTACTG				
WNT4	F: AGGCAAGAACAGAGGGAGATGAG	Human	Proprietary to Primerdesign	No	Primerdesign
	R: TGGGTCTGGGGAGTGGTTA				
IHH	F: GAGAGCCTTCAGGTATCG	Human	Proprietary to Primerdesign	No	Primerdesign
	R: CGTGTGATTGTCAGCCGTAAA				
TGFB1R	F: TGACTGAAGGCTGCTCTGG	Human	Proprietary to Primerdesign	No	Primerdesign
	R: CATCTGCTCAATCTCCAACTTG				
CALM3	F: AACCAAGCCCTGTGATTCCAC	Human	Proprietary to Primerdesign	No	Primerdesign
	R: CAGTCAACGCCACAATTCCCTC				
RPL13A	F: CTCAAGGTGTTGACGGCATC	Human	Previously calculated by Origene	No	Eurogentec
	R: TACTTCCAGCCAACCTCGTG				
RPLPO	F: ATCCAGCAGGTGTTGACCAA	Human	N/A	No	Eurogentec
	R: AGGAAGCGAGAATGCAGAGT				
RPL3	F: TGCTCGTAGCCTCTCTGTG	Human	Previously calculated by Origene	No	Eurogentec
	R: GGTCAAGTCAGTGGAGGCATTG				
RPL4	F: CCGTTGGCATCGTAGAGTGA	Human	N/A	No	Eurogentec
	R: CTTTGCCAGCTCTCATTCGC				
ATP5F1A	F: GCTCCTTACTCTGGCTGTTCCA	Human	Previously calculated by Origene	No	Eurogentec
	R: GCGGAGCAACAGAGACATCTGA				
YWHAE	F: GACAGAACTTCCACCAACGCATC	Human		No	Eurogentec

	R: CACTCAGCGTATCCAGTTCTGC		Previously calculated by Origene		
RHOA	F: GGAAAGACATGCTTGCTCATAGTC	Human	N/A	Yes	Eurogentec
	R: CCAACTCTACCTGCTTCCATC				
HDAC2	F: CATGGCGTACAGTCAAGGAG	Human	N/A	Yes	Eurogentec
	R: CCAATATCACCGTCGTAGTAGTC				
SMAD9	F: CACTCAGTTGACACACCACC	Human	N/A	Yes	Eurogentec
	R: GCACTACATGTCTATCAGCTGTGG				
TNF	F: TGTGTAGCAAACCCCTCAAGCT	Human	N/A	Yes	Eurogentec
	R: GAGGTACAGGCCCTCTGAT				
IRF1	F: GAGGAGGTGAAAGACCAGAGCA	Human	N/A	No	Eurogentec
	R: TAGCATCTCGGCTGGACTTCGA				

## 2.22 Treatment of human primary chondrocytes with IL-1 $\beta$

Lyophilised recombinant human IL-1 $\beta$  (R&D Systems, Abingdon, UK) was reconstituted in sterile PBS containing 0.1% (w/v) Bovine Serum Albumin (BSA) (R&D Systems, Abingdon, UK) according to manufacturer's recommendations. Human primary OA chondrocytes were extracted from knee femoral cartilage and cultured in T75 flasks as described in Section 2.9. Cells were trypsinised as described in Section 2.11 and seeded in 12-well plates at a seeding density of 30,000cell/cm<sup>2</sup>. Cells were seeded in complete media and left to attach and proliferate in a tissue culture incubator at 37°C, supplied with 20% (v/v) O<sub>2</sub> and 5% (v/v) CO<sub>2</sub> overnight. Next day, complete media was removed and replaced with DMEM supplemented with 1% (v/v) P/S and 0.2% (v/v) F/Z. No FBS was added to the culture media. Chondrocytes were serum-starved overnight and the next day cells were treated with FBS-free DMEM

supplemented with 10ng/mL IL-1 $\beta$  (R&D Systems, Abingdon, UK) or PBS/BSA as control. Treated cells and control were then lysed in TRIzol.

IL-1 $\beta$  treatment of human primary chondrocytes from non-OA donors undergoing autologous cartilage transplantation after trauma/sport injury, was undertaken by Dr Caron Marjolein, Assistant Professor, Maastricht UMC+, Netherlands, following ethical approval (ID MEC 08-4-028). The same process was followed. cDNA from these cells was shipped to the Institute of Life Course and Medical Sciences, University of Liverpool, UK and further processed by the author.

## 2.23 Overexpression and knockdown of miRNAs in IL-1 $\beta$ induced human primary chondrocytes

miRNA mimics and inhibitors (Qiagen, Manchester, UK) were used to overexpress and knockdown the expression of four miRNAs in IL-1 $\beta$  induced human primary chondrocytes: hsa-miR-107, hsa-miR-379-5p, hsa-miR-361-5p and hsa-miR-143-3p. Two commercially available systems by Qiagen were used to undertake these experiments. For hsa-miR-107, -379-5p, -361-5p the miScript mimics, inhibitors and controls were used. For hsa-miR-143-3p, the miRCURY LNA mimic, inhibitor and controls were used. These are summarised in **Table 2.7** below.

**Table 2.7: List of miRNA mimics, inhibitors and controls used in this thesis.**

miRNA	Product name	Type	Final concentration	System
hsa-miR-107	Syn-hsa-miR-107 miScript miRNA Mimic	Mimic	5nM	miScript
	Anti-hsa-miR-107 miScript miRNA Inhibitor	Inhibitor	200nM	
hsa-miR-379-5p	Syn-hsa-miR-379-5p miScript miRNA Mimic	Mimic	5nM	

	Anti-hsa-miR-379-5p miScript miRNA Inhibitor	Inhibitor	200nM	
hsa-miR-361-5p	Syn-hsa-miR-361-5p miScript miRNA Mimic	Mimic	5nM	
	Anti-hsa-miR-361-5p miScript miRNA Inhibitor	Inhibitor	200nM	
Control	AllStars Negative Control siRNA	Mimic Negative Control	5nM	miRCURY LNA
	miScript Inhibitor Negative Control	Inhibitor Negative Control	200nM	
hsa-miR-143-3p	hsa-miR-143-3p miRCURY LNA miRNA Mimic	Mimic	0.5nM	
	hsa-miR-143-3p miRCURY LNA miRNA Inhibitor	Inhibitor	50nM	
Control	Negative Control miRCURY LNA miRNA Mimic	Mimic Negative Control	0.5nM	
	miRCURY LNA miRNA Inhibitor Negative Control A	Inhibitor Negative Control	50nM	

Chondrocytes were extracted from the femoral condyles of OA patients undergoing TKA according to Section 2.9 and cultured as described in Section 2.11. Cells were seeded in well-plates in complete media at a density of 25,000-30,000 cells/cm<sup>2</sup>. For experiments concerning

hsa-miR-107, -379-5p, -361-5p, chondrocytes were seeded in 24-well plates for qPCR analysis. For experiments concerning hsa-miR-143-3p, chondrocytes were seeded in 6-well plates for LC-MS/MS. Cells were left to attach and proliferate overnight. Next day, chondrocytes were treated with the respective mimic, inhibitor or control. The HiPerFect Transfection Reagent (Qiagen, Manchester, UK) was used for delivery into the cell. Specifically, working under sterile conditions, the appropriate volume of mimic, mimic negative control, inhibitor and inhibitor negative control was added in sterile 1.5mL tubes, one tube per condition per miRNA. The appropriate volume of HiPerFect Transfection Reagent was added to each tube. The volume of the transfection reagent was dependent on the size of the well. For 24-well plates, 3 $\mu$ L were added per tube, whereas for a 6-well plate, 12 $\mu$ L were added per tube. The volume was brought to a final volume of 100 $\mu$ L by adding DMEM media without FBS, P/S, F/Z and phenol red, but supplemented with 1% (v/v) L-glutamine (Gibco/ThermoFisher Scientific, Paisley, UK). Tubes were vortexed, spun down briefly and left at room temperature for 20min for constructs to form.

In the meantime, complete media was removed from chondrocytes in well plates and cells were washed twice with DMEM supplemented only with 1% (v/v) L-glutamine. For 24-well plates, 300 $\mu$ L of DMEM, supplemented with 1% (v/v) L-glutamine and 10ng/mL IL-1 $\beta$ , was added to each treatment well, whereas for 6-well plates, 900 $\mu$ L of the same media was added. After 20min, 100 $\mu$ L of each construct/treatment was added drop-wise to the respective well. For a 24-well plate, final volume was 400 $\mu$ L, whereas for a 6-well plate, final volume was 1mL. Chondrocytes were treated for 48h and then lysed either in TRIzol for qPCR analysis or as described in Section 2.24 for LC-MS/MS analysis.

## **2.24 Collection and lysis of human primary chondrocytes for LC-MS/MS analysis**

Prior to chondrocyte collection, a fresh 2x protease inhibitor cocktail solution and a fresh 50mM Ammonium Bicarbonate (AmBic) (Sigma-Aldrich, Dorset, UK) solution were prepared. For the 2x protease inhibitor cocktail, one cComplete™ ULTRA, EDTA-free, tablet of protease inhibitor cocktail (Roche Life Science, Penzberg, Germany) was dissolved in 5mL of Pierce™ Water, LC-MS Grade (ThermoFisher Scientific, Paisley, UK). For the 50mM AmBic, 0.04g of

AmBic was dissolved in 10mL of Pierce™ Water, LC-MS Grade. Equal volume of each solution was mixed to prepare a 25mM AmBic solution supplemented with 1x protease inhibitor cocktail and stored on ice.

For chondrocyte collection, media was removed and cells were washed with 1xDPBS. DPBS was removed and 200µL of 25mM AmBic supplemented with 1x protease inhibitor cocktail was added per well. Cells were scrapped off the well surface using a cell scrapper and collected in tubes. 7.5units of benzonase nuclease (Biocompare, San Francisco, USA) was added per sample and mixed slightly to release histones from DNA. Cells were lysed by sonication with a Soniprep 150 ultrasonic disintegrator (MSE, East Sussex, UK). Cells were sonicated on ice, in three rounds of 30sec each, with 1min and 15sec rest between each round. Volume was adjusted to 200µL by adding 25mM AmBic supplemented with 1x protease inhibitor cocktail. 20µL per sample was taken for protein quantification and 10µL was taken for protein quality analysis. The remaining lysate was stored at -80°C for LC-MS/MS analysis.

## **2.25 Pierce™ 660nm Protein Assay for protein quantification**

Prior to LC-MS/MS, protein amount in each sample was quantified using the Pierce™ 660nm Protein Assay (ThermoFisher Scientific, Paisley, UK). For protein standard preparation, two pre-diluted BSA protein assay standards (ThermoFisher Scientific, Paisley, UK) of known concentration, 2000µg/mL and 1000µg/mL, were serially diluted in 25mM AmBic supplemented with 1x protease inhibitor cocktail, according to **Table 2.8**.

**Table 2.8: Protein standard preparation for Pierce™ 660nm Protein Assay.**

<b>Known concentration of pre-made standard (µg/mL)</b>	<b>Volume of pre-diluted BSA protein assay standard (µL)</b>	<b>Volume of 25mM AmBic/1x protein inhibitor cocktail (µL)</b>	<b>Standard - final concentration (µg/mL)</b>
2000	37.5	12.5	<b>1500</b>

2000	25	25	<b>1000</b>
1000	37.5	12.5	<b>750</b>
1000	25	25	<b>500</b>
1000	12.5	37.5	<b>250</b>
1000	5	35	<b>125</b>
1000	2.5	47.5	<b>50</b>
-	-	50	<b>0 (Blank)</b>

10µL of standards, blank and unknown samples was loaded in duplicate onto a Costar® 96-well plate (Corning, Flintshire, UK). 150µL of the Protein Assay Reagent was added to each well. The plate was covered and mixed on a plate shaker at medium speed for 1min, incubated at room temperature for 5min and then absorbance was measured at 600nm using a FLUOstar Omega Microplate Reader (BMG LABTECH, Aylesbury, UK).

For protein quantification, absorbance of the blank was deducted from standards and unknown samples and a standard curve was designed in Excel by plotting the corrected absorbance of the standards against their concentration. Using the standard curve, the protein concentration and total protein amount were calculated for the unknown samples.

## 2.26 SDS-PAGE for protein quality assessment

Sodium dodecyl sulphate–polyacrylamide gel electrophoresis (SDS-PAGE) was used to separate proteins derived from chondrocyte lysates and prepare gel for silver staining or Coomassie Brilliant Blue staining. 7.5µL of 2x Novex™ Tris-Glycine SDS Sample Buffer (ThermoFisher Scientific, Paisley, UK), supplemented with 8% (v/v) of 2-Mercaptoethanol (Sigma-Aldrich, Dorset, UK), was added to 7.5µL of sample (2µg of protein). Samples were mixed and heated at 100°C for 10min to denature proteins. Samples were placed immediately on ice. A NuPAGE™ 4% to 12% (w/v), Bis-Tris gel (ThermoFisher Scientific, Paisley, UK) was placed in the electrophoretic tank and the tank was filled with 1x NuPAGE® MES Running

Buffer (ThermoFisher Scientific, Paisley, UK) (diluted from the 20x stock in ultrapure water). Samples were loaded onto the gel alongside 6 $\mu$ L of the Novex™ Sharp Pre-stained Protein Standard ladder (ThermoFisher Scientific, Paisley, UK). The gel was run at 80V for 10min and then 100V for the remaining time of electrophoresis.

## 2.27 Silver staining of polyacrylamide gels

Silver staining is a sensitive method which allows visualisation of protein bands on a polyacrylamide gel. The Pierce Silver Stain Kit (ThermoFisher Scientific, Paisley, UK) was used to assess quality and molecular weight distribution of proteins run on polyacrylamide gels according to manufacturer's instructions (ThermoFisherScientific, 2016). Prior to staining, the following solutions were prepared in advance:

- Fixing solution [60% (v/v) water:30% (v/v) ethanol:10% (v/v) acetic acid]
- 10% (v/v) ethanol
- Stop solution (5% (v/v) acetic acid)

Then gel was stained as follows:

- The gel was washed twice in ultrapure water for 5min each.
- Then, the gel was fixed in fixing solution in two consecutive rounds, for 15min each.
- After fixing, the gel was washed twice in 10% (v/v) ethanol for 5min each and washed twice in ultrapure water for 5min each.
- Sensitiser working solution was prepared by mixing 1 part of Silver Stain Sensitizer with 500 parts ultrapure water. The gel was incubated in the sensitiser working solution for exactly 1min and then washed twice in ultrapure water for 1min each.
- Stain Working Solution was prepared by mixing 1 part of Silver Stain Enhancer with 50 parts Silver Stain. The gel was incubated in Stain Working Solution for 30min.
- Developer working solution was prepared by mixing 1 part of Silver Stain Enhancer with 50 parts Silver Stain Developer.
- After incubating the gel in Stain Working Solution, the gel was washed twice in ultrapure water for 20sec each.

- Then, Developer Working Solution was added onto the gel and incubated for approximately 2min until protein bands appeared.
- Immediately after 2min, Developer Working Solution was removed and the gel was washed in stop solution for 20sec. The first round of stop solution was replaced by an extra round of stop solution and the gel was incubated in that for 10min.

The gel was visualised using the ChemiDoc XRS+ Gel Imaging System (Bio-Rad, Watford, UK).

## **2.28 Protein sample preparation for LC-MS/MS**

Prior to LC-MS/MS, fresh 25mM and 50mM AmBic solutions were prepared and the total protein amount in each sample was measured as described in Section 2.25. For normalisation purposes, the same amount of protein in the same starting volume was used for all samples. In this protocol, 160µL was used as the starting volume for all samples. The sample with the lowest total protein amount, based on the Pierce™ 660nm protein assay, was the reference sample. The amount of protein contained in 160µL of the reference sample was selected as the amount of protein that would be used for LC-MS/MS for every sample. Thus, per sample, this amount of protein was transferred in protein LoBind tubes (Eppendorf, Stevenage, UK) and volume was brought to 160µL by adding 25mM AmBic. Samples were randomised for processing. Then:

- 10µL of 1% (w/v) RapiGest SF Surfactant (Waters, Herts, UK) (freshly prepared in 25mM AmBic) was added to each sample. The samples were vortexed briefly and incubated at 80°C for 10min, with a quick vortex at the 5min timepoint. The samples were then pulse spun to collect all liquid at the bottom of the tube.
- 11.1mg of Dithiothreitol (DTT) (Sigma-Aldrich, Dorset, UK) was dissolved in 1mL of 25mM AmBic to prepare a 11.1mg/mL solution. 10µL of this solution was added to each sample (final DTT concentration 4mM) and the samples were vortexed briefly. Then, the samples were incubated at 60°C for 10min, with a quick vortex at the 5min time point. The samples were pulse spun briefly and left to cool down at room temperature.

- After cooling down, 46mg of iodoacetamide (IAA) (Sigma-Aldrich, Dorset, UK) was dissolved in 1mL of 25mM AmBic and solution was kept in the dark. 10µL of IAA was added in all samples and the samples were incubated in the dark, at room temperature for 30min.
- To prevent overalkylation, 9.4µL of the 11.1mg/mL DTT solution was added in each sample (final DTT concentration 7mM). Samples were vortexed briefly.
- For protein digestion, Trypsin/Lys-C Mix, Mass Spec Grade (Promega, Southampton, UK), provided as powder, was reconstituted in 50µL of resuspension buffer (provided in the pack) and 50µL of 50mM AmBic. 10µL of Trypsin/Lys-C Mix was added to every sample and then samples were placed in a rotating incubator at 37°C for 2h, at medium speed. After 2h, samples were pulse spun to collect all liquid and an extra 10µL of Trypsin/Lys-C Mix was added to each sample. The samples were placed in a rotating incubator at 37°C, overnight, to achieve complete protein digestion.
- Next day, the samples were pulse spun to collect digest at the bottom of the tube. 1µL of Trifluoroacetic acid (TFA) (Sigma-Aldrich, Dorset, UK) was added per sample and then samples were vortexed briefly and pulse spun. Acidity of the samples was confirmed with pH paper (Camlab, Cambridge, UK) and then the samples were incubated at 37°C for 45 min.
- After incubation, samples were centrifuged at 13,000g at 4°C for 15min to remove all insolubles. Supernatant was transferred to new tubes and the samples were spun again at 13,000g at 4°C for 15min. Supernatant was transferred in new tubes and checked that no precipitate was present in any of the samples. Aliquots containing 1µg of digested protein were taken to confirm digestion on an SDS-PAGE gel with Coomassie Brilliant Blue staining.

## **2.29 Coomassie Brilliant Blue staining of polyacrylamide gels**

To confirm full digestion of proteins, 1µg of digested protein samples was run on an SDS-polyacrylamide gel as described in Section 2.26. After electrophoresis, gel was washed 3x times with ultrapure water for 5min each. The gel was stained with Coomassie Brilliant Blue R-250 Staining Solution (Bio-Rad, Watford, UK) for 2h with gentle agitation. The gel was

destained in Coomassie Brilliant Blue R-250 Destaining Solution (Bio-Rad, Watford, UK) in 4x washes for 30min each with gentle agitation. The gel was visualised using the ChemiDoc XRS+ Gel Imaging System.

## 2.30 LC-MS/MS workflow

Digested proteins, extracted from human primary chondrocytes treated with miRNA mimic, inhibitor, or control, were subjected to LC-MS/MS and run on a 90min gradient with a 30min run of blanks between samples. The procedure was carried out by appropriate personnel at the Centre for Proteome Research (CPR) at the University of Liverpool, as described in (Timur et al., 2020). 500ng of digest per sample was used for LC-MS/MS. Analysis was undertaken using a QExactive HF quadrupole-Orbitrap mass spectrometer (ThermoFisher Scientific, Paisley, UK) coupled to an UltiMate™ 3000 RSLCnano liquid chromatographer (ThermoFisher Scientific, Paisley, UK). The samples were loaded onto a trap column (Acclaim PepMap 100 C18, 75 $\mu$ m  $\times$  2cm, 3 $\mu$ m packing material, 100 $\text{\AA}$ ) for 7 min at a flow rate of 12  $\mu$ L/min, using 0.1% (v/v) TFA in acetonitrile/water [2/98 (v/v)] as the loading buffer. The trap column was set in-line with an analytical column (EASY-Spray PepMap RSLC C18, 75 $\mu$ m  $\times$  50cm, 2 $\mu$ m packing material, 100 $\text{\AA}$ ). The peptides were eluted using a linear gradient of 96.2% A:3.8% B to 50% A:50% B over 90min at a flow rate of 300 nL/min, where A is 0.1% (v/v) formic acid and B is 0.1% (v/v) formic acid in water/acetonitrile [80/20 (v/v)]. This was followed by a washing step at 1% A:99% B for 5min. Then column was re-equilibrated to starting conditions. The column was kept at 40°C and the effluent was introduced into the nano-electrospray ionisation source set in positive ion mode. The mass spectrometer was set to data-dependent acquisition mode with survey scans between mass-to-charge ratio (m/z) 350–2000, acquired at a mass resolution of 60,000 (full width at half maximum) at m/z 200. The maximum injection time was 100msec, and the automatic gain control was set to 3e<sup>6</sup>. The 12 most intense precursor ions with charges states of between 2+ and 5+ were selected for MS/MS with an isolation window of 2 m/z units. The maximum injection time was 100ms, and the automatic gain control was set to 1e<sup>5</sup>. Fragmentation of the peptides was by higher-energy collisional dissociation using normalized collision energy of 30%. Dynamic exclusion of

mass/charge values to prevent repeated fragmentation of the same peptide was used with an exclusion time of 20sec.

## **2.31 Bioinformatic analysis of microarray experiment**

Microarray analysis was performed as described in Section 2.14. Bioinformatic analysis was performed by appropriate personnel at CGR who produced the following report: After scanning the arrays, Affymetrix array .CEL files were generated using the Affymetrix GeneChip Command Console Software. Data was pre-processed using Robust Microarray data Analysis (RMA) to obtain normalised small RNA expression data. Model-based analysis of small RNA expression was applied to data pre-processed with RMA which generated normalised expression values presented on a  $\log_2$  scale. Data quality was assessed by measuring small RNA expression distribution. Two statistical tools were used for data variation assessment. The first was a heatmap of correlation coefficients among arrays and the second was the Principal Component Analysis (PCA) (Abdi et al., 2010). The random variation of the data was formulated following a normal distribution, and the model was linear, taking the mean of each group as a model parameter. Therefore, the number of parameters was equal to the number of sample groups.

The  $\log_2$  Fold Change (logFC) was computed from model fitting results and tested using t-tests to get associated p-values. P-values were adjusted for multiple testing using the False Discovery Rate (FDR) approach (Benjamini et al., 1995). Significantly differentially expressed miRNAs were defined as those with FDR-adjusted p-value < 5%. All the processes were performed in R environment using limma package (Smyth, 2005).

## **2.32 Bioinformatic analysis of small RNA-Seq experiment**

Small RNA-Seq analysis was performed as described in Section 2.15. Bioinformatic analysis was performed by appropriate personnel at CGR who produced the following report: Initial processing and quality assessment of the sequence data was performed using an in-house pipeline (developed by Dr Richard Gregory). Briefly, base-calling and de-multiplexing of

indexed reads were performed by CASAVA version 1.8.2 (Illumina, Cambridge, UK) to produce the sequence data for the samples, in fastq format. The raw fastq files were trimmed to remove Illumina adapter sequences using Cutadapt version 1.2.1 (Martin, 2011). The option “-O 3” was set so that the 3' end of any reads which matched the adapter sequence over at least 3bp could be trimmed off. The reads were further trimmed to remove low quality bases, using Sickle version 1.200 with a minimum window quality score of 20. After trimming, reads shorter than 20bp were removed. If both reads from a pair passed this filter, each was included in the R1 (forward reads) or R2 (reverse reads) file. If only one of a read pair passed this filter, it was included in the R0 (unpaired reads) file.

The genome reference sequence and annotations used for alignment were downloaded from NCBI. The link for the DNA reference sequence is:

[ftp://ftp.ncbi.nlm.nih.gov/genomes/all/GCF/002/863/925/GCF\\_002863925.1\\_EquCab3.0/GCF\\_002863925.1\\_EquCab3.0\\_genomic.fna.gz](ftp://ftp.ncbi.nlm.nih.gov/genomes/all/GCF/002/863/925/GCF_002863925.1_EquCab3.0/GCF_002863925.1_EquCab3.0_genomic.fna.gz)

The link of the annotation GFF is:

[ftp://ftp.ncbi.nlm.nih.gov/genomes/all/GCF/002/863/925/GCF\\_002863925.1\\_EquCab3.0/GCF\\_002863925.1\\_EquCab3.0\\_genomic.gff.gz](ftp://ftp.ncbi.nlm.nih.gov/genomes/all/GCF/002/863/925/GCF_002863925.1_EquCab3.0/GCF_002863925.1_EquCab3.0_genomic.gff.gz)

Annotation information of gene features are also linked to other databases:

<ftp://ftp.ebi.ac.uk/pub/databases/Rfam/14.0/>

<ftp://mirbase.org/pub/mirbase/CURRENT/genomes/eca.gff3>

Alignment of reads was carried out using the above genome references. TopHat version 2.1.0 (Kim et al., 2013) was used as the alignment tool with the option “-g 1”, which instructs the software to report the best hits, or randomly select one if there are more than 1 hits that are equally best. Reads aligning to the reference genome sequences were counted according to the gene features that they mapped to, as defined in the GFF files, using HTSeq-count version 0.6.1p1 (Anders et al., 2010). The features whose biotype belonged to the gene categories, such as miRNA, were extracted to generate a categorised gene reads-count table. Differential gene expression analysis for the genes was applied to the read count data and conducted in R environment, using the EdgeR package (Robinson et al., 2010). Assessment of variation in the count data was visualised using pairwise scatter plots of read counts ( $\log_{10}$  scale),

correlation heatmaps and PCA plots of the 1<sup>st</sup> and 2nd components using the log<sub>10</sub> count data from all libraries.

For differential expression analysis, the random variations in the data were formulated following negative binomial distributions. The data model is a Generalised Linear Model with as many parameters, as the number of the groups compared. Normalisation factors were calculated to correct for differences in library size among samples, which could otherwise cause bias in differential expression analysis. The default method “TMM” in EdgeR was applied, with default parameters. The common, trended (dispersion-mean relationship) and gene-wise dispersion parameters were estimated. Gene-wise dispersion was used for significance testing. The Generalised Linear Model was parametrized using the count data and then used to obtain the logFC values for each required comparison. The estimated logFC were tested in EdgeR using a likelihood ratio test. P-values associated with logFC were adjusted for multiple testing using the FDR approach (Benjamini et al., 1995). Significantly DE miRNAs were defined as those with FDR-adjusted p-value < 5%.

### **2.33 Bioinformatic analysis of LC-MS/MS experiment**

Bioinformatic analysis of LC-MS/MS data was performed by appropriate personnel at CPR, as described in (Timur et al., 2020). For label-free quantification, the raw files of the acquired spectra were aligned by the Progenesis QI for proteomics software (Waters, Manchester, UK), which peak picks for quantification by peptide ion abundance. One reference sample was selected and the retention times of the other samples were aligned. The top five spectra for each feature were exported from Progenesis QI and used for peptide identification with our local Mascot server (Version 2.6.2) searching against the Unihuman Reviewed database, containing 22,640 protein sequences. Search parameters were adjusted to mass tolerance of 10ppm, fragment mass tolerance of 0.01Da, one missed cleavage allowed, with carbamidomethyl cysteine as a fixed modification and methionine, proline, lysine oxidation as variable modifications. For statistical analysis, proteins that had at least two unique peptides were selected. To assessed differences between mimic and control mimic, and inhibitor and control-inhibitor groups, two-tailed paired t-tests were undertaken using the

Stats R package (Version 4.0.2). P values were adjusted for multiple testing. Differences at FDR-adjusted p<0.05 were considered significant.

## **2.34 Primer design**

For primer design, the Primer-Blast tool was used (Ye et al., 2012). The accession number or FASTA sequence of the gene of interest was pulled from NCBI Gene (2004) and inserted into the ‘PCR template’ field of Primer-Blast. Product size was adjusted between 70bp and 200bp and, when possible, the option for the primers to span an exon-exon junction was selected. From the primer pairs proposed by Primer-Blast, the pairs that did not have unintended targets were selected for further assessment. In some cases, proposed primer pairs were edited slightly with the addition or removal of flanking nucleotides from the sequence retrieved from NCBI Gene to create more suitable pairs. The selected primer pair was subjected to further quality control which included the use of the New England Biolabs ‘T<sub>m</sub> Calculator’ tool (2020b), adjusted for Hot Start Taq and Hot Start Taq DNA Polymerase 2X Master Mix, to calculate primer T<sub>m</sub>. In general, most primers were designed approximately at a similar T<sub>m</sub>, between 58°C -60°C, which allowed the use of multiple primer pairs during qPCR amplification. Furthermore, the potential generation of primer dimers or self-dimers was assessed with the ThermoFisher Scientific ‘Multiple Primer Analyzer’ tool (2020a), with primer concentration adjusted at 400nM. Primer pairs that were not predicted to generate primer dimers or self-dimers were selected.

## **2.35 miRNA target prediction tools**

For prediction of miRNA targets, four online prediction tools were used: TargetScan (Agarwal et al., 2015), miRmap (Vejnar et al., 2012), miRTar (Hsu et al., 2011) and miRWalk (Dweep et al., 2015). In TargetScan, the name of the miRNA of interest was inserted in the appropriate field, setting ‘human’ as species. The results tab provided a list of all predicted target genes along with a total score starting from the most probable interaction. In miRmap, human was selected as species, and the miRNA of interested was inserted in the ‘miRNA’ field. In case of an already selected gene candidate, the name of the gene was inserted in the ‘Gene’ field and

the relationship between the miRNA and the gene of interest was assessed and reported through a scoring system. In miRTar, in the ‘Prediction’ tab, either the ‘Single miRNA to single gene’ mode or the ‘Single miRNA to multiple genes’ mode was selected. The mature miRNA sequence in FASTA format and the gene symbol(s) were inserted in the appropriate fields. The ‘miRNA Target Regions’ option was set on ‘3’ UTR’. This tool provided results on an ‘interaction-no interaction’ basis without providing a probability score. Finally, in miRwalk, the ‘predicted target module’ was selected and from the dropdown menu, the ‘MicroRNA-gene Targets’ option was selected. In step 1, human was selected as species, ‘miRBase’ was the chosen database and the identifier was set to MIMATid. The name of the mature miRNA was written in the provided space. In step 2, the following default options were selected: ‘miRNA’, ‘similar seeds’, ‘miR family’, ‘alignment’, ‘Host gene’ and ‘family alignment’. In step 3, ‘3’ UTR’ and ‘minimum seed length=7’ were selected. miRWalk users have the option of viewing miRNA-gene interactions as predicted by miRWalk alone, or interactions predicted by miRwalk in combination with other online tools. For the second option the following tools were selected: ‘miRWalk’ and ‘RNA22’ and ‘miRanda’ and TargetScan. With this option, only the miRNA-gene interactions which were common among the selected tool were displayed.

Genes predicted as miRNAs targets from at least two of the above four online tools were selected for further experimental validation.

## **2.36 Ingenuity Pathway Analysis of miRNA-gene interactions**

Ingenuity Pathway Analysis (IPA) (Qiagen, Manchester, UK) was used for miRNA target prediction and pathway analysis and interaction. IPA was utilised for the three main experiments in this thesis: A) microarray analysis in Chapter 3, B) proteomic analysis in Chapter 5 and C) small RNA-Seq analysis in Chapter 6.

A) Experimentally obtained DE miRNAs and their calculated logFC were inserted in an Excel spreadsheet and uploaded into IPA. For prediction of target genes, the ‘analyze/filter dataset’ option was selected, followed by the ‘microRNA target filter’ option. IPA generated a list of target genes for each miRNA uploaded. To redefine the number of predicted mRNAs, in

addition to the default columns, the following columns were added in order to filter the results:

- Tissue/cells: 'Cartilage' and 'Chondrocytes'
- Disease: 'Connective Tissue Disorders' and 'Skeletal and Muscular Disorders'
- Species: 'Human'

Confidence was set to 'High (predicted)'. Results with predicted mRNAs were saved and downloaded onto an Excel file. Then, predicted mRNAs were re-uploaded into IPA as new dataset and a Core Analysis was run to identify pathways, diseases, functions and upstream regulators specific to the predicted target genes. Filters in Core Analysis were set to default.

B) For proteomic analysis, the list of identified proteins with their p values and expression ratio from each comparison; mimic vs control mimic and inhibitor vs control inhibitor, was uploaded in IPA. Filters were set to default and p value cut-off was set to 0.05. Core analysis was run for each list of proteins.

C) For the small RNA-Seq experiment, the list of DE miRNAs in equine chondrocytes was paired to a list of experimentally obtained DE mRNAs in equine cartilage, generated in a previous project by our group (Peffers et al., 2013). To achieve this, the list of DE miRNAs and their logFC values were uploaded on IPA as described previously. The 'analyze/filter dataset' and 'microRNA target filter' options were selected. In the table generated, the 'Add/Replace mRNA dataset' was selected and a list with DE mRNAs from our previous project, along with their logFC values, was uploaded. The 'Expression Pairing' option was selected so that DE miRNAs were paired to DE mRNA targets, but only if the direction of expression was opposite (upregulation of miRNA-downregulation of mRNA and *vice versa*). mRNAs that passed this filter were re-uploaded on IPA and a 'Core Analysis' was carried out for disease, pathway and network analysis.

## **2.37 Enrichr analysis of predicted target genes**

To confirm results generated by IPA, lists of all highly predicted mRNA targets from IPA were input in Enrichr online tool (Chen et al., 2013, Kuleshov et al., 2016) for gene enrichment

analysis and further pathway identification. Results were listed based on ‘Pathway’, ‘Ontologies’ and ‘Disease/Drugs’ information.

## **2.38 ToppGene Suite, REVIGO and Cytoscape analysis for gene network generation and visualisation**

To generate and visualise gene networks, datasets of predicted mRNAs were uploaded on ToppGene Suite (Chen et al., 2009). This generated a list of gene ontology (GO) terms for biological processes, and each GO term was assigned an FDR value. Go terms with FDR were uploaded onto REVIGO (Supek et al., 2011) and interactive graphs and tree maps were generated. To better visualise the gene networks generated by REVIGO, these were downloaded and then uploaded on Cytoscape (Shannon et al., 2003). Within cytoscape, networks were filtered by ‘value’ and gene interactions were visualised.

## **2.39 STRING analysis for identification of protein-protein interactions**

To identify protein-protein interactions, STRING analysis was undertaken (Szklarczyk et al., 2019). The ‘Multiple proteins’ option was selected and protein lists were uploaded on STRING. Organism was set to ‘*Homo sapiens*’. Network type was set to ‘full STRING network’ and meaning of network edges was set to ‘evidence’. Minimum required interaction score was set to ‘highest confidence (0.900)’.

## **2.40 Selection of reference genes for qPCR data normalisation**

RefFinder (Xie et al., 2012) is a free online tool used to select the best reference genes for qPCR data normalisation between different sample groups. It integrates four different programs: geNorm (Vandesompele et al., 2002), Normfinder (Andersen et al., 2004), BestKeeper (Pfaffl et al., 2004), and the comparative Delta- $C_T$  method (Silver et al., 2006), to rank the best reference genes for the samples of interest.  $C_T$  values of the candidate genes were obtained after qPCR analysis in the sample groups of interest. These  $C_T$  values were input in the field provided on the online tool and analysed. RefFinder suggested the best

reference gene based on each of the four programmes used, but also a comprehensive ranking that takes into account all four programmes together.

## **2.41. Principal Component Analysis using MetaboAnalyst**

For LC-MS/MS and small RNA-Seq experiments, data variation was assessed by PCA plots generated with MetaboAnalyst 5.0 (Chong et al., 2019). Data type was set to ‘Concentrations’ and data were uploaded on MetaboAnalyst. Data were log transformed using ‘Log transformation’ option on MetaboAnalyst and submitted for analysis. 2D PCA plot were generated using the ‘Principal Component Analysis (PCA)’ function and selecting for 2D Scores plots.

## **2.42 Statistical Analysis**

Statistical analysis was undertaken in GraphPad Prism version 8.0.1 for Windows and normality of data was assessed using the Shapiro-Wilk normality test. For radiographic, macroscopic and histological scoring of human cartilage samples, as well as for qPCR quantification of miRNAs and mRNAs in human and equine cartilage tissues, the Mann-Whitney test was used as data did not follow the Gaussian distribution and groups were independent. For qPCR quantification of miRNAs and mRNAs in human primary cells treated with IL-1 $\beta$ , miRNA mimics/inhibitors or control, paired t-tests were undertaken between treated and control groups. Paired t-test was chosen as, for every donor, cells were extracted and cultured in the same flask and were only split in different wells during the time of treatment, thus both groups were homogenous. P values < 0.05 were considered significant.

# **Chapter 3: MicroRNA profiling in young intact, old OA intact and old OA lesioned human knee cartilage using microarray analysis**

### **3.1 Introduction**

Cartilage biology and OA research have advanced considerably in the last decade due to technological improvements in the field of transcriptomics. ‘Whole transcriptome’ techniques, such as microarrays and RNA-Seq, have facilitated a shift from interrogating specific areas of the genome to investigating the global transcriptomic profile of chondrocytes and cartilage, in response to homeostatic changes and disease (Chen et al., 2018, Korostynski et al., 2018, Li et al., 2019b, Rai et al., 2020). This, in combination with the development of specific software and bioinformatic tools to process, filter and analyse the ‘big data’ generated by such experiments, have added significantly to our knowledge regarding cartilage biology and OA, away from the simple ‘wear and tear’ model.

Moreover, scientific advancements in the field have redefined the interrogation of different molecules in cartilage biology and disease, including miRNAs. There is growing interest in the role of miRNAs in OA and their potential use as biomarkers and therapeutic agents. The number of miRNAs involved in OA pathogenesis has increased substantially in the last few years, and this is, in part, due to the use of ‘whole genome’ technologies. Microarrays are a simple and cost-effective way of measuring expression of thousands of miRNAs in different samples at the same time. Miyaki *et al* (2009) used microarrays to detect DE miRNAs between human primary chondrocytes and human MSCs and identified miR-140 as a novel player in human chondrocyte differentiation and OA development (Miyaki et al., 2009). In a similar study, Swingler *et al* (2012) identified a set of miRNAs involved in chondrogenesis and their potential role in OA, such as miR-455 which was shown to regulate TGF- $\beta$  signalling by suppressing the SMAD2/3 pathway (Swingler et al., 2012).

Furthermore, Díaz-Prado *et al* (2012) used microarray analysis to identify DE miRNAs in 3-D cultured chondrocytes, isolated from old healthy and old OA human cartilage tissue. Amongst these, miR-483-5p was upregulated in OA chondrocytes, whereas miR-149-3p, -582-3p, -1227, -634, -576-5p and -641 were downregulated in OA chondrocytes (Díaz-Prado et al., 2012). Microarrays have also been used to identify circulating miRNAs in serum from OA patients (Beyer et al., 2015) and in synovial fluid from early and late-stage OA patients (Li et al., 2016), providing insights into their potential use as biomarkers.

Moreover, ageing is the most prominent risk factor for developing OA. It is believed that age-related effects predispose cartilage to OA development through the accumulation of changes in ECM composition and signalling pathways (Loeser et al., 2016). There is very little research that has addressed the role of miRNAs in cartilage ageing without the effect of OA, mainly due to the difficulty of obtaining relatively healthy cartilage samples from young and old donors. Ukai *et al* (2012) compared the expression of miRNAs between cartilage samples collected from infants with polydactylysm and cartilage collected from young ACL donors and identified three DE miRNAs: miR-199a-3p, -193b and -320c (Ukai et al., 2012). Peffers *et al* (2013) detected significantly higher expression of miR-21 in the metacarpophalangeal joints of old horses compared to young suggesting that this miRNA could potentially have a role in cartilage ageing (Peffers et al., 2013). Given the lack of data, more research is needed in identifying potential miRNA candidates with a role in cartilage ageing.

### **3.2 Study aim and rationale**

OA is a heterogeneous disease and the molecular landscape that underlines it, is complex. There are several risk factors which influence the development and progression of OA, and ageing is the most prominent. Moreover, clinical presentation of cartilage degeneration varies between patients even within the same joint, with some areas being more affected than others. Up to the start of this project (September 2016), there was a limited number of studies on the effect of ageing on miRNA expression in human knee OA cartilage tissue. In addition, to the best of our knowledge, there were not any studies on the expression of miRNAs between areas of different cartilage degeneration within the same knee joint. Therefore, the aim of this study was to identify DE miRNAs between young intact, old OA intact and old OA lesioned human knee cartilage using microarray analysis.

### **3.3 Experimental design**

The experimental procedures, pertinent to this chapter, are described briefly below. For full details on the experimental procedures, please refer to Chapter 2. Appropriate references are provided throughout the text.

### **3.3.1 Human knee cartilage specimens**

To identify DE miRNAs in ageing and OA, three, all male, human knee cartilage groups were used:

- i) Young intact cartilage from patients undergoing ACL reconstruction (n=9, age $\pm$ SD=23.8 $\pm$ 3.8). Samples were collected from the area of the intercondylar notch, as described in Section 2.2.
- ii) Old OA intact cartilage from patients undergoing TKA (n=10, age $\pm$ SD=62.6 $\pm$ 7.3). Intact OA cartilage samples were collected from a relatively intact area of the femoral condyles of OA patients, as described in section 2.1.
- iii) Old OA lesioned cartilage from patients undergoing TKA (n=10, age $\pm$ SD=62.6 $\pm$ 7.3). Lesioned OA cartilage samples were collected from a lesioned area of the femoral condyles of OA patients, as described in section 2.1.

The femoral condyles of OA patients were assessed radiographically prior to TKA, and macroscopically on the day of TKA. Old OA intact and lesioned cartilage samples were collected on the day of TKA. For every patient, a note was made regarding which condyle, lateral or medial, intact and lesioned cartilage was sampled from. Moreover, each intact and lesioned cartilage sample collected was divided into two pieces. One piece was used for histological assessment, and the other piece was used for RNA extraction and microarray analysis. Therefore, from each OA patient, four cartilage pieces were collected: two pieces from an intact area (histology+microarray analysis) and two pieces from a lesioned area (histology+microarray analysis). One cartilage piece was collected from the young intact group for microarray analysis, as the piece was not of sufficient size to be used for histology too.

### **3.3.2 Kellgren-Lawrence grading of human knee OA cartilage samples**

The lateral and medial femoral condyles of the OA patients (which the old OA intact and lesioned cartilage samples were collected from) were radiographically assessed using the KL scoring system. Each femoral condyle of the OA joint was assigned a KL score based on OA

severity, as described in Section 1.5.1 and further explained in **Figure 1.7**. Statistical analysis for KL scores between lateral and medial condyles was undertaken using the Mann-Whitney test in GraphPad Prism version 8.0.1 for Windows (GraphPad, 2018). P values<0.05 were considered significant.

### **3.3.3 Macroscopic assessment of human knee OA cartilage samples**

The area of the femoral condyles, from which the old OA intact and lesioned cartilage samples were collected from, were macroscopically scored using the Outerbridge scoring system, as described in Section 2.3. Scoring was undertaken by two independent scorers, at two different time points per scorer as described in Section 2.3. For scorer agreement, Scorer A-1st time was compared to Scorer B-1st time, and Scorer A-2nd time to Scorer B-2nd time. For agreement calculation, averages were not used to avoid decimal numbers which are incompatible with the online tool used to calculate scorer agreement. For statistical analysis, the average score of intact and lesioned cartilage samples was compared using the Mann-Whitney test in GraphPad Prism version 8.0.1 for Windows. P values<0.05 were considered significant.

### **3.3.4 Histologic assessment of human knee OA cartilage samples**

Histology assessment was undertaken for the old OA intact and lesioned cartilage samples collected. Samples were paraffin embedded and sectioned as described in Sections 2.4 and 2.5A. Sections were stained with H&E and Saf-O/FG as described in sections 2.6 and 2.7. Sections were scored using the Mankin HHGS and the OARSI scoring system as described in Section 2.8. Scoring was undertaken by two independent scorers, in two different time points per scorer, and scorer agreement was calculated as described in Section 2.8. Scorer agreement was calculated as described above in Section 3.3.3. This was undertaken for both scoring systems. For statistical analysis, the same approach as in Section 3.3.3 was followed.

### **3.3.5 RNA extraction from human cartilage samples for microarray analysis**

Young intact, old OA intact and lesioned human cartilage tissue was homogenised as described in Section 2.12. For microarray analysis, RNA was extracted using the mirVana™ miRNA Isolation Kit with phenol, as described in Section 2.13.1.

### **3.3.6 Microarray analysis between young intact, old OA intact and old OA lesioned human knee cartilage samples**

DE miRNAs between young intact, old OA intact and old OA lesioned human knee cartilage samples were identified using the Affymetrix GeneChip® miRNA 4.0 Arrays, as described in Section 2.14. Bioinformatic and statistical analyses of the microarray experiment were undertaken as described in Section 2.31.

### **3.3.7 Target gene prediction and identification of miRNA/mRNA-related biological pathways**

Target prediction of DE miRNAs identified by microarray analysis in cartilage samples was undertaken using IPA as described in Section 2.36. Biological pathways where DE miRNAs might be involved in were identified by the ‘Core Analysis’ feature in IPA, as described in Section 2.36 and Enrichr analysis as described in Section 2.37. GO terms were generated and refined by ToppGene Suite and REVIGO and visualised by Cytoscape, as described in Section 2.38.

## 3.4 Results

### 3.4.1 Kellgren-Lawrence grading of human knee OA femoral condyles

The lateral and medial femoral condyles of the OA patients, recruited for microarray analysis, were assigned a KL score according to radiographic findings. Scores for each patient are listed in **Table 3.1**. KL score of the medial condyles was significantly higher to that of the lateral condyles ( $p=0.03$ ) (**Figure 3.1**). Further analysis showed that for all patients, intact cartilage was collected from the lateral condyle, whereas lesioned cartilage was collected from the medial condyle **Table 3.1**.

**Table 3.1: KL score of each femoral condyle of the OA patients recruited for microarray analysis.** N/A: KL score was not available for these samples (patient 1 and 4).

OA Patient	Condyle	KL Score	Type of sample collected
1	Lateral	N/A	Intact
	Medial	N/A	Lesioned
2	Lateral	2	Intact
	Medial	4	Lesioned
3	Lateral	1	Intact
	Medial	2	Lesioned
4	Lateral	N/A	Intact
	Medial	N/A	Lesioned
5	Lateral	1	Intact
	Medial	3	Lesioned
6	Lateral	1	Intact
	Medial	4	Lesioned

7	Lateral	3	Intact
	Medial	3	Lesioned
8	Lateral	3	Intact
	Medial	3	Lesioned
9	Lateral	2	Intact
	Medial	2	Lesioned
10	Lateral	2	Intact
	Medial	3	Lesioned

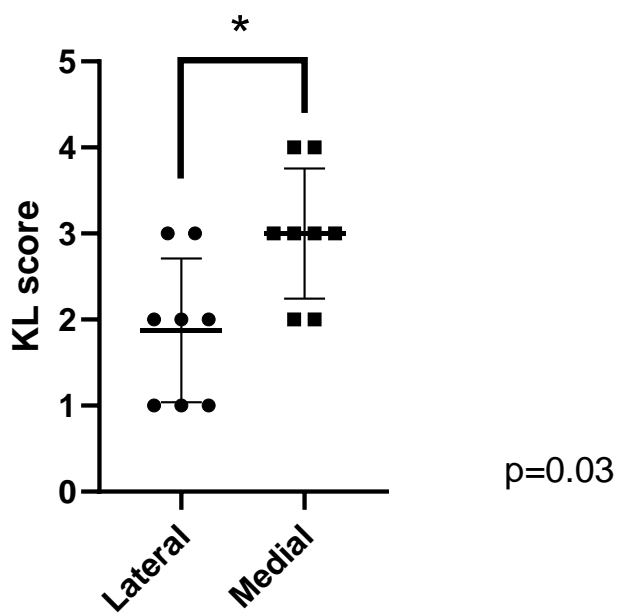


**Figure 3.1: Scatter plot of KL score between lateral and medial condyles of the OA patients, recruited for microarray analysis.** The lateral and medial femoral condyles from knee OA patients (n=8) were assessed radiographically and scored using the KL scoring system. Statistical analysis was undertaken using a Mann-Whitney test in GraphPad Prism (Version 8.0.1). Data are represented as mean±SD. P values<0.05 were considered significant. \*: p<0.05.

### 3.4.2 Outerbridge grading of human knee OA femoral condyles

To assess tissue integrity macroscopically, intact and lesioned human knee cartilage samples from OA patients (**Figure 3.2**) were graded using the Outerbridge scoring system by two independent scorers, scored twice by each scorer. Results for each scorer are listed in **Table 3.2**. Inter-scorer agreement is listed in **Table 3.3**. On average, for both scorers, intact samples were scored significantly lower compared to lesioned samples ( $p=0.002$ ) (**Figure 3.3**).

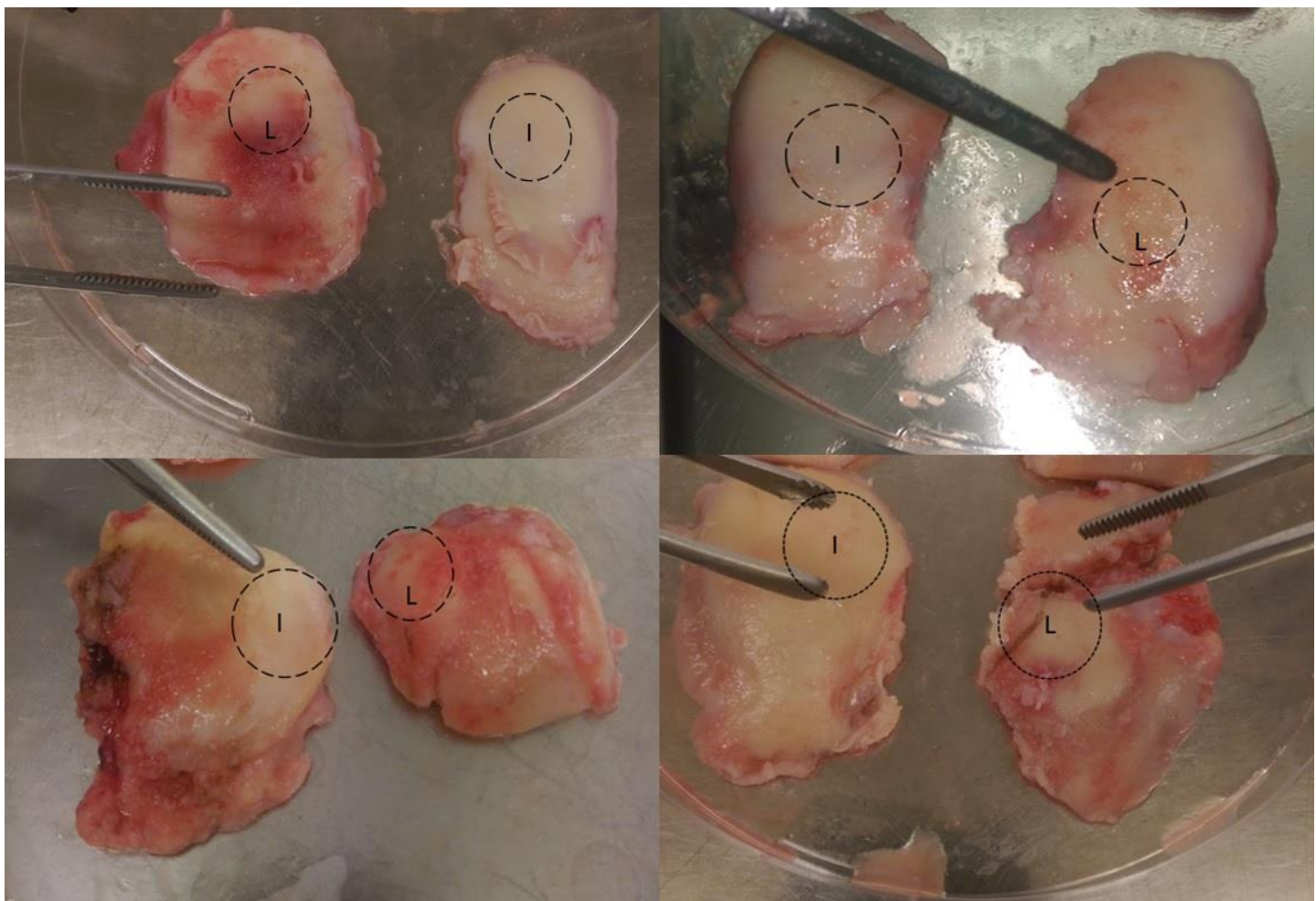


**Figure 3.2: Examples of intact and lesioned cartilage samples collected from knee OA patients.** A cartilage biopsy from intact and lesioned areas of the femoral condyles of OA patients was collected for histology and microarray analysis. For all ten patients, intact samples came from the lateral condyle and lesioned from the medial. I: intact, L: lesioned. Original figure, courtesy of the author.

**Table 3.2: Outerbridge score for intact and lesioned OA cartilage collected from the knee joints of 10 OA patients.** N/A: Outerbridge score was not available for patient 4.

Patient	Sample	Scorer A		Scorer B		Average±SD
		1 <sup>st</sup> Time	2 <sup>nd</sup> Time	1 <sup>st</sup> Time	2 <sup>nd</sup> Time	
1	Intact	0	0	0	0	0±0
	Lesioned	2	2	2	2	2±0
2	Intact	2	2	1	2	1.75±0.5
	Lesioned	4	4	4	4	4±0
3	Intact	0	0	0	0	0±0
	Lesioned	3	3	3	4	3.25±0.5
4	Intact	N/A	N/A	N/A	N/A	N/A
	Lesioned	N/A	N/A	N/A	N/A	N/A
5	Intact	1	1	0	1	0.75±0.5
	Lesioned	2	2	2	2	2±0
6	Intact	1	2	2	2	1.75±0.5
	Lesioned	2	3	4	4	3.25±1
7	Intact	0	0	0	0	0±0
	Lesioned	1	1	0	1	0.75±0.5
8	Intact	1	2	1	1	1.25±0.5
	Lesioned	4	4	4	4	4±0
9	Intact	0	1	0	0	0.25±0.5
	Lesioned	1	1	1	1	1±0
10	Intact	1	0	0	0	0.25±0.5

	Lesioned	2	2	1	2	$1.75 \pm 0.5$
--	----------	---	---	---	---	----------------

**Table 3.3: Inter-scorer agreement between the two independent scorers – macroscopic assessment.** <0.00: poor, 0.00-0.20: slight, 0.20-0.40: fair, 0.41-0.60: moderate, 0.61-0.80: Good, >0.80: Very Good.

		Outerbridge Score	
		1 <sup>st</sup> time	2 <sup>nd</sup> time
<b>Inter-scorer agreement</b>		0.70	0.85
<b>Standard Error</b>		0.10	0.07
<b>95% Confidence Intervals</b>		0.51 to 0.89	0.73 to 0.98
<b>Degree of agreement</b>		Good	Very Good

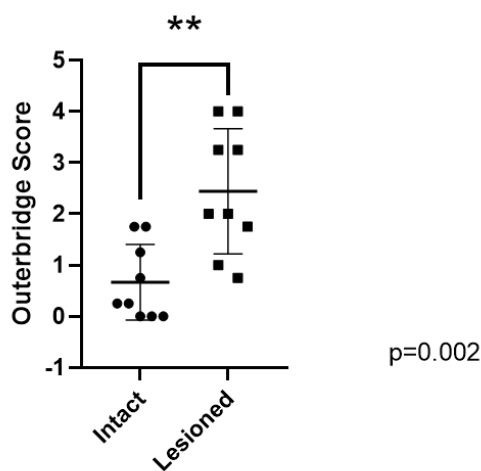


**Figure 3.3: Scatter plot of Outerbridge scores of intact and lesioned OA cartilage samples.** Intact and lesioned cartilage tissue was collected from the lateral and medial femoral condyles of knee OA patients (n=9) after surgery for end-stage OA. Condyles were scored by two independent scorers using the Outerbridge scoring system. For each sample, the score represents the average score of two independent scorers, who each scored the samples twice. Statistical analysis was undertaken using a Mann-Whitney test in GraphPad Prism (Version 8.0.1). Data are represented as mean $\pm$ SD. P values<0.05 were considered significant.

\*\*: p<0.01.

### **3.4.3 Histological scoring of old OA intact and lesioned human knee cartilage**

To assess tissue integrity histologically, intact and lesioned human knee cartilage samples from OA patients were sectioned and stained with H&E and Saf-O/FG (**Figure 3.4**). Sections were graded using the Mankin HHGS and the OARSI scoring system by two independent scorers, scored twice by each scorer. Results for each scorer are listed in **Table 3.4** for the Mankin HHGS, and **Table 3.5** for the OARSI scoring system. Inter-scorer agreement is listed in **Table 3.6**.

For the Mankin HHGS: for patients: 3, 5, 7 and 8, the average score of intact samples was lower compared to that of lesioned samples, for two patients (patients 6 and 10), the average score of intact samples was equal to that of lesioned samples, and for one patient (patient 9), the score of the intact sample was higher than that of the lesioned sample. On average, for both scorers, intact samples were scored lower compared to lesioned samples ( $p=0.12$ ) (**Figure 3.5A**).

When using the OARSI scoring system: for patients 3, 5, 7 and 8, the average score of intact samples was lower compared to that of lesioned samples, whereas for three patients (patients 6, 9 and 10) the average score of intact samples was higher than that of the lesioned samples. On average from both scorers, intact samples were scored lower compared to lesioned samples ( $p=0.26$ ) (**Figure 3.5B**).

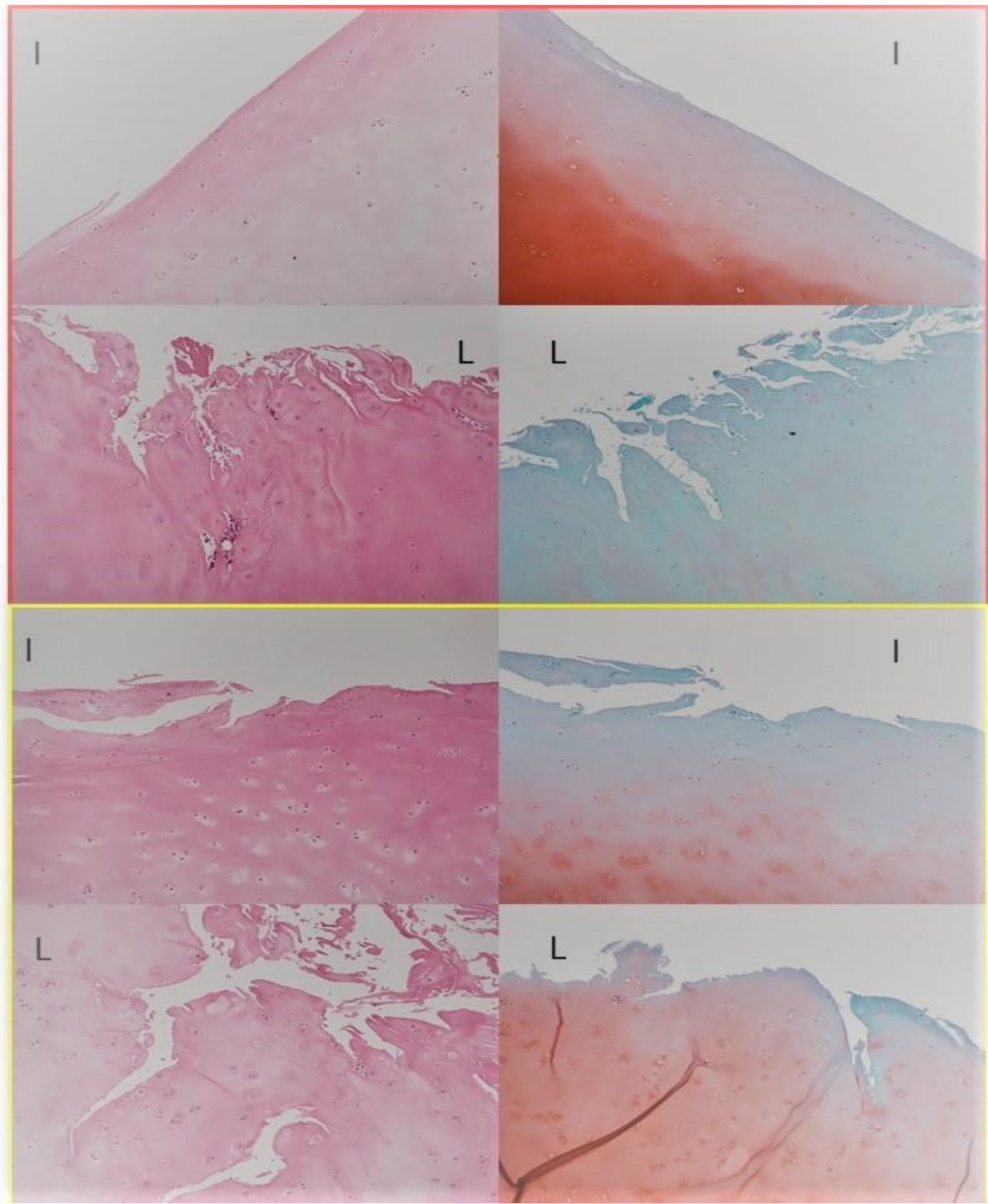


**Figure 3.4: Examples of intact and lesioned cartilage samples stained with H&E and Saf-O/FG.** Intact and lesioned OA cartilage samples were paraffin embedded, sectioned and stained with H&E (left side) and Saf-O/FG (right side) for histologic assessment. Red box depicts sections of intact and lesioned cartilage from one patient, and yellow box from another. Original figure, courtesy of the author. I: intact, L: lesioned.

**Table 3.4: Mankin HHGS for intact and lesioned OA cartilage collected from the knee joints of 10 OA patients.** N/A: Paraffin blocks for these samples were not available.

Patient	Sample	Scorer A		Scorer B		Average±SD
		1 <sup>st</sup> Time	2 <sup>nd</sup> Time	1 <sup>st</sup> Time	2 <sup>nd</sup> Time	
<b>1</b>	Intact	N/A	N/A	N/A	N/A	N/A
	Lesioned	N/A	N/A	N/A	N/A	N/A
<b>2</b>	Intact	4	4	3	3	3.5±0.5
	Lesioned	N/A	N/A	N/A	N/A	N/A
<b>3</b>	Intact	1	1	2	2	1.5±0.5
	Lesioned	5	4	8	7	6±1.6
<b>4</b>	Intact	N/A	N/A	N/A	N/A	N/A
	Lesioned	N/A	N/A	N/A	N/A	N/A
<b>5</b>	Intact	1	2	2	1	1.5±0.5
	Lesioned	7	7	8	6	7±0.7
<b>6</b>	Intact	3	3	4	4	3.5±0.5
	Lesioned	3	4	4	3	3.5±0.5
<b>7</b>	Intact	4	4	4	5	4.25±0.4
	Lesioned	7	7	7	7	7±0
<b>8</b>	Intact	5	5	3	5	4.5±0.9
	Lesioned	9	9	8	9	8.75±0.4
<b>9</b>	Intact	5	2	4	2	3.25±1.3
	Lesioned	1	2	2	2	1.75±0.4
<b>10</b>	Intact	1	1	1	3	1.5±0.9

	Lesioned	2	2	1	1	1.5±0.5
--	----------	---	---	---	---	---------

**Table 3.5: OARSI scoring system for intact and lesioned OA cartilage collected from the knee joints of 10 OA patients.** N/A: Paraffin blocks for these samples were not available.

Patient	Sample	Scorer A		Scorer B		Average±SD
		1 <sup>st</sup> Time	2 <sup>nd</sup> Time	1 <sup>st</sup> Time	2 <sup>nd</sup> Time	
1	Intact	N/A	N/A	N/A	N/A	N/A
	Lesioned	N/A	N/A	N/A	N/A	N/A
2	Intact	2	2	1	1	1.5±0.6
	Lesioned	N/A	N/A	N/A	N/A	N/A
3	Intact	0	0	1	1	0.5±0.6
	Lesioned	3	2	3	3	2.75±0.5
4	Intact	N/A	N/A	N/A	N/A	N/A
	Lesioned	N/A	N/A	N/A	N/A	N/A
5	Intact	1	1	1	0	0.75±0.5
	Lesioned	3	2	3	3	2.75±0.5
6	Intact	1	1	2	2	1.5±0.6
	Lesioned	0	2	1	1	1±0.8
7	Intact	1	2	1	2	1.5±0.6
	Lesioned	4	4	2	3	3.25±1
8	Intact	2	2	1	2	1.75±0.5
	Lesioned	4	3	3	3	3.25±0.5

<b>9</b>	Intact	1	1	1	1	$1\pm 0$
	Lesioned	1	1	0	1	$0.75\pm 0.5$
<b>10</b>	Intact	1	1	1	1	$1\pm 0$
	Lesioned	1	1	1	0	$0.75\pm 0.5$

**Table 3.6: Inter-scorer agreement for the two independent scorers.** <0.00: poor, 0.00-0.20: slight, 0.20-0.40: fair, 0.41-0.60: moderate, 0.61-0.80: Good, >0.80: Very Good.

	Mankin HHGS		OARSI grading system	
	1 <sup>st</sup> time	2 <sup>nd</sup> time	1 <sup>st</sup> time	2 <sup>nd</sup> time
<b>Inter-scorer agreement</b>	0.64	0.66	0.47	0.44
<b>Standard Error</b>	0.07	0.08	0.14	0.12
<b>95% Confidence Intervals</b>	0.50 to 0.77	0.51 to 0.82	0.20 to 0.75	0.22 to 0.67
<b>Degree of agreement</b>	Good	Good	Moderate	Moderate

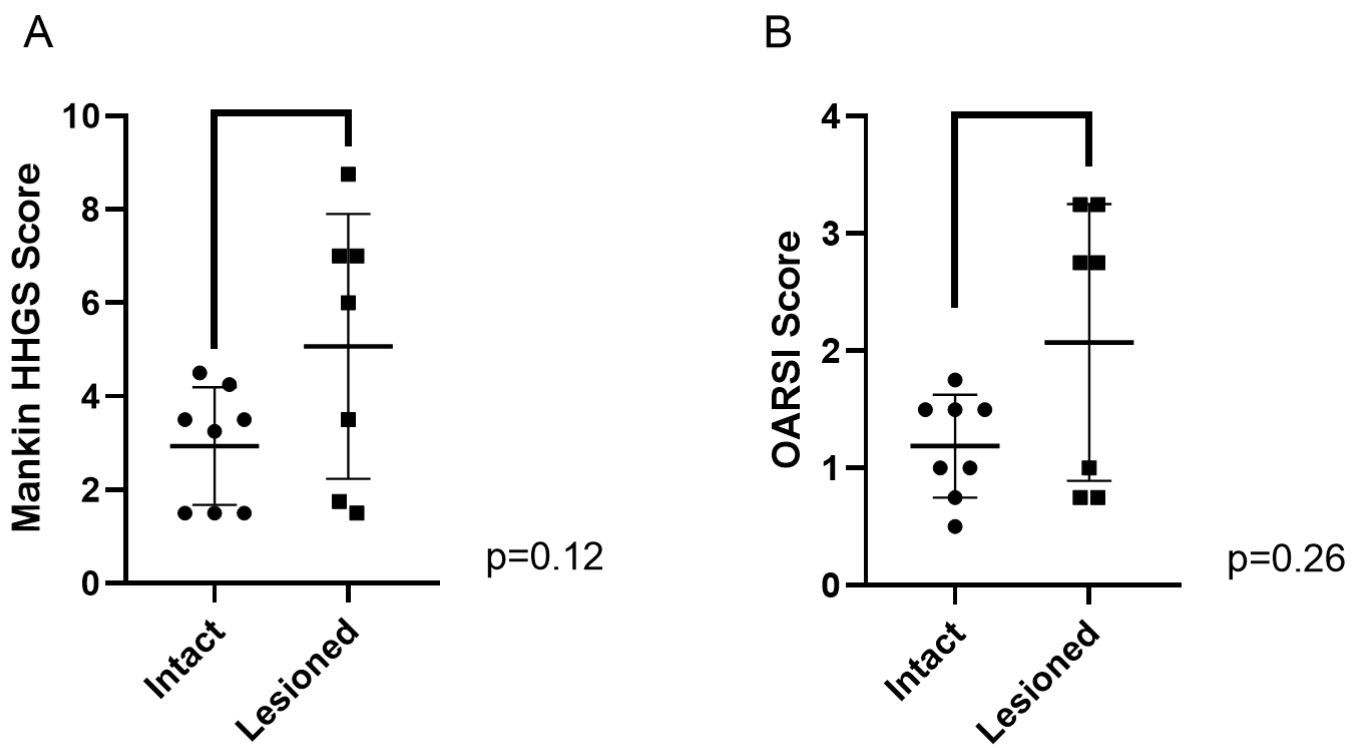


**Figure 3.5: Scatter plot of score of intact and lesioned OA cartilage samples.** Intact (n=8) and lesioned (n=7) OA cartilage samples were stained with H&E and Saf-O/FG and scored using the A) Mankin HHGS and B) OARSI grading system. For each sample, the score represents the average score of two independent scorers, who each scored the sections twice. Statistical analysis was undertaken using a Mann-Whitney test in GraphPad Prism (Version 8.0.1). Data are represented as mean $\pm$ SD. P values $<0.05$  were considered significant.

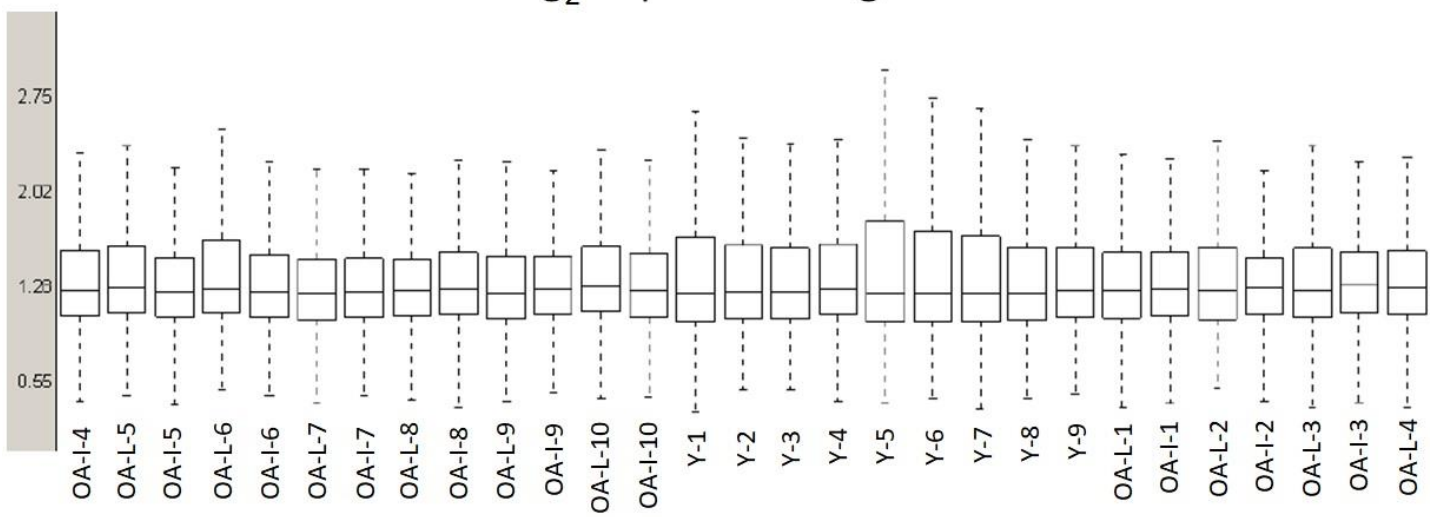
#### 3.4.4 Microarray analysis overview

Data quality was assessed by measuring small RNA expression in nine young intact, 10 old OA intact and 10 old OA lesioned samples. Log<sub>2</sub> small RNA expression distribution (**Figure 3.6A**) and probability density curves (**Figure 3.6B**) for all samples, revealed that there was no notable systematic expression bias between samples and there were no outliers. Assessment of dispersion of expression values across arrays for each miRNA, identified differences in expression for some miRNAs amongst the three groups. Heatmap of correlation coefficients

amongst samples showed that samples in the young group correlated closer to each other and there was no significant biological variation within the group. In contrast, samples in OA intact and OA lesioned groups were more variable and biological variation was stronger within these two groups (**Figure 3.7**).

A

Log<sub>2</sub> Expression Signal



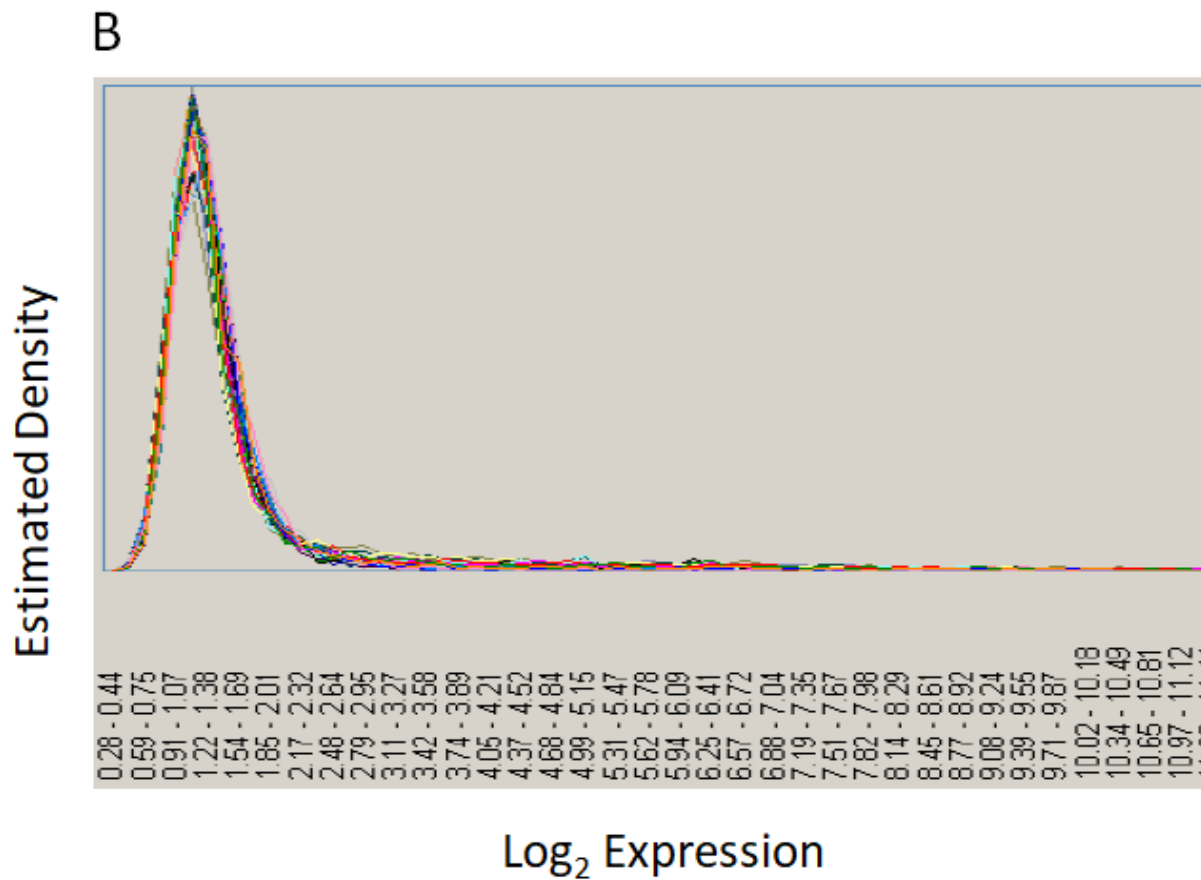


**Figure 3.6: Microarray data quality assessment from young intact, old OA intact and lesioned cartilage samples.** A) Boxplot and B) density curve of miRNA log-transformed expression distribution generated young intact, old OA intact and lesioned cartilage samples. Graphs generated using R. OA-I: OA intact, OA-L: OA lesioned, Y: Young.

## Sample correlation heatmap

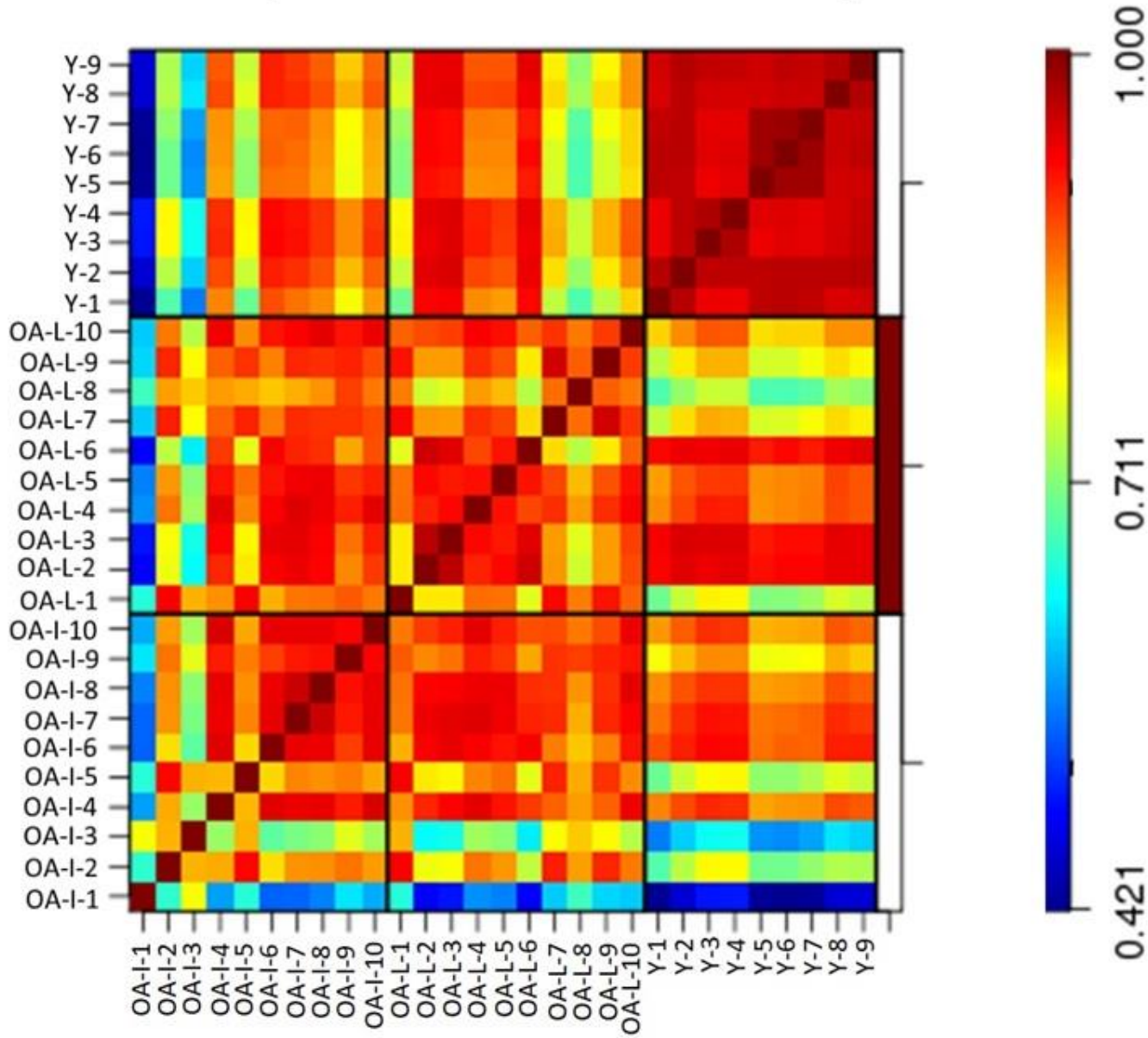


**Figure 3.7: Heatmap of sample correlation coefficients.** Correlation coefficients following microarray analysis between young intact, old OA intact and lesioned cartilage samples were computed using log-transformed expression values of detected miRNAs. Colour gradient from blue to red denotes transition from low to high correlation coefficients. Heatmap generated in R. OA-I: OA intact, OA-L: OA lesioned, Y: Young.

2-D PCA plot of the second and third components of log-transformed miRNA abundance showed that young intact cartilage samples clustered together in one group and were separated from OA intact and OA lesioned groups (**Figure 3.8**). OA intact samples were scattered in a wide range and could be divided into two separate subgroups: OA-Intact-1 (samples OA-I-1, OA-I-2, OA-I-3 and OA-I-5) and OA-Intact-2 (samples OA-I-4, OA-I-6, OA-I-7, OA-I-8, OA-I-9 and OA-I-10).

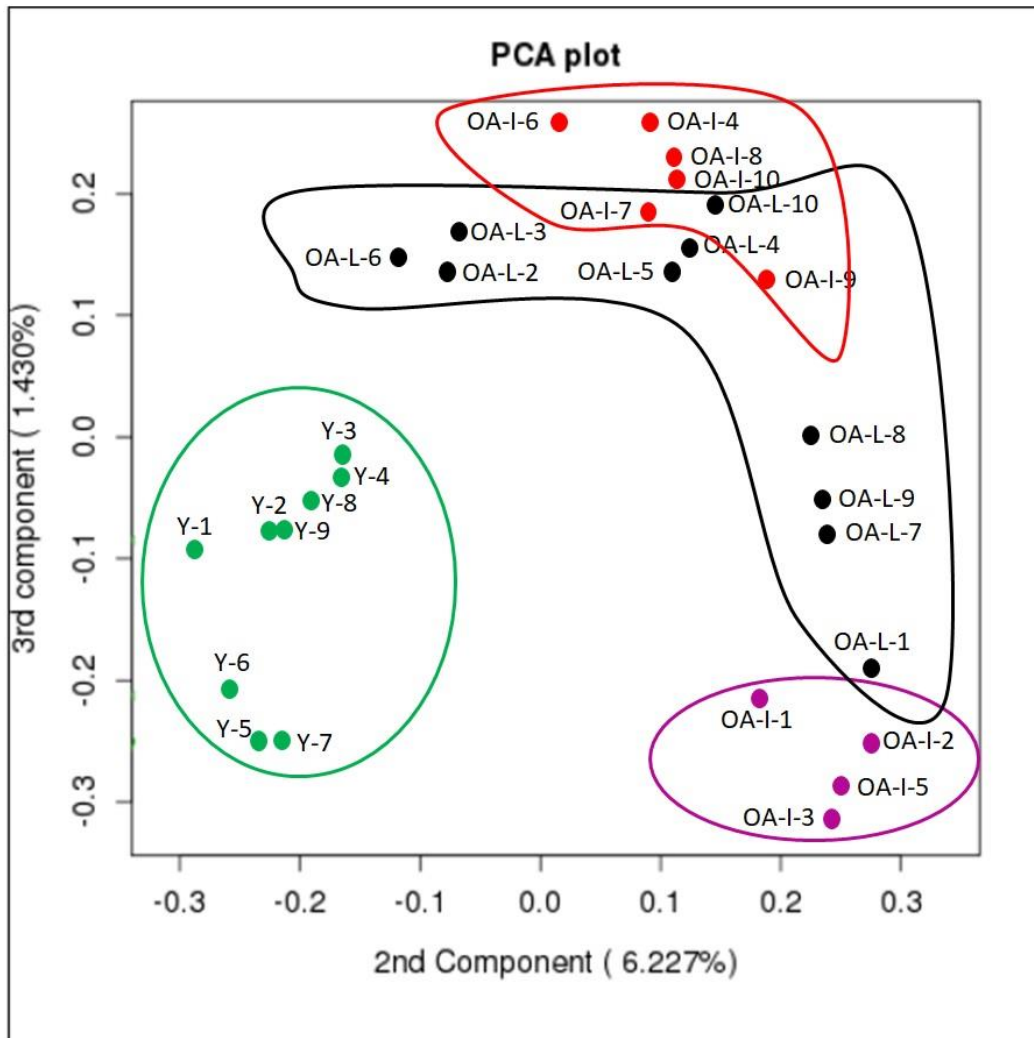


**Figure 3.8: 2-D PCA plot of the second and third components of miRNA abundance in young intact, old OA intact and old OA lesioned samples.** Clustering of young intact (Y), old OA intact (OA-I) and lesioned (OA-L) cartilage samples based on miRNA expression, following microarray analysis. Green: Young intact, magenta: old OA-Intact-1, red: old OA-Intact-2, black: old OA-Lesioned. Numbers (1 to 9 for young intact and 1 to 10 for old OA intact/lesioned) correspond to donor/patient number. PCA plot generated in R.

OA lesioned samples were also scattered, but the degree of variation was not as high as in the OA intact group. Therefore, OA lesioned samples could be clustered into three similar subgroups or remain in one major group. Clustering of OA lesioned samples into three subgroups would complicate further analysis and comparison to the rest of the groups. Therefore, the decision to cluster all OA lesioned samples in one group was made.

To investigate possible reasons for the old OA intact group splitting into two subgroups, I analysed patient data that were available: age, KL score, Outerbridge score, Mankin score and OARSI score (**Table 3.7**). Analysis showed that there is a statistically significant 10-year difference between OA-Intact-1 and OA-Intact-2 groups, with patients in OA-Intact-1 being younger than patients in OA-Intact-2 (**Figure 3.9A**). Although intact and lesioned samples were obtained from the same OA patients, there is little separation in the lesioned group based on age differences, and lesioned samples were grouped together. Moreover, it was observed that samples in Intact-group1 had a lower KL, Outerbridge, Mankin and OARSI score compared to OA-Intact-2, but differences were not significant (**Figure 3.9 B-E**).

**Table 3.7: Characteristics and comparison of OA-Intact-1 and OA-Intact-2 samples.** For each characteristic, the average $\pm$ SD is shown. Statistical analysis undertaken using the Mann-Whitney test. P values are indicated.

	OA-Intact-1	OA-Intact-2	OA-Intact-1 VS OA-Intact-2 (p-value)
<b>Age</b>	56 $\pm$ 3.5	67 $\pm$ 4.6	0.01
<b>KL score</b>	1.33 $\pm$ 0.58	2.20 $\pm$ 0.84	0.23
<b>Outerbridge score</b>	0.63 $\pm$ 0.83	0.70 $\pm$ 0.76	0.74
<b>Mankin score</b>	2.17 $\pm$ 1.15	3.40 $\pm$ 1.18	0.30
<b>OARSI score</b>	0.92 $\pm$ 0.52	1.35 $\pm$ 0.34	0.20

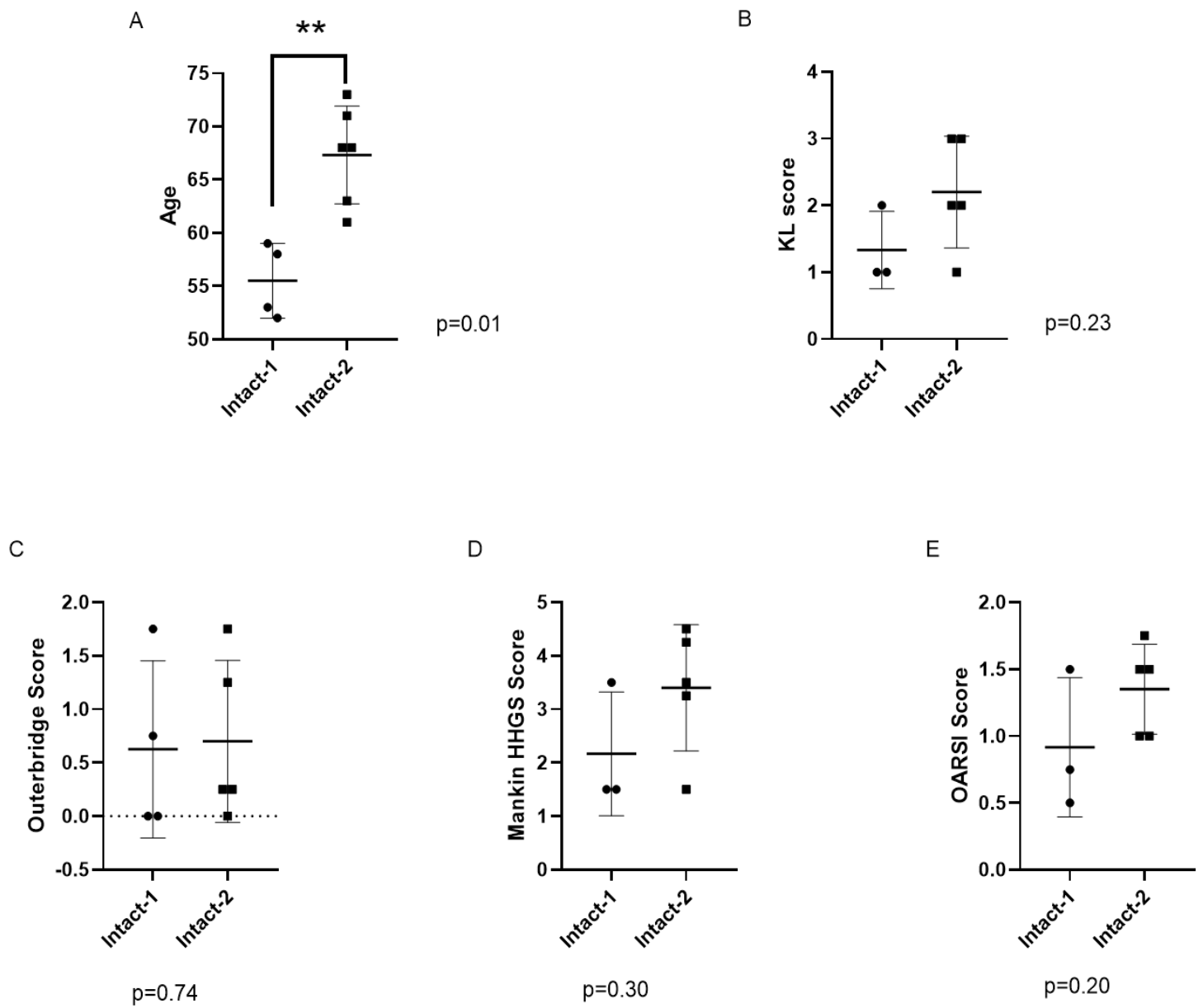


**Figure 3.9: Comparison of OA-Intact-1 and OA-Intact-2 cartilage samples.** OA-Intact-1 (n=3-4) and OA-Intact-2 (n=5-6) samples were compared to each other based on the following characteristics: age of donors, KL score, Outerbridge score, Mankin HHGS score and OARSI score. Statistical analysis was undertaken using a Mann-Whitney test in GraphPad Prism (Version 8.0.1). Data are represented as mean $\pm$ SD. P values $<0.05$  were considered significant.  
 \*\*: p<0.01. Outerbridge, Mankin HHGS and OARSI scores represent the average score of two independent scorers, who each scored samples twice.

### **3.4.5 Differentially expressed miRNAs in young intact, old OA intact and old OA lesioned human cartilage**

To identify DE miRNAs, the following comparisons were investigated:

- Old OA lesioned vs Young (OA-Lesioned vs Y)
- Old OA intact subgroup 1 vs Young (OA-Intact-1 vs Y)
- Old OA intact subgroup 2 vs Young (OA-Intact-2 vs Y)
- Old OA lesioned vs OA intact subgroup 1 (OA-Lesioned vs OA-Intact-1)
- Old OA lesioned vs OA intact subgroup 2 (OA-Lesioned vs OA-Intact-2)
- OA intact subgroup 1 vs OA intact subgroup 2 (OA-Intact-1 vs OA-Intact-2)

In the above comparisons, the first group mentioned is the group of interest and the second group is the reference group. For this thesis, changes in miRNA expression (increased/decreased expression) refer to changes of miRNA expression in the group of interest compared to the reference group.

A list of DE miRNAs was identified for each of the above comparisons and differential expression was reported as logFC (**Figure 3.10**). Significantly DE miRNAs were defined as those with FDR-adjusted p-value < 5%, as described in Section 2.31. **Table 3.8** summarises the total number of significantly DE miRNAs and direction of dysregulation for each comparison.

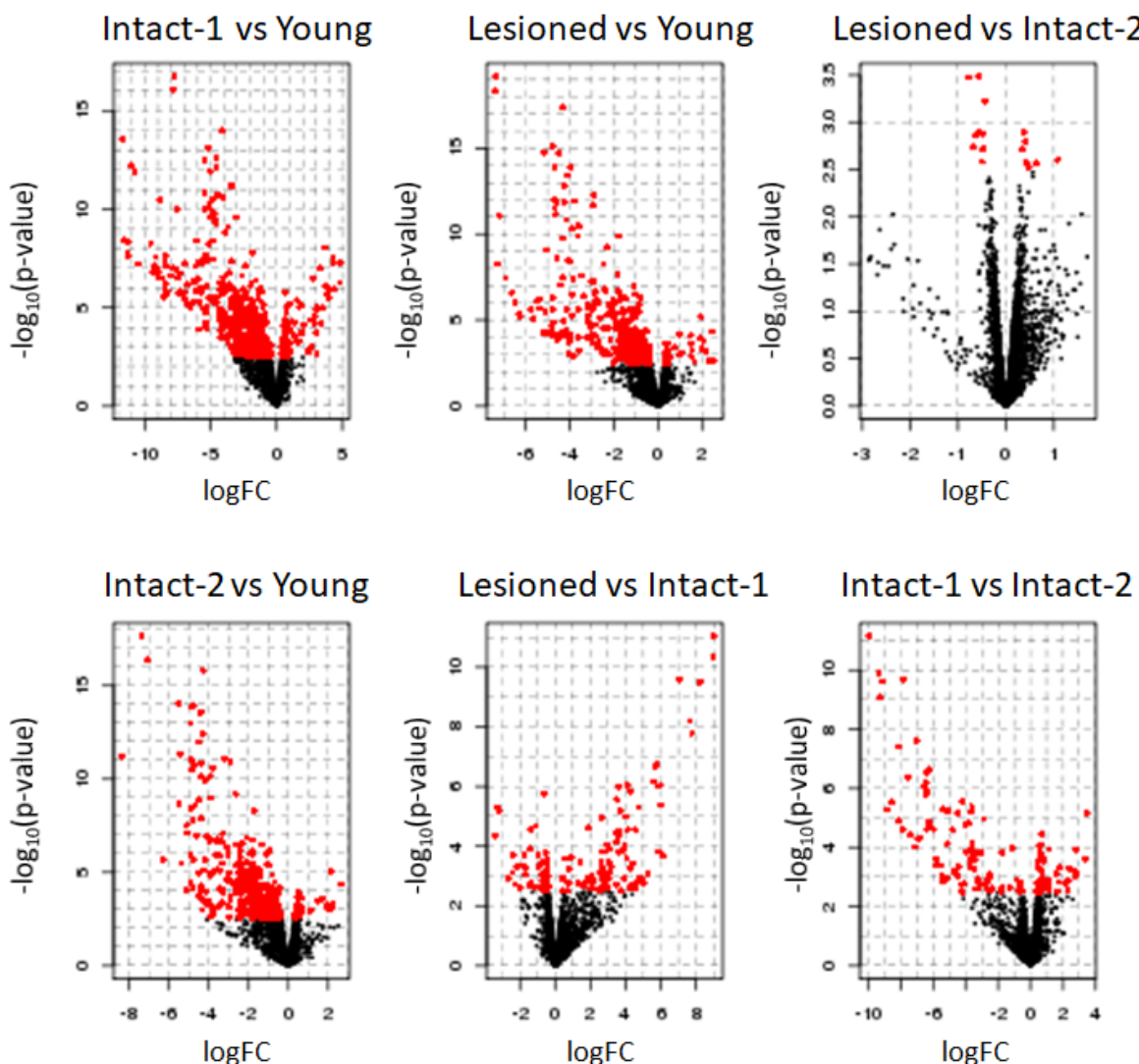


**Figure 3.10: Visual identification of significantly DE miRNAs in human cartilage samples, detected by microarray analysis.** Volcano plots were used to contrast statistical significance [ $-\log_{10}(p\text{-value})$ ] to magnitude of differential expression ( $\log FC$ ) of miRNAs identified in six comparisons. Red dots represent individual miRNAs which are significantly differentially expressed. The further away from 0 on x axis, the higher the level of differential expression (either positive or negative) for an individual miRNA. The higher an individual miRNA scores on the y axis, the more statistically significant its differential expression is. Thus, red dots in the upper left and right corner of each volcano plot represent miRNAs with the highest degree of statistically significant differential expression. Plots generated in R. Intact-1: OA intact subgroup 1, Intact-2: OA intact subgroup 2, Lesioned: OA-Lesioned, Young: Young intact.

**Table 3.8.: Number of significantly DE miRNAs in human cartilage samples.** Significant DE miRNAs are defined as those with FDR-adjusted p-value<5%.

	OA-Lesioned vs Y	OA-Intact-1 vs Y	OA-Intact-2 vs Y
<b>No of DE miRNAs with higher expression in the group of interest</b>	20	69	19
<b>No of DE miRNAs with lower expression in the group of interest</b>	298	408	313
<b>Total</b>	318	477	332

	OA-Lesioned vs OA-Intact-1	OA-Lesioned vs OA-Intact-2	OA-Intact-1 vs OA-Intact-2
<b>No of DE miRNAs with higher expression in the group of interest</b>	90	3	30
<b>No of DE miRNAs with lower expression in the group of interest</b>	33	9	85
<b>Total</b>	123	12	115

The full list of significantly DE miRNAs for every comparison is in Appendix to Chapter 3.

Analysis showed that the list of significantly DE miRNAs was similar in the following three comparisons: OA-Lesioned vs Y, OA-Intact-1 vs Y and OA-Intact-2 vs Y, indicating that OA intact and OA lesioned cartilage samples were more similar to each other than to the young cartilage samples. Of the old OA groups, OA-Lesioned and OA-Intact-2 were more similar to each other and less similar when compared to OA-Intact-1 group. Since the list of DE miRNAs was similar for the first three comparisons, I selected these for analysis in IPA. MicroRNA Target filter analysis generated a list of experimentally validated and highly predicted mRNA targets. Due to the high number of DE miRNA input, the number of predicted mRNAs was also

high (>10,000). For core analysis, there is a cut off of 8,000 genes. To meet this requirement and redefine the number of predicted mRNAs appropriate filters for cartilage and OA were selected. As expected, the list of mRNA targets was highly similar for all three comparisons and included transcription factors, cytokines and ligands, receptors and ECM components.

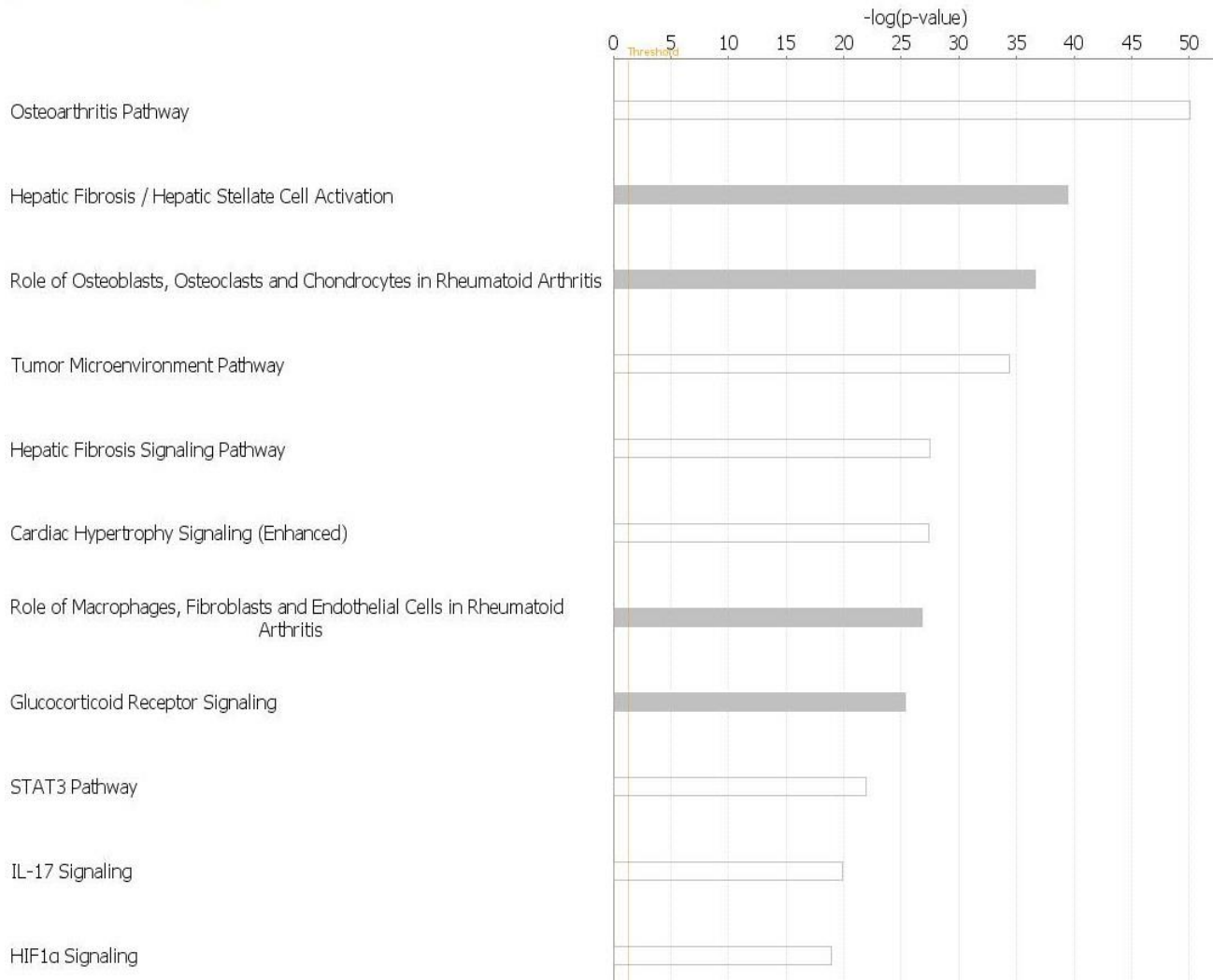


**Figure 3.11: Top canonical pathways of validated and predicted mRNA targets of DE miRNAs in human cartilage samples.** Core analysis of highly predicted mRNA targets of DE miRNAs in OA-Lesioned vs Y, OA-Intact-1 vs Y and OA-Intact-2 vs Y, revealed the most important pathways that these mRNAs are involved in. Pathways were ranked based on level of significance [ $-\log(p\text{-value})$ ], dependent on the number of mRNAs involved in each pathway. The figure depicts biological pathways generated from validated and predicted mRNA targets of the DE miRNAs identified in the OA-Lesioned vs Y comparison. DE miRNAs in OA-Intact-1 vs Y and OA-Intact-2 vs Y comparisons were similar and, therefore, top biological pathways were also similar. Graph generated in IPA Version 60467501.

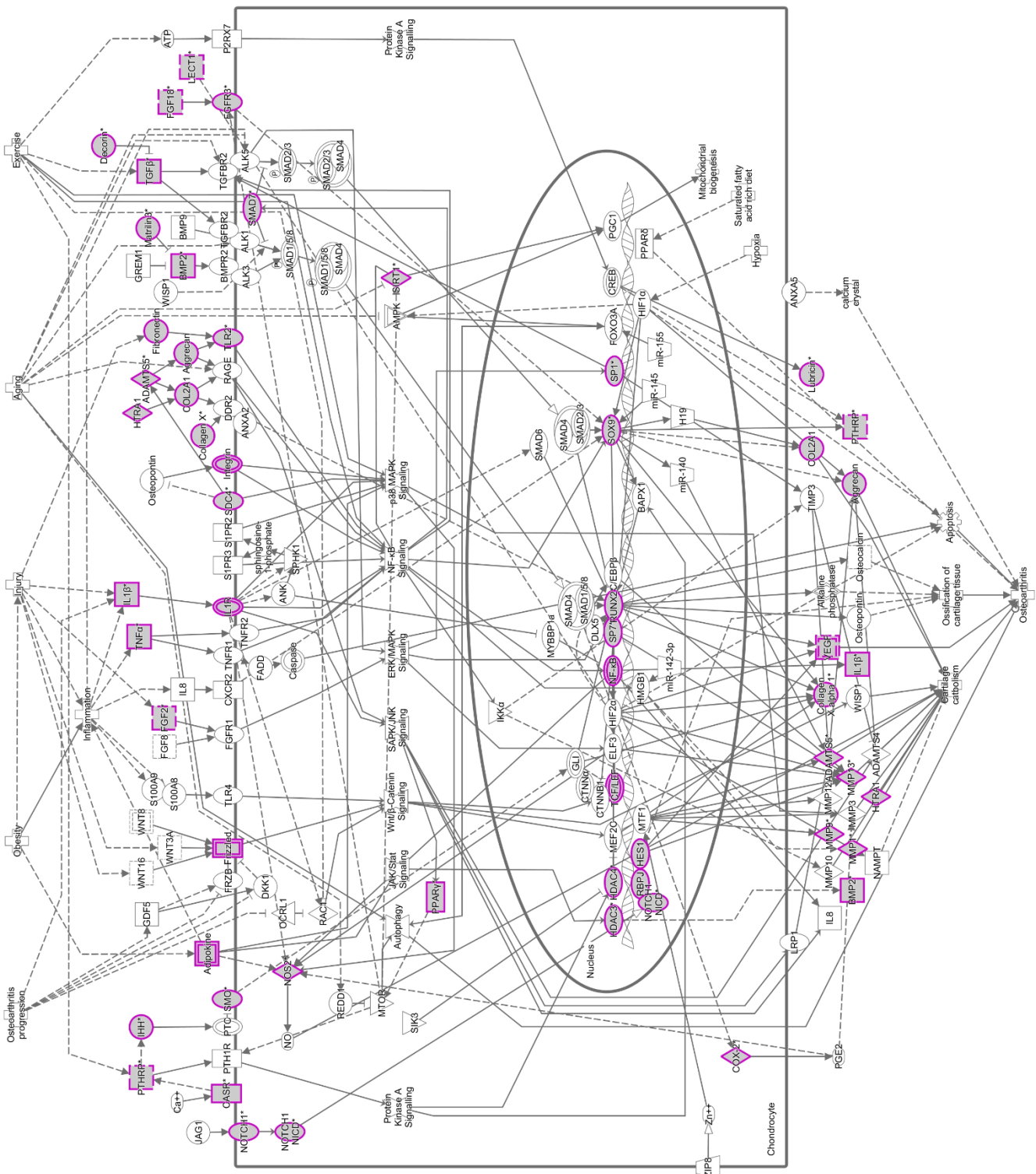


**Figure 3.12: The osteoarthritis pathway generated by IPA based on predicted target genes of DE miRNAs.** Osteoarthritis pathway was one of the top canonical pathways associated with the predicted target genes of DE miRNAs. Predicted target genes were involved in several OA-related mechanisms and were linked to ageing, injury, physical exercise and obesity. Figure generated with IPA Version 60467501.

IPA Core Analysis generated similar results for the three comparisons. Specifically, predicted mRNA targets of DE miRNAs were involved in significant canonical pathways, including osteoarthritis pathway [-log(p-value)=50.04], hepatic fibrosis [-log(p-value)=39.46], role of osteoblasts and chondrocytes in rheumatoid arthritis [-log(p-value)=36.67], IL-17 signalling [-log(p-value)=19.86], HIF1 $\alpha$  signalling [-log(p-value)=18.89] and others (**Figure 3.11**) (**Figure 3.12**). Top diseases and disorders associated with these mRNAs are listed in **Table 3.9**, and top molecular and cellular functions are listed in **Table 3.10**. Moreover, IPA generated a list of potential upstream regulators of the predicted target genes. Amongst these, there were molecules involved in inflammation, such as IL-1 $\beta$  ( $p= 1.92\times 10^{-66}$ ) and TNF- $\alpha$  ( $p=5.33\times 10^{-62}$ ), as well as cell signalling, such as TGF- $\beta$  ( $p=2.11\times 10^{-55}$ ). IPA report is in Appendix to Chapter 3.

**Table 3.9: Top diseases and disorders associated with predicted targets genes of DE miRNAs.**

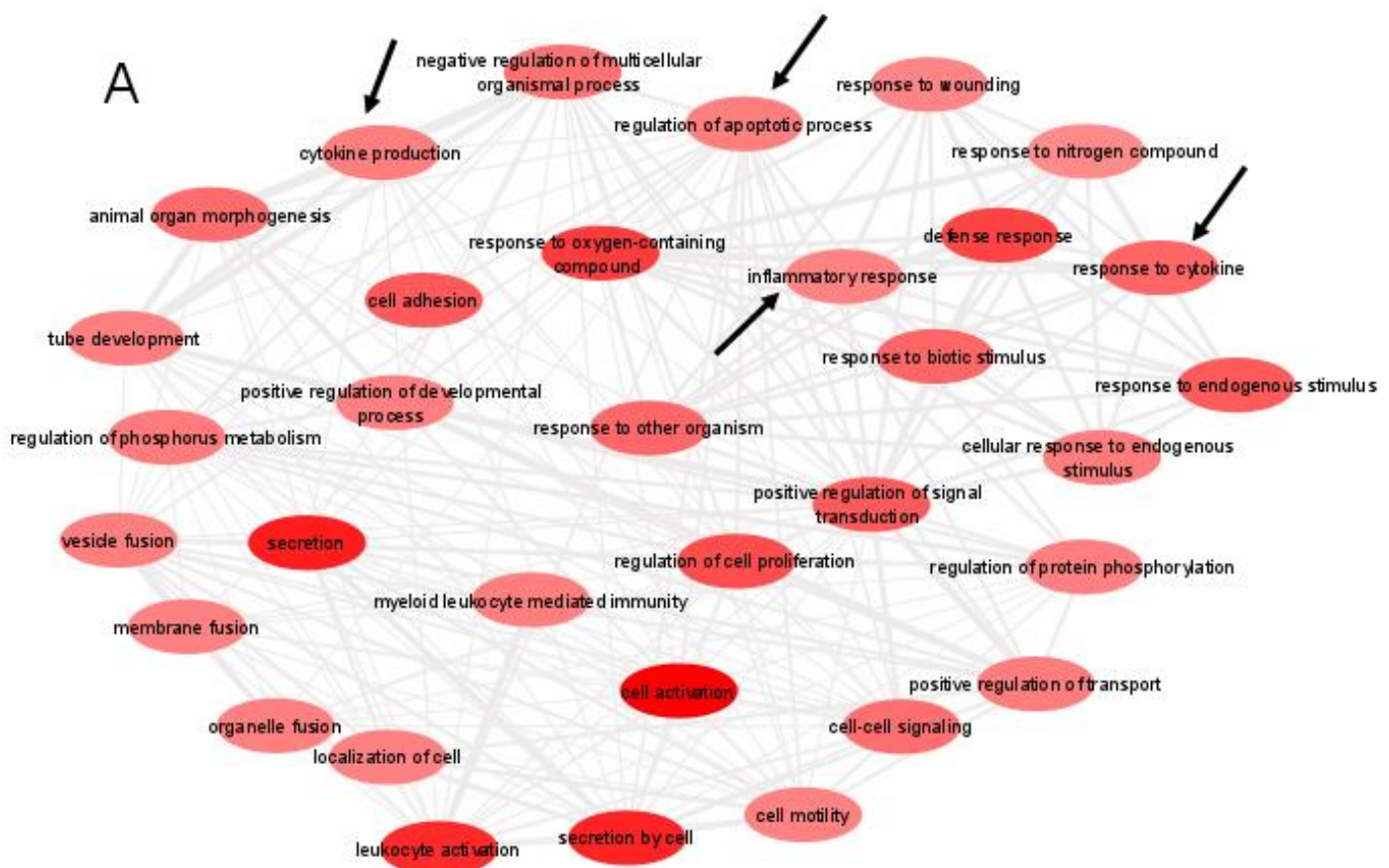
Name	p-value range	Number of target genes involved
Cancer	$1.11\times 10^{-22} - 4.69\times 10^{-63}$	188
Organismal Injury and Abnormalities	$1.69\times 10^{-22} - 4.69\times 10^{-63}$	212
Cardiovascular Disease	$5.46\times 10^{-23} - 1.51\times 10^{-56}$	139
Inflammatory Response	$2.28\times 10^{-22} - 7.97\times 10^{-50}$	155
Connective Tissue Disorders	$8.87\times 10^{-23} - 2.96\times 10^{-48}$	147

**Table 3.10: Top molecular and cellular functions associated with predicted mRNA targets of DE miRNAs.**

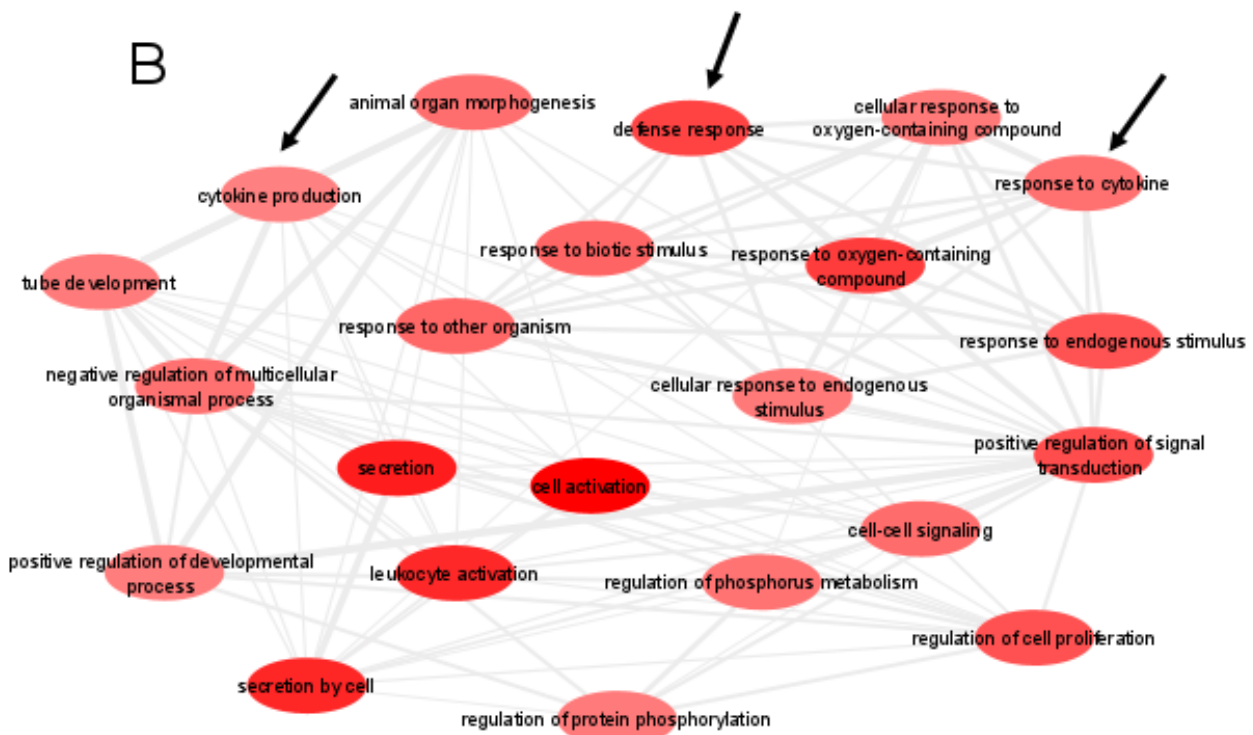
Name	p-value range	Number of mRNAs involved
Cellular Movement	$9.40\times 10^{-23} - 5.42\times 10^{-72}$	157
Cellular Development	$2.13\times 10^{-22} - 1.17\times 10^{-69}$	185

Cellular Growth and Proliferation	$2.13 \times 10^{-22} - 3.33 \times 10^{-64}$	178
Cell Death and Survival	$1.69 \times 10^{-22} - 3.33 \times 10^{-60}$	162
Cell-To-Cell Signalling and Interaction	$1.81 \times 10^{-22} - 3.98 \times 10^{-56}$	141

To investigate further the potential pathways that the DE miRNAs and their predicted target genes are associated with, the Enrichr online tool was used. Analysis showed that predicted mRNAs of DE miRNAs from OA-Lesioned vs Y, OA-Intact-1 vs Y and OA-Intact-2 vs Y were involved in pathways such as inflammatory response, cytokine production, cytokine response, regulation of apoptosis and regulation of cell proliferation amongst others. To create pathway interactions, gene ontology terms were generated with ToppGene Suite and redefined with Revigo and then visualised in Cytoscape. Gene interaction analysis agreed with IPA and



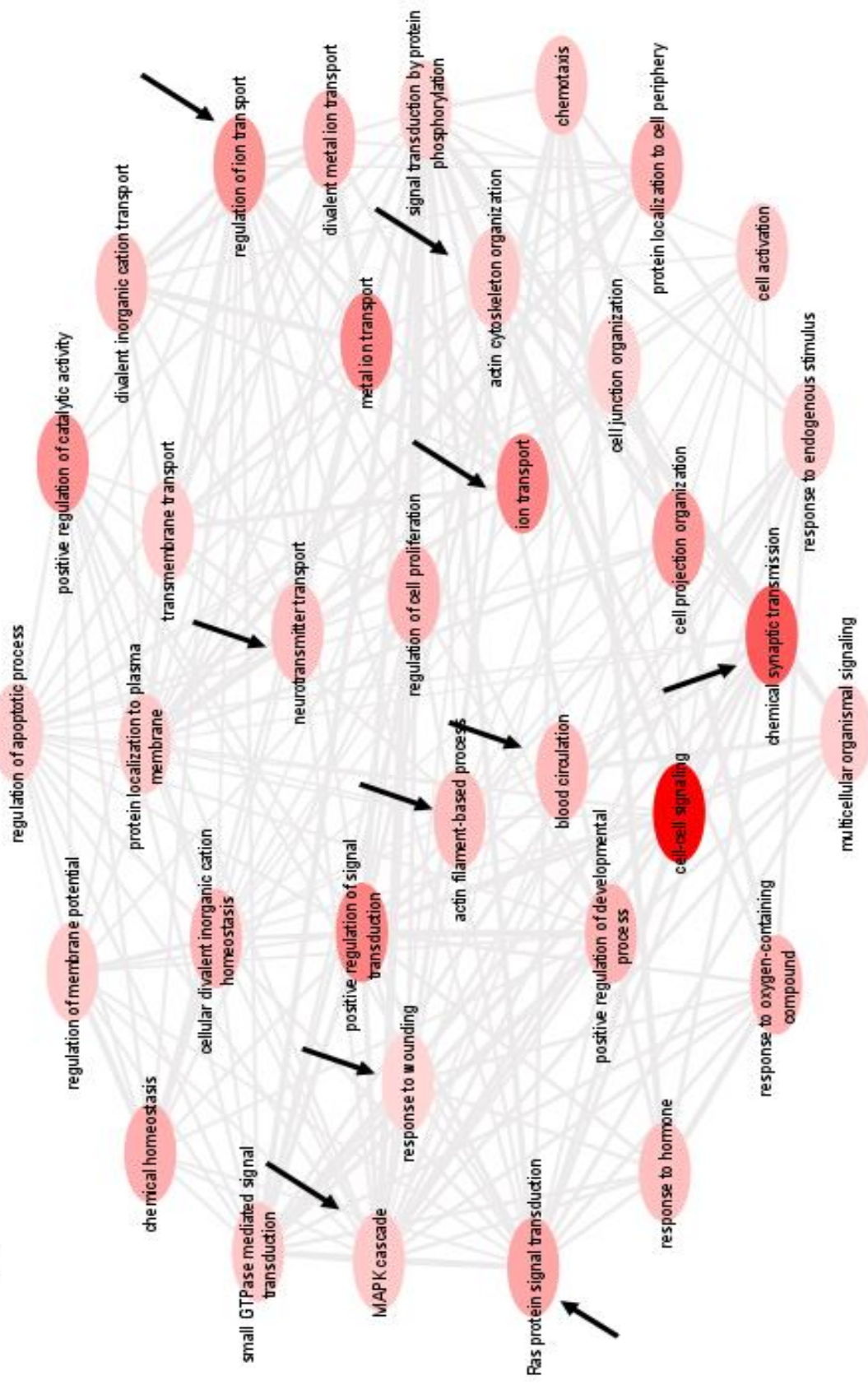
Enrichr analyses, and the networks that were generated included similar pathways as before (Figure 3.13A&B).



**Figure 3.13: Pathway interaction analysis of predicted targets of DE miRNAs from comparisons OA-Intact-1 vs Young Intact and OA-Intact-2 vs Young Intact.** Predicted target genes of DE miRNAs from comparisons A) OA-Intact-1 vs Young Intact and B) OA-Intact-2 vs Young Intact were uploaded on ToppGene Suite which generated a list of GO terms. GO terms were pasted in REVIGO for selection of key biological pathways. Biological pathways were visualised with Cytoscape Version 3.8.2, which generated the figures. Pathways of interest are indicated with black arrows.

After identifying biological pathways from the first three comparisons (OA-Lesioned vs Y, OA-Intact-1 vs Y and OA-Intact-2 vs Y), I sought to identify pathways relevant to the other three comparisons that were generated by microarray analysis: OA-Lesioned vs OA-Intact-1, OA-Lesioned vs OA-Intact-2 and OA-Intact-1 vs OA-Intact-2. Enrichr analysis was undertaken to investigate the biological processes that the predicted targets of DE miRNAs from these three comparisons were involved in. Analysis revealed that these were involved in pathways such as regulation of ion transport, actin and cytoskeleton regulation, MAPK cascade, Ras signalling, regulation of apoptosis, neuronal signalling, synaptic transmission, response to wounding and blood circulation (**Figure 3.14A&B**).

A



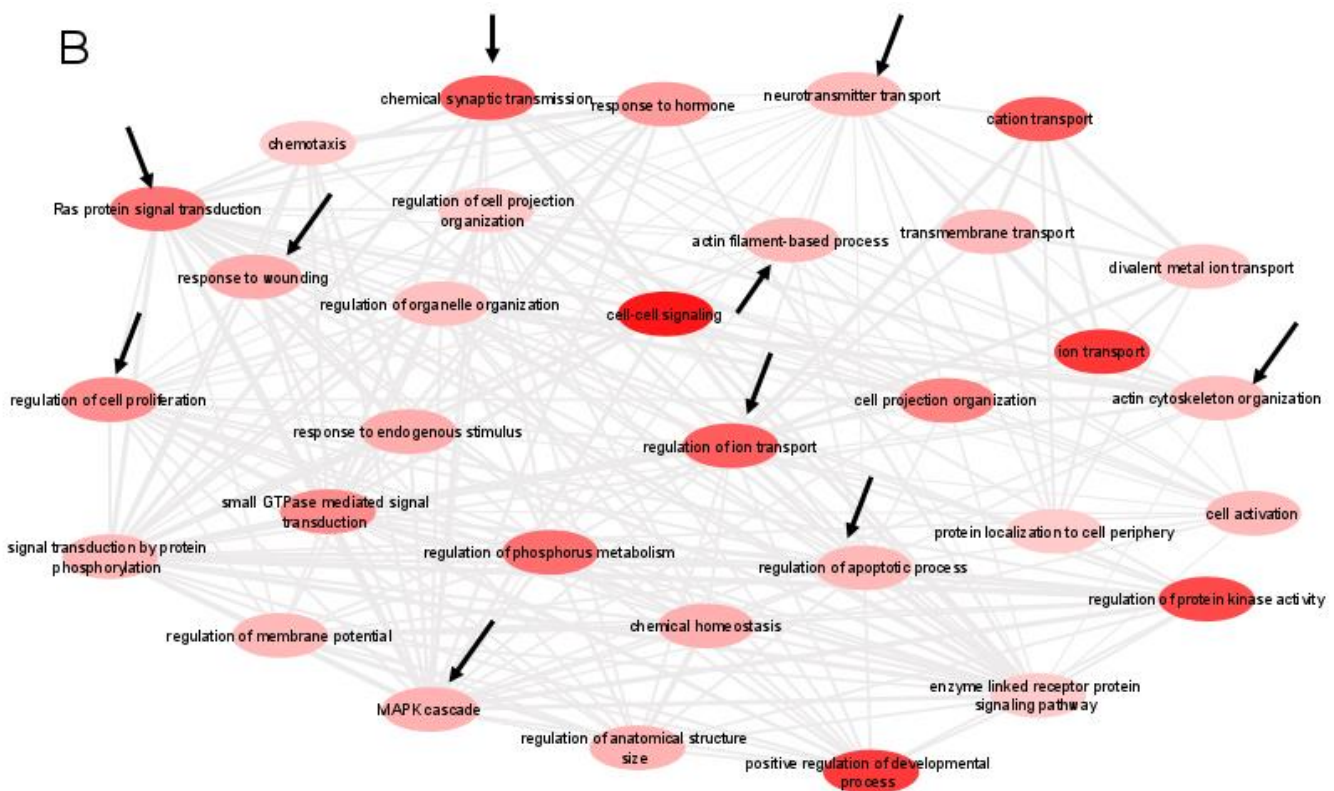


**Figure 3.14: Pathway interactions of predicted gene targets of DE miRNAs from comparison OA-Lesioned vs OA-Intact-1 and OA-Intact-1 vs OA-Intact-2.** Predicted targets of DE miRNAs from comparisons A) OA-Lesioned vs OA-Intact-1 and B) OA-Intact-1 vs OA-Intact-2 were uploaded on ToppGene Suite which generated a list of GO terms. GO terms were pasted in REViGO for selection of key biological pathways. Biological pathways were visualised with Cytoscape Version 3.8.2, which generated the figures. Pathways of interest are indicated with black arrows.

### **3.5 Discussion**

OA is the most common joint disease that affects millions of people worldwide and especially the elderly population. It is considered a whole joint disease with several joint tissues affected. Amongst them, cartilage is, by far, the most researched tissue in OA. Ageing is the most prevalent risk factor for OA and it is thought that cartilage changes that accumulate with increasing ageing contribute to OA. An evolving area in cartilage ageing and OA that has attracted scientific interest is epigenetic alterations and, specifically, changes in miRNA expression. Scientific and technical advancements have enabled the interrogation of the whole miRNAome in tissue homeostasis and disease. In this project, I undertook a microarray analysis approach to detect changes in miRNA expression between young intact, old OA intact and old OA lesioned cartilage and investigate how differentially expressed miRNAs could contribute to cartilage ageing and disease.

Old OA intact and lesioned cartilage samples were collected from patients undergoing TKA. Prior to surgery, lateral and medial condyles were assessed radiographically and scored, based on the KL grading system. Analysis showed that, per patient, OA intact samples were collected from the lateral condyle and OA lesioned samples from the medial condyle. Moreover, it was shown that lateral condyles were graded significantly lower than medial condyles ( $p=0.03$ ). This is to be expected as the medial is the most weight-bearing condyle between the two and usually more affected than the lateral (Pelletier et al., 2007). Macroscopic scoring using the Outerbridge grading system confirmed that the lateral condyles were less damaged than the medial condyles, per patient. To avoid scorer bias, two independent scorers graded the sections in two different time points. Results showed that there was a good level of agreement between the scorers and analysis was reproducible.

Histologic assessment and scoring using the Mankin HHGS and the OARSI grading system generally confirmed radiographic and macroscopic assessments. For all but two patients, intact samples were graded lower than lesioned samples with the Mankin HHGS, although the difference between these scores was small. For patient 9, the intact sample was scored higher than the lesioned sample (average 3.5 compared to 1.75) and for patient 10, intact sample had the same score as the lesioned sample (average 1.5 for both), in contrast to KL and Outerbridge scores for these patients, where intact samples were graded lower than

lesioned. One possible explanation for this, is that biopsies taken from specific parts of the condyles were not representative of the joint as a whole (Moskowitz, 2006). This could explain partially why results for the Mankin HHGS did not reach statistical significance ( $p=0.12$ ). This also applies to the OARSI scoring system ( $p=0.26$ ). The OARSI scoring system utilises not only the depth of the lesion (grade) but also the extent of damage in the articular surface (stage) to assess OA severity. However, this implies that sections be prepared from the whole condyle which was not possible for this project. Moreover, the OARSI system assesses bone deformation and remodelling (Pritzker et al., 2006) which was beyond the scope of this project. Therefore, partial use of the parameters outlined for each scoring system could lead to skewed or biased results. However, this does not undermine the use of histology, or suggests that KL and macroscopic scoring systems are better at assessing OA severity. This is because KL and Outerbridge scoring systems take into account specific criteria and the grades assigned have a limited range (from 0 to 4) and cannot distinguish between samples that are similar and only differ slightly. For such samples histologic assessment is more reliable in identifying underlying tissue differences, as long as different parts of the joint are assessed. Although there was a good agreement between radiographic, macroscopic and histologic assessment for most patients in our study, it is preferred, when possible, to utilize different scoring approaches for better assessment of tissue integrity and OA severity. Moreover, another point that should be taken into account is donor variability. Even though for the same patient, intact samples are generally graded lower than lesioned samples, this might not be the case when comparing different patients to each other, as the intact sample from one patient could have the same or slightly higher score than the lesioned sample of another patient. All samples came from end-stage OA patients following TKA, however, this does not mean that lateral and medial condyles from different patients have the same degree of cartilage damage. As OA is a heterogeneous disease, there are many factors, apart from cartilage loss, that could affect a patient's decision to have TKA, including pain in the joint, level of discomfort, degree of disability and interference with everyday activities (Skou et al., 2015). In our data set, this is also evident from the error bars in the scatter plots for the Mankin and OARSI scores (**Figure 3.5**), which implies some degree of patient variability, even though our data suggests that the general trend is that intact samples had lower scores than the lesioned samples.

For microarray analysis, three different groups were used: young intact cartilage from patients undergoing ACL reconstruction, old OA intact and lesioned cartilage from patients undergoing TKA (collected from the same OA patients). This project aimed to identify DE miRNAs in ageing and diseased cartilage, hence the use of young intact samples. An important note here is the suitability of cartilage from young ACL patients as the control/reference group. Rupture of the cruciate ligament is a known risk factor for developing PTOA as the rupture destabilises the knee joint if left untreated or in some cases even after reconstruction (Ajued et al., 2014). In a follow up study, about 34% of patients who had ACL surgery showed signs of slight joint degeneration (KL=1) and approximately 30% showed moderate degeneration (KL=2), ten years after surgery. Perhaps, changes in the joint following ACL injury that lead to OA might not appear until years after rupture. In this project, all young samples were collected from patients who had reconstruction weeks to a few months after injury and therefore this time frame may not have been enough for changes to be established in cartilage. Moreover, young cartilage was collected from the intercondylar notch, an area which is not heavily affected by OA. MRI longitudinal studies in weight-bearing knee areas of OA patients showed that the most cartilage volume loss over a period of 24 months was observed in the medial condyle, followed by the lateral condyle and the area less affected was that of the intercondylar notch (Pelletier et al., 2007). In our study, young cartilage from the notch was inspected for any pathological changes during collection and intact tissue was collected. Histologic assessment would have provided more details about to tissue integrity of young intact cartilage samples and their suitability to be used as the control group in our microarray analysis. However, that was not possible due to the small amount of cartilage tissue collected from these young ACL patients, which was enough for RNA extraction only and did not allow its use for histologic assessment as well.

Following microarray analysis, the 2-D PCA plot generated showed a wide distribution of samples. Even though young intact samples clustered tighter together, old OA samples clustered more widely. Old OA lesioned samples did not cluster as tight as young samples but could still be considered as one group. However, old OA intact samples clustered in two distinctive subgroups: OA-Intact-1 and OA-Intact-2. This could be due to the 10-year age difference (OA-Intact-1:  $56 \pm 3.5$  years, OA-Intact-2:  $67 \pm 4.6$  years) or tissue integrity of the samples in these subgroups. Our results showed that OA-Intact-1 group had lower KL,

Outerbridge, Mankin and OARSI scores compared to OA-Intact-2 group (**Table 3.7**) even though differences between the two groups were not significant. Therefore, the separation of the OA intact group observed in our microarray data could be the result of different OA severity amongst the samples of the group. In our experience, this was not generally unexpected. In a previous microarray study published by our group, I compared the expression of miRNAs between a smaller number of young cartilage samples from ACL donors and old OA intact cartilage from TKA donors (Balaskas et al., 2017). Analysis showed that old OA intact cartilage samples were separated in three different clusters based on OA severity, defined by KL radiographic assessment. Results from our previous study and this study suggest the accumulation of biological variation in miRNA expression with ageing and OA. Furthermore, as already discussed, OA is a heterogeneous disease characterised by different phenotypes, risk factors and clinical symptoms amongst patients (Roman-Blas et al., 2020). Therefore, subgrouping might indicate underlying molecular differences.

Several DE miRNAs were identified in each comparison. First, I compared the old OA intact group to the young group and the old OA lesioned group to the young group, as this was the primary focus of the project. Most of DE miRNAs identified in these comparisons had lower expression in the old OA groups compared to the young intact group. This was in accordance with our previous study in cartilage, discussed previously (Balaskas et al., 2017). In fact, the list of DE miRNAs was similar in all three comparisons (OA-Lesioned vs Y, OA-Intact-1 vs Y and OA-Intact-2 vs Y). This indicated that, as expected, old OA groups were more similar to each other than to young samples. This was also apparent by the number of DE miRNAs between all comparisons, as there were more DE miRNAs when old OA groups were compared to the young intact group than to each other. This is expected as there are more biological factors that could drive miRNA differences when comparing the young group to the old OA groups. These include mainly ageing and OA. Apart from the fact that disease is one of the major differences between young ACL and old OA donors in our data set, there was also an approximate 40-year age difference between young donors and old OA donors. In contrast, old OA intact and lesioned cartilage was collected from the same OA donors and therefore ageing was not a critical factor driving miRNA expression when the old OA groups were compared to each other. Therefore, it is expected that the number of DE miRNAs would be higher when the old OA groups were compared to the young group than to each other. In

fact, most dysregulation was observed in the OA-Intact-1 vs Y comparison, based on the number of DE miRNAs. Predicted gene targets of DE miRNAs from these three comparisons revealed that these are involved in cartilage and OA-related pathways including inflammation, cytokine production, secretion and signalling all of which are linked to cartilage ageing and OA (Chow et al., 2020, Sokolove et al., 2013, Wojdasiewicz et al., 2014).

Following initial analysis, old OA groups were compared to each other. Of the three OA groups, OA-Intact-2 and OA-Lesioned groups were more similar to each other than to OA-Intact-1 group, also evident by the number of DE miRNAs between these comparisons (**Table 3.8**). When comparing OA-Intact-1 group to OA-Lesioned and OA-Intact-2, there were 123 and 115 DE miRNAs, respectively, in contrast to OA-Lesioned vs OA-Intact-2 comparison, where there were only 12 DE miRNAs. This could be due to the differences between OA-Intact-1 and 2 groups mentioned previously. Samples in OA-Intact-1 were graded lower (less severe OA) compared to samples in OA-Intact-2 and OA-Lesioned groups. Tissue integrity was more compromised in OA-Intact-2 group, thus more similar to the OA-Lesioned group. By looking at the biological processes and the predicted targets of DE miRNAs from each of these comparisons, it was found that DE miRNAs in OA-Lesioned vs OA-Intact-1 and OA-Intact-1 vs OA-Intact-2, were involved in regulation of cell proliferation, actin and cytoskeleton organisation, chemokine signalling, ion transport, responses to wounding, apoptosis and neurotransmitter transport. This is in agreement with the results reported by Soul *et al* (2018), where they compared gene expression between old OA intact cartilage samples and age-matched non-OA cartilage samples (Soul et al., 2018). In this study, old OA intact samples were clustered into two sub-groups: Group A and Group B. As in our study, Group A had lower Mankin Score and age mean compared to Group B and Group B included genes related to mechanotransduction, actin and cytoskeleton regulation and ion transport. Comparison of these two subgroups revealed DE genes involved in oxidative stress, immune responses, chemokine signalling, apoptosis, calcium and ion regulation (Soul et al., 2018), which are similar to our study when I compared OA-Intact-1 to OA-Intact-2. In fact, our study showed that there was a shift in the biological pathways/molecular mechanisms, when comparing young samples to old OA groups and when comparing old OA groups amongst each other. When old OA groups were compared to the young group, inflammation and cytokine-related pathways were more prominent. In contrast, when old OA groups were compared to each

other, inflammation-related pathways were not the prominent pathways identified. This may suggest that after inflammation is established in the joint, there are not major changes in the levels of inflammatory cytokines that are released as OA progresses. This is in agreement with other studies where they failed to identify major changes in inflammatory genes between intact and lesioned OA samples (Dunn et al., 2016).

Pathways identified when comparing old OA groups to each other, such as cell morphology, cell proliferation, apoptosis, ion transport, wound healing, blood circulation and neuron-related pathways, highlight the biological processes that take place during OA progression. These include changes in tissue integrity as cartilage breaks down and chondrocytes become hypertrophic and apoptotic. The wound healing pathway identified in the analysis is closely linked to transition from intact to lesioned cartilage. As the process of cartilage break down begins, there is a tissue reaction to compensate for the loss of ECM (Goldring et al., 2016). The results reported here indicate that such alterations in tissue morphology and wound healing are also reflected on the cartilage miRNAome. Of note is the identification of cation/ion-transport related pathways when the old OA groups were compared, and especially when the OA-Lesioned group was compared to the OA-Intact-1 group. Chondrocytes have a defined channelome which responds to mechanical and physical stimuli (Mobasher et al., 2019). Our analysis revealed, intact samples came from the lateral condyle and lesioned samples from the medial condyle. During OA, the medial condyle is subjected to higher mechanical pressures compared to the lateral condyle. This could affect ion channel responsiveness between the two areas of cartilage, leading to altered ion and biomechanical-related pathways between areas of high and low loading. When Dunn *et al* (2016) compared gene expression between intact and lesioned areas of cartilage, they identified DE genes involved in, amongst others, mechanical loading and stimuli. The fact that predicted target genes of DE miRNAs identified in OA-Lesioned vs OA-Intact-1 were also involved in mechanotransduction, confirms the important function of miRNAs in several aspects of cartilage biology and homeostasis.

Finally, two other biological processes that were identified as significant when comparing old OA intact and lesioned groups were blood circulation and neuronal signalling. Cartilage is devoid of blood vessels and neurons. However, in advanced stages of OA, when significant tissue has been lost, increased angiogenesis is observed in subchondral bone and blood

vessels penetrate calcified cartilage (Mapp et al., 2012). Blood invasion is also accompanied by innervation in areas of the joint that normally do not have any sensory neurons, leading to increased pain in the joint (Mapp et al., 2012). At first, pain is nociceptive occurring when the joint moves. However, as OA progresses, pain can be present even during resting phases or during the night and this coincides with greater cartilage damage (Schaible, 2012). Even though there is not a direct correlation between radiographic findings and pain, it was reported that OA patients with higher KL score have more incidents of pain and this was linked to more loss of cartilage damage in the medial condyle (Eckstein et al., 2011). This is consistent with our analysis, as the comparison between OA-Intact-1 and OA-Lesioned samples, where the biggest differences in scoring/cartilage loss were observed, identified DE miRNAs that could be involved in neuronal/pain-related pathways, further cementing the role of miRNAs in cartilage homeostasis and different stages of disease and highlighting the interplay between different tissues in the joint and their contribution to OA.

### **3.6 Conclusion**

Microarray analysis between young intact, old OA intact and old OA lesioned human knee cartilage samples identified a distinctive profile of DE miRNAs in ageing and OA cartilage of different damage stages. Analysis suggested that there are several disease mechanisms that can contribute to OA and within these mechanisms, miRNAs play an important role from initiation to disease progression. This highlights that gene regulation in cartilage is a multi-layered process and is indicative of the complex molecular landscape that underlies cartilage damage and OA. In the next chapters, I validated a selected set of DE miRNAs from our microarray results and further investigated their role in cartilage homeostasis and OA.

**Chapter 4: Validation of miRNA profiling in  
young intact, old OA intact and old OA  
lesioned human cartilage and investigation  
of selected miRNAs in an in vitro OA  
inflammatory model**

## 4.1 Introduction

There has been a significant increase in the number of publications regarding miRNAs and OA in the last decade. MiRNAs have been linked to important biological pathways in cartilage and OA such as inflammation, hypertrophy, apoptosis and mechanotransduction (Chen et al., 2016b, Gu et al., 2021, Hecht et al., 2019, Liao et al., 2020). Inflammation is one of the most prominent changes that characterise ageing and OA cartilage. Aged senescent chondrocytes exhibit a secretory phenotype by producing higher levels of pro-inflammatory cytokines, leading to the establishment of low-grade inflammation in the joint, called inflammingeing (Loeser, 2010). Inflammingeing, together with other factors, such as injury and mechanical stress, contributes to the development of OA and of a more severe inflammatory response. This leads to extended changes in the joint and contributes to cell apoptosis and cartilage loss (He et al., 2020).

Inflammation of the OA joint is evident, not only in the tissue level, but at a molecular level. A key part of this inflammatory response is IL-1 $\beta$ , a pro-inflammatory cytokine which has major roles in OA-related molecular pathways (for more detailed information please refer to Chapter 1, **Figure 1.12**). IL-1 $\beta$  affects expression of important cartilage and ECM components, such as collagens, aggrecan, MMPs and ADAMTSs, but also promotes the expression of other pro-inflammatory cytokines, such as TNF- $\alpha$  and IL-6 (Chow et al., 2020). Moreover, inflammation, and IL-1 $\beta$  specifically, affect the expression of several miRNAs and their target genes. *In vitro* experiments using IL-1 $\beta$ -treated primary chondrocytes have shed light on the role of IL-1 $\beta$  in miRNA expression (Papanagnou et al., 2016). These experimental conditions mimic an OA inflammatory environment and provide the opportunity to investigate OA-related gene responses and disease mechanisms *in vitro*. Of significant use are microarray studies which compare miRNA expression in IL-1 $\beta$  treated chondrocytes compared to control, as they provide the opportunity to investigate several miRNA changes in response to IL-1 $\beta$ . One such study, from Akhtar et al (2010,) identified 44 DE miRNAs (2 upregulated and 42 downregulated) in OA chondrocytes treated with 5ng/ml or 10ng/ml IL-1 $\beta$  for 6h (Akhtar et al., 2010). In a similar study, Rasheed et al (2016) identified one upregulated and 35 downregulated miRNAs in OA chondrocytes treated with 5ng/ml IL-1 $\beta$  for 24h, including several miRNAs from the *let-7* family (Rasheed et al., 2016). Therefore, this experimental system is useful in studying OA-like inflammatory changes in chondrocytes *in vitro*.

## **4.2 Study aim and rationale**

Microarray analysis in Chapter 3 identified DE miRNAs between young intact, old OA intact and old OA lesioned cartilage collected from knee joints of young patients undergoing ACL reconstruction, and old OA patients undergoing TKA. In this chapter, qPCR validation of selected miRNAs was carried out in:

- i) the same cartilage samples used in the microarrays (dependent cohort)
- ii) an additional cohort of young intact, old OA intact and old OA lesioned cartilage samples (independent cohort)
- iii) young healthy and old healthy cartilage samples from cadavers

Moreover, in Chapter 3, IPA analysis of DE miRNAs from comparisons OA-Intact vs Young, and OA-Lesioned vs Young identified inflammatory response and cytokine signalling amongst the main pathways that these miRNAs are involved in. Furthermore, IL-1 $\beta$  was identified as an upstream regulators of these DE miRNAs and their predicted targets. Therefore, to further investigate the expression of selected miRNAs in an OA *in vitro* inflammatory model, primary OA chondrocytes were treated with human IL-1 $\beta$  for different time points.

## **4.3 Experimental design**

The experimental procedures, pertinent to this chapter, are described briefly below. For full details on the experimental procedures, please refer to Chapter 2. Appropriate references are provided throughout the text.

### **4.3.1 Selection of specific DE miRNAs for follow up studies following microarray analysis**

For validation of microarray results by qPCR, specific DE miRNAs were selected for follow up studies. As described in Chapter 3, the list of DE miRNAs in comparisons OA-Lesioned vs Y, OA-Intact-1 vs Y and OA-Intact-2 vs Y were similar and therefore I selected miRNAs from these

three comparisons as I was interested in including all three major cartilage groups (young, old OA intact and lesioned). Specific DE miRNAs were selected based on the following criteria:

- only mature miRNA forms were selected for further validation
- fold change, as I chose those with logFC <-3 or >3 in all three comparisons
- known and predicted importance in cartilage biology, based on the available literature and known/predicted target genes generated by target prediction tools as described in Section 2.35.

Additionally, miRNAs that belonged to families with very similar sequences, such as miRNAs of the let-7 family and miRNA isoforms (miRNAs denoted with -a, -b, -c and so on) were excluded from further follow up, as qPCR technology may not be sufficient to conclusively distinguish between these. Finally, other candidates were selected for qPCR validation, based on known function in cartilage biology from the available literature.

In addition, miRNAs with no/limited data regarding their function in cartilage were also selected for qPCR validation. These miRNAs were investigated further in young healthy and old healthy cartilage samples from cadavers, and primary chondrocytes treated with IL-1 $\beta$ .

#### **4.3.2 Human knee cartilage specimens used for qPCR validation of microarray results**

Validation of microarray results was carried out by qPCR in the same samples that were used for microarray analysis (dependent cohort), as well as in an independent cohort of cartilage samples also from male donors. Patient characteristics for the dependent cohort can be found in Chapter 3, Section 3.3.1. For the independent cohort, the following samples were used:

- i) Young intact cartilage from patients undergoing ACL reconstruction (n=8, age $\pm$ SD=21 $\pm$ 6.5). Samples were collected from the area of the intercondylar notch, as described in Section 2.2.

- ii) Old OA intact cartilage from patients undergoing TKA (n=7, age $\pm$ SD=62.1 $\pm$ 3.7). Intact OA cartilage samples were collected from the most grossly intact area of the femoral condyles of OA patients, as described in Section 2.1.
- iii) Old OA lesioned cartilage from patients undergoing TKA (n=7, age $\pm$ SD=62.1 $\pm$ 3.7). Lesioned OA cartilage samples were collected from a lesioned area of the femoral condyles of OA patients, as described in Section 2.1.

#### **4.3.3 Young healthy and old healthy human knee cartilage specimens for the investigation of ageing in selected miRNAs**

Microarray analysis identified DE miRNAs between young intact and old OA intact and lesioned cartilage samples from knee joints of young patients undergoing ACL reconstruction and old OA patients undergoing TKA. There were two main variables driving the differential expression between these groups: ageing and OA. To further clarify whether ageing alone could affect the expression of selected miRNAs, young healthy and old healthy human knee cartilage samples were collected from male cadavers with no history of knee pain and disease and an unrelated cause of death (ProteoGenex, Inglewood, USA). These samples were macroscopically normal. Specifically, the following samples were used:

- i) Young healthy cartilage from cadavers (n=5, age $\pm$ SD=32 $\pm$ 3.7). Samples were collected from the knee femoral lateral and medial condyles.
- ii) Old healthy cartilage from cadavers (n=5, age $\pm$ SD=62 $\pm$ 6.6). Samples were collected from the knee femoral lateral and medial condyles.

Further characteristics of these donors are listed in **Table 4.1** below.

**Table 4.1: Characteristics of young healthy and old healthy cartilage donors.**

Donor	Age	BMI	Comorbidities
Young-Healthy-1	32	30.9	N/A

Young-Healthy -2	35	24.8	N/A
Young-Healthy -3	32	29.6	Hypertension, chronic tonsillitis, impaired glucose tolerance
Young-Healthy -4	26	25.3	N/A
Young-Healthy -5	35	24.7	N/A
Old-Healthy-1	70	24.9	Gastric ulcer perforation, peritonitis
Old-Healthy-2	67	26.1	Coronary artery disease, atherosclerosis, hypertension, pelvic vein thrombosis, cardiosclerosis, prostatitis
Old-Healthy-3	56	25.7	Coronary artery disease, atherosclerosis, hypertension, history of cholecystectomy
Old-Healthy-4	63	25.9	Hypertension, atherosclerosis, myocardial hypertrophy, impaired glucose tolerance, coronary artery disease
Old-Healthy-5	55	24.2	Chronic alcoholism, secondary cardiomyopathy, liver steatosis

#### **4.3.4 Histologic assessment of young healthy and old healthy cartilage samples**

To confirm that young healthy and old healthy cartilage samples collected from cadavers had no pathologic perturbations, histologic assessment with H&E staining was undertaken to examine tissue integrity. Samples were cryosectioned as described in Section 2.5B and then stained with H&E as described in Section 2.6. Tissue sections were examined under the microscope for pathological perturbations.

#### **4.3.5 Treatment of human primary chondrocytes with human recombinant IL-1 $\beta$**

To investigate the effect of IL-1 $\beta$  on the expression of selected miRNAs, primary articular chondrocytes were extracted from non-OA donors undergoing autologous cartilage

transplantation after trauma/sport injury, and OA donors undergoing TKA (n=2 per group), as described in Section 2.22. Donor details are as below:

- i) Non-OA primary chondrocytes from autologous cartilage repair donors (n=2, age $\pm$ SD=48 $\pm$ 5.7, 1 male/1 female)
- ii) OA primary chondrocytes from OA patients (n=2, age $\pm$ SD=64.5 $\pm$ 4.9, 1 male/1 female)

Due to the limited number of non-OA donors available, and to optimise treatment time points, OA chondrocytes from one donor were treated for 6h and 24h. Based on these results further treatments in more donors were undertaken for 24h and 5 days (n=5 OA donors). Furthermore, to investigate the extent of the inflammatory response in chondrocytes *in vitro*, the effect of IL-1 $\beta$  on the following cartilage and OA-related markers was measured: *COL2A1*, *ACAN*, *MMP13* and *ADAMTS4*, after 24h and 5-day treatments.

#### **4.3.6 Total RNA extraction from human cartilage samples and primary chondrocytes for qPCR validation**

For the dependent cohort of microarray analysis, total RNA was extracted as described in Section 2.13.1. This consisted of total RNA that was not used for microarray analysis.

For the independent cohort, additional samples of young intact, old OA intact and lesioned human cartilage tissue were homogenised as described in Section 2.12. Total RNA was extracted using the mirVana™ miRNA Isolation Kit with phenol, as described in Section 2.13.1.

For the young healthy and old healthy cartilage samples, plus the human primary chondrocytes, total RNA was extracted as described in Section 2.13.3. Total RNA was extracted using the guanidinium thiocyanate-phenol-chloroform method (TRIzol).

#### **4.3.7 Poly(A) cDNA synthesis for miRNA quantification**

Poly(A) cDNA for miRNA quantification by qPCR was synthesised from total RNA as described in Section 2.16.

#### **4.3.8 cDNA synthesis for mRNA quantification**

cDNA synthesis for mRNA quantification by qPCR was synthesised from total RNA as described in Section 2.17.

#### **4.3.9 qPCR for miRNA and mRNA quantification**

miRNA and mRNA quantification by qPCR was undertaken as described in Section 2.18 and 2.19, respectively. Statistical analysis was undertaken in GraphPad Prism version 8.0.1 for Windows and normality of data was assessed using the Shapiro-Wilk normality test. For miRNA quantification in human cartilage tissue, statistical significance was calculated using the Mann-Whitney test, as data did not follow the Gaussian distribution. For miRNA and mRNA quantification in IL-1 $\beta$  treated and control human primary chondrocytes, statistical significance was calculated using a two-tailed paired t-test, as data followed the Gaussian distribution. P values<0.05 were considered significant.

#### **4.3.10 Selection of endogenous reference genes for qPCR data normalisation**

For qPCR validation of microarray analysis, five potential reference genes were selected for testing. Two of them, RNU6 and SNORD61, were widely used in the literature for miRNA normalisation, and three of them, miR-1915-3p, miR-6786-5p and miR-6087, were selected from the microarray results as having high and stable expression in all samples (mean log expression >10 and SD <0.5). For IL-1 $\beta$  treatment, three potential reference genes were selected for testing: SNORD68, miR-6786-5p and RNU6. Selection of the appropriate reference genes for qPCR data normalisation was carried out as described in Section 2.40.

## 4.4 Results

### 4.4.1 Selection of specific DE miRNAs from microarray analysis

For selection of DE miRNAs from microarray analysis, I focused on three comparisons: OA-Lesioned vs Y, OA-Intact-1 vs Y and OA-Intact-2 vs Y. After applying filters of logFC <-3 and >3, the list of DE miRNAs was reduced to 66 DE mature miRNAs, of which all had lower expression in the old OA groups compared to young (logFC<-3). There were no common mature miRNAs with logFC>3 in these three comparisons. The only comparison that contained mature miRNAs with logFC>3 was the OA-Intact-1 vs Y comparison and therefore no miRNAs with logFC>3 were selected for validation.

To further reduce the number of mature DE miRNAs, miRNAs with high sequence similarity, such as miRNAs of the *let-7* family, and miRNA isoforms were excluded from further analysis. This way the list was reduced to 35 DE mature miRNAs (**Table 4.2**).

**Table 4.2: Important DE mature miRNAs in young intact, old OA intact and old OA lesioned cartilage.**

miRNA	LogFC		
	OA-Lesioned vs Y	OA-Intact-1 vs Y	OA-Intact-2 vs Y
hsa-miR-107	-4.65	-8.97	-3.40
hsa-miR-1231	-3.07	-4.16	-3.26
hsa-miR-126-3p	-7.36	-7.86	-7.07
hsa-miR-127-3p	-4.01	-6.54	-3.75
hsa-miR-132-3p	-4.02	-5.14	-4.70
hsa-miR-139-5p	-4.31	-4.14	-4.30
hsa-miR-140-5p	-5.11	-6.99	-3.82
hsa-miR-143-3p	-7.35	-7.75	-7.36
hsa-miR-145-5p	-7.20	-8.85	-8.35
hsa-miR-152-3p	-5.37	-7.98	-4.80

hsa-miR-155-5p	-4.77	-6.25	-4.51
hsa-miR-16-5p	-6.62	-9.25	-5.11
hsa-miR-17-5p	-4.42	-5.96	-5.11
hsa-miR-185-5p	-3.59	-5.84	-4.10
hsa-miR-195-5p	-7.30	-9.55	-4.90
hsa-miR-21-5p	-3.20	-3.22	-3.07
hsa-miR-221-3p	-4.23	-6.69	-4.38
hsa-miR-222-3p	-4.80	-7.43	-3.80
hsa-miR-25-3p	-3.96	-4.56	-4.39
hsa-miR-28-3p	-3.35	-4.32	-4.10
hsa-miR-28-5p	-4.14	-4.10	-4.31
hsa-miR-342-3p	-4.40	-6.99	-4.13
hsa-miR-361-5p	-4.20	-7.54	-4.04
hsa-miR-379-5p	-4.50	-4.58	-4.77
hsa-miR-382-5p	-4.16	-4.98	-4.72
hsa-miR-409-3p	-3.92	-4.61	-3.90
hsa-miR-432-5p	-4.58	-5.11	-4.72
hsa-miR-4417	-3.30	-4.97	-4.88
hsa-miR-4485	-3.20	-4.08	-3.06
hsa-miR-455-5p	-3.62	-4.69	-4.18
hsa-miR-532-5p	-3.17	-4.06	-3.71
hsa-miR-6807-5p	-3.17	-3.58	-3.56
hsa-miR-6824-5p	-3.01	-3.53	-3.31
hsa-miR-8071	-3.61	-4.15	-4.17
hsa-miR-93-5p	-3.89	-5.66	-4.91

To narrow down further the number of DE miRNAs for validation I searched the available literature and investigated the predicted target genes or pathways that these miRNAs were involved in (predicted targets are analysed further in Chapter 5). Based on this criteria, I selected miRNAs that had previously been linked to cartilage biology and OA, but also novel

candidate miRNAs with limited or no data regarding their role in cartilage and OA. The final list of miRNAs for qPCR validation is in **Table 4.3**.

**Table 4.3: Final list of DE mature miRNAs for qPCR validation in young intact, old OA intact and old OA lesioned cartilage**

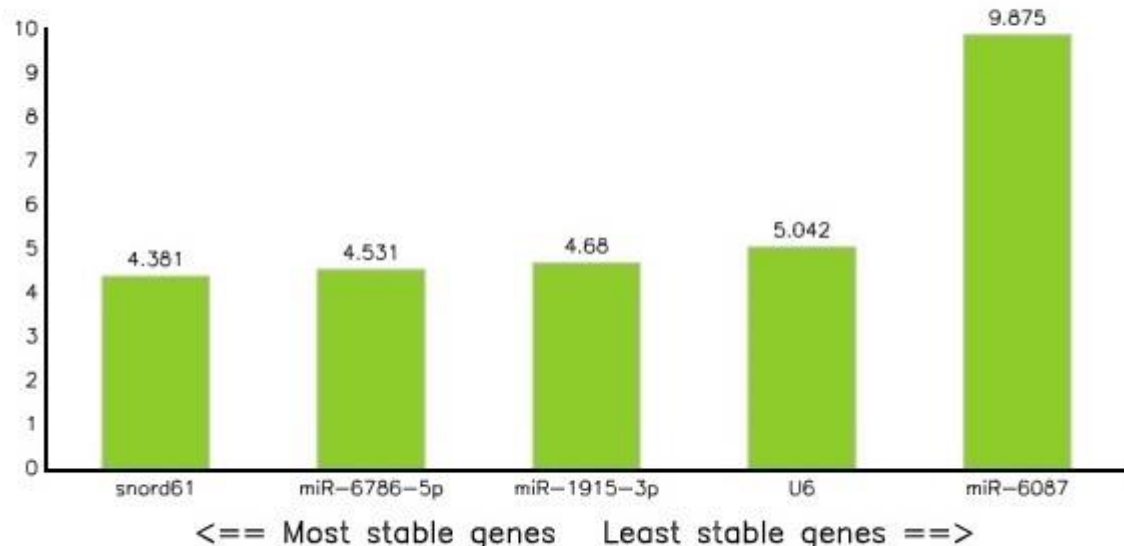
miRNA	Previously reported in cartilage-OA/novel candidate
miR-140-5p	Previously reported (Karlsen et al., 2014, Miyaki et al., 2009, Miyaki et al., 2010, Swingler et al., 2012)
miR-155-5p	Previously reported (Xu et al., 2015)
miR-143-3p	novel candidate
miR-107	novel candidate
miR-379-5p	novel candidate
miR-361-5p	novel candidate
miR-132-3p	novel candidate

#### 4.4.2 Selection of reference genes for qPCR data normalisation

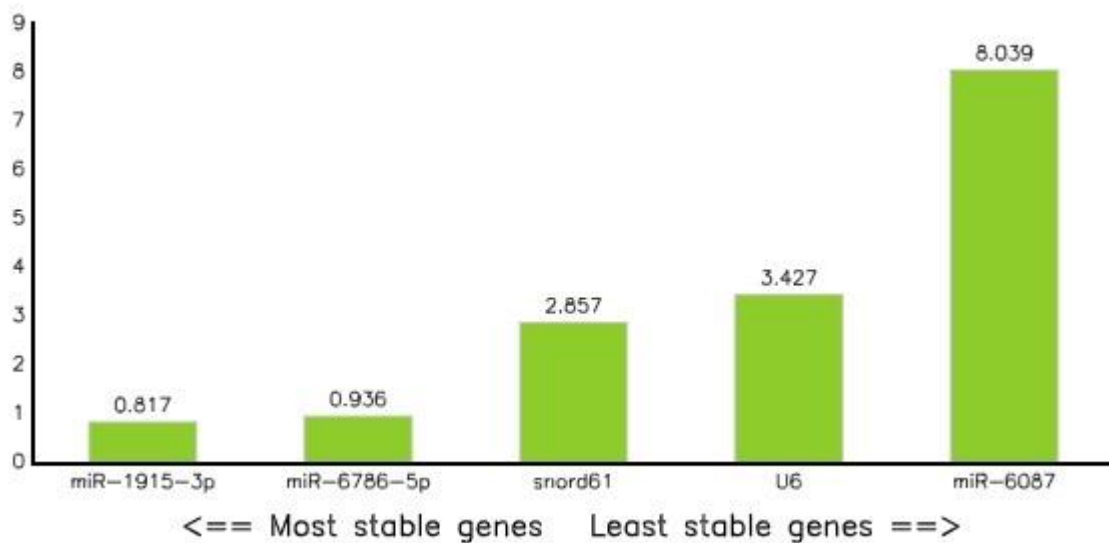
Appropriate reference gene was selected using RefFinder (Xie et al., 2012). RefFinder utilises four different tools for reference gene selection and one comprehensive ranking, based on all four tools. Results are shown in **Figure 4.1**. miR-6786-5p was selected as the reference gene for miRNA data normalisation in the dependent and independent cohort for qPCR validation of microarray findings.

**A**

Gene stability by Delta CT method

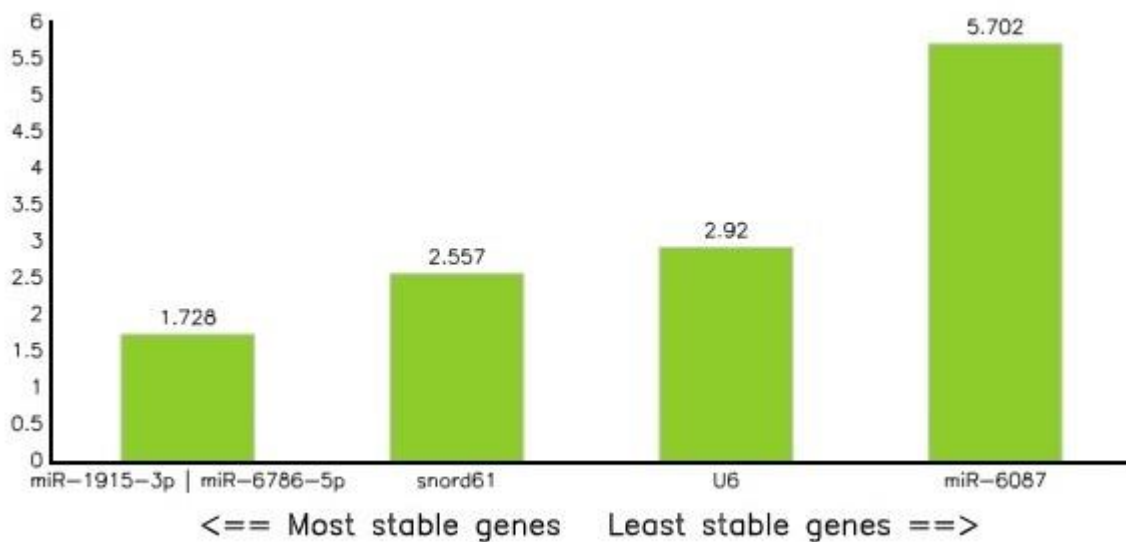
**B**

Gene stability by BestKeeper



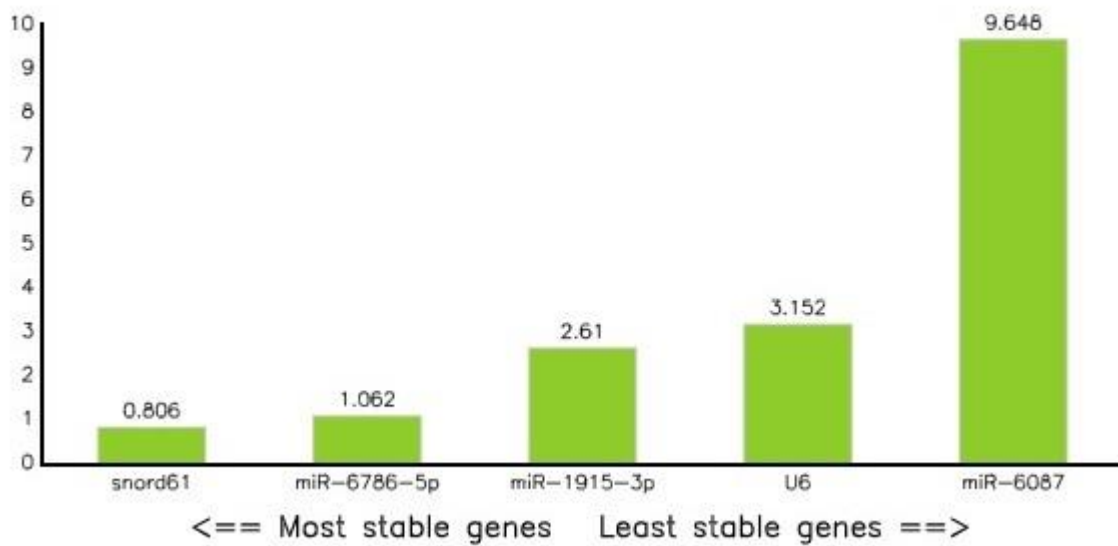
C

Gene stability by Genorm



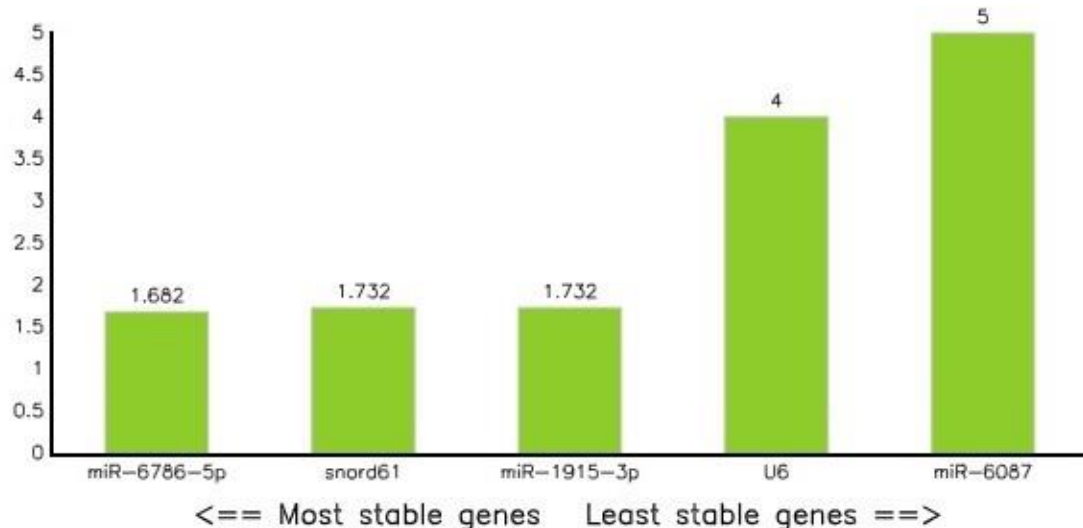
D

Gene stability by normFinder



E

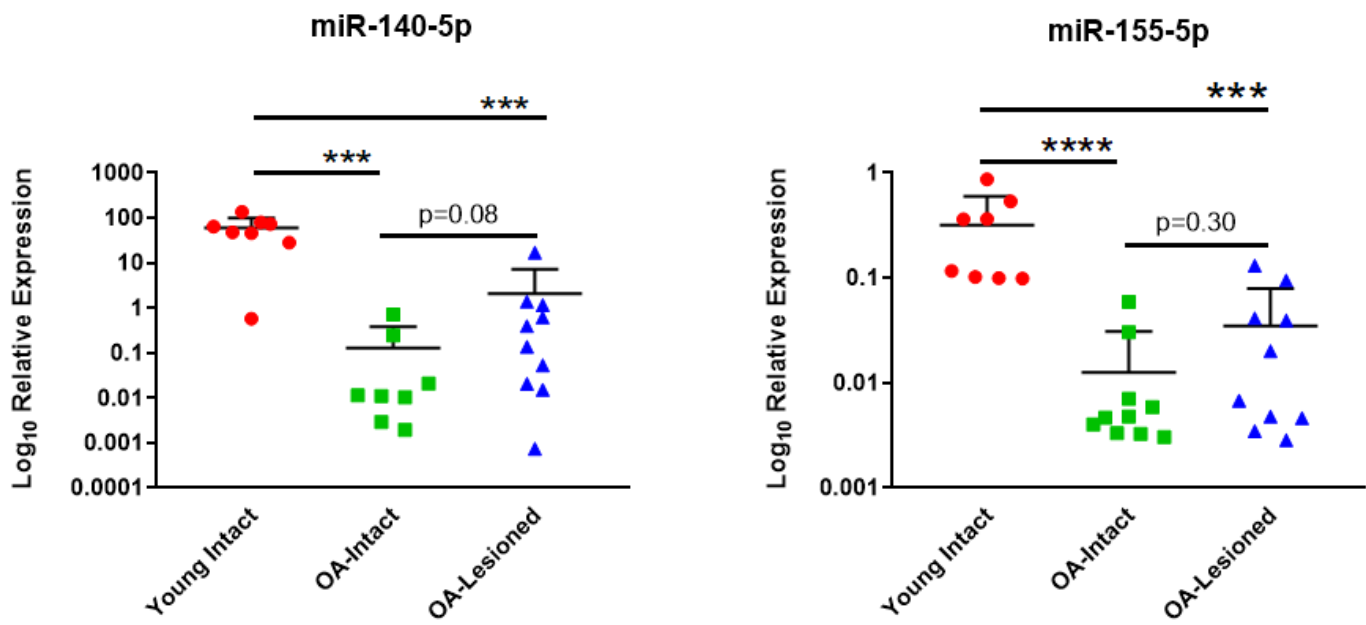
Comprehensive gene stability

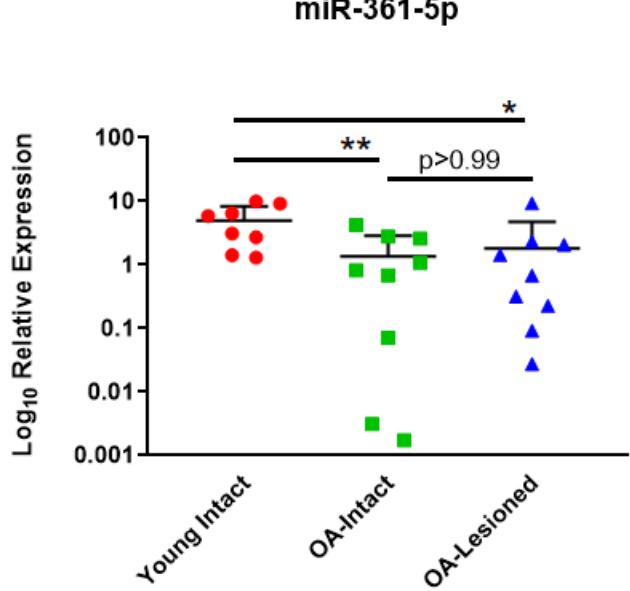
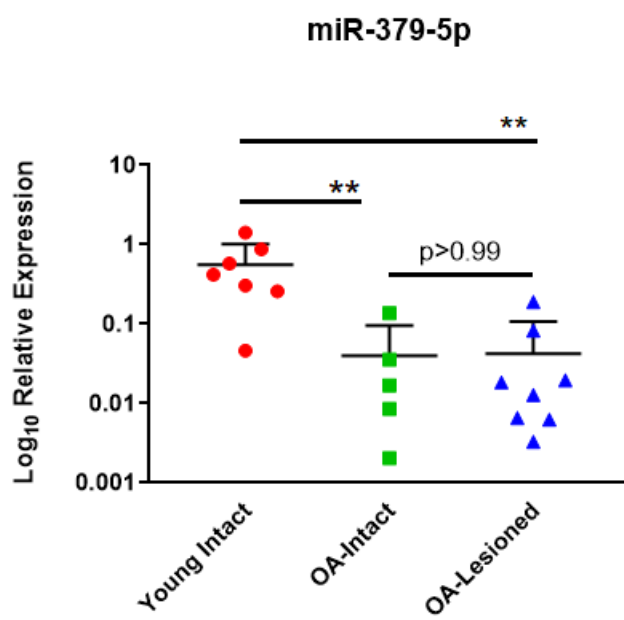
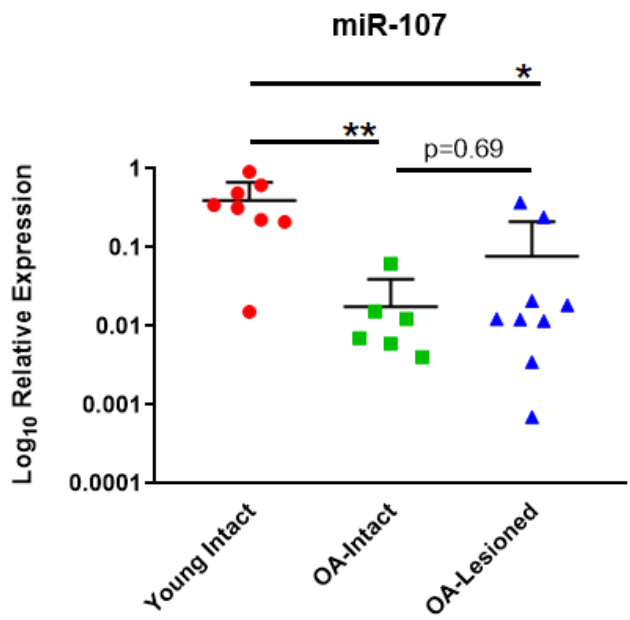
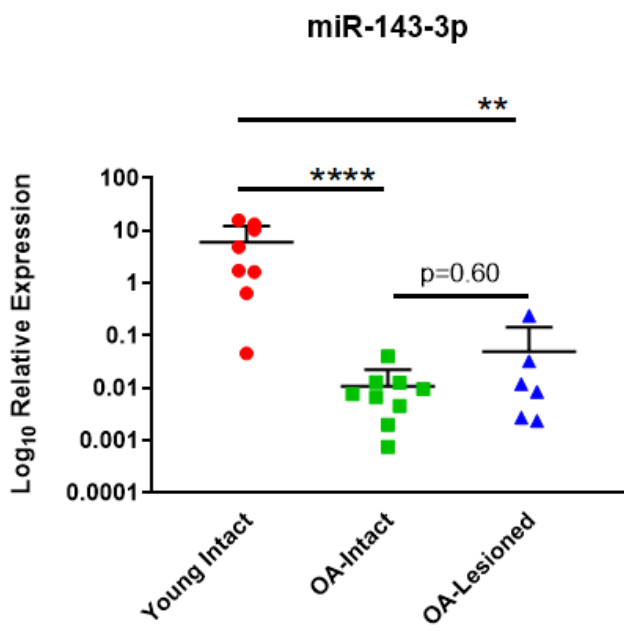


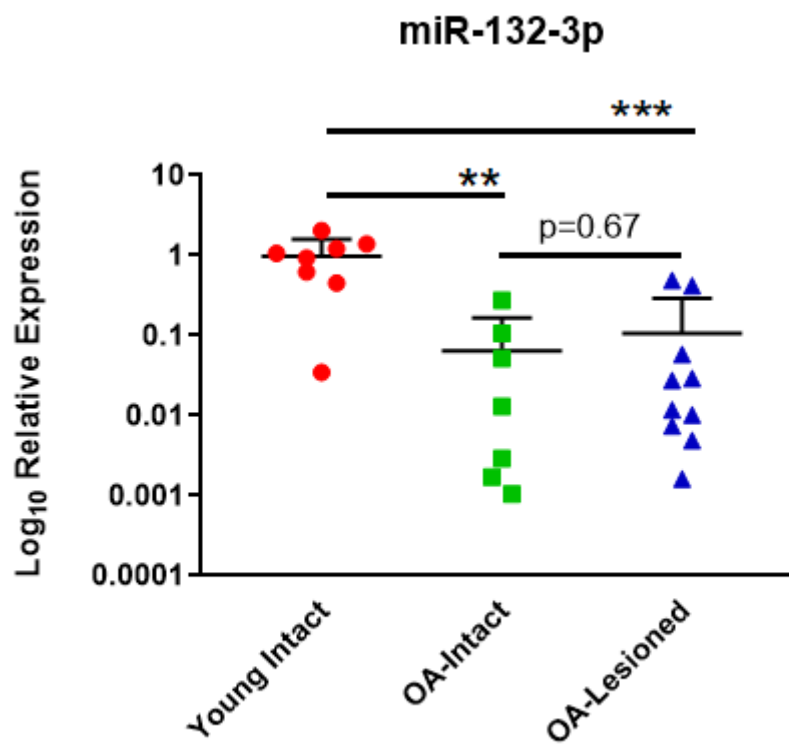
**Figure 4.1: Selection of appropriate reference gene for qPCR validation of microarray analysis.** RefFinder was used to select the appropriate reference gene for qPCR validation of microarray analysis. Five potential reference genes, SNORD61, RNU6, miR-6786-5p, miR-1915-3p and miR-6087, were ranked by each one of RefFinder tools (A, B, C, D) and a stability value was generated for each potential reference gene. The lower the value, the most stable the gene. A comprehensive gene stability ranking (E), integrating all results, showed that miR-6786-5p was the best reference genes out of the five. Graphs generated with RefFinder.

#### 4.4.3 qPCR validation of microarray findings in the dependent cohort

To validate microarray results from Chapter 3, I carried out qPCR analysis for a selected set of DE miRNAs, using RNA from the same donors as in the microarrays. Selected miRNAs had significantly lower expression in the OA-Intact and Lesioned groups when compared to Young group and followed the same trend as in microarray analysis (**Figure 4.2**). OA-Intact-1 and -2 groups, which were separated during microarray analysis, were grouped together in one cluster as both groups showed similar direction of dysregulation when compared to Young group. Moreover, as in microarray analysis, selected miRNAs were not significantly different between OA-Intact and OA-Lesioned groups and their expression was similar between the two groups.



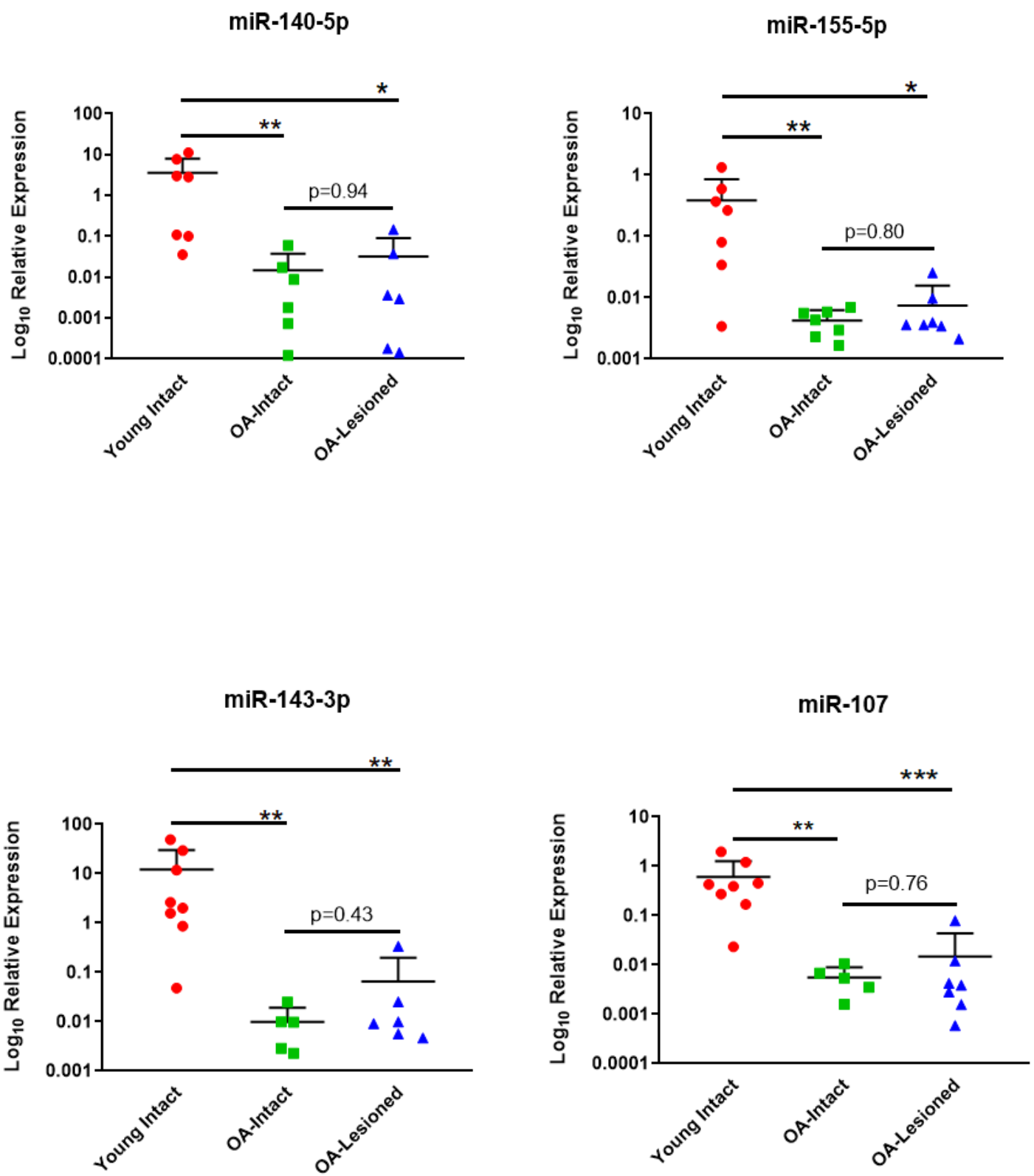




**Figure 4.2: qPCR validation of selected DE miRNAs in the dependent cohort.** Seven miRNAs which were DE in microarray analysis were selected for validation with qPCR in the same samples. N=5-10 samples/group. Y axis represents log-transformed expression relative to miR-6786-5p. Statistical analysis was undertaken using a Mann Whitney test in GraphPad Prism (Version 8.0.1). Data are represented as mean+SD (due to the logarithmic scale on Y axis, negative SD values cannot be plotted). P values<0.05 were considered significant. \*: p<0.05, \*\*: p<0.01, \*\*\*: p<0.001, \*\*\*\*: p<0.0001.

#### 4.4.4 qPCR validation of microarray findings in the independent cohort

After validating microarray findings in the dependent cohort, I sought to investigate expression of DE miRNAs in an independent cohort of Young, OA-Intact and OA-Lesioned cartilage samples. Analysis was undertaken by qPCR. Validation in the independent cohort is shown in **Figure 4.3**. Results indicated that selected miRNAs had significantly lower expression in OA-intact and lesioned groups compared to Young intact group. Moreover, as with the dependent cohort, expression of these miRNAs in the OA-intact group was lower than in the OA-lesioned group, but this change was not statistically significant.



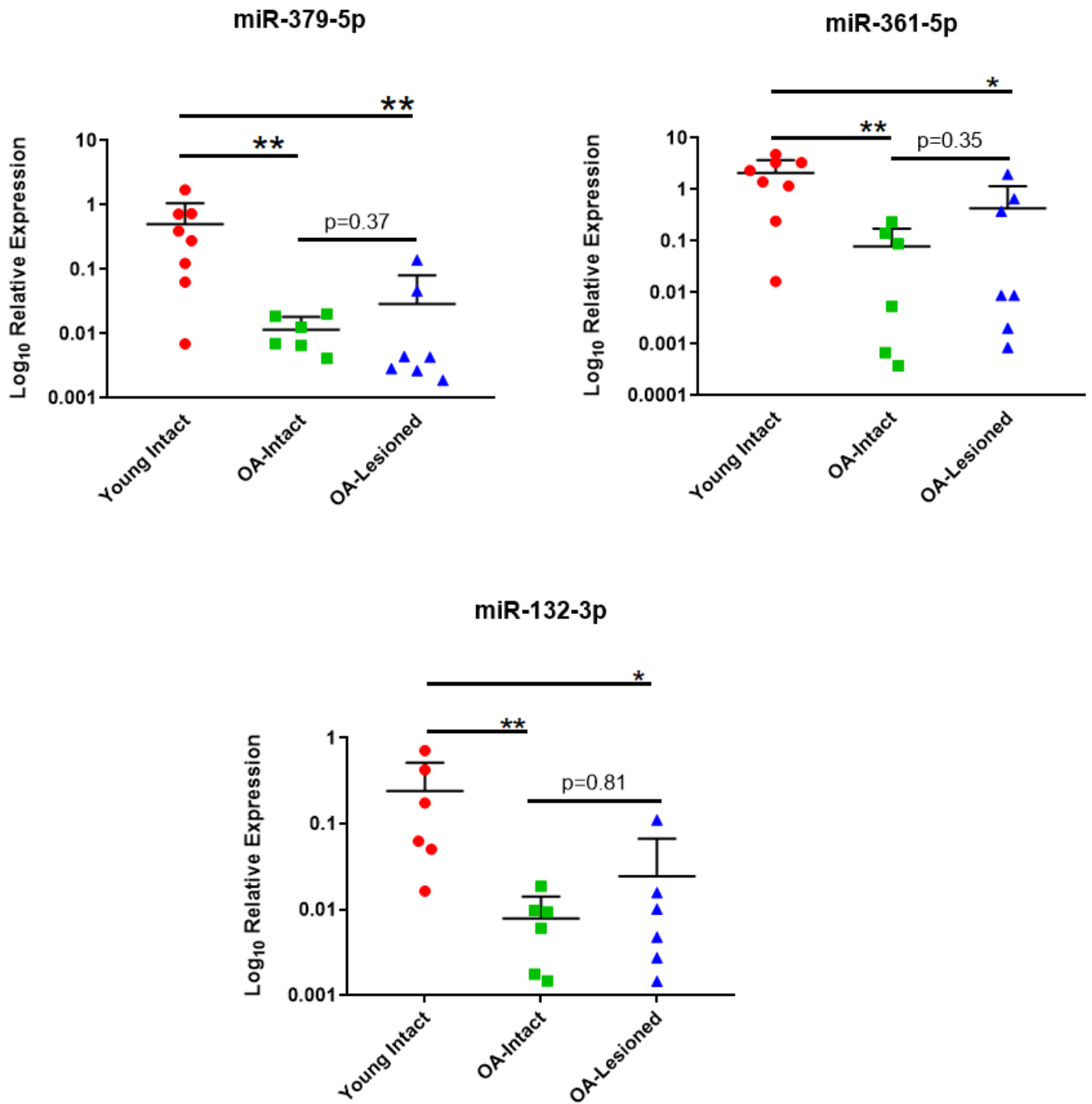


**Figure 4.3: qPCR validation of selected DE miRNAs in the independent cohort.** Seven miRNAs which were DE in microarray analysis were selected for validation with qPCR in an independent cohort of cartilage samples. N=5-10 samples/group. Y axis represents log-transformed expression relative to miR-6786-5p. Statistical analysis was undertaken using a Mann Whitney test in GraphPad Prism (Version 8.0.1). Data are represented as mean+SD (due to the logarithmic scale on Y axis, negative SD values cannot be plotted). P values<0.05 were considered significant. \*: p<0.05, \*\*: p<0.01, \*\*\*: p<0.001.

**Table 4.3** summarises and compares findings between microarray analysis and qPCR in the dependent and independent cohorts. Results showed that there was good agreement between microarray findings and qPCR validation for both cohorts. Specifically, the direction of dysregulation was the same for both microarray and qPCR analyses for all seven miRNAs selected. In addition, LogFC of expression was similar between microarray and qPCR results for OA-Intact vs Y, and OA-Lesioned vs Y. The largest difference was observed for miR-140-5p in OA-Intact vs Y comparison. miR-140-5p had logFC= -5.09 in the microarray analysis, and logFC= -10.40 in qPCR validation of the dependent cohort. However, for the independent cohort, miR-140-5p had logFC= -5.71, which agrees with the microarray findings. A similar finding was observed for miR-361-5p in comparison OA-Lesioned vs Y. miR-361-5p had logFC= -4.20 in microarray analysis, and logFC= -2.59 in qPCR validation for the dependent cohort. For the independent cohort, logFC of this miRNA was -3.74.

**Table 4.3 Comparison of direction of dysregulation and logFC between microarray analysis and qPCR validation in same samples used for microarray analysis and an independent cohort of cartilage samples.**

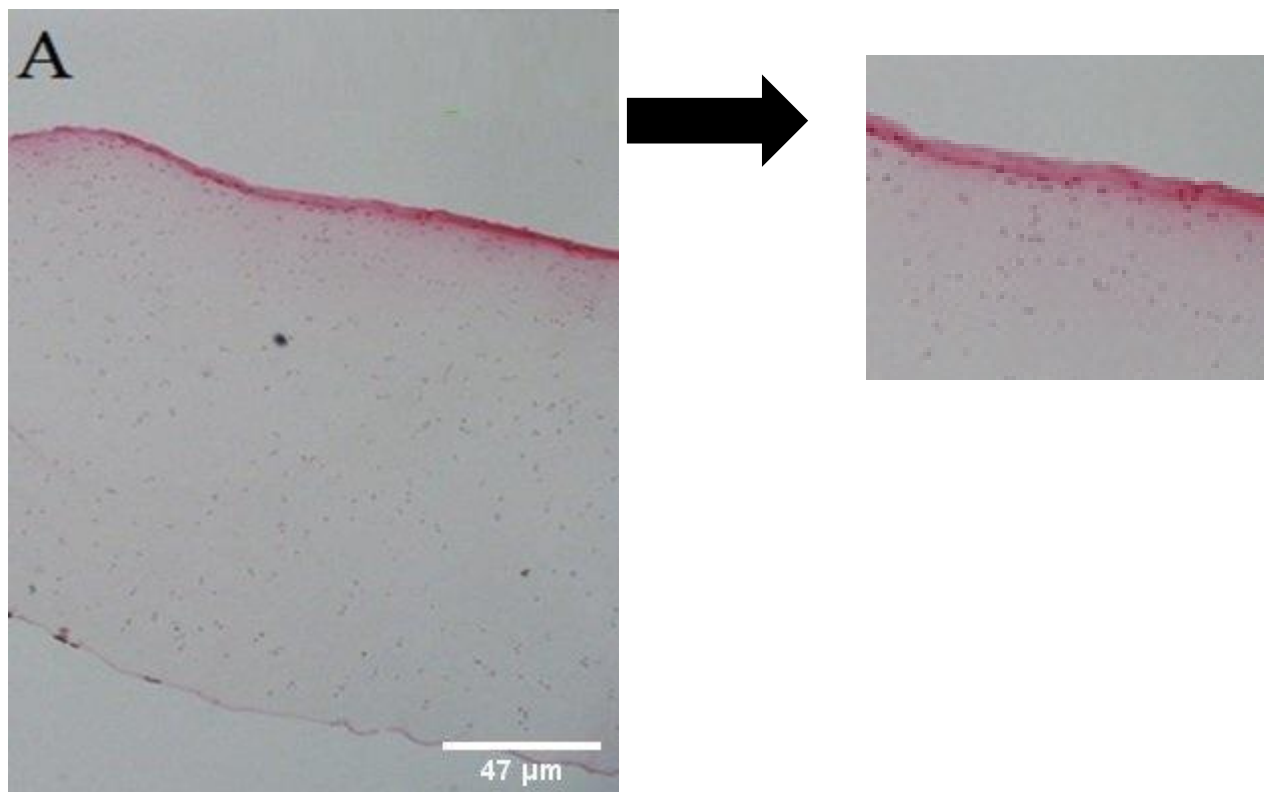
	Microarray (dependent cohort)		qPCR (dependent cohort)		qPCR (independent cohort)	
	OA-Intact vs Y		OA-Intact vs Y		OA-Intact vs Y	
	Direction	LogFC	Direction	LogFC	Direction	LogFC
miR-140-5p	Lower in OA intact	-5.09	Lower in OA intact	-10.40	Lower in OA intact	-5.71
miR-155-5p		-5.20		5.09		-4.80
miR-143-3p	Lower in OA intact	-7.52	Lower in OA intact	-8.58	Lower in OA intact	-6.54
miR-107		-5.63		-4.52		-5.13
miR-379-5p		-4.69		-4.00		-4.27

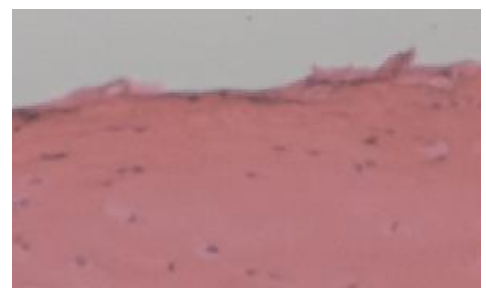
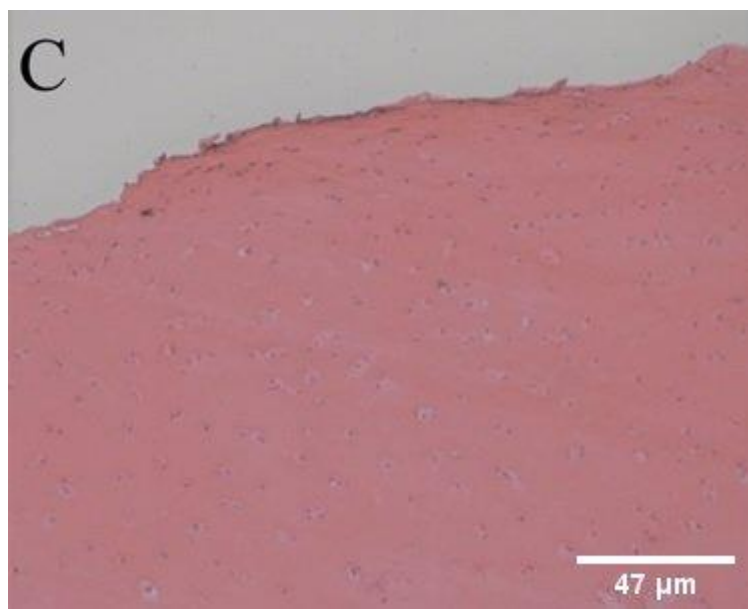
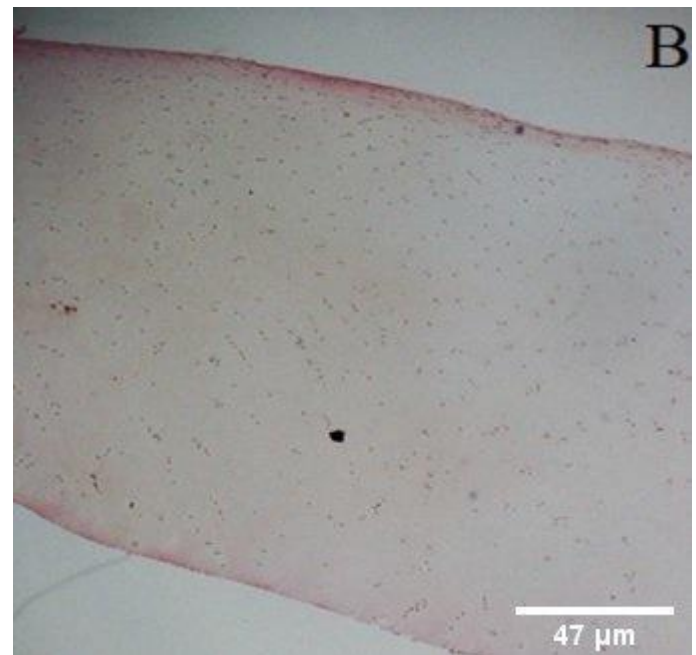
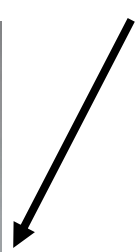
miR-361-5p		-5.44		-3.09	-4.51
		-4.87		-4.34	
miR-132-3p					-4.63

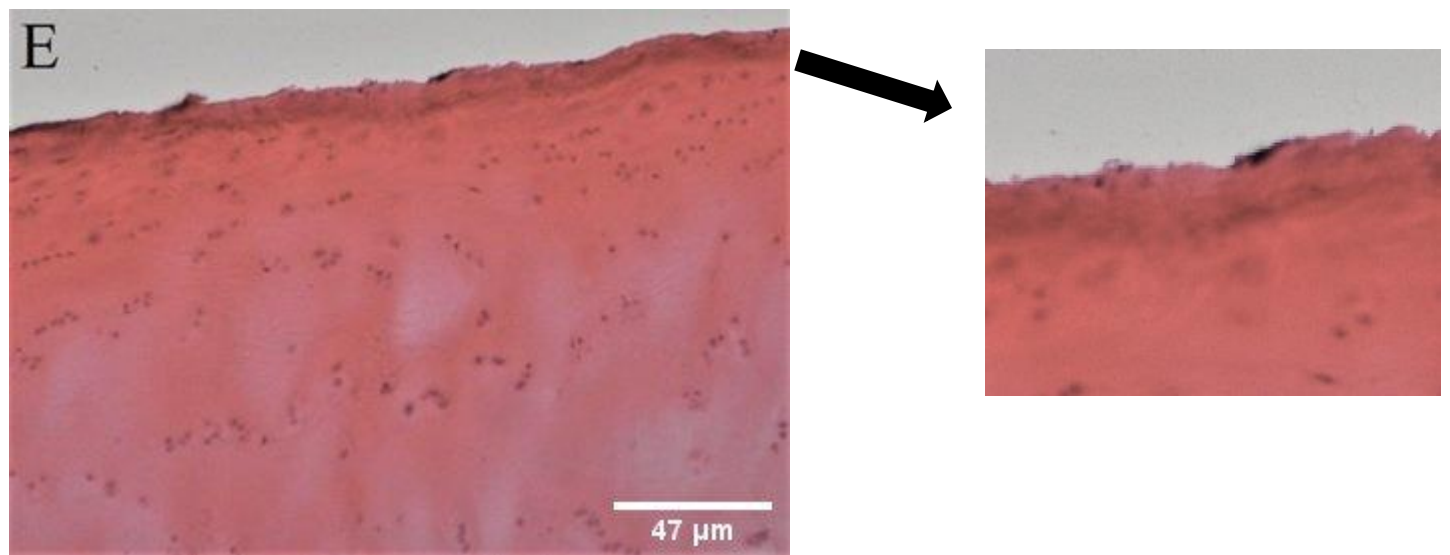
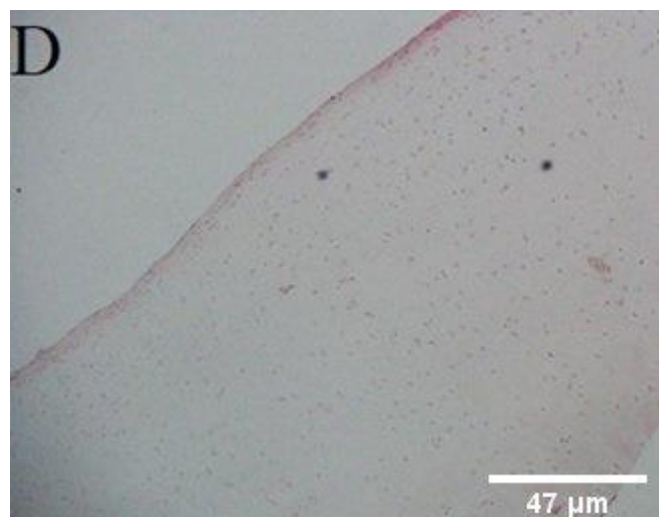
	Microarray (dependent cohort)		qPCR (dependent cohort)		qPCR (independent cohort)	
	OA-Lesioned vs Y		OA-Lesioned vs Y		OA-Lesioned vs Y	
	Direction	LogFC	Direction	LogFC	Direction	LogFC
miR-140-5p	Lower in OA lesioned	-5.11	Lower in OA lesioned	-7.48	Lower in OA lesioned	-5.72
miR-155-5p		-4.77		-3.74		-4.41
miR-143-3p		-7.36		-7.20		-5.81
miR-107		-4.65		-3.80		-4.77
miR-379-5p		-4.50		-4.28		-3.98
miR-361-5p		-4.20		-2.59		-3.74
		-4.02		-4.23		-3.83
miR-132-3p						

#### 4.4.5 Investigation of selected miRNAs in cartilage ageing

Microarray analysis and qPCR validation of selected miRNAs was carried out in young cartilage samples from ACL donors and old OA intact and lesioned cartilage samples from TKA patients. There were two main variables between these groups: ageing and OA. To investigate the effect of ageing on selected miRNAs without the effect of OA, further analysis was carried out on young healthy and old healthy human knee cartilage samples collected from the femoral lateral and medial condyles of male cadavers with no history of knee disease. To confirm that samples, and especially old ones, had no extended pathologic perturbations, cartilage was stained with H&E to visualise tissue integrity and any pathological perturbations. Staining showed that both young and old samples were quite intact with no extended pathological perturbations (**Figure 4.4**). In old samples there was some superficial fibrillation and surface irregularities but there was no cartilage loss or clefts extending into the lower superficial zone or middle zone. Therefore, samples were considered healthy with no pathological perturbations and suitable for further analysis.







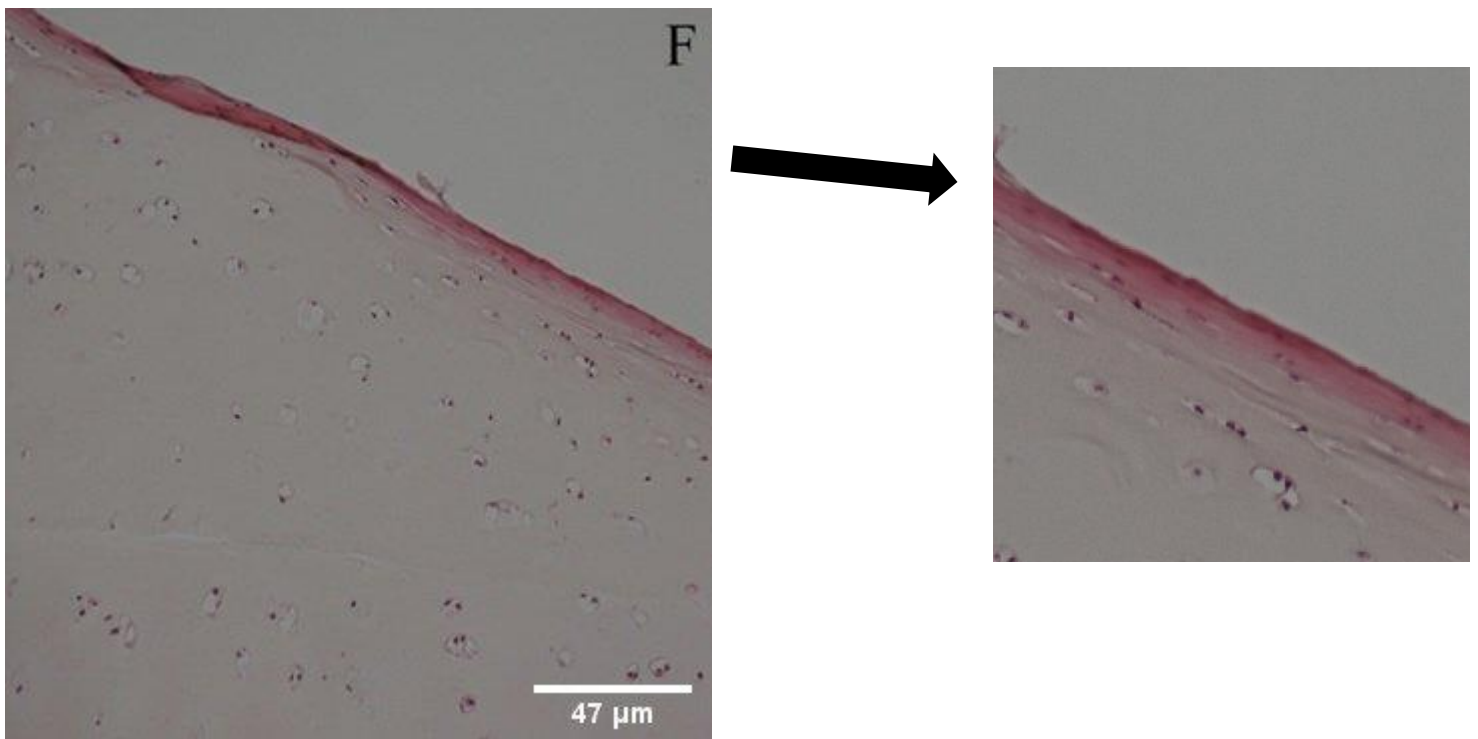


**Figure 4.4: Examples of H&E staining of human young and old healthy knee cartilage.**

Cartilage samples collected from the knee femoral condyles of cadavers with no history of knee disease were stained with H&E to assess tissue integrity. A and B represent young healthy human cartilage samples. C, D, E and F represent old healthy human cartilage samples. For each sample shown here, there are two figures: one showing a greater area of the tissue (magnification 10x) and the other one showing the surface of the section in greater magnification (20x). Scale bars are indicated. Photographed using a Nikon Eclipse 80i microscope (Nikon, UK). Original figures. Figure A and B are courtesy of Aibek Smagul (used with his permission). Figures C-F are courtesy of the author.

After histologic assessment of young and old healthy samples, expression of selected miRNAs from microarray analysis was measured to assess the impact of ageing. Of the seven miRNAs that were validated previously, four of these were selected for investigation in young healthy and old healthy cartilage: miR-107, miR-379-5p, miR-361-5p and miR-143-3p. This selection was based on novelty, as there was little or no data regarding their role in cartilage and OA. SNORD6B was used as the reference gene as it was more stable than miR-6786-5p that was used previously for microarray validation (data not shown). In the microarrays and

subsequent qPCR validation in the dependent and independent cohorts, these four miRNAs had lower expression in OA intact and lesioned cartilage samples when compared to young cartilage samples from ACL donors. However, qPCR analysis of these four miRNAs in young healthy and old healthy cartilage samples, showed that there was no significant difference in their expression in these samples (**Figure 4.5**). miR-107 had higher expression in the old healthy group compared to young but the difference did not reach significance ( $p=0.06$ ).

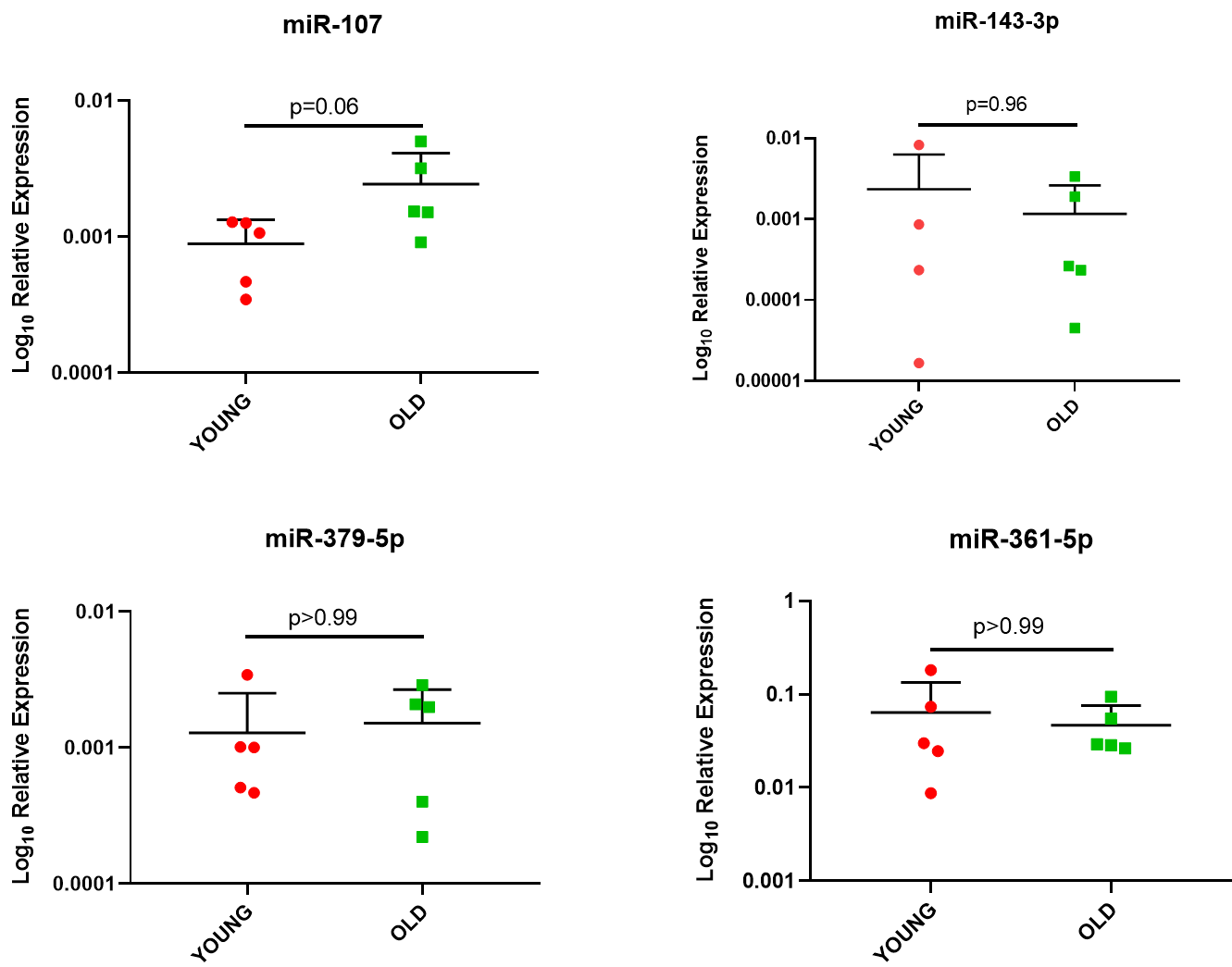


**Figure 4.5: Expression of selected miRNAs in young healthy and old healthy human knee cartilage.** Expression of four selected miRNAs was investigated with qPCR in young and old human healthy cartilage samples from cadavers with no history of knee disease. Y axis represents log-transformed expression relative to SNORD68. N=4-5 samples/group. Statistical analysis was undertaken using a Mann Whitney test in GraphPad Prism (Version 8.0.1). Data are represented as mean+SD. P values<0.05 were considered significant.

#### 4.4.6 Investigation of selected miRNAs in an OA *in vitro* inflammatory model

To investigate miRNA response in an OA-like inflammatory system, I undertook a number of approaches. Initially, I tested the effect of inflammation on chondrocytes from non-OA donors and compared them to OA chondrocytes from donors undergoing TKA. I first assessed the appropriate reference gene to be used for IL-1 $\beta$  treated human chondrocytes. I tested three reference genes: miR-6786-5p, SNORD68 and RNU6. RefFinder indicated that the best reference gene was SNORD68, followed closely by miR-6786-5p and then RNU6 (**Figure 4.6**).

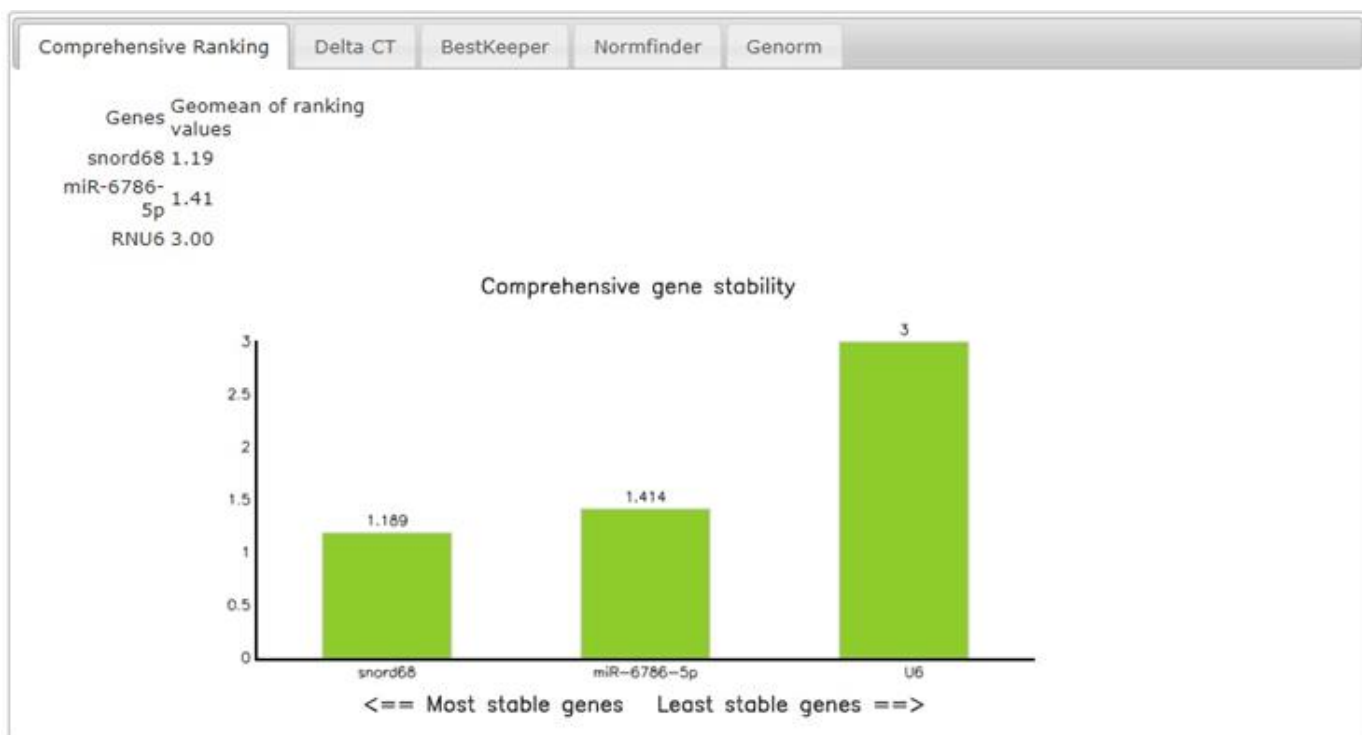


**Figure 4.6: Selection of appropriate reference genes in human chondrocytes treated with IL-1 $\beta$ .** Three reference genes were tested for stability in human chondrocytes treated with IL-1 $\beta$ : SNORD68, miR-6786-5p and U6. Comprehensive gene stability for the three candidates is shown. Y axis represents ranking values. Graphs generated with RefFinder.

Having tested for suitable reference gene and due to the limited starting material for the non-OA group, only two miRNAs were selected during this first treatment: miR-143-3p and miR-107. Chondrocytes from non-OA donors treated with 10ng/ml IL-1 $\beta$  had reduced expression of miR-143-3p and miR-107 in the treated group compared to control. In contrast, OA

chondrocytes treated with IL-1 $\beta$  for 24h showed a less clear expression profile and changes in miRNA expression were less prominent between the treated and control group. In fact, in treated non-OA chondrocytes, expression of these miRNAs reached similar levels to OA chondrocytes (**Figure 4.7**).

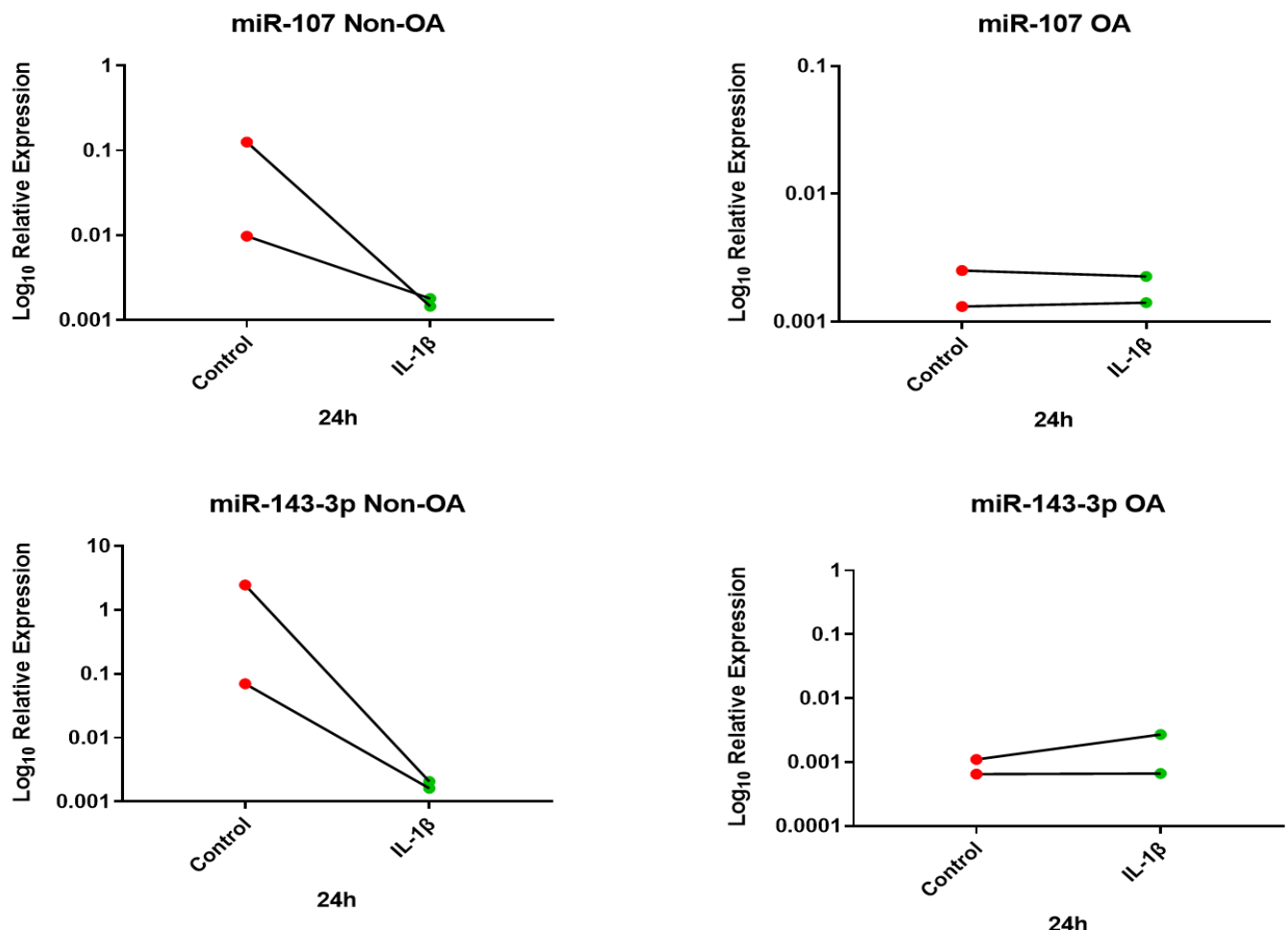


**Figure 4.7: Before-after plot showing expression of miR-143-3p and miR-107 in IL-1 $\beta$  treated chondrocytes extracted from non-OA and OA cartilage.** Non-OA and OA chondrocytes were treated with 10ng/ml of human recombinant IL-1 $\beta$  for 24h. Y axis represents log-transformed expression relative to SNORD68. N=2 donors/group. Each line connects the control and treated group of the same donor.

I, next, focused on further IL-1 $\beta$  treatment of human OA chondrocytes due to the availability of the cells. Given that little difference in miRNA expression was observed in the 24h time point, I performed an initial experiment for a shorter amount of time using primary OA chondrocytes from one patient to investigate whether shorter treatments were more appropriate. Chondrocytes were treated for 6h and 24h for comparison and RNA was collected and subjected to poly(A) cDNA synthesis and qPCR. I also checked chondrocyte morphology under the microscope to identify potential morphological changes between treated and control. I observed changes in cell morphology for both the 6h and 24h treatments. Chondrocytes in control groups had the typical fibroblastic appearance that they acquire in monolayer culture, with axonal projections present. In treated groups, even from the 6h time point, cells became rounder, their extensions became shorter and cells looked more apoptotic. Changes were more prominent in the 24h time point (**Figure 4.8**).

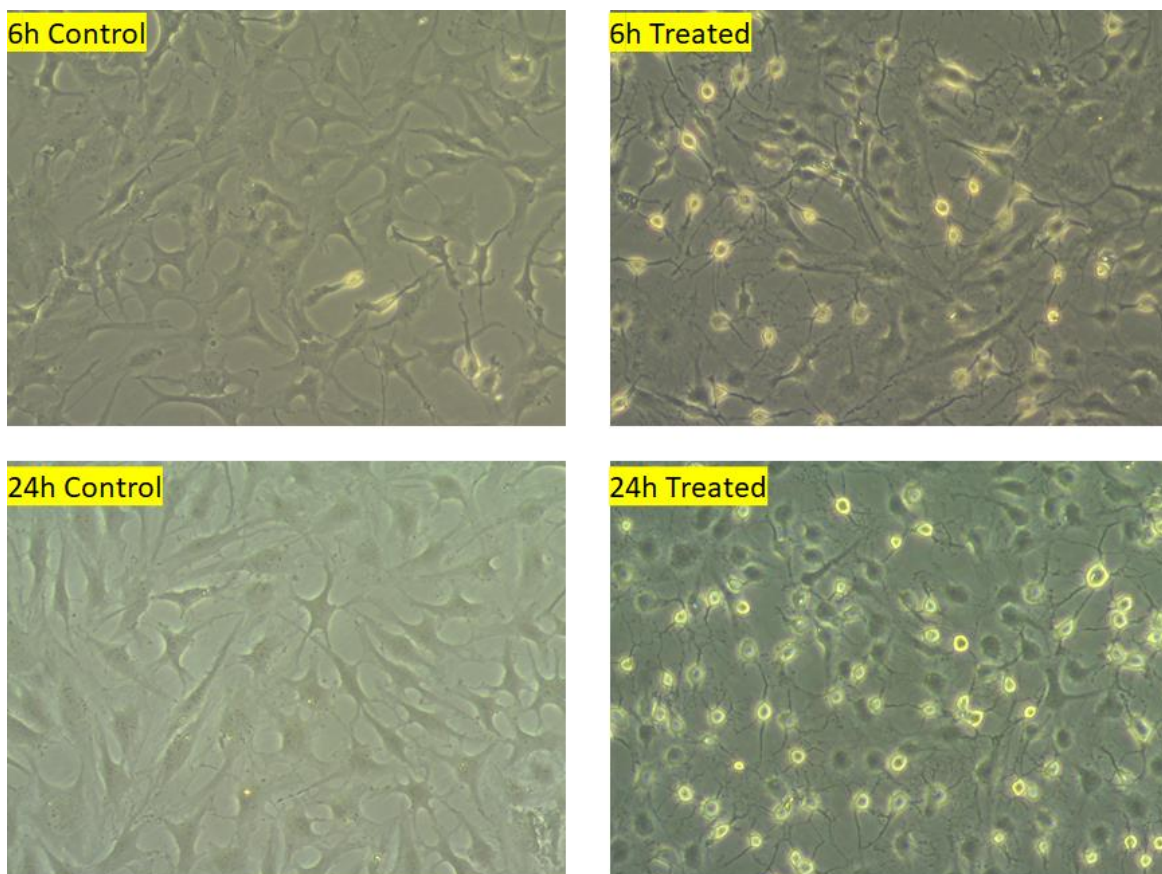


**Figure 4.8: OA chondrocyte morphology after treatment with IL-1 $\beta$  or control for 6h and 24h.** Human OA chondrocytes were treated with 10ng/ml human recombinant IL-1 $\beta$  or control for 6h and 24h. Cells were photographed at the 6h and 24h time points using a ZEISS Axio Vert.A1 Inverted Microscope at 10x magnification. Original figure, courtesy of the author.

qPCR analysis of cell lysates showed that selected miRNAs responded even less to the 6h treatment compared to the 24h treatment (**Figure 4.9**). None of the four selected miRNAs, showed any differences in their expression at the 6h time point when compared to control.

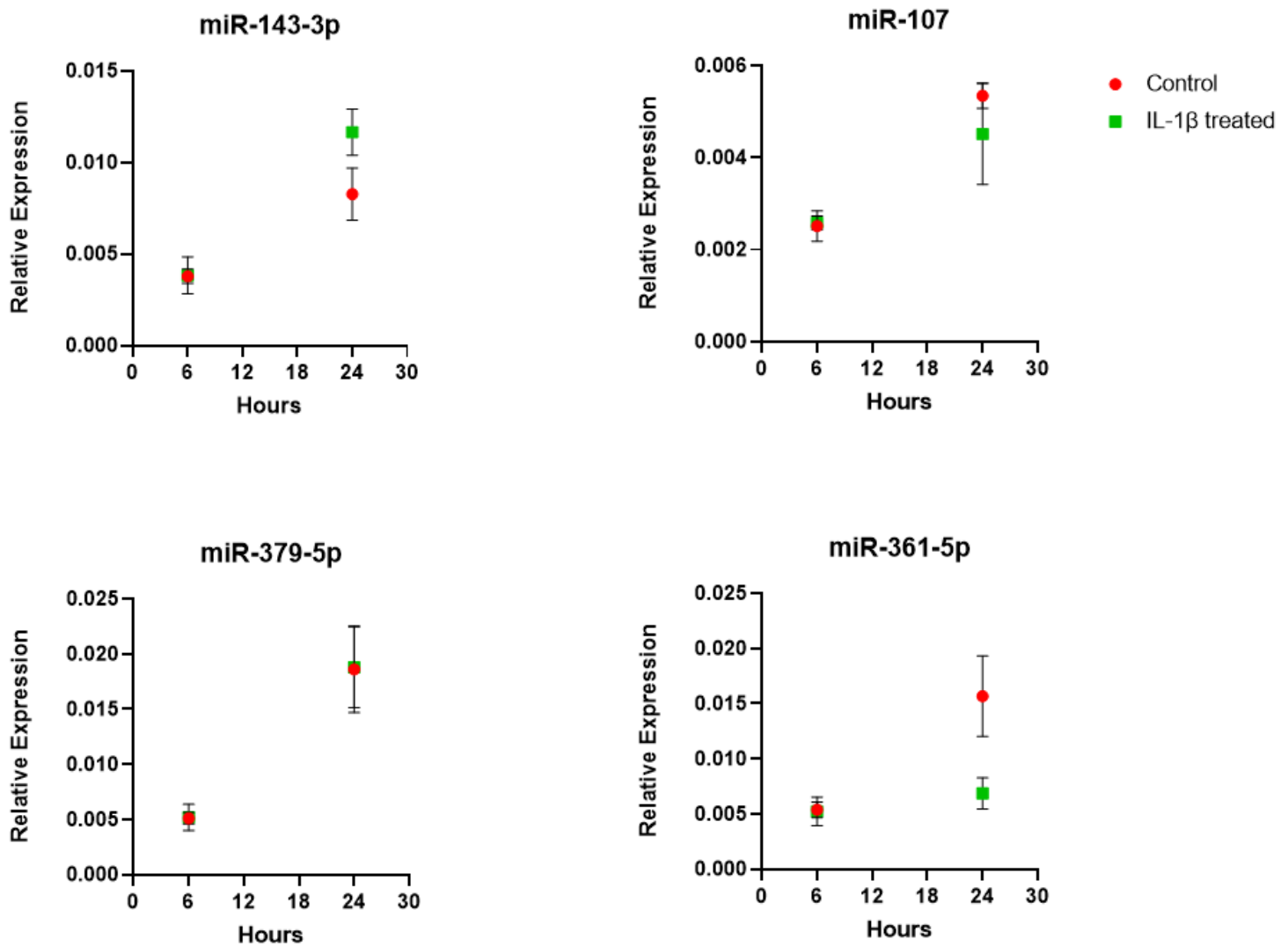
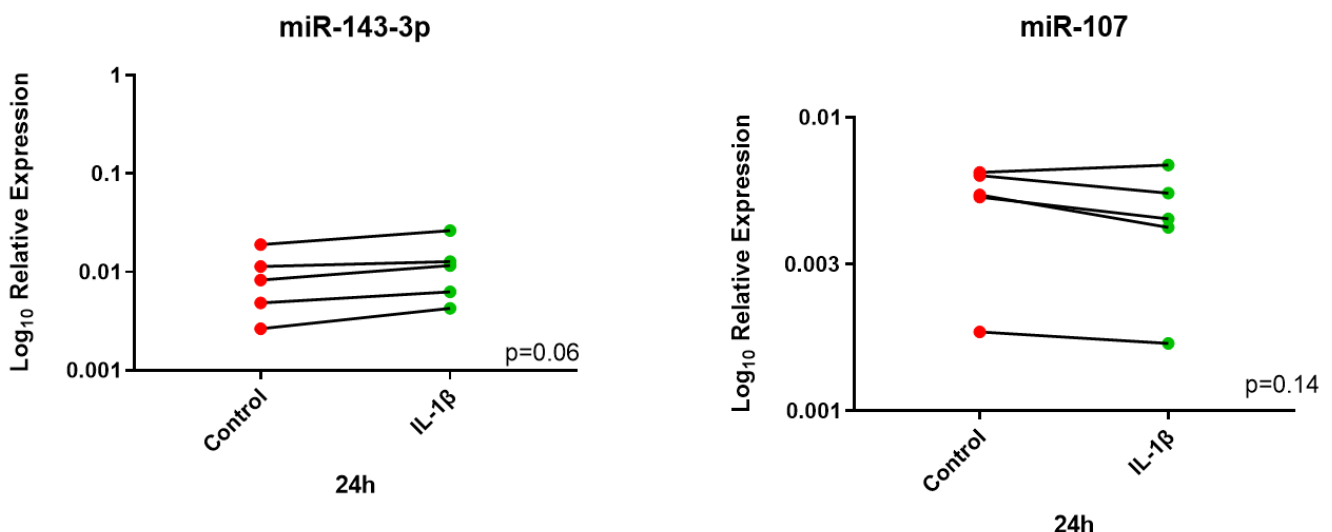


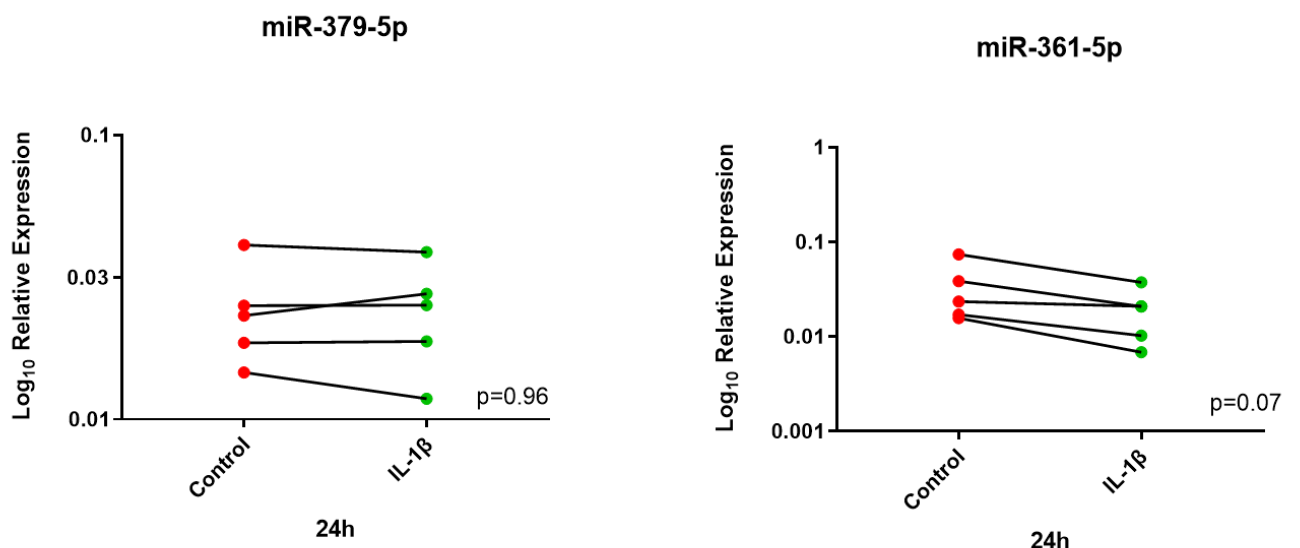
**Figure 4.9 Expression of selected miRNAs in human OA chondrocytes treated with IL-1 $\beta$  in a time course of 6h and 24h.** Human OA chondrocytes from one patient were treated with 10ng/ml of human recombinant IL-1 $\beta$  or control for 6h and 24h. miRNA expression is relative to SNORD68. Key is indicated.

At the 24h time point, expression of miR-107 and miR-143-3p followed a similar trend to the previous experiment. For miR-107 there was slightly lower expression in the treated group compared to control, whereas expression of miR-143-3p was slightly higher compared to control. miR-361-5p showed the largest decrease in expression in the treated group compared to control, and miR-379-5p did not show any difference at the 24h time point.

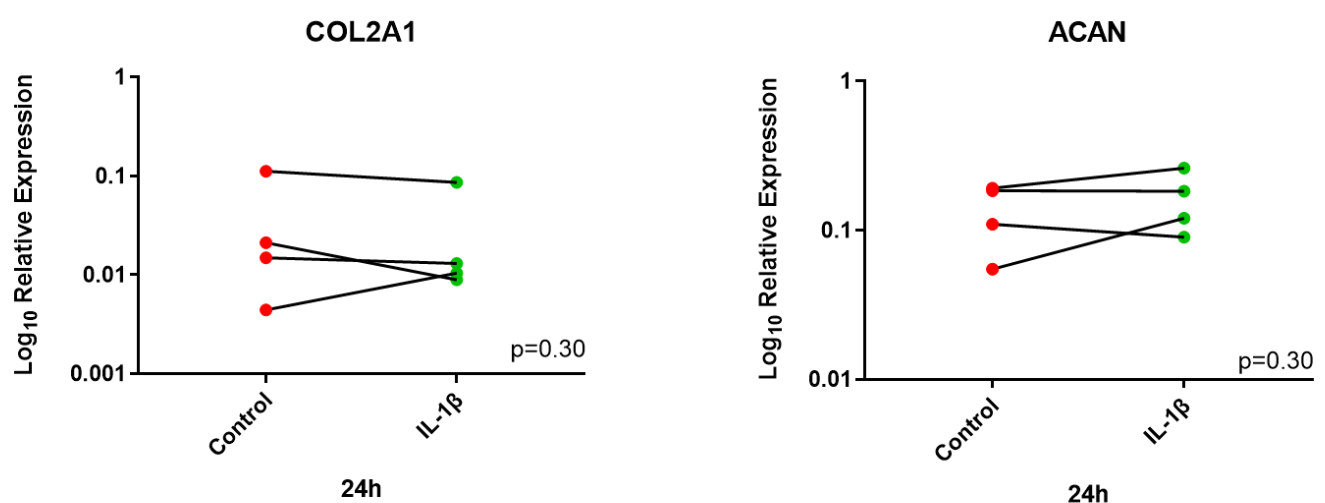
Based on the above results, I decided to further test the expression of selected miRNAs at the 24h time point but this time include longer treatments as well, specifically treatment for 5 days, to see if larger changes were observed. Furthermore, with this series of experiments, in addition to miRNA expression, I determined the expression of specific cartilage and OA markers, namely *COL2A1*, *ACAN*, *MMP13* and *ADAMTS4*, in order to investigate how effective IL-1 $\beta$  treatment is in the establishment of an OA inflammatory response. Analysis showed that for the 24h time point, miR-107 and miR-361-5p had lower expression in the treated group and the difference was almost significant for the latter. Expression was almost significantly higher in the treated group for miR-143-3p, whereas miR-379-5p did not show any difference (**Figure 4.10A**). Analysis of cartilage markers in OA chondrocytes treated with IL-1 $\beta$  for 24h showed that *COL2A1* and *ACAN* did not have significant changes between treated cells and control, although there was a slight increase in *ACAN* expression in the treated group. In contrast, *MMP13* and *ADAMTS4* had significantly higher expression in treated chondrocytes when compared to control (**Figure 4.10B**).

**A**





**B**



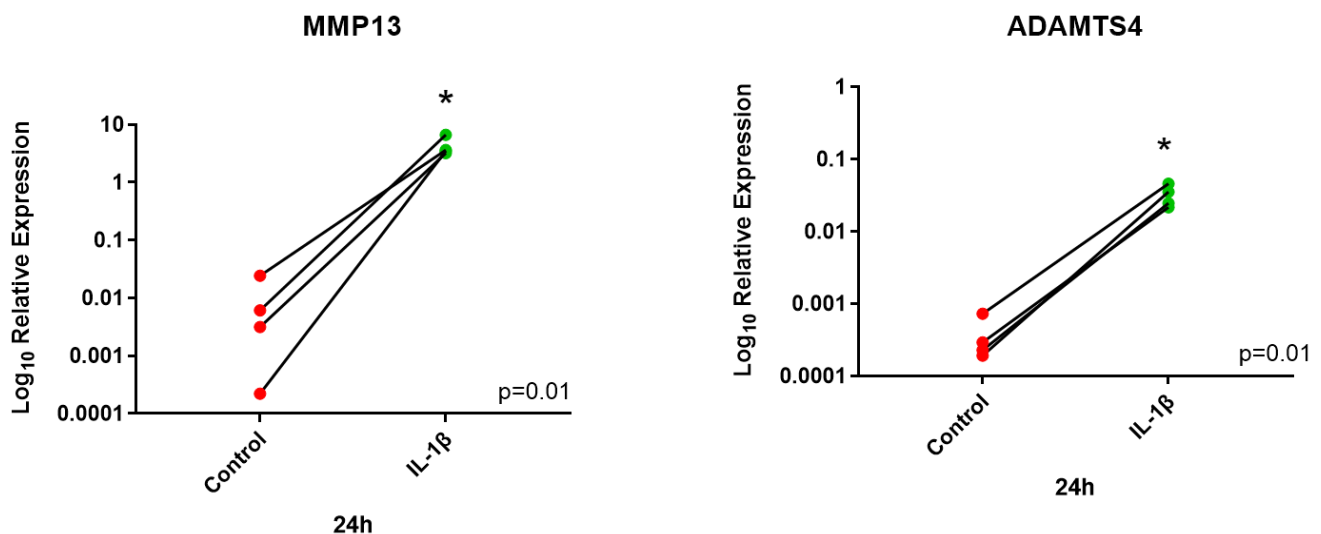


**Figure 4.10: Before-after plot showing expression of selected (A) miRNAs and (B) cartilage markers in human OA chondrocytes treated with IL-1 $\beta$  or control for 24h.** Human OA chondrocytes were treated with 10ng/ml human recombinant IL-1 $\beta$  or control for 24h and expression of selected miRNAs and cartilage markers was measured. N=4-5 donors. Y axis represents log-transformed expression relative to SNORD68 for miRNAs and relative to GAPDH for OA markers. Statistical analysis was undertaken using a two-tailed paired t-test in GraphPad Prism (Version 8.0.1). P values<0.05 were considered significant. \*: p<0.05. Each line connects the control and treated group of the same donor.

Next, I sought to investigate the expression of miRNAs and cartilage markers in chondrocytes treated with IL-1 $\beta$  for 5 days. As before, I also visualised cell morphology under the microscope. I observed similar morphological changes as in the 24h time point, mainly rounder cells with less protrusions and apoptotic appearance (**Figure 4.11**).

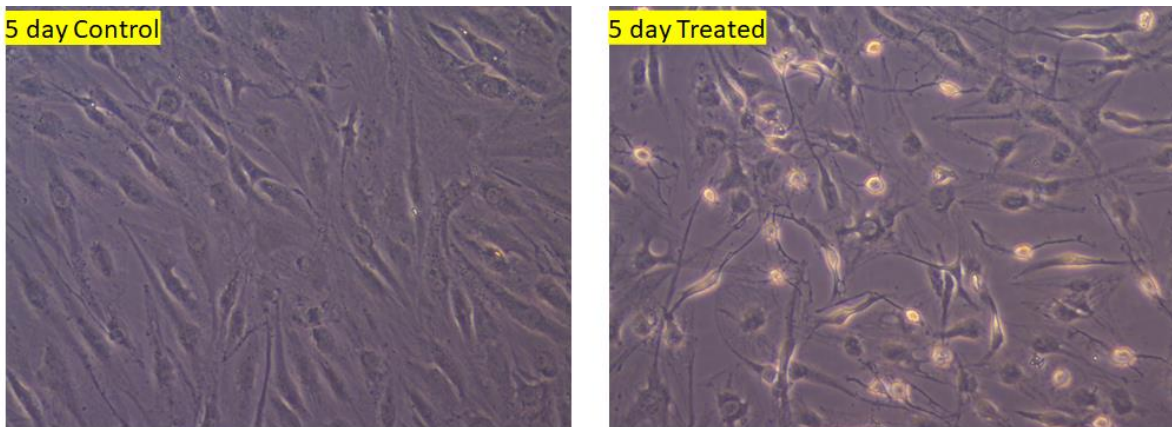


**Figure 4.11: OA chondrocyte morphology after treatment with 10ng/ml IL-1 $\beta$  or control for 5 days.** Human OA chondrocytes were treated with 10ng/ml human recombinant IL-1 $\beta$  or control for 5 days. Cells were photographed at the 5-day time point using a ZEISS Axio Vert.A1 Inverted Microscope at 10x magnification. Original figure, courtesy of the author.

Regarding gene expression, IL-1 $\beta$  treatment of OA chondrocytes for 5 days resulted in a miRNA expression profile that resembled that of our microarray experiment. While miR-143-3p had higher expression in chondrocytes treated with IL-1 $\beta$  for 24h, its expression was almost significantly lower in chondrocytes treated for 5 days when compared to control. Therefore, there was a shift in its expression levels from the 24h time point to the 5-day time point. For miR-107 and miR-361-5p the trend was the same as in the 24h time point, with lower expression in the treated group compared to control. However, the difference between treated and control cells was much larger in the 5-day time point and reached statistical significance, whereas this did not happen in the 24h time point for these two miRNAs. miR-379-5p showed the largest difference between the 24h and 5-day time points. There was no difference in expression between treated and control chondrocytes in the 24h time point for this miRNA ( $p=0.96$ ). However, after 5 days of treatment, miR-379-5p had significantly lower expression in the treated group compared to control ( $p=0.0002$ ). Results for the 5-day time point are shown in **Figure 4.12**.

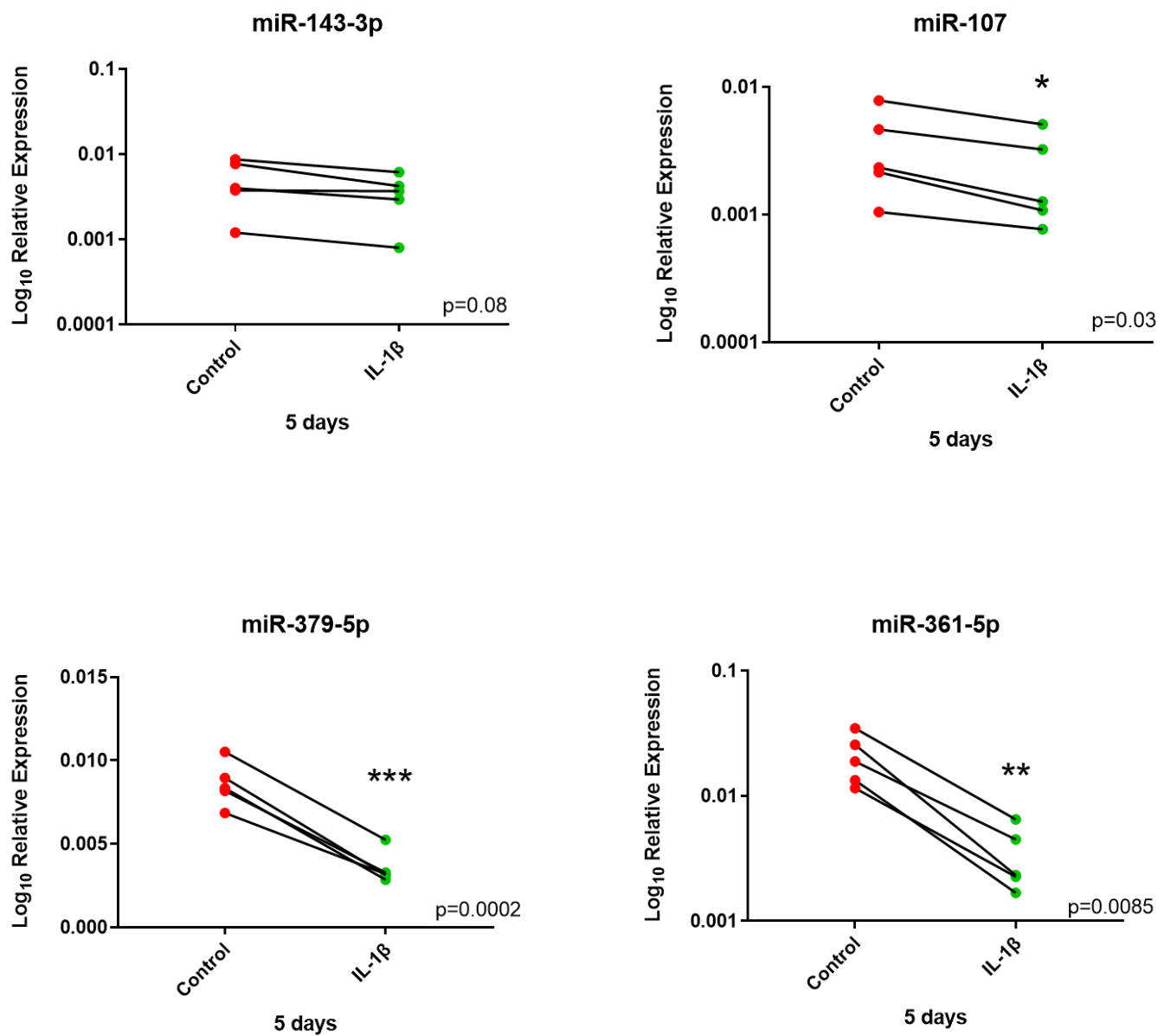


**Figure 4.12: Before-after plot showing expression of selected miRNAs in human OA chondrocytes treated with 10ng/ml IL-1 $\beta$  for 5 days.** Human OA chondrocytes were treated with 10ng/ml human recombinant IL-1 $\beta$  or control for 5 days and expression of selected miRNAs was measured. N=5 donors. Y axis represents log-transformed expression relative to SNORD68. Statistical analysis was undertaken using a two-tailed paired t-test in GraphPad Prism (Version 8.0.1). P values<0.05 were considered significant. \*: p<0.05, \*\*: p<0.01, \*\*\*: p<0.001. Each line connects the control and treated group of the same donor.

Following the same approach as for the 24h time point, I investigated the expression of selected cartilage markers in OA chondrocytes treated with IL-1 $\beta$ . Analysis showed that chondrogenic markers *COL2A1* and *ACAN* had significantly lower expression in the treated group compared to control after 5 days of treatment and in contrast to the 24h time point where there was no significant difference between treated and control groups. Moreover catabolic markers *MMP13* and *ADAMTS4* had significantly higher expression in the treated groups (**Figure 4.13**), similar to the 24h time point. For *MMP13* the difference was larger in the 5-day treated group compared to the 24h treated group when these were compared to their respective controls.

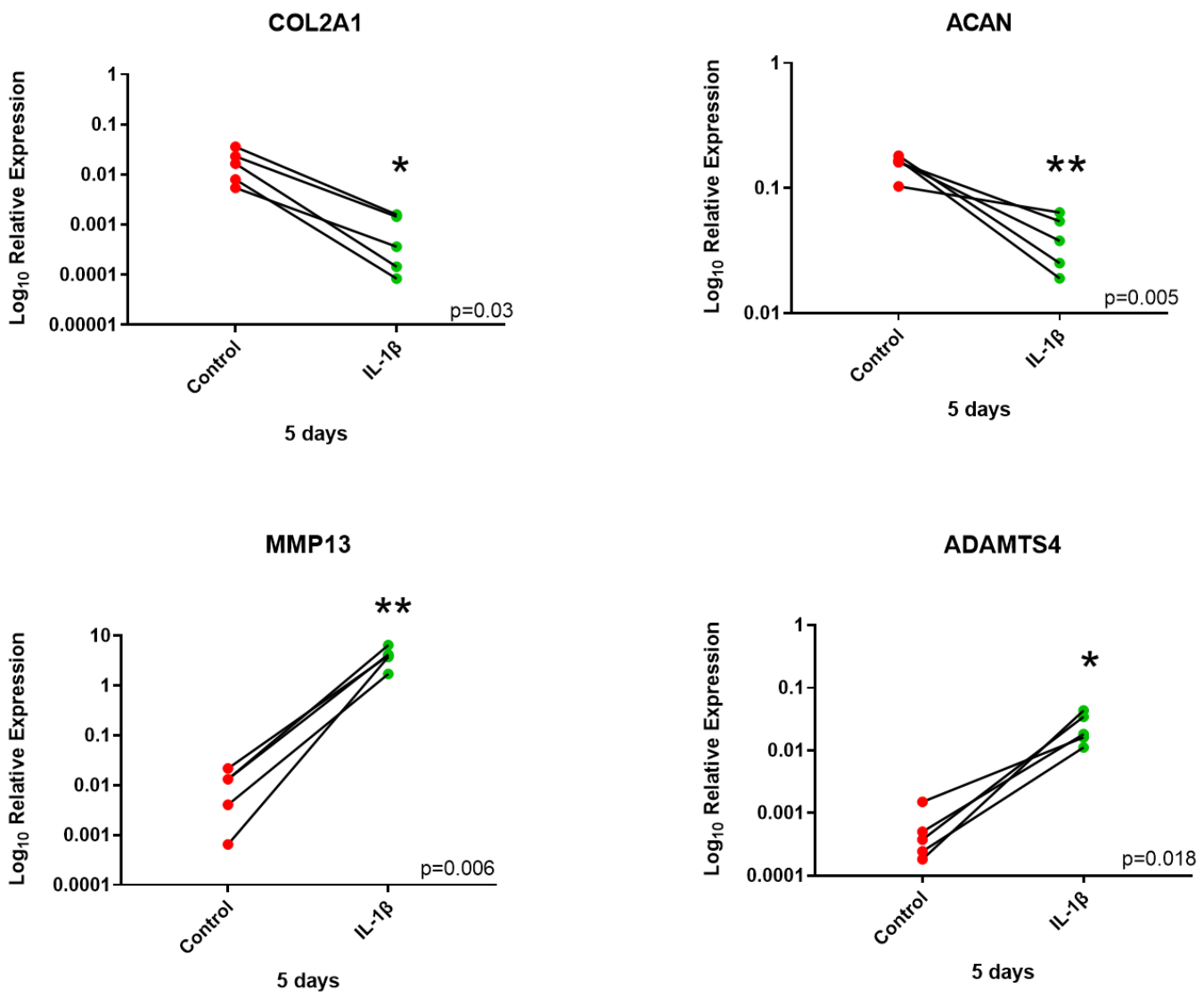


**Figure 4.13: Expression of selected miRNAs in human OA chondrocytes treated with 10ng/ml IL-1 $\beta$  for 5 days.** Human OA chondrocytes were treated with 10ng/ml human recombinant IL-1 $\beta$  or control for 5 days and expression of selected cartilage markers was measured. N=5 donors. Y axis represents log-transformed expression relative to GAPDH. Statistical analysis was undertaken using a two-tailed paired t-test in GraphPad Prism (Version 8.0.1). P values<0.05 were considered significant. \*:  $p<0.05$ , \*\*:  $p<0.01$ . Each line connects the control and treated group of the same donor.

## **4.5 Discussion**

In the current thesis I sought to investigate the expression of miRNAs in cartilage ageing and OA. To achieve this, I undertook a microarray analysis using cartilage tissue from young patients undergoing ACL reconstruction and old OA patients. Two areas were used from OA patients. A macroscopically intact area of OA cartilage and a lesioned area of OA cartilage. In Chapter 3 I described the results of this microarray analysis between these three main groups and identified DE miRNAs between young and old OA intact and lesioned cartilage. In this chapter I validated selected DE miRNAs by qPCR in the same samples, as well as in an independent cohort of cartilage tissue. Moreover, I investigated the expression of selected miRNAs in young healthy and old healthy cartilage tissue. Finally, to investigate expression of selected miRNAs and specific cartilage markers in an *in vitro* OA inflammatory model, I treated primary chondrocytes with IL-1 $\beta$  for different time points.

### **4.5.1 Validation of microarray results**

The first step in our analysis was to validate the microarray results from Chapter 3 using qPCR. For this reason I selected seven miRNAs based on logFC from the microarray results and known or predicted function in cartilage and OA. The selected miRNAs were: miR-140-5p, miR-155-5p, miR-143-3p, miR-107, miR-379-5p, miR-361-5p and miR-132-3p. I undertook qPCR analysis in two sample cohorts: a cohort consisting of the same samples that were used in our microarray analysis (dependent cohort), and an additional independent cohort of young and old OA intact and lesioned cartilage samples, from ACL and OA patients, respectively. In our microarray analysis, old OA intact samples were separated into two subgroups based on univariate analysis: OA-Intact-1 and 2. However, for qPCR validation I decided to group these samples together in one group again. This was done for the following reasons. First of all, I focused on the following comparisons: OA-Intact-1 vs Young, OA-Intact-2 vs Young and OA-Lesioned vs Young. Selected miRNAs had the same direction of dysregulation in both OA-Intact-1 vs Young and OA-Intact-2 vs Young, therefore I decided to group OA-Intact-1 and 2 together into OA-Intact and compare that to the Young group. This would also increase power as our microarray finding showed that there was no significant difference for the seven selected miRNAs between OA-Intact 1 and 2 (OA-Intact-1 vs OA-

Intact-2). Moreover, I would use an independent cohort of cartilage samples to validate our microarray findings with qPCR. It would not have been possible to know whether OA-intact samples from the independent cohort would be more similar to the OA-Intact-1 or 2 group of the dependent cohort, hence, for qPCR validation, I decided to have only three main groups for each cohort of samples: Young, OA-Intact and OA-Lesioned.

qPCR analysis in the dependent cohort validated the microarray results for these seven selected miRNAs. Analysis showed that all selected miRNAs had significantly lower expression in the old OA-Intact and Lesioned groups when these were compared to the Young group from ACL donors, similar to our microarray results. Moreover, there was no significant difference for these selected miRNAs when old OA-Intact and Lesioned groups were compared to each other, in agreement with our microarray findings. Therefore, there was a good agreement between microarrays and qPCR.

qPCR analysis in an additional independent cohort of cartilage samples, further validated our findings. Similar to the dependent cohort, all seven miRNAs had significantly lower expression in old OA-Intact and Lesioned groups when these were compared to the Young group. There was no significant difference for these miRNAs when old OA-Intact and Lesioned groups of the independent cohort were compared to each other. This confirmed that our microarray findings were reproducible in a wider range of biological samples. Indeed, comparison of fold changes between microarray results and qPCR validation in the dependent and independent cohort indicated that for the selected miRNAs there was agreement not only in the direction of dysregulation but in the magnitude of differential expression also. This further confirmed the biological significance of our microarray findings and indicated that observed changes in miRNA expression are applicable to a larger cohort of patients.

From the seven selected miRNAs, two of them had been studied previously in cartilage and OA. miR-140-5p is amongst the best studied miRNAs in cartilage homeostasis and OA. In agreement with our results, miR-140-5p was downregulated in OA human cartilage (Miyaki et al., 2009) and multiple studies have identified miR-140-5p as an important mediator of chondrogenesis and differentiation of MSCs into chondrocytes (Karlsen et al., 2014, Swingler et al., 2012). Tao *et al* (2017) showed that exosomes derived from MSCs overexpressing miR-140-5p could promote knee cartilage regeneration and chondrocyte proliferation and could inhibit OA in a rat model (Tao et al., 2017). Moreover, important targets of miR-140-5p include

*MMP13* and *ADAMTS5*, further validating the role of this miRNA in cartilage and OA (Miyaki et al., 2010). In addition, miR-155-5p is also implicated in OA. Expression of miR-155 was decreased in OA patients compared to control and increased in OA patients who received hyaluronic acid injection in the knee joint compared to those who did not (Xu et al., 2015). Furthermore, miR-132-3p had lower expression in the microarrays and in qPCR validation in the dependent and independent cohort. There were no available studies on the role of miR-132-3p on cartilage and OA at the time of our microarray validation. However, recent studies have shown that this miRNA was involved in chondrogenic differentiation of rat MSCs and promoted proteoglycan deposition and increased expression of *Sox9*, *Col2a1* and *Acan* by targeting *Adamts5* (Zhou et al., 2018). Moreover, miR-132-3p was identified as an important regulator of the NF-κB pathway in ATDC5 cells treated with lipopolysaccharides (LPS) (Li et al., 2019a). LPS is a proinflammatory agent that activates the NF-κB signalling pathway and leads to the release of proinflammatory cytokines. In LPS-treated ATDC5 cells, expression of miR-132-3p was inhibited which led to increased levels of NF-κB and pro-inflammatory cytokines such as IL-6 and TNF-α (Li et al., 2019a). Upregulation of miR-132-3p attenuated these effects. The significant role of miR-132-3p in OA was further confirmed by Wang *et al* (2020), who carried out a meta-analysis of microarray expression data to generate OA dysfunctional modules and their transcriptional regulators (Wang et al., 2020). Amongst these, miR-132-3p and NF-κB were identified as important transcriptional regulators of the OA-modules generated and had a significant regulatory effect on OA (Wang et al., 2020). The remaining four miRNAs, miR-107, -379-5p, -361-5p and 143-3p were selected for further studies and their role in cartilage and OA will be discussed later on and in the next chapter.

#### **4.5.2 Investigation of selected miRNAs in cartilage ageing**

Ageing is the most common risk factor for OA. Age-related changes in cartilage can predispose individuals to the development of OA. In our microarray experiment and subsequent qPCR validation I compared young intact cartilage from ACL donors to old OA intact and lesioned cartilage from OA donors. In this dataset there were at least two major variables that could drive results: ageing and OA. To have a better understanding of how ageing can affect the results and whether ageing, disease or both drive differential expression in our dataset, I

measured by qPCR the expression of four selected miRNAs, miR-107, -379-5p, -361-5p and 143-3p, in young healthy and old healthy cartilage tissue, collected from male cadavers without any known history of knee damage or OA. To confirm that tissues were indeed healthy, especially the old samples, I carried out H&E staining which confirmed that cartilage samples were mainly intact. Small perturbations, such as surface irregularities are to be expected in the old samples given that average age was  $62 \pm 6.6$  and these were not considered pathological changes. qPCR analysis in these samples showed that there were not any age-related changes in the expression of these miRNAs between young and old healthy cartilage samples, indicating that the results I observed from the microarrays were most likely driven by disease rather than ageing. This is not unexpected as pathological alterations in the tissue are probably of greater extent compared to alterations due to ageing. Indeed, our group has recently carried out small RNAseq between young and old healthy human knee cartilage samples and none of these miRNAs were identified as DE (unpublished data). Moreover, the number of DE miRNAs in this ageing study was much lower compared to the number of DE miRNAs from our microarray study, further supporting that pathology is mostly driving results rather than ageing. There is very limited information in the literature on the effect of ageing on miRNAs in cartilage tissue without the effect of OA. To the best of our knowledge the only study that has investigated the effect of cartilage ageing on miRNA expression is from Ukai *et al* (2012), where they compared expression of miRNAs in cartilage from infants with polydactylyism to cartilage collected from young ACL donors and identified three DE miRNAs (miR-199a-3p, -193b and -320c) (Ukai et al., 2012). Such studies are very limited in human cartilage given the difficulty in obtaining healthy tissue, but would shed much light on the effect of age on miRNA expression and help define better potential miRNA candidates in OA.

#### **4.5.3 Investigation of selected miRNAs in an *in vitro* OA inflammatory model**

Chapter 3 described the bioinformatic analysis of microarray findings using IPA to identify relevant biological pathways that our DE miRNAs are involved in. In comparisons OA-Intact-1 vs Y, OA-Intact-2 vs Y and OA-Lesioned vs Y, inflammation was one of the main pathways identified as relevant to our dataset. Further analysis with ToppGene, Revigo and Cytoscape confirmed that inflammation and cytokine production was amongst the top relevant

processes that our DE miRNAs are involved in. Furthermore, key pro-inflammatory cytokines, such as IL-1 $\beta$  and TNF- $\alpha$ , were identified by IPA as upstream regulators of our dataset. To investigate the effect of inflammation on our selected list of four miRNAs (miR-107, -379-5p, -361-5p and -143-3p), I treated human primary chondrocytes with human recombinant IL-1 $\beta$ . First, I treated non-OA chondrocytes extracted from donors undergoing autologous chondrocyte transplantation and OA chondrocytes extracted from patients undergoing TKA. There was limited number of non-OA donors available, so I was only able to interrogate two donors. For this part of the experiment, I also included two OA donors for direct comparison. There was limited amount of cDNA available for the non-OA samples so only two miRNAs were tested: miR-107 and miR-143-3p. Results showed that non-OA chondrocytes were more responsive to the treatment compared to OA chondrocytes. Both miR-107 and miR-143-3p had lower expression in non-OA treated cells compared to non-OA control cells. In contrast, miR-143-3p and miR-107 showed minor changes in treated OA cells compared to control OA cells. This is in contrast to a study from Lee *et al* (2002) where they treated chondrocytes from non-OA and OA donors with IL-1 $\beta$  and they concluded that OA chondrocytes responded better to IL-1 $\beta$  treatment than non-OA chondrocytes, due to the higher number of IL-1 $\beta$  receptors in OA chondrocytes (Lee *et al.*, 2002). However, in the same study the authors concluded that chondrocytes become more tolerant to IL-1 $\beta$  with time (Lee *et al.*, 2002). Taking into account that OA chondrocytes were extracted from patients with chronic OA, and therefore possibly subjected to an inflammatory environment for longer compared to non-OA chondrocytes from autologous transplantation patients, one could justify the limited response seen in OA chondrocytes in our study compared to non-OA chondrocytes. Moreover, a point to consider is the use of different markers to assess chondrocyte responsiveness. While Lee *et al* (2002) measured expression of selected gene markers, such as *MMP13*, *NO* and *PGE2* to assess chondrocyte responsiveness, I tested the expression of specific miRNAs and therefore differences in the markers used with regards to their responsiveness are to be expected and no direct contrast can be made. Indeed, Moulin *et al* (2017) carried out microarray analysis in non-OA chondrocytes treated with 10ng/ml IL-1 $\beta$  for 48h and identified a list of DE miRNAs, including miR-140-5p (Moulin *et al.*, 2017), which suggests that response of non-OA chondrocytes varies dependent on the markers that are assessed. Moreover, in our study, comparison of the control groups between non-OA and OA chondrocytes showed that expression levels for miR-143-3p and miR-107 differed between the two controls, with higher

levels seen in the non-OA control group compared to the OA control group. This was consistent with our microarray findings where both of the miRNAs had lower expression in the OA groups compared to the young intact group. This also suggests that chondrocytes retain some phenotypic characteristics after extraction from cartilage tissue, at least during the early passages. It is known that chondrocytes dedifferentiate following tissue extraction and passaging as they lose their characteristic ECM organisation and mechanical stimuli (Caron et al., 2012). This is accompanied by morphological changes and a shift in the expression of specific chondrogenic and hypertrophic markers, especially when chondrocytes are cultured in monolayer (Charlier et al., 2019). After treatment, expression of these two miRNAs was similar between non-OA and OA treated chondrocytes, mainly because non-OA chondrocytes responded to IL-1 $\beta$  treatment, whereas OA chondrocytes only had minor/moderate changes after 24h of treatment. This could be due to the fact that expression of these miRNAs in OA chondrocytes was low even in the control group and IL-1 $\beta$  treatment for 24h could not reduce expression significantly. This was also confirmed when I tested the expression of all four selected miRNAs in IL-1 $\beta$ -treated OA chondrocytes from the same donor for 6h and 24h. As before, I observed moderate changes in the expression of miRNAs in the 24h time point and the changes were even smaller in the 6h time point. At the 24h time point, the larger change was observed for miR-361-5p and the smaller for miR-379-5p. Ji et al (2016) carried out a similar experiment for miR-30a in OA chondrocytes treated with 10ng/ml and observed larger changes in miRNA expression at the 24h time point compared to the 6h time point (Ji et al., 2016). Moreover, in a similar experiment, Mao et al (2017) treated OA chondrocytes with 10ng/ml IL-1 $\beta$  and observed greater changes in expression of miR-92a-3p after 24h of treatment compared to 6h of treatment (Mao et al., 2017).

The above experiments prompted us to treat OA chondrocytes from more donors for longer periods, mainly for 5 days and compare that to the 24h time point where I observed moderate changes. The 6h time point was not used for further experiments. Indeed, analysis showed greater IL-1 $\beta$  response in OA chondrocytes after 5 days of treatment and miRNA expression profile matched that of microarray analysis. I was not able to identify any studies from the available literature where they checked the miRNA expression profile in OA chondrocytes treated with IL-1 $\beta$  for longer time points, as most studies have looked at shorter time points, ranging from a few hours up to 24h (Mao et al., 2017, Moulin et al., 2017, Zheng et al., 2017).

Some studies have looked at the expression of specific OA markers, such as collagens and MMPs after treatment for longer periods. Lee *et al* (2002) treated OA chondrocytes with IL-1 $\beta$  for up to 14 days and reported increased expression of *MMP13* starting from the earlier time points and up to 14 days in the treated group compared to control (Lee et al., 2002). In another study, Lv et al (2019) treated bovine cartilage explants for 24 days and observed increased collagen and GAG content loss in the treated group (Lv et al., 2019). In the same study, Lv et al (2019) undertook RNA sequencing to assess differential expression of extracted chondrocytes treated with IL-1 $\beta$  for 48h. It was shown that *COL2A1* and *ACAN* had decreased expression and *MMP13* and *ADMATS4* increased expression in treated chondrocytes (Lv et al., 2019). Cortial *et al* (2006) treated bovine chondrocytes with IL-1 $\beta$  for 24h and 3 days and checked expression of specific cartilage markers for the two time points. The authors reported decreased expression for *COL2A1* and *ACAN* and increased expression of *MMP13* and *ADMATS4* for both time points. In our experiment, *MMP13* and *ADMATS4* had significantly higher expression at both the 24h and 5-day time points. *COL2A1* and *ACAN* did not show any significant changes at the 24h time point but had significant changes at the 5-day time point.

There are limited data on the role of our selected miRNAs in chondrocyte inflammation. Nonetheless, there were specific trends observed for some of the miRNAs even from the 24h time point. miR-361-5p had lower expression in the treated group compared to control and this almost reached significance ( $p= 0.07$ ). This trend was significant at the 5-day time point ( $p=0.0085$ ). Therefore, this miRNA might respond to early inflammatory stimuli in chondrocytes. It is now accepted that inflammation is present in early stages of OA even before any marked changes in cartilage structure or radiographic findings (Sokolove et al., 2013, van Dalen et al., 2016). Discovery of biomarkers in early-stage disease is of utmost importance. miR-361-5p was shown to be downregulated in the plasma of patients with chronic gouty arthritis and treatment of these patients with Chuanhutongfeng, a herb mixture with anti-inflammatory properties, increased levels of miR-361-5p (Wang et al., 2019b), suggesting an opposite relationship between inflammation and miR-361-5p levels, in agreement with our IL-1 $\beta$  experiment. Furthermore, miR-379-5p did not show any difference in OA chondrocytes treated with IL-1 $\beta$  for 24h ( $p=0.96$ ), but had the largest difference at the 5-day time point ( $p=0.0002$ ). As with miR-361-5p, there is limited data on the relationship between this miRNA and IL-1 $\beta$ . Li *et al* (2019) showed that decreased levels of miR-379-5p in

arsenite-treated human liver cells resulted in increased secretion of IL-1 $\beta$  and contributed to fibrosis (Li et al., 2019c). miR-107 expression was reduced in chondrocytes treated with LPS, an inflammatory mediator in OA, while it upregulated the expression of IL-1 $\beta$ . Overexpression of miR-107 resulted in decreased IL-1 $\beta$  levels in chondrocytes (Qian et al., 2021). Moreover, an interesting finding was that miR-143-3p showed increased expression at the 24h time point, which almost reached significance ( $p=0.06$ ). However, treatment for 5 days resulted in this miRNA having lower expression in treated cells compared to control ( $p=0.08$ ). Thus, there was a shift in its expression moving from 24h to 5 days of treatment. miR-143-3p was shown to have higher expression in the superficial zone of bovine cartilage compared to middle zone (Dunn et al., 2009, Hong et al., 2013). Expression of miR-143-3p, *COL2A1* and *ACAN* was decreased in dedifferentiated chondrocytes but was restored with TGF- $\beta$ 1 treatment, indicating that miR-143-3p might play a role in cartilage homeostasis. It is known that during early stages of OA, there is an upregulation of chondrogenic markers as an attempt of the tissue to compensate for cartilage loss, but expression gradually decreases as disease progresses (Goldring et al., 2016). This shift in miR-143-3p expression from the 24h time point to the 5-day time point could potentially indicate a role for this miRNA in cartilage homeostasis. By looking at the expression of specific cartilage markers, such as *COL2A1* and *ACAN*, starting from the 24h treatment and then up to the 5-day treatment, I also observed a similar pattern. This is more prominent for *ACAN*, which had higher expression in the treated group at 24h, but then its expression decreased significantly at the 5-day treatment group, further implying a compensation mechanism during the early stages of disease.

Another point to take into account is the dose of IL-1 $\beta$  used and how closely this *in vitro* inflammatory system resembles OA. In our study I used 10ng/ml to treat OA chondrocytes for all time points. This concentration is one of the most used in the literature (Chang et al., 2016, Yang et al., 2016, Zheng et al., 2017). However, the physiological levels of IL-1 $\beta$  in synovial fluid of OA patients has been reported to be between 0.021 – 0.146 ng/mL (McNulty et al., 2013), which is much lower than the levels used in our study and the literature. One reason for using higher concentration is time constraints. OA is a chronic disease progressing over several years. Systemic low-level inflammation is present in ageing and OA joints and production of pro-inflammatory cytokines by the synovium increases with ageing and in OA (Loeser, 2010). To reinstate an inflammatory response that resembles, in part, the

inflammatory response observed in an OA joint and in less time, higher levels or IL-1 $\beta$  were used. Moreover, an OA joint is subjected to the release of other pro-inflammatory cytokines, such as TNF- $\alpha$  and IL-6, which work synergistically to influence the inflammatory response in the joint. In most *in vitro* experiments and in our study, only IL-1 $\beta$  was used, therefore higher concentrations were selected to account for the absence of other pro-inflammatory and mechanically stimuli. That said, treatment of OA chondrocytes with IL-1 $\beta$  for these relatively shorter periods could resemble more acute inflammatory responses rather than the chronic low-level inflammation seen in OA patients. IL-1 $\beta$  has a short half-life of a few hours (Hazuda et al., 1988, Lopez-Castejon et al., 2011). In our experiment IL-1 $\beta$  was added in the cultures at day 0 and day 3 and cells were collected 24h and 5 days after day 0. In addition, while inflammation is one of the main features in an OA joint, and specifically during the early stage, other important factors have a significant effect as well. *In vivo*, chondrocytes are subjected to a sheer amount of mechanical force and are organised into zones, with different cell characteristics. In our IL-1 $\beta$  cultures, these stimuli and structure were absent and cells were grown in a monolayer. While IL-1 $\beta$  treatment induced changes in our selected miRNAs and specific cartilage markers, it cannot mimic the OA environment completely. Moreover, it is known that chondrocytes growing in monolayer cultures lose their OA and hypertrophic phenotype and dedifferentiate (Hong et al., 2013). Therefore, while IL-1 $\beta$  can be used to successfully induce inflammatory responses in chondrocytes, it cannot reinstate the complete pathological profile seen in OA and more combinatory studies would be needed for further interpretation of results. A more accurate approach would have been the treatment of 3-D cultures of healthy chondrocytes with low levels (0.05-0.1ng/ml) of IL-1 $\beta$  or a mixture of inflammatory cytokines for longer periods (weeks rather than days), where chondrocytes are also subjected to mechanical stress. Still, this model comes with challenges and does not fully represent physiological conditions.

## 4.6 Conclusion

qPCR analysis validated a selected list of DE miRNAs from our microarray results in the same samples as well as in an independent cohort of cartilage samples and confirmed reproducibility of results. Analysis in a separate cohort of young and old healthy cartilage

samples did not identify any of the selected miRNAs as DE, suggesting that changes reported in our microarray analysis were driven mainly by disease, rather than ageing. Treatment of OA chondrocytes with IL-1 $\beta$  showed that selected miRNAs responded better to longer treatments and the changes observed were similar to our data from the microarray analysis.

**Chapter 5: Modulation of expression of  
selected miRNAs in human primary OA  
chondrocytes and investigation of  
selected target gene expression**

## 5.1 Introduction

Over the last decade, miRNAs have become increasingly popular and a lot of research has been focused on elucidating their role and function. miRNAs exert their function by targeting complementary sequences in mRNAs, and either preventing them from being translated, or promoting their degradation (Dexheimer et al., 2020). miRNAs participate in all developmental stages by fine tuning the expression of important genes and their use as therapeutic targets or disease biomarkers is being realised (Bottani et al., 2020). The number of miRNAs implicated in cartilage and OA has steadily increased, and important cartilage and OA-related genes have been reported as miRNA targets (Jeffries, 2019, Reynard et al., 2020). Due to their short sequence length, the same miRNA can target many different mRNAs, and the same mRNA is targeted by many miRNAs. Several bioinformatic tools have been developed to predict miRNA-mRNA target interactions and provide insights into the potential targets of miRNAs, and therefore the potential functions of these (Huang et al., 2010). These tools take into account several parameters for target recognition, and amongst the most important is complementarity between the miRNA and the mRNA sequence. However, current predicting algorithms are not perfect and can generate many false positive results (Cloonan, 2015). Therefore, experimental validation must be undertaken for any miRNA target predicted by such algorithms.

Experimental validation of miRNA targets can be undertaken using different approaches. It is still not clear whether miRNA-mRNA interactions result in the degradation of the mRNA molecule or not (Cloonan, 2015). Data suggests that both mechanisms can take place and work synergistically to re-define gene expression (Dexheimer et al., 2020, Iwakawa et al., 2015). Taking this into account, to confirm miRNA targets numerous experimental approaches can be utilised, both at the transcriptional and protein level, using techniques such qPCR quantification, RNA-Seq, Western blotting, LC-MS/MS, luciferase reporter assays, crosslinking immunoprecipitation sequencing, and others. Confirmation of a miRNA-mRNA interaction allows the investigation of the biological pathways that the pair is involved in.

## **5.2 Study aim and rationale**

In Chapter 3 I undertook a microarray analysis to identify DE miRNAs between young cartilage from ACL donors and old OA intact and lesioned cartilage from TKA patients. In Chapter 4, a selected list of miRNAs that were DE between young and old OA intact/lesioned samples was selected for further validation. Selected miRNAs were validated by qPCR in additional cartilage samples and four of these; miR-361-5p, -379-5p, -107 and -143-3p, were selected for investigation using an *in vitro* OA inflammatory cell model. To investigate further the role and function of selected miRNAs in cartilage homeostasis and OA, I overexpressed and inhibited these four miRNAs in human primary OA chondrocytes using miRNA mimics and inhibitors. OA chondrocytes were treated in media supplemented with 10ng/ml IL-1 $\beta$  to mimic the inflammatory environment of an OA joint. Selected target genes and relevant biological pathways were investigated using qPCR for experiments investigating miR-361-5p, -379-5p and -107, and by LC-MS/MS for experiments investigating miR-143-3p. Selected target genes were investigated in the independent cohort of human cartilage samples that were used to validate microarray findings in Chapter 4.

## **5.3 Experimental design**

The experimental procedures, pertinent to this chapter are described briefly below. For full details on the experimental procedures, please refer to Chapter 2. Appropriate references are provided throughout the text.

### **5.3.1 Selection of predicted target genes**

Targets genes of selected miRNAs were predicted as described in Section 2.35. For experiments regarding miR-361-5p, -379-5p and -107, genes that were predicted as targets by at least two bioinformatic tools/databases were selected for validation. Target genes were selected based on their known or predicted function in cartilage and OA and novelty. Target genes which had previously been validated at the time of selection (as identified through literature) were not considered for further investigation. For miR-143-3p I followed a

prediction-free approach by undertaking LC-MS/MS using OA chondrocytes treated with mimics and inhibitors.

### 5.3.2 Treatment of human OA chondrocytes with miRNA mimics and inhibitors

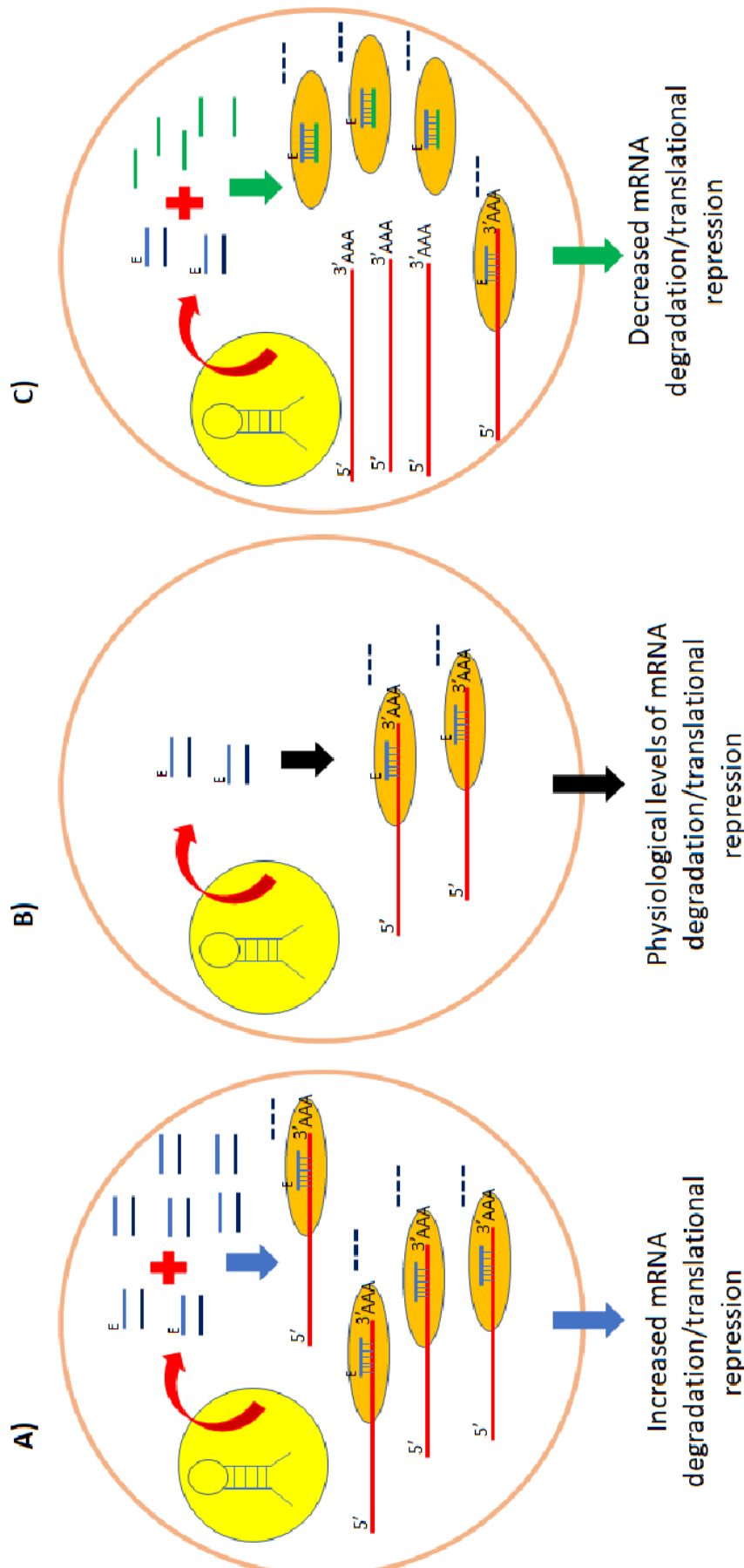
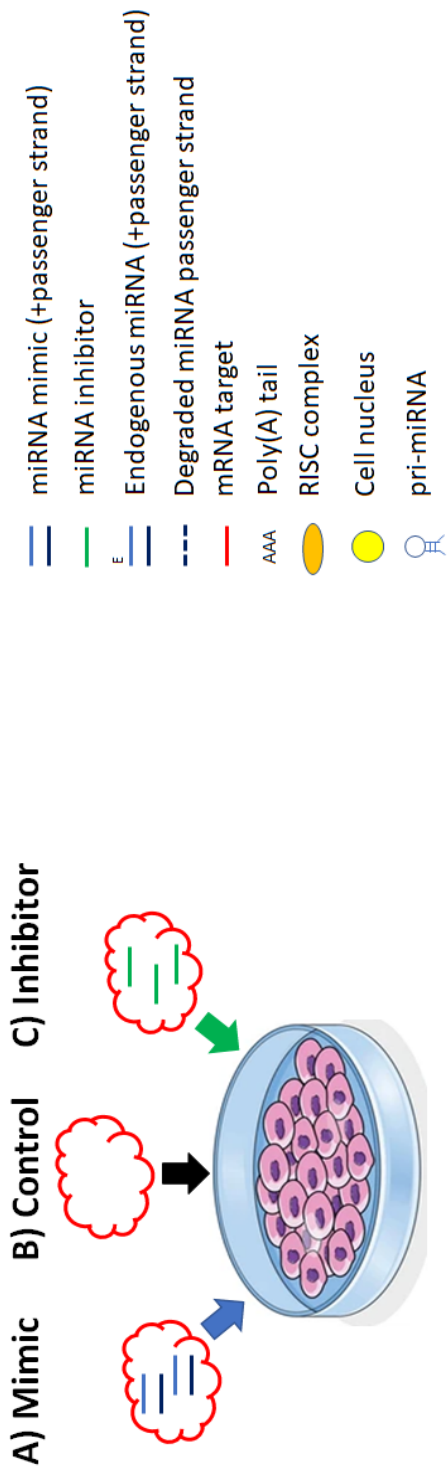
Isolation of human primary chondrocytes from OA patients was undertaken as described in Section 2.9. Cells were grown in T75 flasks until they reached 85-90% confluence, and then passaged and seeded in well plates as described in Section 2.11. Donor characteristics for each experiment are in **Table 5.1**. Cells plated in well plates were treated as described in Section 2.23. Function of miRNA mimics and inhibitors is shown in **Figure 5.1**.

**Table 5.1: Characteristics of OA donors whose chondrocytes were used to overexpress and inhibit selected miRNAs.** N/A: Sample details were not available.

miRNA	Donor	Age	Sex
miR-361-5p	1	73	M
	2	61	F
	3	62	M
	4	63	F
	5	N/A	F
miR-379-5p	1	N/A	N/A
	2	85	M
	3	70	M
	4	71	M
	5	80	M
	6	80	F

<b>miR-107</b>	1	75	F
	2	80	F
	3	73	M
	4	59	M
	5	51	F
	6	65	M
	7	77	M
	8	62	M
	9	78	M
	10	77	M
	11	80	M
<b>miR-143-3p</b>	1	78	M
	2	66	M
	3	81	M
	4	78	M
	5	68	F

**Figure 5.1 Function of miRNA mimics and inhibitors for modulation of miRNA expression.** miRNA mimics and inhibitors are synthetic compounds commonly used in research for overexpression and knockdown of the miRNA of interest. miRNA mimics (A) ‘mimic’ the structure and sequence of the endogenous miRNA of interest resulting in an increased number of miRNA copies in the cell compared to control (B), thus enhancing the downstream effect of the miRNA on its target genes. Inhibitors (C) are compounds complementary to the miRNA of interest and by binding it, they prevent the miRNA from binding its mRNA targets, thus inhibiting the miRNA from functioning. Original figure, key is indicated.



### **5.3.3 Total RNA extraction from human primary OA chondrocytes for qPCR validation of selected target genes**

Total RNA was extracted from human primary OA chondrocytes treated with mimics and inhibitors for miR-361-5, -379-5p and -107, or control, using TRIzol as described in Section 2.13.3.

### **5.3.4 cDNA synthesis for miRNA and mRNA quantification**

Poly(A) cDNA for miRNA quantification by qPCR was synthesised from total RNA as described in Section 2.16. cDNA synthesis for mRNA quantification by qPCR was synthesised from total RNA as described in Section 2.17.

### **5.3.5 qPCR for miRNA and mRNA quantification**

miRNA and mRNA quantification by qPCR was undertaken as described in Section 2.18 and 2.19, respectively. Statistical analysis was undertaken in GraphPad Prism version 8.0.1 for Windows and normality of data was assessed using the Shapiro-Wilk normality test. For miRNA and mRNA quantification in treated and control human primary chondrocytes, statistical significance was calculated using a two-tailed paired t-test as data followed the Gaussian distribution. For mRNA quantification in human cartilage tissue, statistical significance was calculated using the Mann-Whitney test, as data did not follow the Gaussian distribution. P values<0.05 were considered significant.

### **5.3.6 Selection of endogenous reference genes for qPCR data normalisation**

For qPCR validation of target genes in cartilage tissue samples, seven potential reference genes were selected for testing: *RPL13A*, *RPLPO*, *RPL3*, *ATP5F1A*, *RPL4*, *YWHAE* and *GAPDH*. Potential reference genes were either selected from the literature or from an RNA-Seq project undertaken by our group in which I compared the mRNA expression between young normal,

old normal and old OA human cartilage tissue (unpublished data). Selection of the appropriate reference genes for qPCR data normalisation was carried out as described in Section 2.40.

### **5.3.7 Collection, lysis and preparation of human primary chondrocytes for LC-MS/MS analysis**

Human primary OA chondrocytes treated with mimics and inhibitors for miR-143-3p or control were collected and lysed for LC-MS/MS analysis as described in Section 2.24. Proteins in chondrocyte lysates were quantified using the Pierce™ 660nm Protein Assay as described in Section 2.25 and protein quality was assessed using Silver Staining as described in Sections 2.26 and 2.27. Cell lysates were trypsin digested and prepared for LC-MS/M as described in Section 2.28. Complete digestion was assessed using Coomassie Brilliant Blue staining as described in Section 2.29. Trypsin digests were subjected to LC-MS/MS analysis as described in Section 2.30. Label-free quantification was undertaken using the Progenesis QI for proteomics software as described in Section 2.33. Briefly, the raw files of the spectra were aligned and peak picking was carried out by the Progenesis software for ion quantification. Lists of peptide ions were exported to our local Mascot server (Version 2.6.2) for peptide identification. Proteins that had at least two unique peptides were selected. Protein abundances were  $\log_{10}$  transformed and normalised relative to a selected reference sample. Statistical analysis was undertaken using two-tailed paired t-tests in R (Version 4.0.2). P values were adjusted for multiple testing. Differences at FDR-adjusted  $p < 0.05$  were considered significant.

### **5.3.8 STRING analysis for identification of protein interactions**

To identify protein interactions between DE proteins from LC-MS/MS, I undertook a STRING analysis as described in Section 2.39. Minimum required interaction score was set to highest confidence (0.900).

### **5.3.9 IPA analysis for identification of miR-143-3p relevant biological pathways following LC-MS/MS analysis**

To identify relevant biological pathways that miR-143-3p is involved in, IPA was used to analyse the DE proteins identified by label-free quantification following LC-MS/MS of primary OA chondrocytes treated with mimics and inhibitors of miR-143-3p. IPA analysis was undertaken as described in Section 2.36B. P value cut-off was set to 0.05.

## 5.4 Results

### 5.4.1 Selection of predicted targets for miR-361-5p, -379-5p and -107

Predicted target genes of miR-361-5p, -379-5p and -107 were selected using bioinformatic tools available online. The following tools were used to predict the target genes of selected miRNAs: TargetScan (Agarwal et al., 2015), miRWalk (Dweep et al., 2015), miRmap (Vejnar et al., 2012) and miRTar (Hsu et al., 2011). TargetScan and miRWalk generated lists of all predicted target genes for these specific miRNAs of interest. The following target genes were selected for each of the three miRNAs of interest: for miR-361-5p: *CALM3* and *RHOA*, for miR-379-5p: *TGFBR1*, *HDAC2* and *SMAD9*, and for miR-107: *WNT4*, *IHH*, *FGF2*, *TNF* and *IRF1*.

**Table 5.2** summarises the predicted targets that were selected for further validation for each miRNA, as well as which of the four databases predicted each interaction.

**Table 5.2: Selected predicted targets of miR-361-5p, -379-5p and -107 by four prediction algorithms.**

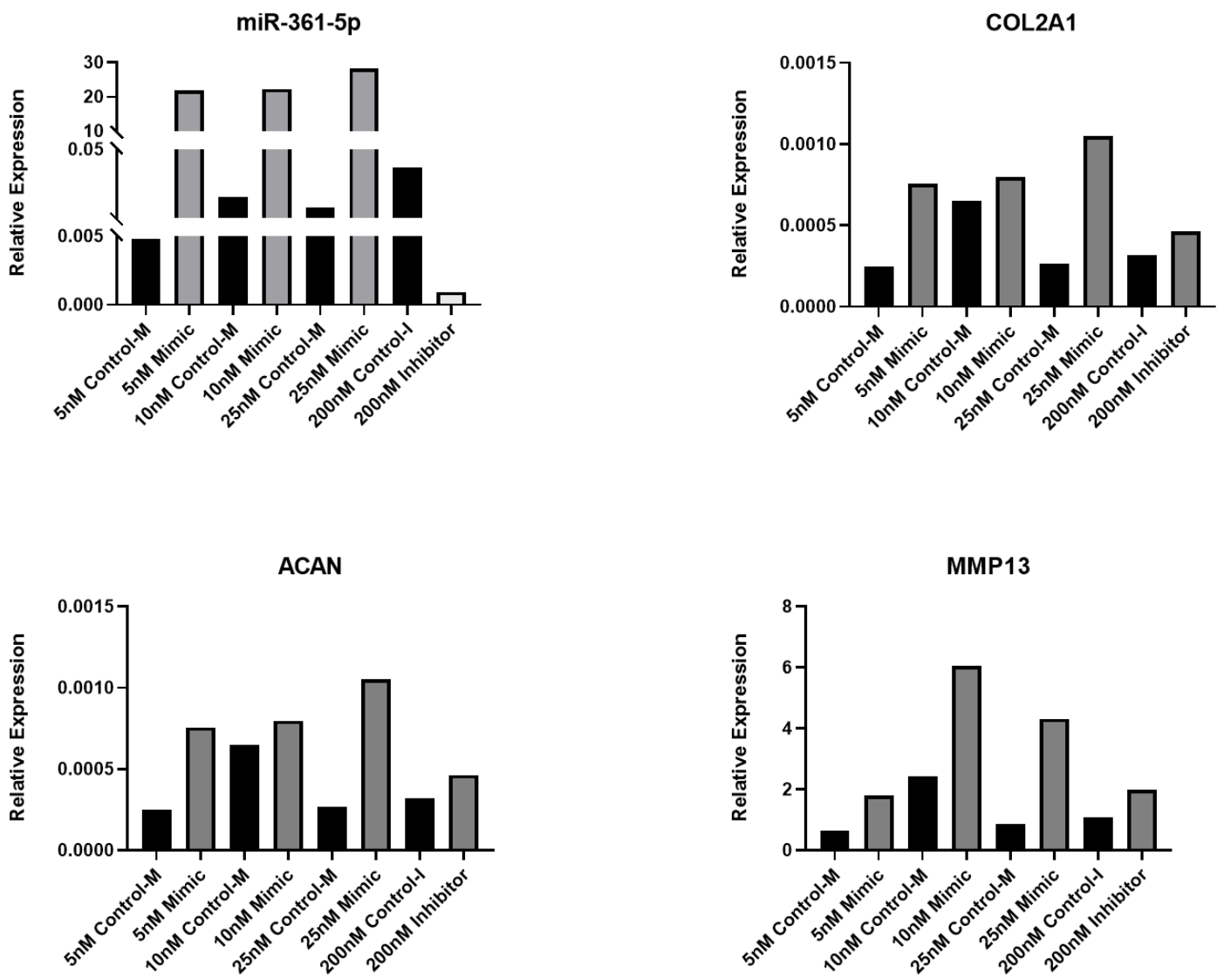
miRNA	Target	TargetScan	miRWalk	miRmap	miRTar
miR-361-5p	<b><i>CALM3</i></b>	✓	✓	✓	✓
	<b><i>RHOA</i></b>	✓	✓	✓	x
miR-379-5p	<b><i>TGFBR1</i></b>	✓	✓	✓	✓
	<b><i>HDAC2</i></b>	x	✓	✓	✓
	<b><i>SMAD9</i></b>	x	x	✓	✓
miR-107	<b><i>WNT4</i></b>	✓	✓	x	✓
	<b><i>IHH</i></b>	✓	✓	✓	✓
	<b><i>FGF2</i></b>	✓	✓	✓	✓
	<b><i>TNF</i></b>	x	✓	x	✓
	<b><i>IRF1</i></b>	x	✓	✓	x

#### **5.4.2 Expression of selected target genes in human primary OA chondrocytes treated with miR-361-5p mimics and inhibitors in an *in vitro* OA inflammatory model**

Human primary OA chondrocytes, cultured to passage 1, were treated with miR-361-5p mimic or control-mimic and miR-361-5p inhibitor or control-inhibitor, in media supplemented with 10ng/ml IL-1 $\beta$  for 48h. According to the manufacturer of mimics and inhibitors, successful overexpression or inhibition should not be confirmed by looking at the expression of the miRNA itself, but at the expression of the target genes or other relevant gene markers that might be influenced by the miRNA (Qiagen, 2015, Qiagen, 2017). Nonetheless, for some of the experiments I also looked at the expression of the miRNA itself following its overexpression/inhibition. I also investigated the effect of transfection on predicted target genes or relevant cartilage markers.

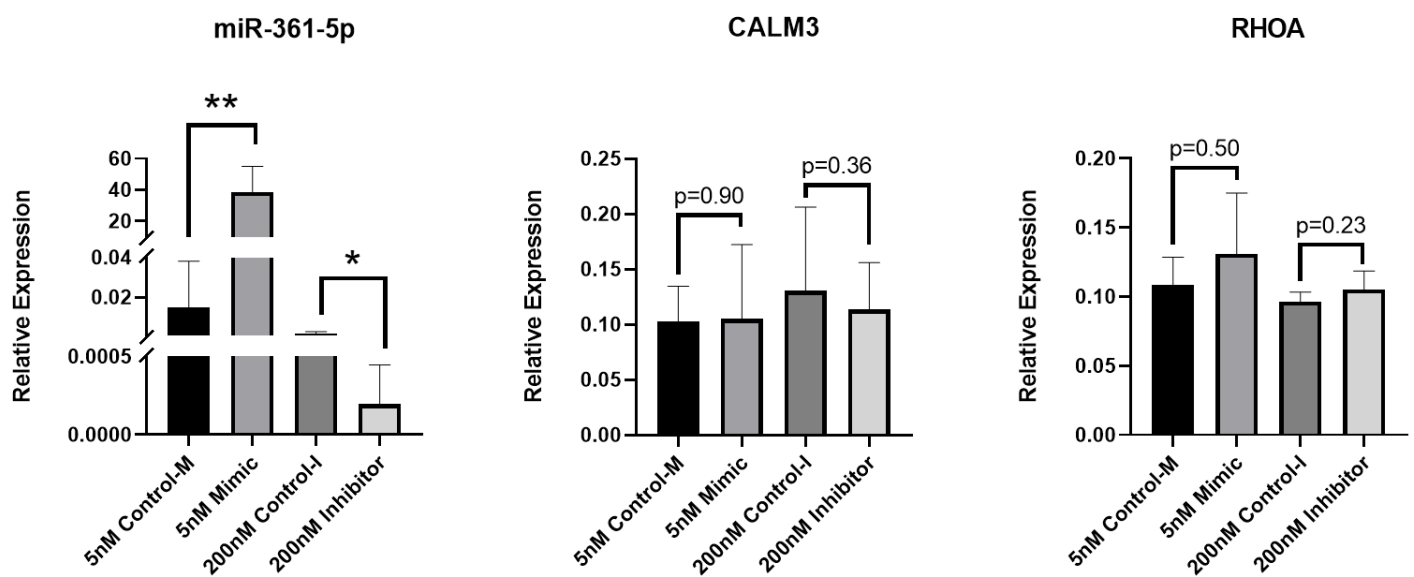
Our microarray analysis identified that miR-361-5p had a lower expression in OA intact and lesioned cartilage compared to young cartilage from ACL donors (Chapter 3), and also that its expression was lower in IL-1 $\beta$  treated cells compared to control (Chapter 4). Thus, I expected miR-361-5p to exert a positive effect on cartilage homeostasis and increase the expression of anabolic markers such as *COL2A1* and *ACAN*, and decrease the expression of catabolic markers such as *MMP13*. First, I assessed the optimal concentration for the miR-361-5p mimic by measuring the expression of *COL2A1*, *ACAN* and *MMP13* in human primary OA chondrocytes from the same donor treated with three different concentrations of miR-361-5p mimic: 5nM, 10nM and 25nM. The optimum concentration would be the one that would exert the strongest positive effect on the anabolic markers *COL2A1* and *ACAN*, and the strongest negative effect on the catabolic marker *MMP13*. For the inhibitor, I selected a concentration of 200nM based on previous experience from our colleagues and collaborators. Analysis showed that miR-361-5p had higher expression in all cells treated with any concentration of the mimic, compared to control, but all three different concentrations resulted in similar levels for miR-361-5p in the treated cells (**Figure 5.2**). *COL2A1*, *ACAN* and *MMP13* behaved similarly in all three different concentrations and all had higher expression in the treated cells compared to control. Chondrocytes treated with the inhibitor had lower expression compared to control, whereas all selected markers had slightly higher expression in the inhibitor group compared to control. Since all concentrations had a similar effect on selected cartilage markers and on miRNA expression, I selected 5nM as the concentration to

be used for further experiments. This was also the recommended starting concentration by the manufacturer (Qiagen, 2015).



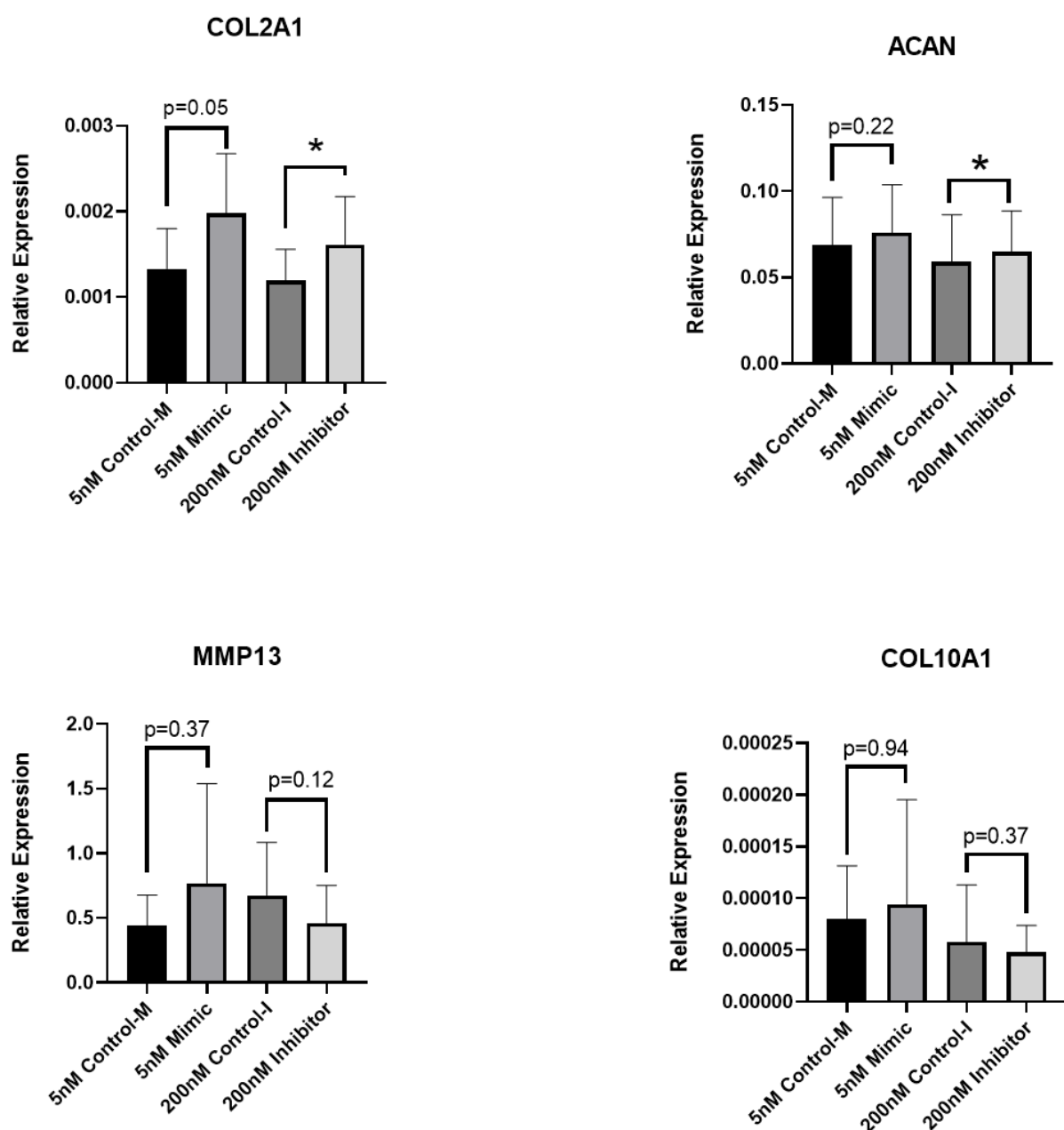
**Figure 5.2: Expression of miR-361-5p and selected cartilage markers in human OA chondrocytes treated with a gradient of miR-361-5p mimic or control and inhibitor or control.** Human OA chondrocytes were treated in media supplemented with 10ng/ml IL-1 $\beta$  with miR-361-5p 5nM/10nM/25nM mimic or control-mimic and 200nM inhibitor or control-inhibitor, for 48h. Expression of miR-361-5p and of cartilage markers is shown. N=1 donor. Expression is relative to SNORD68 for miR-361-5p and relative to GAPDH for cartilage markers. Control-M=control-mimic, control-I=control-inhibitor.

Based on the preliminary results, I treated OA chondrocytes from additional donors with 5nM mimic/control-mimic and 200nM inhibitor/control-inhibitor for miR-361-5p, and measured the expression of miR-361-5p, of selected cartilage markers: *COL2A1*, *ACAN*, *MMP13*, *SOX9*, *RUNX2*, *COL10A1*, as well as the expression of two predicted target genes: *CALM3* and *RHOA*. Analysis showed that expression of miR-361-5p was significantly higher in chondrocytes treated with mimics compared to control ( $p=0.006$ ) and significantly lower in chondrocytes treated with the inhibitor compared to control ( $p=0.01$ ). The percentage of knockdown was 90%. However, as already mentioned this is not a clear indication that the treatments were successful. When I assessed the expression of predicted target genes, *CALM3* and *RHOA*, there was no significant change in their expression (Figure 5.3).



**Figure 5.3: Expression of miR-361-5p and its two predicted target genes in human OA chondrocytes treated with miR-361-5p mimic, inhibitor or control.** Human OA chondrocytes were treated in media supplemented with 10ng/ml IL-1 $\beta$  with miR-361-5p 5nM mimic, 200nM inhibitor or control for 48h. Expression of miR-361-5p and of predicted targets is shown. N=4-5 donors. Expression is relative to SNORD6B for miR-361-5p and relative to GAPDH for predicted target genes. Statistical analysis was undertaken using a two-tailed paired t-test in GraphPad Prism (Version 8.0.1). Data are represented as mean+SD. P values<0.05 were considered significant. \*: p<0.05, \*\*: p<0.01. Control-M=control-mimic, control-I=control-inhibitor.

For miR-361-5p mimic and inhibitor treatments, I also looked at the expression of specific chondrogenic and hypertrophic cartilage markers, to investigate whether modulation of the miRNA expression had an effect on them. Analysis showed that most cartilage markers did not significantly change between mimic and control or inhibitor and control. *COL2A1* and *ACAN* expression was significantly higher in the inhibitor group compared to control ( $p=0.04$  in both), and *COL2A1* expression was higher in the mimic group compared to control but did not reach significant levels ( $p=0.05$ ) (Figure 5.4).



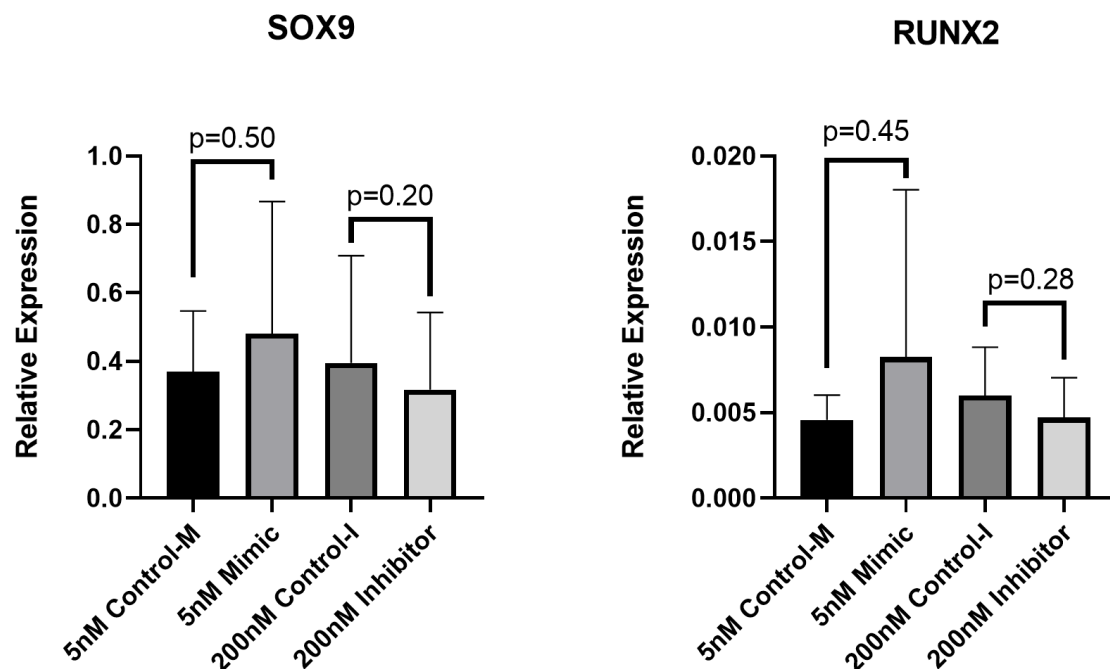
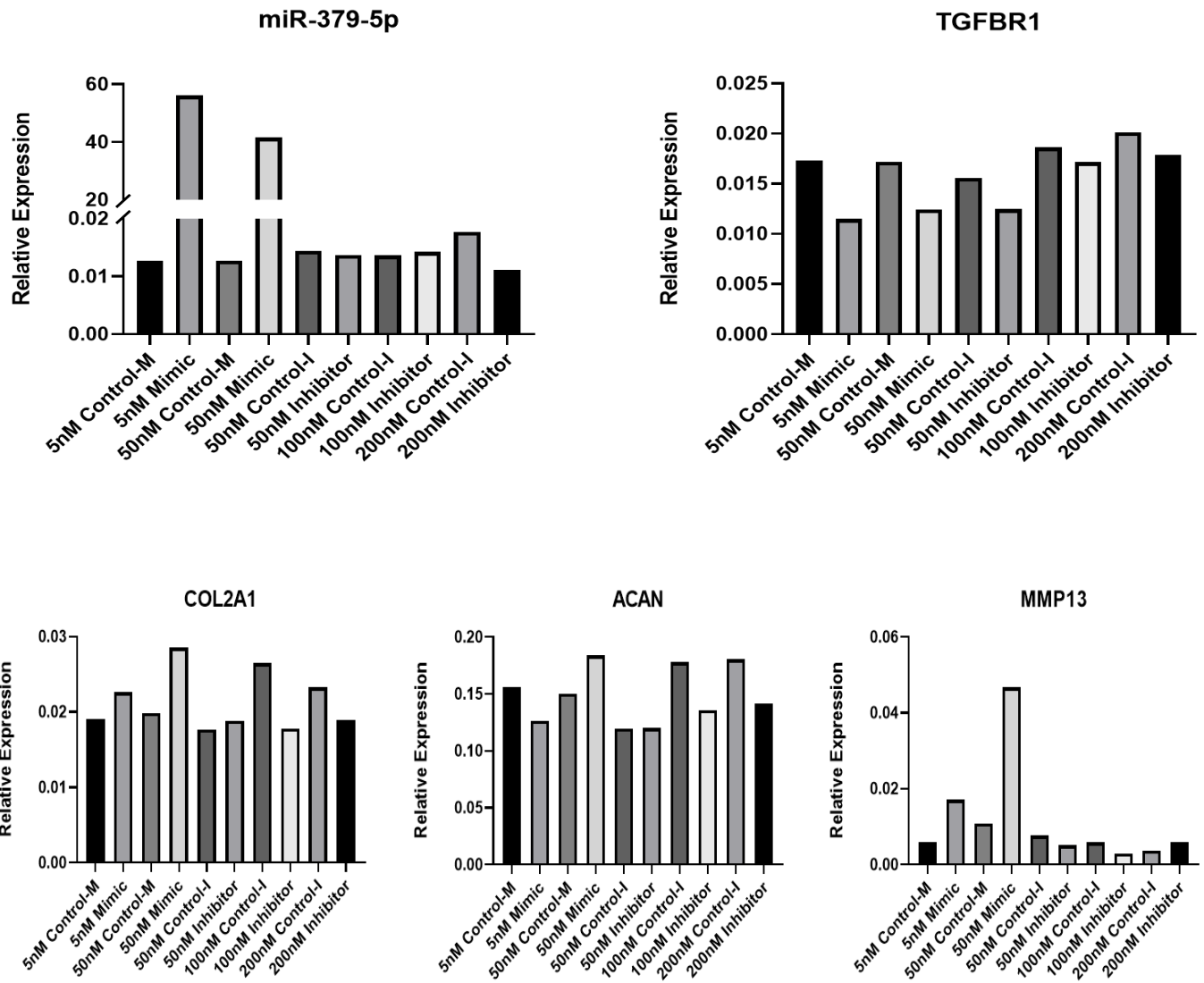


**Figure 5.4: Expression of selected cartilage markers in human OA chondrocytes treated with miR-361-5p mimic, inhibitor or control.** Human OA chondrocytes were treated in media supplemented with 10ng/ml IL-1 $\beta$  with miR-361-5p 5nM mimic, 200nM inhibitor or control for 48h. Expression of specific chondrogenic and hypertrophic cartilage markers is shown. N=4-5 donors. Expression is relative to GAPDH. Statistical analysis was undertaken using a two-tailed paired t-test in GraphPad Prism (Version 8.0.1). Data are represented as mean+SD. P values<0.05 were considered significant. \*: p<0.05. Control-M=control-mimic, control-I=control-inhibitor.

#### 5.4.3 Expression of selected target genes in human primary OA chondrocytes treated with miR-379-5p mimics and inhibitors in an *in vitro* OA inflammatory model

To investigate the role of miR-379-5p in cartilage and OA, the same approach was taken as with miR-361-5p. Human primary OA chondrocytes, were treated with miR-379-5p mimic or control-mimic and miR-379-5p inhibitor or control-inhibitor, in media supplemented with 10ng/ml IL-1 $\beta$  for 48h. Following overexpression and inhibition, I investigated the expression of miR-379-5p. Additionally I investigated the effect of mimic and inhibitor on the predicted target genes or relevant cartilage markers.

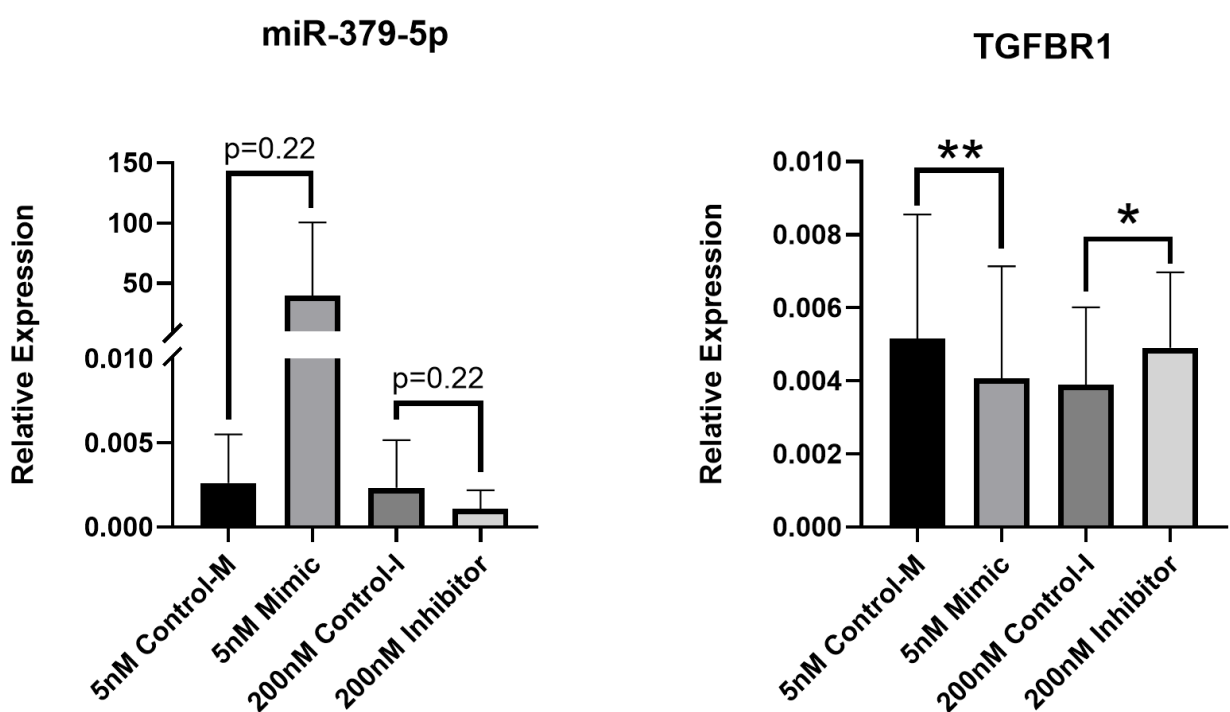
First, I assessed the optimum concentration for miR-379-5p mimic and inhibitor using chondrocytes from one donor. I used two concentrations for the mimic: 5nM (recommended starting concentration) and 50nM. From our miR-361-5p experiments, I observed that there were no significant differences between the concentrations initially tested (5nM, 10nM and 25nM). Therefore, I utilised a higher concentration to see the effect compared to 5nM. For the inhibitor, 200nM was the selected concentration, as before. Additionally, I also included initial treatments of 50nM and 100nM for direct comparison and confirmation. Following treatment, I measured the relative expression of miR-379-5p, its predicted target: *TGFBR1*, and also of three cartilage markers: *COL2A1*, *ACAN* and *MMP13*. Results indicated that 5nM and 50nM mimic produced similar results and in fact the 5nM concentration led to higher miR-379-5p expression compared to the 50nM treatment. Both treatments led to reduced *TGFBR1* expression and at similar levels. The effect of the mimics on cartilage markers was less clear. Of note was that the 50nM mimic treatment led to a larger increase in *MMP13*, compared to the 5nM mimic treatment. I selected the 5nM mimic treatment as it had the same effect on *TGFBR1* and did not lead to an extremely high increase in *MMP13* expression. For the inhibitor treatments, 50nM and 100nM did not have any effect on miR-379-5p expression, whereas 200nM treatment led to a decrease in miR-379-5p expression. The effect on *TGFBR1* expression was the same for all concentrations with *TGFBR1* having lower expression in all three treatments. This was opposite to what was expected. 50nM inhibitor treatment did not have any effect on cartilage markers, whereas 100nM and 200nM led to decrease *COL2A1* and *ACAN* expression. Only the 200nM treatment led to increased *MMP13* expression (**Figure 5.5**). Based on these results I selected the 200nM treatment for follow up studies.



**Figure 5.5: Expression of miR-379-5p, TGFBR1 and selected cartilage markers in human OA chondrocytes treated with a gradient of miR-379-5p mimic/control and inhibitor/control.**

Human OA chondrocytes were treated in media supplemented with 10ng/ml IL-1 $\beta$  with miR-379-5p 5nM/50nM mimic-control-mimic and 50nM/100nM/200nM inhibitor-control-inhibitor, for 48h. Expression of miR-379-5p, predicted targets and cartilage markers is shown. N=1 donor. Expression is relative to SNORD68 for miR-379-5p, and relative to GAPDH for protein-coding genes. Control-M=control-mimic, control-I=control-inhibitor.

Based on these preliminary results, I treated OA chondrocytes from additional donors with 5nM mimic/control-mimic and 200nM inhibitor/control-inhibitor for miR-379-5p, and checked the expression of miR-379-5p, of selected cartilage markers: *COL2A1*, *ACAN*, *MMP13*, as well as the expression of the predicted target genes: *TGFBR1*, *SMAD9* and *HDAC2*. Results showed that expression of miR-379-5p was higher in chondrocytes treated with mimics compared to control ( $p=0.22$ ), and lower in chondrocytes treated with the inhibitor compared to control ( $p=0.22$ ), but neither reached statistical significance. However, when I looked at the expression of the predicted target gene, *TGFBR1*, there were significant changes observed in its expression. Specifically, expression of *TGFBR1* was significantly lower in chondrocytes treated with the mimic ( $p=0.001$ ), and significantly higher in chondrocytes treated with the inhibitor ( $p=0.02$ ), consistent with the direction of dysregulation expected after overexpressing or inhibiting miR-379-5p. Predicted targets *SMAD9* and *HDAC2* as well as cartilage markers did not show any statistically significant changes between treated groups and controls (**Figure 5.6**).



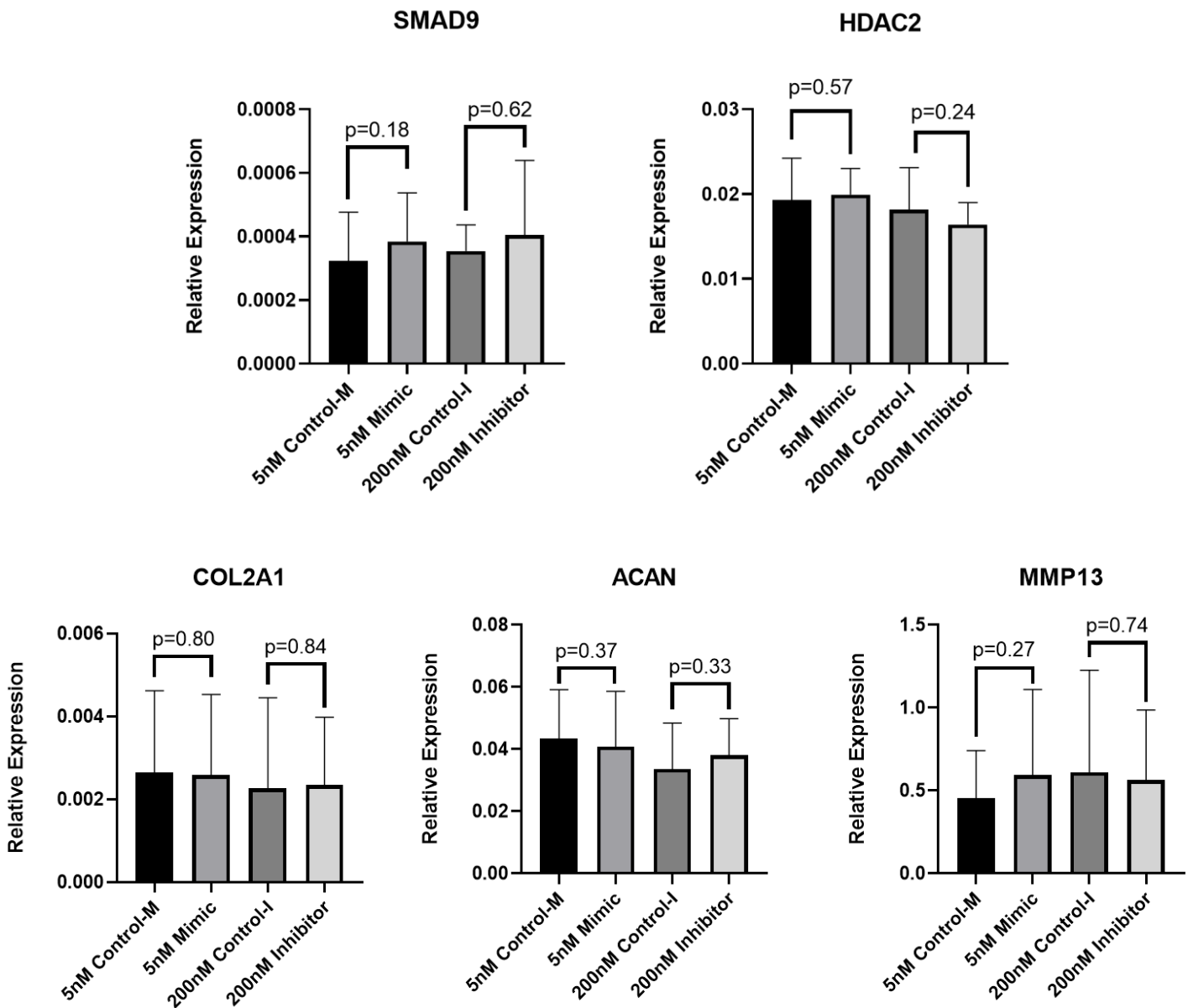
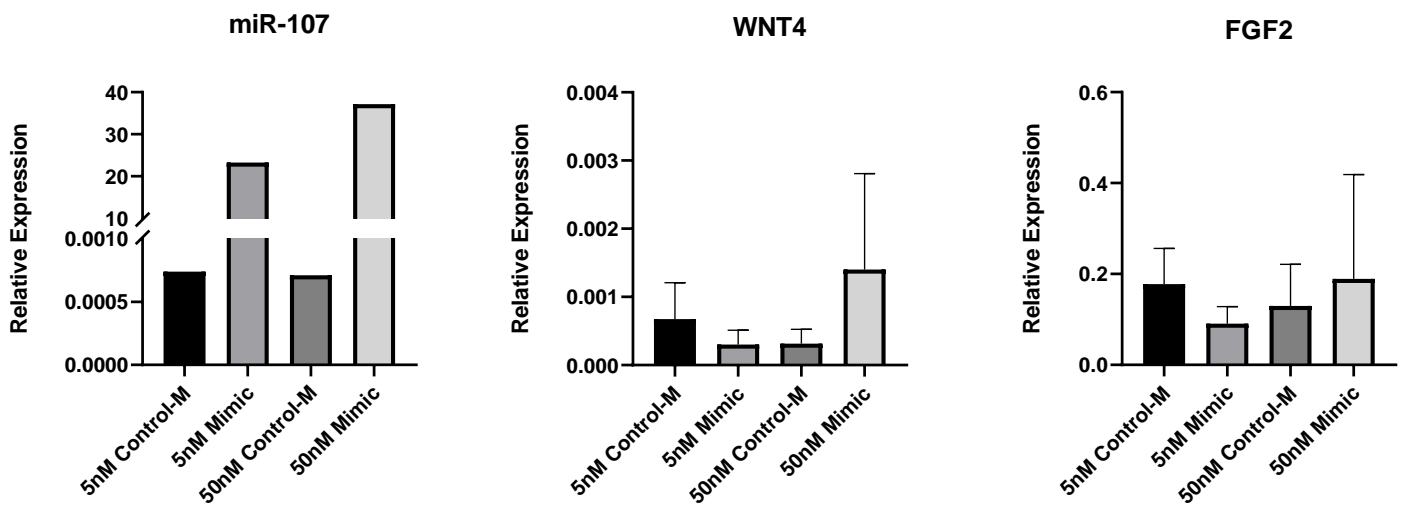


**Figure 5.6: Expression of miR-379-5p, its predicted target gene and cartilage markers in human OA chondrocytes treated with miR-379-5p mimic, inhibitor or control.** Human OA chondrocytes were treated in media supplemented with 10ng/ml IL-1 $\beta$  with miR-379-5p 5nM mimic, 200nM inhibitor or control, for 48h. Expression of miR-379-5p, predicted targets and cartilage markers is shown. N=5-6 donors. Expression is relative to SNORD68 for miR-379-5p and relative to GAPDH for protein-coding genes. Statistical analysis was undertaken using a two-tailed paired t-test in GraphPad Prism (Version 8.0.1). Data are represented as mean+SD. P values<0.05 were considered significant. \*: p<0.05, \*\*: p<0.01. Control-M=control-mimic, control-I=control-inhibitor.

#### **5.4.4 Expression of selected target genes in human primary OA chondrocytes treated with miR-107 mimics and inhibitors in an *in vitro* OA inflammatory model**

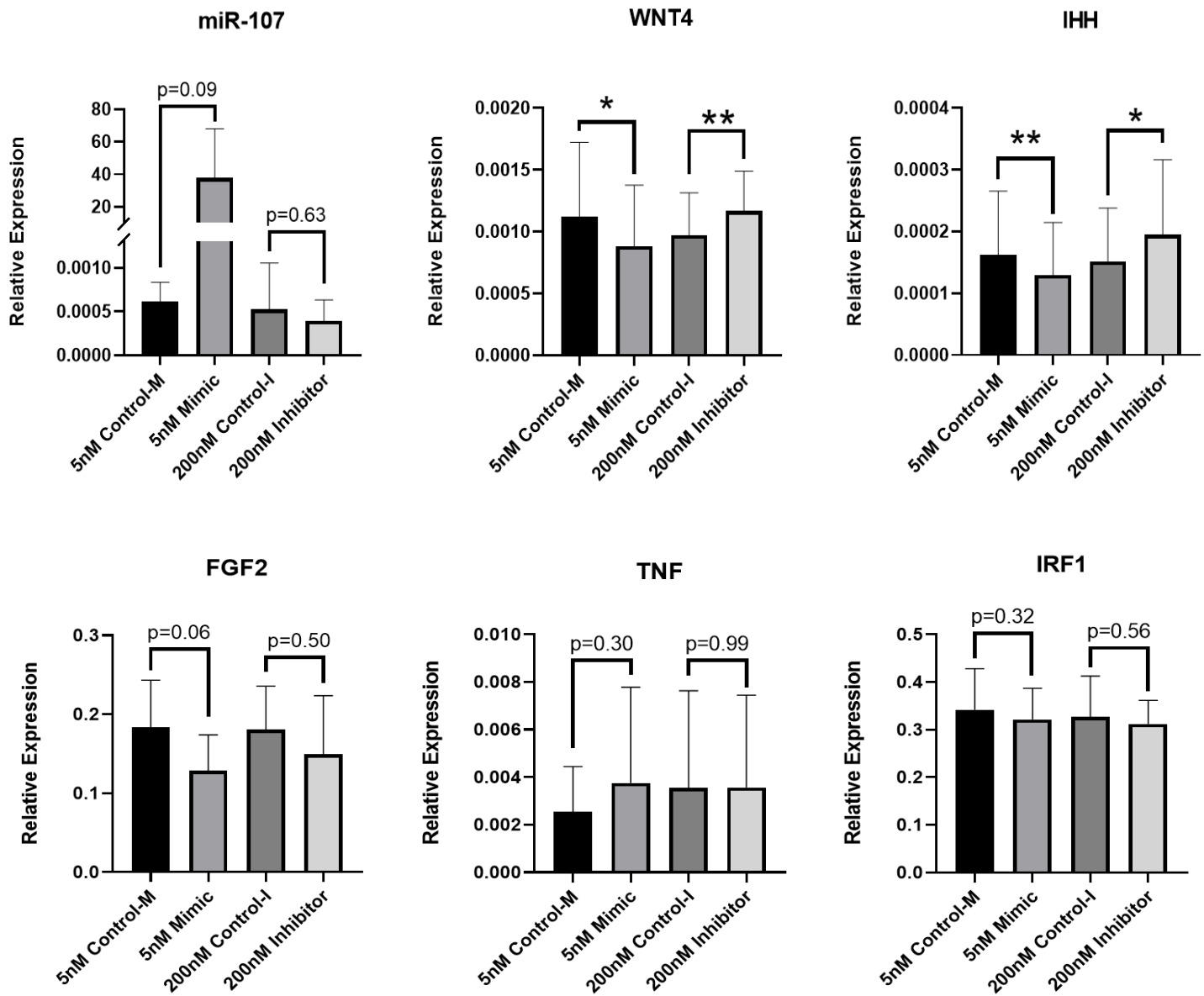
To investigate the role of miR-107 in cartilage and OA, I undertook a similar set of experiments. Human primary OA chondrocytes were treated with miR-107 mimic or control-mimic and miR-107 inhibitor or control-inhibitor, in media supplemented with 10ng/ml IL-1 $\beta$  for 48h. Following overexpression and inhibition, I focused primarily on the expression of predicted target genes, *WNT4*, *IHH*, *FGF2*, *TNF* and *IRF1*.

Based on results from our previous experiments, initially I used chondrocytes from two donors and investigated a 5nM and a 50nM concentration for the mimic treatment and measured the relative expression of miR-107 and two target genes: *WNT4* and *FGF2*. Results showed that expression of miR-107 was higher in chondrocytes treated with either concentration compared to control, and reached higher levels in chondrocytes treated with 50nM. However, when I investigated the expression of selected predicted target genes, I observed that *WNT4* and *FGF2* had an improved response to 5nM mimic treatment compared to 50nM. Specifically, both *WNT4* and *FGF2* had lower expression in chondrocytes treated with 5nM compared to control and higher expression in chondrocytes treated with 50nM mimic compared to control (**Figure 5.7**). Therefore, only the 5nM mimic treatment generated the expected results. Based on this, I selected 5nM as the concentration for follow up experiments. For the inhibitor, I used 200nM as in previous experiments.



**Figure 5.7: Expression of miR-107, WNT4 and FGF2 in human OA chondrocytes treated with a 5nM and 50nM miR-107 mimic and control.** Human OA chondrocytes were treated in media supplemented with 10ng/ml IL-1 $\beta$  with miR-107 5nM or 50nM mimic or control, for 48h. Expression of miR-107 and targets is shown. N=1-2 donors. Expression is relative to SNORD68 for miR-107 and relative to GAPDH for WNT4 and FGF2. Data are represented as mean+SD. Control-M=control-mimic, control-I=control-inhibitor.

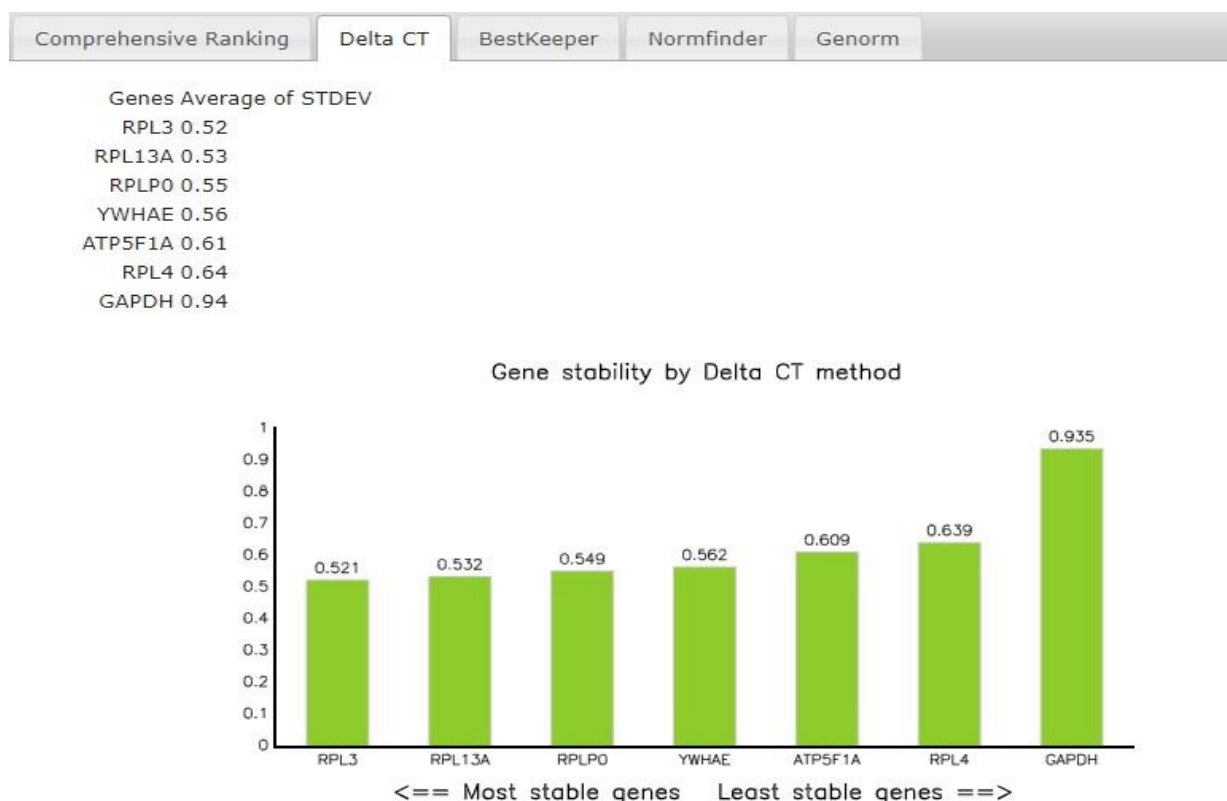
Based on these preliminary results, I treated chondrocytes from additional donors with 5nM mimic and 200nM inhibitor and measured the relative expression of predicted target genes: *WNT4*, *IHH*, *FGF2*, *TNF* and *IRF1*. Results demonstrated that expression of miR-107 was higher in chondrocytes treated with the mimic and lower in chondrocytes treated with the inhibitor. However, neither reached statistical significance. Moreover, chondrocytes had significantly lower *WNT4* and *IHH* expression in the mimic group and significantly higher expression in the inhibitor group, as expected. *FGF2* expression was lower in the mimic group ( $p=0.06$ ) but did not show significant change in the inhibitor group. *TNF* and *IRF1* did not show any significant change in the mimic, nor in the inhibitor group. Results are shown in **Figure 5.8**.

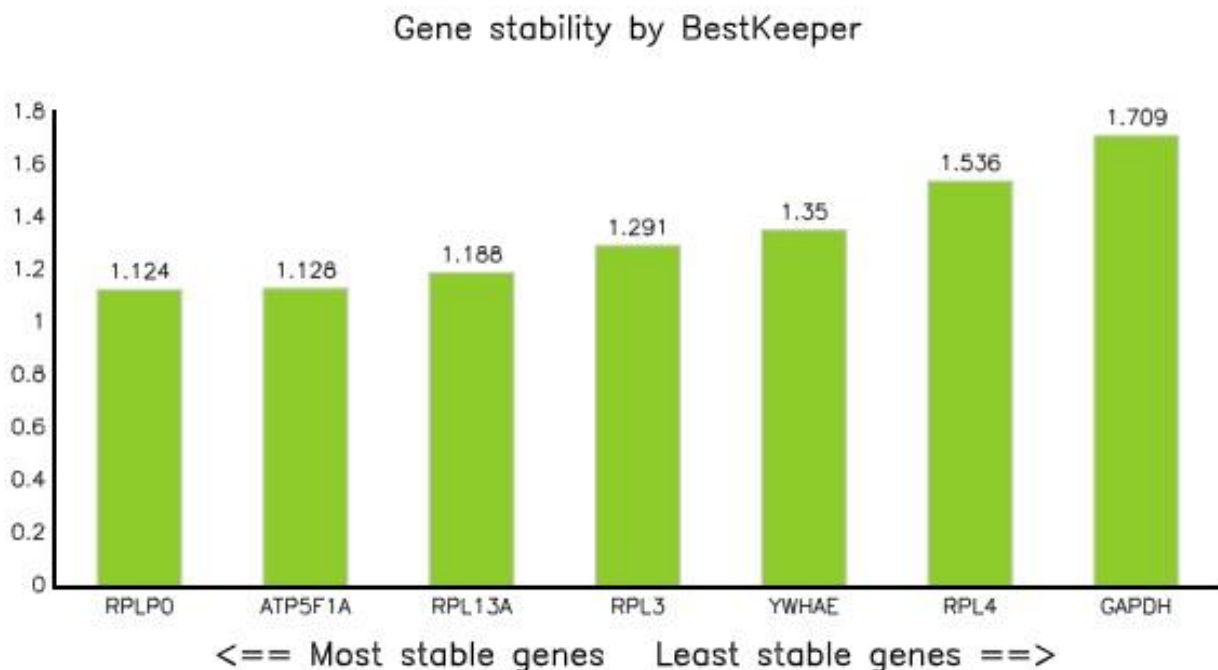


**Figure 5.8: Expression of miR-107 and its predicted target genes in human primary OA chondrocytes treated with miR-107 mimic, inhibitor or control.** Human OA chondrocytes were treated in media supplemented with 10ng/ml IL-1 $\beta$  with miR-107 5nM mimic, 200nM inhibitor or control. Expression of miR-107 and predicted targets is shown. N=8-11 donors. Expression is relative to SNORD68 for miR-107, and relative to GAPDH for predicted target genes. Statistical analysis was undertaken using a two-tailed paired t-test in GraphPad Prism (Version 8.0.1). Data are represented as mean+SD. P values<0.05 were considered significant.  
\*: p<0.05, \*\*: p<0.01. Control-M=control-mimic, control-I=control-inhibitor.

#### 5.4.5 Investigation of miRNA predicted target genes in human articular cartilage tissue

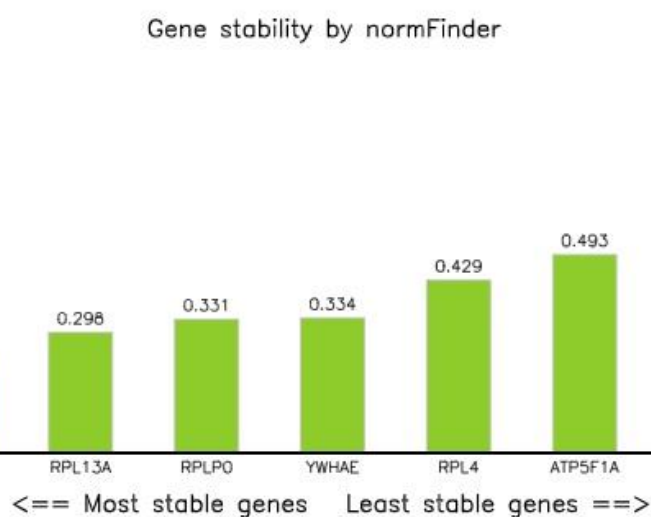
Overexpression and knockdown of selected miRNAs in human primary OA chondrocytes offered insights on some potential target genes of these miRNAs. *CALM3* and *RHOA* did not show any significant changes in chondrocytes treated with miR-361-5p mimic and inhibitor. *TGFB1* had significantly lower expression in chondrocytes treated with miR-379-5p mimic and significantly higher expression in chondrocytes treated with miR-379-5p inhibitor. Likewise, *WNT4* and *IHH* had significantly lower expression in chondrocytes treated with miR-107 mimic and significantly higher expression in chondrocytes treated with miR-107 inhibitor. In Chapter 3, I identified that miR-379-5p and miR-107 had significantly lower expression in old OA intact and lesioned cartilage tissue compared to young cartilage tissue from ACL donors. To investigate further whether these genes are indeed targeted by these miRNAs, I interrogated their expression in the independent cohort of cartilage tissue samples that were used to validate microarray findings in Chapter 4. First, I identified the most appropriate endogenous reference gene to use. I investigated the following potential reference genes: *RPL13A*, *RPLPO*, *RPL3*, *ATP5F1A*, *RPL4*, *YWHAE* and *GAPDH*. Analysis with RefFinder showed that the best reference gene for our cartilage tissue samples was *RPL3* (**Figure 5.9**), and thus it was selected as the reference gene.





Gene name Stability value

RPL3	0.237
RPL13A	0.298
RPLP0	0.331
YWHAE	0.334
RPL4	0.429
ATP5F1A	0.493
GAPDH	0.888

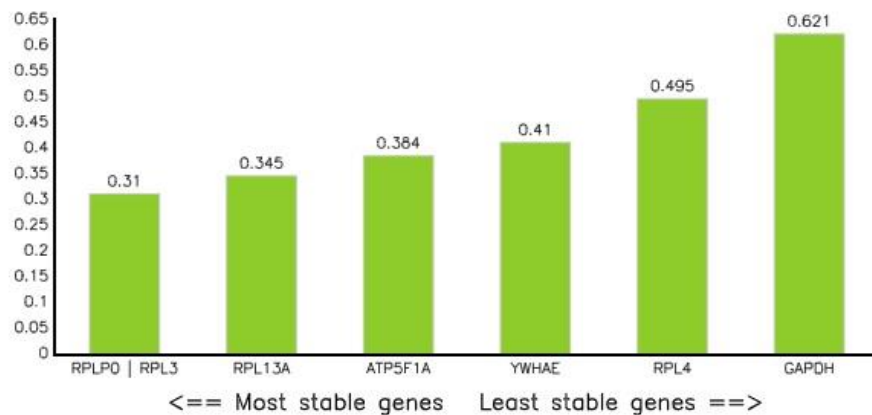


Comprehensive Ranking Delta CT BestKeeper Normfinder Genorm

Gene name Stability value

RPLP0   RPL3	0.310
RPL13A	0.345
ATP5F1A	0.384
YWHAE	0.410
RPL4	0.495
GAPDH	0.621

Gene stability by Genorm



Comprehensive Ranking Delta CT BestKeeper Normfinder Genorm

Genes Geomean of ranking values

RPL3	1.41
RPLP0	1.73
RPL13A	2.45
ATP5F1A	3.94
YWHAE	4.47
RPL4	5.73
GAPDH	7.00

Comprehensive gene stability

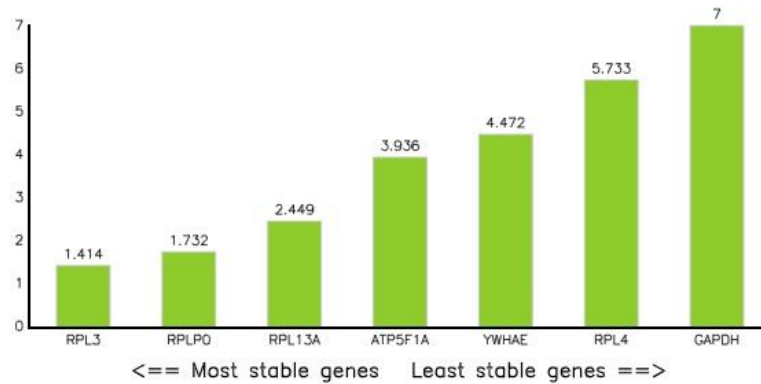


**Figure 5.9: Selection of the best endogenous reference gene in human articular cartilage.**

From a list of seven potential reference genes, RefFinder identified *RPL3* as the best gene to use for qPCR normalisation in human articular cartilage tissue.

Results showed that *TGFBR1* had lower expression in OA intact and lesioned cartilage samples compared to young intact cartilage from ACL donors, similar to miR-379-5p and opposite to what was expected (**Figure 5.10**). In addition, *TGFBR1* had a significantly higher expression in OA-intact cartilage samples compared to OA-lesioned cartilage. However, as described in Chapter 3 and 4 there was no significant difference between OA-intact and OA-lesioned cartilage for miR-379-5p. Therefore, results indicated that *TGFBR1* was not likely a target of miR-379-5p in our cartilage dataset, as they both showed the same direction of dysregulation between young and old OA cartilage tissues.

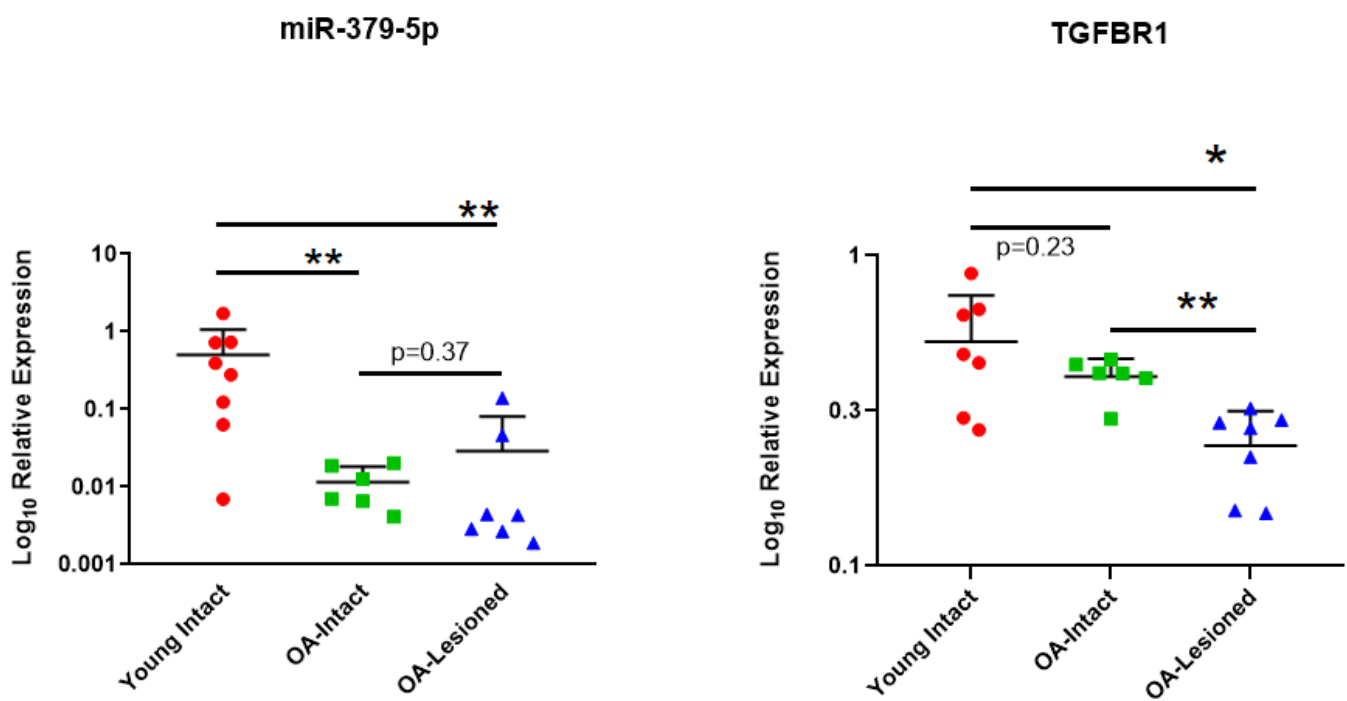


**Figure 5.10: Expression of *TGFBR1* in the independent cohort of young intact and old OA intact and lesioned cartilage samples.** Expression of miR-379-5p and *TGFBR1* in young intact cartilage from ACL donors and old OA intact and lesioned cartilage is shown. N=6-8 donors. Y-axis represents log-transformed expression relative to SNORD68 for miR-379-5p, and relative to *RPL3* for *TGFBR1*. Statistical analysis was undertaken using a Mann Whitney test in GraphPad Prism (Version 8.0.1). Data are represented as mean+SD. P values<0.05 were considered significant. \*: p<0.05, \*\*: p<0.01.

Results for *WNT4* and *IHH* showed that these genes had significantly higher expression in old OA intact and lesioned cartilage tissue from OA patients compared to young intact cartilage from ACL donors (**Figure 5.11**). This is consistent with *WNT4* and *IHH* being targets of miR-107, since miR-107 had lower expression in old OA intact and lesioned cartilage tissue compared to young intact cartilage tissue. **Table 5.3** summarises findings for all three miRNAs in OA chondrocytes and cartilage tissue.

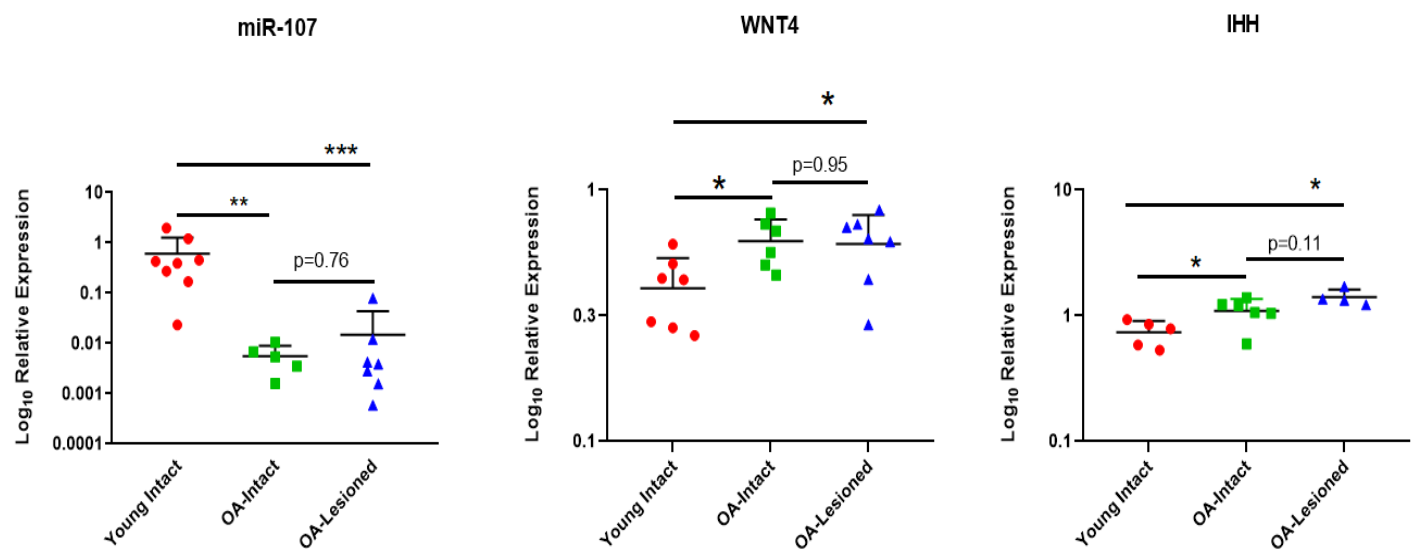


**Figure 5.11: Expression of *WNT4* and *IHH* in the independent cohort of young intact and old OA intact and lesioned cartilage samples.** Expression of miR-107, *WNT4* and *IHH* in young intact cartilage from ACL donors and old OA intact and lesioned cartilage is shown. N=5-8 donors. Y axis represents log-transformed expression relative to SNORD68 for miR-107, and relative to *RPL3* for *WNT4* and *IHH*. Statistical analysis was undertaken using a Mann Whitney test in GraphPad Prism (Version 8.0.1). Data are represented as mean+SD. P values<0.05 were considered significant. \*: p<0.05, \*\*: p<0.01, \*\*\*: p<0.001.

Note: I had planned to investigate the protein levels of *WNT4* and *IHH* by Western blotting, using human primary chondrocytes treated with miR-107 mimic and inhibitor. However, due to the unexpected shutdown of our laboratory facilities in March 2020 due to COVID-19, I was unable to carry out these experiments. By the time the facilities were open again, the studentship that supported this project and the author of this thesis had ended, and the author had already relocated back to his home country.

**Table 5.3: Summary of findings of miRNA-target gene validation in human chondrocytes and human cartilage.** Validation of miRNA-target gene interactions was undertaken in human primary OA chondrocytes treated with mimics, inhibitors and control and in human young intact cartilage from ACL donors and human OA cartilage from end-stage OA patients. ‘Yes/No’ denotes validated/not validated findings at p<0.05. N/A denotes expression measurement was not undertaken in these groups.

miRNA	Predicted Target gene	Validated in human OA chondrocytes	Validated in human young intact and old OA cartilage
miR-361-5p	<i>RHOA</i>	No	N/A
	<i>CALM3</i>	No	N/A
miR-379-5p	<i>TGFBR1</i>	Yes	No
	<i>HDAC2</i>	No	N/A
	<i>SMAD9</i>	No	N/A
miR-107	<i>WNT4</i>	Yes	Yes
	<i>IHH</i>	Yes	Yes
	<i>FGF2</i>	No	N/A
	<i>TNF</i>	No	N/A
	<i>IRF1</i>	No	N/A

#### 5.4.6 Proteomic investigation of human primary OA chondrocytes treated with miR-143-3p mimic and inhibitor

To investigate the role of miR-143-3p in cartilage and OA, I undertook a proteomic approach, using LC-MS/MS and label-free quantification in human primary OA chondrocytes treated with 10ng/ml human recombinant IL-1 $\beta$  and miR-143-3p mimic, or miR-143-3p inhibitor, or control-mimic, or control-inhibitor. Firstly, cell lysates were collected and amount of protein

in each sample was quantified using the Pierce™ 660nm Protein Assay. To calculate protein concentration for each sample, a standard curve was prepared using the absorbance of samples with known protein concentration. The amount of protein for each unknown sample is listed in **Table 5.4**.

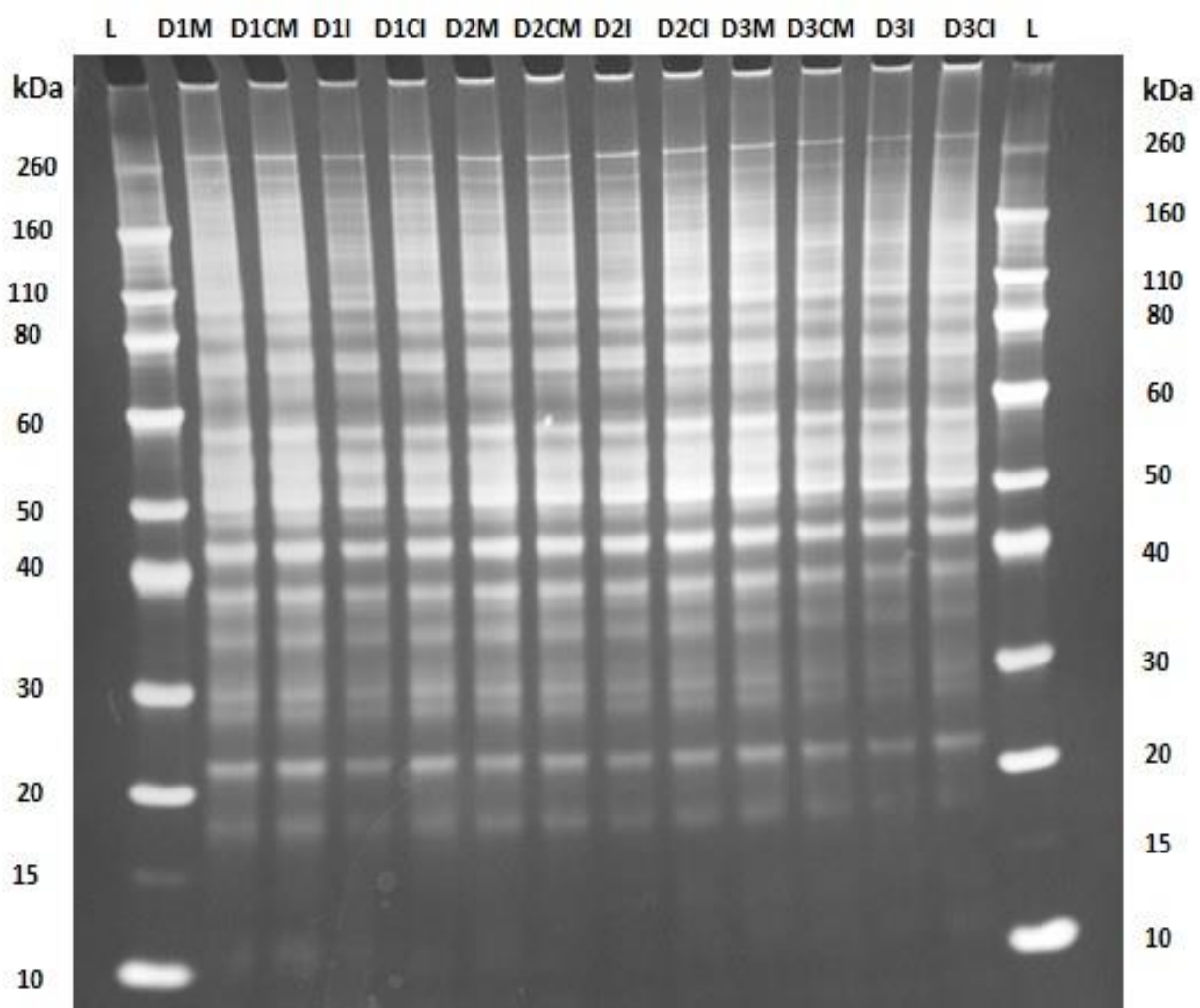
**Table 5.4: Amount of protein contained in chondrocyte lysates per treatment per donor.**

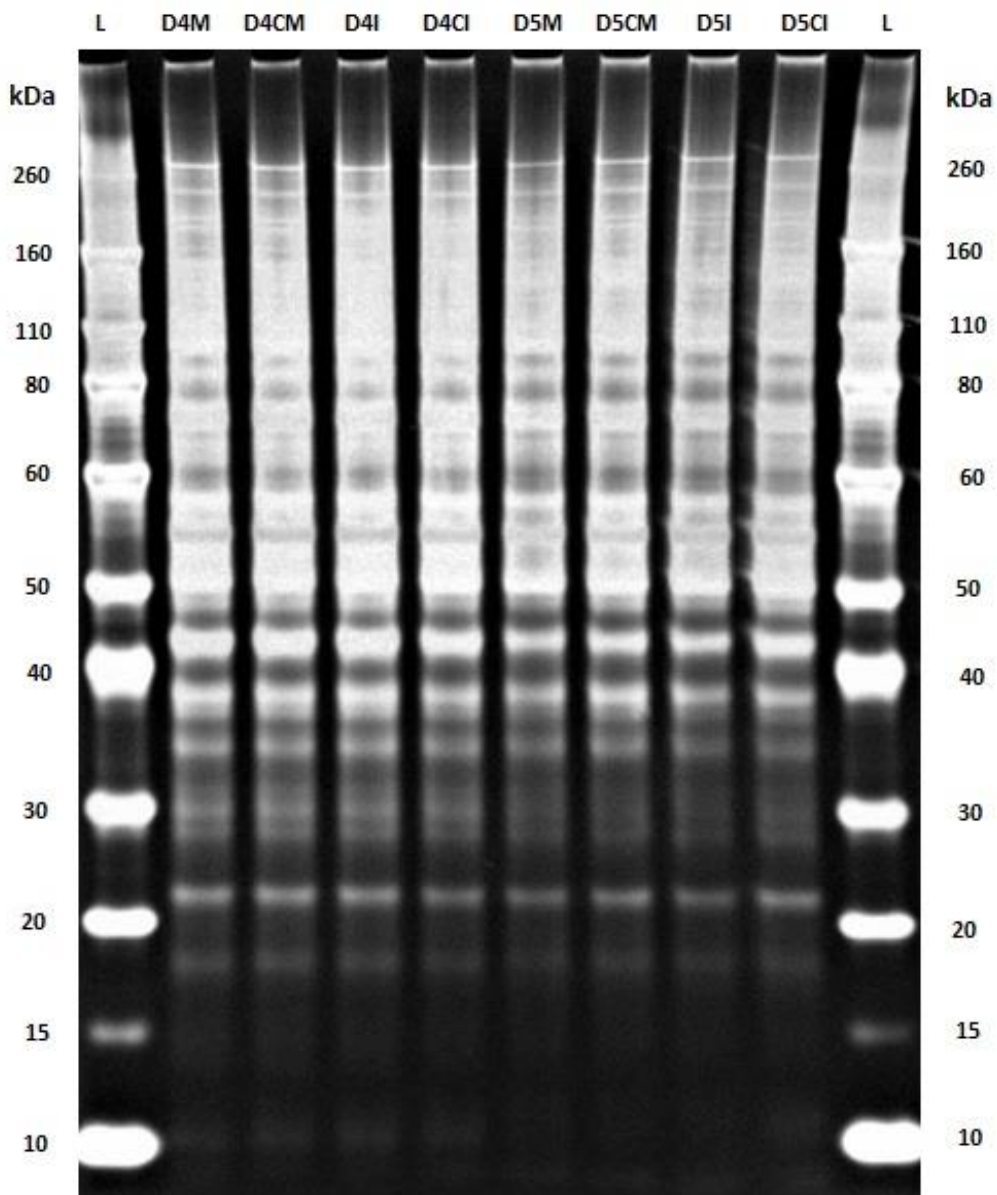
Donor	Treatment	Amount of protein (µg)
1	Mimic	52.3
	Control-Mimic	46.8
	Inhibitor	44.2
	Control-Inhibitor	45.9
2	Mimic	62.9
	Control-Mimic	64.2
	Inhibitor	68
	Control-Inhibitor	61.7
3	Mimic	48.5
	Control-Mimic	53.2
	Inhibitor	43
	Control-Inhibitor	35.3
4	Mimic	55.7
	Control-Mimic	54.4
	Inhibitor	50.2
	Control-Inhibitor	44.7
5	Mimic	51.5

	Control-Mimic	46.8
	Inhibitor	52.3
	Control-Inhibitor	53.6

To evaluate the quality and gross profile of the total protein content in chondrocyte lysates, prior to trypsin digestion and LC-MS/MS, all samples were subjected to SDS-PAGE using a NuPAGE™ 4% to 12% (w/v), Bis-Tris gel. After SDS-PAGE, the gel was silver stained. Silver staining showed that quality of total protein was good for all samples. Moreover, all samples had protein bands in the expected range of molecular weights (10kDa-260kDa), which was a further indication of good protein quality (**Figure 5.12A&B**).

## A

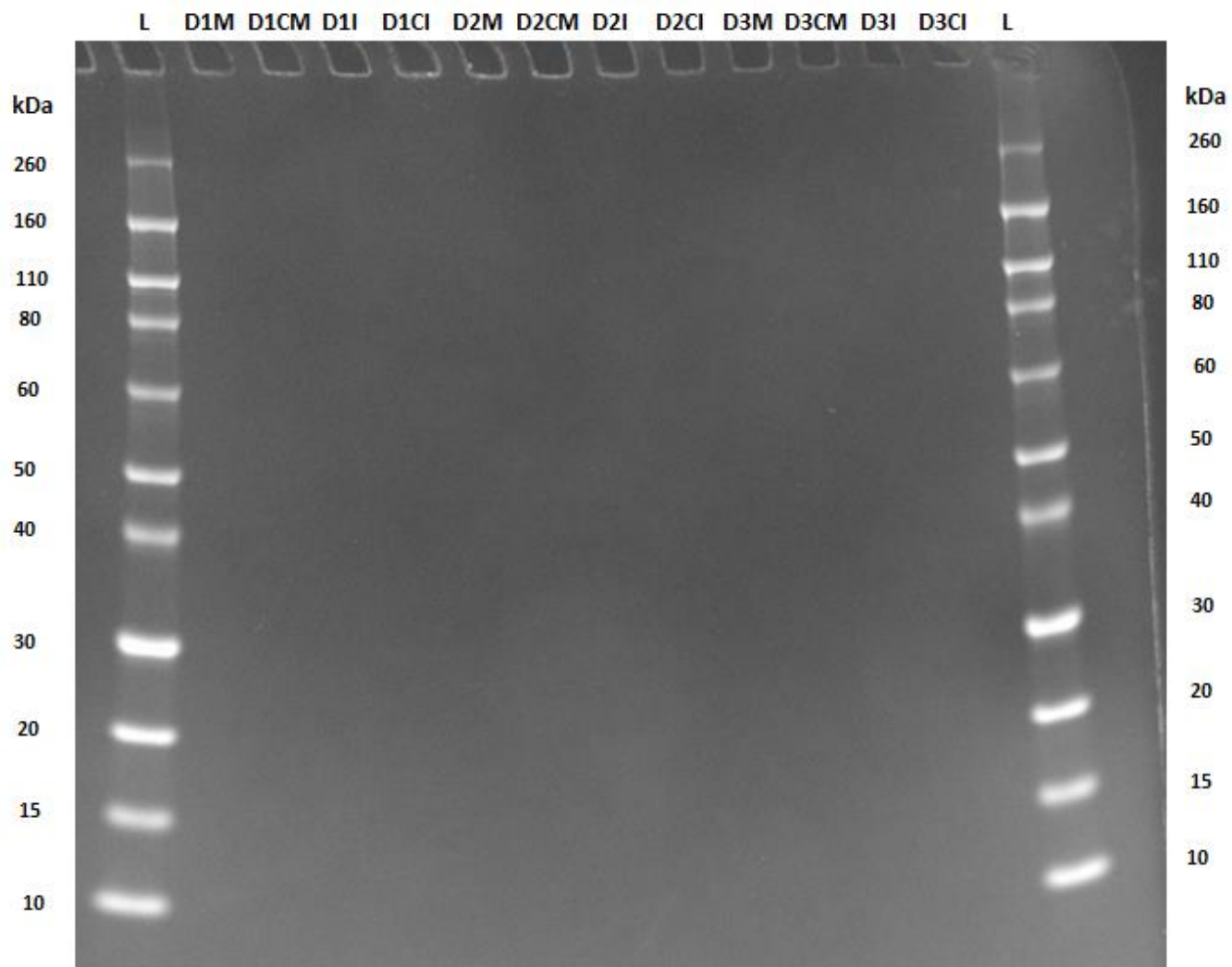


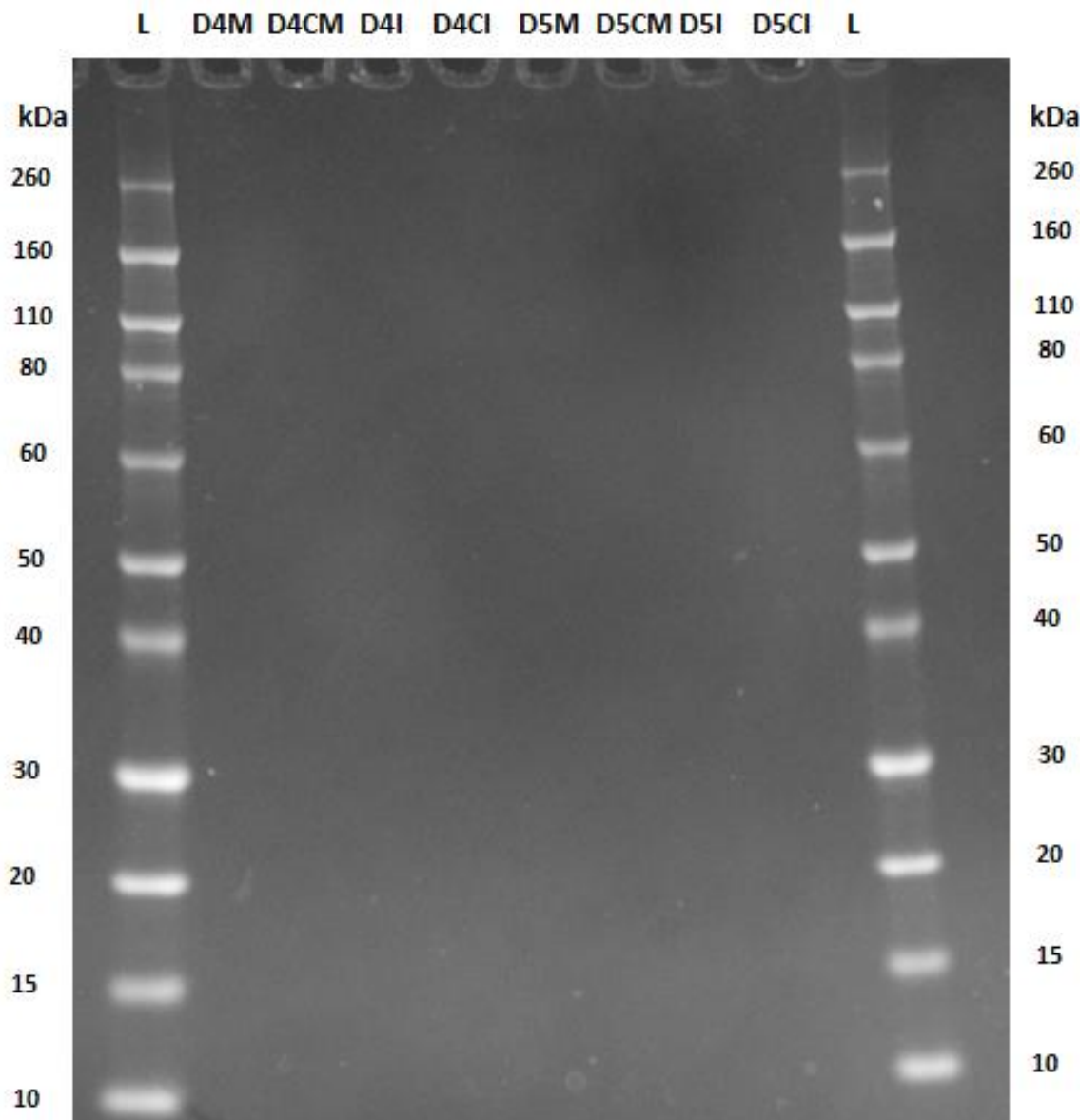
**B**

**Figure 5.12: Total protein detection by silver staining in chondrocyte lysates treated with miR-143-3p mimic, inhibitor or control.** Human OA chondrocytes were treated with miR-143-3p mimic, inhibitor or control. Cell lysates were collected 48h after treatment. 2 $\mu$ g of total protein per sample was run on a NuPAGE™ 4% to 12% (w/v), Bis-Tris gel at 100V for 90min, alongside a Novex™ Sharp Pre-stained Protein Standard ladder. Following electrophoresis, gel was silver stained and visualised using a ChemiDoc XRS+. N=5 donors per treatment. D: Donor, M: mimic, CM: control-mimic, I: inhibitor, CI: control-inhibitor, L: Pre-stained Protein Standard ladder, kDa: kilodalton.

To investigate digestion efficiency prior to LC-MS/MS, all digests were run on a NuPAGE™ 4% to 12% (w/v), Bis-Tris gel. Gel was stained with Coomassie Brilliant Blue and destained in Coomassie Brilliant Blue Destaining Solution. Staining showed that all samples were completely digested (**Figure 5.13A&B**).

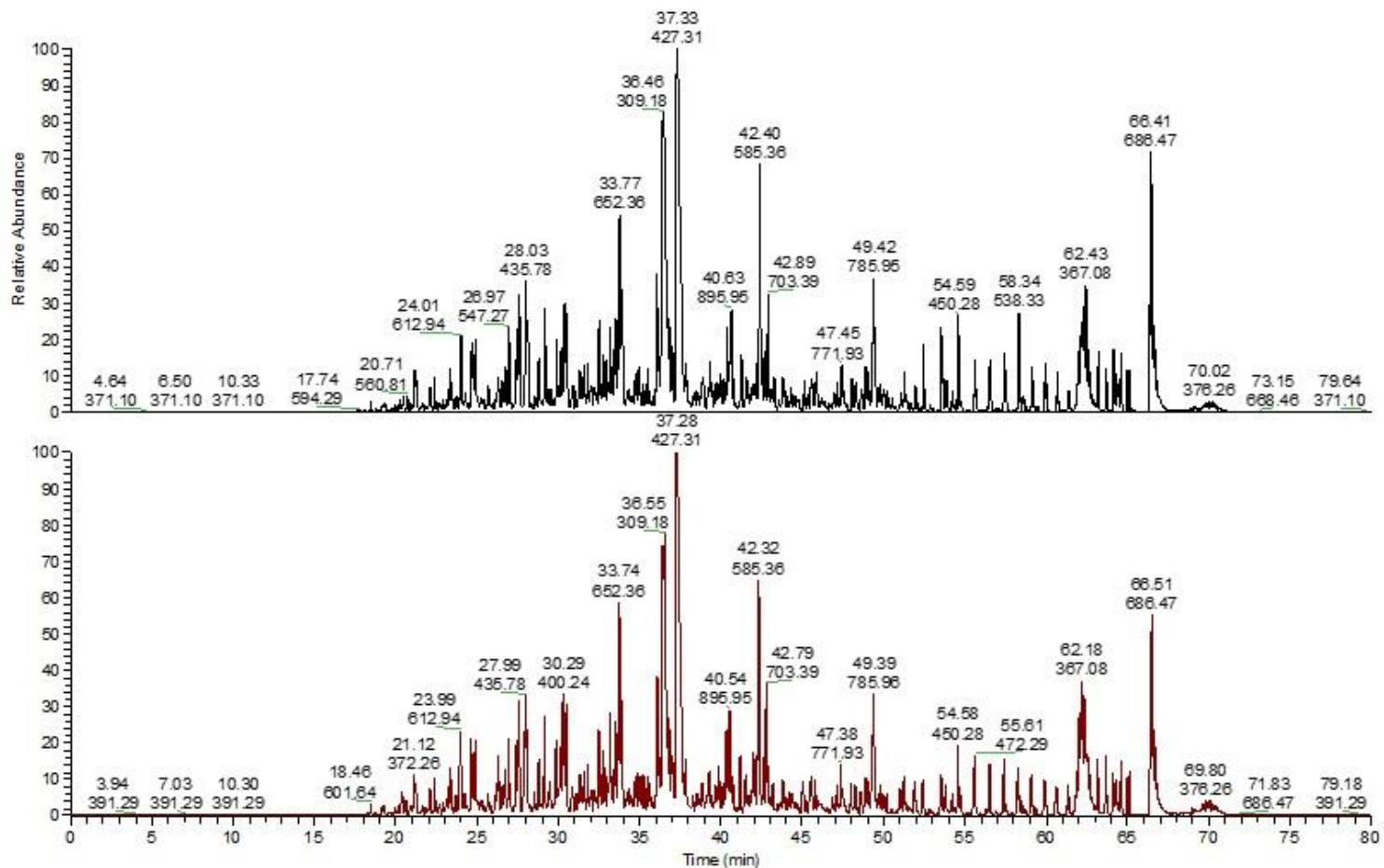
A



**B**

**Figure 5.13: Digestion quality assessment by Coomassie Brilliant Blue staining in chondrocyte lysates treated with miR-143-3p mimic, inhibitor or control.** To confirm complete digestion of proteins, 1 $\mu$ g of digest was run on a NuPAGE™ 4% to 12% (w/v), Bis-Tris gel at 100V for 90min, alongside a Novex™ Sharp Pre-stained Protein Standard ladder. Gel was stained with Coomassie Brilliant Blue for 2h and destained in Destaining Solution for 2h. The gel was visualised using a ChemiDoc XRS+. N=5 donors. D: Donor, M: mimic, CM: control-mimic, I: inhibitor, CI: control-inhibitor, L: Pre-stained Protein Standard ladder, kDa: kilodalton.

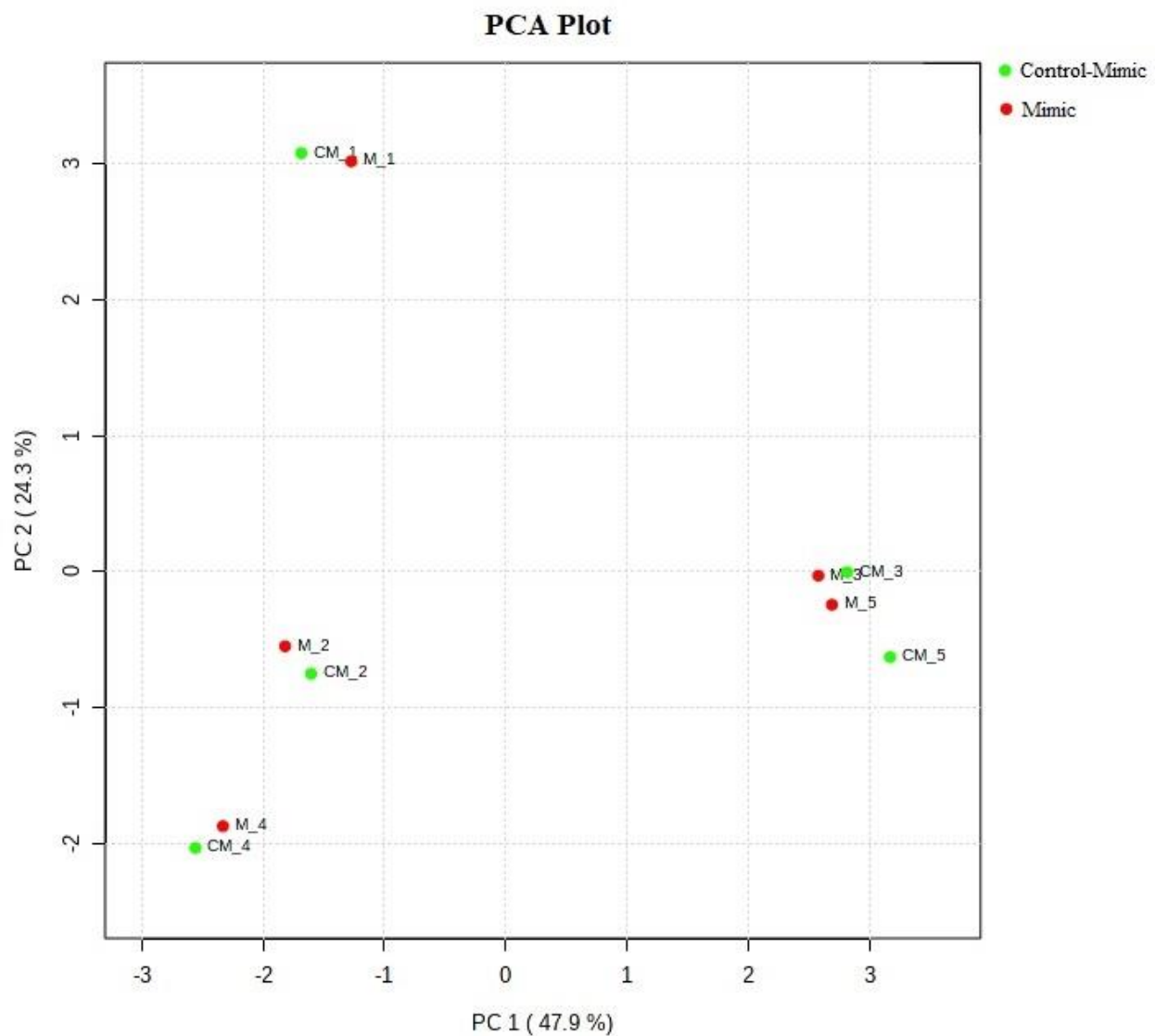
Digests were subjected to LC-MS/MS using a 90min gradient with 30min blanks between each sample. Chromatograms showed that there was good separation of ions, and of sufficient complexity representative of cell lysates (**Figure 5.14**).

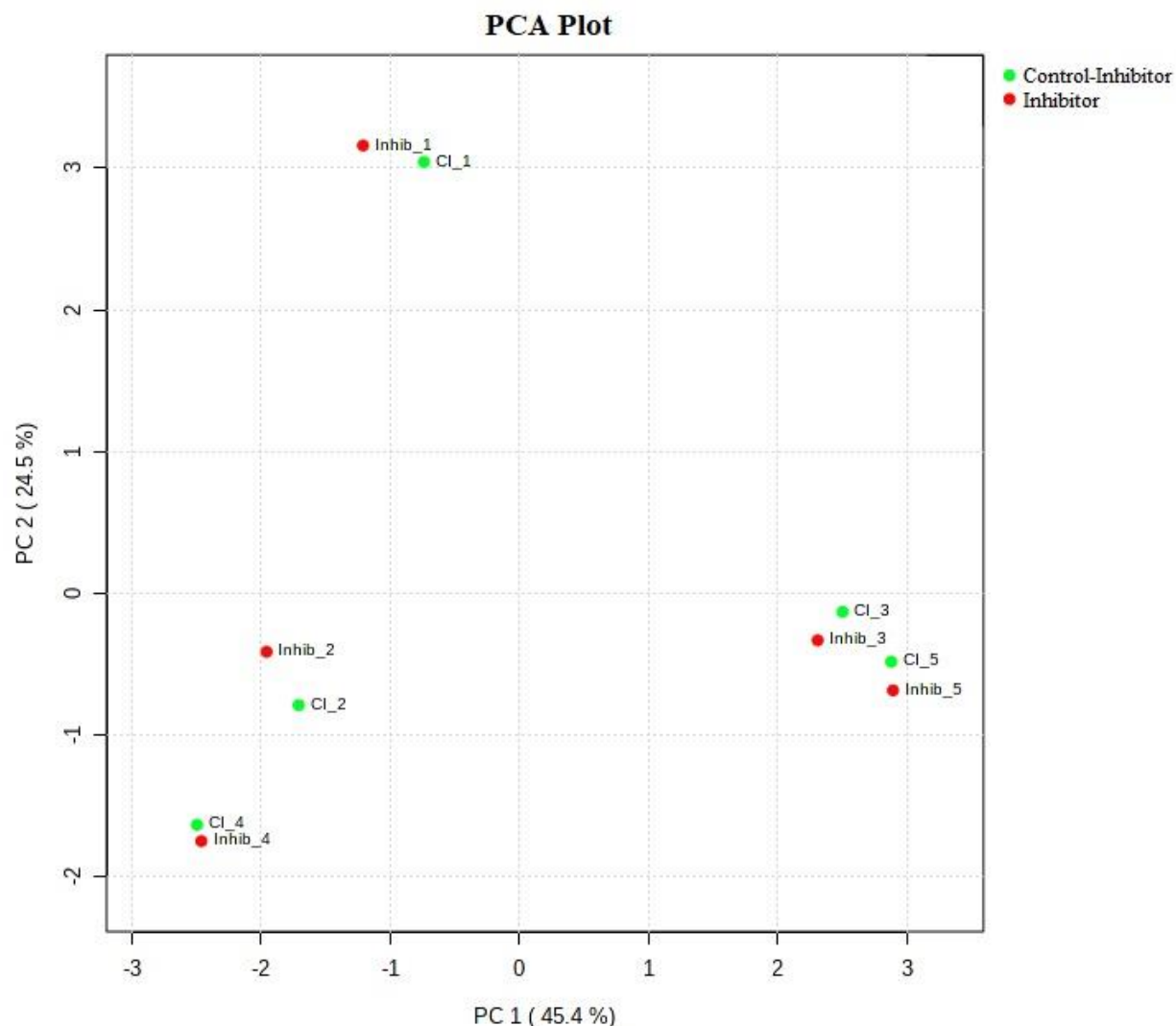


**Figure 5.14: Example of chromatograms generated following LC-MS/MS in human primary chondrocytes treated with miR-143-3p mimic, inhibitor or control.** OA human chondrocytes were treated with miR-143-3p mimic, inhibitor or control for 48h. Total proteins were digested and 500ng of digest per sample was subjected to LC-MS/MS for identification of protein abundance. Samples were run on a 90min gradient. Figure depicts two basic peak ion chromatograms, generated by LC-MS/MS. Chromatograms plot the retention time in the column for each analyte against their relative abundance in the sample. Each peak represents the detector response for a different ion. The height of each peak represents the amount of the particular ion in the sample.

A total of 2252 proteins were identified, of which 1628 were identified with two or more peptides. PCA plots of the 1<sup>st</sup> and 2<sup>nd</sup> component for proteins identified with two or more peptides showed that there were not many changes between the mimic and the control-mimic group (**Figure 5.15A**), or between the inhibitor and the control-inhibitor group (**Figure 5.15B**). There was no specific clustering observed between the groups and samples seemed to cluster based on individual donors rather than treatment.

**A**

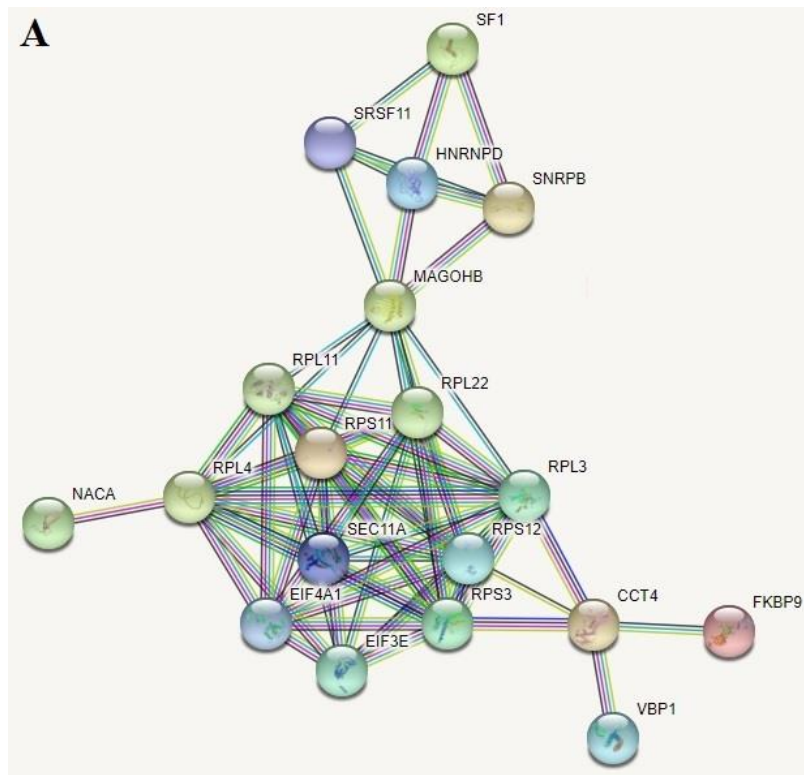


**B**

**Figure 5.15: PCA of the 1<sup>st</sup> and 2<sup>nd</sup> components for proteins identified with at least two peptides following chondrocyte lysates subjected to LC-MS/MS after treatment with miR-143-3p mimic, inhibitor or control.** Human OA chondrocytes were treated with miR-143-3p mimic, inhibitor or control for 48h and subjected to LC-MS/MS. Figure depicts PCA plots of 1<sup>st</sup> and 2<sup>nd</sup> components for proteins identified with at least two peptides in comparisons: A) mimic vs control-mimic and B) inhibitor vs control-inhibitor. N=5. Numbers 1-5 correspond to different donors. Figure produced with MetaboAnalyst 5.0.

Statistical analysis following label-free quantification was carried out using two-tailed paired t-tests between the mimic and the control-mimic group, and also between the inhibitor and

the control-inhibitor group. Paired t-test analysis identified 87 DE proteins at  $p<0.05$  in the mimic/control-mimic comparison and 50 DE proteins at  $p<0.05$  in the inhibitor/control-inhibitor group (Appendix to Chapter 5). However, when I adjusted for multiple testing, I did not identify any significantly DE proteins in the two comparisons (FDR-adjusted  $p<0.05$ ). Therefore, I continued our analysis with proteins that were DE at  $p<0.05$ . First, I sought to identify common DE proteins between the two comparisons, and then investigate those which have opposite direction of expression between the two comparisons, lower in the mimic vs control-mimic and higher in the inhibitor vs control-inhibitor, as this would suggest that these DE proteins could be potential targets of miR-143-3p. Analysis showed that there were no common DE proteins between the two comparisons and, therefore, I was not able to directly identify target genes of miR-143-3p. Nonetheless, to characterise the sets of DE proteins from the two comparisons, I uploaded them on STRING, to check whether these proteins were interacting with each other. STRING analysis showed that for each comparison, most proteins were strongly interacting with each other and were forming specific networks (**Figure 5.16A&B**). Of interest is that the proteins forming these networks were ribosomal proteins and translation initiation factors.



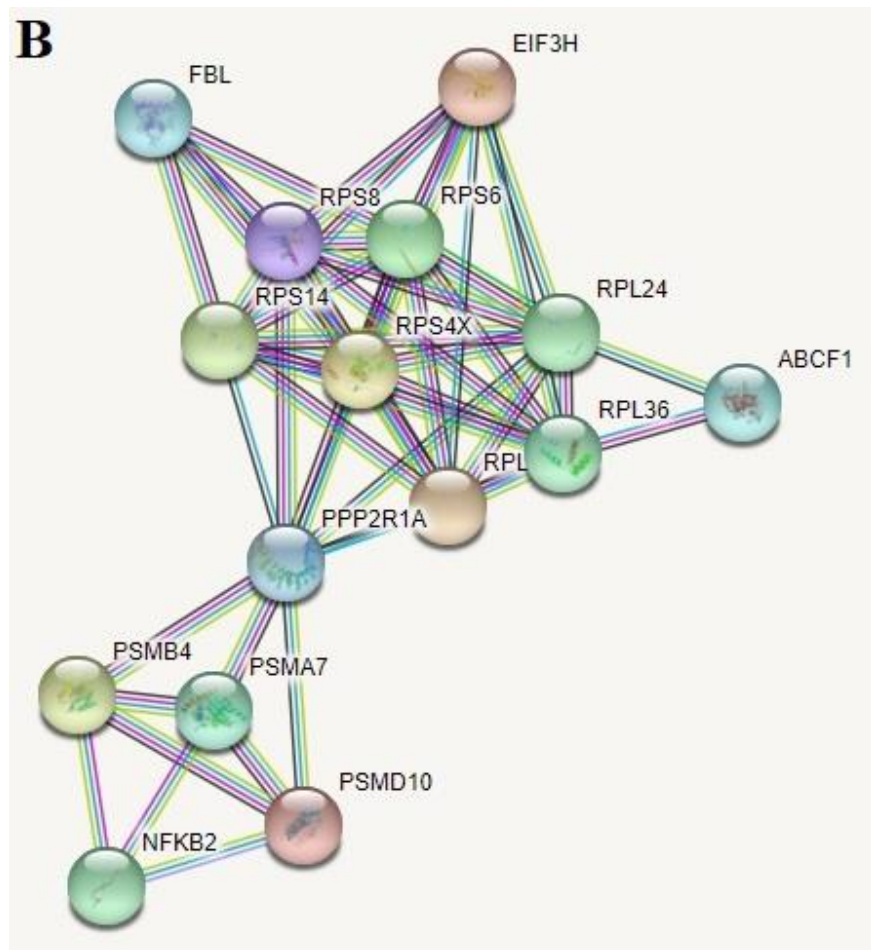
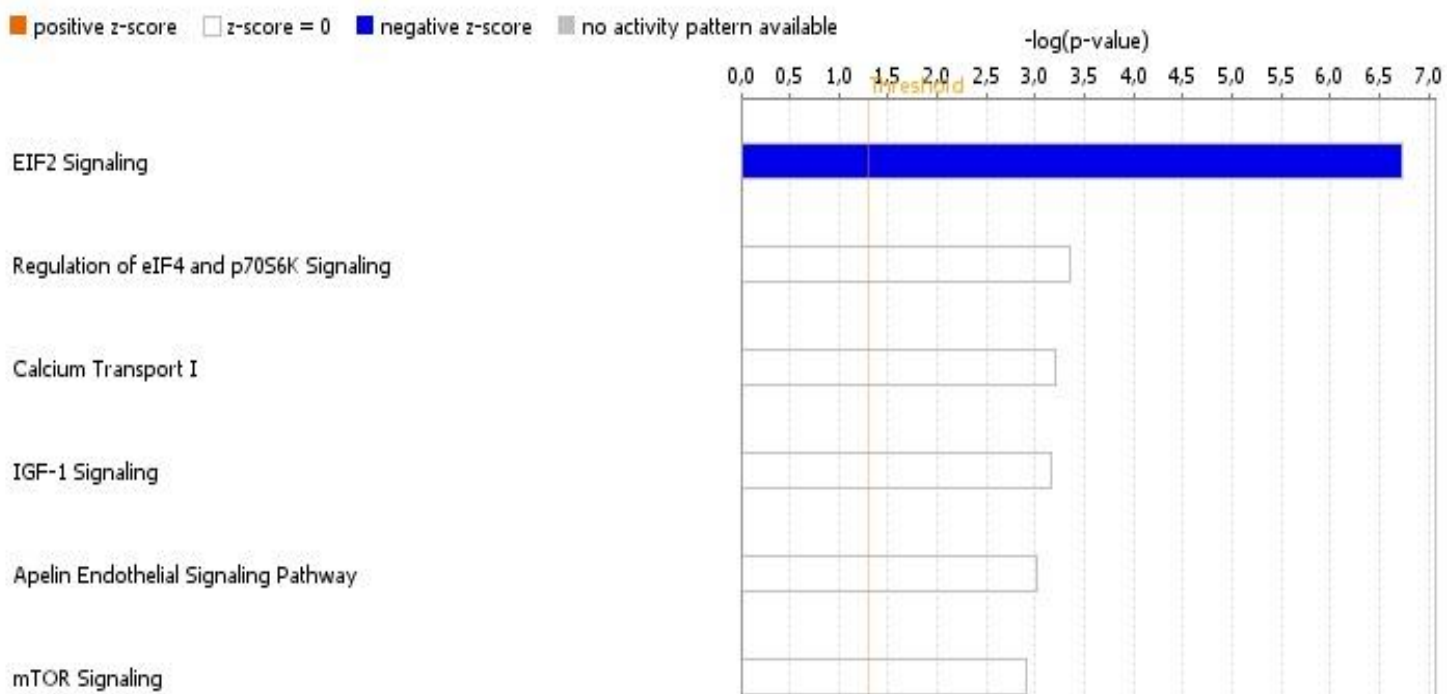


**Figure 5.16: STRING analysis of DE proteins identified in chondrocytes treated with miR-143-3p mimic, inhibitor or control following LC-MS/MS.** DE proteins ( $p < 0.05$ ) between A) mimic vs control-mimic group and B) inhibitor vs control-inhibitor group, were uploaded on STRING for protein network analysis and to identify protein-protein interactions. Filters were set to show both functional and physical protein associations, and highest confidence (0.900) was selected. Line colour indicates the type of interaction evidence. Stronger associations are represented by thicker lines. Figures generated with STRING.

I hypothesised that the DE proteins might be part of specific pathways regulated by miR-143-3p through targeting of genes that were not identified by LC-MS/MS. To investigate this hypothesis further, I uploaded the list of identified proteins for each comparison in IPA and carried out a ‘Core Analysis’ for each list, setting a  $p$  value cut-off at 0.05. Core Analysis showed that though they were not any common DE proteins between the two lists,

surprisingly, for both mimic vs control-mimic and inhibitor vs control-inhibitor, the top canonical pathway identified was EIF2 signalling (**Figure 5.17A&B**). In fact, in the mimic vs control-mimic comparison, EIF2 signalling had a negative z score [z-score= -1,  $-\log(p\text{-value})$ = 6.72], whereas, in the inhibitor vs control-inhibitor comparison, EIF2 signalling had a positive z score [z-score= 2,  $-\log(p\text{-value})$ = 7.54]. This suggests activation of EIF2 signalling in the inhibitor group and inhibition in the mimic group. Therefore, miR-143-3p could potentially be involved in translational initiation regulation either directly or indirectly via its target genes. Other common pathways identified by IPA between the two comparisons included: regulation of eIF4 and p70S6K signalling and mTOR signalling. IPA reports for both datasets are in Appendix to Chapter 5.

A



B

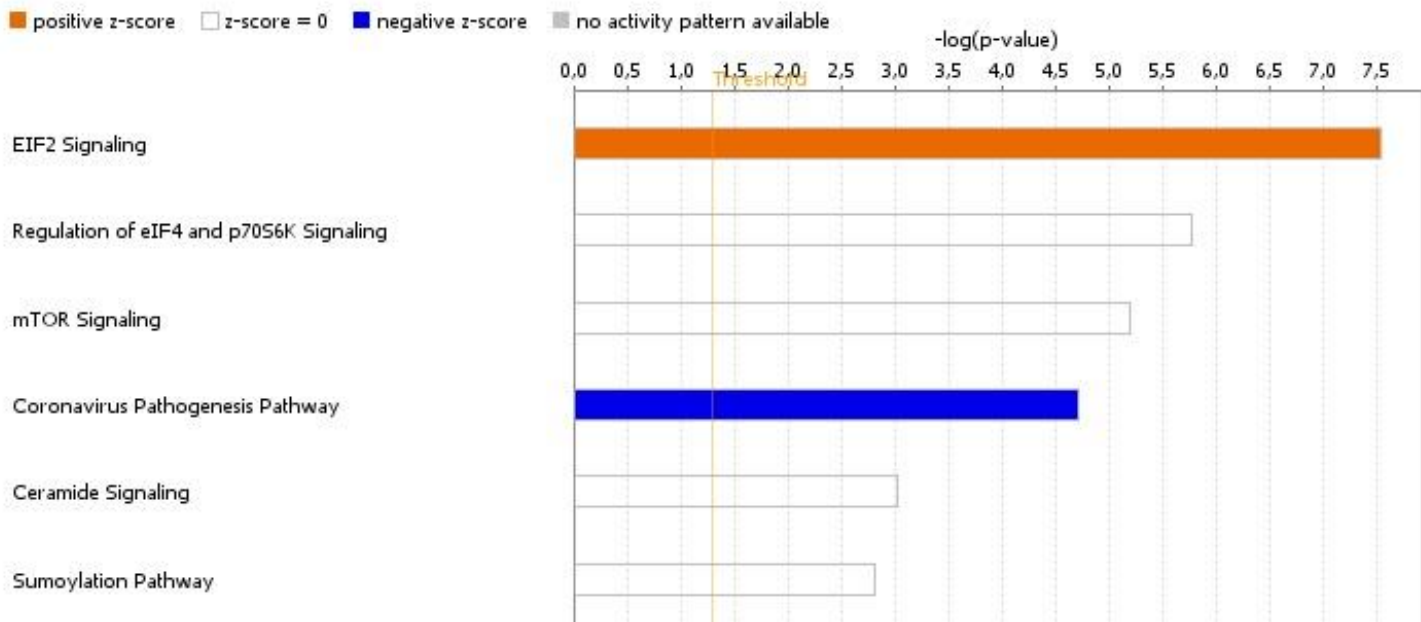


**Figure 5.17: Top canonical pathways linked to DE proteins from human OA chondrocytes treated with miR-143-3p mimic, inhibitor or control.** Human OA chondrocytes were treated in media supplemented with 10ng/ml IL-1 $\beta$  with miR-143-3p mimic, inhibitor or control for 48h. Cell lysates were collected and subjected to LC-MS/MS. Figure depicts IPA Core Analysis of DE proteins from chondrocytes treated with A) miR-143-3p mimic or control and B) miR-143-3p inhibitor or control. Top canonical pathways associated with each dataset and z activation scores for each canonical pathways are shown. Figures generated with IPA Version 60467501.

Further to our analysis, I also checked the upstream regulators of the pathways identified in IPA for each comparison. In the mimic vs control-mimic comparison, La ribonucleoprotein 1 translational regulator (*LARP1*) was predicted to be an activated upstream regulator (activation z-score= 2.12). Other upstream regulators in this comparison include CCAAT enhancer binding protein alpha (*CEBPA*) and *TNF*. These were predicted to be inhibited (activation z-score= -2.40 and -2.17, respectively) (Figure 5.18A).

The same analysis was undertaken in IPA for the inhibitor vs control-inhibitor comparison. Interestingly, in this comparison, *LARP1* was identified as being an inhibited upstream

regulator (activation score  $z = -2.83$ ), opposite to what I observed in the mimic vs control-mimic group. Furthermore, an activated upstream regulator in this comparison was MLX interacting protein like (*MLXIPL*) (activation  $z$ -score= 2.24) (Figure 5.18B). Of interest is that, even though there were no common DE proteins between the two comparisons, both sets of proteins were involved in similar pathways and IPA generated similar but opposite results for these sets. Moreover, according to IPA, both sets of DE proteins were involved in skeletal and muscular disorders ( $p=1.31 \times 10^{-2} - 7.80 \times 10^{-4}$ ) and skeletal and muscular system development and function ( $p=3.81 \times 10^{-3} - 1.46 \times 10^{-6}$ ).

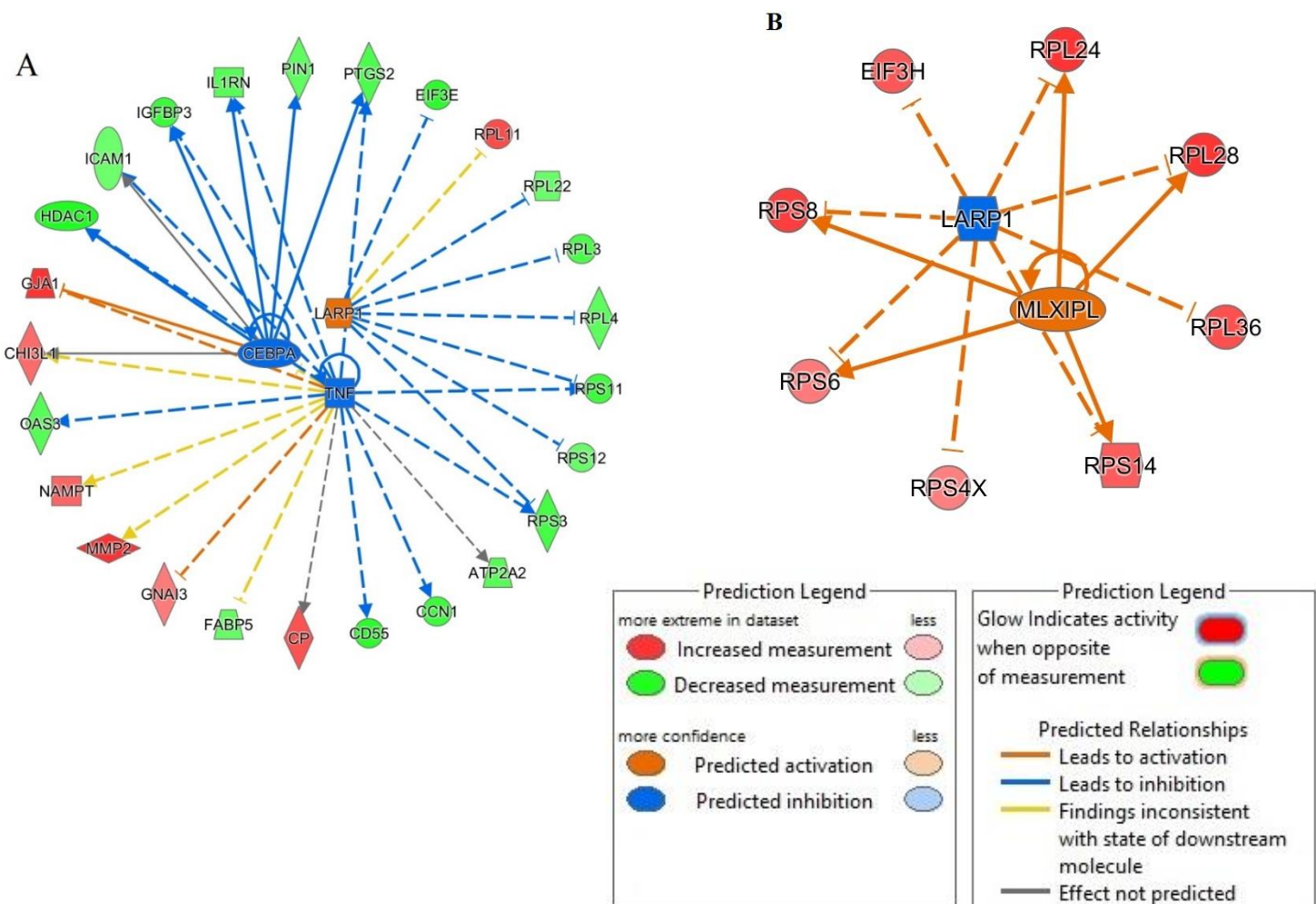


**Figure 5.18: Network analysis of predicted upstream regulators of DE proteins in human OA chondrocytes treated with miR-143-3p mimic, inhibitor or control.** IPA analysis of DE proteins ( $p<0.05$ ) in human OA chondrocytes treated with miR-143-3p A) mimic or control-mimic and B) inhibitor or control-inhibitor, identified a set of predicted upstream regulators in each comparison. Figure generated with IPA. Key is indicated.

## 5.5 Discussion

In this thesis I identified DE miRNAs between young intact cartilage from ACL donors and old OA intact and lesioned cartilage from OA patients. I selected a list of four miRNAs for follow up studies: miR-361-5p, -379-5p, -107 and -143-3p. To evaluate the role and function of these specific miRNAs in cartilage and OA, I overexpressed and knocked down their expression in human primary OA chondrocytes and measured the expression of selected predicted target genes, or of cartilage-related markers. For miRNAs miR-361-5p, -379-5p and -107, I selected specific target genes to investigate. I aimed at selecting genes that had not been identified previously as targets of our selected miRNAs, at least up to the time I selected these targets. Moreover, I selected genes that are or could potentially be relevant to cartilage biology and OA. Given that our miRNAs had significantly lower expression in OA intact and lesioned cartilage tissue compared to young intact cartilage from ACL donors, when possible, I selected genes that were reported as overexpressed in OA cartilage, so that they matched the opposite expression of our selected miRNAs.

### 5.5.1 Justification of target gene selection

For miR-361-5p, I selected two predicted target genes, *CALM3* and *RHOA*. *CALM3*, along with *CALM1* and *CALM2*, is an important gene involved in calcium transport and mechanical stimuli in chondrocytes, and its expression was shown to be upregulated in OA cartilage compared to normal cartilage (Mototani et al., 2010). *RHOA* is another important gene linked to cartilage and OA. It is involved in actin re-organization, cell maturation and apoptosis as well as in the remodelling of the ECM. *RHOA* is activated in OA cartilage and acts through the Rho associated coiled-coil containing protein kinase (*ROCK*) signalling pathway to induce chondrocyte hypertrophy and ECM degradation (Deng et al., 2019b). For miR-379-5p, I selected three predicted target genes: *TGFBR1*, *HDAC2* and *SMAD9*. *TGFBR1* is one of the receptors of TGF- $\beta$ , a ligand that has major roles in cartilage development. Physiological loading has been shown to induce low concentrations of active TGF- $\beta$  in healthy articular cartilage, which is necessary for cartilage homeostasis (van der Kraan, 2018). However, during OA, levels of TGF- $\beta$  are increased and chondrocytes become exposed to higher levels of the growth factor. This results in altered signalling that could potentially contribute to the

development of the disease, rather than cartilage homeostasis (van der Kraan, 2018). Therefore, I thought to investigate further the relationship of miR-379-5p and *TGFBR1*. Following this rationale, I also included *SMAD9* (also known as *SMAD8*) in our analysis, as SMADs are downstream targets of TGF- $\beta$  signalling and are involved transcription regulation. The role of *SMAD9* in cartilage seems limited compared to other SMAD proteins (Retting et al., 2009). Furthermore, *HDAC2* is another gene involved in cartilage and OA. Studies have shown *HDAC2* is increased in primary chondrocytes extracted from OA patients compared to non-OA and it can inhibit expression of ECM components, such as collagen type II and aggrecan (Hong et al., 2009).

For miR-107, I selected four predicted target genes to investigate: *WNT4*, *IHH*, *TNF* and *IRF1*. *WNT4* is a member of the WNT signalling pathway which is an important regulator of chondrocyte proliferation and maintenance (Wang et al., 2019c). Even though, another WNT family member, *WNT3A*, is more studied in cartilage and OA, *WNT4* was also shown to be upregulated in hip and knee OA patients (Velasco et al., 2010). Moreover, *IHH* was upregulated in human OA articular cartilage and OA synovial fluid and induced collagen type X and MMP13 expression, suggesting a role for *IHH* in chondrocyte hypertrophy and cartilage degeneration in OA (Wei et al., 2012). Finally, the role of *TNF* and of other inflammatory cytokines has already been discussed in this thesis, and based on this; I chose to investigate whether *TNF* and *IRF1*, which is induced by *TNF* signalling, are targeted by miR-107.

### **5.5.2 Evaluation of predicted targets of miR-361-6p, -379-5p and -107**

To evaluate whether the selected predicted target genes were targets of our three miRNAs of interest, I overexpressed and inhibited the expression of these miRNAs in human primary OA chondrocytes grown in media supplemented with 10ng/ml IL-1 $\beta$  for 48h. The use of IL-1 $\beta$  has been discussed more extensively in Chapter 4. As already discussed there, chondrocytes dedifferentiate in monolayer passaged cultures and tend to lose their phenotypic characteristics (Caron et al., 2012). The rationale behind the addition of IL-1 $\beta$  in chondrocytes treated with mimics or inhibitors, is to evaluate the benefit of these overexpressing or inhibitory agents when chondrocytes are in an inflammatory environment, and also to investigate whether these could be used to treat patients *in vivo*, as some studies suggest an

inflammatory component in early OA (Benito et al., 2005, Sokolove et al., 2013). Adding IL-1 $\beta$  treatment to OA chondrocytes treated with miRNA mimics and inhibitors is a common practice in the literature (Chang et al., 2016, Yuan et al., 2016, Zheng et al., 2017), and in our experiments all groups, mimic, inhibitor and controls, were treated with IL-1 $\beta$ . In addition, treatment time was kept to 48h, as from our IL-1 $\beta$  experiments in Chapter 4, I observed that longer treatments generated a more satisfactory response in human primary chondrocytes, compared to 24h. 48h is also sufficient time to observe any effects from the mimic and inhibitor treatments. From our experience, longer treatments for 72h and 96h did not produce different results (data not shown).

Overexpression and inhibition of selected miRNAs and analysis of their predicted target genes showed that *CALM3*, *RHOA*, *SMAD9*, *HDAC2*, *TNF* and *IRF1* were not validated as targets of using our approaches in our cell systems. This could be due to a number of reasons. First of all, these genes may not be actual targets of these miRNAs in chondrocytes. Even though these genes were predicted as targets by at least two prediction tools, these predictions could be false positives. Cloonan (2015) reported that the percentage of false positive predictions by miRNA target prediction tools ranges from 20% to 50% (Cloonan, 2015). With that said, *RHOA* was recently validated as one of miR-361-5p target genes in triple-negative breast cancer (Bhattacharya et al., 2020). This example points to another reason for not validating some of the selected target genes, and that is tissue specificity. Gene expression is a very tightly regulated process in eukaryotic cells and differs significantly from one cell/tissue type to another. Therefore, the relationship between a miRNA and its predicted targets could change dependent on the tissue type, developmental stage and health/disease state (Fiannaca et al., 2018, Sood et al., 2006). Also, it is worth mentioning that miRNAs are not the only regulators of gene expression. Gene expression is regulated at many different levels by an array of genetic and epigenetic modifiers, such as enhancers, transcription factors, DNA methylation, histone modifications and other classes of non-coding RNAs, which indicates the complex molecular landscape that underlies gene interactions. Another point to take into consideration is the approach taken to validate the predicted target genes from these three miRNAs. I used qPCR to detect expression of the miRNA of interest and of predicted target genes. As already mentioned, qPCR for the miRNA itself is not the recommended method to confirm whether the mimics or the inhibitors have worked properly (Qiagen, 2017), and I did

not consider results from miRNA quantification as confirmation of successful or unsuccessful overexpression/knockdown. For the overexpression experiments, even though the expression of the miRNA itself was increased in the mimic group by several folds compared to control in all three miRNAs tested, this did not guarantee that all these mimics were actually functional within the cells. This is also evident by the fact that using 5nM and 50nM mimics did not result in significant differences between the two treatments that would justify that the 50nM concentration should be used instead of the 5nM one. In fact, using higher concentrations of miRNA mimics could potentially lead to accumulation of mutated and unnatural passenger strands, off-target effects and saturation of the RISC complex (Jin et al., 2015). For the knockdown experiments, qPCR should not be used to assess transfection efficiency. These inhibitors usually bind the miRNA of interest and prevent it from binding the target gene, but usually do not lead to miRNA degradation (Qiagen, 2017). From our experiments, I observed that miR-361-5p had significantly lower expression in the inhibitor group compared to control, but none of the predicted target genes expression were altered. Instead, even though expression of miR-379-5p and miR-107 was not significantly lower in the inhibitor group compared to control, *TGFBR1*, *WNT4* and *IHH* had significantly higher expression in the inhibitor group compared to control, suggesting successful miRNA inhibition. This further supports that the evaluation of overexpressing and inhibitory experiments should be based on the expression of the target genes, rather than the miRNA itself. Another possible reason for the unsuccessful validation of some of the predicted target genes could be the experimental method used to assess this. I used qPCR to check the expression of the mRNA of the predicted target genes. However, changes on target genes may not be detectable at the mRNA level, but could be present at the protein level. This is because miRNA pairing does not always lead to mRNA degradation, but to translational repression. The contribution of each mechanism is still unclear and in certain cases one might be the prominent mechanism compared to the other (Cloonan, 2015). Therefore, it is possible that some of these target genes could show differences at the protein level. However, it was not possible to undertake Western blotting for all predicted targets. I had planned to undertake Western blot analysis for *WNT4* and *IHH*, which were also validated by qPCR, but that was not possible due to the COVID-19 pandemic. Additional mechanistic experiments, such as proliferation or migration assays, or luciferase assays would have been useful to assess miRNA function and validate predicted target genes.

Following validation of *TGFBR1*, *WNT4* and *IHH* in chondrocytes treated with mimics and inhibitors, I sought to investigate the expression of these predicted targets in human cartilage tissue. Our microarray experiment was undertaken between young intact cartilage from ACL donors and old OA intact and lesioned cartilage from OA patients undergoing TKA. miR-379-5p and miR-107 had significantly lower expression in the old OA cartilage samples compared to young cartilage. Our results showed that *WNT4* and *IHH* had significantly higher expression in old OA intact and lesioned cartilage compared to young intact cartilage, in agreement with previous studies (Velasco et al., 2010, Wei et al., 2012). This further confirmed that these two genes could represent actual targets of miR-107, since they had opposite expression to that of miR-107. However, our analysis showed that *TGFBR1* had lower expression in old OA cartilage tissues compared to young cartilage tissue, following the same direction of dysregulation as miR-379-5p. This suggested that *TGFBR1* might not represent a true target of miR-379-5p, at least in cartilage tissue. The fact that *TGFBR1* responded to miR-379-5p mimic and inhibitor as I would have expected if it were a real target, could potentially indicate differences between cartilage tissue and cultured chondrocytes, or could be a culture artifact.

Given the above results, it is difficult to describe the role of miR-361-5p and miR-379-5p in cartilage and OA. Wang et al (2019) reported that expression of miR-361-5p was upregulated in OA chondrocytes compared to normal chondrocytes and that it promoted chondrocyte apoptosis and ECM degradation (Wang et al., 2019a) . This is in contrast with our study, as miR-361-5p had lower expression in OA cartilage tissues. However, the experimental design between the two studies was different, as I used cartilage tissue and not extracted chondrocytes for our initial microarray analysis. Moreover, I compared OA cartilage tissues to young intact tissue from ACL donors, whereas Wang et al (2019) compared OA chondrocytes to normal chondrocytes from age-matched donors.

Regarding miR-379-5p, there is limited data on its role in cartilage and OA. Jee et al (2018) reported that miR-379-5p had lower expression in the hypertrophic zone of murine growth plate compared to the proliferative zone and this led to increased expression of hypertrophic markers (Jee et al., 2018).

miR-107 is a well-researched miRNA. A few studies have shown that miR-107 has lower expression in OA cartilage tissue and chondrocytes compared to normal controls, in agreement with our study (Qian et al., 2021, Tian et al., 2019, Zhao et al., 2019). These studies

have shown that miR-107 can promote chondrocyte proliferation, and inhibition of its expression can lead to apoptosis. It was shown that this function of miR-107 is achieved by targeting genes involved in cell survival and proliferation and autophagy, such as *TRAF3*, phosphatase and tensin homolog (*PTEN*), and caspase 1 (*CASP1*). In our study, I found that *WNT4* and *IHH* could be potential target genes of miR-107. *WNT4* was found to be overexpressed in human OA hip and knee cartilage (Velasco et al., 2010), and in mice with induced-OA (Gu et al., 2019). In the latter study, induced-OA led to increased levels of *Wnt4* and activated the WNT signalling pathway leading to increased expression of *Mmp2* and *Mmp9* through β-catenin. In another study, inhibition of *IHH* signalling led to increased chondrocyte proliferation and reduced apoptosis and cartilage degeneration by treating cells with ipriflavone, a compound that inhibits *IHH* signalling (Guo et al., 2019). Given the biological pathways that *WNT4* and *IHH* are involved in, our analyses indicate that if miR-107 targets these genes, then it could also be involved in chondrocyte survival and proliferation.

### **5.5.3 Investigation of miR-143-3p in cartilage and OA**

To investigate the role of miR-143-3p in cartilage and OA, I took a different approach compared to the first three miRNAs. Instead of looking at the expression of specific predicted target genes, I undertook LC-MS/MS analysis in lysates from chondrocytes treated with miR-143-3p mimic, inhibitor, or control. I analysed results using two-tailed paired t-tests for chondrocytes treated with mimic or control mimic and inhibitor or control-inhibitor, as I was interested in comparing each treatment to its respective control. Analysis did not identify any statistically significant changes when I corrected for multiple testing, using a cut-off of FDR-adjusted p value<0.05. This could have resulted from reduced transfection efficiency. Given that assaying for the miRNA itself is not a reliable approach to confirm overexpression or inhibition of the miRNA, it was not possible to assess the magnitude of overexpression of inhibition in chondrocytes treated the miR-143-3p mimics and inhibitors. Another possible reason could have been donor variability, as I used chondrocytes extracted from five different donors and this could have masked any treatment-related differences, given the small number of samples. This was also evident from the PCA plots, as samples clustered based on the donors rather than the type of treatment. However, paired t-test analysis between

comparisons mimic vs control-mimic, and inhibitor vs control-inhibitor, identified DE proteins at  $p < 0.05$  for each comparison. Analysis showed that there were no common DE proteins between the two comparisons that would have pointed to specific targets of miR-143-3p. However, analysis of these DE proteins from each comparison with IPA indicated that both sets of DE proteins were involved in EIF2 signalling. In fact, IPA predicted that DE proteins from the mimic vs control-mimic comparison were involved in inhibition of EIF2 signalling. In contrast, IPA predicted that DE proteins from the inhibitor vs control-inhibitor comparison were involved in activation of EIF2 signalling. The potential regulation of EIF2 signalling could be through specific miR-143-3p target genes that were not identified by LC-MS/MS, either because their detection was outside of the sensitivity range of the technique, or because they act at an early point (a few hours after transfection), but their results can still be observed several hours and until collection of lysates, 48h after transfection. Either way, our results provided a useful insight into the potential role of miR-143-3p and its association with EIF2 signalling.

EIF2 signalling is involved in protein translation and protein synthesis and plays a crucial role in cellular response due to stress-related stimuli, such as oxidative stress, injury, and others (Wek, 2018). Under such stress stimuli, eIF2a is phosphorylated and this leads to its inhibition and to reduced global protein translation. Instead, specific genes are expressed which promote cellular adaptation and survival and exert an anti-apoptotic effect. In a relevant study, it was shown that curcumin could inhibit EIF2 signalling in oxidative stress-induced rat chondrocytes and alleviate OA progression and chondrocyte apoptosis (Feng et al., 2019). Interestingly, in a study assessing the transcriptomic differences between ovaries from young and middle-aged mice, the authors reported increased miR-143 expression and reduced EIF2 signalling in middle-aged ovaries compared to young (Cuomo et al., 2018). Even though the authors did not discuss the potential association of miR-143 to EIF2 signalling, our results also suggest a potential link between miR-143-3p and EIF2. Perhaps, miR-143-3p is involved in cartilage homeostasis through regulating EIF2 signalling. Specifically, overexpression of miR-143-3p could inhibit EIF2 signalling, leading to repression of global protein synthesis, but promoting the expression of genes that assist chondrocyte survival during stress. In contrast, inhibition of miR-143-3p during OA (as suggested by our microarray study), could induce EIF2 signalling, which, under stress conditions, could result in depletion of cellular components

important for cell survival, thus leading to increased apoptosis. Perhaps, this could explain the upregulation of miR-143-3p in chondrocytes treated with IL-1 $\beta$  for 24h, reported in Chapter 4. IL-1 $\beta$ -induced stress in treated chondrocytes could result in a stress response, which could promote increased expression of miR-143-3p. Increased expression of miR-143-3p could, in turn, inhibit global protein translation by inhibiting EIF2 signalling, in an attempt of the cell to survive and adapt to the inflammatory stress. Continuous treatment with IL-1 $\beta$ , could eventually lead to inhibition of miR-143-3p, as observed by chondrocytes treated with IL-1 $\beta$  for 5 days, and subsequently to chondrocyte apoptosis. In fact, it has been suggested that the result of the stress response depends on the duration and intensity of the stress stimulus (Bevilacqua et al., 2010). During the early stages of the response, inhibition of EIF2 signalling leads to activation of genes important for cell survival. However, with persisting stress stimuli, there is a shift in stress responses and eventually apoptosis is favoured over survival.

Moreover, IPA identified upstream regulators of these DE proteins for each comparison. Amongst these, *LARP1* was a common upstream regulator in both comparisons, and it was predicted to be activated in chondrocytes treated with the mimic, and inhibited in chondrocytes treated with the inhibitor. *LARP1* is involved in protein translation, cell proliferation and cell survival and has been shown to interact with ribosomal proteins and also be part of the mTOR signalling pathway, suggesting a role for LARP1 in miR-143-3p related pathways (Berman et al., 2020). Though there are contradictory data on its role, it is believed that LARP1 inhibits the translation of ribosomal proteins and translation factors (Fonseca, Lahr, Damgaard, Alain, & Berman, 2018). However further studies are needed to elucidate its exact role, especially with regards to cartilage biology, as there are currently no data on its role in OA.

## 5.6 Conclusion

I was able to interrogate the role of selected miRNAs in cartilage and OA, by modulating their expression in human primary OA chondrocytes. Investigation of their predicted target genes showed that miR-107 could target *WNT4* and *IHH* and that it could be involved in chondrocyte proliferation and cell survival. Moreover, I showed that even though I was not able to pinpoint

at specific target genes of miR-143-3 following LC-MS/MS, I was still able to identify pathways that this miRNA could be involved in, such as the EIF2 signalling pathway, and propose a link between this miRNA and cartilage homeostasis through regulation of protein translation.

# **Chapter 6: Investigation of miRNA expression in equine ageing chondrocytes using small RNA Sequencing**

## 6.1 Introduction

Articular cartilage displays a limited repairing capacity, low chondrocyte proliferation and low collagen turnover (Decker, 2017). There are a number of factors affecting the homeostatic properties of cartilage, such as genetics and obesity. However, ageing is the leading risk factor that predisposes cartilage to pathological changes and OA. Although OA is not the direct result of ageing, it is believed that age-related changes in the joint make articular cartilage susceptible to OA (Loeser et al., 2016), since they affect both chondrocyte physiology and ECM properties (Mobasher et al., 2015). Aged chondrocytes display increased senescence and higher expression of catabolic markers; features also evident in OA chondrocytes (Sacitharan et al., 2016). Moreover, in humans, aged knee cartilage is thinner compared to younger cartilage and is characterised by increased collagen crosslinking and altered proteoglycan content. These changes affect matrix stiffness, make cartilage susceptible to fractures and lower its ability to sense mechanical stimuli (Verzijl et al., 2002, Zhang et al., 2019).

The exact mechanisms through which age can affect cartilage health remain elusive, though it is believed to be a cumulative combination of many molecular pathways rather than a single aetiology. MiRNAs have been linked to ageing cartilage. miR-140, one of the best studied miRNAs in cartilage, is important for cartilage development and deletion of miR-140 in mice resulted in age-related OA-like changes and skeletal defects (Miyaki et al., 2010). Moreover, OA chondrocytes show decreased expression of miR-24, resulting in increased expression of the senescent marker p16INK4a, highlighting the link between OA and senescence, which is one of the hallmarks of ageing (Philipot et al., 2014). Ukai *et al* (2012) identified miRNA changes in chondrocytes isolated from the fingers of infants diagnosed with polydactylism (average age: 13 months) and normal, non-load bearing articular cartilage from young patients undergoing ACL reconstruction (average age: 22.3 years) (Ukai et al., 2012). They found elevated expression of miR-199a-3p and miR-193b, and decreased expression of miR-320c in the ACL group compared to the infant group. Overexpression of miR-199a-3p and miR-193b in chondrocytes resulted in reduced expression of *COL2A1*, *ACAN* and *SOX9* compared to control, whereas the opposite occurred when they inhibited the expression of these two miRNAs in chondrocytes. The group concluded that miR-199a-3p and miR-193b could be potentially involved in chondrocyte senescence. However, it is quite challenging to

investigate, purely, age-related changes in human cartilage without the effect of OA, given the difficulty in obtaining young and old healthy articular cartilage. Our group previously carried out RNA-Seq in cartilage tissue from the metacarpophalangeal joints of young (4 years) and old (>15 years) horses and detected significantly higher expression of miR-21 in the old group, suggesting that this miRNA could potentially be involved in cartilage ageing (Peffers et al., 2013). There is very limited data on the effect of ageing on miRNA expression in cartilage and chondrocytes, without the effect of OA, therefore such studies are needed to elucidate age-related mechanisms that could help diagnose early-stage OA.

*Note: The analyses described in this chapter are included in the published research article: Small Non-Coding RNAome of Ageing Chondrocytes (Balaskas et al., 2020). The article is available in the Appendix to Chapter 6.*

## 6.2 Study aim and rationale

In this study, I undertook small RNA-Seq to investigate the expression changes of miRNAs in chondrocytes isolated from healthy metacarpophalangeal joints of young and old horses. I used chondrocytes instead of cartilage tissue to obtain high quality RNA suitable for small RNA-Seq. Results were validated with qPCR using RNA from the same equine samples, as well as an independent cohort of young and old chondrocytes isolated from healthy metacarpophalangeal joints.

## 6.3 Experimental design

The experimental procedures, pertinent to this chapter are described briefly below. For full details on the experimental procedures, please refer to Chapter 2. Appropriate references are provided throughout the text.

### **6.3.1 Isolation of young and old healthy equine chondrocytes**

For small RNA-Seq, healthy primary chondrocytes were isolated from the metacarpophalangeal joints of young ( $n = 5$ , age mean $\pm$  SD=  $4\pm 1$  years) and old ( $n = 5$ , age mean $\pm$  SD=  $17.4\pm 1.9$  years) non-Thoroughbred horses as described in Section 2.10. Joints were grossly inspected for pathological perturbations and only grossly normal joints were selected for chondrocyte isolation.

In addition to the above samples, RNA from chondrocytes from young ( $n=2$ , age mean $\pm$  SD=  $0.75\pm 0.3$  years) and old ( $n=6$ , age mean $\pm$  SD;  $19.3 \pm 3.6$  years) non-Thoroughbred horses were used for validation with qPCR.

### **6.3.2 Equine chondrocyte culture, passaging and total RNA extraction**

Isolated chondrocytes were cultured up to 90% confluence and collected as described in Section 2.11. Total RNA was extracted from young and old healthy equine chondrocytes using the miRNeasy Mini Kit (Qiagen, Manchester, UK), as described in Section 2.13.2.

### **6.3.3 Small RNASeq analysis for detection of differentially expressed miRNAs in young and old healthy equine chondrocytes**

To detect DE miRNAs between young and old healthy equine chondrocytes, small RNA-Seq was undertaken using the Illumina MiSeq platform (Illumina, Cambridge, UK), as described in Section 2.15. Following small RNA-Seq, sequence data were processed through a number of steps to obtain miRNA expression values, including base-calling, trimming of fastq files to remove Illumina adapter sequences and low-quality bases, read alignment, as described in Section 2.32. Differential expression analysis was undertaken in R environment using package EdgeR. The estimated logFC were tested in EdgeR using a likelihood ratio test. Significantly DE miRNAs were defined as those with FDR-adjusted p-value $<5\%$ , as described in Section 2.32.

### **6.3.4 Pathway analysis of DE miRNAs between young and old equine chondrocytes**

In order to identify miRNA targets, bioinformatic analysis was performed by uploading DE miRNA data into the MicroRNA Target Filter module within IPA, along with previously identified DE mRNAs from our ageing equine cartilage study (Peffers et al., 2013). In IPA I selected miRNA-target genes based on the direction of differential expression (for example, if a miRNA was reduced in expression, it was only matched to mRNAs that demonstrated increased expression). I then identified the networks, functions, and canonical pathways of these miRNA-target genes, as described in Section 2.36.

### **6.3.5 cDNA synthesis and qPCR for miRNA quantification**

Poly(A) cDNA for miRNA quantification using qPCR, was synthesised from total RNA as described in Section 2.16. miRNA quantification was undertaken as described in Section 2.18. Statistical analysis was undertaken in GraphPad Prism version 8.0.1 for Windows and normality of data was assessed using the Shapiro-Wilk normality test. For miRNA quantification in equine primary chondrocytes, statistical significance was calculated using the Mann-Whitney test, as data did not follow the Gaussian distribution. Expression levels were normalised to U6 (as this was stable in the small RNA-Seq data set) and calculated using the  $2^{-\Delta Ct}$  method. P values $<0.05$  were considered significant.

## 6.4 Results

### 6.4.1 Differential Expression Analysis of Small RNA-Seq Data

To identify differential expression of miRNAs in ageing, small RNA-Seq between young healthy and old healthy equine chondrocytes was undertaken using the Illumina MiSeq platform. Reads mapping percentages were between 92 to 94.3%. There were 266 mature miRNAs identified.

The effect of age on the expression of miRNAs was weak and the separation of young and old samples was not clear. The 2-D PCA plot indicated that few, but very specific changes in the expression of miRNAs were found, and samples from old donors were more variable than those from young (**Figure 6.1**).

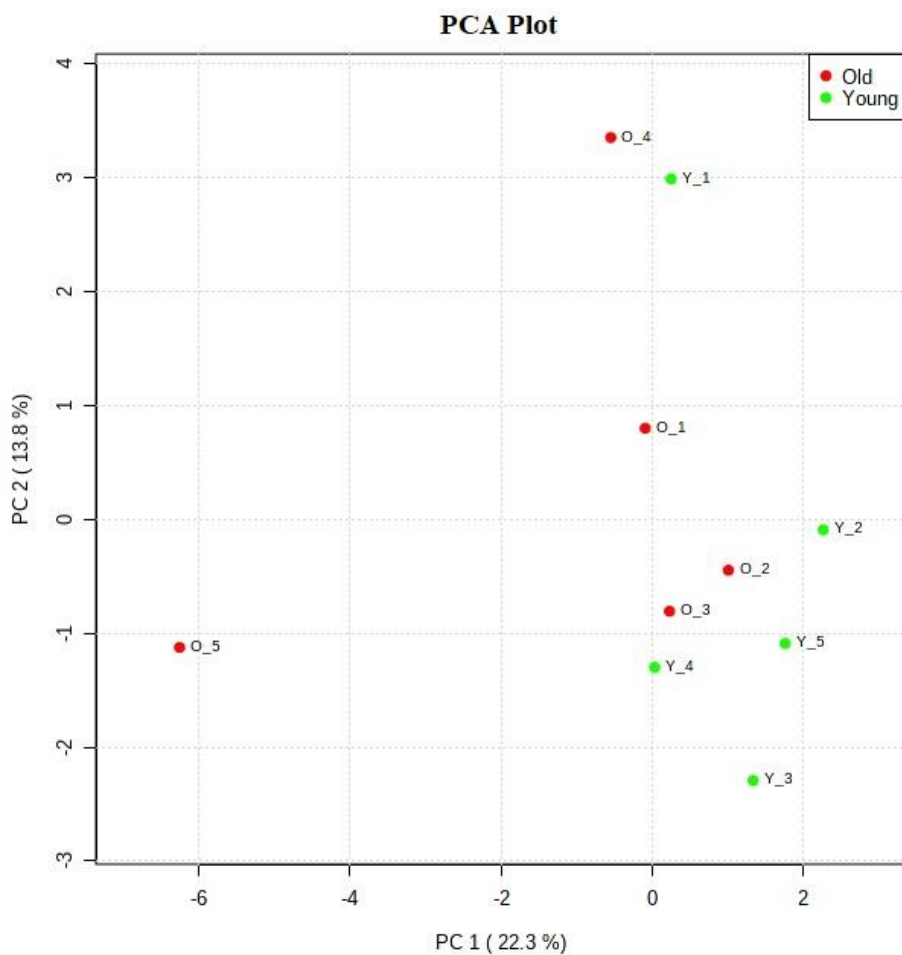


**Figure 6.1: 2D PCA plot of the first and second components of miRNA abundance in young and old equine chondrocytes.** PCA plot created using the logarithm-transformed data from all libraries. Plot produced using MetaboAnalyst 5.0.

A heat map of hierarchical clusters of correlations among samples depicted that the miRNA expression of young and old groups was not very different (**Figure 6.2**). Analysis showed that there were five DE miRNAs between young and old equine chondrocytes at FDR-adjusted  $p<0.05$ . Two of the DE miRNAs had significantly higher expression in the old group, whereas the other three had significantly lower expression in the old group. **Table 6.1** summarises results.

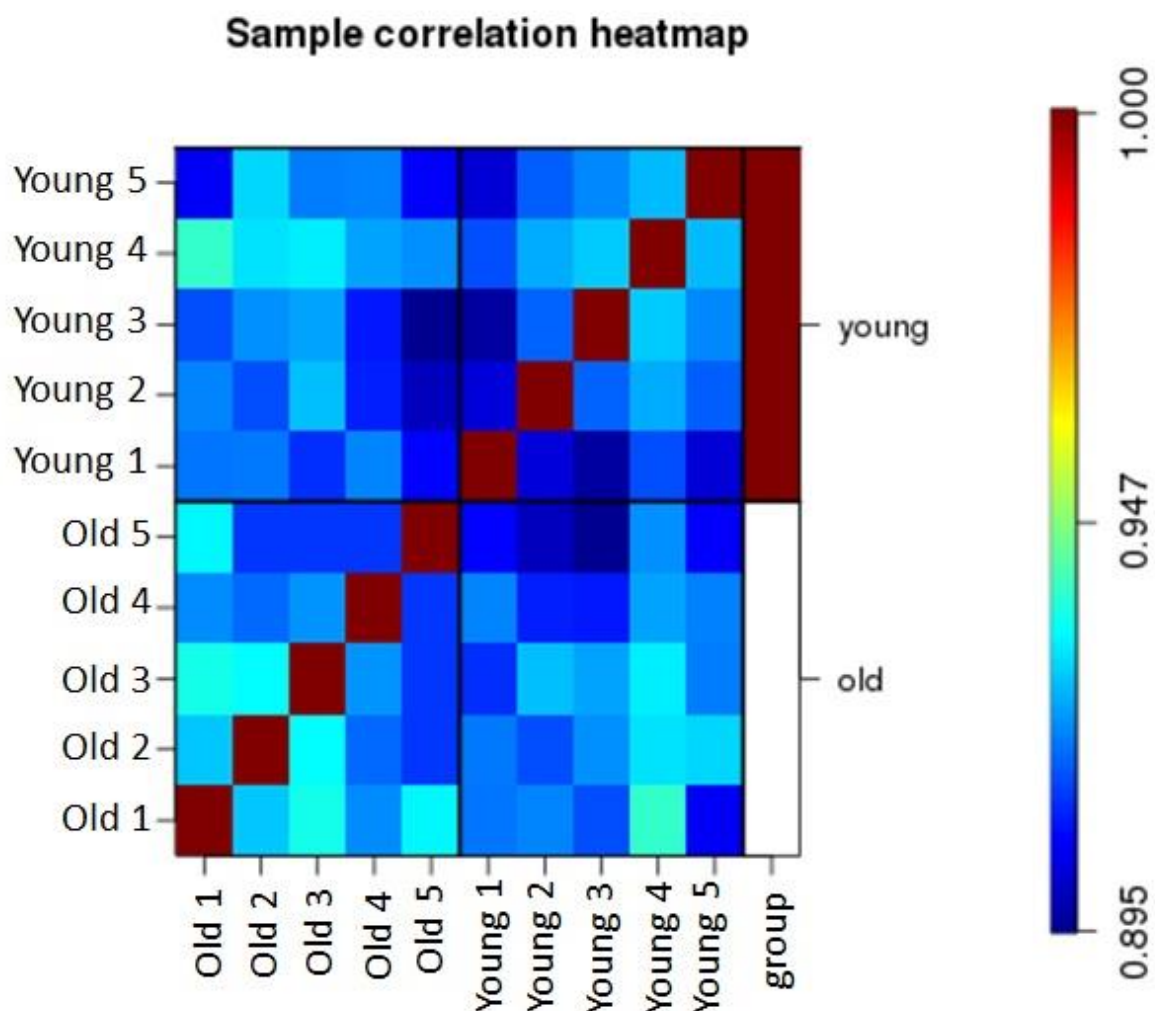


**Figure 6.2: Heatmap of correlation coefficients among young and old chondrocyte samples.**

Correlation coefficients among five young and five old equine chondrocyte samples were computed using logarithm-transformed expression values of detected miRNAs. Colour gradient from blue to red denotes transition from lower to higher correlation coefficients.

Produced in R environment using Stats Package.

**Table 6.1: Differentially expressed miRNAs in ageing chondrocytes.** Log<sub>2</sub> FC values were derived with young as the reference group. A positive log<sub>2</sub> fold change equates to higher expression in old, whereas a negative log<sub>2</sub> fold change equates to lower expression in old. Significant at FDR-adjusted p< 0.05.

miRNA	Log <sub>2</sub> FC (old vs young)
eca-miR-143	-1.3
eca-miR-145	-1.8
eca-miR-181b	-1.8
eca-miR-122	2.3
eca-miR-148a	1.3

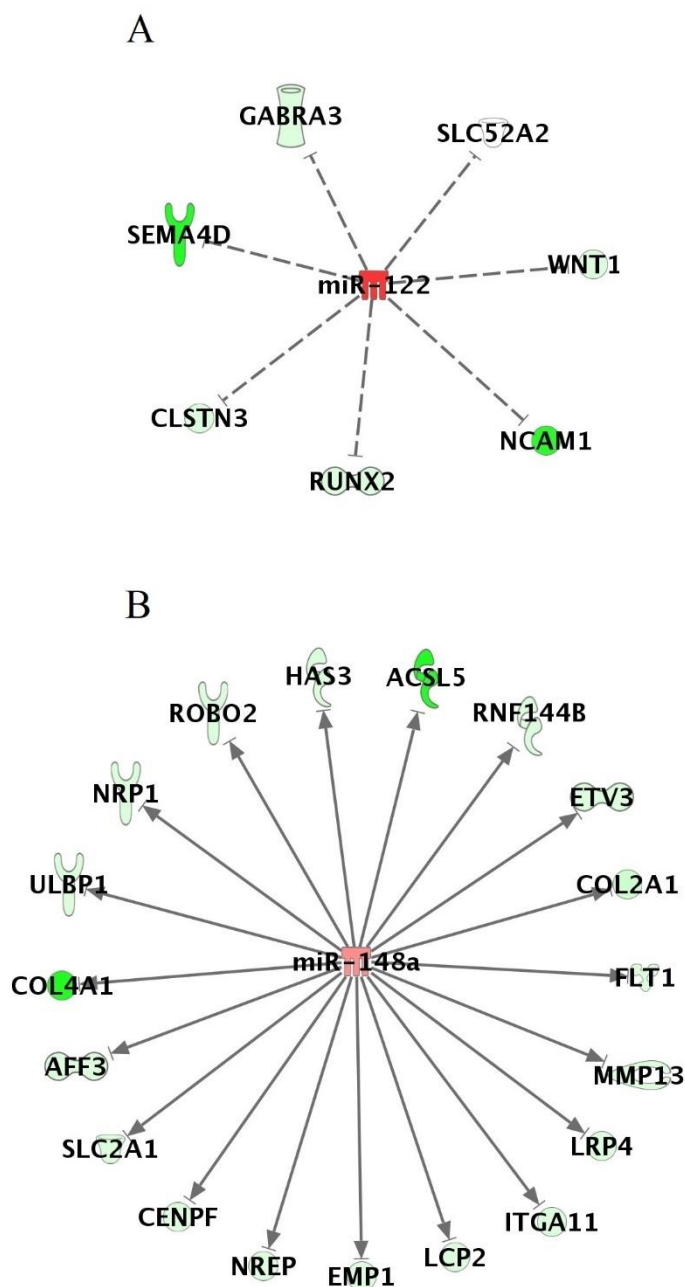
#### 6.4.2 IPA analysis of DE miRNAs in equine chondrocyte ageing

To investigate the role of the five DE miRNAs (miR-143, miR-145, miR-181b, miR-122, miR-148a), and their potential implication in cartilage and chondrocyte ageing, I undertook further analysis of our dataset using IPA. Our group had previously carried out RNA-Seq between young and old equine cartilage tissue to identify age-related DE mRNAs (Peffers et al., 2013). In IPA, the five DE miRNAs were paired with the 351 DE protein coding genes from our RNA-Seq study, to identify likely miRNA-mRNA interactions. Expression pairing was adjusted to show only miRNA-mRNA interactions that followed the correct pairing direction (miR increase and mRNA decrease or vice versa). Analysis showed that four out of five miRNAs interacted with 31 DE mRNAs from our RNA-Seq experiment (**Table 6.2**).

**Table 6.2: Predicted and experimentally validated miRNA-mRNA interactions in equine cartilage/chondrocyte ageing.** IPA analysis generated a list of experimentally validated or predicted (with high/moderate confidence) miRNA-mRNA interactions in cartilage/chondrocyte ageing. Expression pairing was set to only show pairings with opposite direction of expression between the miRNA and the mRNA target. Upward arrow denotes significantly higher expression in the old group, whereas a downward arrow denotes lower expression in the old group. Young group was the reference group.

miRNA	Direction	mRNA	Direction	Confidence
miR-122	↑	CLSTN3	↓	Moderate (predicted)
miR-122	↑	GABRA3	↓	Moderate (predicted)
miR-122	↑	NCAM1	↓	Experimentally Observed
miR-122	↑	RUNX2	↓	Moderate (predicted)
miR-122	↑	SEMA4D	↓	High (predicted)
miR-122	↑	SLC52A2	↓	High (predicted)
miR-122	↑	WNT11	↓	Moderate (predicted)
miR-143	↓	FST	↑	Moderate (predicted)
miR-143	↓	KCNN3	↑	Moderate (predicted)
miR-143	↓	MGARP	↑	Moderate (predicted)
miR-148a	↑	ACSL5	↓	Moderate (predicted)
miR-148a	↑	AFF3	↓	Moderate (predicted)
miR-148a	↑	CENPF	↓	Moderate (predicted)
miR-148a	↑	COL2A1	↓	Moderate (predicted)
miR-148a	↑	COL4A1	↓	Moderate (predicted)
miR-148a	↑	EMP1	↓	High (predicted)
miR-148a	↑	ETV3	↓	Moderate (predicted)
miR-148a	↑	FLT1	↓	High (predicted)
miR-148a	↑	HAS3	↓	Moderate (predicted)
miR-148a	↑	ITGA11	↓	Moderate (predicted)
miR-148a	↑	LCP2	↓	Moderate (predicted)
miR-148a	↑	LRP4	↓	Moderate (predicted)
miR-148a	↑	MMP13	↓	Moderate (predicted)
miR-148a	↑	NREP	↓	Moderate (predicted)
miR-148a	↑	NRP1	↓	High (predicted)
miR-148a	↑	RNF144B	↓	Moderate (predicted)
miR-148a	↑	ROBO2	↓	Moderate (predicted)
miR-148a	↑	SLC2A1	↓	High (predicted)
miR-148a	↑	ULBP1	↓	Moderate (predicted)
miR-181b	↓	HEY2	↑	Moderate (predicted)
miR-181b	↓	TNFSF11	↑	Moderate (predicted)

The 31 mRNAs which interacted with our four DE miRNAs were used in IPA as network-eligible molecules and overlaid onto molecular networks based on information from the IPA database. Networks were generated based on miRNA-mRNA interactions (**Figure 6.3A-D**). IPA Core Analysis for the 31 mRNA targets identified that among the top canonical pathways were hepatic fibrosis ( $p = 1.51 \times 10^{-3}$ ), glycoprotein 6 signalling ( $p = 5.67 \times 10^{-4}$ ), and OA pathway ( $p = 2.93 \times 10^{-3}$ ). The top diseases and cellular functions associated with this network are shown in **Figure 6.4** and **Table 6.3**. IPA Core Analysis Report is in Appendix to Chapter 6.



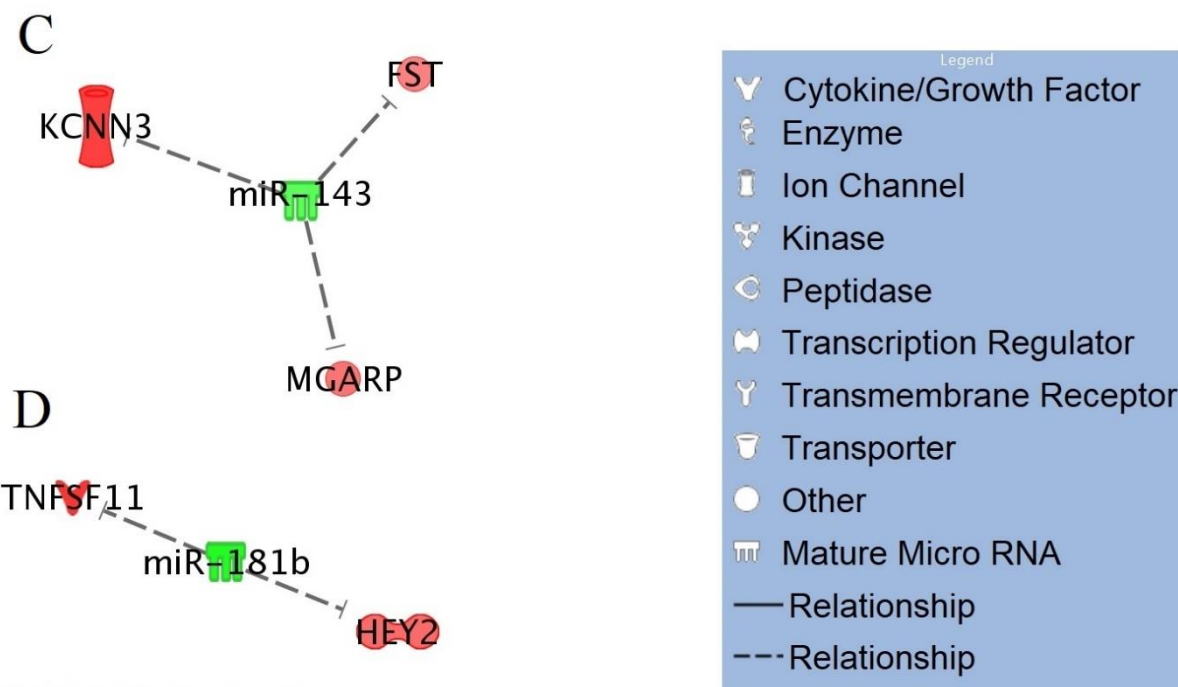


**Figure 6.3: miRNA-mRNA interactome for differentially expressed miRs in ageing.**

Significantly DE miRNAs were paired with DE mRNAs from our original RNA-Seq cartilage study. A) miR-122, B) miR-148a, C) miR-143 and D) miR-181b. The legend for individual molecules is shown. Genes in red are upregulated and green downregulated in old chondrocytes/cartilage compared to young, and depth of colour correlates to fold expression change. Figure produced in IPA using Path Designer tool. Uploaded datasets were overlaid onto molecular networks based on miRNA-mRNA interactions predicted by IPA.

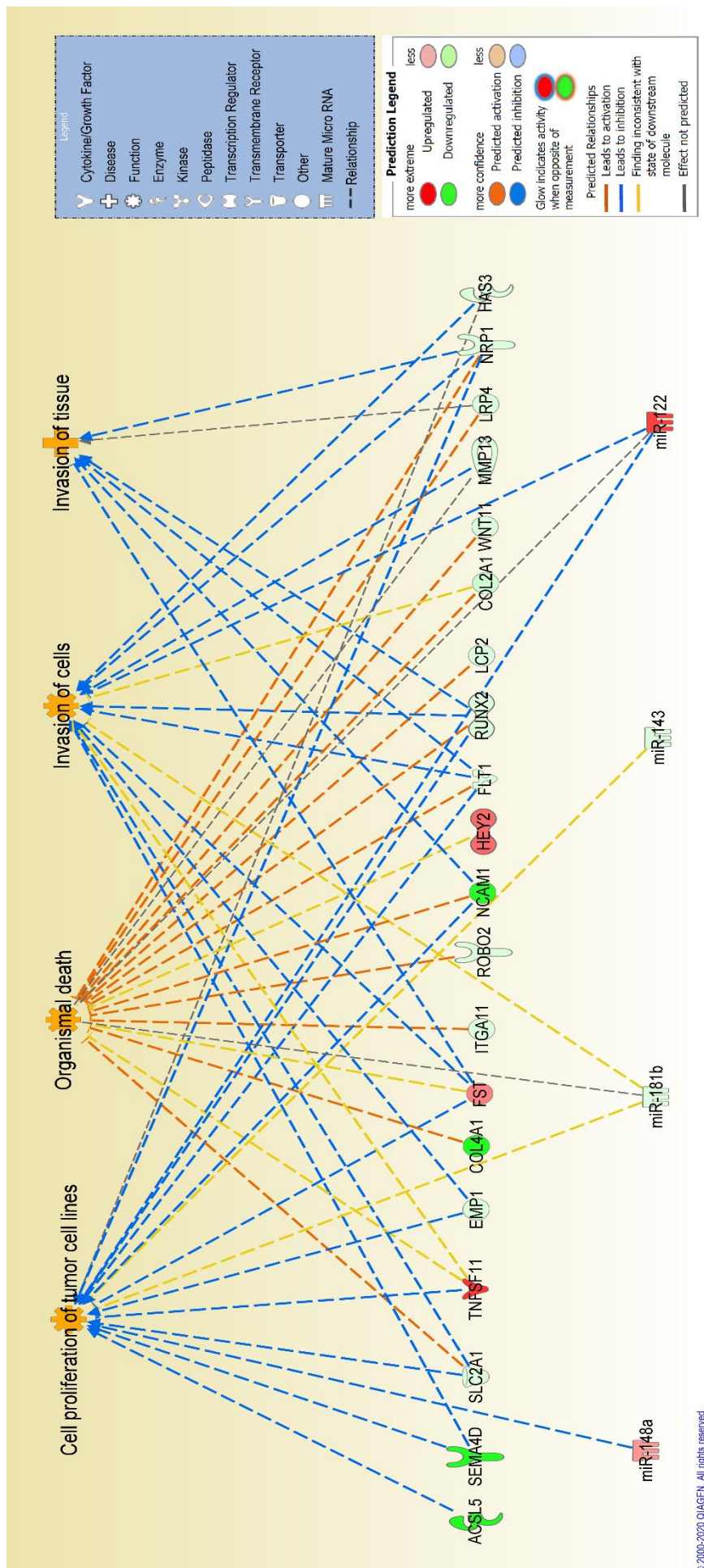


**Figure 6.4: Significant pathways and networks affected in cartilage ageing.** IPA was used to pair differentially expressed mRNA and miRNA data from ageing equine cartilage and chondrocytes. Figure is a graphical representation between molecules identified in our data in their respective networks. Red nodes denote upregulated gene expression in old group and green nodes denote downregulated gene expression in old group. Intensity of colour is related to higher fold-change. The key to the main features in the networks is shown. Figure produced in IPA and top predicted cellular functions were displayed as networks based on miRNA-mRNA interactions.

**Table 6.3: IPA mRNA target diseases and functions.** 1<sup>st</sup> column shows A) top molecular and cellular functions and B) top diseases and disorders associated with predicted miRNA-mRNA interactions in ageing chondrocytes. 2<sup>nd</sup> column lists the level of significance for each network, calculated by IPA. 3rd column denotes the number of DE mRNA targets involved in each function/disease listed in the 1<sup>st</sup> column.

A. Top Molecular and Cellular Functions	p-Value Range	Number of Molecules
Cellular Movement	$1.41 \times 10^{-3} - 4.23 \times 10^{-10}$	21
Cell Morphology	$1.37 \times 10^{-3} - 3.52 \times 10^{-8}$	16
Cellular Development	$1.42 \times 10^{-3} - 4.94 \times 10^{-7}$	24
Cell Death and Survival	$1.37 \times 10^{-3} - 1.08 \times 10^{-5}$	18
Cell-To-Cell Signalling and Interaction	$1.37 \times 10^{-3} - 1.88 \times 10^{-5}$	20
B. Top Diseases and Disorders		
Skeletal and Muscular Disorders	$1.50 \times 10^{-3} - 1.22 \times 10^{-9}$	16
Connective Tissue Disorders	$1.50 \times 10^{-3} - 3.52 \times 10^{-8}$	16
Organismal Injury and Abnormalities	$1.50 \times 10^{-3} - 3.52 \times 10^{-8}$	31
Cancer	$1.49 \times 10^{-3} - 5.30 \times 10^{-7}$	31
Developmental Disorder	$1.37 \times 10^{-3} - 5.30 \times 10^{-7}$	17

#### 6.4.3 Validation of DE miRNAs in young and old equine chondrocytes using qPCR

To validate our findings from the small RNA-Seq experiment, I undertook qPCR analysis in an extended cohort of young and old equine chondrocytes. The validation cohort consisted of RNA samples from the same donors used in small RNA-Seq, and RNA from additional young and old equine chondrocyte samples. qPCR analysis showed that miR-143, miR-145, and miR-181b had significantly lower expression in the old group compared to young group. miR-122 had significantly higher expression in the old group compared to young, whereas miR-148a did not show any significant expression differences between young and old groups (**Figure 6.5**). Therefore, four out of five miRNAs were validated with qPCR analysis.

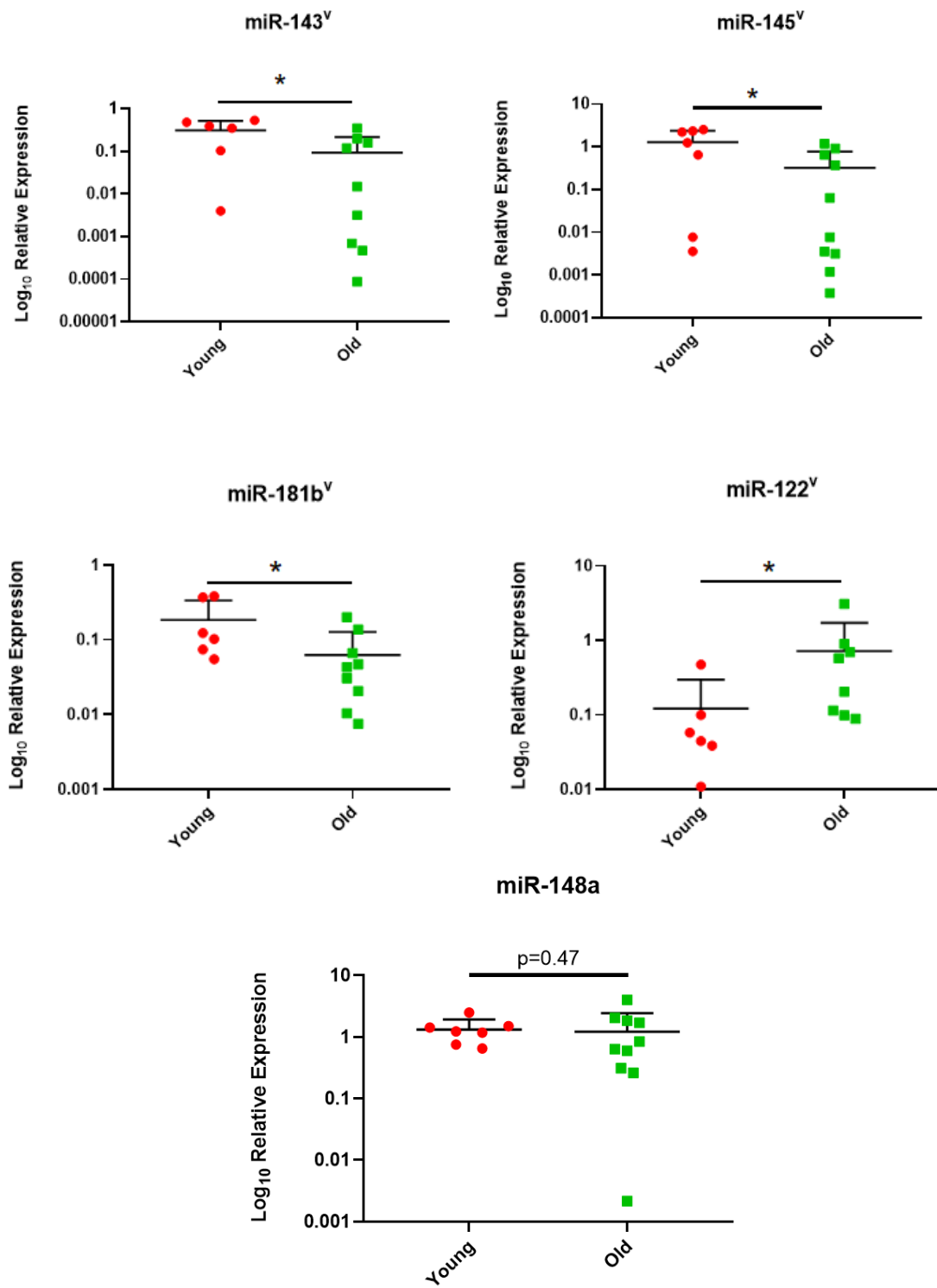


**Figure 6.5: Validation of selected miRNAs in an extended cohort of equine young and old chondrocytes.** qPCR was used to validate DE miRNAs identified from the small RNA-Seq analysis. N= 6-10 per group. Y axis shows log<sub>10</sub> expression relative to U6. V denotes DE miRNAs that were validated with qPCR. Statistical analysis was undertaken using a Mann Whitney test in GraphPad Prism. Data are represented as mean+SD. P values<0.05 were considered significant. \*: p<0.05.

## 6.5 Discussion

In Chapter 3 I undertook a microarray analysis to identify DE miRNAs between young intact cartilage from ACL donors and old OA intact and lesioned cartilage from TKA patients. Changes identified were driven by at least two major variables: ageing and OA. Even though it is likely that, in our study, disease-related changes could mask age-related changes, ageing is one of the leading risk factors contributing to OA (Lotz et al., 2012). Many studies have shown that ageing can affect cartilage in different ways, both at cellular and molecular level. Increased chondrocyte death, apoptosis, and a shift towards a catabolic profile have been observed in aged chondrocytes (Li et al., 2013). Additional age-related changes in articular cartilage include increased chondrocyte senescence (Martin et al., 2001), oxidative stress (Jallali et al., 2005), and changes in the composition and structure of ECM (Rahmati et al., 2017). Although the underlying molecular causes of these changes are not completely understood, it is hypothesised that aged chondrocytes respond differently to various stimuli, such as growth factors (Hodgson et al., 2019) and demonstrate altered molecular signatures (Zhang et al., 2019). Previously, our group undertook an RNA-Seq analysis in young and old equine cartilage tissue to identify DE mRNAs (Peffers et al., 2013). In this chapter, I used small RNA-Seq to identify alterations in miRNA expression between young and old equine chondrocytes from non-OA joints. The horse is a good model to study musculoskeletal ageing and disease as I could assess the whole joint for pathological perturbations during tissue collection. It is very challenging to source aged human cartilage that has no OA changes, whereas this is easily undertaken in equine samples. Moreover, the horse has been used as a model of OA and there has been significant research on equine joint anatomy and pathophysiology (Goodrich et al., 2006b, McIlwraith et al., 2012).

Within our dataset, I identified two miRNAs with higher expression in the old group: miR-122 and miR-148a, and three miRNAs with lower expression in the old group: miR-143, miR-145 and miR-181b. Of these five miRNAs, all except miR-148a were validated in an extended cohort of young and old equine chondrocytes with qPCR. Studies have shown that miR-122 is upregulated in OA cartilage compared to normal cartilage and can induce the expression of catabolic markers, such as MMPs and ADAMTSs (Bai et al., 2020). In a rat bilateral ACL transection model, miR-122 had higher expression in joints from OA rats compared to control (Scott et al., 2021). However, its role in ageing is less studied. miR-122 was decreased in the

serum and plasma of patients with osteoporosis, the most common age-related bone disease (Mandourah et al., 2018), but was significantly upregulated in senescent human fibroblasts (Markopoulos et al., 2017). Interestingly, I have recently carried out small RNA-Seq in young and old healthy human cartilage and miR-122 was one of the miRNAs upregulated in the old group (unpublished data), which furthers supports a role for this miRNA in cartilage and chondrocyte ageing.

Another important finding of this study is the implication of miR-143 in chondrocyte ageing. miR-143 was one of the miRNAs in our microarray study that was selected for further validation as it had significantly lower expression in old OA intact and lesioned cartilage compared to young intact cartilage from ACL donors. The findings here further support a role for this miRNA in cartilage ageing and OA. However, in Chapter 4, when I compared the expression of miR-143 in young and old healthy, non-OA cartilage from human cadavers, I failed to identify differential expression for miR-143. This could be due to species differences between human and equine, or sample differences between cartilage tissue and chondrocytes. Studies have shown that miR-143 was downregulated in muscle satellite cells from old mice and primary myoblasts from old humans and mice (Soriano-Arroquia et al., 2016). In addition, circulating miR-143 was upregulated in young individuals following resistant exercise, but was downregulated in older individuals after resistant exercise (Margolis et al., 2016). In Chapter 5, when I overexpressed and knockdown miR-143 in human OA chondrocytes and investigated the proteomic profile of the cells, I reported a possible link between miR-143 and EIF2 signalling. It would be interesting to evaluate this interaction in ageing chondrocytes, without the effect of OA, by modulating the expression of miR-143 and investigating whether a similar link exists. While collection of human aged chondrocytes without OA is quite challenging, these experiments could be carried out in animal models, given that our data suggest a role for miR-143 in cartilage among difference species.

Two other miRNAs that were validated were miR-145 and miR-181b. miR-145 belongs to the same cluster as miR-143 and they share similar functions (Qiu et al., 2021). There is very limited data on the role of this miRNA in ageing cartilage since most studies have been conducted using OA specimens. Specifically, miR-145 was downregulated in cartilage from old OA patients compared to non-OA cartilage (Liu et al., 2019a), as well as in OA rat chondrocytes treated with TNF- $\alpha$  (Hu et al., 2017a). Similarly, there is very limited data on the role of miR-

181b in ageing. Most data on its role in musculoskeletal ageing come from muscle studies. miR-181b was downregulated in skeletal muscle of old rhesus monkeys compared to young (Mercken et al., 2013), was downregulated in myogenic progenitors of old mice compared to adult mice, and its overexpression promoted myogenesis (Proctor et al., 2017).

To further investigate the potential role of the DE miRNAs identified between young and old equine chondrocytes, I used IPA to combine them with DE mRNAs between young and old cartilage from our previous equine cartilage study (Peffers et al., 2013). IPA miRNA ‘Target Filter and Expression Pairing’ identified 31 potential target genes. IPA core analysis of these genes revealed canonical pathways associated with cartilage physiology, such as role of chondrocytes in rheumatoid arthritis ( $p=2.2\times10^{-4}$ ), OA-related pathways ( $p=2.93\times10^{-3}$ ) and BMP signalling ( $p=6\times10^{-3}$ ), all of which have been linked to ageing (Collins et al., 2018, Thielen et al., 2019). Of note, follistatin (*FST*) which was upregulated in old equine cartilage and was predicted by IPA as a target of the downregulated miR-143, was overexpressed in human OA chondrocytes compared to normal chondrocytes (Tardif et al., 2004), and in canine OA cartilage compared to normal cartilage (Tardif et al., 2009). In another study, FST was induced by telomere shortening (Liu et al., 2019b), a process closely related to ageing. Moreover, TNF ligand superfamily member 11 (*TNFSF11*), also known as receptor activator of nuclear factor kappa-B ligand (*RANKL*), was upregulated in old equine cartilage and was identified as a predicted target of the downregulated miR-181b. Higher expression of TNFSF11/RANKL, which correlated with bone loss, was reported in old C57BL/6 mice (Cao et al., 2003), rabbits with chronic antigen-induced arthritis (Martínez-Calatrava et al., 2012), and in human high grade OA cartilage (Upton et al., 2012), suggesting that miR-181b could also be involved in these pathways through the targeting of TNFSF11/RANKL.

I am aware that the effect of ageing between young and old equine chondrocytes was small as only five DE miRNAs were identified. I cannot rule out changes related to the use of chondrocytes instead of cartilage tissue. Even though chondrocytes of low passage (P0) were used, collagenase digestion and plating of cells could have affected their phenotype and gene expression. I have discussed in previous chapters of this thesis that primary chondrocytes dedifferentiate when in culture due to the loss of stimuli they normally receive from the ECM (Caron et al., 2012, Charlier et al., 2019). The choice of chondrocytes over cartilage tissue was made based on the observation that RNA extracted from cartilage tissue was of low quality

(in our hands) and heavily contaminated with proteoglycans (Ali et al., 2012), usually making it challenging for sequencing. With that said, with the use of chondrocytes instead of cartilage tissue, it is likely that I am interrogating highly specific changes that are age-dependent and persist even with culturing of chondrocytes. Another point that should be taken into account is the use of the Illumina MiSeq platform which may have contributed to the low number of DE miRNAs as it offers less depth coverage (12-15 million paired-end reads per run) compared to other systems, such as the HiSeq platform (~280 million paired-end reads per run). Finally, I have used a relatively small number of samples per group. Given the use of primary cells and the degree of variability observed, especially for the old group, the inclusion of five samples pre group may have contributed to the small number of differentially expressed miRNAs in ageing equine chondrocytes.

## 6.6 Conclusion

In this chapter I have investigated, using unbiased methods, the effect of ageing on the expression of miRNAs in equine chondrocytes. Even though the effect of ageing on equine chondrocytes was small, I detected five miRNAs, which are predicted to play a role in the development of the musculoskeletal system and in skeletal disorders. Amongst them, I identified miR-143, a miRNA which has been one of the main miRNAs discussed in this thesis for its role in cartilage and OA. Further research is needed to elucidate the role and function of these molecules in ageing cartilage and their potential link to disease.

# **Chapter 7: General Discussion and Future Directions**

## 7.1 General Discussion

In this thesis, I aimed to define the miRNA signatures of ageing and OA cartilage and investigate the role and targetome of specific miRNAs in cartilage ageing and disease. To interrogate biological pathways of selected miRNAs, I undertook transcriptomic and proteomic analyses in human cartilage, and human and equine chondrocytes, and utilised bioinformatics tools and experimental approaches to explore relevant miRNA targets and disease-related mechanisms. The first objective of this thesis, to establish DE miRNAs in OA cartilage, was achieved by undertaking microarray analysis on young intact cartilage from donors undergoing ACL reconstruction and OA patients undergoing TKA for end-stage OA. The second objective, to evaluate the response of selected DE miRNAs in an *in vitro* OA inflammatory cell model, was achieved by treating human primary OA chondrocytes with human recombinant IL-1 $\beta$  for a series of time points. This thesis achieved its third objective, to characterise selected target genes of a set of DE miRNAs, by undertaking gain and loss of function approaches in human primary chondrocytes, as well as transcriptomic and proteomic investigation of miRNA-target interactions. Finally, this thesis achieved its fourth objective, to establish DE miRNAs in ageing chondrocytes, by undertaking small RNA-Seq between young and old healthy equine chondrocytes. The work in this thesis supports the hypothesis that there is aberrant miRNA expression in aged and OA cartilage and chondrocytes, which results in changes in gene expression and could potentially contribute to altered cellular mechanisms in chondrocytes.

The starting point for this thesis was the microarray analysis between young intact cartilage and old OA cartilage. Young cartilage was sampled from donors undergoing ACL reconstruction. Time of surgery ranged from weeks to a few months after rupture. Since ACL is a risk factor for PTOA, I chose to refer this group as ‘Young intact’ cartilage rather than ‘Young healthy’. Studies showed that 30% of patients who have ACL reconstruction surgery, show signs of cartilage degeneration, evident by KL scoring (KL=1 or 2), ten years after surgery (Ajuedo et al., 2014). However, such alterations seem to appear years after reconstruction, therefore, for the purposes of the thesis, I mainly considered young intact cartilage as non-OA. It would have been beneficial to assess these tissues histologically and confirm integrity of the tissue, but given the limited size of cartilage tissue collected during these surgeries, that was not possible. Another option would have been to include old healthy cartilage in our

microarray analysis and contrast that to aged-matched OA cartilage samples. It is true that in Chapter 4 I used young and old healthy human knee cartilage from cadavers to look at the age effect of selected miRNAs. However, at the time of the microarray analysis those samples were not available to us to use in our microarray analysis and compare to OA tissue. Moreover, the limited number of these samples ( $n=5$ ) would have reduced the power of the experiment.

Microarray analysis between young intact, old OA intact and old OA lesioned samples identified significant changes (FDR-adjusted  $p<0.05$ ) in the expression of multiple miRNAs between the contrasted groups. There were at least two variables that drove those changes: ageing and OA. I hypothesise that these changes were driven mainly by disease rather than ageing. In Chapter 4, by using qPCR, I validated our findings for a selected set of DE miRNAs in the samples from the microarray analysis, as well as in an additional independent cohort of samples. qPCR analysis validated the miRNA expression changes observed in microarray analysis. However, when I interrogated the expression of the same set of miRNAs in young and old healthy cartilage tissue from human cadavers with no history of OA and with normal histology, I did not observe any differences in the expression of these miRNAs. Moreover, in Chapter 6, I carried out small RNA-Seq between young and old equine chondrocytes from donors with no OA and macroscopically normal joints, and identified only five DE miRNAs (FDR-adjusted  $p<0.05$ ) between the two groups. While a direct comparison cannot be made, given species differences, the use of different starting material (cartilage tissue versus chondrocytes), and the use of different experimental approach (qPCR versus small RNA-Seq), in both experiments I observed moderate miRNA expression changes with ageing. Though limited in number, other studies which have interrogated the expression of miRNAs in cartilage ageing without the effect of OA, support our findings (Ukai et al., 2012). In addition, our group has carried out small RNA-Seq between young and old healthy human cartilage from donors with no history of OA, and only a small number of miRNAs were DE at FDR-adjusted  $p<0.05$  (unpublished data). This is not to say that ageing does not affect cartilage integrity and chondrocyte homeostasis, as age is a principal risk factor for OA, but it supports our initial hypothesis that our microarray findings are mainly driven by OA. With that said, our results indicated that there was more variability in miRNA expression of old samples compared to young. In microarray analysis, old OA intact samples were clustered in two

separate subgroups: OA intact 1 and 2. Old OA lesioned samples were also more variable and could be clustered as different subgroups. In contrast, young samples were clustered more tightly together. Similar trends were observed in Chapter 6, as young equine chondrocyte samples clustered more tightly together, whereas old equine samples showed more variability. Studies using monozygotic twins have reported that epigenetic variation increases with ageing (Talens et al., 2012). Furthermore, OA is a heterogeneous disease with a number of different phenotypes and endotypes, therefore, subgrouping of old OA samples was not unexpected (Berenbaum, 2019).

In our microarray analysis, a high number of miRNAs were DE between young intact cartilage and old OA cartilage. It is quite challenging to differentiate between miRNAs that are driving the disease and have a causal relationship in OA, and those whose differential expression is the result of the disease. This would require the use of early-stage cartilage samples, which is difficult to obtain in humans. An alternative is the use of synovial fluid from early-stage OA from animal models. Recently, our group undertook small RNA-Seq in synovial fluid from horses with early-OA and control horses and one of the miRNAs that had significantly lower expression in the early-OA samples was miR-143 (Castanheira et al., 2021). miR-143-3p is one of the miRNAs investigated in this thesis and had significantly lower expression in human old OA cartilage compared to young intact and in old equine chondrocytes compared to young chondrocytes. The horse is a good model to study musculoskeletal ageing and disease as the whole joint can be assessed for pathological perturbations during tissue collection. It is very challenging to source aged human cartilage that has no OA changes, whereas this is easily undertaken in equine samples. Moreover, the horse has been used as a model of OA and there has been significant research on equine joint anatomy and pathophysiology (Goodrich et al., 2006a, McIlwraith et al., 2012).

By using pathway prediction tools, such as IPA, ToppGene, Revigo and Cytoscape, I identified distinctive mechanisms between young intact and old OA cartilage tissues. When OA intact-1, OA intact-2 and OA lesioned groups were compared to the young intact group, the list of DE miRNAs and relevant biological pathways was quite similar. These included inflammation-related pathways, such as cytokine signalling, production and secretion of cytokines and defence response mechanisms. This indicated that DE miRNAs between OA groups and young group, were mainly involved in inflammatory responses in chondrocytes. However, when I

compared the OA intact and lesioned groups to each other, I identified a different set of biological pathways, including ion transport, wound response, actin cytoskeleton organisation, blood circulation and neuronal signalling. These results suggested that inflammation plays a more prominent role when transitioning from normal cartilage to OA cartilage and perhaps during the early stages of the disease. However, once inflammation has been established in the joint, and OA progresses, there are little changes in inflammatory-related pathways. This is supported by studies where they have identified inflammatory changes in early-stage OA (Benito et al., 2005, Sokolove et al., 2013), but not at later stages (Dunn et al., 2016). Indeed, our results indicate that as OA progresses, pathways related to mechanotransduction (ion transport), wounding, blood cell and neuron formation become more significant. As already discussed in Chapter 3, this is expected given that with disease progression, there is blood cell invasion from the subchondral bone in cartilage, and also innervation which is related to pain in late-stage OA. Moreover, wounding pathways are related to damage and degeneration as intact cartilage becomes lesioned. An interesting finding is the ion transport pathways identified when OA intact and OA lesioned cartilage were compared. Ion transport is linked to mechanotransduction and mechanical stimuli. All of our OA intact samples came from the lateral condyle, whereas the OA lesioned samples came from the medial condyles. The medial condyle is subjected to higher mechanical pressure than the lateral, and therefore, it is expected that DE miRNAs between OA intact and lesioned tissue could be involved in mechanical stimuli.

An interesting finding from our microarray analysis, was that the majority of DE miRNAs had lower expression in the old OA cartilage groups compared to the young intact group. This could be due to disruption of the miRNA processing machinery during OA. Studies have shown that expression of DGCR8, which is part of the microprocessor complex, decreased with ageing in human MSCs, and overexpression of DGCR8 alleviated cartilage degradation in mice with ACL-induced OA (Deng et al., 2019a). Similarly, genetic deletion of DICER and DROSHA led to increased numbers of hypertrophic chondrocytes, increased chondrocyte death and decreased chondrocyte proliferation and OA-like symptoms in murine joints (Kobayashi et al., 2008, Kobayashi et al., 2015). These studies suggest that changes in the cellular components involved in miRNA biogenesis could lead to decreased miRNA processing and, therefore,

decreased miRNA expression. This may also justify the high number of DE miRNAs in our microarray study.

Following microarray analysis and pathway identification, a set of miRNAs was selected for qPCR validation and further experimental analysis. All selected DE miRNAs were validated with qPCR in the samples used for microarrays as well as in an independent cohort of cartilage samples. Agreement between the two techniques was confirmed, not only for DE miRNAs, but also for miRNAs that were not DE. To select appropriate endogenous reference genes, I looked at the microarray data to identify miRNAs with stable expression between the different groups. miR-1915-3p, -6786-5p and -6087 had stable expression in the microarrays, and that was also confirmed with qPCR, indicating that there was a good agreement between microarrays and qPCR. Of the validated DE miRNAs, four were chosen for follow up analysis: miR-361-5p, -379-5p, -107 and -143-3p. All four miRNAs were downregulated in human primary OA chondrocytes treated with IL-1 $\beta$ , one of the major pro-inflammatory cytokines. IL-1 $\beta$  treatment of primary chondrocytes is a common approach in miRNA research in OA. Microarray analyses in OA primary chondrocytes stimulated with IL-1 $\beta$ , revealed that most miRNAs which responded to the treatment were downregulated, whereas only few were upregulated (Akhtar et al., 2010, Rasheed et al., 2016). This is consistent with our microarray findings and the IL-1 $\beta$  treatments carried out in this thesis. I discussed previously that disruption of the miRNA processing machinery could lead to decreased expression of several miRNAs in disease. It is possible that inflammation in the joint could contribute to such disruption. Studies have shown that overexpression of components involved in miRNA biogenesis, such as DGCR8, reduced the level of inflammatory markers, such as IL-1 $\beta$  and IL-6 (Deng et al., 2019a). However, it is also important to note that the duration of treatment can affect miRNA response. In our dataset, miR-361-5p and miR-107 showed changes in their expression even from the 24h timepoint, whereas miR-379-5p was unchanged after 24h of treatment, but showed the largest decrease after 5days of treatment. In addition, miR-143-3p was upregulated after 24h of treatment, but was downregulated at the 5-day timepoint. This shows the complex regulatory mechanisms that characterise inflammatory response in chondrocytes. With that said, it is important to consider additional factors that contribute to OA, such as mechanical stress, injury, obesity, genetics, joint structure and others. Even though this *in vitro* OA inflammatory model is commonly used in miRNA research in OA, it

does not fully represent the underlying molecular landscape of OA. As already mentioned, when I compared miRNA expression between OA intact and lesioned cartilage samples, I discovered a set of pathways related to mechanotransduction, ECM remodelling and wounding rather than inflammation. Therefore, it would have been useful to investigate the role of our selected miRNAs using alternative methods, such as subjecting chondrocytes under mechanical pressure to evaluate miRNA response. This could have been combined with chondrocytes embedded in 3D scaffolds to better represent the zonal organisation of chondrocytes *in vivo*. Even though I did not have the opportunity to carry out such experiments in this thesis, it would have been very informative to interrogate miRNA responses under such conditions, given that most miRNA research in OA is being undertaken in monolayer cultures.

In Chapter 5, I evaluated predicted target genes of our set of four DE miRNAs. To achieve this, I overexpressed and inhibited these four miRNAs using mimic and inhibitors, specific for each miRNA. For miR-361-5p, -379-5p and -107, I used qPCR to look at the predicted targets, whereas for miR-143-3p I used LC-MS/MS to investigate proteomic changes in treated chondrocytes. An important point to consider regarding miRNA-target interactions, is the complex regulation of gene expression at different levels, including post-transcriptionally and post-translationally. miRNAs fine tune the expression of their target genes, but they are not the only cellular mechanism that regulates gene expression, as other mechanisms, such as DNA methylation, long non-coding RNAs, transcription factor regulation, protein folding, contribute to regulation of gene expression. The effect of miRNA binding on their target genes can differ, based on the tissue/cell type, developmental stage and sequence complementarity amongst others (Fiannaca et al., 2018, Sood et al., 2006). In our dataset, while I was able to show that OA chondrocytes treated with miR-379-5p mimic and inhibitor had significantly higher and lower expression of *TGFBR1*, respectively, this interaction was not validated in cartilage tissues; OA cartilage tissue had lower miR-379-5p and *TGFBR1* expression compared to young intact cartilage, suggesting that *TGFBR1* was not targeted by miR-379-5p in our cartilage dataset. Moreover, I was not able to validate *RHOA* and *CALM3* as targets of miR-361-5p using qPCR. This could be due to the fact that the effect of a miRNA on its target genes cannot always be observed at the mRNA level. It is still unclear if the preferred way of gene silencing by miRNAs, is through mRNA decay or translational inhibition. Evidence suggests

that both mechanisms contribute to gene silencing (Cloonan, 2015). Therefore, analysis at the protein level, for instance with Western blotting, would have provided further evidence about whether *RHOA* and *CALM3* are targeted by miR-361-5p in cartilage. In contrast, our experimental results support the hypothesis that miR-107 targets *WNT4* and *IHH* in cartilage. OA primary chondrocytes treated with miR-107 mimic and inhibitor had lower and higher *WNT4* and *IHH* expression respectively, compared to control. Moreover, I showed that *WNT4* and *IHH* are expressed significantly higher in OA cartilage tissue compared to young intact cartilage, opposite to miR-107. To further evaluate whether *WNT4* and *IHH* are targeted by miR-107, I had planned to investigate their protein levels with Western blotting in treated chondrocytes. However, as already mentioned in Chapter 5, due to the unexpected closing of our laboratory facilities due to COVID-19, I was not able to carry out these experiments. Nonetheless, our preliminary results agree with recent studies concerning the role of miR-107 in OA, where it was shown that miR-107 promoted chondrocyte proliferation and inhibited apoptosis (Qian et al., 2021, Tian et al., 2019). Excessive WNT and IHH signalling in OA promoted chondrocyte hypertrophy and induced expression of MMPs (Wang et al., 2019c, Wei et al., 2012, Zhou et al., 2014). Therefore, had I confirmed that *WNT4* and *IHH* were targets of miR-107, that would have provided further evidence on the role of miR-107 in chondrocyte proliferation.

One of the most promising miRNAs researched in this thesis, is miR-143-3p. Both our microarray analysis in Chapter 3, and our small RNA-Seq data from Chapter 6, have hinted at an important role for this miRNA in cartilage and OA. miR-143-3p was one of the most downregulated miRNAs in our microarray study. Moreover, it was downregulated in old equine chondrocytes compared to young. As already mentioned previously, additional work from our group, identified miR-143-3p as one of the miRNAs downregulated in early OA equine synovial fluid compared to non-OA (Castanheira et al., 2021). Our proteomics data from treating OA primary chondrocytes with miR-143-3p mimic and inhibitor, did not identify any proteins that were consistently downregulated in the mimic group and upregulated in the inhibitor group, that would have suggested potential targets of miR-143-3p. This could have been due to the detection limit of LC-MS/MS, as it can identify the most abundant proteins in the sample and not the total proteome. However, abundance of proteins may not always correlate to protein function. Another possible reason could have been the experimental

setup. Chondrocytes were treated for 48h before collection and lysis of cells. Changes in specific targets of miR-143-3p could have occurred at a prior time point, and may have no longer been detectable at the 48h time point. With that said, the downstream effect of those changes could still be detectable. Therefore, to further analyse the proteomics data, I carried out analysis in IPA using the list of DE proteins ( $p$  value $<0.05$ ) from the mimic vs control comparison and from the inhibitor vs control comparison. Analysis suggested a link between miR-143-3p and EIF2 signalling. EIF2 signalling is involved in protein translation and stress-response in the cell (Wek, 2018). Reduced EIF2 signalling leads to decreased global protein translation and activation of specific genes important for cell survival. Bioinformatics analysis with IPA, predicted inhibition of EIF2 signalling in the mimic group and activation of the pathway in the inhibition group. This hints at a potential role of miR-143-3p in chondrocyte survival. In Chapter 4, I reported increased expression of miR-143-3p in chondrocytes treated with IL-1 $\beta$  for 24h, but reduced expression in chondrocytes treated for 5 days. It is possible that miR-143-3p is initially upregulated in chondrocytes treated with IL-1 $\beta$ , to aid the cells adapt to the effect of the cytokine, but continued treatment with IL-1 $\beta$ , could result in a shift towards apoptosis. In fact, it has been proposed that prolonged or excessive stimulus by a stress factor, leads to a shift in the stress response, from survival to apoptosis via phosphorylation of eIF2a (Bevilacqua et al., 2010). It is worth mentioning that our analysis in IPA, identified LARP1 as an upstream regulator of the DE expressed proteins both in the mimic vs control group and in the inhibitor vs control group. In fact, LARP1 was predicted to be activated in the mimic group, and inhibited in the inhibitor group. It is believed that LARP1 binds and inhibits the translation of mRNA of ribosomal proteins and translation factors, although the data on its role are still contradictory (Fonseca et al., 2018), and there are currently no data on its role in OA. However, evidence suggests that inactivation of LARP1 leads to reduced chondrocyte proliferation and cellular growth (Berman et al., 2020). It would be interesting to observe future findings regarding the role of LARP1 and how these relate to our data which suggest a role for miR-143-3p in regulating protein translation in chondrocytes through the EIF2 signalling pathway.

## 7.2 Future Directions

There are several future directions for the project described in this thesis. In Chapter 5, I described that *WNT4* and *IHH* could be potential targets of miR-107 in cartilage. Western blotting analysis could be undertaken in chondrocytes treated with miR-107 mimic and inhibitor to confirm targeting of *WNT4* and *IHH* by this miRNA. Luciferase assays could also be carried out to confirm targeting, by using constructs that contain the 3' UTR of these genes. Transfection of cells with these constructs and the miRNA mimic could further confirm whether these specific genes are targets of miR-107. Moreover, given that our data suggest the involvement of miR-107 in chondrocyte proliferation and inhibition of apoptosis, proliferation assays could be undertaken to measure proliferation capacity of chondrocytes treated with mimic and inhibitors. Another important direction that this project could follow is the investigation of the role of miR-143-3p in the translational capacity of chondrocytes. Puromycin assays in chondrocytes treated with miR-143-3p mimic and inhibitor would shed light on the role of this miRNA in translational capacity of chondrocytes. Ideally, treatment of chondrocytes with miR-143-3p mimic and inhibitors for different time points would be desirable. As mentioned previously, in our experiments, chondrocytes were treated for 48h and I measured proteomic changes for this time point. However, early changes, including changes in specific target genes, especially in transcription factors, may not have been detectable at the 48h time point. Therefore, treatment for earlier time points could assist in the identification of relevant miR-143-3p target genes. Moreover, investigation of LARP1 expression in treated chondrocytes could provide more insights on its potential implication to our proteomics findings.

In addition, the results described in this thesis offer the opportunity to investigate additional miRNAs in cartilage ageing and OA. Microarray analysis identified a high number of DE miRNAs between young intact cartilage from ACL donors and old OA intact and lesioned cartilage from patients undergoing TKA. Additional miRNAs could be selected for follow up analysis. It would be of interest to analyse specific miRNAs that were DE between OA intact and lesioned cartilage, as these would represent miRNAs involved in disease progression and other OA-related pathways, such as mechanotransduction. Similarly, DE miRNAs from Chapter 6, between young and old equine chondrocytes, could be further investigated to

identify age-related mechanisms in chondrocytes, by carrying out gain and loss of function experiments.

### **7.3 Conclusion**

This thesis undertook a number of studies in human knee cartilage and human and equine chondrocytes, to identify aberrant expression of miRNAs in ageing and diseased cartilage, and to characterise the role of a specific set of miRNAs in cartilage biology. It utilised omics approaches to investigate transcriptomic and proteomic changes relevant to miRNA function and interrogate disease mechanisms in cartilage. Analyses in this thesis have pointed to the complex mechanistic networks that underlie cartilage pathology and have set the ground for further research in the field.

## References

2004. Gene [Internet].
- 2020a. Multiple Primer Analyzer.
- 2020b. Tm Calculator.
- ABDI, H. & WILLIAMS, L. J. 2010. Principal component analysis. 2, 433-459.
- ADAMS, C. S. & HORTON, W. E., JR. 1998. Chondrocyte apoptosis increases with age in the articular cartilage of adult animals. *Anat Rec*, 250, 418-25.
- AFFYMETRIX. 2012. FlashTag™ Biotin HSR RNA Labeling Kit: User Manual. Available: [https://media.affymetrix.com/support/downloads/manuals/mirna\\_flashtag\\_manual.pdf](https://media.affymetrix.com/support/downloads/manuals/mirna_flashtag_manual.pdf) [Accessed 28/11/2020].
- AFFYMETRIX. 2016. Array content description Available: <https://www.thermofisher.com/order/catalog/product/902411#/902411> [Accessed 27/11/2020].
- AGARWAL, V., BELL, G. W., NAM, J. W. & BARTEL, D. P. 2015. Predicting effective microRNA target sites in mammalian mRNAs. *Elife*, 4.
- AIGNER, T., HEMMEL, M., NEUREITER, D., GEBHARD, P. M., ZEILER, G., KIRCHNER, T. & MCKENNA, L. 2001. Apoptotic cell death is not a widespread phenomenon in normal aging and osteoarthritis human articular knee cartilage: a study of proliferation, programmed cell death (apoptosis), and viability of chondrocytes in normal and osteoarthritic human knee cartilage. *Arthritis Rheum*, 44, 1304-12.
- AJUIED, A., WONG, F., SMITH, C., NORRIS, M., EARNSHAW, P., BACK, D. & DAVIES, A. 2014. Anterior cruciate ligament injury and radiologic progression of knee osteoarthritis: a systematic review and meta-analysis. *Am J Sports Med*, 42, 2242-52.
- AKHTAR, N., RASHEED, Z., RAMAMURTHY, S., ANBAZHAGAN, A. N., VOSS, F. R. & HAQQI, T. M. 2010. MicroRNA-27b regulates the expression of matrix metalloproteinase 13 in human osteoarthritis chondrocytes. *Arthritis Rheum*, 62, 1361-71.
- ALI, S. A. & ALMAN, B. 2012. RNA extraction from human articular cartilage by chondrocyte isolation. *Analytical Biochemistry*, 429, 39-41.
- ALLES, J., FEHLMANN, T., FISCHER, U., BACKES, C., GALATA, V., MINET, M., HART, M., ABU-HALIMA, M., GRÄSSER, F. A., LENHOF, H. P., KELLER, A. & MEESE, E. 2019. An estimate of the total number of true human miRNAs. *Nucleic Acids Res*, 47, 3353-3364.
- AMANO, K., ICHIDA, F., SUGITA, A., HATA, K., WADA, M., TAKIGAWA, Y., NAKANISHI, M., KOGO, M., NISHIMURA, R. & YONEDA, T. 2008. MSX2 stimulates chondrocyte maturation by controlling Ihh expression. *J Biol Chem*, 283, 29513-21.
- AMBION. 2011. mirVana™ miRNA Isolation Kit protocol. Available: [https://www.thermofisher.com/document-connect/document-connect.html?url=https%3A%2F%2Fassets.thermofisher.com%2FTFS-Assets%2FLSG%2Fmanuals%2Fcms\\_055423.pdf&title=bWlyVmFuYSZ0cmFkZTsgbWISTkEgSXNvbGF0aW9uItpdCAoRW5nbGlzaCAp](https://www.thermofisher.com/document-connect/document-connect.html?url=https%3A%2F%2Fassets.thermofisher.com%2FTFS-Assets%2FLSG%2Fmanuals%2Fcms_055423.pdf&title=bWlyVmFuYSZ0cmFkZTsgbWISTkEgSXNvbGF0aW9uItpdCAoRW5nbGlzaCAp) [Accessed 21/11/2020].
- AMBROS, V., BARTEL, B., BARTEL, D. P., BURGE, C. B., CARRINGTON, J. C., CHEN, X., DREYFUSS, G., EDDY, S. R., GRIFFITHS-JONES, S., MARSHALL, M., MATZKE, M., RUVKUN, G. & TUSCHL, T. 2003. A uniform system for microRNA annotation. *Rna*, 9, 277-9.
- ANDERS, S. & HUBER, W. 2010. Differential expression analysis for sequence count data. *Genome Biol*, 11, R106.
- ANDERSEN, C. L., JENSEN, J. L. & ØRNTOFT, T. F. 2004. Normalization of real-time quantitative reverse transcription-PCR data: a model-based variance estimation approach to identify genes suited for normalization, applied to bladder and colon cancer data sets. *Cancer Res*, 64, 5245-50.
- ARMIENTO, A. R., STODDART, M. J., ALINI, M. & EGLIN, D. 2018. Biomaterials for articular cartilage tissue engineering: Learning from biology. *Acta Biomater*, 65, 1-20.

- ASAHARA, H. 2016. Current Status and Strategy of microRNA Research for Cartilage Development and Osteoarthritis Pathogenesis. *J Bone Metab*, 23, 121-7.
- BAI, Y., CHEN, K., ZHAN, J. & WU, M. 2020. miR-122/SIRT1 axis regulates chondrocyte extracellular matrix degradation in osteoarthritis. *Biosci Rep*, 40.
- BALASKAS, P., GOLJANEK-WHYSALL, K., CLEGG, P., FANG, Y., CREMERS, A., EMANS, P., WELTING, T. & PEFFERS, M. 2017. MicroRNA Profiling in Cartilage Ageing. *Int J Genomics*, 2017, 2713725.
- BALASKAS, P., GREEN, J. A., HAQQI, T. M., DYER, P., KHARAZ, Y. A., FANG, Y., LIU, X., WELTING, T. J. M. & PEFFERS, M. J. 2020. Small Non-Coding RNAome of Ageing Chondrocytes. *Int J Mol Sci*, 21.
- BENITO, M. J., VEALE, D. J., FITZGERALD, O., VAN DEN BERG, W. B. & BRESNIHAN, B. 2005. Synovial tissue inflammation in early and late osteoarthritis. *Ann Rheum Dis*, 64, 1263-7.
- BENJAMINI, Y. & HOCHBERG, Y. 1995. Controlling the False Discovery Rate: A Practical and Powerful Approach to Multiple Testing. 57, 289-300.
- BERENBAUM, F. 2019. Deep phenotyping of osteoarthritis: a step forward. *Ann Rheum Dis*, 78, 3-5.
- BERMAN, A. J., THOREEN, C. C., DEDEIC, Z., CHETTLE, J., ROUX, P. P. & BLAGDEN, S. P. 2020. Controversies around the function of LARP1. *RNA Biol*, 1-11.
- BESWICK, A. D., WYLDE, V., GOOBERMAN-HILL, R., BLOM, A. & DIEPPE, P. 2012. What proportion of patients report long-term pain after total hip or knee replacement for osteoarthritis? A systematic review of prospective studies in unselected patients. *BMJ Open*, 2, e000435.
- BEVILACQUA, E., WANG, X., MAJUMDER, M., GACCIOLE, F., YUAN, C. L., WANG, C., ZHU, X., JORDAN, L. E., SCHEUNER, D., KAUFMAN, R. J., KOROMILAS, A. E., SNIDER, M. D., HOLCIK, M. & HATZOGLOU, M. 2010. eIF2alpha phosphorylation tips the balance to apoptosis during osmotic stress. *J Biol Chem*, 285, 17098-111.
- BEYER, C., ZAMPETAKI, A., LIN, N. Y., KLEYER, A., PERRICONE, C., IAGNOCCO, A., DISTLER, A., LANGLEY, S. R., GELSE, K., SESSELMANN, S., LORENZINI, R., NIEMEIER, A., SWOBODA, B., DISTLER, J. H., SANTER, P., EGGER, G., WILLEIT, J., MAYR, M., SCHETT, G. & KIECHL, S. 2015. Signature of circulating microRNAs in osteoarthritis. *Ann Rheum Dis*, 74, e18.
- BHATTACHARYA, S., GHOSH, A., MAITI, S., AHIR, M., DEBNATH, G. H., GUPTA, P., BHATTACHARJEE, M., GHOSH, S., CHATTOPADHYAY, S., MUKHERJEE, P. & ADHIKARY, A. 2020. Delivery of thymoquinone through hyaluronic acid-decorated mixed Pluronic® nanoparticles to attenuate angiogenesis and metastasis of triple-negative breast cancer. *Journal of Controlled Release*, 322, 357-374.
- BOHAČEK, I., BOJANIĆ, I., GAJOVIĆ, S., JOSIPOVIĆ, M. & JELIĆ, M. 2015. Articular cartilage repair techniques exploiting intrinsic healing capacity – which one is the best? *PERIODICUM BIOLOGORUM*, 117, 125–133.
- BORGONIO CUADRA, V. M., GONZÁLEZ-HUERTA, N. C., ROMERO-CÓRDOBA, S., HIDALGO-MIRANDA, A. & MIRANDA-DUARTE, A. 2014. Altered expression of circulating microRNA in plasma of patients with primary osteoarthritis and in silico analysis of their pathways. *PLoS One*, 9, e97690.
- BOTTANI, M., BANFI, G. & LOMBARDI, G. 2020. The Clinical Potential of Circulating miRNAs as Biomarkers: Present and Future Applications for Diagnosis and Prognosis of Age-Associated Bone Diseases. *Biomolecules*, 10.
- BURDAN, F., SZUMIŁO, J., KOROBOWICZ, A., FAROOQUEE, R., PATEL, S., PATEL, A., DAVE, A., SZUMIŁO, M., SOLECKI, M., KLEPACZ, R. & DUDKA, J. 2009. Morphology and physiology of the epiphyseal growth plate. *Folia Histochem Cytobiol*, 47, 5-16.
- CAMARERO-ESPINOSA, S., ROTHEN-RUTISHAUSER, B., FOSTER, E. J. & WEDER, C. 2016. Articular cartilage: from formation to tissue engineering. *Biomater Sci*, 4, 734-67.
- CAO, J., VENTON, L., SAKATA, T. & HALLORAN, B. P. 2003. Expression of RANKL and OPG Correlates With Age-Related Bone Loss in Male C57BL/6 Mice. 18, 270-277.
- CARAMÉS, B., OLMER, M., KIOSSES, W. B. & LOTZ, M. K. 2015. The relationship of autophagy defects to cartilage damage during joint aging in a mouse model. *Arthritis Rheumatol*, 67, 1568-76.

- CARAMÉS, B., TANIGUCHI, N., OTSUKI, S., BLANCO, F. J. & LOTZ, M. 2010. Autophagy is a protective mechanism in normal cartilage, and its aging-related loss is linked with cell death and osteoarthritis. *Arthritis Rheum*, 62, 791-801.
- CARON, M. M., EMANS, P. J., COOLSEN, M. M., VOSS, L., SURTEL, D. A., CREMERS, A., VAN RHIJN, L. W. & WELTING, T. J. 2012. Redifferentiation of dedifferentiated human articular chondrocytes: comparison of 2D and 3D cultures. *Osteoarthritis Cartilage*, 20, 1170-8.
- CASTANHEIRA, C., BALASKAS, P., FALLS, C., ASHRAF-KHARAZ, Y., CLEGG, P., BURKE, K., FANG, Y., DYER, P., WELTING, T. J. M. & PEFFERS, M. J. 2021. Equine synovial fluid small non-coding RNA signatures in early osteoarthritis. *BMC Vet Res*, 17, 26.
- CHANG, T., XIE, J., LI, H., LI, D., LIU, P. & HU, Y. 2016. MicroRNA-30a promotes extracellular matrix degradation in articular cartilage via downregulation of Sox9. *Cell Proliferation*, 49, 207-218.
- CHARLIER, E., DEROYER, C., CIREGIA, F., MALAISE, O., NEUVILLE, S., PLENER, Z., MALAISE, M. & DE SENY, D. 2019. Chondrocyte dedifferentiation and osteoarthritis (OA). *Biochem Pharmacol*, 165, 49-65.
- CHEN, E. Y., TAN, C. M., KOU, Y., DUAN, Q., WANG, Z., MEIRELLES, G. V., CLARK, N. R. & MA'AYAN, A. 2013. Enrichr: interactive and collaborative HTML5 gene list enrichment analysis tool. *BMC Bioinformatics*, 14, 128.
- CHEN, J., BARDES, E. E., ARONOW, B. J. & JEGGA, A. G. 2009. ToppGene Suite for gene list enrichment analysis and candidate gene prioritization. *Nucleic Acids Res*, 37, W305-11.
- CHEN, P., GAO, L., SHI, X., ALLEN, K. & YANG, L. 2019. Fully automatic knee osteoarthritis severity grading using deep neural networks with a novel ordinal loss. *Comput Med Imaging Graph*, 75, 84-92.
- CHEN, W., CHEN, L., ZHANG, Z., MENG, F., HUANG, G., SHENG, P., ZHANG, Z. & LIAO, W. 2016a. MicroRNA-455-3p modulates cartilage development and degeneration through modification of histone H3 acetylation. *Biochim Biophys Acta*, 1863, 2881-2891.
- CHEN, W., SHENG, P., HUANG, Z., MENG, F., KANG, Y., HUANG, G., ZHANG, Z., LIAO, W. & ZHANG, Z. 2016b. MicroRNA-381 Regulates Chondrocyte Hypertrophy by Inhibiting Histone Deacetylase 4 Expression. *Int J Mol Sci*, 17.
- CHEN, Y. & WANG, X. 2020. miRDB: an online database for prediction of functional microRNA targets. *Nucleic Acids Res*, 48, D127-d131.
- CHEN, Y. J., CHANG, W. A., WU, L. Y., HSU, Y. L., CHEN, C. H. & KUO, P. L. 2018. Systematic Analysis of Transcriptomic Profile of Chondrocytes in Osteoarthritic Knee Using Next-Generation Sequencing and Bioinformatics. *J Clin Med*, 7.
- CHOMCZYNSKI, P. & SACCHI, N. 1987. Single-step method of RNA isolation by acid guanidinium thiocyanate-phenol-chloroform extraction. *Anal Biochem*, 162, 156-9.
- CHONG, J., WISHART, D. S. & XIA, J. 2019. Using MetaboAnalyst 4.0 for Comprehensive and Integrative Metabolomics Data Analysis. 68, e86.
- CHOU, C. H., SHRESTHA, S., YANG, C. D., CHANG, N. W., LIN, Y. L., LIAO, K. W., HUANG, W. C., SUN, T. H., TU, S. J., LEE, W. H., CHIEW, M. Y., TAI, C. S., WEI, T. Y., TSAI, T. R., HUANG, H. T., WANG, C. Y., WU, H. Y., HO, S. Y., CHEN, P. R., CHUANG, C. H., HSIEH, P. J., WU, Y. S., CHEN, W. L., LI, M. J., WU, Y. C., HUANG, X. Y., NG, F. L., BUDDHAKOSAI, W., HUANG, P. C., LAN, K. C., HUANG, C. Y., WENG, S. L., CHENG, Y. N., LIANG, C., HSU, W. L. & HUANG, H. D. 2018. miRTarBase update 2018: a resource for experimentally validated microRNA-target interactions. *Nucleic Acids Res*, 46, D296-d302.
- CHOW, Y. Y. & CHIN, K. Y. 2020. The Role of Inflammation in the Pathogenesis of Osteoarthritis. *Mediators Inflamm*, 2020, 8293921.
- CLOONAN, N. 2015. Re-thinking miRNA-mRNA interactions: intertwining issues confound target discovery. *Bioessays*, 37, 379-88.
- COHEN, J. 1960. A Coefficient of Agreement for Nominal Scales. 20, 37-46.
- COLLINS, J. A., DIEKMAN, B. O. & LOESER, R. F. 2018. Targeting aging for disease modification in osteoarthritis. 30, 101-107.

- COLLINS, J. A., WOOD, S. T., NELSON, K. J., ROWE, M. A., CARLSON, C. S., CHUBINSKAYA, S., POOLE, L. B., FURDUI, C. M. & LOESER, R. F. 2016. Oxidative Stress Promotes Peroxiredoxin Hyperoxidation and Attenuates Pro-survival Signaling in Aging Chondrocytes. *J Biol Chem*, 291, 6641-54.
- CORREA, D. & LIETMAN, S. A. 2017. Articular cartilage repair: Current needs, methods and research directions. *Semin Cell Dev Biol*, 62, 67-77.
- CUOMO, D., PORRECA, I., CECCARELLI, M., THREADGILL, D. W., BARRINGTON, W. T., PETRIELLA, A., D'ANGELO, F., COBELLIS, G., DE STEFANO, F., D'AGOSTINO, M. N., DE FELICE, M., MALLARDO, M. & AMBROSINO, C. 2018. Transcriptional landscape of mouse-aged ovaries reveals a unique set of non-coding RNAs associated with physiological and environmental ovarian dysfunctions. *Cell Death Discov*, 4, 112.
- CURL, W. W., KROME, J., GORDON, E. S., RUSHING, J., SMITH, B. P. & POEHLING, G. G. 1997. Cartilage injuries: a review of 31,516 knee arthroscopies. *Arthroscopy*, 13, 456-60.
- DECKER, R. S. 2017. Articular cartilage and joint development from embryogenesis to adulthood. *Semin Cell Dev Biol*, 62, 50-56.
- DECKER, R. S., KOYAMA, E. & PACIFICI, M. 2015. Articular Cartilage: Structural and Developmental Intricacies and Questions. *Curr Osteoporos Rep*, 13, 407-14.
- DENG, L., REN, R., LIU, Z., SONG, M., LI, J., WU, Z., REN, X., FU, L., LI, W., ZHANG, W., GUILLEN, P., IZPISUA BELMONTE, J. C., CHAN, P., QU, J. & LIU, G. H. 2019a. Stabilizing heterochromatin by DGCR8 alleviates senescence and osteoarthritis. *Nat Commun*, 10, 3329.
- DENG, Z., JIA, Y., LIU, H., HE, M., YANG, Y., XIAO, W. & LI, Y. 2019b. RhoA/ROCK pathway: implication in osteoarthritis and therapeutic targets. *Am J Transl Res*, 11, 5324-5331.
- DEXHEIMER, P. J. & COCHELLA, L. 2020. MicroRNAs: From Mechanism to Organism. *Front Cell Dev Biol*, 8, 409.
- DÍAZ-PRADO, S., CICIONE, C., MUIÑOS-LÓPEZ, E., HERMIDA-GÓMEZ, T., OREIRO, N., FERNÁNDEZ-LÓPEZ, C. & BLANCO, F. J. 2012. Characterization of microRNA expression profiles in normal and osteoarthritic human chondrocytes. *BMC Musculoskelet Disord*, 13, 144.
- DUDHIA, J. 2005. Aggrecan, aging and assembly in articular cartilage. *Cell Mol Life Sci*, 62, 2241-56.
- DUNN, S. L., SOUL, J., ANAND, S., SCHWARTZ, J. M., BOOT-HANDFORD, R. P. & HARDINGHAM, T. E. 2016. Gene expression changes in damaged osteoarthritic cartilage identify a signature of non-chondrogenic and mechanical responses. *Osteoarthritis Cartilage*, 24, 1431-40.
- DUNN, W., DURAINE, G. & REDDI, A. H. 2009. Profiling microRNA expression in bovine articular cartilage and implications for mechanotransduction. *Arthritis Rheum*, 60, 2333-9.
- DWEEP, H. & GRETZ, N. 2015. miRWalk2.0: a comprehensive atlas of microRNA-target interactions. *Nat Methods*, 12, 697.
- ECKSTEIN, F., COTOFANA, S., WIRTH, W., NEVITT, M., JOHN, M. R., DREHER, D. & FROBELL, R. 2011. Greater rates of cartilage loss in painful knees than in pain-free knees after adjustment for radiographic disease stage: data from the osteoarthritis initiative. *Arthritis Rheum*, 63, 2257-67.
- ENDISHA, H., ROCKEL, J., JURISICA, I. & KAPOOR, M. 2018. The complex landscape of microRNAs in articular cartilage: biology, pathology, and therapeutic targets. *JCI Insight*, 3.
- EYRE, D. 2002. Collagen of articular cartilage. *Arthritis Res*, 4, 30-5.
- EYRE, D. R. 2004. Collagens and cartilage matrix homeostasis. *Clin Orthop Relat Res*, S118-22.
- EYRE, D. R., WEIS, M. A. & WU, J. J. 2006. Articular cartilage collagen: an irreplaceable framework? *Eur Cell Mater*, 12, 57-63.
- FELSON, D. T., ZHANG, Y., ANTHONY, J. M., NAIMARK, A. & ANDERSON, J. J. 1992. Weight loss reduces the risk for symptomatic knee osteoarthritis in women. The Framingham Study. *Ann Intern Med*, 116, 535-9.
- FENG, K., GE, Y., CHEN, Z., LI, X., LIU, Z., LI, X., LI, H., TANG, T., YANG, F. & WANG, X. 2019. Curcumin Inhibits the PERK-eIF2 $\alpha$ -CHOP Pathway through Promoting SIRT1 Expression in Oxidative

- Stress-induced Rat Chondrocytes and Ameliorates Osteoarthritis Progression in a Rat Model. *Oxid Med Cell Longev*, 2019, 8574386.
- FIANNACA, A., LA ROSA, M., LA PAGLIA, L. & URSO, A. 2018. miRTissue: a web application for the analysis of miRNA-target interactions in human tissues. *BMC Bioinformatics*, 19, 434.
- FONSECA, B. D., LAHR, R. M., DAMGAARD, C. K., ALAIN, T. & BERMAN, A. J. 2018. LARP1 on TOP of ribosome production. *Wiley interdisciplinary reviews. RNA*, e1480-e1480.
- FRANCESCHI, C., BONAFÈ, M., VALENSIN, S., OLIVIERI, F., DE LUCA, M., OTTAVIANI, E. & DE BENEDICTIS, G. 2000. Inflamm-aging. An evolutionary perspective on immunosenescence. *Ann N Y Acad Sci*, 908, 244-54.
- FU, Y., KINTER, M., HUDSON, J., HUMPHRIES, K. M., LANE, R. S., WHITE, J. R., HAKIM, M., PAN, Y., VERDIN, E. & GRIFFIN, T. M. 2016. Aging Promotes Sirtuin 3-Dependent Cartilage Superoxide Dismutase 2 Acetylation and Osteoarthritis. *Arthritis Rheumatol*, 68, 1887-98.
- GINZINGER, D. G. 2002. Gene quantification using real-time quantitative PCR: an emerging technology hits the mainstream. *Exp Hematol*, 30, 503-12.
- GOLDRING, M. B. 2012. Chondrogenesis, chondrocyte differentiation, and articular cartilage metabolism in health and osteoarthritis. *Ther Adv Musculoskelet Dis*, 4, 269-85.
- GOLDRING, M. B., TSUCHIMOCHI, K. & IJIRI, K. 2006. The control of chondrogenesis. *J Cell Biochem*, 97, 33-44.
- GOLDRING, S. R. & GOLDRING, M. B. 2016. Changes in the osteochondral unit during osteoarthritis: structure, function and cartilage-bone crosstalk. *Nat Rev Rheumatol*, 12, 632-644.
- GOODRICH, L. R. & NIXON, A. J. 2006a. Medical treatment of osteoarthritis in the horse - a review. *Vet J*, 171, 51-69.
- GOODRICH, L. R. & NIXON, A. J. 2006b. Medical treatment of osteoarthritis in the horse – A review. *The Veterinary Journal*, 171, 51-69.
- GRAPHPAD 2018. GraphPad Software. 8.0.1 ed.
- GRESS, K., CHARPOVA, K., AN, D., HASOON, J., KAYE, A. D., PALADINI, A., VARRASSI, G., VISWANATH, O., ABD-ELSAYED, A. & URITS, I. 2020. Treatment recommendations for chronic knee osteoarthritis. *Best Pract Res Clin Anaesthesiol*, 34, 369-382.
- GRIFFITHS-JONES, S., GROCOCK, R. J., VAN DONGEN, S., BATEMAN, A. & ENRIGHT, A. J. 2006. miRBase: microRNA sequences, targets and gene nomenclature. *Nucleic Acids Res*, 34, D140-4.
- GU, W., SHI, Z., SONG, G. & ZHANG, H. 2021. MicroRNA-199-3p up-regulation enhances chondrocyte proliferation and inhibits apoptosis in knee osteoarthritis via DNMT3A repression. *Inflamm Res*.
- GU, Y., REN, K., WANG, L. & YAO, Q. 2019. Loss of Klotho contributes to cartilage damage by derepression of canonical Wnt/β-catenin signaling in osteoarthritis mice. *Aging (Albany NY)*, 11, 12793-12809.
- GUÉRIT, D., BRONDELLO, J. M., CHUCHANA, P., PHILIPOT, D., TOUPET, K., BONY, C., JORGENSEN, C. & NOËL, D. 2014. FOXO3A regulation by miRNA-29a Controls chondrogenic differentiation of mesenchymal stem cells and cartilage formation. *Stem Cells Dev*, 23, 1195-205.
- GUO, L., WEI, X., ZHANG, Z., WANG, X., WANG, C., LI, P., WANG, C. & WEI, L. 2019. Ipriflavone attenuates the degeneration of cartilage by blocking the Indian hedgehog pathway. *Arthritis Res Ther*, 21, 109.
- HA, M. & KIM, V. N. 2014. Regulation of microRNA biogenesis. *Nat Rev Mol Cell Biol*, 15, 509-24.
- HALLETT, S. A., ONO, W. & ONO, N. 2019. Growth Plate Chondrocytes: Skeletal Development, Growth and Beyond. *Int J Mol Sci*, 20.
- HAM, O., SONG, B. W., LEE, S. Y., CHOI, E., CHA, M. J., LEE, C. Y., PARK, J. H., KIM, I. K., CHANG, W., LIM, S., LEE, C. H., KIM, S., JANG, Y. & HWANG, K. C. 2012. The role of microRNA-23b in the differentiation of MSC into chondrocyte by targeting protein kinase A signaling. *Biomaterials*, 33, 4500-7.

- HANNAN, M. T., FELSON, D. T. & PINCUS, T. 2000. Analysis of the discordance between radiographic changes and knee pain in osteoarthritis of the knee. *J Rheumatol*, 27, 1513-7.
- HAWKER, G. A., BADLEY, E. M., BORKHOFF, C. M., CROXFORD, R., DAVIS, A. M., DUNN, S., GIGNAC, M. A., JAGLAL, S. B., KREDER, H. J. & SALE, J. E. 2013. Which patients are most likely to benefit from total joint arthroplasty? *Arthritis Rheum*, 65, 1243-52.
- HAYES, A. J., MACPHERSON, S., MORRISON, H., DOWTHWAITE, G. & ARCHER, C. W. 2001. The development of articular cartilage: evidence for an appositional growth mechanism. *Anat Embryol (Berl)*, 203, 469-79.
- HAZUDA, D. J., LEE, J. C. & YOUNG, P. R. 1988. The kinetics of interleukin 1 secretion from activated monocytes. Differences between interleukin 1 alpha and interleukin 1 beta. *J Biol Chem*, 263, 8473-9.
- HE, Y., LI, Z., ALEXANDER, P. G., OCASIO-NIEVES, B. D., YOCUM, L., LIN, H. & TUAN, R. S. 2020. Pathogenesis of Osteoarthritis: Risk Factors, Regulatory Pathways in Chondrocytes, and Experimental Models. *Biology (Basel)*, 9.
- HECHT, N., JOHNSTONE, B., ANGELE, P., WALKER, T. & RICHTER, W. 2019. Mechanosensitive MiRs regulated by anabolic and catabolic loading of human cartilage. *Osteoarthritis Cartilage*, 27, 1208-1218.
- HILIGSMANN, M., COOPER, C., ARDEN, N., BOERS, M., BRANCO, J. C., LUISA BRANDI, M., BRUYÈRE, O., GUILLEMIN, F., HOCHBERG, M. C., HUNTER, D. J., KANIS, J. A., KVÍEN, T. K., LASLOP, A., PELLETIER, J. P., PINTO, D., REITER-NIESERT, S., RIZZOLI, R., ROVATI, L. C., SEVERENS, J. L., SILVERMAN, S., TSOUDEROS, Y., TUGWELL, P. & REGINSTER, J. Y. 2013. Health economics in the field of osteoarthritis: an expert's consensus paper from the European Society for Clinical and Economic Aspects of Osteoporosis and Osteoarthritis (ESCEO). *Semin Arthritis Rheum*, 43, 303-13.
- HODGSON, D., ROWAN, A. D., FALCIANI, F. & PROCTOR, C. J. 2019. Systems biology reveals how altered TGF $\beta$  signalling with age reduces protection against pro-inflammatory stimuli. *PLOS Computational Biology*, 15, e1006685.
- HONG, E. & REDDI, A. H. 2013. Dedifferentiation and redifferentiation of articular chondrocytes from surface and middle zones: changes in microRNAs-221/-222, -140, and -143/145 expression. *Tissue Eng Part A*, 19, 1015-22.
- HONG, S., DERFOUL, A., PEREIRA-MOURIES, L. & HALL, D. J. 2009. A novel domain in histone deacetylase 1 and 2 mediates repression of cartilage-specific genes in human chondrocytes. *Faseb j*, 23, 3539-52.
- HSU, J. B., CHIU, C. M., HSU, S. D., HUANG, W. Y., CHIEN, C. H., LEE, T. Y. & HUANG, H. D. 2011. miRTar: an integrated system for identifying miRNA-target interactions in human. *BMC Bioinformatics*, 12, 300.
- HU, G., ZHAO, X., WANG, C., GENG, Y., ZHAO, J., XU, J., ZUO, B., ZHAO, C., WANG, C. & ZHANG, X. 2017a. MicroRNA-145 attenuates TNF- $\alpha$ -driven cartilage matrix degradation in osteoarthritis via direct suppression of MKK4. *Cell Death & Disease*, 8, e3140-e3140.
- HU, G., ZHAO, X., WANG, C., GENG, Y., ZHAO, J., XU, J., ZUO, B., ZHAO, C., WANG, C. & ZHANG, X. 2017b. MicroRNA-145 attenuates TNF- $\alpha$ -driven cartilage matrix degradation in osteoarthritis via direct suppression of MKK4. *Cell Death Dis*, 8, e3140.
- HUANG, Y., ZOU, Q., SONG, H., SONG, F., WANG, L., ZHANG, G. & SHEN, X. 2010. A study of miRNAs targets prediction and experimental validation. *Protein Cell*, 1, 979-86.
- HUDELMAIER, M., GLASER, C., HOHE, J., ENGLMEIER, K. H., REISER, M., PUTZ, R. & ECKSTEIN, F. 2001. Age-related changes in the morphology and deformational behavior of knee joint cartilage. *Arthritis Rheum*, 44, 2556-61.
- HUNZIKER, E. B., KAPFINGER, E. & GEISS, J. 2007. The structural architecture of adult mammalian articular cartilage evolves by a synchronized process of tissue resorption and neoformation during postnatal development. *Osteoarthritis Cartilage*, 15, 403-13.

- IWAKAWA, H. O. & TOMARI, Y. 2015. The Functions of MicroRNAs: mRNA Decay and Translational Repression. *Trends Cell Biol*, 25, 651-65.
- JALLALI, N., RIDHA, H., THRASIVOULOU, C., UNDERWOOD, C., BUTLER, P. E. & COWEN, T. 2005. Vulnerability to ROS-induced cell death in ageing articular cartilage: the role of antioxidant enzyme activity. *Osteoarthritis Cartilage*, 13, 614-22.
- JEE, Y. H., WANG, J., YUE, S., JENNINGS, M., CLOKIE, S. J., NILSSON, O., LUI, J. C. & BARON, J. 2018. mir-374-5p, mir-379-5p, and mir-503-5p Regulate Proliferation and Hypertrophic Differentiation of Growth Plate Chondrocytes in Male Rats. *Endocrinology*, 159, 1469-1478.
- JEFFRIES, M. A. 2019. Osteoarthritis year in review 2018: genetics and epigenetics. *Osteoarthritis Cartilage*, 27, 371-377.
- JI, Q., XU, X., ZHANG, Q., KANG, L., XU, Y., ZHANG, K., LI, L., LIANG, Y., HONG, T., YE, Q. & WANG, Y. 2016. The IL-1 $\beta$ /AP-1/miR-30a/ADAMTS-5 axis regulates cartilage matrix degradation in human osteoarthritis. *Journal of Molecular Medicine*, 94, 771-785.
- JIN, H. Y., GONZALEZ-MARTIN, A., MILETIC, A. V., LAI, M., KNIGHT, S., SABOURI-GHOMI, M., HEAD, S. R., MACAULEY, M. S., RICKERT, R. C. & XIAO, C. 2015. Transfection of microRNA Mimics Should Be Used with Caution. *Front Genet*, 6, 340.
- JOHNSON, S. C., RABINOVITCH, P. S. & KAEBERLEIN, M. 2013. mTOR is a key modulator of ageing and age-related disease. *Nature*, 493, 338-45.
- KALACHE, A. 1999. Ageing: a global perspective. *Community Eye Health*, 12, 1-4.
- KARAGKOUNI, D., PARASKEVOPOULOU, M. D., CHATZOPOULOS, S., VLACHOS, I. S., TASTSOGLOU, S., KANELLOS, I., PAPADIMITRIOU, D., KAVAKIOTIS, I., MANIOU, S., SKOUFOS, G., VERGOULIS, T., DALAMAGAS, T. & HATZIGEORGIOU, A. G. 2018. DIANA-TarBase v8: a decade-long collection of experimentally supported miRNA-gene interactions. *Nucleic Acids Res*, 46, D239-d245.
- KARLSEN, T. A., JAKOBSEN, R. B., MIKKELSEN, T. S. & BRINCHMANN, J. E. 2014. microRNA-140 targets RALA and regulates chondrogenic differentiation of human mesenchymal stem cells by translational enhancement of SOX9 and ACAN. *Stem Cells Dev*, 23, 290-304.
- KELLGREN, J. H. & LAWRENCE, J. S. 1957. Radiological assessment of osteo-arthrosis. *Ann Rheum Dis*, 16, 494-502.
- KIM, D., PERTEA, G., TRAPNELL, C., PIMENTEL, H., KELLEY, R. & SALZBERG, S. L. 2013. TopHat2: accurate alignment of transcriptomes in the presence of insertions, deletions and gene fusions. *Genome Biol*, 14, R36.
- KIM, J., KUNDU, M., VIOLET, B. & GUAN, K. L. 2011. AMPK and mTOR regulate autophagy through direct phosphorylation of Ulk1. *Nat Cell Biol*, 13, 132-41.
- KNUDSON, C. B. & KNUDSON, W. 2001. Cartilage proteoglycans. *Semin Cell Dev Biol*, 12, 69-78.
- KNUTSEN, G., DROGSET, J. O., ENGBRETSEN, L., GRØNTVEDT, T., LUDVIGSEN, T. C., LØKEN, S., SOLHEIM, E., STRAND, T. & JOHANSEN, O. 2016. A Randomized Multicenter Trial Comparing Autologous Chondrocyte Implantation with Microfracture: Long-Term Follow-up at 14 to 15 Years. *J Bone Joint Surg Am*, 98, 1332-9.
- KOBAYASHI, T., LU, J., COBB, B. S., RODDA, S. J., MCMAHON, A. P., SCHIPANI, E., MERKENSCHLAGER, M. & KRONENBERG, H. M. 2008. Dicer-dependent pathways regulate chondrocyte proliferation and differentiation. *Proc Natl Acad Sci U S A*, 105, 1949-54.
- KOBAYASHI, T., PAPAIOANNOU, G., MIRZAMOHAMMADI, F., KOZHEMYAKINA, E., ZHANG, M., BLELLOCH, R. & CHONG, M. W. 2015. Early postnatal ablation of the microRNA-processing enzyme, Drosha, causes chondrocyte death and impairs the structural integrity of the articular cartilage. *Osteoarthritis Cartilage*, 23, 1214-20.
- KOIKE, M., NOJIRI, H., OZAWA, Y., WATANABE, K., MURAMATSU, Y., KANEKO, H., MORIKAWA, D., KOBAYASHI, K., SAITA, Y., SASHO, T., SHIRASAWA, T., YOKOTE, K., KANEKO, K. & SHIMIZU, T. 2015. Mechanical overloading causes mitochondrial superoxide and SOD2 imbalance in chondrocytes resulting in cartilage degeneration. *Sci Rep*, 5, 11722.
- KOMORI, T. 2018. Runx2, an inducer of osteoblast and chondrocyte differentiation. *Histochem Cell Biol*, 149, 313-323.

- KOMORI, T. 2020. Molecular Mechanism of Runx2-Dependent Bone Development. *Mol Cells*, 43, 168-175.
- KONG, R., GAO, J., SI, Y. & ZHAO, D. 2017. Combination of circulating miR-19b-3p, miR-122-5p and miR-486-5p expressions correlates with risk and disease severity of knee osteoarthritis. *Am J Transl Res*, 9, 2852-2864.
- KOROSTYNSKI, M., MALEK, N., PIECHOTA, M. & STAROWICZ, K. 2018. Cell-type-specific gene expression patterns in the knee cartilage in an osteoarthritis rat model. *Funct Integr Genomics*, 18, 79-87.
- KOZHEMYAKINA, E., LASSAR, A. B. & ZELZER, E. 2015. A pathway to bone: signaling molecules and transcription factors involved in chondrocyte development and maturation. *Development*, 142, 817-31.
- KOZOMARA, A., BIRGAOANU, M. & GRIFFITHS-JONES, S. 2019. miRBase: from microRNA sequences to function. *Nucleic Acids Res*, 47, D155-d162.
- KRISHNAN, Y. & GRODZINSKY, A. J. 2018. Cartilage diseases. *Matrix Biol*.
- KULESHOV, M. V., JONES, M. R., ROUILLARD, A. D., FERNANDEZ, N. F., DUAN, Q., WANG, Z., KOPLEV, S., JENKINS, S. L., JAGODNIK, K. M., LACHMANN, A., MCDERMOTT, M. G., MONTEIRO, C. D., GUNDERSEN, G. W. & MA'AYAN, A. 2016. Enrichr: a comprehensive gene set enrichment analysis web server 2016 update. *Nucleic Acids Res*, 44, W90-7.
- LEE, G. M., TIORAN, M. E., JANSEN, M., GRAFF, R. D., KELLEY, S. S. & LIN, P. 2002. Development of selective tolerance to interleukin-1beta by human chondrocytes in vitro. *J Cell Physiol*, 192, 113-24.
- LEE, R. C., FEINBAUM, R. L. & AMBROS, V. 1993. The *C. elegans* heterochronic gene lin-4 encodes small RNAs with antisense complementarity to lin-14. *Cell*, 75, 843-54.
- LEFEBVRE, V. & SMITS, P. 2005. Transcriptional control of chondrocyte fate and differentiation. *Birth Defects Res C Embryo Today*, 75, 200-12.
- LI, C., PAN, S., SONG, Y., LI, Y. & QU, J. 2019a. Silence of lncRNA MIAT protects ATDC5 cells against lipopolysaccharides challenge via up-regulating miR-132. *Artif Cells Nanomed Biotechnol*, 47, 2521-2527.
- LI, H., YANG, H. H., SUN, Z. G., TANG, H. B. & MIN, J. K. 2019b. Whole-transcriptome sequencing of knee joint cartilage from osteoarthritis patients. *Bone Joint Res*, 8, 290-303.
- LI, J., XUE, J., WANG, D., DAI, X., SUN, Q., XIAO, T., WU, L., XIA, H., MOSTOFA, G., CHEN, X., WEI, Y., CHEN, F., QUAMRUZZAMAN, Q., ZHANG, A. & LIU, Q. 2019c. Regulation of gasdermin D by miR-379-5p is involved in arsenite-induced activation of hepatic stellate cells and in fibrosis via secretion of IL-1 $\beta$  from human hepatic cells. *Metalomics*, 11, 483-495.
- LI, Y., WEI, X., ZHOU, J. & WEI, L. 2013. The age-related changes in cartilage and osteoarthritis. *Biomed Res Int*, 2013, 916530.
- LI, Y. H., TAVALLAEE, G., TOKAR, T., NAKAMURA, A., SUNDARARAJAN, K., WESTON, A., SHARMA, A., MAHOMED, N. N., GANDHI, R., JURISICA, I. & KAPOOR, M. 2016. Identification of synovial fluid microRNA signature in knee osteoarthritis: differentiating early- and late-stage knee osteoarthritis. *Osteoarthritis Cartilage*, 24, 1577-86.
- LI, Y. P., WEI, X. C., LI, P. C., CHEN, C. W., WANG, X. H., JIAO, Q., WANG, D. M., WEI, F. Y., ZHANG, J. Z. & WEI, L. 2015. The Role of miRNAs in Cartilage Homeostasis. *Curr Genomics*, 16, 393-404.
- LI, Y. S., XIAO, W. F. & LUO, W. 2017. Cellular aging towards osteoarthritis. *Mech Ageing Dev*, 162, 80-84.
- LIAO, H., ZHANG, Z., LIU, Z., LIN, W., HUANG, J. & HUANG, Y. 2020. Inhibited microRNA-218-5p attenuates synovial inflammation and cartilage injury in rats with knee osteoarthritis by promoting sclerostin. *Life Sci*, 267, 118893.
- LIU, C., REN, S., ZHAO, S. & WANG, Y. 2019a. LncRNA MALAT1/MiR-145 Adjusts IL-1 $\beta$ -Induced Chondrocytes Viability and Cartilage Matrix Degradation by Regulating ADAMTS5 in Human Osteoarthritis. *Yonsei Med J*, 60, 1081-1092.

- LIU, N., YIN, Y., WANG, H., ZHOU, Z., SHENG, X., FU, H., GUO, R., WANG, H., YANG, J., GONG, P., NING, W., JU, Z., LIU, Y. & LIU, L. 2019b. Telomere dysfunction impairs epidermal stem cell specification and differentiation by disrupting BMP/pSmad/P63 signaling. *PLoS Genet*, 15, e1008368.
- LIU, X., SHE, Y., WU, H., ZHONG, D. & ZHANG, J. 2018. Long non-coding RNA Gas5 regulates proliferation and apoptosis in HCS-2/8 cells and growth plate chondrocytes by controlling FGF1 expression via miR-21 regulation. *J Biomed Sci*, 25, 18.
- LIVAK, K. J. & SCHMITTGEN, T. D. 2001. Analysis of relative gene expression data using real-time quantitative PCR and the 2(-Delta Delta C(T)) Method. *Methods*, 25, 402-8.
- LOESER, R. F. 2010. Age-related changes in the musculoskeletal system and the development of osteoarthritis. *Clin Geriatr Med*, 26, 371-86.
- LOESER, R. F., CARLSON, C. S., DEL CARLO, M. & COLE, A. 2002. Detection of nitrotyrosine in aging and osteoarthritic cartilage: Correlation of oxidative damage with the presence of interleukin-1beta and with chondrocyte resistance to insulin-like growth factor 1. *Arthritis Rheum*, 46, 2349-57.
- LOESER, R. F., COLLINS, J. A. & DIEKMAN, B. O. 2016. Ageing and the pathogenesis of osteoarthritis. *Nat Rev Rheumatol*, 12, 412-20.
- LOESER, R. F., GANDHI, U., LONG, D. L., YIN, W. & CHUBINSKAYA, S. 2014. Aging and oxidative stress reduce the response of human articular chondrocytes to insulin-like growth factor 1 and osteogenic protein 1. *Arthritis Rheumatol*, 66, 2201-9.
- LOPEZ-CASTEJON, G. & BROUGH, D. 2011. Understanding the mechanism of IL-1 $\beta$  secretion. *Cytokine & growth factor reviews*, 22, 189-195.
- LOTZ, M. & LOESER, R. F. 2012. Effects of aging on articular cartilage homeostasis. *Bone*, 51, 241-8.
- LUO, Y., SINKEVICIUTE, D., HE, Y., KARSDAL, M., HENROTIN, Y., MOBASHERI, A., ÖNNERFJORD, P. & BAY-JENSEN, A. 2017. The minor collagens in articular cartilage. *Protein Cell*, 8, 560-572.
- LV, M., ZHOU, Y., POLSON, S. W., WAN, L. Q., WANG, M., HAN, L., WANG, L. & LU, X. L. 2019. Identification of Chondrocyte Genes and Signaling Pathways in Response to Acute Joint Inflammation. *Scientific reports*, 9, 93-93.
- MALEMUD, C. J. 2006. Matrix metalloproteinases: role in skeletal development and growth plate disorders. *Front Biosci*, 11, 1702-15.
- MANDOURAH, A. Y., RANGANATH, L., BARRACLOUGH, R., VINJAMURI, S., HOF, R. V., HAMILL, S., CZANNER, G., DERA, A. A., WANG, D. & BARRACLOUGH, D. L. 2018. Circulating microRNAs as potential diagnostic biomarkers for osteoporosis. *Sci Rep*, 8, 8421.
- MANKIN, H. J., DORFMAN, H., LIPPIELLO, L. & ZARINS, A. 1971. Biochemical and metabolic abnormalities in articular cartilage from osteo-arthritis human hips. II. Correlation of morphology with biochemical and metabolic data. *J Bone Joint Surg Am*, 53, 523-37.
- MAO, G., WU, P., ZHANG, Z., ZHANG, Z., LIAO, W., LI, Y. & KANG, Y. 2017. MicroRNA-92a-3p Regulates Aggrecanase-1 and Aggrecanase-2 Expression in Chondrogenesis and IL-1 $\beta$ -Induced Catabolism in Human Articular Chondrocytes. *Cellular Physiology and Biochemistry*, 44, 38-52.
- MAO, G., ZHANG, Z., HU, S., ZHANG, Z., CHANG, Z., HUANG, Z., LIAO, W. & KANG, Y. 2018. Exosomes derived from miR-92a-3p-overexpressing human mesenchymal stem cells enhance chondrogenesis and suppress cartilage degradation via targeting WNT5A. *Stem Cell Res Ther*, 9, 247.
- MAPP, P. I. & WALSH, D. A. 2012. Mechanisms and targets of angiogenesis and nerve growth in osteoarthritis. *Nat Rev Rheumatol*, 8, 390-8.
- MARGOLIS, L. M., LESSARD, S. J., EZZYAT, Y., FIELDING, R. A. & RIVAS, D. A. 2016. Circulating MicroRNA Are Predictive of Aging and Acute Adaptive Response to Resistance Exercise in Men. *The Journals of Gerontology: Series A*, 72, 1319-1326.
- MARKOPOULOS, G. S., ROUPAKIA, E., TOKAMANI, M., VARTHOLOMOTOS, G., TZAVARAS, T., HATZIAPOSTOLOU, M., FACKELMAYER, F. O., SANDALTZOPOULOS, R., POLYTARCHOU, C. &

- KOLETTAS, E. 2017. Senescence-associated microRNAs target cell cycle regulatory genes in normal human lung fibroblasts. *Exp Gerontol*, 96, 110-122.
- MARTEL-PELLETIER, J., BARR, A. J., CICUTTINI, F. M., CONAGHAN, P. G., COOPER, C., GOLDRING, M. B., GOLDRING, S. R., JONES, G., TEICHTAHL, A. J. & PELLETIER, J. P. 2016. Osteoarthritis. *Nat Rev Dis Primers*, 2, 16072.
- MARTIN, J. A. & BUCKWALTER, J. A. 2001. Telomere erosion and senescence in human articular cartilage chondrocytes. *J Gerontol A Biol Sci Med Sci*, 56, B172-9.
- MARTIN, M. 2011. Cutadapt removes adapter sequences from high-throughput sequencing reads. *2011*, 17, 3 %J EMBnet.journal.
- MARTÍNEZ-CALATRAVA, M. J., PRIETO-POTÍN, I., ROMAN-BLAS, J. A., TARDIO, L., LARGO, R. & HERRERO-BEAUMONT, G. 2012. RANKL synthesized by articular chondrocytes contributes to juxta-articular bone loss in chronic arthritis. *Arthritis Research & Therapy*, 14, R149.
- MARTINEZ-SANCHEZ, A., DUDEK, K. A. & MURPHY, C. L. 2012. Regulation of human chondrocyte function through direct inhibition of cartilage master regulator SOX9 by microRNA-145 (miRNA-145). *J Biol Chem*, 287, 916-24.
- MATSUYAMA, H. & SUZUKI, H. I. 2019. Systems and Synthetic microRNA Biology: From Biogenesis to Disease Pathogenesis. *Int J Mol Sci*, 21.
- MCALINDON, T. E., WILSON, P. W., ALIABADI, P., WEISSMAN, B. & FELSON, D. T. 1999. Level of physical activity and the risk of radiographic and symptomatic knee osteoarthritis in the elderly: the Framingham study. *Am J Med*, 106, 151-7.
- MCILWRAITH, C. W., FRISBIE, D. D. & KAWCAK, C. E. 2012. The horse as a model of naturally occurring osteoarthritis. *Bone Joint Res*, 1, 297-309.
- MCNULTY, A. L., ROTHFUSZ, N. E., LEDDY, H. A. & GUILAK, F. 2013. Synovial fluid concentrations and relative potency of interleukin-1 alpha and beta in cartilage and meniscus degradation. *J Orthop Res*, 31, 1039-45.
- MELROSE, J., SHU, C., WHITELOCK, J. M. & LORD, M. S. 2016. The cartilage extracellular matrix as a transient developmental scaffold for growth plate maturation. *Matrix Biol*, 52-54, 363-383.
- MERCKEN, E. M., MAJOUNIE, E., DING, J., GUO, R., KIM, J., BERNIER, M., MATTISON, J., COOKSON, M. R., GOROSPE, M., DE CABO, R. & ABDELMOHSEN, K. 2013. Age-associated miRNA alterations in skeletal muscle from rhesus monkeys reversed by caloric restriction. *Aging (Albany NY)*, 5, 692-703.
- MIYAKI, S. & ASAHARA, H. 2012. Macro view of microRNA function in osteoarthritis. *Nat Rev Rheumatol*, 8, 543-52.
- MIYAKI, S., NAKASA, T., OTSUKI, S., GROGAN, S. P., HIGASHIYAMA, R., INOUE, A., KATO, Y., SATO, T., LOTZ, M. K. & ASAHARA, H. 2009. MicroRNA-140 is expressed in differentiated human articular chondrocytes and modulates interleukin-1 responses. *Arthritis Rheum*, 60, 2723-30.
- MIYAKI, S., SATO, T., INOUE, A., OTSUKI, S., ITO, Y., YOKOYAMA, S., KATO, Y., TAKEMOTO, F., NAKASA, T., YAMASHITA, S., TAKADA, S., LOTZ, M. K., UENO-KUDO, H. & ASAHARA, H. 2010. MicroRNA-140 plays dual roles in both cartilage development and homeostasis. *Genes Dev*, 24, 1173-85.
- MOBASHERI, A., MATTÀ, C., UZIELIENÈ, I., BUDD, E., MARTÍN-VASALLO, P. & BERNOTIENE, E. 2019. The chondrocyte channelome: A narrative review. *Joint Bone Spine*, 86, 29-35.
- MOBASHERI, A., MATTÀ, C., ZÁKÁNY, R. & MUSUMECI, G. 2015. Chondrosenescence: definition, hallmarks and potential role in the pathogenesis of osteoarthritis. *Maturitas*, 80, 237-44.
- MOSKOWITZ, R. W. 2006. Osteoarthritis cartilage histopathology: grading and staging. *Osteoarthritis Cartilage*, 14, 1-2.
- MOTOTANI, H., IIDA, A., NAKAMURA, Y. & IKEGAWA, S. 2010. Identification of sequence polymorphisms in CALM2 and analysis of association with hip osteoarthritis in a Japanese population. *J Bone Miner Metab*, 28, 547-53.
- MOULIN, D., SALONE, V., KOUFANY, M., CLÉMENT, T., BEHM-ANSMANT, I., BRANLANT, C., CHARPENTIER, B. & JOUZEAU, J.-Y. 2017. MicroRNA-29b Contributes to Collagens Imbalance

- in Human Osteoarthritic and Dedifferentiated Articular Chondrocytes. *BioMed Research International*, 2017, 9792512.
- MURATA, K., YOSHITOMI, H., TANIDA, S., ISHIKAWA, M., NISHITANI, K., ITO, H. & NAKAMURA, T. 2010. Plasma and synovial fluid microRNAs as potential biomarkers of rheumatoid arthritis and osteoarthritis. *Arthritis Res Ther*, 12, R86.
- NEEFJES, M., VAN CAAM, A. P. M. & VAN DER KRAAN, P. M. 2020. Transcription Factors in Cartilage Homeostasis and Osteoarthritis. *Biology (Basel)*, 9.
- NEWENGLAND-BIOLABS. 2020. Multiplex Small RNA Library Prep Workflow. Available: [https://international.neb.com/-/media/nebus/files/manuals/manuale7300\\_e7330\\_e7560\\_e7580.pdf?rev=c1c5ab8864234a62b78401f83acb2205&hash=6C1E8073384F307864018EA87D3638EF](https://international.neb.com/-/media/nebus/files/manuals/manuale7300_e7330_e7560_e7580.pdf?rev=c1c5ab8864234a62b78401f83acb2205&hash=6C1E8073384F307864018EA87D3638EF) [Accessed 29/11/2020].
- NISHIMURA, R., HATA, K., NAKAMURA, E., MURAKAMI, T. & TAKAHATA, Y. 2018. Transcriptional network systems in cartilage development and disease. *Histochem Cell Biol*, 149, 353-363.
- NISHIMURA, R., HATA, K., TAKAHATA, Y., MURAKAMI, T., NAKAMURA, E., OHKAWA, M. & RUENGSPININYA, L. 2020. Role of Signal Transduction Pathways and Transcription Factors in Cartilage and Joint Diseases. *Int J Mol Sci*, 21.
- NTOUMOU, E., TZETIS, M., BRAOUDAKI, M., LAMBOU, G., POULOU, M., MALIZOS, K., STEFANOPOULOU, N., ANASTASOPOULOU, L. & TSEZOU, A. 2017. Serum microRNA array analysis identifies miR-140-3p, miR-33b-3p and miR-671-3p as potential osteoarthritis biomarkers involved in metabolic processes. *Clin Epigenetics*, 9, 127.
- NUGENT, M. 2016. MicroRNAs: exploring new horizons in osteoarthritis. *Osteoarthritis Cartilage*, 24, 573-80.
- O'NEILL, T. W., MCCABE, P. S. & MCBETH, J. 2018. Update on the epidemiology, risk factors and disease outcomes of osteoarthritis. *Best Pract Res Clin Rheumatol*, 32, 312-326.
- OLIVERIA, S. A., FELSON, D. T., REED, J. I., CIRILLO, P. A. & WALKER, A. M. 1995. Incidence of symptomatic hand, hip, and knee osteoarthritis among patients in a health maintenance organization. *Arthritis Rheum*, 38, 1134-41.
- OSTERGAARD, K., ANDERSEN, C. B., PETERSEN, J., BENDTZEN, K. & SALTER, D. M. 1999. Validity of histopathological grading of articular cartilage from osteoarthritic knee joints. *Ann Rheum Dis*, 58, 208-13.
- OUTERBRIDGE, R. E. 1961. The etiology of chondromalacia patellae. *J Bone Joint Surg Br*, 43-b, 752-7.
- PAPANAGNOU, P., STIVAROU, T. & TSIRONI, M. 2016. The Role of miRNAs in Common Inflammatory Arthropathies: Osteoarthritis and Gouty Arthritis. *Biomolecules*, 6.
- PASQUINELLI, A. E., REINHART, B. J., SLACK, F., MARTINDALE, M. Q., KURODA, M. I., MALLER, B., HAYWARD, D. C., BALL, E. E., DEGNAN, B., MELLER, P., SPRING, J., SRINIVASAN, A., FISHMAN, M., FINNERTY, J., CORBO, J., LEVINE, M., LEAHY, P., DAVIDSON, E. & RUVKUN, G. 2000. Conservation of the sequence and temporal expression of let-7 heterochronic regulatory RNA. *Nature*, 408, 86-9.
- PEARSON, R. G., KURIEN, T., SHU, K. S. & SCAMMELL, B. E. 2011. Histopathology grading systems for characterisation of human knee osteoarthritis--reproducibility, variability, reliability, correlation, and validity. *Osteoarthritis Cartilage*, 19, 324-31.
- PEFFERS, M., LIU, X. & CLEGG, P. 2013. Transcriptomic signatures in cartilage ageing. *Arthritis Res Ther*, 15, R98.
- PELLETIER, J. P., RAYNAULD, J. P., BERTHIAUME, M. J., ABRAM, F., CHOQUETTE, D., HARAOUI, B., BEARY, J. F., CLINE, G. A., MEYER, J. M. & MARTEL-PELLETIER, J. 2007. Risk factors associated with the loss of cartilage volume on weight-bearing areas in knee osteoarthritis patients assessed by quantitative magnetic resonance imaging: a longitudinal study. *Arthritis Res Ther*, 9, R74.

- PETURSSON, F., HUSA, M., JUNE, R., LOTZ, M., TERKELTAUB, R. & LIU-BRYAN, R. 2013. Linked decreases in liver kinase B1 and AMP-activated protein kinase activity modulate matrix catabolic responses to biomechanical injury in chondrocytes. *Arthritis Res Ther*, 15, R77.
- PFAFFL, M. W., TICHOPAD, A., PRGOMET, C. & NEUVIANS, T. P. 2004. Determination of stable housekeeping genes, differentially regulated target genes and sample integrity: BestKeeper--Excel-based tool using pair-wise correlations. *Biotechnol Lett*, 26, 509-15.
- PHILIPOT, D., GUÉRIT, D., PLATANO, D., CHUCHANA, P., OLIVOTTO, E., ESPINOZA, F., DORANDEU, A., PERS, Y. M., PIETTE, J., BORZI, R. M., JORGENSEN, C., NOEL, D. & BRONDELLO, J. M. 2014. p16INK4a and its regulator miR-24 link senescence and chondrocyte terminal differentiation-associated matrix remodeling in osteoarthritis. *Arthritis Res Ther*, 16, R58.
- PRITZKER, K. P., GAY, S., JIMENEZ, S. A., OSTERGAARD, K., PELLETIER, J. P., REVELL, P. A., SALTER, D. & VAN DEN BERG, W. B. 2006. Osteoarthritis cartilage histopathology: grading and staging. *Osteoarthritis Cartilage*, 14, 13-29.
- PROCTOR, C. J. & GOLJANEK-WHYSALL, K. 2017. Using computer simulation models to investigate the most promising microRNAs to improve muscle regeneration during ageing. *Sci Rep*, 7, 12314.
- PROMEGA. 2016. M-MLV Reverse Transcriptase protocol. Available: <https://worldwide.promega.com/Products/PCR/RT-PCR/M-MLV-Reverse-Transcriptase/?catNum=M1701> [Accessed 21/11/2020].
- QIAGEN. 2011a. Protocol: Real-Time PCR for Detection of Mature miRNA or Noncoding RNA. Available: <https://www.qiagen.com/gb/resources/resourcedetail?id=7954ef25-3a39-4b0a-a27e-42689dbb4f5f&lang=en> [Accessed 22/11/2020].
- QIAGEN. 2011b. Reverse transcription in miScript HiSpec Buffer Available: <https://www.qiagen.com/gb/resources/resourcedetail?id=7954ef25-3a39-4b0a-a27e-42689dbb4f5f&lang=en> [Accessed 21/11/2020].
- QIAGEN. 2015. *Guidelines for miRNA mimic and miRNA inhibitor experiments* [Online]. Available: <https://www.qiagen.com/gb/resources/resourcedetail?id=3e1477ad-74a2-4ee6-9c31-54b1997f2941&lang=en> [Accessed 15/02/2021].
- QIAGEN. 2017. *miRCURY® LNA® miRNA Inhibitors and Target Site Blockers Handbook* [Online]. Available: <https://www.qiagen.com/gb/resources/resourcedetail?id=c035dbe7-933f-4b11-b36f-b99c8e93aad9&lang=en> [Accessed 15/02/2021].
- QIAGEN. 2020. Protocol: Purification of Total RNA, Including Small RNAs, from Animal Cells Available: <https://www.qiagen.com/gb/resources/resourcedetail?id=da6c8d17-58c4-411c-a334-bc1754876db3&lang=en> [Accessed 21/11/20].
- QIAN, J., FU, P., LI, S., LI, X., CHEN, Y. & LIN, Z. 2021. miR-107 affects cartilage matrix degradation in the pathogenesis of knee osteoarthritis by regulating caspase-1. *J Orthop Surg Res*, 16, 40.
- QIU, X., SHI, Q., HUANG, Y., JIANG, H. & QIN, S. 2021. miR-143/145 inhibits Th9 cell differentiation by targeting NFATc1. *Molecular Immunology*.
- RACUNICA, T. L., TEICHTAHL, A. J., WANG, Y., WLUKA, A. E., ENGLISH, D. R., GILES, G. G., O'SULLIVAN, R. & CICUTTINI, F. M. 2007. Effect of physical activity on articular knee joint structures in community-based adults. *Arthritis Rheum*, 57, 1261-8.
- RAHMATI, M., NALESSO, G., MOBASHERI, A. & MOZAFARI, M. 2017. Aging and osteoarthritis: Central role of the extracellular matrix. *Ageing Res Rev*, 40, 20-30.
- RAI, M. F., SANDELL, L. J., BARRACK, T. N., CAI, L., TYCKSEN, E. D., TANG, S. Y., SILVA, M. J. & BARRACK, R. L. 2020. A Microarray Study of Articular Cartilage in Relation to Obesity and Severity of Knee Osteoarthritis. *Cartilage*, 11, 458-472.
- RASHEED, Z., AL-SHOBAILI, H. A., RASHEED, N., AL SALLOOM, A. A., AL-SHAYA, O., MAHMOOD, A., ALAJEZ, N. M., ALGHAMDI, A. S. & MEHANA EL, S. E. 2016. Integrated Study of Globally Expressed microRNAs in IL-1 $\beta$ -stimulated Human Osteoarthritis Chondrocytes and Osteoarthritis Relevant Genes: A Microarray and Bioinformatics Analysis. *Nucleosides Nucleotides Nucleic Acids*, 35, 335-55.

- RETTING, K. N., SONG, B., YOON, B. S. & LYONS, K. M. 2009. BMP canonical Smad signaling through Smad1 and Smad5 is required for endochondral bone formation. *Development*, 136, 1093-104.
- REYNARD, L. N. & BARTER, M. J. 2020. Osteoarthritis year in review 2019: genetics, genomics and epigenetics. *Osteoarthritis Cartilage*, 28, 275-284.
- ROBINSON, M. D., MCCARTHY, D. J. & SMYTH, G. K. 2010. edgeR: a Bioconductor package for differential expression analysis of digital gene expression data. *Bioinformatics*, 26, 139-40.
- ROMAN-BLAS, J. A., MENDOZA-TORRES, L. A., LARGO, R. & HERRERO-BEAUMONT, G. 2020. Setting up distinctive outcome measures for each osteoarthritis phenotype. *Ther Adv Musculoskeletal Dis*, 12, 1759720x20937966.
- ROSE, J., SÖDER, S., SKHIRTLADZE, C., SCHMITZ, N., GEBHARD, P. M., SESSELMANN, S. & AIGNER, T. 2012. DNA damage, disordinated gene expression and cellular senescence in osteoarthritic chondrocytes. *Osteoarthritis Cartilage*, 20, 1020-8.
- ROUGHLEY, P. J. 2006. The structure and function of cartilage proteoglycans. *Eur Cell Mater*, 12, 92-101.
- RUANE, J. J. 2016. *Knee Osteoarthritis Diagnosis* [Online].  
<https://www.practicalpainmanagement.com/>. Available:  
<https://www.practicalpainmanagement.com/patient/conditions/osteoarthritis/knee-osteoarthritis/knee-osteoarthritis-diagnosis> [Accessed 15/11/2020 2020].
- SACITHARAN, P. K. & VINCENT, T. L. 2016. Cellular ageing mechanisms in osteoarthritis. *Mamm Genome*, 27, 421-9.
- SANCHEZ-ADAMS, J., LEDDY, H. A., MCNULTY, A. L., O'CONOR, C. J. & GUILAK, F. 2014. The mechanobiology of articular cartilage: bearing the burden of osteoarthritis. *Curr Rheumatol Rep*, 16, 451.
- SCHAIBLE, H. G. 2012. Mechanisms of chronic pain in osteoarthritis. *Curr Rheumatol Rep*, 14, 549-56.
- SCHMITZ, N., LAVERTY, S., KRAUS, V. B. & AIGNER, T. 2010. Basic methods in histopathology of joint tissues. *Osteoarthritis Cartilage*, 18 Suppl 3, S113-6.
- SCOTT, K. M., COHEN, D. J., HAYS, M., NIELSON, D. W., GRINSTAFF, M. W., LAWSON, T. B., SNYDER, B. D., BOYAN, B. D. & SCHWARTZ, Z. 2021. Regulation of inflammatory and catabolic responses to IL-1 $\beta$  in rat articular chondrocytes by microRNAs miR-122 and miR-451. *Osteoarthritis Cartilage*, 29, 113-123.
- SHAKER, F., NIKRAVESH, A., AREZUMAND, R. & AGHAEE-BAKHTIARI, S. H. 2020. Web-based tools for miRNA studies analysis. *Comput Biol Med*, 127, 104060.
- SHANNON, P., MARKIEL, A., OZIER, O., BALIGA, N. S., WANG, J. T., RAMAGE, D., AMIN, N., SCHWIJKOWSKI, B. & IDEKER, T. 2003. Cytoscape: a software environment for integrated models of biomolecular interaction networks. *Genome Res*, 13, 2498-504.
- SHARMA, L., SONG, J., DUNLOP, D., FELSON, D., LEWIS, C. E., SEGAL, N., TORNER, J., COOKE, T. D., HIETPAS, J., LYNCH, J. & NEVITT, M. 2010. Varus and valgus alignment and incident and progressive knee osteoarthritis. *Ann Rheum Dis*, 69, 1940-5.
- SHEN, G. 2005. The role of type X collagen in facilitating and regulating endochondral ossification of articular cartilage. *Orthod Craniofac Res*, 8, 11-7.
- SHEN, P., LI, X., XIE, G., HUANGFU, X. & ZHAO, J. 2016. Time-Dependent Effects of Arthroscopic Conditions on Human Articular Cartilage: An In Vivo Study. *Arthroscopy*, 32, 2582-2591.
- SHIBAKAWA, A., AOKI, H., MASUKO-HONGO, K., KATO, T., TANAKA, M., NISHIOKA, K. & NAKAMURA, H. 2003. Presence of pannus-like tissue on osteoarthritic cartilage and its histological character. *Osteoarthritis Cartilage*, 11, 133-40.
- SILVER, N., BEST, S., JIANG, J. & THEIN, S. L. 2006. Selection of housekeeping genes for gene expression studies in human reticulocytes using real-time PCR. *BMC Mol Biol*, 7, 33.
- SILVERWOOD, V., BLAGOJEVIC-BUCKNALL, M., JINKS, C., JORDAN, J. L., PROTHEROE, J. & JORDAN, K. P. 2015. Current evidence on risk factors for knee osteoarthritis in older adults: a systematic review and meta-analysis. *Osteoarthritis Cartilage*, 23, 507-15.

- SINGH, P., MARCU, K. B., GOLDRING, M. B. & OTERO, M. 2018. Phenotypic instability of chondrocytes in osteoarthritis: on a path to hypertrophy. *Ann N Y Acad Sci*.
- SKOU, S. T., ROOS, E. M., LAURSEN, M. B., RATHLEFF, M. S., ARENDT-NIELSEN, L., SIMONSEN, O. & RASMUSSEN, S. 2015. A Randomized, Controlled Trial of Total Knee Replacement. *N Engl J Med*, 373, 1597-606.
- SLATTERY, C. & KWEON, C. Y. 2018. Classifications in Brief: Outerbridge Classification of Chondral Lesions. *Clin Orthop Relat Res*, 476, 2101-2104.
- SMYTH, G. K. 2005. limma: Linear Models for Microarray Data. In: GENTLEMAN, R., CAREY, V. J., HUBER, W., IRIZARRY, R. A. & DUDOIT, S. (eds.) *Bioinformatics and Computational Biology Solutions Using R and Bioconductor*. New York, NY: Springer New York.
- SOKOLOVE, J. & LEPUS, C. M. 2013. Role of inflammation in the pathogenesis of osteoarthritis: latest findings and interpretations. *Ther Adv Musculoskeletal Dis*, 5, 77-94.
- SONG, H. & PARK, K. H. 2020. Regulation and function of SOX9 during cartilage development and regeneration. *Semin Cancer Biol*.
- SONG, J., KIM, D., LEE, C. H., LEE, M. S., CHUN, C. H. & JIN, E. J. 2013. MicroRNA-488 regulates zinc transporter SLC39A8/ZIP8 during pathogenesis of osteoarthritis. *J Biomed Sci*, 20, 31.
- SOOD, P., KREK, A., ZAVOLAN, M., MACINO, G. & RAJEWSKY, N. 2006. Cell-type-specific signatures of microRNAs on target mRNA expression. *Proc Natl Acad Sci U S A*, 103, 2746-51.
- SOPHIA FOX, A. J., BEDI, A. & RODEO, S. A. 2009. The basic science of articular cartilage: structure, composition, and function. *Sports Health*, 1, 461-8.
- SORIANO-ARROQUIA, A., MCCORMICK, R., MOLLOY, A. P., MCARDLE, A. & GOLJANEK-WHYSALL, K. 2016. Age-related changes in miR-143-3p:Igfbp5 interactions affect muscle regeneration. *Aging Cell*, 15, 361-9.
- SOUL, J., DUNN, S. L., ANAND, S., SERRACINO-INGLOTT, F., SCHWARTZ, J. M., BOOT-HANDFORD, R. P. & HARDINGHAM, T. E. 2018. Stratification of knee osteoarthritis: two major patient subgroups identified by genome-wide expression analysis of articular cartilage. *Ann Rheum Dis*, 77, 423.
- STATSTODO. 2020. *StatsToDo : Kappa (Cohen and Fleiss) for Ordinal Data Program* [Online]. Available: [http://www.statstodo.com/CohenFleissKappa\\_Pgm.php](http://www.statstodo.com/CohenFleissKappa_Pgm.php) [Accessed 27/12/2020].
- SULZBACHER, I. 2013. Osteoarthritis: histology and pathogenesis. *Wien Med Wochenschr*, 123, 212-9.
- SUPEK, F., BOŠNJAK, M., ŠKUNCA, N. & ŠMUC, T. 2011. REVIGO summarizes and visualizes long lists of gene ontology terms. *PLoS One*, 6, e21800.
- SWINGLER, T. E., NIU, L., SMITH, P., PADDY, P., LE, L., BARTER, M. J., YOUNG, D. A. & CLARK, I. M. 2019. The function of microRNAs in cartilage and osteoarthritis. *Clin Exp Rheumatol*, 37 Suppl 120, 40-47.
- SWINGLER, T. E., WHEELER, G., CARMONT, V., ELLIOTT, H. R., BARTER, M. J., ABU-ELMAGD, M., DONELL, S. T., BOOT-HANDFORD, R. P., HAJIHOSSEINI, M. K., MÖNSTERBERG, A., DALMAY, T., YOUNG, D. A. & CLARK, I. M. 2012. The expression and function of microRNAs in chondrogenesis and osteoarthritis. *Arthritis Rheum*, 64, 1909-19.
- SZKLARCZYK, D., GABLE, A. L., LYON, D., JUNGE, A., WYDER, S., HUERTA-CEPAS, J., SIMONOVIC, M., DONCHEVA, N. T., MORRIS, J. H., BORK, P., JENSEN, L. J. & MERING, C. V. 2019. STRING v11: protein-protein association networks with increased coverage, supporting functional discovery in genome-wide experimental datasets. *Nucleic Acids Res*, 47, D607-d613.
- TALENS, R. P., CHRISTENSEN, K., PUTTER, H., WILLEMSEN, G., CHRISTIANSEN, L., KREMER, D., SUCHIMAN, H. E., SLAGBOOM, P. E., BOOMSMA, D. I. & HEIJMANS, B. T. 2012. Epigenetic variation during the adult lifespan: cross-sectional and longitudinal data on monozygotic twin pairs. *Aging Cell*, 11, 694-703.
- TANIGUCHI, N., CARAMÉS, B., RONFANI, L., ULMER, U., KOMIYA, S., BIANCHI, M. E. & LOTZ, M. 2009. Aging-related loss of the chromatin protein HMGB2 in articular cartilage is linked to reduced cellularity and osteoarthritis. *Proc Natl Acad Sci U S A*, 106, 1181-6.

- TAO, S. C., YUAN, T., ZHANG, Y. L., YIN, W. J., GUO, S. C. & ZHANG, C. Q. 2017. Exosomes derived from miR-140-5p-overexpressing human synovial mesenchymal stem cells enhance cartilage tissue regeneration and prevent osteoarthritis of the knee in a rat model. *Theranostics*, 7, 180-195.
- TARDIF, G., HUM, D., PELLETIER, J. P., BOILEAU, C., RANGER, P. & MARTEL-PELLETIER, J. 2004. Differential gene expression and regulation of the bone morphogenetic protein antagonists follistatin and gremlin in normal and osteoarthritic human chondrocytes and synovial fibroblasts. *Arthritis Rheum*, 50, 2521-30.
- TARDIF, G., PELLETIER, J. P., BOILEAU, C. & MARTEL-PELLETIER, J. 2009. The BMP antagonists follistatin and gremlin in normal and early osteoarthritic cartilage: an immunohistochemical study. *Osteoarthritis Cartilage*, 17, 263-70.
- THERMOFISHERSCIENTIFIC. 2016. Procedure for Silver Staining Proteins in Polyacrylamide Gels. Available: <https://www.thermofisher.com/order/catalog/product/24612#/24612> [Accessed 26/11/2020].
- THIELEN, N. G. M., VAN DER KRAAN, P. M. & VAN CAAM, A. P. M. 2019. TGF $\beta$ /BMP Signaling Pathway in Cartilage Homeostasis. *Cells*, 8.
- TIAN, F., WANG, J., ZHANG, Z. & YANG, J. 2019. miR-107 modulates chondrocyte proliferation, apoptosis, and extracellular matrix synthesis by targeting PTEN. *Int J Clin Exp Pathol*, 12, 488-497.
- TIMUR, U. T., JAHR, H., ANDERSON, J., GREEN, D. C., EMANS, P. J., SMAGUL, A., VAN RHIJN, L. W., PEFFERS, M. J. & WELTING, T. J. M. 2020. Identification of tissue-dependent proteins in knee OA synovial fluid. *Osteoarthritis Cartilage*.
- UKAI, T., SATO, M., AKUTSU, H., UMEZAWA, A. & MOCHIDA, J. 2012. MicroRNA-199a-3p, microRNA-193b, and microRNA-320c are correlated to aging and regulate human cartilage metabolism. *J Orthop Res*, 30, 1915-22.
- ULGHERAIT, M., RANA, A., RERA, M., GRANIEL, J. & WALKER, D. W. 2014. AMPK modulates tissue and organismal aging in a non-cell-autonomous manner. *Cell Rep*, 8, 1767-1780.
- UPTON, A. R., HOLDING, C. A., DHARMAPATNI, A. A. S. S. K. & HAYNES, D. R. 2012. The expression of RANKL and OPG in the various grades of osteoarthritic cartilage. *Rheumatology International*, 32, 535-540.
- VADALÀ, G., RUSSO, F., MUSUMECI, M., GIACALONE, A., PAPALIA, R. & DENARO, V. 2018. Targeting VEGF-A in cartilage repair and regeneration: state of the art and perspectives. *J Biol Regul Homeost Agents*, 32, 217-224.
- VALDES, A. M. & SPECTOR, T. D. 2011. Genetic epidemiology of hip and knee osteoarthritis. *Nat Rev Rheumatol*, 7, 23-32.
- VAN DALEN, S., BLOM, A., JOOSTEN, L., SLOETJES, A., HELSEN, M., VAN DEN BERG, W. & VAN LENT, P. 2016. Interleukin-1 does not aggravate joint inflammation and cartilage destruction in experimental osteoarthritis. *Osteoarthritis and Cartilage*, 24, S326.
- VAN DER KRAAN, P. M. 2018. Differential Role of Transforming Growth Factor-beta in an Osteoarthritic or a Healthy Joint. *J Bone Metab*, 25, 65-72.
- VANDESOMPELE, J., DE PRETER, K., PATTYN, F., POPPE, B., VAN ROY, N., DE PAEPE, A. & SPELEMAN, F. 2002. Accurate normalization of real-time quantitative RT-PCR data by geometric averaging of multiple internal control genes. *Genome Biol*, 3, Research0034.
- VEJNAR, C. E. & ZDOBNOV, E. M. 2012. MiRmap: comprehensive prediction of microRNA target repression strength. *Nucleic Acids Res*, 40, 11673-83.
- VELASCO, J., ZARRABEITIA, M. T., PRIETO, J. R., PEREZ-CASTRILLON, J. L., PEREZ-AGUILAR, M. D., PEREZ-NUÑEZ, M. I., SAÑUDO, C., HERNANDEZ-ELENA, J., CALVO, I., ORTIZ, F., GONZALEZ-MACIAS, J. & RIANCHO, J. A. 2010. Wnt pathway genes in osteoporosis and osteoarthritis: differential expression and genetic association study. *Osteoporos Int*, 21, 109-18.
- VERZIJL, N., DE GROOT, J., BEN, Z. C., BRAU-BENJAMIN, O., MAROUDAS, A., BANK, R. A., MIZRAHI, J., SCHALKWIJK, C. G., THORPE, S. R., BAYNES, J. W., BIJLSMA, J. W., LAFEBER, F. P. &

- TEKOPPELE, J. M. 2002. Crosslinking by advanced glycation end products increases the stiffness of the collagen network in human articular cartilage: a possible mechanism through which age is a risk factor for osteoarthritis. *Arthritis Rheum*, 46, 114-23.
- VIGNON, E., ARLOT, M., PATRICOT, L. M. & VIGNON, G. 1976. The cell density of human femoral head cartilage. *Clin Orthop Relat Res*, 303-8.
- VYNIOS, D. H. 2014. Metabolism of cartilage proteoglycans in health and disease. *Biomed Res Int*, 2014, 452315.
- WANG, A., HU, N., ZHANG, Y., CHEN, Y., SU, C., LV, Y. & SHEN, Y. 2019a. MEG3 promotes proliferation and inhibits apoptosis in osteoarthritis chondrocytes by miR-361-5p/FOXO1 axis. *BMC Med Genomics*, 12, 201.
- WANG, F., GUO, Z. & YUAN, Y. 2020. STAT3 speeds up progression of osteoarthritis through NF-κB signaling pathway. *Exp Ther Med*, 19, 722-728.
- WANG, Y., DONG, L., LIU, P., CHEN, Y., JIA, S. & WANG, Y. 2019b. A Randomized Controlled Trial of Chuanhutongfeng Mixture for the Treatment of Chronic Gouty Arthritis by Regulating miRNAs. *Evid Based Complement Alternat Med*, 2019, 5917269.
- WANG, Y., FAN, X., XING, L. & TIAN, F. 2019c. Wnt signaling: a promising target for osteoarthritis therapy. *Cell Communication and Signaling*, 17, 97.
- WANG, Y., SIMPSON, J. A., WLUKA, A. E., TEICHTAHL, A. J., ENGLISH, D. R., GILES, G. G., GRAVES, S. & CICUTTINI, F. M. 2011. Is physical activity a risk factor for primary knee or hip replacement due to osteoarthritis? A prospective cohort study. *J Rheumatol*, 38, 350-7.
- WANG, Y., WEI, L., ZENG, L., HE, D. & WEI, X. 2013. Nutrition and degeneration of articular cartilage. *Knee Surg Sports Traumatol Arthrosc*, 21, 1751-62.
- WEI, F., ZHOU, J., WEI, X., ZHANG, J., FLEMING, B. C., TEREK, R., PEI, M., CHEN, Q., LIU, T. & WEI, L. 2012. Activation of Indian hedgehog promotes chondrocyte hypertrophy and upregulation of MMP-13 in human osteoarthritic cartilage. *Osteoarthritis and Cartilage*, 20, 755-763.
- WEILNER, S., GRILLARI-VOGLAUER, R., REDL, H., GRILLARI, J. & NAU, T. 2015. The role of microRNAs in cellular senescence and age-related conditions of cartilage and bone. *Acta Orthop*, 86, 92-9.
- WEK, R. C. 2018. Role of eIF2 $\alpha$  Kinases in Translational Control and Adaptation to Cellular Stress. *Cold Spring Harb Perspect Biol*, 10.
- WELLS, T., DAVIDSON, C., MÖRGELIN, M., BIRD, J. L., BAYLISS, M. T. & DUDHIA, J. 2003. Age-related changes in the composition, the molecular stoichiometry and the stability of proteoglycan aggregates extracted from human articular cartilage. *Biochem J*, 370, 69-79.
- WITHROW, J., MURPHY, C., DUKES, A., FULZELE, S., LIU, Y., HUNTER, M. & HAMRICK, M. 2016. Synovial Fluid Exosomal MicroRNA Profiling of Osteoarthritis Patients and Identification of Synoviocyte-Chondrocyte Communication Pathway. *ORS 2016 Annual Meeting*. Orlando.
- WITTENAUER, R., SMITH, L. & KAMAL, A. 2013. Update on 2004 Background Paper, BP 6.12 Osteoarthritis. Geneva, World Health Organization.
- WOJDASIEWICZ, P., PONIATOWSKI Ł, A. & SZUKIEWICZ, D. 2014. The role of inflammatory and anti-inflammatory cytokines in the pathogenesis of osteoarthritis. *Mediators Inflamm*, 2014, 561459.
- WU, J. J., WEIS, M. A., KIM, L. S. & EYRE, D. R. 2010. Type III collagen, a fibril network modifier in articular cartilage. *J Biol Chem*, 285, 18537-44.
- WU, X. F., ZHOU, Z. H. & ZOU, J. 2017. MicroRNA-181 inhibits proliferation and promotes apoptosis of chondrocytes in osteoarthritis by targeting PTEN. *Biochem Cell Biol*.
- XIE, F., XIAO, P., CHEN, D., XU, L. & ZHANG, B. 2012. miRDeepFinder: a miRNA analysis tool for deep sequencing of plant small RNAs. *Plant Mol Biol*.
- XU, J. F., ZHANG, S. J., ZHAO, C., QIU, B. S., GU, H. F., HONG, J. F., CAO, L., CHEN, Y., XIA, B., BI, Q. & WANG, Y. P. 2015. Altered microRNA expression profile in synovial fluid from patients with knee osteoarthritis with treatment of hyaluronic acid. *Mol Diagn Ther*, 19, 299-308.

- YANG, B., KANG, X., XING, Y., DOU, C., KANG, F., LI, J., QUAN, Y. & DONG, S. 2014. Effect of microRNA-145 on IL-1 $\beta$ -induced cartilage degradation in human chondrocytes. *FEBS Lett.*, 588, 2344-52.
- YANG, X., GUAN, Y., TIAN, S., WANG, Y., SUN, K. & CHEN, Q. 2016. Mechanical and IL-1 $\beta$  Responsive miR-365 Contributes to Osteoarthritis Development by Targeting Histone Deacetylase 4. *Int J Mol Sci.*, 17, 436.
- YATES, L. A., NORBURY, C. J. & GILBERT, R. J. 2013. The long and short of microRNA. *Cell*, 153, 516-9.
- YE, J., COULOURIS, G., ZARETSKAYA, I., CUTCUTACHE, I., ROZEN, S. & MADDEN, T. L. 2012. Primer-BLAST: a tool to design target-specific primers for polymerase chain reaction. *BMC Bioinformatics*, 13, 134.
- YU, X. M., MENG, H. Y., YUAN, X. L., WANG, Y., GUO, Q. Y., PENG, J., WANG, A. Y. & LU, S. B. 2015. MicroRNAs' Involvement in Osteoarthritis and the Prospects for Treatments. *Evid Based Complement Alternat Med*, 2015, 236179.
- YUAN, Y., ZHANG, G. Q., CHAI, W., NI, M., XU, C. & CHEN, J. Y. 2016. Silencing of microRNA-138-5p promotes IL-1 $\beta$ -induced cartilage degradation in human chondrocytes by targeting FOXC1: miR-138 promotes cartilage degradation. *Bone Joint Res*, 5, 523-530.
- ZENGINI, E., HATZIKOTULAS, K., TACHMAZIDOU, I., STEINBERG, J., HARTWIG, F. P., SOUTHAM, L., HACKINGER, S., BOER, C. G., STYRKARSDOTTIR, U., GILLY, A., SUVEGES, D., KILLIAN, B., INGVARSSON, T., JONSSON, H., BABIS, G. C., MCCASKIE, A., UITTERLINDEN, A. G., VAN MEURS, J. B. J., THORSTEINSDOTTIR, U., STEFANSSON, K., DAVEY SMITH, G., WILKINSON, J. M. & ZEGGINI, E. 2018. Genome-wide analyses using UK Biobank data provide insights into the genetic architecture of osteoarthritis. *Nat Genet*, 50, 549-558.
- ZHANG, G., SUN, Y., WANG, Y., LIU, R., BAO, Y. & LI, Q. 2016. MiR-502-5p inhibits IL-1 $\beta$ -induced chondrocyte injury by targeting TRAF2. *Cell Immunol*, 302, 50-57.
- ZHANG, M., THELEMAN, J. L., LYGRISSE, K. A. & WANG, J. 2019. Epigenetic Mechanisms Underlying the Aging of Articular Cartilage and Osteoarthritis. *Gerontology*, 65, 387-396.
- ZHANG, Q., JI, Q., WANG, X., KANG, L., FU, Y., YIN, Y., LI, Z., LIU, Y., XU, X. & WANG, Y. 2015a. SOX9 is a regulator of ADAMTSs-induced cartilage degeneration at the early stage of human osteoarthritis. *Osteoarthritis Cartilage*, 23, 2259-2268.
- ZHANG, X., WANG, C., ZHAO, J., XU, J., GENG, Y., DAI, L., HUANG, Y., FU, S. C., DAI, K. & ZHANG, X. 2017. miR-146a facilitates osteoarthritis by regulating cartilage homeostasis via targeting Camk2d and Ppp3r2. *Cell Death Dis*, 8, e2734.
- ZHANG, Y., VASHEGHANI, F., LI, Y. H., BLATI, M., SIMEONE, K., FAHMI, H., LUSSIER, B., ROUGHLEY, P., LAGARES, D., PELLETIER, J. P., MARTEL-PELLETIER, J. & KAPOOR, M. 2015b. Cartilage-specific deletion of mTOR upregulates autophagy and protects mice from osteoarthritis. *Ann Rheum Dis*, 74, 1432-40.
- ZHAO, X., LI, H. & WANG, L. 2019. MicroRNA-107 regulates autophagy and apoptosis of osteoarthritis chondrocytes by targeting TRAF3. *Int Immunopharmacol*, 71, 181-187.
- ZHENG, X., ZHAO, F.-C., PANG, Y., LI, D.-Y., YAO, S.-C., SUN, S.-S. & GUO, K.-J. 2017. Downregulation of miR-221-3p contributes to IL-1 $\beta$ -induced cartilage degradation by directly targeting the SDF1/CXCR4 signaling pathway. *Journal of Molecular Medicine*, 95, 615-627.
- ZHONG, L., HUANG, X., KARPERIEN, M. & POST, J. N. 2016. Correlation between Gene Expression and Osteoarthritis Progression in Human. *Int J Mol Sci.*, 17.
- ZHOU, J., CHEN, Q., LANSKE, B., FLEMING, B. C., TEREK, R., WEI, X., ZHANG, G., WANG, S., LI, K. & WEI, L. 2014. Disrupting the Indian hedgehog signaling pathway in vivo attenuates surgically induced osteoarthritis progression in Col2a1-CreERT2; Ihhfl/fl mice. *Arthritis Research & Therapy*, 16, R11.
- ZHOU, X., LUO, D., SUN, H., QI, Y., XU, W., JIN, X., LI, C., LIN, Z. & LI, G. 2018. MiR-132-3p regulates ADAMTS-5 expression and promotes chondrogenic differentiation of rat mesenchymal stem cells. *J Cell Biochem*, 119, 2579-2587.

## **Appendix to Chapter 3**

Microarray analysis between young intact cartilage from donors undergoing anterior cruciate ligament surgery and old osteoarthritic intact and lesioned cartilage from patients undergoing total knee replacement, identified sets of differentially expressed miRNAs. The full lists of differentially expressed miRNAs, their fold change and FDR-adjusted p values are shown here for the following comparisons:

- A. Old OA Intact-1 vs Young Intact**
- B. Old OA Intact-2 vs Young Intact**
- C. Old OA Lesioned vs Young Intact**
- D. Old OA Lesioned vs Old OA Intact-1**
- E. Old OA Lesioned vs Old OA Intact-2**
- F. Old OA Intact-1 vs Old OA Intact-2**

Moreover, The IPA Core Analysis Report for comparison old OA-Lesioned vs Young Intact is included at the end of the Appendix. This comparison was chosen as it is also discussed in Chapter 3.

### **Old OA Intact-1 vs Young Intact (Columns A, B and C)**

### **Old OA Intact-2 vs Young Intact (Columns D, E and F)**

(FC=log<sub>2</sub> Fold change, FDR=False Discover Rate, Int=OA-Intact, Y= Young Intact)

<b>Transcript ID</b>	<b>FC Int-1 vs Y</b>	<b>FDR Int-1 vs Y</b>	<b>Transcript ID</b>	<b>FC Int-2 vs Y</b>	<b>FDR Int-2 vs Y</b>
hsa-miR-143-3p	-7.75	9.46E-14	hsa-miR-143-3p	-7.37	1.98E-14
hsa-miR-126-3p	-7.86	3.13E-13	hsa-miR-126-3p	-7.08	1.86E-13
hsa-miR-139-5p	-4.14	2.03E-11	hsa-miR-139-5p	-4.3	4.88E-13
hsa-let-7c-5p	-11.7	3.98E-11	hsa-miR-30c-5p	-5.53	1.94E-11
hsa-miR-148a-3p	-5.17	9.36E-11	hsa-miR-148a-3p	-4.87	2.03E-11
hsa-miR-25-3p	-4.56	2.83E-10	hsa-miR-379-5p	-4.77	2.03E-11
hsa-miR-30c-5p	-5.45	3.21E-10	hsa-miR-25-3p	-4.39	3.98E-11
hsa-let-7b-5p	-11.04	5.64E-10	hsa-miR-20a-5p	-4.92	1.21E-10
hsa-miR-379-5p	-4.58	7.06E-10	hsa-miR-28-5p	-4.31	3.84E-10
hsa-miR-20a-5p	-5.05	9.35E-10	hsa-miR-15a-5p	-4.46	8.90E-10
hsa-miR-125b-5p	-10.76	9.35E-10	hsa-let-7g-5p	-5.45	3.13E-09
hsa-miR-628-3p	-3.42	4.18E-09	hsa-miR-145-5p	-8.35	4.16E-09
hsa-miR-30a-5p	-5.46	7.66E-09	hsa-miR-150-5p	-3.2	4.73E-09
hsa-miR-15a-5p	-4.49	9.10E-09	hsa-miR-30a-5p	-4.89	5.10E-09

hsa-miR-28-5p	-4.1	1.17E-08	hsa-miR-628-3p	-2.91	7.25E-09
hsa-miR-10b-5p	-4.81	1.44E-08	hsa-miR-10b-5p	-4.37	7.79E-09
hsa-miR-145-5p	-8.85	1.45E-08	hsa-miR-432-5p	-4.72	8.58E-09
hsa-miR-432-5p	-5.11	2.24E-08	hsa-miR-382-5p	-4.72	9.33E-09
hsa-miR-4454	-7.53	3.88E-08	hsa-miR-30b-5p	-3.8	1.22E-08
hsa-let-7g-5p	-5.41	4.01E-08	hsa-miR-181b-5p	-4.85	1.37E-08
hsa-miR-382-5p	-4.98	4.03E-08	hsa-miR-151b	-4.39	2.85E-08
hsa-miR-455-5p	-4.69	5.82E-08	hsa-miR-487b-3p	-3.95	2.94E-08
hsa-miR-181b-5p	-5.02	8.46E-08	hsa-miR-455-5p	-4.18	4.29E-08
hsa-miR-150-5p	-3.12	8.46E-08	hsa-miR-30a-3p	-2.66	1.91E-07
hsa-miR-151b	-4.68	9.60E-08	hsa-miR-409-3p	-3.9	3.11E-07
hsa-miR-409-3p	-4.61	1.55E-07	hsa-miR-19b-3p	-4.51	3.90E-07
hsa-miR-30b-5p	-3.7	2.41E-07	hsa-miR-106b-5p	-5.5	6.61E-07
hsa-miR-487b-3p	-3.9	4.62E-07	hsa-miR-132-3p	-4.69	7.36E-07
hsa-miR-24-3p	-11.54	1.03E-06	hsa-miR-4417	-4.88	1.03E-06
hsa-miR-19b-3p	-4.88	1.04E-06	hsa-miR-196a-5p	-4.38	2.98E-06
hsa-miR-106b-5p	-6.1	1.06E-06	hsa-let-7f-5p	-4.8	3.79E-06
hsa-miR-26a-5p	-11.26	1.20E-06	hsa-miR-378a-3p	-5.12	6.68E-06
hsa-miR-195-5p	-9.55	1.37E-06	hsa-miR-17-5p	-5.11	1.44E-05
hsa-miR-132-3p	-5.14	1.47E-06	hsa-miR-146a-5p	-3.3	1.54E-05
hsa-miR-23b-3p	-11.31	4.16E-06	hsa-miR-106a-5p	-4.61	2.03E-05
hsa-let-7f-5p	-5.37	5.24E-06	hsa-miR-28-3p	-4.11	2.18E-05
hsa-let-7i-5p	-8.43	5.32E-06	hsa-miR-505-5p	-2.1	2.42E-05
hsa-miR-23a-3p	-11.27	5.53E-06	hsa-miR-4253	-3.91	2.80E-05
hsa-miR-199a-3p	-9.18	5.89E-06	hsa-miR-146b-5p	-3.57	2.88E-05
hsa-miR-1281	4.3	5.89E-06	hsa-miR-654-5p	-1.87	2.88E-05
hsa-miR-4417	-4.97	7.23E-06	hsa-miR-139-3p	-1.79	3.02E-05
hsa-miR-196a-5p	-4.73	7.42E-06	hsa-miR-324-5p	-3.95	3.37E-05
hsa-miR-106a-5p	-5.57	8.39E-06	hsa-miR-3687	-3.64	3.40E-05
hsa-miR-885-3p	-3.4	8.80E-06	hsa-miR-27b-5p	-3.33	3.55E-05
hsa-miR-151a-5p	-8.44	9.06E-06	hsa-miR-424-3p	-2.3	4.01E-05
hsa-miR-744-5p	-5.33	9.37E-06	hsa-miR-24-2-5p	-2.64	4.55E-05
hsa-miR-17-5p	-5.96	1.03E-05	hsa-miR-378c	-3.06	6.80E-05
hsa-miR-4750-3p	4.87	1.03E-05	hsa-miR-485-5p	-2.41	8.45E-05
hsa-miR-940	4.31	1.05E-05	hsa-miR-3907	-1.83	8.86E-05
hsa-miR-5100	-6.96	1.08E-05	hsa-miR-196b-5p	-1.88	0.000117224
hsa-miR-378a-3p	-5.65	1.08E-05	hsa-miR-331-5p	-1.1	0.000118605
hsa-let-7a-5p	-10.47	1.12E-05	hsa-miR-10a-5p	-1.8	0.000119464
hsa-miR-30a-3p	-2.38	1.39E-05	hsa-miR-23b-5p	-3.03	0.000120825
hsa-miR-16-5p	-9.25	1.40E-05	hsa-miR-130a-3p	-3.63	0.000121044
hsa-let-7e-5p	-8.43	1.44E-05	hsa-miR-93-5p	-4.92	0.000128241
hsa-miR-320c	-6.15	1.45E-05	hsa-miR-3609	-3.4	0.00013218
hsa-miR-125a-5p	-7.84	1.73E-05	hsa-miR-885-3p	-2.43	0.000153135
hsa-miR-6732-5p	3.34	1.73E-05	hsa-miR-151a-3p	-4.78	0.00018438
hsa-miR-99a-5p	-9.07	1.93E-05	hsa-miR-199a-3p	-6.28	0.000190099

hsa-miR-193b-3p	-7.58	2.03E-05	hsa-miR-8071	-4.17	0.000195326
hsa-miR-103a-3p	-9.37	2.57E-05	hsa-miR-6753-5p	-2.09	0.000239052
hsa-miR-107	-8.97	2.66E-05	hsa-miR-708-5p	-3.32	0.000270084
hsa-miR-146a-5p	-3.62	2.83E-05	hsa-miR-181a-5p	-5.37	0.000273639
hsa-miR-181a-5p	-7.26	3.08E-05	hsa-miR-181d-5p	-1.76	0.0002814
hsa-miR-152-3p	-7.98	3.61E-05	hsa-miR-584-5p	-1.06	0.000293246
hsa-miR-6806-5p	-2.63	3.61E-05	hsa-miR-195-3p	-2.36	0.000314473
hsa-let-7d-5p	-8.92	4.26E-05	hsa-miR-378f	-2.61	0.000314473
hsa-miR-3687	-4.07	4.43E-05	hsa-miR-6846-5p	-1.77	0.0003262
hsa-miR-361-5p	-7.54	4.46E-05	hsa-miR-6886-5p	-1.01	0.000345523
hsa-miR-191-5p	-8.73	4.46E-05	hsa-miR-433-3p	-2.4	0.000350689
hsa-miR-320d	-5.93	5.03E-05	hsa-miR-664a-5p	-2.49	0.000386843
hsa-miR-4447	-1.57	5.46E-05	hsa-miR-6875-5p	-1.54	0.000462972
hsa-miR-214-3p	-6.3	6.41E-05	hsa-miR-6796-5p	-1.84	0.000495271
hsa-miR-320b	-6.25	6.45E-05	hsa-miR-6807-5p	-3.56	0.000509695
hsa-miR-155-5p	-6.25	6.54E-05	hsa-miR-1246	-4.27	0.000531525
hsa-miR-28-3p	-4.32	6.71E-05	hsa-miR-370-3p	-2.25	0.000535333
hsa-miR-6800-3p	4.83	6.71E-05	hsa-miR-339-5p	-2.29	0.000535333
hsa-miR-3180	-4.07	7.12E-05	hsa-miR-10b-3p	-1.97	0.000546296
hsa-miR-27b-3p	-8.44	7.62E-05	hsa-miR-34a-5p	-3.45	0.000576343
hsa-miR-23b-5p	-3.57	8.05E-05	hsa-miR-20b-5p	-1.8	0.000576343
hsa-miR-29a-3p	-6.74	8.23E-05	hsa-miR-532-5p	-3.71	0.000597097
hsa-miR-146b-5p	-3.74	8.82E-05	hsa-miR-1273h-5p	-2.07	0.000608926
hsa-miR-654-5p	-1.96	8.89E-05	hsa-miR-5739	-2.51	0.00061492
hsa-miR-134-5p	-5.3	8.94E-05	hsa-miR-4462	-2.49	0.00065135
hsa-miR-6796-3p	3.73	9.23E-05	hsa-miR-3180	-2.97	0.000655815
hsa-miR-130a-3p	-4.22	9.56E-05	hsa-miR-6746-5p	-2.07	0.000656731
hsa-miR-324-5p	-4.16	9.56E-05	hsa-miR-3124-5p	-1.71	0.000676276
hsa-miR-378c	-3.37	0.000102245	hsa-miR-155-5p	-4.51	0.000687995
hsa-miR-3921	3.88	0.000114082	hsa-miR-4685-5p	-2.25	0.000693232
hsa-miR-320e	-5.8	0.000117224	hsa-miR-134-5p	-3.91	0.000714332
hsa-miR-6802-5p	-4.1	0.000117856	hsa-miR-331-3p	-1.63	0.000844346
hsa-miR-93-5p	-5.66	0.000118244	hsa-miR-3180-3p	-3.92	0.0008676
hsa-miR-331-5p	-1.25	0.000118855	hsa-miR-422a	-2.21	0.000905027
hsa-miR-7112-5p	-2.57	0.000121044	hsa-miR-6871-5p	-1.38	0.000905027
hsa-miR-27b-5p	-3.45	0.000121075	hsa-miR-7112-5p	-1.89	0.001013763
hsa-miR-6805-3p	4.41	0.000121075	hsa-miR-135a-3p	-2.13	0.00101779
hsa-miR-150-3p	-4.35	0.000122273	hsa-miR-4485	-3.06	0.001107098
hsa-miR-151a-3p	-5.62	0.000123739	hsa-miR-557	-1.68	0.001173658
hsa-miR-100-5p	-8.46	0.000132444	hsa-miR-6825-5p	-2.1	0.001231898
hsa-miR-584-5p	-1.28	0.000140985	hsa-miR-6847-5p	-2.92	0.001441414
hsa-miR-664a-5p	-3.08	0.000142031	hsa-miR-21-5p	-3.07	0.001444229
hsa-miR-6808-5p	-3.9	0.000142444	hsa-miR-5195-3p	-2.31	0.001493174
hsa-miR-199a-5p	-7.33	0.000143393	hsa-miR-6728-5p	-2.04	0.001632517
hsa-miR-1273g-3p	-6.14	0.000143393	hsa-miR-6080	-1.68	0.001665757

hsa-miR-22-3p	-8.26	0.000153322	hsa-miR-345-5p	-2.82	0.001754583
hsa-miR-30d-5p	-5.68	0.00015985	hsa-miR-6768-5p	-2.11	0.001845833
hsa-miR-140-5p	-6.99	0.000163318	hsa-miR-195-5p	-4.9	0.001995035
hsa-miR-548n	0.65	0.00016529	hsa-miR-1254	-1.41	0.002043351
hsa-miR-4485	-4.08	0.000174078	hsa-miR-4284	-2.21	0.00207681
hsa-miR-424-3p	-2.34	0.000176524	hsa-miR-1273f	-2.11	0.00207681
hsa-miR-92a-3p	-8.41	0.000180577	hsa-miR-30c-2-3p	-1.22	0.002077768
hsa-miR-222-3p	-7.43	0.000187578	hsa-miR-3921	2.64	0.002102616
hsa-miR-8075	3.85	0.000193438	hsa-miR-342-5p	-2.48	0.002105049
hsa-miR-27a-3p	-8.43	0.000203144	hsa-miR-106b-3p	-2.8	0.002107936
			hsa-miR-1185-2-3p		
hsa-miR-6753-5p	-2.4	0.000218591		-1.53	0.002107936
hsa-miR-6768-5p	-2.88	0.000227446	hsa-miR-6808-5p	-2.7	0.002136132
hsa-miR-7641	-8.53	0.000245329	hsa-miR-199b-5p	-1.67	0.002386854
hsa-miR-3135b	-4.5	0.000249544	hsa-miR-409-5p	-2.01	0.002420057
hsa-miR-6797-3p	3.98	0.000261087	hsa-miR-6797-5p	-1.73	0.002420057
hsa-miR-342-3p	-6.99	0.000261215	hsa-miR-29a-3p	-4.4	0.002456404
hsa-miR-485-5p	-2.5	0.000273251	hsa-miR-18a-5p	-1.92	0.002534195
hsa-miR-5739	-3.06	0.000275272	hsa-miR-196b-3p	-1.47	0.002572415
hsa-miR-210-3p	-4.91	0.0002814	hsa-miR-4535	-1.3	0.002733129
hsa-miR-125b-2-3p	-5.13	0.000283777	hsa-miR-23c	-1.2	0.002806701
hsa-miR-4665-5p	-3.44	0.000295996	hsa-miR-30e-5p	-1.87	0.002854737
hsa-miR-6846-5p	-2.03	0.000306108	hsa-miR-7114-5p	-2.51	0.002862332
			hsa-miR-1185-1-3p		
hsa-miR-2467-3p	-1.36	0.00030878		-1.59	0.002882896
hsa-miR-505-5p	-1.96	0.000325312	hsa-miR-660-5p	-1.85	0.002895429
hsa-miR-320a	-4.88	0.000334095	hsa-miR-3652	-1.61	0.002957094
hsa-miR-339-5p	-2.71	0.00034457	hsa-miR-152-3p	-4.8	0.003051751
hsa-miR-7111-3p	1.59	0.000345523	hsa-miR-130b-3p	-3.49	0.003109917
hsa-miR-574-3p	-6.24	0.000361938	hsa-miR-6880-5p	-1.98	0.003126194
hsa-miR-185-5p	-5.84	0.000386843	hsa-miR-371a-5p	-1.17	0.003196903
hsa-miR-423-5p	-4.7	0.000390237	hsa-miR-1231	-3.26	0.003215076
hsa-miR-4449	-4.51	0.000410978	hsa-miR-6515-5p	-1.09	0.003488964
hsa-miR-99b-5p	-6.81	0.000417914	hsa-miR-378i	-2.23	0.003543658
hsa-miR-221-3p	-6.69	0.000451063	hsa-miR-16-5p	-5.11	0.003698292
hsa-miR-497-5p	-6.43	0.000462686	hsa-miR-4783-3p	-1.89	0.003752725
hsa-miR-6861-5p	-3.46	0.000462686	hsa-miR-6737-5p	-1.54	0.003774195
hsa-miR-4715-5p	-0.96	0.000487737	hsa-miR-487a-5p	-1.51	0.00382499
hsa-miR-4462	-2.91	0.000497922	hsa-miR-3154	-1.59	0.003858826
hsa-miR-4728-5p	-2.82	0.000535141	hsa-let-7i-5p	-4.35	0.003890183
hsa-miR-8064	-2.59	0.000566738	hsa-miR-4732-5p	-1.7	0.003912236
hsa-miR-6743-5p	-2.72	0.000567477	hsa-miR-6742-5p	-1.69	0.00393803
hsa-miR-877-3p	1.76	0.000597097	hsa-miR-125a-3p	-2.61	0.004162044
hsa-miR-1228-3p	3.05	0.000605928	hsa-miR-185-5p	-4.1	0.004162044

hsa-miR-6737-5p	-2.09	0.000608926	hsa-miR-4525	-1.72	0.004258758
hsa-miR-6845-5p	-1.93	0.000614127	hsa-miR-148b-3p	-1.93	0.004365419
hsa-miR-433-3p	-2.6	0.000627411	hsa-miR-6824-5p	-3.31	0.004560258
hsa-miR-3609	-3.4	0.000637676	hsa-miR-498	-1.38	0.004622029
hsa-miR-7977	-5.32	0.000640689	hsa-miR-4760-3p	0.52	0.004654825
hsa-miR-127-3p	-6.54	0.000656731	hsa-miR-7106-3p	0.57	0.004850173
hsa-miR-4274	3.5	0.000661762	hsa-miR-29c-3p	-1.47	0.004852427
hsa-miR-652-3p	-4.28	0.000677707	hsa-miR-6881-5p	-0.52	0.004852427
hsa-miR-345-5p	-3.49	0.000681972	hsa-miR-7109-5p	-1.99	0.004866435
hsa-miR-4498	-2.92	0.000710743	hsa-miR-214-5p	-2.59	0.004868667
hsa-miR-504-3p	-2.57	0.000716385	hsa-miR-224-3p	-1.38	0.005027193
hsa-miR-139-3p	-1.57	0.000728571	hsa-miR-6861-5p	-2.41	0.00511519
hsa-miR-3651	-5.54	0.00073299	hsa-miR-194-5p	-1.63	0.005483256
hsa-miR-6086	-2.03	0.000737983	hsa-miR-6795-5p	-1.44	0.005617057
hsa-miR-557	-1.98	0.000771848	hsa-miR-6829-5p	-1.53	0.005629179
hsa-miR-24-2-5p	-2.39	0.000772999	hsa-miR-4447	-0.91	0.005749882
hsa-miR-181d-5p	-1.84	0.000772999	hsa-miR-200c-3p	-1.4	0.005916613
hsa-miR-140-3p	-2.35	0.000905027	hsa-miR-3135b	-2.9	0.006435194
hsa-miR-532-5p	-4.06	0.000913852	hsa-miR-4534	-1.75	0.006450207
hsa-miR-8071	-4.15	0.000959389	hsa-miR-199a-5p	-4.51	0.006489928
hsa-miR-4688	-2.71	0.000978197	hsa-miR-330-3p	-1.12	0.006531402
hsa-miR-1231	-4.16	0.000985092	hsa-miR-504-3p	-1.81	0.006779604
hsa-miR-193b-5p	-5.34	0.000989895	hsa-miR-654-3p	-1.84	0.007081132
hsa-miR-3195	-4.29	0.001044369	hsa-miR-381-3p	-1.49	0.007195121
hsa-miR-7847-3p	-3.85	0.001173658	hsa-miR-3127-3p	0.68	0.007336022
hsa-miR-3679-5p	-3.03	0.001323095	hsa-miR-2467-3p	-0.87	0.007741871
hsa-miR-3907	-1.66	0.001353107	hsa-miR-99a-3p	-1.3	0.00777261
hsa-miR-4783-3p	-2.39	0.001358729	hsa-miR-6806-5p	-1.42	0.007789795
hsa-miR-4685-5p	-2.42	0.001379127	hsa-miR-6732-5p	1.71	0.007961221
hsa-miR-3162-3p	2.93	0.001459343	hsa-miR-665	-2.05	0.008166454
hsa-miR-20b-5p	-1.88	0.001497287	hsa-miR-3911	-1.59	0.008274196
hsa-miR-324-3p	-3.91	0.001608828	hsa-miR-127-5p	-1	0.008341602
hsa-miR-106b-3p	-3.29	0.001617047	hsa-miR-8064	-1.73	0.008341602
hsa-miR-378f	-2.58	0.001622679	hsa-miR-493-3p	-1.81	0.008420047
hsa-miR-34a-5p	-3.58	0.001642706	hsa-miR-221-3p	-4.38	0.008487899
hsa-miR-370-3p	-2.32	0.001679508	hsa-miR-3181	-0.86	0.008496729
hsa-miR-224-3p	-1.76	0.001720577	hsa-miR-1972	-2.15	0.008645408
hsa-miR-331-3p	-1.74	0.001744228	hsa-miR-615-3p	-1.71	0.008668275
hsa-miR-342-5p	-2.88	0.001754193	hsa-miR-642b-3p	-1.8	0.008864404
hsa-miR-5572	-3.3	0.00176222	hsa-miR-362-5p	-2.18	0.009060965
hsa-miR-3154	-1.96	0.001794172	hsa-miR-339-3p	-2.92	0.009110792
hsa-miR-6742-5p	-2.1	0.00180264	hsa-miR-6774-5p	-1.32	0.009415942
hsa-miR-6746-5p	-2.15	0.001813198	hsa-miR-361-5p	-4.04	0.009695982
hsa-miR-4429	-4.34	0.001842869	hsa-miR-4800-3p	-1.51	0.009723741
hsa-miR-6820-5p	-3.21	0.001868487	hsa-miR-5093	-2.17	0.009882725

hsa-miR-425-5p	-4.39	0.0019177	hsa-miR-6754-3p	-0.98	0.009882725
hsa-miR-6716-5p	-3.55	0.0019177	hsa-miR-1238-5p	-1.33	0.010077951
hsa-miR-6889-5p	-2.8	0.001947297	hsa-miR-337-5p	-1.95	0.010270926
hsa-miR-7109-5p	-2.49	0.00197038	hsa-miR-6753-3p	-1.4	0.010270926
hsa-miR-4656	-2.81	0.001988616	hsa-miR-6862-5p	-0.82	0.010438325
hsa-miR-196b-5p	-1.68	0.00202093	hsa-miR-3178	-1.86	0.01061259
hsa-miR-6807-5p	-3.58	0.00204258	hsa-miR-5006-5p	-2.29	0.010960124
hsa-miR-130b-3p	-4.14	0.002089534	hsa-miR-5585-3p	-0.72	0.011055727
hsa-miR-4253	-3.11	0.002089534	hsa-miR-5572	-2.37	0.01107774
hsa-miR-6825-5p	-2.27	0.002089534	hsa-miR-30d-5p	-3.3	0.011209751
hsa-miR-1185-1-3p	-1.87	0.002126497	hsa-miR-3130-3p	-0.71	0.011446767
hsa-miR-494-3p	-4.17	0.002155109	hsa-miR-6893-5p	-1.74	0.01171248
hsa-miR-1909-3p	-3.74	0.002225003	hsa-miR-4436b-5p	-1.62	0.011939261
hsa-miR-4758-3p	1.14	0.002444246	hsa-miR-365b-5p	-1.1	0.012024387
hsa-miR-4433b-5p	1.39	0.002568336	hsa-miR-7-2-3p	0.48	0.01216102
hsa-miR-6860	-2.04	0.002575532	hsa-miR-151a-5p	-3.93	0.01279353
hsa-miR-708-5p	-3.08	0.002663473	hsa-miR-6781-5p	-2.19	0.013051141
hsa-miR-193a-5p	-5.26	0.002682754	hsa-miR-8075	2.22	0.013558665
hsa-miR-1254	-1.57	0.00269632	hsa-miR-212-3p	-1.06	0.013785842
hsa-miR-423-3p	-5.39	0.002722742	hsa-miR-342-3p	-4.13	0.013785842
hsa-miR-1246	-4.19	0.002728825	hsa-miR-6762-5p	-1.14	0.013954549
hsa-miR-937-5p	-2.77	0.002736254	hsa-miR-198	-1.38	0.013982956
hsa-miR-3157-3p	3.35	0.002762931	hsa-miR-1281	1.93	0.014014488
hsa-miR-4726-5p	-1.45	0.002843541	hsa-miR-664b-5p	-1.52	0.014112386
hsa-miR-6819-3p	2.88	0.002882896	hsa-miR-6133	-1.36	0.01411325
hsa-miR-4284	-2.42	0.003030259	hsa-miR-4257	-0.97	0.014513209
hsa-miR-195-3p	-2.17	0.003238888	hsa-miR-6830-5p	-0.97	0.0147239
hsa-miR-6886-5p	-0.93	0.003274526	hsa-miR-4669	-1.68	0.014913489
hsa-miR-4669	-2.28	0.003293414	hsa-miR-6084	-1.74	0.015110703
hsa-miR-21-5p	-3.22	0.00331709	hsa-miR-6792-5p	-1.37	0.015201006
hsa-miR-548u	0.66	0.00331709	hsa-miR-6757-5p	-1.86	0.015996339
hsa-miR-4463	-3.86	0.00331709	hsa-miR-744-3p	0.46	0.016059468
hsa-miR-520c-3p	0.5	0.003320306	hsa-miR-425-5p	-3.02	0.01618786
hsa-miR-6728-5p	-2.16	0.003321912	hsa-miR-4688	-1.75	0.016250206
hsa-miR-498	-1.63	0.003457299	hsa-miR-3197	-3.46	0.016536143
hsa-miR-339-3p	-3.72	0.003469378	hsa-miR-93-3p	-1.28	0.016850054
hsa-miR-30e-5p	-2.09	0.003472747	hsa-miR-637	-1.29	0.016951337
hsa-miR-23a-5p	-3.87	0.003479787	hsa-miR-377-5p	-1.13	0.017143659
hsa-miR-6829-5p	-1.82	0.003707175	hsa-miR-6820-3p	0.69	0.017143659
hsa-miR-6132	-3.45	0.003808028	hsa-miR-30b-3p	-1.16	0.017157079
hsa-miR-6778-5p	-2.9	0.003825326	hsa-miR-149-5p	-1.2	0.01786989
hsa-miR-6875-5p	-1.44	0.003825326	hsa-miR-125b-2-3p	-2.94	0.017887562
hsa-miR-3175	-5.45	0.003858826	hsa-miR-181c-5p	-1.3	0.017902095

hsa-miR-8089	-3.24	0.00392948	hsa-miR-376c-3p	-1.64	0.01810689
hsa-miR-500a-3p	-3.91	0.00393803	hsa-miR-6819-5p	-2.42	0.018281427
hsa-miR-660-5p	-2.04	0.003995135	hsa-miR-140-5p	-3.82	0.018341677
hsa-miR-4505	-3	0.004162044	hsa-miR-3162-3p	1.93	0.018552813
hsa-miR-3124-5p	-1.63	0.004260023	hsa-miR-26b-5p	-0.91	0.018756299
hsa-miR-6165	-2.78	0.004360367	hsa-miR-6877-3p	-1.48	0.018867937
hsa-miR-4436b-5p	-2.07	0.004464979	hsa-miR-4750-3p	2.16	0.019552606
hsa-miR-15b-5p	-5.29	0.004514169	hsa-miR-6845-5p	-1.17	0.019609517
hsa-miR-6792-5p	-1.8	0.004524906	hsa-miR-3187-3p	-2.47	0.019910339
hsa-miR-10a-5p	-1.47	0.004652409	hsa-miR-1538	-1.33	0.0200721
hsa-miR-6763-5p	-2.79	0.004654825	hsa-miR-711	-0.88	0.020093343
hsa-miR-31-5p	-5.88	0.004755497	hsa-miR-625-5p	-1.17	0.020127481
hsa-miR-6080	-1.71	0.00490227	hsa-miR-1224-5p	-2.2	0.02043889
hsa-miR-591	0.55	0.004996519	hsa-miR-874-5p	-0.76	0.02043889
hsa-miR-1228-5p	-3.12	0.004996519	hsa-miR-421	-1.37	0.021040138
hsa-miR-371a-5p	-1.27	0.005000899	hsa-miR-4715-5p	-0.56	0.021190402
hsa-miR-502-3p	-4.24	0.005027193	hsa-miR-3917	-0.81	0.021987354
hsa-miR-125a-3p	-2.89	0.005314777	hsa-miR-26a-5p	-4.33	0.02207693
hsa-miR-548ap-5p	0.57	0.005416354	hsa-miR-1273d	-1.16	0.022347306
hsa-miR-6795-5p	-1.64	0.005507729	hsa-miR-1471	-1.02	0.022578038
hsa-miR-4324	-1.12	0.005617057	hsa-miR-4646-5p	-1.71	0.022631013
hsa-miR-6754-3p	-1.2	0.005669525	hsa-miR-4271	-1.12	0.02279463
hsa-miR-3925-5p	0.7	0.005866333	hsa-miR-920	-1.06	0.022839029
hsa-miR-4750-5p	-3.43	0.005866333	hsa-miR-652-3p	-2.55	0.02306791
hsa-miR-6749-5p	-3.24	0.005916613	hsa-miR-487a-3p	-1.16	0.023579731
hsa-miR-4651	-3.29	0.006010373	hsa-miR-142-3p	0.43	0.023724432
hsa-miR-7114-3p	2	0.00609262	hsa-miR-425-3p	-1.79	0.023855959
hsa-miR-4525	-1.89	0.006196579	hsa-miR-5001-3p	-0.46	0.024136726
hsa-miR-4534	-2	0.006196579	hsa-miR-4446-3p	-0.87	0.024687865
hsa-miR-4433b-3p	-3.54	0.006196579	hsa-miR-5196-5p	-2.14	0.024969322
hsa-miR-378h	3.01	0.006274829	hsa-miR-513c-3p	0.52	0.025288878
hsa-miR-4689	-3.54	0.006275409	hsa-miR-629-5p	-1.54	0.025466238
hsa-miR-422a	-2.07	0.006407152	hsa-miR-296-3p	-1.38	0.025492523
hsa-miR-6817-3p	0.66	0.006423896	hsa-miR-6793-5p	-1.06	0.025811529
hsa-miR-194-5p	-1.82	0.006587779	hsa-miR-6889-5p	-1.8	0.026373888
hsa-miR-135a-3p	-2	0.006851215	hsa-miR-6865-5p	-1.11	0.026450886
hsa-miR-6798-3p	1.78	0.006854653	hsa-miR-154-5p	-1.6	0.026616163
hsa-miR-3180-3p	-3.63	0.006929516	hsa-miR-4292	-0.75	0.026616163
hsa-miR-6779-5p	-2.87	0.007048073	hsa-miR-3607-5p	-1.12	0.026708138
hsa-miR-6796-5p	-1.62	0.00712704	hsa-miR-4717-3p	-1.39	0.026839532
hsa-miR-1273h-5p	-1.85	0.007130903	hsa-miR-194-3p	-0.84	0.026839732
hsa-miR-1185-2-3p	-1.53	0.007195121	hsa-miR-6875-3p	-1.53	0.027042314
hsa-miR-3622b-5p	-1.58	0.007213331	hsa-miR-3147	-1.34	0.027278639
hsa-miR-6893-5p	-2.1	0.00735397	hsa-miR-503-5p	-1.31	0.027542247

hsa-miR-6757-5p	-2.34	0.007501909	hsa-miR-548q	-0.51	0.027581844
hsa-miR-3652	-1.65	0.007510878	hsa-miR-3914	0.55	0.02799789
hsa-miR-6727-3p	1.27	0.00756791	hsa-miR-4327	-1.31	0.028433616
hsa-miR-6819-5p	-3.09	0.007573482	hsa-miR-6782-5p	-2.15	0.029095398
hsa-miR-149-5p	-1.52	0.007638362	hsa-miR-127-3p	-3.75	0.029247388
hsa-miR-1238-5p	-1.57	0.007705708	hsa-miR-4725-3p	-1.54	0.03016603
hsa-miR-149-3p	-2.93	0.007714749	hsa-miR-1301-3p	-1.54	0.030272493
hsa-miR-197-5p	-2.77	0.00777261	hsa-miR-222-3p	-3.8	0.030435319
hsa-miR-6824-5p	-3.53	0.008159633	hsa-miR-378d	-1.26	0.030525108
hsa-miR-4741	-3.59	0.008166454	hsa-miR-6785-5p	-1.53	0.03054425
hsa-miR-6090	-1.09	0.008166454	hsa-miR-551b-5p	-0.88	0.031274952
hsa-miR-4513	-1.34	0.008177907	hsa-miR-4304	-0.66	0.031826119
hsa-miR-4538	-1.01	0.008252148	hsa-miR-4655-5p	-1.71	0.032459246
hsa-miR-877-5p	-2.17	0.008287102	hsa-miR-1973	-1.5	0.032854268
hsa-miR-3911	-1.81	0.008341602	hsa-miR-6860	-1.3	0.032854268
hsa-miR-7114-5p	-2.53	0.008674587	hsa-miR-150-3p	-2.13	0.033160545
hsa-miR-10b-3p	-1.7	0.008690179	hsa-miR-887-3p	-0.92	0.033234756
hsa-miR-4430	-2.13	0.008800452	hsa-miR-3944-3p	-1.14	0.033441344
hsa-miR-6797-5p	-1.71	0.009151004	hsa-miR-128-3p	-1.12	0.033824674
hsa-miR-4638-5p	-1.02	0.009264268	hsa-miR-6831-5p	-1.6	0.033958521
hsa-miR-4725-5p	1.43	0.009576507	hsa-miR-6857-5p	-0.5	0.035346605
hsa-miR-4752	0.64	0.009612778	hsa-miR-6878-5p	0.36	0.03536274
hsa-miR-92b-3p	-4.25	0.009796128	hsa-miR-185-3p	-1.27	0.035535417
hsa-miR-4687-3p	-2.66	0.009882725	hsa-miR-7111-5p	-1.65	0.035812204
hsa-miR-1273f	-2.02	0.010103903	hsa-miR-6815-5p	-1.14	0.035891018
hsa-miR-6812-5p	-2.83	0.01011316	hsa-miR-6748-5p	-0.78	0.036317463
hsa-miR-6748-5p	-1.07	0.010128175	hsa-miR-500a-5p	-1.57	0.036447589
hsa-miR-6790-5p	-3.92	0.010193975	hsa-miR-4750-5p	-2.35	0.036452091
hsa-miR-6752-5p	-3.68	0.010483633	hsa-miR-4430	-1.53	0.036584504
hsa-miR-6515-5p	-1.09	0.010890161	hsa-miR-1287-5p	-0.86	0.037522356
hsa-miR-6851-5p	-1.88	0.010933575	hsa-miR-6751-5p	-0.93	0.03756757
hsa-miR-337-5p	-2.2	0.010966853	hsa-miR-31-5p	-3.92	0.03765947
hsa-miR-449c-3p	0.45	0.011229996	hsa-miR-642a-3p	-1.79	0.037915098
hsa-miR-6781-5p	-2.54	0.011390111	hsa-miR-191-3p	-0.97	0.03977905
hsa-miR-5195-3p	-2.1	0.011837947	hsa-miR-1324	0.53	0.03983022
hsa-miR-4433-5p	1.53	0.012042094	hsa-miR-4726-5p	-0.9	0.039906025
hsa-miR-6831-5p	-2.12	0.012042094	hsa-miR-4731-3p	0.47	0.039906025
hsa-miR-4633-5p	0.75	0.012293318	hsa-miR-138-5p	-0.94	0.04101721
hsa-miR-6738-5p	-2.14	0.01251978	hsa-miR-297	-2.99	0.042908321
hsa-miR-214-5p	-2.63	0.012817184	hsa-miR-500a-3p	-2.5	0.042954705
hsa-miR-18a-5p	-1.82	0.01306157	hsa-miR-4513	-0.93	0.04347851
hsa-miR-194-3p	-1.07	0.01322058	hsa-miR-5010-5p	-1.11	0.043636922
hsa-miR-637	-1.51	0.013443792	hsa-miR-518d-3p	0.34	0.044004551
hsa-miR-4535	-1.24	0.013525862	hsa-miR-6734-5p	-1.09	0.044371063
hsa-miR-6715a-3p	1.59	0.013871386	hsa-miR-3648	-2.41	0.044646132

hsa-miR-548ar-3p	0.56	0.013954549	hsa-miR-936	-1.05	0.045640594
hsa-miR-519d-3p	0.67	0.014035875	hsa-miR-8060	-0.95	0.045883963
hsa-miR-548x-3p	0.64	0.014035875	hsa-miR-615-5p	-0.78	0.0460425
hsa-miR-377-5p	-1.32	0.014066587	hsa-miR-6851-5p	-1.33	0.047192511
hsa-miR-6089	-1.05	0.014173144	hsa-miR-6877-5p	-1.1	0.047669336
hsa-miR-4279	1.71	0.014202757	hsa-miR-29b-1-5p	-0.73	0.04771584
hsa-miR-378i	-2.16	0.014422422	hsa-miR-5189-5p	-1.79	0.048559286
hsa-miR-4499	-0.66	0.014513209	hsa-miR-34c-5p	-0.46	0.048585262
hsa-miR-6793-5p	-1.31	0.014534341	hsa-miR-6890-5p	-0.79	0.04866001
hsa-miR-4758-5p	-2.87	0.014538588			
hsa-miR-6785-5p	-1.94	0.01471883			
hsa-miR-148b-3p	-1.9	0.015289263			
hsa-miR-2110	-2.99	0.01534092			
hsa-miR-29c-3p	-1.45	0.015976882			
hsa-miR-4732-5p	-1.64	0.016334818			
hsa-miR-579-3p	0.46	0.016364921			
hsa-miR-4484	-3.67	0.016573589			
hsa-miR-6880-5p	-1.85	0.016878918			
hsa-miR-487a-5p	-1.45	0.016904712			
hsa-miR-135b-5p	0.66	0.01694863			
hsa-miR-6717-5p	-0.88	0.017081955			
hsa-miR-409-5p	-1.82	0.017183563			
hsa-miR-4298	-2.72	0.017562998			
hsa-miR-191-3p	-1.25	0.017628394			
hsa-miR-212-3p	-1.16	0.018281427			
hsa-miR-6770-5p	-0.66	0.018521471			
hsa-miR-1468-3p	0.51	0.018629451			
hsa-miR-526a	0.48	0.019626103			
hsa-miR-5189-5p	-2.35	0.019837133			
hsa-miR-6741-5p	-2.17	0.019910339			
hsa-miR-325	-0.53	0.020132941			
hsa-miR-330-3p	-1.11	0.020165819			
hsa-miR-8073	-1.86	0.020186228			
hsa-miR-374a-5p	0.62	0.020193757			
hsa-miR-425-3p	-2.09	0.020261839			
hsa-miR-6753-3p	-1.46	0.020635601			
hsa-miR-4441	-0.72	0.020783898			
hsa-miR-4749-5p	-3.45	0.020904314			
hsa-miR-493-3p	-1.83	0.021175313			
hsa-miR-3151-3p	0.77	0.02180052			
hsa-miR-3117-5p	-0.46	0.021882546			
hsa-miR-4539	-2.41	0.021893588			
hsa-miR-1234-3p	2.67	0.02207693			
hsa-miR-4271	-1.29	0.022105275			

hsa-miR-760	-1.36	0.022263219
hsa-miR-198	-1.47	0.022499945
hsa-miR-7106-5p	-1.62	0.022542405
hsa-miR-296-3p	-1.6	0.022631013
hsa-miR-642b-3p	-1.82	0.022948361
hsa-miR-6076	-0.92	0.02313208
hsa-miR-501-3p	-2.98	0.023193618
hsa-miR-4673	-1.18	0.02334592
hsa-miR-663b	-1.58	0.02351927
hsa-miR-6871-5p	-1.09	0.023917144
hsa-miR-744-3p	0.49	0.024287151
hsa-miR-4530	-2.72	0.024379332
hsa-miR-6847-5p	-2.39	0.024629893
hsa-miR-4662a-3p	0.67	0.024912413
hsa-miR-671-3p	-0.93	0.025003838
hsa-miR-3936	-0.74	0.02522075
hsa-miR-4488	-1.75	0.025288878
hsa-miR-362-5p	-2.17	0.025320337
hsa-miR-6499-3p	0.68	0.025320337
hsa-miR-6774-5p	-1.32	0.025326955
hsa-miR-5008-5p	-0.61	0.025470007
hsa-miR-483-3p	0.66	0.02549318
hsa-miR-6877-3p	-1.62	0.02549318
hsa-miR-125b-1-3p	-2.38	0.025666532
hsa-miR-6729-3p	0.96	0.025886722
hsa-miR-421	-1.51	0.026450886
hsa-miR-6894-5p	-1.53	0.026450886
hsa-miR-532-3p	-2.6	0.026645285
hsa-miR-6752-3p	0.99	0.026650544
hsa-miR-4743-5p	-1.69	0.027042314
hsa-miR-665	-1.99	0.027241071
hsa-miR-381-3p	-1.42	0.027514504
hsa-miR-4634	-2.64	0.027582678
hsa-miR-6857-5p	-0.59	0.02826417
hsa-miR-7845-5p	-2.62	0.02826417
hsa-miR-4507	-2.54	0.028433616
hsa-miR-6848-5p	-3.22	0.02851159
hsa-miR-197-3p	-2.74	0.028943187
hsa-miR-3147	-1.51	0.030282347
hsa-miR-4270	-2.63	0.030862063
hsa-miR-1266-5p	-0.68	0.030868094
hsa-miR-6134	-0.63	0.031462893
hsa-miR-7107-5p	2.41	0.031868737
hsa-miR-1307-3p	-2.73	0.032235917

hsa-miR-6836-5p	-3.01	0.032501419
hsa-miR-8063	-2.73	0.032517167
hsa-miR-200c-3p	-1.27	0.032688591
hsa-miR-7160-5p	-0.96	0.032865598
hsa-miR-1225-5p	-3.07	0.032888287
hsa-miR-5193	0.93	0.032972441
hsa-miR-137	0.4	0.033128216
hsa-miR-3622a-5p	-1.44	0.033182605
hsa-miR-3937	-2.93	0.033995173
hsa-miR-30b-3p	-1.2	0.034265918
hsa-miR-4433-3p	-2.9	0.034291438
hsa-miR-1202	-3.03	0.034504385
hsa-miR-5703	-0.86	0.034504385
hsa-miR-6722-3p	-3.25	0.035087165
hsa-miR-4731-5p	-0.65	0.035322337
hsa-miR-6881-5p	-0.45	0.035322337
hsa-miR-6762-5p	-1.13	0.035357908
hsa-miR-4649-5p	-3.23	0.035509574
hsa-miR-376c-3p	-1.69	0.036317463
hsa-miR-4257	-0.97	0.036360381
hsa-miR-6830-5p	-0.97	0.036733345
hsa-miR-548a-3p	3.05	0.036767885
hsa-miR-1273d	-1.22	0.036959839
hsa-miR-3181	-0.8	0.037290482
hsa-miR-4283	-0.57	0.037522356
hsa-miR-196b-3p	-1.2	0.037619599
hsa-miR-1271-5p	-2.99	0.037696361
hsa-miR-4718	0.44	0.037696361
hsa-miR-6827-5p	-1.12	0.037855461
hsa-miR-518d-3p	0.4	0.037915961
hsa-miR-625-5p	-1.21	0.037916868
hsa-miR-23c	-0.98	0.037958487
hsa-miR-29c-5p	-0.68	0.039341038
hsa-miR-1301-3p	-1.68	0.039825618
hsa-miR-6088	-0.71	0.040551784
hsa-miR-6858-5p	-2.45	0.040815743
hsa-miR-6878-5p	0.4	0.04101721
hsa-miR-1182	-1.06	0.041450019
hsa-miR-29b-2-5p	-2.03	0.041450822
hsa-miR-93-3p	-1.27	0.042121201
hsa-miR-3156-3p	0.48	0.042121201
hsa-miR-6850-3p	-0.53	0.04216548
hsa-miR-4327	-1.41	0.042355872
hsa-miR-575	-2.58	0.042406187
hsa-miR-762	-1.98	0.04329673

hsa-miR-4491	0.59	0.043435267
hsa-miR-98-5p	-0.75	0.04347851
hsa-miR-6784-5p	-2.29	0.044371063
hsa-miR-500a-5p	-1.73	0.045096056
hsa-miR-920	-1.08	0.045179402
hsa-miR-29b-1-5p	-0.84	0.046243573
hsa-miR-6890-5p	-0.9	0.046581809
hsa-miR-499a-5p	0.61	0.047474071
hsa-miR-3917	-0.81	0.04771584
hsa-miR-6803-3p	0.65	0.04771584
hsa-miR-548e-3p	0.46	0.047933337
hsa-miR-1260a	0.88	0.048113067
hsa-miR-323a-5p	-0.52	0.048206137
hsa-miR-3614-3p	0.57	0.048585262
hsa-miR-874-5p	-0.75	0.048818559
hsa-miR-4481	-1.78	0.049081251
hsa-miR-615-3p	-1.52	0.049115816
hsa-miR-1972	-1.91	0.049342031
hsa-miR-6738-3p	0.56	0.049342606
hsa-miR-642a-3p	-1.96	0.04937258
hsa-miR-3152-3p	0.77	0.049446002

### Old OA Lesioned vs Young Intact (Columns A, B and C)

### Old OA Lesioned vs Old OA Intact-1 (Columns D, E and F)

(FC= $\log_2$  Fold change, FDR=False Discover Rate, Les=OA-Lesioned, Int=OA-Intact, Y= Young Intact)

Transcript ID	FC Les vs Y	FDR Les vs Y	Transcript ID	FC Les vs Int-1	FDR Les vs Int-1
hsa-miR-143-3p	-7.35	1.73E-15	hsa-let-7c-5p	9.03	5.10E-09
hsa-miR-126-3p	-7.36	5.92E-15	hsa-let-7b-5p	8.98	2.02E-08
hsa-miR-139-5p	-4.31	2.68E-14	hsa-miR-4454	7.09	8.46E-08
hsa-miR-148a-3p	-4.77	2.15E-12	hsa-miR-125b-5p	8.25	1.04E-07
hsa-miR-30c-5p	-5.15	4.37E-12	hsa-miR-5100	7.66	1.59E-06
hsa-miR-379-5p	-4.5	4.37E-12	hsa-miR-1273g-3p	7.78	3.80E-06
hsa-miR-20a-5p	-4.69	2.03E-11	hsa-miR-210-3p	5.79	2.76E-05
hsa-miR-25-3p	-3.96	2.03E-11	hsa-miR-320c	5.73	3.32E-05

hsa-miR-28-5p	-4.14	4.88E-11	hsa-miR-320d	5.63	8.34E-05
hsa-miR-15a-5p	-4.22	1.76E-10	hsa-miR-4505	4.12	9.90E-05
hsa-miR-628-3p	-2.92	5.07E-10	hsa-miR-214-3p	5.96	0.000105409
hsa-miR-30a-5p	-4.71	7.93E-10	hsa-miR-320b	5.91	0.000107991
hsa-miR-30b-5p	-3.79	9.35E-10	hsa-miR-937-5p	3.61	0.000112999
hsa-miR-10b-5p	-4.23	1.02E-09	hsa-miR-744-5p	4.31	0.000143393
hsa-miR-432-5p	-4.58	1.08E-09	hsa-miR-548n	-0.64	0.000166987
hsa-miR-150-5p	-2.96	1.48E-09	hsa-miR-193b-3p	6.03	0.000325919
hsa-miR-181b-5p	-4.68	2.03E-09	hsa-miR-320a	4.75	0.000377914
hsa-let-7g-5p	-4.66	4.37E-09	hsa-miR-6796-3p	-3.26	0.000386843
hsa-miR-145-5p	-7.2	4.73E-09	hsa-miR-6779-5p	3.7	0.000451063
hsa-miR-382-5p	-4.16	7.66E-09	hsa-miR-940	-3.19	0.000462686
hsa-miR-487b-3p	-3.58	1.42E-08	hsa-miR-6132	4.01	0.000647846
hsa-miR-151b	-3.9	1.93E-08	hsa-miR-6743-5p	2.63	0.000677707
hsa-miR-409-3p	-3.92	2.07E-08	hsa-miR-1180-5p	-1.1	0.001185151
hsa-miR-455-5p	-3.62	4.70E-08	hsa-miR-3620-5p	1.88	0.001303606
hsa-miR-19b-3p	-4.34	5.94E-08	hsa-miR-7111-3p	-1.38	0.001447619
hsa-miR-30a-3p	-2.33	1.82E-07	hsa-miR-320e	4.59	0.001516529
hsa-miR-106b-5p	-5.04	2.45E-07	hsa-miR-423-5p	4.1	0.001525621
hsa-let-7f-5p	-4.58	7.25E-07	hsa-miR-6749-5p	3.65	0.001623862
hsa-miR-196a-5p	-4.07	9.98E-07	hsa-miR-4507	3.5	0.001753448
hsa-miR-132-3p	-4.02	1.03E-06	hsa-miR-4530	3.62	0.001942065
hsa-miR-424-3p	-2.48	1.34E-06	hsa-miR-6805-3p	-3.39	0.00207681
hsa-miR-195-5p	-7.3	1.37E-06	hsa-miR-7847-3p	3.53	0.002445626
hsa-miR-654-5p	-1.82	5.39E-06	hsa-miR-4651	3.48	0.003115063
hsa-miR-146b-5p	-3.45	5.78E-06	hsa-miR-4687-3p	2.94	0.003543971
hsa-miR-106a-5p	-4.32	6.72E-06	hsa-miR-4429	3.95	0.00392948
hsa-miR-199a-3p	-6.92	7.44E-06	hsa-miR-877-3p	-1.43	0.004396775
hsa-miR-130a-3p	-3.83	8.22E-06	hsa-miR-149-3p	3.06	0.004622029
hsa-miR-378c	-3.03	1.08E-05	hsa-miR-1202	3.84	0.005077995
hsa-miR-146a-5p	-2.94	1.08E-05	hsa-miR-4492	3.79	0.005255682
hsa-miR-17-5p	-4.42	1.63E-05	hsa-miR-4508	2.7	0.005255682
hsa-miR-331-5p	-1.09	1.92E-05	hsa-miR-6802-5p	2.85	0.005297532
hsa-miR-885-3p	-2.42	2.66E-05	hsa-miR-24-3p	5.88	0.005360181
hsa-miR-196b-5p	-1.81	3.29E-05	hsa-miR-4463	3.59	0.005484815
hsa-miR-24-2-5p	-2.35	3.48E-05	hsa-miR-591	-0.54	0.005669525
hsa-miR-505-5p	-1.78	3.52E-05	hsa-miR-6798-3p	-1.77	0.006284396
hsa-miR-16-5p	-6.62	3.71E-05	hsa-miR-1281	-2.37	0.006531402
hsa-miR-23b-5p	-2.87	4.08E-05	hsa-miR-7641	6.12	0.006813824
hsa-miR-584-5p	-1.07	4.54E-05	hsa-miR-6803-5p	0.92	0.007563374
hsa-miR-378a-3p	-3.92	4.55E-05	hsa-miR-7977	4.07	0.00777261
hsa-miR-28-3p	-3.35	5.56E-05	hsa-miR-4270	3.04	0.009882725
hsa-miR-4417	-3.3	5.87E-05	hsa-miR-6845-5p	1.43	0.009968
hsa-miR-10a-5p	-1.65	6.08E-05	hsa-miR-6820-5p	2.62	0.010210203
hsa-miR-139-3p	-1.47	6.64E-05	hsa-miR-4718	-0.52	0.010438325

hsa-miR-181d-5p	-1.73	6.64E-05	hsa-miR-574-3p	4.39	0.010630373
hsa-miR-155-5p	-4.77	6.66E-05	hsa-miR-520c-3p	-0.43	0.01107774
hsa-miR-3907	-1.62	6.89E-05	hsa-miR-6732-5p	-1.83	0.01234311
hsa-let-7i-5p	-5.4	7.12E-05	hsa-miR-4433b-3p	3.2	0.01274064
hsa-miR-331-3p	-1.73	8.13E-05	hsa-miR-4758-3p	-0.93	0.013085771
hsa-miR-7112-5p	-2.03	8.45E-05	hsa-miR-193a-5p	4.29	0.014008818
hsa-miR-151a-5p	-5.5	8.94E-05	hsa-miR-150-3p	2.7	0.014201627
hsa-miR-20b-5p	-1.83	8.94E-05	hsa-miR-1228-5p	2.71	0.014241987
hsa-miR-26a-5p	-6.47	9.90E-05	hsa-miR-4279	-1.69	0.014357896
hsa-miR-27b-5p	-2.68	9.94E-05	hsa-miR-6088	0.82	0.014534341
hsa-miR-3687	-2.9	0.000112753	hsa-miR-4758-5p	2.79	0.016250206
hsa-miR-4485	-3.2	0.000127989	hsa-miR-4689	3.09	0.016956046
hsa-miR-485-5p	-2.03	0.000129982	hsa-miR-548x-3p	-0.61	0.017274059
hsa-miR-433-3p	-2.25	0.000140101	hsa-miR-4750-3p	-2.45	0.018089108
hsa-miR-30e-5p	-2.12	0.000143842	hsa-miR-575	2.88	0.018281427
hsa-miR-4253	-2.97	0.000163384	hsa-miR-6812-5p	2.58	0.018281427
hsa-miR-708-5p	-3	0.000176524	hsa-let-7a-5p	5.29	0.01841332
hsa-miR-21-5p	-3.2	0.00017822	hsa-miR-8089	2.65	0.018569716
hsa-miR-152-3p	-5.37	0.000188522	hsa-miR-7114-3p	-1.7	0.019399484
hsa-miR-370-3p	-2.13	0.000195326	hsa-miR-6889-5p	2.1	0.020186228
hsa-miR-151a-3p	-4.13	0.000208347	hsa-miR-3120-3p	-0.43	0.02207693
hsa-miR-181a-5p	-4.78	0.000211265	hsa-miR-3664-5p	0.39	0.02309227
hsa-miR-224-3p	-1.62	0.000211265	hsa-miR-877-5p	1.86	0.023601894
hsa-miR-99a-5p	-5.78	0.000213852	hsa-miR-26a-5p	4.79	0.024219472
hsa-miR-8071	-3.61	0.000214268	hsa-miR-6800-3p	-2.65	0.024287151
hsa-miR-324-5p	-2.97	0.000220311	hsa-miR-125a-5p	3.91	0.024379332
hsa-miR-140-5p	-5.11	0.000282594	hsa-miR-548u	-0.51	0.025003838
hsa-miR-1185-1-3p	-1.7	0.000314473	hsa-miR-4741	3.04	0.025437702
hsa-miR-6846-5p	-1.55	0.00031561	hsa-miR-4690-5p	2.69	0.026202577
hsa-miR-378f	-2.27	0.000334095	hsa-miR-3180	2.19	0.02826417
hsa-miR-23b-3p	-6.3	0.00033649	hsa-miR-4665-5p	2.07	0.02851159
hsa-miR-127-5p	-1.19	0.00033649	hsa-miR-23b-3p	5.01	0.02883199
hsa-miR-664a-5p	-2.19	0.000343187	hsa-miR-4728-5p	1.78	0.028977053
hsa-miR-660-5p	-1.95	0.000361938	hsa-miR-103a-3p	4.65	0.029082141
hsa-miR-337-5p	-2.35	0.000390237	hsa-miR-3151-3p	-0.72	0.029091686
hsa-miR-6807-5p	-3.17	0.000392715	hsa-miR-4449	2.78	0.029924576
hsa-miR-93-5p	-3.89	0.000419735	hsa-miR-6086	1.31	0.030032856
hsa-miR-23a-3p	-6.25	0.000439315	hsa-miR-6087	0.67	0.030282347
hsa-miR-3609	-2.65	0.000523689	hsa-miR-4256	-0.46	0.030525108
hsa-miR-339-5p	-2	0.000531525	hsa-miR-23a-3p	5.02	0.030946742
hsa-miR-24-3p	-5.66	0.000597694	hsa-miR-455-3p	-1.37	0.031274952
hsa-miR-3124-5p	-1.5	0.000641191	hsa-miR-2467-3p	0.81	0.031960642
hsa-miR-6080	-1.59	0.000662042	hsa-miR-6763-5p	2.14	0.031995581

hsa-miR-6871-5p	-1.24	0.000662042	hsa-miR-6806-5p	1.31	0.032985466
hsa-miR-1185-2-3p	-1.48	0.000671598	hsa-miR-6797-3p	-2.31	0.033535453
hsa-miR-1254	-1.36	0.000677707	hsa-miR-3651	3.51	0.034504385
hsa-miR-532-5p	-3.17	0.000728571	hsa-miR-2355-5p	-0.6	0.035322337
hsa-miR-29a-3p	-4.29	0.00073299	hsa-miR-134-5p	2.8	0.03536274
hsa-miR-409-5p	-1.94	0.000779596	hsa-miR-4488	1.63	0.035742022
hsa-let-7e-5p	-4.71	0.000798209	hsa-miR-107	4.32	0.035812204
hsa-miR-503-5p	-1.69	0.000856562	hsa-miR-6799-5p	2.94	0.037229481
hsa-miR-18a-5p	-1.84	0.000912747	hsa-miR-4725-5p	-1.15	0.039092445
hsa-miR-34a-5p	-2.85	0.001050485	hsa-miR-6752-5p	2.99	0.04020963
hsa-miR-3154	-1.57	0.00110757	hsa-miR-449c-3p	-0.37	0.040815573
hsa-miR-422a	-1.87	0.001265341	hsa-miR-6819-3p	-2.02	0.040815743
hsa-miR-3135b	-2.99	0.001292101	hsa-miR-5193	-0.89	0.04103568
hsa-miR-222-3p	-4.81	0.001326578	hsa-miR-23a-5p	2.76	0.041649658
hsa-miR-194-5p	-1.64	0.001334904	hsa-miR-6085	2.11	0.04192142
hsa-miR-29c-3p	-1.46	0.001416766	hsa-miR-92a-3p	4.58	0.041977162
hsa-miR-1231	-3.07	0.001456386	hsa-miR-762	1.95	0.043348753
hsa-miR-376c-3p	-1.9	0.001492759	hsa-miR-1468-3p	-0.44	0.044071792
hsa-miR-345-5p	-2.49	0.001493174	hsa-let-7d-5p	4.3	0.044254966
hsa-miR-6742-5p	-1.63	0.001497287	hsa-miR-4539	2.12	0.04432732
hsa-miR-342-5p	-2.23	0.001518563	hsa-miR-3162-5p	2.66	0.046461316
hsa-miR-557	-1.42	0.001617047	hsa-miR-8063	2.53	0.047552766
hsa-miR-6754-3p	-1.04	0.001666376	hsa-let-7e-5p	3.72	0.048308578
hsa-miR-6875-5p	-1.2	0.001737063	hsa-miR-6513-5p	0.68	0.048323174
hsa-miR-711	-1.01	0.001876322	hsa-miR-135b-5p	-0.55	0.048818559
hsa-miR-135a-3p	-1.75	0.001957012	hsa-miR-3126-3p	0.41	0.048818559
hsa-miR-6825-5p	-1.75	0.001957012	hsa-miR-1279	-0.42	0.049007779
hsa-miR-361-5p	-4.2	0.001968107			
hsa-miR-6881-5p	-0.49	0.002102616			
hsa-miR-4726-5p	-1.14	0.002166785			
hsa-miR-4750-3p	2.42	0.002225163			
hsa-miR-342-3p	-4.4	0.002337632			
hsa-miR-191-5p	-4.76	0.002386854			
hsa-let-7a-5p	-5.19	0.002505639			
hsa-miR-100-5p	-5.01	0.002511593			
hsa-miR-4447	-0.86	0.002511593			
hsa-miR-4673	-1.16	0.002721069			
hsa-miR-107	-4.65	0.002746171			
hsa-miR-1273h-5p	-1.57	0.002750484			
hsa-miR-30c-2-3p	-1.03	0.00286679			
hsa-miR-125a-5p	-3.93	0.002892642			
hsa-miR-487a-5p	-1.36	0.002897906			
hsa-miR-6746-5p	-1.57	0.002899101			
hsa-miR-191-3p	-1.18	0.003067062			

hsa-miR-1260a	0.96	0.003085032
hsa-miR-6824-5p	-3.01	0.003112842
hsa-miR-10b-3p	-1.44	0.003401744
hsa-miR-221-3p	-4.23	0.003401744
hsa-miR-652-3p	-2.81	0.003401744
hsa-miR-103a-3p	-4.72	0.003494151
hsa-miR-654-3p	-1.73	0.003507044
hsa-miR-30b-3p	-1.22	0.003537269
hsa-miR-199a-5p	-4.2	0.003543971
hsa-miR-421	-1.48	0.00359403
hsa-miR-93-3p	-1.34	0.003808028
hsa-let-7d-5p	-4.62	0.003825326
hsa-miR-185-5p	-3.59	0.003991644
hsa-miR-30d-5p	-3.24	0.004018527
hsa-miR-125b-2-3p	-3.05	0.004262891
hsa-miR-1281	1.93	0.004302475
hsa-miR-27b-3p	-4.5	0.004360367
hsa-miR-4324	-0.88	0.004652409
hsa-miR-497-5p	-3.94	0.00475851
hsa-miR-4525	-1.48	0.00475851
hsa-miR-330-3p	-1.01	0.004762611
hsa-miR-6806-5p	-1.31	0.004762611
hsa-miR-1273d	-1.22	0.004839803
hsa-miR-199b-5p	-1.35	0.004852427
hsa-miR-1273f	-1.68	0.005022798
hsa-miR-6753-5p	-1.37	0.005094831
hsa-miR-6737-5p	-1.29	0.005285477
hsa-miR-22-3p	-4.55	0.005363484
hsa-miR-6808-5p	-2.14	0.005363484
hsa-miR-212-3p	-1.03	0.005441535
hsa-miR-4783-3p	-1.58	0.005491503
hsa-miR-663b	-1.44	0.005749882
hsa-miR-3921	2.06	0.005916613
hsa-miR-196b-3p	-1.17	0.006009435
hsa-miR-127-3p	-4.01	0.006274829
hsa-miR-5698	-0.93	0.006332704
hsa-miR-6865-5p	-1.16	0.006470483
hsa-miR-6768-5p	-1.61	0.006509487
hsa-let-7c-5p	-2.68	0.006620239
hsa-miR-425-5p	-2.94	0.006630423
hsa-miR-3181	-0.77	0.00686925
hsa-miR-381-3p	-1.3	0.007081132
hsa-miR-154-5p	-1.67	0.007091225
hsa-miR-3664-5p	0.35	0.007230224

hsa-miR-4685-5p	-1.56	0.007242272
hsa-miR-6732-5p	1.51	0.00735397
hsa-miR-6829-5p	-1.29	0.00736005
hsa-miR-377-5p	-1.09	0.007380505
hsa-miR-625-5p	-1.16	0.00762787
hsa-miR-5739	-1.69	0.00777261
hsa-miR-26b-5p	-0.89	0.007972968
hsa-miR-205-3p	-1.12	0.008108465
hsa-miR-4284	-1.66	0.008144449
hsa-miR-99a-3p	-1.12	0.008541873
hsa-miR-4535	-0.99	0.009550382
hsa-miR-642b-3p	-1.55	0.009850767
hsa-miR-4436b-5p	-1.43	0.010578176
hsa-miR-378i	-1.72	0.01061259
hsa-miR-6780b-3p	0.75	0.010794095
hsa-miR-6830-5p	-0.88	0.011055727
hsa-miR-106b-3p	-2.03	0.011254494
hsa-miR-23c	-0.89	0.011288326
hsa-miR-29b-1-5p	-0.79	0.01138115
hsa-miR-1246	-2.72	0.011686501
hsa-miR-4725-3p	-1.53	0.011816716
hsa-miR-8075	1.96	0.012196033
hsa-miR-7109-5p	-1.55	0.012279843
hsa-miR-149-5p	-1.09	0.012649417
hsa-miR-487a-3p	-1.11	0.012649417
hsa-miR-198	-1.21	0.013085771
hsa-miR-134-5p	-2.5	0.014005469
hsa-miR-130b-3p	-2.56	0.014035875
hsa-miR-128-3p	-1.11	0.014112386
hsa-miR-493-3p	-1.48	0.01411325
hsa-miR-3652	-1.17	0.01411325
hsa-miR-3180	-1.88	0.01411325
hsa-miR-664b-5p	-1.32	0.01437568
hsa-miR-548av-3p	0.41	0.014513209
hsa-miR-200c-3p	-1.09	0.015110703
hsa-miR-1973	-1.47	0.015110703
hsa-miR-371a-5p	-0.85	0.015201006
hsa-miR-181d-3p	-0.87	0.01522335
hsa-miR-4715-5p	-0.51	0.015262529
hsa-miR-4462	-1.56	0.01534453
hsa-miR-99b-5p	-3.58	0.015745485
hsa-miR-615-5p	-0.8	0.01583846
hsa-miR-6800-3p	2.18	0.016095452
hsa-miR-214-5p	-1.94	0.016866823
hsa-miR-181c-5p	-1.14	0.016908868

hsa-miR-3180-3p	-2.48	0.017002329
hsa-miR-195-3p	-1.36	0.017081955
hsa-miR-551b-5p	-0.84	0.017081955
hsa-miR-5589-5p	-0.65	0.017081955
hsa-miR-6762-5p	-0.96	0.017081955
hsa-miR-6880-5p	-1.41	0.017199414
hsa-miR-339-3p	-2.35	0.017379213
hsa-miR-17-3p	-1.19	0.017588632
hsa-miR-10a-3p	0.35	0.017664904
hsa-miR-3130-3p	-0.59	0.017675837
hsa-miR-135a-5p	0.34	0.017973088
hsa-miR-4316	-0.43	0.017998864
hsa-miR-6862-5p	-0.67	0.01810689
hsa-miR-194-3p	-0.78	0.018281427
hsa-miR-29c-5p	-0.59	0.018818872
hsa-miR-378d	-1.18	0.018948272
hsa-miR-504-3p	-1.38	0.019062771
hsa-miR-27a-3p	-4.06	0.019241152
hsa-miR-3620-5p	1.08	0.019241152
hsa-miR-125b-5p	-2.51	0.019837133
hsa-miR-7114-5p	-1.73	0.020204866
hsa-miR-6861-5p	-1.77	0.020223768
hsa-miR-486-3p	-0.48	0.020709085
hsa-miR-494-3p	-2.45	0.020740883
hsa-miR-30e-3p	-1.01	0.02207693
hsa-miR-6747-5p	-0.54	0.02207693
hsa-miR-324-3p	-2.2	0.022171147
hsa-miR-148b-5p	0.46	0.022263219
hsa-miR-3121-3p	-0.39	0.022327552
hsa-miR-5195-3p	-1.47	0.023252314
hsa-miR-1266-5p	-0.54	0.023917144
hsa-miR-4257	-0.79	0.023917144
hsa-miR-192-5p	-0.7	0.023933082
hsa-miR-362-5p	-1.67	0.023947018
hsa-miR-6774-5p	-1.01	0.024750316
hsa-miR-22-5p	-0.78	0.02522075
hsa-miR-4292	-0.65	0.025326955
hsa-miR-4534	-1.27	0.025466238
hsa-miR-325	-0.39	0.02558789
hsa-miR-143-5p	-0.71	0.025972491
hsa-miR-92a-3p	-3.83	0.026450886
hsa-miR-6797-5p	-1.13	0.026450886
hsa-miR-6820-3p	0.56	0.02677921
hsa-miR-6847-5p	-1.8	0.02677921
hsa-miR-1299	-0.59	0.027042314

hsa-miR-181a-2-3p	-0.99	0.027159044
hsa-miR-1228-3p	1.53	0.027159044
hsa-miR-6757-5p	-1.5	0.027890698
hsa-miR-6781-5p	-1.7	0.028943187
hsa-miR-3607-5p	-0.96	0.029277098
hsa-miR-4498	-1.46	0.02991739
hsa-miR-377-3p	-0.4	0.030312165
hsa-miR-6717-5p	-0.61	0.031256427
hsa-miR-7-2-3p	0.36	0.031995581
hsa-miR-4283	-0.45	0.032612083
hsa-miR-6887-5p	-1.09	0.033234756
hsa-miR-6785-5p	-1.32	0.033478894
hsa-miR-4446-3p	-0.72	0.033868155
hsa-miR-4748	-0.43	0.03449092
hsa-miR-148b-3p	-1.28	0.034549781
hsa-miR-498	-0.92	0.035322337
hsa-miR-6515-5p	-0.7	0.035551052
hsa-miR-6721-5p	-1.26	0.035791098
hsa-miR-1914-3p	-0.83	0.036800847
hsa-miR-6890-5p	-0.72	0.036885636
hsa-miR-4786-3p	-0.66	0.037517115
hsa-miR-6753-3p	-1.02	0.037517115
hsa-miR-6819-5p	-1.89	0.038062423
hsa-miR-6084	-1.31	0.03884799
hsa-miR-4655-5p	-1.44	0.04020963
hsa-miR-3613-5p	2.53	0.04049252
hsa-miR-542-5p	-0.72	0.041215152
hsa-miR-548a-3p	2.29	0.041450822
hsa-miR-500a-5p	-1.34	0.041856784
hsa-miR-34a-3p	-0.5	0.042547139
hsa-miR-4274	1.65	0.042660611
hsa-miR-4746-3p	-0.54	0.043597083
hsa-miR-4685-3p	-0.62	0.044254966
hsa-miR-4327	-1.06	0.044815606
hsa-miR-4732-5p	-1.07	0.045208942
hsa-miR-4430	-1.29	0.045640594
hsa-miR-1538	-1.02	0.046232489
hsa-miR-4278	-0.37	0.047089566
hsa-miR-3178	-1.29	0.048886666
hsa-miR-548y	-0.38	0.049342606
hsa-miR-3195	-2.05	0.049492783
hsa-miR-548q	-0.41	0.049581805
hsa-miR-3622b-5p	-0.92	0.049584947
hsa-miR-6728-5p	-1.16	0.049584947

**Old OA Lesioned vs Old OA Intact-2 (Columns A, B and C)****Old OA Intact-1 vs Old OA Intact-2 (Columns D, E and F)**(FC= $\log_2$  Fold change, FDR=False Discover Rate, Les=OA-Lesioned, Int=OA-Intact)

Transcript ID	FC Les vs Int-2	FDR Les vs Int-2	Transcript ID	FC Int-1 vs Int-2	FDR Int-1 vs Int-2
hsa-miR-1180-5p	-0.77	0.009694881	hsa-let-7c-5p	-9.97	4.35E-09
hsa-miR-1343-3p	-0.44	0.014885525	hsa-let-7b-5p	-9.36	4.70E-08
hsa-miR-3934-5p	-0.57	0.02549318	hsa-miR-4454	-7.83	6.94E-08
hsa-miR-548ad	0.38	0.025821697	hsa-miR-125b-5p	-9.14	8.14E-08
hsa-miR-4666b	-0.48	0.026301219	hsa-miR-5100	-9.27	2.41E-07
hsa-miR-3202	-0.63	0.027159044	hsa-miR-210-3p	-7.01	5.53E-06
hsa-miR-668-3p	-0.68	0.032902968	hsa-miR-1273g-3p	-8.11	8.00E-06
hsa-miR-5591-5p	-0.46	0.033719929	hsa-miR-320c	-6.23	3.44E-05
hsa-miR-513c-3p	-0.48	0.034512295	hsa-miR-320d	-6.45	4.26E-05
hsa-miR-6796-5p	1.09	0.041376783	hsa-miR-193b-3p	-7.57	5.71E-05
hsa-miR-3914	-0.5	0.042694986	hsa-miR-320e	-6.43	7.86E-05
hsa-miR-3688-3p	0.48	0.047257571	hsa-miR-214-3p	-6.53	9.90E-05
			hsa-miR-320b	-6.35	0.000128241
			hsa-miR-7977	-6.44	0.000152838
			hsa-miR-4505	-4.2	0.000229215
			hsa-miR-24-3p	-8.56	0.000250603
			hsa-miR-937-5p	-3.61	0.000330464
			hsa-miR-4429	-5.37	0.00037246
			hsa-miR-423-5p	-5.05	0.000390237
			hsa-miR-7641	-8.81	0.000390237
			hsa-miR-320a	-5.12	0.00043626
			hsa-miR-6132	-4.5	0.000471017
			hsa-miR-6796-3p	3.49	0.000490611
			hsa-miR-6743-5p	-2.87	0.000677707
			hsa-let-7a-5p	-8.13	0.000756652
			hsa-miR-125a-5p	-6.25	0.000772999
			hsa-miR-6779-5p	-3.81	0.000868949
			hsa-miR-193a-5p	-6.22	0.000960541
			hsa-miR-744-5p	-4	0.000978197
			hsa-let-7e-5p	-6.36	0.001291066
			hsa-miR-574-3p	-6.01	0.001292257

hsa-miR-23b-3p	-7.87	0.001303606
hsa-miR-1202	-4.8	0.001360182
hsa-miR-591	0.66	0.001754193
hsa-miR-92a-3p	-7.41	0.00180264
hsa-let-7d-5p	-6.86	0.0022226
hsa-miR-26a-5p	-6.94	0.002234389
hsa-miR-193b-5p	-5.14	0.003157938
hsa-miR-4507	-3.59	0.003157938
hsa-miR-548n	0.53	0.003519406
hsa-miR-23a-3p	-7.16	0.003808028
hsa-miR-668-3p	-1.12	0.00392948
hsa-miR-7847-3p	-3.63	0.004291367
hsa-miR-4758-3p	1.16	0.004362096
hsa-miR-940	2.8	0.004590493
hsa-miR-23a-5p	-3.99	0.005104545
hsa-miR-4530	-3.55	0.005214083
hsa-miR-3620-5p	-1.78	0.005248823
hsa-miR-149-3p	-3.29	0.005255682
hsa-miR-4687-3p	-3.06	0.005441535
hsa-miR-6749-5p	-3.45	0.006405887
hsa-miR-548ad	0.56	0.007332888
hsa-miR-191-5p	-5.91	0.007533354
hsa-miR-3688-3p	0.77	0.00777261
hsa-miR-4651	-3.42	0.00777261
hsa-miR-6800-3p	3.36	0.00777261
hsa-miR-99a-5p	-5.75	0.007942131
hsa-miR-4463	-3.74	0.008166454
hsa-miR-520c-3p	0.48	0.008875159
hsa-miR-107	-5.57	0.011180246
hsa-miR-103a-3p	-5.79	0.011423186
hsa-miR-4492	-3.74	0.012293318
hsa-miR-3651	-4.45	0.01234311
hsa-miR-6798-3p	1.78	0.01239332
hsa-miR-1281	2.37	0.013354375
hsa-miR-4689	-3.45	0.014113385
hsa-miR-3925-5p	0.67	0.01487736
hsa-miR-423-3p	-4.73	0.015460671
hsa-miR-4750-3p	2.71	0.01621448
hsa-miR-6805-3p	2.88	0.018136072
hsa-miR-195-5p	-4.65	0.018281427
hsa-miR-455-3p	1.61	0.018281427
hsa-miR-4508	-2.52	0.018796817
hsa-miR-6738-3p	0.7	0.019363363
hsa-miR-22-3p	-5.42	0.02043889
hsa-miR-151a-5p	-4.51	0.020539631

hsa-miR-7107-5p	2.75	0.021882546
hsa-miR-100-5p	-5.39	0.023298086
hsa-miR-27b-3p	-5.12	0.023579731
hsa-miR-6802-5p	-2.57	0.023855959
hsa-miR-4433b-3p	-3.19	0.024379332
hsa-miR-6803-5p	-0.86	0.024833007
hsa-miR-7111-3p	1.08	0.024898966
hsa-miR-6812-5p	-2.69	0.025003838
hsa-miR-6511b-5p	2.36	0.026450886
hsa-miR-6745	0.7	0.027005534
hsa-miR-27a-3p	-5.4	0.027677414
hsa-miR-1228-5p	-2.68	0.028013555
hsa-miR-4741	-3.24	0.029247388
hsa-miR-4758-5p	-2.78	0.029488342
hsa-let-7i-5p	-4.08	0.031252384
hsa-miR-4693-5p	0.4	0.031868737
hsa-miR-34c-5p	0.6	0.032336957
hsa-miR-135b-5p	0.64	0.032974733
hsa-miR-497-5p	-4.29	0.033160545
hsa-miR-3195	-3.07	0.033441344
hsa-miR-1288-3p	0.49	0.035334136
hsa-miR-4270	-2.74	0.037581379
hsa-miR-4488	-1.76	0.039244011
hsa-miR-3914	-0.63	0.039873533
hsa-miR-328-3p	-3.27	0.041225284
hsa-miR-6820-5p	-2.34	0.041273018
hsa-miR-6790-5p	-3.44	0.041856784
hsa-miR-6727-3p	1.08	0.042547139
hsa-miR-4690-5p	-2.72	0.042667117
hsa-miR-6088	-0.75	0.044646132
hsa-miR-4274	2.29	0.045559612
hsa-miR-3175	-4.2	0.046788181
hsa-miR-877-3p	1.13	0.046973053
hsa-miR-8089	-2.5	0.047257571
hsa-miR-4728-5p	-1.78	0.048818559
hsa-miR-6499-3p	0.65	0.048818559
hsa-miR-6732-5p	1.62	0.048818559
hsa-miR-6866-5p	0.5	0.049392034
hsa-miR-99b-5p	-4.21	0.049964737



Analysis Name: OA-Lesioned vs Young Intact Core Analysis

Analysis Creation Date: 2021-02-06

Build version: exported

Content version: 60467501 (Release Date: 2020-11-19)

## Experiment Metadata

Name	Value

## Analysis Settings

## Top Canonical Pathways

Name	p-value	Overlap
Osteoarthritis Pathway	9,23E-51	21,4 % 47/220
Hepatic Fibrosis / Hepatic Stellate Cell Activation	3,50E-40	20,4 % 38/186
Role of Osteoblasts, Osteoclasts and Chondrocytes in Rheumatoid Arthritis	2,16E-37	17,4 % 38/218
Tumor Microenvironment Pathway	4,31E-35	19,3 % 34/176



**Top Upstream Regulators****Upstream Regulators**

Name	p-value	Predicted Activation
IL1B	1,92E-66	
TNF	5,33E-62	
beta-estradiol	2,11E-55	
TGFB1	2,11E-55	
HIF1A	3,58E-54	

**Causal Network**

Name	p-value	Predicted Activation
EAF2	3,75E-65	
RUNX2	2,56E-62	
gallium nitrate	2,53E-60	
PAQR3	1,85E-59	
PROTEASE	2,29E-59	

**Top Diseases and Bio Functions**



## Summary of Analysis - OA-Lesioned vs Young Intact Core Analysis

---

### Diseases and Disorders

Name	p-value range	# Molecules
Cancer	1,11E-22 - 4,69E-63	188
Organismal Injury and Abnormalities	1,69E-22 - 4,69E-63	212
Cardiovascular Disease	5,46E-23 - 1,51E-56	139
Inflammatory Response	2,28E-22 - 7,97E-50	155
Connective Tissue Disorders	8,87E-23 - 2,96E-48	147

### Molecular and Cellular Functions

Name	p-value range	# Molecules
Cellular Movement	9,40E-23 - 5,42E-72	157
Cellular Development	2,13E-22 - 1,17E-69	185
Cellular Growth and Proliferation	2,13E-22 - 3,33E-64	178
Cell Death and Survival	1,69E-22 - 3,33E-60	162
Cell-To-Cell Signaling and Interaction	1,81E-22 - 3,98E-56	141

### Physiological System Development and Function

Name	p-value range	# Molecules
Embryonic Development	2,09E-22 - 6,66E-72	162
Organismal Development	2,09E-22 - 6,66E-72	182
Connective Tissue Development and Function	7,96E-24 - 1,17E-69	153



**Skeletal and Muscular System Development and Function**

8,87E-23 - 4,65E-68

165

**Top Tox Functions****Assays: Clinical Chemistry and Hematology**

Name	p-value range	# Molecules
<a href="#">Increased Levels of Alkaline Phosphatase</a>	4,56E-02 - 3,73E-35	27
<a href="#">Increased Levels of LDH</a>	5,33E-03 - 7,77E-07	6
<a href="#">Decreased Levels of Albumin</a>	6,33E-02 - 9,25E-07	6
<a href="#">Increased Levels of ALT</a>	1,26E-03 - 1,51E-06	6
<a href="#">Increased Levels of Creatinine</a>	1,31E-01 - 2,17E-05	6

**Cardiotoxicity**

Name	p-value range	# Molecules
<a href="#">Cardiac Enlargement</a>	2,23E-01 - 3,24E-42	67
<a href="#">Cardiac Dysfunction</a>	3,12E-01 - 3,10E-26	37
<a href="#">Heart Failure</a>	9,76E-02 - 1,33E-21	32
<a href="#">Cardiac Infarction</a>	1,55E-01 - 1,60E-20	29
<a href="#">Cardiac Fibrosis</a>	5,45E-02 - 5,02E-18	25

## Hepatotoxicity

---

(c) 2000-2021 QIAGEN. All rights reserved.

INGENUITY  
PATHWAY ANALYSIS

## Summary of Analysis - OA-Lesioned vs Young Intact Core Analysis

Name	p-value range	# Molecules
Liver Proliferation	1,93E-01 - 6,04E-38	40
Hepatocellular carcinoma	1,06E-01 - 2,44E-24	72
Liver Hyperplasia/Hyperproliferation	1,63E-01 - 2,44E-24	128
Liver Fibrosis	1,23E-01 - 7,32E-23	49
Liver Inflammation/Hepatitis	1,86E-01 - 3,68E-18	32

## Nephrotoxicity

Name	p-value range	# Molecules
Renal Necrosis/Cell Death	4,56E-02 - 7,35E-21	40
Renal Damage	8,91E-02 - 1,02E-18	27
Kidney Failure	8,91E-02 - 1,80E-18	27
Renal Proliferation	7,20E-02 - 1,40E-16	23
Glomerular Injury	2,86E-01 - 4,54E-15	43

## Top Regulator Effect Networks

## Top Networks

ID	Associated Network Functions	Score
----	------------------------------	-------



## Summary of Analysis - OA-Lesioned vs Young Intact Core Analysis

	Cellular Development, Connective Tissue Development and Function, Skeletal and Muscular System Development and Function	37
1		
2	Tissue Development, Carbohydrate Metabolism, Small Molecule Biochemistry	30
3	Tissue Development, Connective Tissue Disorders, Organismal Injury and Abnormalities	30
4	Cardiovascular Disease, Cardiovascular System Development and Function, Organ Morphology	28
5	Inflammatory Disease, Inflammatory Response, Organismal Injury and Abnormalities	26

### Top Tox Lists

Name	p-value	Overlap
Hepatic Fibrosis	2,14E-38	13,0 % 45/346
Liver Proliferation	5,91E-37	15,3 % 40/262

**Cardiac Hypertrophy**

**Renal Necrosis/Cell Death**

1,28E-28

1,56E-22

9,9 % 39/395

6,5 % 40/613

---

(c) 2000-2021 QIAGEN. All rights reserved.

**INGENUITY**  
PATHWAY ANALYSIS

## Summary of Analysis - OA-Lesioned vs Young Intact Core Analysis

---

**Increases Glomerular Injury**

1,43E-20

15,2 % 22/145

**Top My Lists**

**Top My Pathways**

**Top Analysis-Ready Molecules**



## **Appendix to Chapter 5**

Appendix to Chapter 5 contains the list of differentially expressed proteins ( $p<0.05$ ) that were identified in human primary OA chondrocytes treated with miR-143-3p mimic or control and inhibitor or control, following liquid chromatography-tandem mass spectrometry. Differentially expressed proteins were identified by undertaking two-tailed paired t-tests. T-statistic and gene ID for each protein is indicated. Moreover, for each set of differentially expressed proteins, a Core Analysis was undertaken in Ingenuity PathwayAnalysis (Qiagen, UK), to identify biological pathways of interest. The report generated for each set of proteins is included here.

### **A. Mimic vs Control-mimic comparison**

Protein ID	Gene Name	P value	T-statistic
P11413	G6PD	0.000322	11.54044
Q9Y678	COPG1	0.000732	-9.34029
P50991	CCT4	0.004404	-5.79679
Q07866	KLC1	0.005327	5.500224
P09871	C1S	0.005463	5.461922
P11387	TOP1	0.005622	-5.41861
Q9Y383	LUC7L2	0.005772	-5.37924
P08253	MMP2	0.007066	5.083034
P02792	FTL	0.007693	4.962408
Q96HY6	DDRGK1	0.007844	4.935131
P21796	VDAC1	0.007911	4.92333
Q9Y6N5	SQOR	0.009081	-4.73348
P51659	HSD17B4	0.010273	4.568451
O95433	AHSA1	0.01041	-4.55094
Q15233	NONO	0.010582	-4.52944
P17302	GJA1	0.010824	4.499773
P14550	AKR1A1	0.011041	4.474002
Q3SY69	ALDH1L2	0.011281	4.446105
Q8NB5J	COLGALT1	0.011311	-4.44265
Q96AZ6	ISG20	0.012599	-4.3047
Q13547	HDAC1	0.013085	-4.25698
P68431	H3C1	0.013131	-4.25261
Q13098	GPS1	0.013437	4.223782
P61758	VBP1	0.014133	-4.16106

P49773	HINT1	0.014288	-4.1476
P67812	SEC11A	0.014403	-4.13774
Q9UL25	RAB21	0.015146	-4.07614
P08174	CD55	0.015383	-4.0573
Q96S97	MYADM	0.015659	-4.03572
P60228	EIF3E	0.015752	-4.0286
P14678	SNRPB	0.016904	-3.94392
Q9UHB6	LIMA1	0.017461	-3.90541
P62913	RPL11	0.017514	3.901823
Q15637	SF1	0.017994	-3.86994
Q5T9A4	ATAD3B	0.018104	-3.86282
P29992	GNA11	0.018214	3.855679
P17936	IGFBP3	0.019169	-3.79602
O00622	CCN1	0.019274	-3.78969
P00450	CP	0.019582	3.771305
P08758	ANXA5	0.019871	3.754414
P27348	YWHAQ	0.01995	3.749816
P49591	SARS1	0.020372	3.725744
Q8TCT9	HM13	0.020929	-3.69487
P62280	RPS11	0.020939	-3.69433
Q8IXQ6	PARP9	0.021497	-3.66441
O95302	FKBP9	0.024072	3.537306
P23396	RPS3	0.024587	-3.51382
Q08257	CRYZ	0.025097	3.491142
P39023	RPL3	0.025697	-3.46516
Q96T51	RUFY1	0.025815	-3.4601
P09622	DLD	0.025958	-3.45408
Q96QK1	VPS35	0.026461	3.433089
Q9BXJ9	NAA15	0.026874	-3.41621
P35354	PTGS2	0.027714	-3.38277
Q9H488	POFUT1	0.028009	-3.37136
P07741	APRT	0.028046	-3.36992
P43490	NAMPT	0.028548	3.350769
P16615	ATP2A2	0.031647	-3.24089
P18510	IL1RN	0.032101	-3.22588
P36222	CHI3L1	0.032672	3.20734
Q15758	SLC1A5	0.032701	3.2064
Q9H4F8	SMOC1	0.032887	-3.20044
Q9Y6K5	OAS3	0.033132	-3.19267
Q9BRF8	CPPED1	0.034055	3.163939
P0DP23	CALM1	0.034057	-3.16388
P63104	YWHAZ	0.034853	3.139847
P31689	DNAJA1	0.03669	-3.08676
Q9NS69	TOMM22	0.037337	-3.06879
P36578	RPL4	0.03775	-3.05751

Q13526	PIN1	0.03814	-3.04699
Q9BTM4	TMEM43	0.039491	3.011527
Q01469	FABP5	0.041955	-2.95034
O95373	IPO7	0.042596	-2.9351
Q14103	HNRNPD	0.044061	-2.90128
Q9Y3A5	SBDS	0.044124	-2.89985
O00410	IPO5	0.0442	-2.89816
P60842	EIF4A1	0.044666	-2.88771
P08754	GNAI3	0.045856	2.861581
P25398	RPS12	0.045998	-2.85853
Q96A26	FAM162A	0.04622	-2.85375
Q9Y2W1	THRAP3	0.046755	-2.84238
Q05519	SRSF11	0.046876	-2.83983
P35268	RPL22	0.047159	-2.83388
Q96A72	MAGOHB	0.047517	-2.82642
E9PAV3	NACA	0.047521	2.826351
Q4ZH4	FNDC1	0.049184	-2.79255
P12814	ACTN1	0.049379	2.788674
P05362	ICAM1	0.049861	-2.77916

# INGENUITY® PATHWAY ANALYSIS



Analysis Name: Mimic vs Control-mimic

Analysis Creation Date: 2021-02-20

Build version: exported

Content version: 60467501 (Release Date: 2020-11-19)

## Experiment Metadata

Name

Value

## Analysis Settings

## Top Canonical Pathways

Name	p-value	Overlap
EIF2 Signaling	1,90E-07	4,0 % 9/224
Regulation of eIF4 and p70S6K Signaling	4,38E-04	3,0 % 5/166
Calcium Transport I	6,34E-04	20,0 % 2/10
IGF-1 Signaling	6,78E-04	3,8 % 4/104
Apelin Endothelial Signaling Pathway	9,88E-04	3,5 % 4/115

**Top Upstream Regulators****Upstream Regulators**

Name	p-value	Predicted Activation
LARP1	1,18E-09	Activated
MYC	1,25E-09	
tretinoïn	9,45E-09	
torin1	4,00E-08	
MYCN	1,74E-07	

**Causal Network**

Name	p-value	Predicted Activation
MNK1/2	1,71E-11	
L-asparagine	4,66E-11	Inhibited
VWF	6,53E-11	
MLKL	1,15E-10	
TSPAN33	1,51E-10	

**Top Diseases and Bio Functions****Diseases and Disorders**

## Summary of Analysis - Mimic vs Control-mimic

---

Name	p-value range	# Molecules
Cancer	3,81E-03 - 5,09E-08	85
Organismal Injury and Abnormalities	3,81E-03 - 5,09E-08	86
Tumor Morphology	3,32E-03 - 5,09E-08	18
Dermatological Diseases and Conditions	3,81E-03 - 2,84E-07	23
Reproductive System Disease	3,81E-03 - 9,90E-07	58

## Molecular and Cellular Functions

Name	p-value range	# Molecules
RNA Damage and Repair	4,10E-10 - 2,66E-11	10
Protein Synthesis	5,75E-05 - 7,57E-11	28
Cell Death and Survival	3,81E-03 - 5,09E-08	46
Cellular Development	3,81E-03 - 5,21E-08	37
Cellular Growth and Proliferation	3,81E-03 - 5,21E-08	36

## Physiological System Development and Function

Name	p-value range	# Molecules
Skeletal and Muscular System Development and Function	3,81E-03 - 1,46E-06	14
Organ Development	3,81E-03 - 1,87E-06	13
Tissue Development	3,81E-03 - 1,87E-06	27
Cardiovascular System Development and Function	3,81E-03 - 5,97E-06	17
Organismal Development	3,81E-03 - 5,97E-06	27

## Top Tox Functions

### Assays: Clinical Chemistry and Hematology

Name	p-value range	# Molecules
Decreased Levels of Albumin	4,48E-02 - 8,32E-03	2
Increased Levels of Albumin	2,27E-02 - 2,27E-02	1
Increased Levels of Creatinine	5,57E-02 - 2,27E-02	2
Increased Levels of Hematocrit	4,64E-02 - 4,64E-02	2
Increased Levels of AST	7,00E-02 - 7,00E-02	1

### Cardiotoxicity

Name	p-value range	# Molecules
Cardiac Arrhythmia	1,87E-01 - 4,18E-04	7
Cardiac Stenosis	4,48E-02 - 9,25E-04	3
Cardiac Dilation	2,58E-01 - 3,81E-03	5
Cardiac Enlargement	3,39E-01 - 3,81E-03	7
Cardiac Necrosis/Cell Death	1,52E-02 - 3,81E-03	5

### Hepatotoxicity

## Summary of Analysis - Mimic vs Control-mimic

Name	p-value range	# Molecules
Liver Hemorrhaging	5,83E-03 - 3,81E-03	2
Hepatocellular carcinoma	3,54E-01 - 4,24E-03	16
Liver Hyperplasia/Hyperproliferation	3,54E-01 - 4,24E-03	41
Liver Cholestasis	2,27E-02 - 1,52E-02	1
Liver Proliferation	2,05E-01 - 1,52E-02	4

## Nephrotoxicity

Name	p-value range	# Molecules
Renal Enlargement	2,64E-02 - 8,38E-06	4
Renal Atrophy	3,01E-02 - 6,78E-05	3
Renal Inflammation	2,15E-01 - 6,34E-04	5
Renal Nephritis	2,15E-01 - 6,34E-04	5
Renal Damage	1,22E-01 - 7,89E-04	8

## Top Regulator Effect Networks

ID	Regulators	Disease & Functions	Consistency Score
1	LARP1	Cell death of osteosarcoma cells	-4,082

## Top Networks

## Summary of Analysis - Mimic vs Control-mimic

ID	Associated Network Functions	Score
1	RNA Damage and Repair, Protein Synthesis, Cancer	55
2	Lipid Metabolism, Molecular Transport, Small Molecule Biochemistry	25
3	Cancer, Organismal Injury and Abnormalities, Reproductive System Disease	25
4	Cell Morphology, Tissue Development, Cancer	22
5	Cellular Assembly and Organization, Connective Tissue Disorders, Developmental Disorder	20

### Top Tox Lists

Name	p-value	Overlap
<a href="#">Renal Necrosis/Cell Death</a>	2,35E-03	1,3 % 8/613
<a href="#">Genes associated with Chronic Allograft Nephropathy (Human)</a>	2,88E-03	9,5 % 2/21
<a href="#">Cardiac Necrosis/Cell Death</a>	6,42E-03	1,6 % 5/307
<a href="#">Decreases Depolarization of Mitochondria and Mitochondrial Membrane</a>		<a href="#">Cell Cycle: G2/M DNA Damage CheckpointRegulation</a>

7,03E-03

6,1 % 2/33

1,68E-02

3,8 % 2/52

**Top My Lists****Top My Pathways****Top Analysis-Ready Molecules****Expr Log Ratio**

Molecules	Expr. Value	Chart
G6PD	↑ 11,540	
KLC1	↑ 5,500	
C1S	↑ 5,462	
MMP2	↑ 5,083	
FTL	↑ 4,962	
DDRGK1	↑ 4,935	
VDAC1	↑ 4,923	
HSD17B4	↑ 4,568	
GJA1	↑ 4,500	
AKR1A1	↑ 4,474	

**Expr Log Ratio**

Molecules	Expr. Value	Chart
COPG1	▲ -9,340	
CCT4	▲ -5,797	
TOP1	▲ -5,419	
LUC7L2	▲ -5,379	
SQOR	▲ -4,733	
AHSA1	▲ -4,551	
NONO	▲ -4,529	
COLGALT1	▲ -4,443	
ISG20	▲ -4,305	
HDAC1	▲ -4,257	

**B. Inhibitor vs Control-inhibitor comparison**

Protein ID	Gene Name	P value	T-statistic
Q00653	RTCB	0.000251908	12.28835438
P83731	PSMA7	0.001065084	8.469575083
Q9UQ35	SUCLG1	0.001108887	8.380726513
Q92544	RPS14	0.001337117	7.979125686
P46779	DPM3	0.001591248	7.621415253
Q96PK6	PCNA	0.002557425	6.717220544
P28070	RPL24	0.003801506	-6.034610437
Q9H3P7	CZIB	0.003919213	5.984625312
P61970	DIABLO	0.004349442	-5.816480827
Q969V3	PPP2R1A	0.007511386	4.996052903
Q9P2X0	FBL	0.008635439	4.802016541
O14818	PABPC4	0.010496386	-4.540090438
P62241	ARL3	0.010705504	4.514216211
Q6RW13	RPS8	0.010790073	4.503925891
Q9NTK5	PSMD10	0.013018177	4.263413144
Q96HS1	CYFIP1	0.013899665	-4.181660869
Q9Y3U8	COASY	0.014343976	4.142790024
P52565	SRSF3	0.014381598	-4.139565433
Q8NE71	RPS4X	0.014632643	4.118305436
P53597	TAP1	0.016579706	3.967037805
Q13057	FLOT1	0.017125741	-3.928422169
O15372	ACBD3	0.017299555	3.916439265
P54920	SRRM2	0.01823709	3.854204449
P62263	AGTRAP	0.018965309	3.808454163
Q96AE4	RPL36	0.021263801	3.676791799
Q9Y3C8	ATP13A1	0.022939718	3.591080103
Q7L576	NUTF2	0.023043737	3.58600809
Q9Y3I0	PRKRA	0.02372768	3.553324049
O75569	EIF3H	0.025360874	3.479614385
Q14247	PSMB4	0.02560612	3.469034257
O60784	OXSR1	0.027999361	3.371709973
O95747	CTTN	0.029434239	3.317972057
Q13310	S100A6	0.030412006	3.283099137
Q03518	TOM1	0.030611964	-3.27613065
O75955	UFC1	0.031447202	3.247593376
Q9HD20	CSTB	0.03253923	-3.211603675
P22087	PGAM5	0.033745974	3.17345373
P30153	ARHGDIA	0.033859545	3.169946259
Q9NWV4	SSBP1	0.034116629	3.162057514
P62753	NCLN	0.035792278	3.112295836
O75832	NAPA	0.037864224	3.054421691
P36405	NFKB2	0.038648716	3.033471715

Q04837	RPS6	0.039912623	3.000745357
P62701	FUBP1	0.040557684	2.984506937
O43681	RBM14	0.040745867	2.979826568
P84103	OLA1	0.042144184	2.945821145
P12004	TM9SF4	0.04304244	2.924664305
Q9NR28	GET3	0.043275804	-2.919252059
P06703	ABCF1	0.046067123	2.857036148
P04080	RPL28	0.048344186	-2.809445957

# INGENUITY® PATHWAY ANALYSIS



Analysis Name: Inhibitor vs Control-inhibitor

Analysis Creation Date: 2021-02-20

Build version: exported

Content version: 60467501 (Release Date: 2020-11-19)

## Experiment Metadata

Name

Value

## Analysis Settings

## Top Canonical Pathways

Name	p-value	Overlap
EIF2 Signaling	2,87E-08	3,6 % 8/224
Regulation of eIF4 and p70S6K Signaling	1,65E-06	3,6 % 6/166
mTOR Signaling	6,42E-06	2,9 % 6/210
Coronavirus Pathogenesis Pathway	1,92E-05	3,3 % 5/150
Ceramide Signaling	9,53E-04	3,4 % 3/88

**Top Upstream Regulators****Upstream Regulators**

Name	p-value	Predicted Activation
LARP1	1,21E-11	Inhibited
torin1	6,91E-09	
MYCN	3,32E-06	
5-fluorouracil	1,13E-05	
MLXIPL	1,98E-05	Activated

**Causal Network**

Name	p-value	Predicted Activation
LARP1	1,09E-11	Inhibited
EPOR dimer	1,56E-07	
HABP2	3,84E-07	
PPP1R3A	4,09E-07	
ADP-beta-S	7,22E-07	

**Top Diseases and Bio Functions****Diseases and Disorders**

## Summary of Analysis - Inhibitor vs Control-inhibitor

Name	p-value range	# Molecules
<b>Neurological Disease</b>	4,33E-02 - 1,59E-04	20
<b>Organismal Injury and Abnormalities</b>	4,92E-02 - 1,59E-04	50
<b>Psychological Disorders</b>	2,60E-02 - 1,59E-04	12
<b>Skeletal and Muscular Disorders</b>	1,31E-02 - 7,80E-04	16
<b>Developmental Disorder</b>	4,92E-02 - 7,94E-04	17

## Molecular and Cellular Functions

Name	p-value range	# Molecules
<b>Protein Synthesis</b>	3,62E-02 - 2,74E-11	20
<b>RNA Damage and Repair</b>	2,23E-02 - 1,10E-10	13
<b>Gene Expression</b>	1,01E-02 - 4,65E-07	12
<b>Cell Death and Survival</b>	4,92E-02 - 8,49E-05	26
<b>Cellular Assembly and Organization</b>	4,92E-02 - 1,68E-04	16

## Physiological System Development and Function

Name	p-value range	# Molecules
<b>Nervous System Development and Function</b>	4,92E-02 - 2,56E-04	11
<b>Tissue Morphology</b>	4,92E-02 - 2,56E-04	15
<b>Embryonic Development</b>	4,92E-02 - 1,06E-03	13
<b>Cardiovascular System Development and Function</b>	4,92E-02 - 2,19E-03	3
<b>Connective Tissue Development and Function</b>	3,92E-02 - 2,19E-03	10

## Top Tox Functions

### Assays: Clinical Chemistry and Hematology

Name	p-value range	# Molecules
<a href="#">Increased Levels of Creatinine</a>	3,24E-02 - 3,24E-02	1
<a href="#">Increased Levels of Potassium</a>	3,87E-02 - 3,87E-02	1

### Cardiotoxicity

Name	p-value range	# Molecules
<a href="#">Cardiac Fibrosis</a>	1,96E-02 - 1,96E-02	1
<a href="#">Heart Failure</a>	2,38E-02 - 2,38E-02	1
<a href="#">Cardiac Dilation</a>	6,58E-02 - 6,58E-02	1
<a href="#">Cardiac Enlargement</a>	3,59E-01 - 6,58E-02	3
<a href="#">Cardiac Arrhythmia</a>	3,32E-01 - 3,32E-01	1

### Hepatotoxicity

Name	p-value range	# Molecules
<a href="#">Liver Cirrhosis</a>	1,96E-02 - 1,96E-02	1
<a href="#">Liver Fibrosis</a>	1,96E-02 - 1,96E-02	1

## Summary of Analysis - Inhibitor vs Control-inhibitor

<b>Liver Hyperplasia/Hyperproliferation</b>	1,00E00 - 5,34E-02	22
<b>Hepatocellular carcinoma</b>	1,00E00 - 6,17E-02	4

## Nephrotoxicity

Name	p-value range	# Molecules
<b>Nephrosis</b>	1,09E-02 - 2,19E-03	1
<b>Renal Degeneration</b>	4,38E-03 - 4,38E-03	1
<b>Glomerular Injury</b>	3,46E-01 - 6,56E-03	1
<b>Renal Hypoplasia</b>	6,56E-03 - 6,56E-03	1
<b>Renal Dilation</b>	1,09E-02 - 1,09E-02	1

## Top Regulator Effect Networks

## Top Networks

ID	Associated Network Functions	Score
1	Protein Synthesis, RNA Damage and Repair, Cellular Assembly and Organization	59
2	Carbohydrate Metabolism, Developmental Disorder, Hereditary	46

Disorder

**Top Tox Lists**

Name	p-value	Overlap
<a href="#">Nongenotoxic Hepatocarcinogenicity Biomarker Panel</a>	4,71E-02	4,5 % 1/22
<a href="#">Decreases Depolarization of Mitochondria and Mitochondrial Membrane</a>	6,99E-02	3,0 % 1/33
<a href="#">Hepatic Stellate Cell Activation</a>	7,40E-02	2,9 % 1/35
<a href="#">Pro-Apoptosis</a>	8,81E-02	2,4 % 1/42
<a href="#">Oxidative Stress</a>	1,18E-01	1,8 % 1/57

**Top My Lists****Top My Pathways****Top Analysis-Ready Molecules****Expr Log Ratio**

## Summary of Analysis - Inhibitor vs Control-inhibitor

Molecules	Expr. Value	Chart
NFKB2	↑ 12,288	
RPL24	↑ 8,470	
SRRM2	↑ 8,381	
TM9SF4	↑ 7,979	
RPL28	↑ 7,621	
RBM14	↑ 6,717	
ACBD3	↑ 5,985	
NCLN	↑ 4,996	
DPM3	↑ 4,802	
RPS8	↑ 4,514	

## Expr Log Ratio

Molecules	Expr. Value	Chart
PSMB4	↓ -6,035	
NUTF2	↓ -5,816	
PSMA7	↓ -4,540	
PGAM5	↓ -4,182	
ARHGDIA	↓ -4,140	
COASY	↓ -3,928	
TAP1	↓ -3,276	
ATP13A1	↓ -3,212	
DIABLO	↓ -2,919	
CSTB	↓ -2,809	

## **Appendix to Chapter 6**

Small RNA-Seq analysis between young healthy and old healthy equine chondrocytes identified a set of differentially expressed miRNAs. This dataset was coupled to differentially expressed mRNAs from our group's RNA-Seq experiment in young and old equine cartilage (Peffers, Liu, & Clegg, 2013). miRNA-mRNA pairs were uploaded in IPA and Core Analysis was undertaken for identification of significant biological pathways. The IPA Core Analysis report generated is included here. Moreover, results described in Chapter 6 are included in the published research article: Small Non-Coding RNAome of Ageing Chondrocytes (Balaskas et al., 2020). The article is included at the end of this Appendix.

- Balaskas, P., Green, J. A., Haqqi, T. M., Dyer, P., Kharaz, Y. A., Fang, Y., . . . Peffers, M. J. (2020). Small Non-Coding RNAome of Ageing Chondrocytes. *Int J Mol Sci*, 21(16). doi:10.3390/ijms21165675
- Peffers, M., Liu, X., & Clegg, P. (2013). Transcriptomic signatures in cartilage ageing. *Arthritis Res Ther*, 15(4), R98. doi:10.1186/ar4278



Analysis Name: Young vs old equine chondrocytes

Analysis Creation Date: 2020-05-23

Build version: exported

Content version: 51963813 (Release Date: 2020-03-11)

## Experiment Metadata

Name	Value

## Analysis Settings

Reference set: Ingenuity Knowledge Base (Genes Only)

Relationship to include: Direct and Indirect

Includes Endogenous Chemicals

Optional Analyses: My Pathways My List

Filter Summary:

Consider only molecules and/or relationships where

(species = Rat OR Human OR Uncategorized OR Mouse) AND

(confidence = Experimentally Observed) AND

(tissues/cell lines = Large Intestine OR A2780 OR White Matter OR INS-1 OR Melanoma Cell Lines not otherwise specified OR Myeloma Cell Lines not otherwise specified OR CD34+ cells OR Placenta OR Corpus Callosum OR Lymph node OR Other Dendritic cells OR Cornea OR Hematopoietic progenitor cells OR COLO205 OR H460 OR Skeletal Muscle OR U937 OR Stromal cells OR MDA-MB-361 OR P19 OR

Neutrophils OR Plasma cells OR Granule cells OR Cytotoxic T cells OR Forestomach OR Th2 cells OR Vd2 Gamma-delta T cells OR Nucleus Accumbens OR U2OS OR Granulocytes not otherwise specified OR Striatum OR Trigeminal Ganglion OR NCI-H226 OR M14 OR Other Pancreatic Cancer Cell Lines OR HCT-15 OR THP-1 OR Murine NKT cells OR CCRF-CEM OR DU-145 OR Monocytes not otherwise specified OR T47-D OR Hep3B OR Other Immune cell lines OR Peritoneal macrophages OR Prostate Gland OR Splenocytes OR Subventricular Zone OR J774 OR LNCaP cells OR HOP-62 OR OVCAR-5 OR Bone marrow cells not otherwise specified OR Other Kidney Cancer Cell Lines OR Embryonic stem cells OR KM-12 OR Jurkat OR HUVEC cells OR Central memory helper T cells OR Esophagus OR Thymocytes OR Hypothalamus OR Breast Cancer Cell Lines not otherwise specified OR Olfactory Bulb OR Other Endothelial cells OR HeLa OR Keratinocytes OR NIH/3T3 cells OR Memory T lymphocytes not otherwise specified OR Other Smooth muscle cells OR U87MG OR SK-OV-3 OR Cervical cancer cell line not otherwise specified OR Other CNS Cell Lines OR Sertoli cells OR Effector memory helper T cells OR Kidney cell lines not otherwise specified OR Macrophage Cancer Cell Lines not otherwise specified OR Pheochromocytoma cell lines not otherwise specified OR Hepatocytes OR Other Tissues and Primary Cells OR RAW 264.7 OR SK-N-SH OR Skin OR Smooth muscle cells not otherwise specified OR Lung Cancer Cell Lines not otherwise specified OR Neurons not otherwise specified OR SNB-75 OR Organ Systems not otherwise specified OR Pre-B lymphocytes OR Other Osteosarcoma Cell Lines OR Spinal Cord OR HS 578T OR BT-474 OR Bone marrow-derived dendritic cells OR Lymphoma Cell Lines not otherwise specified OR Granule Cell Layer OR Other Ovarian Cancer Cell Lines OR Ovary OR B lymphocytes not otherwise specified OR Intraepithelial T lymphocytes OR Lung OR 3T3-L1 cells OR Mononuclear leukocytes not otherwise specified OR Adipocytes OR CD56bright NK cells OR TK-10 OR Immature monocyte-derived dendritic cells OR Ventricular Zone OR Neuroblastoma Cell Lines not otherwise specified OR NCI-H332M OR Cardiomyocytes OR Nervous System not otherwise specified OR Peripheral blood monocytes OR Brain OR Hepatoma Cell Lines not otherwise specified OR Hippocampus OR BA/F3 OR RXF-393 OR NT2/D1 OR Other Nervous System OR Activated CD56dim NK cells OR Activated Vd1 Gamma-delta T cells OR Other Prostate Cancer Cell Lines OR PC-12 cells OR SK-MEL-5 OR Naive helper T cells OR NCI-H23 OR Bladder OR Other Kidney cell lines OR Beta islet cells OR Cell Line not otherwise specified OR Cos-7 cells OR Amygdala OR Melanocytes OR Peripheral blood leukocytes not otherwise specified OR Medulla Oblongata OR Granulosa cells OR Lens OR Central memory cytotoxic T cells OR Monocyte-derived dendritic cells not otherwise specified OR Uterus OR 786-0 OR Macrophages not otherwise specified OR T lymphocytes not otherwise specified OR Other Monocyte-derived dendritic cells OR Astrocytes OR Min6 OR Salivary Gland OR BDCA-3+ dendritic cells OR Immune cell lines not otherwise specified OR Choroid Plexus OR Chondrocytes OR Other Cells OR Small Intestine OR MDA-MB-231 OR Other Bone marrow cells OR RKO OR UACC-257 OR Brainstem OR Tissues and Primary Cells not otherwise specified OR RBL-2H3 OR Other Peripheral blood leukocytes OR BDCA-1+ dendritic cells OR K-562 OR CAKI-1 OR Liver OR Sciatic Nerve OR Parietal Lobe OR Crypt OR EKVX OR MOLT-4 OR Dermis OR A375 OR Memory B cells OR Thyroid Gland OR Activated Vd2 Gamma-delta T cells OR PC-3 OR Cerebellum OR Calvaria OR A549-ATCC OR HOP-92 OR LOX IMVI OR Cartilage Tissue OR CD4+ T-lymphocytes OR Natural T-regulatory cells OR Colon Cancer Cell Lines not otherwise specified OR NB4 OR MCF7 OR Myeloid dendritic cells

OR Pyramidal neurons OR Other Neuroblastoma Cell Lines OR Other Macrophages OR NK cells not otherwise specified OR Substantia Nigra OR UACC-62 OR Naive B cells OR Osteoblasts OR Mammary Gland OR CNS Cell Lines not otherwise specified OR Other Teratocarcinoma Cell Lines OR Other T lymphocytes OR Effector memory RA+ cytotoxic T cells OR Adrenal Gland OR MG-63 OR Ovarian Cancer Cell Lines not otherwise specified OR PBMCs OR RPMI-8266 OR Gray Matter OR Fibroblast cell lines not otherwise specified OR Heart OR Stem cells not otherwise specified OR Testis OR Other Melanoma Cell Lines OR Smooth Muscle OR MEF cells OR Eosinophils OR Other Fibroblast cell lines OR 293 cells OR Vd1 Gamma-delta T cells OR SF-268 OR Cortical neurons OR Megakaryocytes OR Caco2 cells OR MDA-MB-435 OR Kidney OR Pro-B lymphocytes OR Epithelial cells not otherwise specified OR Oocytes OR Other Lymphocytes OR Other NK cells OR SK-MEL-2 OR MDA-N OR Other Epithelial cells OR Other B lymphocytes OR HepG2 OR NCI-ADR-RES OR U266 OR Microvascular endothelial cells OR MDA-MB-468 OR Trachea OR SF-295 OR A498 OR Stomach OR Other Immune cells OR HCC-2998 OR Mesenchymal stem cells OR Effector T cells OR Dendritic cells not otherwise specified OR ACHN OR Other Cervical cancer cell line OR Putamen OR Teratocarcinoma Cell Lines not otherwise specified OR Lymphocytes not otherwise specified OR Th17 cells OR Kidney Cancer Cell Lines not otherwise specified OR Plasmacytoid dendritic cells OR Other Mononuclear leukocytes OR SW-620 OR Monocyte-derived macrophage OR Endothelial cells not otherwise specified OR Retina OR HT29 OR IGROV1 OR OVCAR-3 OR Immune cells not otherwise specified OR Other Pheochromocytoma cell lines OR Other Granulocytes OR Other Neurons OR Other Colon Cancer Cell Lines OR Mature monocyte-derived dendritic cells OR Activated CD56bright NK cells OR Langerhans cells OR Thalamus OR Other Leukemia Cell Lines OR Purkinje cells OR Spleen OR SF-539 OR WEHI-231 OR Leukemia Cell Lines not otherwise specified OR Other Breast Cancer Cell Lines OR Dorsal Root Ganglion OR Vascular smooth muscle cells OR Prostate Cancer Cell Lines not otherwise specified OR Other Memory T lymphocytes OR Cerebral Ventricle OR HMC-1 OR Bone marrow-derived macrophages OR OVCAR-4 OR Cerebral Cortex OR HCT-116 OR UO-31 OR OVCAR-8 OR Pancreatic Cancer Cell Lines not otherwise specified OR SW-480 OR Other Stem cells OR CD56dim NK cells OR Other Lymphoma Cell Lines OR SK-MEL-28 OR Caudate Nucleus OR Mast cells OR HuH7 OR PANC-1 OR Other Hepatoma Cell Lines OR Epidermis OR J-774A.1 OR Cells not otherwise specified OR Thymus OR U251 OR HL-60 OR Effector memory cytotoxic T cells OR Adipose OR Th1 cells OR SR OR Peripheral blood lymphocytes OR BT-549 OR Other Myeloma Cell Lines OR Microglia OR Other Lung Cancer Cell Lines OR NCI-H522 OR Pancreas OR Swiss 3T3 cells OR Osteosarcoma Cell Lines not otherwise specified OR Other Organ Systems OR MALME-3M OR Pituitary Gland OR Other Monocytes OR HEL OR Other Cell Line OR Fibroblasts OR Other Macrophage Cancer Cell Lines OR Blood platelets OR SN12C OR Activated helper T cells) AND (mol. types = biologic drug OR canonical pathway OR chemical - endogenous mammalian OR chemical - endogenous non-mammalian OR chemical - kinase inhibitor OR chemical - other OR chemical - protease inhibitor OR chemical drug OR chemical reagent OR chemical toxicant OR complex OR cytokine OR disease OR enzyme OR function OR fusion gene/product OR G-protein coupled receptor OR group OR growth factor OR ion channel OR kinase OR ligand-dependent nuclear receptor OR mature microRNA OR microRNA OR other OR peptidase OR phosphatase OR transcription regulator OR translation regulator OR transmembrane receptor OR transporter) AND

(data sources = An Open Access Database of Genome-wide Association Results OR BIND OR BioGRID OR Catalogue Of Somatic Mutations In Cancer (COSMIC) OR Chemical Carcinogenesis Research Information System (CCRIS) OR ClinicalTrials.gov OR ClinVar OR Cognia OR DIP OR DrugBank OR Gene Ontology (GO) OR GVK Biosciences OR Hazardous Substances Data Bank (HSDB) OR HumanCyc OR Ingenuity Expert Findings OR Ingenuity ExpertAssist Findings OR IntAct OR Interactome studies OR MIPS OR miRBase OR miRecords OR Mouse Genome Database (MGD) OR Obesity Gene Map Database OR Online Mendelian Inheritance in Man (OMIM) OR TarBase OR TargetScan Human)

## Top Canonical Pathways

Name	p-value	Overlap
Hepatic Fibrosis / Hepatic Stellate Cell Activation	1,15E-04	2,2 % 4/186
Role of Osteoblasts, Osteoclasts and Chondrocytes in Rheumatoid Arthritis	2,20E-04	1,8 % 4/220
Axonal Guidance Signaling	4,63E-04	1,0 % 5/484
GP6 Signaling Pathway	5,67E-04	2,5 % 3/119
Hepatic Fibrosis Signaling Pathway	1,51E-03	1,1 % 4/368

## Top Upstream Regulators

### Upstream Regulators

Name	p-value	Predicted Activation
WNT3A	5,03E-09	
NOG	1,05E-08	

**ERK**

4,02E-08

**TGFB1**

5,21E-08

**FOXO1**

1,66E-07

Inhibited

**Causal Network**

Name	p-value	Predicted Activation
<b>benzodiazepines</b>	2,09E-13	
<b>SKF-38393</b>	2,05E-12	
<b>BRAF</b>	1,19E-11	
<b>Sch-23390</b>	2,65E-11	
<b>IL3RA</b>	3,30E-11	

**Top Diseases and Bio Functions****Diseases and Disorders**

Name	p-value range	# Molecules
<b>Skeletal and Muscular Disorders</b>	1,50E-03 - 1,22E-09	16
<b>Connective Tissue Disorders</b>	1,50E-03 - 3,52E-08	16
<b>Organismal Injury and Abnormalities</b>	1,50E-03 - 3,52E-08	31
<b>Cancer</b>	1,49E-03 - 5,30E-07	31
<b>Developmental Disorder</b>	1,37E-03 - 5,30E-07	17

**Molecular and Cellular Functions**

Name	p-value range	# Molecules
<a href="#">Cellular Movement</a>	1,41E-03 - 4,23E-10	21
<a href="#">Cell Morphology</a>	1,37E-03 - 3,52E-08	16
<a href="#">Cellular Development</a>	1,42E-03 - 4,94E-07	24
<a href="#">Cell Death and Survival</a>	1,37E-03 - 1,08E-05	18
<a href="#">Cell-To-Cell Signaling and Interaction</a>	1,37E-03 - 1,88E-05	20

**Physiological System Development and Function**

Name	p-value range	# Molecules
<a href="#">Embryonic Development</a>	1,37E-03 - 6,19E-09	20
<a href="#">Organismal Development</a>	1,50E-03 - 6,19E-09	24
<a href="#">Cardiovascular System Development and Function</a>	1,37E-03 - 2,51E-08	13
<a href="#">Connective Tissue Development and Function</a>	1,50E-03 - 3,52E-08	15
<a href="#">Skeletal and Muscular System Development and Function</a>	1,50E-03 - 3,52E-08	15

**Top Tox Functions****Assays: Clinical Chemistry and Hematology**

Name	p-value range	# Molecules
<a href="#">Increased Levels of Alkaline Phosphatase</a>	6,81E-03 - 4,34E-03	2

**Decreased Levels of Albumin**

8,16E-03 - 8,16E-03

1

**Cardiotoxicity**

Name	p-value range	# Molecules
<a href="#">Cardiac Stenosis</a>	1,63E-02 - 1,40E-06	4
<a href="#">Cardiac Dysfunction</a>	9,51E-02 - 8,01E-04	4
<a href="#">Congenital Heart Anomaly</a>	4,67E-02 - 4,09E-03	3
<a href="#">Cardiac Transformation</a>	5,45E-03 - 5,45E-03	1
<a href="#">Cardiac Arrhythmia</a>	2,20E-01 - 1,14E-02	3

**Hepatotoxicity**

Name	p-value range	# Molecules
<a href="#">Congestion of liver</a>	2,73E-03 - 2,73E-03	1
<a href="#">Hepatocellular carcinoma</a>	1,02E-01 - 1,36E-02	4
<a href="#">Liver Hyperplasia/Hyperproliferation</a>	1,02E-01 - 1,36E-02	15
<a href="#">Liver Inflammation/Hepatitis</a>	1,02E-01 - 2,22E-02	3
<a href="#">Liver Proliferation</a>	2,24E-01 - 4,17E-02	2

**Nephrotoxicity**

Name	p-value range	# Molecules
<a href="#">Renal Inflammation</a>	1,37E-03 - 1,37E-03	1

<b>Renal Nephritis</b>	1,37E-03 - 1,37E-03	1
<b>Renal Necrosis/Cell Death</b>	3,44E-01 - 4,43E-03	5
<b>Renal Hypoplasia</b>	5,84E-02 - 4,70E-03	2
<b>Glomerular Injury</b>	4,54E-02 - 5,45E-03	2

**Top Regulator Effect Networks**

ID	Regulators	Disease & Functions	Consistency Score
<b>1</b>	CEBPA	Invasion of cells, Invasion of tissue	3,5
<b>2</b>	IL4	Cell proliferation of tumor cell lines	1,789
<b>3</b>	IL4	Cell survival	-5,367

**Top Networks**

ID	Associated Network Functions	Score
	Cellular Movement, Skeletal and Muscular	
<b>1</b>	Disorders, Cardiovascular System Development and Function	44
<b>2</b>	Cell-To-Cell Signaling and Interaction, Hematological System Development and Function, Auditory Disease	20

3

Cell-To-Cell Signaling  
and Interaction,  
Nervous System  
Development and  
Function, Cellular  
Assembly and  
Organization

12

## Top Tox Lists

Name	p-value	Overlap
<a href="#">Renal Necrosis/Cell Death</a>	1,04E-03	0,9 % 5/579
<a href="#">VDR/RXR Activation</a>	5,08E-03	2,6 % 2/78
<a href="#">Protection from Hypoxia-induced Renal Ischemic Injury (Rat)</a>	5,45E-03	25,0 % 1/4
<a href="#">Hepatic Fibrosis</a>	1,09E-02	1,7 % 2/116
<a href="#">Recovery from Ischemic Acute Renal Failure (Rat)</a>	1,89E-02	7,1 % 1/14

## Top My Lists

## Top My Pathways

## Top Analysis-Ready Molecules

Molecules	Expr. Value	Chart
TNFSF11	↑ 2,537	
KCNN3	↑ 2,369	
HEY2	↑ 1,844	
MGARP	↑ 1,720	
FST	↑ 1,555	

**Expr Fold Change**

Molecules	Expr. Value	Chart
ACSL5	↓ -30,131	
COL4A1	↓ -30,114	
SEMA4D	↓ -29,748	
NCAM1	↓ -29,075	
COL2A1	↓ -6,533	
CLSTN3	↓ -3,960	
WNT11	↓ -3,806	
FLT1	↓ -3,452	
ROBO2	↓ -3,343	
ITGA11	↓ -3,232	



Article

# Small Non-Coding RNAome of Ageing Chondrocytes

Panagiotis Balaskas <sup>1,\*</sup>, Jonathan A. Green <sup>2</sup>, Tariq M. Haqqi <sup>2</sup>, Philip Dyer <sup>1</sup>, Yalda A. Kharaz <sup>1</sup>, Yongxiang Fang <sup>3</sup>, Xuan Liu <sup>3</sup>, Tim J.M. Welting <sup>4</sup> and Mandy J. Peffers <sup>1,\*</sup>

<sup>1</sup> Institute of Life Course and Medical Sciences, William Henry Duncan Building, 6 West Derby Street, Liverpool L7 8TX, UK; pddyer@liv.ac.uk (P.D.); yalda@liverpool.ac.uk (Y.A.K.)

<sup>2</sup> Department of Anatomy and Neurobiology, Northeast Ohio Medical University, Rootstown, OH 44272, USA; dun06hpu@googlemail.com (J.A.G.); thaqqi@neomed.edu (T.M.H.)

<sup>3</sup> Centre for Genomic Research, Institute of Integrative Biology, Biosciences Building, Crown Street, University of Liverpool, Liverpool L69 7ZB, UK; fangy@liv.ac.uk (Y.F.); xuanliu@liverpool.ac.uk (X.L.)

<sup>4</sup> Department of Orthopaedic Surgery, Maastricht University Medical Centre, 6202 AZ Maastricht, The Netherlands; t.welting@maastrichtuniversity.nl

\* Correspondence: panbalas@liverpool.ac.uk (P.B.); peffs@liv.ac.uk (M.J.P.); Tel.: +44-0787-269-2102 (M.J.P.)

Received: 20 July 2020; Accepted: 4 August 2020; Published: 7 August 2020



**Abstract:** Ageing is a leading risk factor predisposing cartilage to osteoarthritis. However, little research has been conducted on the effect of ageing on the expression of small non-coding RNAs (sncRNAs). RNA from young and old chondrocytes from macroscopically normal equine metacarpophalangeal joints was extracted and subjected to small RNA sequencing (RNA-seq). Differential expression analysis was performed in R using package DESeq2. For transfer RNA (tRNA) fragment analysis, tRNA reads were aligned to horse tRNA sequences using Bowtie2 version 2.2.5. Selected microRNA (miRNAs or miRs) and small nucleolar RNA (snoRNA) findings were validated using real-time quantitative Polymerase Chain Reaction (qRT-PCR) in an extended cohort of equine chondrocytes. tRNA fragments were further investigated in low- and high-grade OA human cartilage tissue. In total, 83 sncRNAs were differentially expressed between young and old equine chondrocytes, including miRNAs, snoRNAs, small nuclear RNAs (snRNAs), and tRNAs. qRT-PCR analysis confirmed findings. tRNA fragment analysis revealed that tRNA halves (tiRNAs), tiRNA-5035-GluCTC and tiRNA-5031-GluCTC-1 were reduced in both high grade OA human cartilage and old equine chondrocytes. For the first time, we have measured the effect of ageing on the expression of sncRNAs in equine chondrocytes. Changes were detected in a number of different sncRNA species. This study supports a role for sncRNAs in ageing cartilage and their potential involvement in age-related cartilage diseases.

**Keywords:** chondrocyte; ageing; equine; small non-coding RNA

## 1. Introduction

Articular cartilage is a specialised connective tissue of diarthrodial joints. Its smooth lubricated surface assists joint movement and its mechanical properties facilitate load bearing in the joint. The tissue harbours one cell type; the chondrocyte, and is devoid of blood vessels and nerves, receiving nutrients from synovial fluid and subchondral bone [1]. Articular cartilage is characterised by an extracellular matrix (ECM) consisting of mainly collagen type 2 and proteoglycans, which give the tissue many of its properties. After reaching maturity, cartilage displays a limited repairing capacity as indicated by low chondrocyte proliferation and low collagen turnover [2].

There are a number of factors affecting the homeostatic properties of cartilage such as genetics and obesity [3]. However, ageing is a leading risk factor that predisposes cartilage to pathological changes and disease, such as osteoarthritis (OA), the most common joint disease [3]. These age-related

changes affect both chondrocyte physiology and ECM properties. Aged chondrocytes display increased senescence and higher expression of catabolic markers; features also evident in OA chondrocytes [3,4]. Moreover, in humans, aged knee cartilage is thinner compared to younger cartilage and is characterised by increased collagen crosslinking and altered proteoglycan content. These changes affect matrix stiffness, make cartilage susceptible to fractures and lower its ability to sense mechanical stimuli [3,5,6].

The exact mechanisms through which age can affect cartilage health remain elusive, though it is believed to be a cumulative combination of many molecular pathways rather than a single aetiology. Recent advances in the field have recognised epigenetics in ageing and diseased articular cartilage as an area of growing interest [6,7]. A class of epigenetic modifications that have attracted increasing attention are small non-coding RNAs (sncRNAs). They are short, typically <200 bp, RNA species, which are not translated into protein but have other structural or regulatory biological roles. These include microRNAs (miRNAs or miRs), small nuclear RNAs (snRNAs), small nucleolar RNAs (snoRNAs), piwi-interacting RNAs and transfer RNAs (tRNAs). SncRNAs are promising candidates for targeted therapeutics due to their small size and diverse cellular functions. By using specific synthetic oligonucleotides, aberrant expression of sncRNAs in disease could be modified, resulting in delay or reversal of pathological changes [8]. Furthermore, sncRNAs could be used as biomarkers to monitor disease initiation and progression or response to treatment [9,10]. This is of high importance in OA, as treatment is currently symptomatic and most patients with end-stage OA require joint replacement; a procedure with a high social and economic burden for patients and the healthcare system respectively [11].

MiRNAs, the most studied sncRNAs, regulate gene expression by binding complementary sequences in the 3' untranslated region of their messenger RNA (mRNA) targets, thus inhibiting mRNA translation [8]. MiRNAs have been linked to ageing and diseased cartilage; miR-140 is important for cartilage development and deletion of miR-140 in mice causes skeletal defects [12]. Moreover, OA chondrocytes show decreased expression of miR-24, resulting in increased expression of the senescent marker p16INK4a, highlighting the link between OA and senescence; a hallmark of ageing [4].

In addition to miRNAs, snoRNAs are increasingly studied in ageing and OA. Snora73 expression increases in the joint and serum of old mice compared to young mice [9] and we have also previously identified a catalogue of age-related snoRNAs in human knee cartilage [13]. SnoRNAs have canonical roles in the post transcriptional modification of RNA substrates including ribosomal RNAs, and mRNAs, but can also exhibit non-canonical functions such as miRNA-like activity [14]. Their aberrant expression has also been associated with the development of some diseases [15]. Our previously conducted mouse study demonstrated alterations in the snoRNA profile of young, old and OA joints in mice when compared to healthy controls, highlighting the potential of snoRNAs to be used as novel markers for this disease [9]. We have also identified changing snoRNA profiles in ageing and OA human cartilage [16], synovial fluid from horses with early OA and diseased anterior cruciate ligaments from OA joints [17].

tRNAs are adaptor molecules of ~73–90 nucleotides long consisting of a T-loop, D-loop, variable loop, and the anticodon loop. Protein translation requires amino acids to be linked together into polypeptides and tRNAs recruit these amino acids to the translating ribosome. Recent studies have shown that tRNAs are a major source of sncRNAs with an active role in gene regulation [18]. tRNA fragments result from specific processing of tRNAs. These include tRNA halves (tiRNAs), which are 28–36 nucleotide long fragments formed by Angiogenin (ANG). ANG divides the tRNA into two halves at the anticodon loop [19] giving rise to the 3' tiRNA and 5' tiRNA halves. tRNAs are also processed into smaller fragments; tRNA-derived small RNA fragments (tRFs); tRF-1, tRF-2, tRF-3 and tRF-5, however the naming conventions of these classes is still not consistent [20]. RNase Z, or its cytoplasmic homologue ELAC2, [21] cleaves the 3' trailer fragment of pre-tRNAs resulting in tRF-1 formation. The enzyme responsible for the cleavage of tRF-2 fragments is still unclear. The tRF-2 fragment consists of the anticodon loop of the tRNA and has been detected in breast cancer MDA-231 cells [22]. Dicer and ANG cleave tRNAs into ~15–30 nucleotide tRF-3 and tRF-5 fragments. TRF-3

fragments are cleaved at the T loop by Dicer [23] and ANG [24] and tRF-5 fragments are derived from the cleavage of the D-loop by Dicer [23]. The final category of tRFs are i-tRFs, which are internal to the respective tRNA and can straddle the anticodon loop [25]. Limited knowledge of the expression and role of tRNA and tRFs is available in health and disease [26] with even less in musculoskeletal biology [27,28].

In this study, we investigated the expression changes of sncRNAs in chondrocytes isolated from healthy metacarpophalangeal joints of young and old horses. Findings for tRNAs are compared to a human OA data set. Age-related changes may predispose cartilage to disease by altering the complex sncRNA expression profile. This provides a sncRNA-wide insight into age-related targets for future therapeutic approaches.

## 2. Materials and Methods

All reagents were from Thermo-Fisher-Scientific, Loughborough, UK unless stated.

### 2.1. Sample Collection and Preparation

Samples were collected from an abattoir as a by-product of the agricultural industry. Specifically, the Animal (Scientific procedures) Act 1986, Schedule 2, does not define collection from these sources as scientific procedures. Ethical approval was therefore not required. Full thickness equine cartilage was removed from the entire surface of macroscopically normal metacarpophalangeal joints of young  $n = 5$  (age mean  $\pm$  standard deviation;  $4 \pm 1$  years) and old  $n = 5$  ( $17.4 \pm 1.9$  years) non-Thoroughbred horses. Scoring of the metacarpophalangeal joint was undertaken using a macroscopic grading system, as previously described [29] and samples with no macroscopic perturbations were selected (combined score of zero). Freshly isolated chondrocytes were removed from all 10 samples of harvested cartilage, as previously described [30], plated to confluence and RNA extracted from two million cells per donor.

In addition to the above samples, RNA from chondrocytes from young  $n = 2$  (age mean  $\pm$  standard deviation;  $0.75 \pm 0.3$  years) and old  $n = 6$  (age mean  $\pm$  standard deviation;  $19.3 \pm 3.6$  years) non-Thoroughbred horses were used for validation.

### 2.2. RNA Isolation, cDNA Library Preparation, and Small RNA Sequencing (RNA-seq)

Total RNA including small RNAs was extracted, as previously described [31], and purified using the miRNAeasy kit (Qiagen, Crawley, UK) according to manufacturer's instructions and including an on-column DNase step to remove residual genomic DNA. The integrity of the RNA was assessed on the Agilent 2100 Bioanalyser system using an RNA Pico chip (Agilent, Stockport, UK). The NEBNext®Small RNA Library Prep Set for Illumina®was used for library preparation (New England Biolabs, Ipswich, MA, USA) but with the addition of a Cap-Clip™ Acid Pyrophosphatase (Cell script, Madison, WI, USA) step to remove potential 5' caps found on some snoRNAs. Samples were amplified for 15 cycles and size was selected. The libraries were sequenced on an Illumina MiSeq platform (Illumina, San Diego, CA, USA) with version 2 chemistry using sequencing by synthesis technology to generate  $2 \times 150$  bp paired-end reads with >12 million clusters per run.

### 2.3. Data Processing

Sequence data were processed through a number of steps to obtain sncRNA expression values including basecalling and de-multiplexing of indexed reads using CASAVA version 1.8.2 [32]; adapter and quality trimming using Cutadapt version 1.2.1 [33] and Sickle version 1.200 to obtain fastq files of trimmed reads; aligning reads to horse genome reference sequences (GCF\_002863925.1) using Tophat version 2.0.10 [34] with option “-g 1”; counting aligned reads using HTSeq-count against the annotated features which are combined annotation information from the sources: NCBI *Equus caballus* 3.0 genome annotation, miRBase horse micro RNA annotation, Rfam snoRNA annotation.

Differential expression analysis was performed in R environment using package DESeq2 [35]. The processes and technical details of the analysis included: assessing data variation and detecting

outlier samples through comparing variations of within and between sample groups using principle component analysis (PCA) and correlation analysis; handling library size variation using the DESeq2 default method; formulating data variation using negative binomial distributions; modelling data using a generalised linear model; computing log<sub>2</sub> Fold Change (logFC) values for required contrasts based on model fitting results through contrast fitting approach, evaluating the significance of estimated logFC values by Wald test; adjusting the effects of multiple tests using False Discovery Rate (FDR) approach to obtain FDR [36] adjusted P-values.

#### 2.4. Pathway Analysis

In order to identify miRNA targets, bioinformatic analysis was performed by uploading differentially expressed miRNA data into the MicroRNA Target Filter module within Ingenuity Pathway Analysis software (IPA) (Qiagen Redwood City, CA, USA) along with previously identified differentially expressed mRNAs from our ageing equine cartilage study following RNA-seq [31]. In IPA we selected miRNA-target genes based on the direction of differential expression (for example, if a miRNA was reduced in expression it was only matched to mRNAs that demonstrated increased expression). We then identified the networks, functions, and canonical pathways of these miRNA-target genes.

#### 2.5. qRT-PCR Validation

Validation of the small RNA-seq results was undertaken using real-time quantitative PCR (qRT-PCR) analysis in the samples used for sequencing as well as additional samples. SncRNAs were chosen based on level of differential expression. Total RNA was extracted and quantified as above. cDNA was synthesized using 200 ng RNA and the miScript II RT Kit according to the manufacturer's protocol (Qiagen, Crawley, UK). qRT-PCR mastermix was prepared using the miScript SYBR Green PCR Kit (Qiagen, Crawley, UK) and the appropriate miScript Primer Assay (Qiagen, Crawley, UK) (File S1) using 1 ng/μL cDNA according to manufacturer's guidelines. qRT-PCR was undertaken using a LightCycler®96 system (Roche, Welwyn Garden City, UK). Relative expression levels were normalised to U6 (as this was stable in the small RNA-seq data set) and calculated using the 2-ΔCt method [37].

#### 2.6. tRNA Fragment Analysis

Following the alignment of trimmed reads to NCBI horse genome reference sequences (version 3.0) using Tophat version 2.1.0 [38], the candidate tRNA reads were extracted from the BAM files according to whether they overlapped the ranges covered by tRNA features. The read pairs were stitched into RNA fragments using PEAR (version 0.9.10) [39]. The output reads were aligned to horse tRNA sequences (defined in NCBI GCF\_002863925.1\_EquCab3.0\_genomic.gff) using Bowtie2 version 2.2.5. Only the perfectly mapped fragments were extracted and taken as tRNA fragments for further explorations. Finally, statistical analyses were mainly focused on the fragment length and the mapping start location, which generated the length distribution and the mapping start position distribution of observed tRNA fragments, as well as the summary table for observed tRNA fragments and their target tRNAs.

#### 2.7. Novel snoRNA Analysis

Putative snoRNAs were detected from the raw pair-end reads using ShortStack 3.8.4 [40] with the setting “–mincov 5”, which specifies that the clusters of small RNAs must have at least five alignments. The ShortStack results were subsequently fed into SnoReport 2.0 [41], which uses RNA secondary structure prediction combined with machine learning as the basis to identify the two main classes of snoRNAs; the box H/ACA and the box C/D. Putative snoRNAs were annotated from our experimental small RNA-seq data using ShortStack and SnoReport.

## 2.8. Statistical Analysis

3D PCA score plots and heat maps were carried out using MetaboAnalyst 3.5 [42] (<http://www.metaboanalyst.ca>) which uses the R package of statistical computing software [43].

For statistical evaluation of qRT-PCR results, following normality testing, Mann-Whitney tests were performed using GraphPad Prism version 7.03 for Windows, (GraphPad Software, La Jolla, CA, USA); p values are indicated.

## 2.9. Human Sample Collection and Preparation

De-identified human OA cartilage approved by Northeast Ohio Medical University (NEOMED) Institutional Review Board and Summa Health Systems, Barberton, Ohio as ‘non-human subject study under 45 CFR’ was used. Total RNA was extracted from smooth, macroscopically intact human OA cartilage with a Mankin score of 2 or less ( $n = 1$ , female, 60 years old) and damaged OA cartilage with a Mankin score of 4 or higher ( $n = 1$ , female, 80 years old) using MiRNeasy Kit (Qiagen, Germantown, MD, USA). RNA was quantified using the Nanodrop 1000 Spectrophotometer (Thermo Fisher, Waltham, MA, USA). TapeStation 4200 (Agilent Technologies, Santa Clara, CA, USA) was used to determine RNA integrity using High Sensitivity RNA ScreenTape analysis kit (Agilent, Santa Clara, CA, USA).

## 2.10. Removal of tRF Modifications from Human Cartilage RNA

The rtStar™ tRF&tiRNA Pretreatment Kit (ArrayStar, Rockville, MD, USA) was used according to the manufacturer’s description. For cDNA qRT-PCR library construction, tRF modifications were removed from RNA. The kit removes 3'-aminoacyl and 3'-cP for 3' adaptor ligation, phosphorylates 5'-OH for 5'-adaptor ligation, and demethylates m1A, m1G, and m3C for efficient cDNA reverse transcription.

## 2.11. tRF 3' and 5' Adaptor Ligation for Human Cartilage cDNA Synthesis

The rtStar™ First-Strand cDNA Synthesis Kit (ArrayStar, Rockville, MD USA) was used according to the manufacturer’s description. The kit sequentially ligates 3'-Adaptor with its 5'-end to the 3'-end of the RNAs, and 5'-Adaptor with its 3'-end to the 5'-end of the RNAs. The non-ligation ends of 3' and 5' Adaptors were blocked by modifications. A universal priming site for reverse transcription was contained within the 3' adaptor. Spike-in RNA was used for monitoring the cDNA synthesis efficiency and as a quantitative reference.

## 2.12. tRF and tRNA Human qPCR Arrays

The nrStar™ Human tRF and tiRNA PCR Array (ArrayStar, Rockville, MD, USA) was used according to the manufacturers description to profile 185 tRF and tiRNA fragments, of which 101 are derived from tRF and tiRNA database [44,45] and the other 84 from recently published papers [46–48]. RNA Spike in control and a positive PCR control were used to evaluate PCR efficiency and a genomic DNA control was used to monitor genomic DNA contamination. To profile parent tRNAs, the nrStat Human tRNA PCR Array (ArrayStar, Rockville, MD, USA) was used according to the manufacturer’s protocol. This array consisted of 163 PCR-distinguishable nuclear tRNA isodecoders and 22 PCR distinguishable mitochondrial tRNA species covering all anti-codons compiled in GtTNAdb [49,50] and tRNAdb [51] databases. Genomic DNA and positive PCR controls were included to monitor the quality of RNA sample.

qRT-PCR reactions were conducted using Power SYBR Green master mix (Life technologies, Carlsbad, CA, USA) on a Step One Plus (Applied Biosystems, Waltham, MA, USA) machine. U6, SNORD43 and SNORD45 were used as endogenous controls for normalisation of tRF, tiRNA and tRNA detection. Target tRNA, tiRNA and tRF levels were determined as fold change differences utilising the  $\Delta\Delta Ct$  method [37].

### 3. Results

#### 3.1. Preliminary Analysis of Small RNA-seq Data

To identify differential expression of sncRNAs in ageing, Illumina MiSeq was utilised. Summaries of raw, trimmed reads, and mapped reads to *Equus caballus* database can be found in File S2. Reads mapping percentages were between 92 to 94.3%. There were 2128 sncRNAs identified. The categories of non-coding RNAs identified are in Figure 1A and File S3 and included miRNAs, snoRNAs, novel snoRNAs, tRNAs, snRNAs, and long non-coding RNAs (lncRNAs).

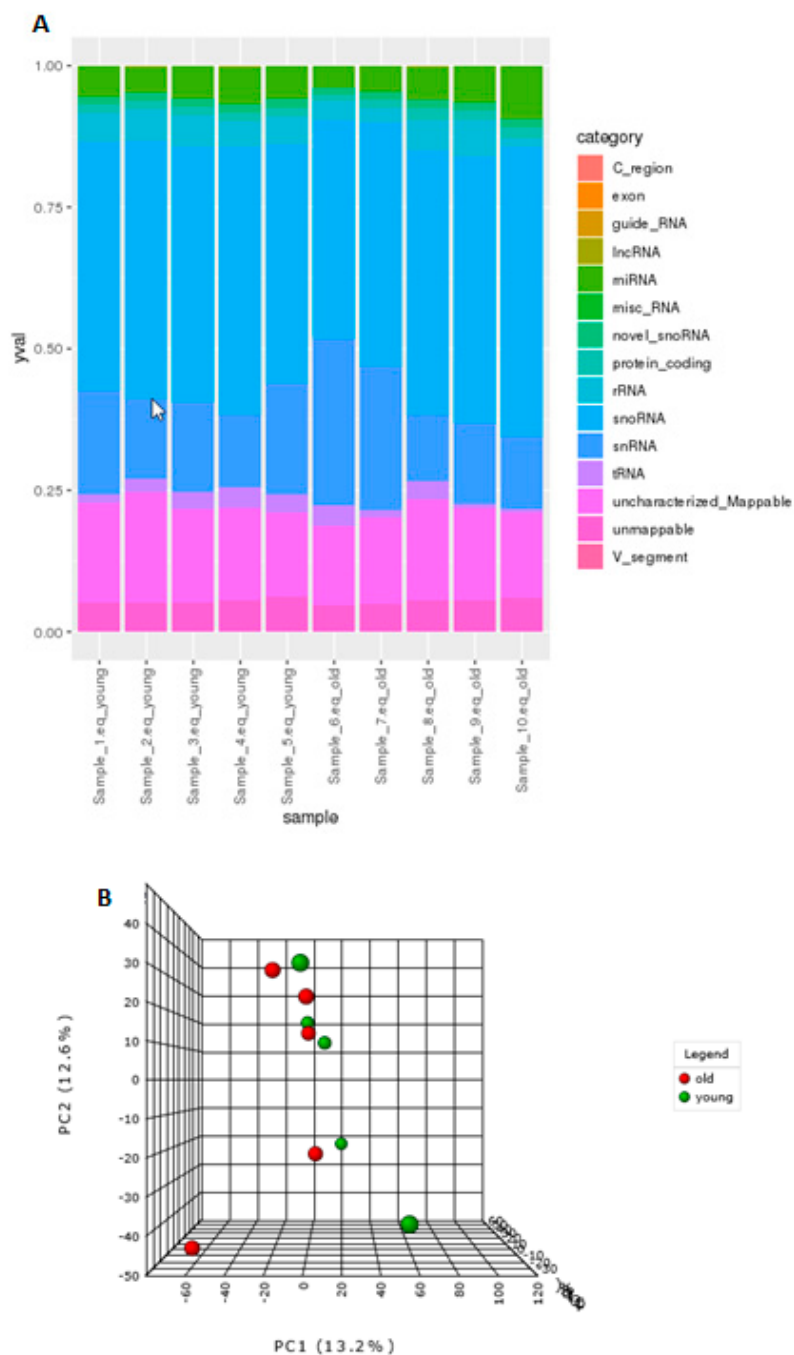
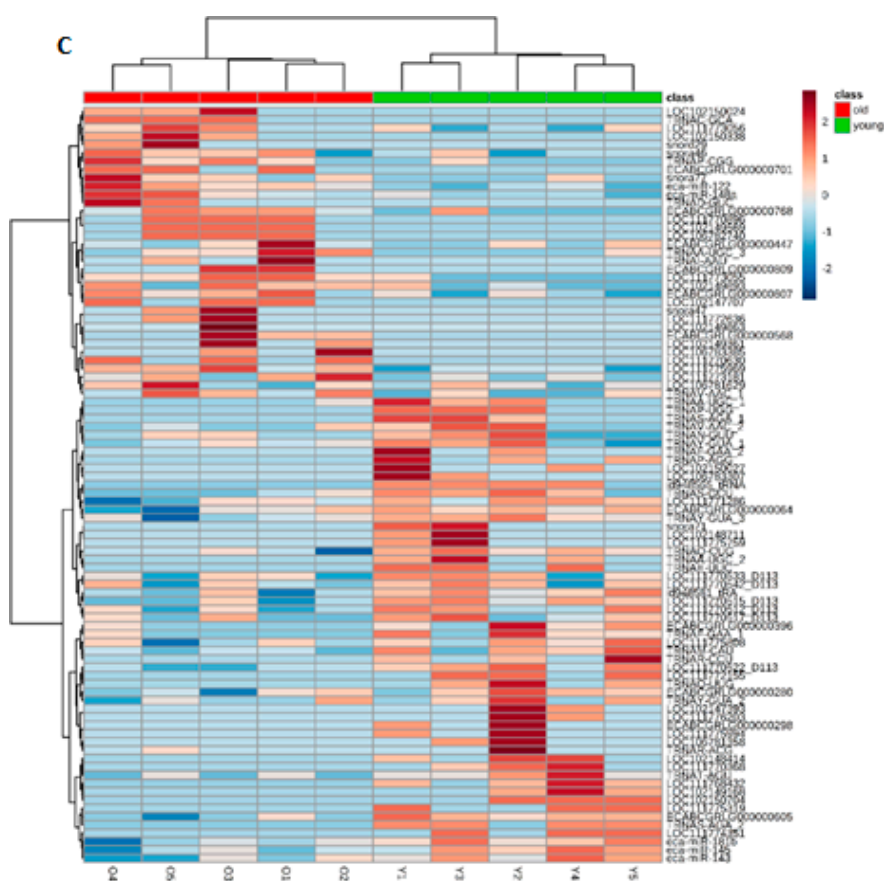


Figure 1. Cont.



**Figure 1.** Age-related differential small non-coding RNA (sncRNA) gene expression. (A) The categories of non-coding RNAs identified in young and old equine chondrocytes; long non-coding RNAs (lncRNAs), microRNAs (miRNAs or miRs), small nucleolar RNAs (snoRNAs), small nuclear RNAs (snRNAs), transfer RNAs (tRNAs). (B) 3D principle component analysis (PCA) plot between the selected principle components (PCs). The explained variances are shown in brackets. (C). Clustering results shown as a heatmap (distance measure using Euclidean, and clustering algorithm using Ward) for the top 90 molecules.

### 3.2. Age-Related Differential Small Non-Coding RNA Gene Expression

There were no overall differences in the distribution of classes of sncRNAs in ageing. The effect of age on the expression of sncRNAs was weak and the separation of young and old samples was not clear. The 3D PCA plot (Figure 1B) indicated that few, but very specific changes in the expression of sncRNAs were found, and samples from old donors were more variable than those from young. A heat map of hierarchical clusters of correlations among samples (Figure 1C) depicts that the sncRNA expression of young and old groups are not very different.

There were 83 sncRNAs differentially expressed with age; six snoRNAs, 11 novel snoRNAs, three snRNAs, 31 lncRNAs, 27 tRNAs ( $p < 0.05$ ) and five miRNAs (FDR-adjusted  $p < 0.05$ ) (Table 1). Data is deposited on NCBI GEO, accession; E-MTAB-8112.

**Table 1.** Differentially expressed sncRNAs in ageing chondrocytes. Log<sub>2</sub> fold change values were derived with young as the reference group. A positive log<sub>2</sub> fold change equates to higher expression in old, whereas a negative log<sub>2</sub> fold change equates to lower expression in old. All are significant at  $p < 0.05$ , except for miRNAs that are significant with a false-discovery rate (FDR)-adjusted p value of  $p < 0.05$ .

Gene/Transcript Name	Gene Biotype	Log <sub>2</sub> Fold Change
eca-miR-143	miRNA	-1.3
eca-miR-145	miRNA	-1.8
eca-miR-181b	miRNA	-1.8
eca-miR-122	miRNA	2.3
eca-miR-148a	miRNA	1.3
snora71	snoRNA	-3.2
snord113	snoRNA	-2.4
snora46	snoRNA	1.0
snora77	snoRNA	2.0
snora47	snoRNA	2.5
snord29	snoRNA	2.5
ECABCGRLG0000003960	novel snoRNA	-2.6
ECABCGRLG0000002980	novel snoRNA	-2.5
ECABCGRLG0000006050	novel snoRNA	-1.6
ECABCGRLG000000640	novel snoRNA	-1.1
ECABCGRLG0000002800	novel snoRNA	-1.0
ECABCGRLG0000007680	novel snoRNA	1.8
ECABCGRLG0000008070	novel snoRNA	2.0
ECABCGRLG0000007010	novel snoRNA	2.5
ECABCGRLG0000008090	novel snoRNA	2.9
ECABCGRLG0000004470	novel snoRNA	3.0
ECABCGRLG0000005680	novel snoRNA	3.1
LOC111775808	snRNA	-1.3
LOC111773055	snRNA	2.2
LOC111772636	snRNA	2.5
LOC111770368	lncRNA	-3.4
LOC111768432	lncRNA	-3.2
LOC102148414	lncRNA	-3.2
LOC102149168	lncRNA	-2.9
LOC111772155	lncRNA	-2.5
LOC106783307	lncRNA	-2.5
LOC111775319	lncRNA	-2.5
LOC102148711	lncRNA	-2.5
LOC111775759	lncRNA	-2.5
LOC111774351	lncRNA	-2.5
LOC102150704	lncRNA	-2.5
LOC111775994	lncRNA	-2.5
LOC102150027	lncRNA	-2.5
LOC106781358	lncRNA	-2.5
LOC102147393	lncRNA	-2.5
LOC111776203	lncRNA	-2.5
LOC111771286	lncRNA	-1.3
LOC102149893	lncRNA	1.7
LOC111775969	lncRNA	1.7
LOC106781629	lncRNA	1.9
LOC111773181	lncRNA	2.0
LOC102149863	lncRNA	2.5
LOC102149361	lncRNA	2.5
LOC111770630	lncRNA	2.5
LOC102147707	lncRNA	2.5
LOC106783385	lncRNA	2.5
LOC102149569	lncRNA	2.5

**Table 1.** Cont.

Gene/Transcript Name	Gene Biotype	Log <sub>2</sub> Fold Change
LOC106782740	lncRNA	2.5
LOC111770896	lncRNA	2.5
LOC102150024	lncRNA	2.9
LOC102150338	lncRNA	2.9
TRNAR-ACG	tRNA	-3.4
TRNAR-CCU	tRNA	-3.2
TRNAS-AGA	tRNA	-3.2
TRNAS-GCU	tRNA	-3.1
TRNAU-UGC	tRNA	-3.0
TRNAP-AGG	tRNA	-2.9
TRNAQ-UUG	tRNA	-2.9
TRNAS-AGA	tRNA	-2.9
TRNAA-UGC	tRNA	-2.9
TRNAF-GAA	tRNA	-2.5
TRNAP-UGG	tRNA	-2.5
TRNAE-UUC	tRNA	-2.5
TRNAF-GAA	tRNA	-2.2
TRNAV-AAC	tRNA	-2.2
TRNAM-CAU	tRNA	-2.1
TRNAT-AGU	tRNA	-1.9
TRNAY-GUA	tRNA	-1.9
TRNAQ-CUG	tRNA	-1.4
TRNAN-GUU	tRNA	-1.4
TRNAY-GUA	tRNA	-1.4
TRNAY-GUA	tRNA	-1.2
TRNAV-AAC	tRNA	1.9
TRNAP-CGG	tRNA	2.2
TRNAA-UGC	tRNA	2.4
TRNAC-GCA	tRNA	2.5
TRNAI-AAU	tRNA	2.9
TRNAD-GUC	tRNA	3.4

### 3.3. Age Specific miRNA Interactome

To generate an age-specific miRNA interactome of the most likely miRNA-mRNA target pairs, analysis was performed to identify miRNA targets of the five differentially expressed miRNAs from this study. In IPA, the five miRNAs (miR-143, miR-145, miR-181b, miR-122, miR-148a) were paired with 351 protein coding genes differentially expressed in our previous RNA-seq study on ageing equine cartilage [31]. In File S4, the miRNA-mRNA pairings in the correct direction (miR increase and mRNA decrease or vice versa) are shown, including the target predictions and /or experimental validation in the respective database. Four of the five miRNAs interacted in IPA with 31 different differentially expressed target genes reflecting that miRNAs target many mRNAs. These mRNAs targeted by the miRNAs were used in IPA as network-eligible molecules and overlaid onto molecular networks based on information from the IPA Database. Networks for the four miRNAs (miR-148a, miR-122, miR-143, and miR-181b) were generated based on connectivity (Figure 2A–D). Interesting age-related features were determined from the gene networks inferred. Among the top canonical pathways were hepatic fibrosis ( $p = 1.51 \times 10^{-3}$ ), glycoprotein 6 (GP6) signalling ( $p = 5.67 \times 10^{-4}$ ), and osteoarthritis pathway ( $p = 2.93 \times 10^{-3}$ ). The top diseases and cellular functions associated with this network are shown in Table 2 and Figure 3. All IPA results are in File S5.

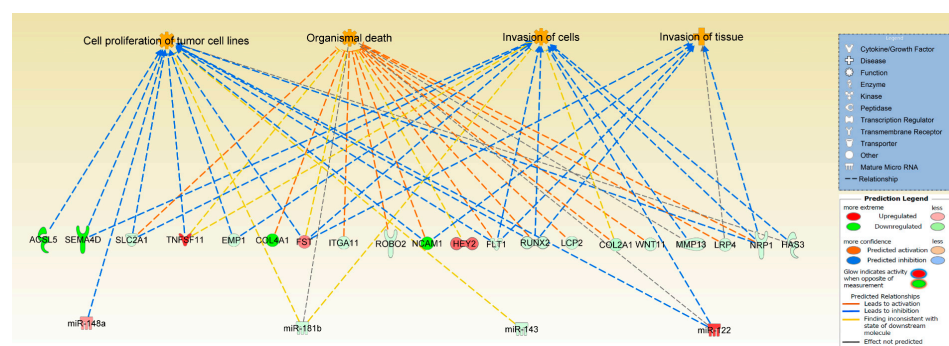
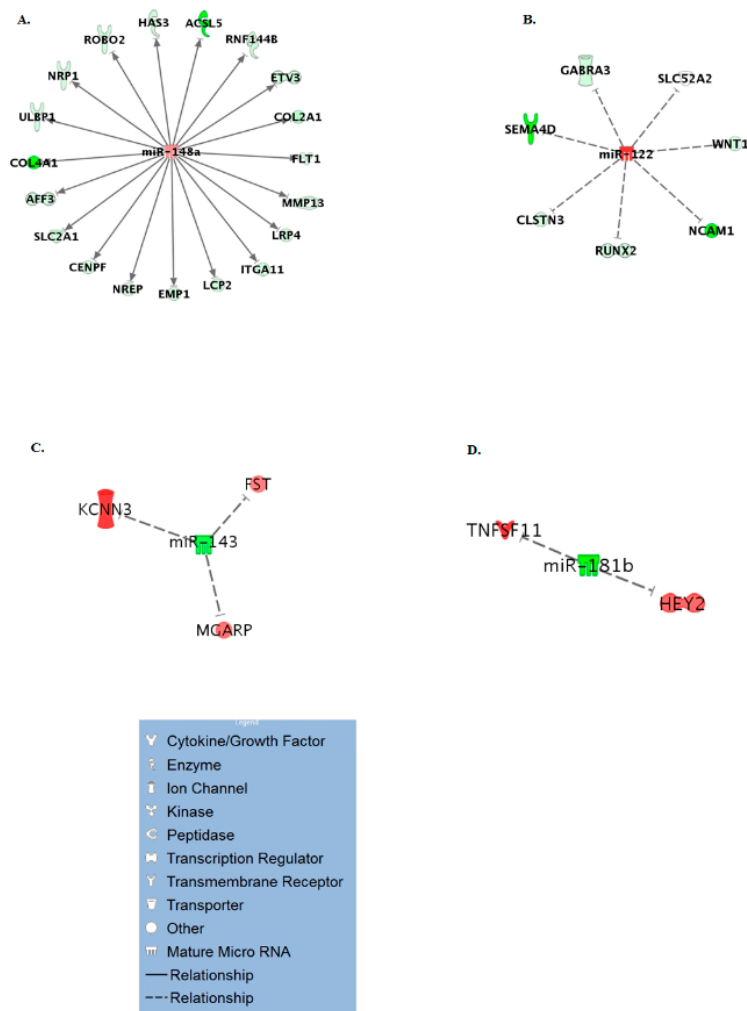


**Table 2.** IPA mRNA target diseases and functions.

a. Top Molecular and Cellular Functions	p-Value Range	Number of Molecules
Cellular Movement	$1.41 \times 10^{-3}$ – $4.23 \times 10^{-10}$	21
Cell Morphology	$1.37 \times 10^{-3}$ – $3.52 \times 10^{-8}$	16
Cellular Development	$1.42 \times 10^{-3}$ – $4.94 \times 10^{-7}$	24
Cell Death and Survival	$1.37 \times 10^{-3}$ – $1.08 \times 10^{-5}$	18
Cell-To-Cell Signalling and Interaction	$1.37 \times 10^{-3}$ – $1.88 \times 10^{-5}$	20
b. Top Diseases and Disorders		
Skeletal and Muscular Disorders	$1.50 \times 10^{-3}$ – $1.22 \times 10^{-9}$	16
Connective Tissue Disorders	$1.50 \times 10^{-3}$ – $3.52 \times 10^{-8}$	16
Organismal Injury and Abnormalities	$1.50 \times 10^{-3}$ – $3.52 \times 10^{-8}$	31
Cancer	$1.49 \times 10^{-3}$ – $5.30 \times 10^{-7}$	31
Developmental Disorder	$1.37 \times 10^{-3}$ – $5.30 \times 10^{-7}$	17

### 3.4. Confirmation of Differential Gene Expression Using qRT-PCR

For selected snoRNAs (snora46, snora71, snora77, and snord113) and miRNAs (miR-143, miR-145, miR-148a, miR-122, and miR-181b) we used qRT-PCR to validate the small RNA-Seq findings in an extended cohort of chondrocytes. Findings for snora71, snord113, miR-143, miR-145, miR-122, and miR-181b were validated (Figure 4).

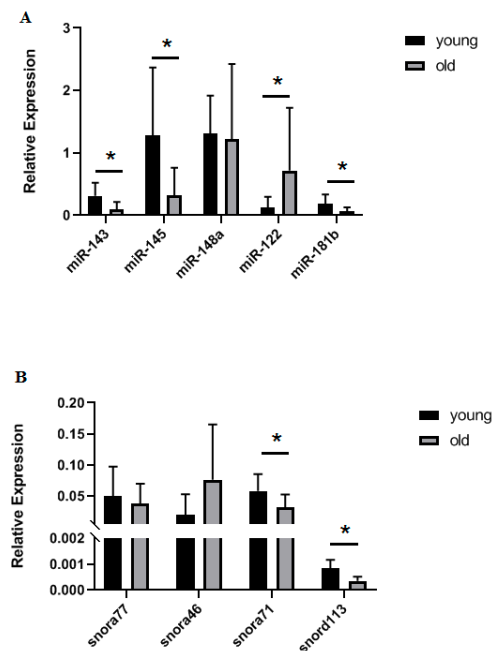


**Figure 4.** Validation of selected sncRNAs in an extended cohort of equine young and old chondrocytes. Real-time quantitative Polymerase Chain Reaction (qRT-PCR) was used to validate findings from the small RNA sequencing (A) microRNAs and (B) snoRNAs,  $n = 5$ –12 per group. Statistical analysis was undertaken using a Mann Whitney test in GraphPad Prism. Mean and standard errors are shown with \* denoting  $p < 0.05$ .

### 3.5. tRNA Fragment Changes in Equine Ageing

As we identified differentially expressed tRNAs in ageing equine chondrocytes, we undertook additional analysis to identify tRNAs and tRFs, as increasing experimental evidence suggests their

functional roles in OA [27]. Figure 5 shows cumulative density of tRNA fragment length, alignment length, gene counts, and map start position. On the assessment of data variation using PCA, samples in group “old” did not scatter very closely. Differential expression analysis of all young versus all old did not identify any differentially expressed tRFs ( $FDR < 0.05$ ). Therefore, we reanalysed the data with the old group divided into two subgroups based on PCA findings: ‘old 1’ (samples 6, 7, 8) and ‘old 2’ (samples 9 and 10) for further differential expression analysis. There were 81 differentially expressed tRNAs/tRFs; 44 higher in ‘old 2’ and 37 lower in ‘old 2’ compared to young (File S6).

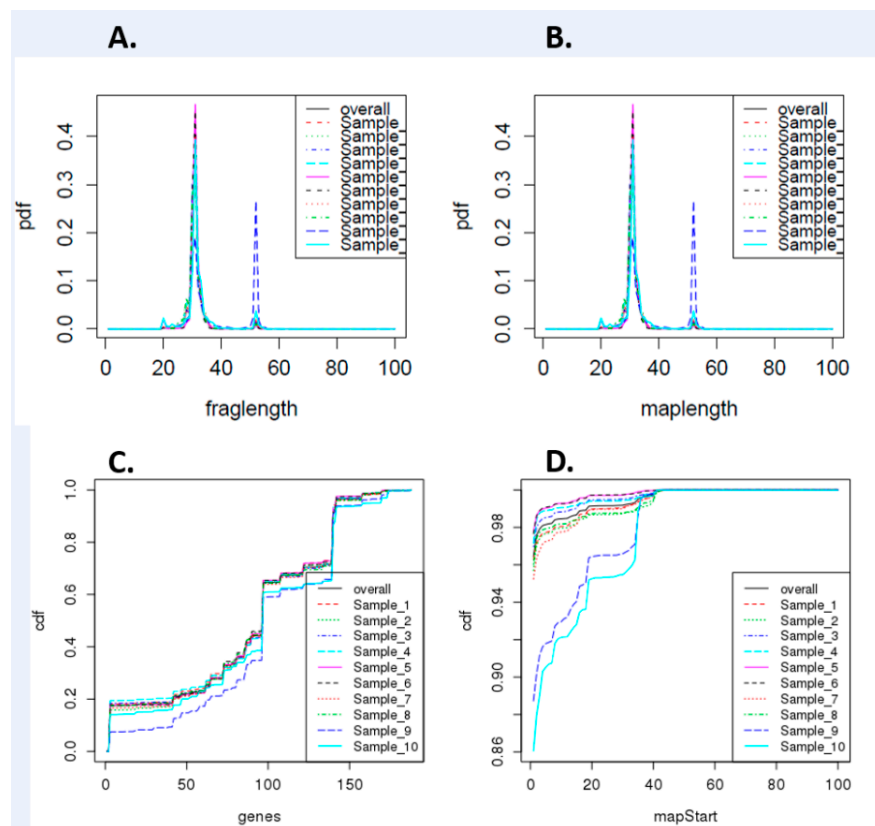


**Figure 5.** Summary of differentially expressed tRNA fragment data. **(A)** Cumulative density of tRNA fragment length, **(B)** alignment length, **(C)** gene counts, and **(D)** map start position. Samples 1–5 are derived from young donors and 6–10 are old donors.

### 3.6. Human tRNA and tRF Profiles Compared to Equine tRNA and tRF Profiles

In both human and equine samples, 26 parent tRNAs were detected. Of these 26 tRNAs, 13 tRNAs were induced and 13 were reduced in cartilage from high grade OA compared to cartilage from low grade OA. In equine chondrocytes, 6 parent tRNAs were expressed higher and 20 parent tRNAs were expressed lower in old samples compared to young. Four parent tRNAs were induced in both high grade OA cartilage compared to low grade OA cartilage and in old versus young equine samples. Eleven parent tRNAs were reduced in high grade OA cartilage compared to low grade OA cartilage and in the old versus young equine samples (Figure 6A).

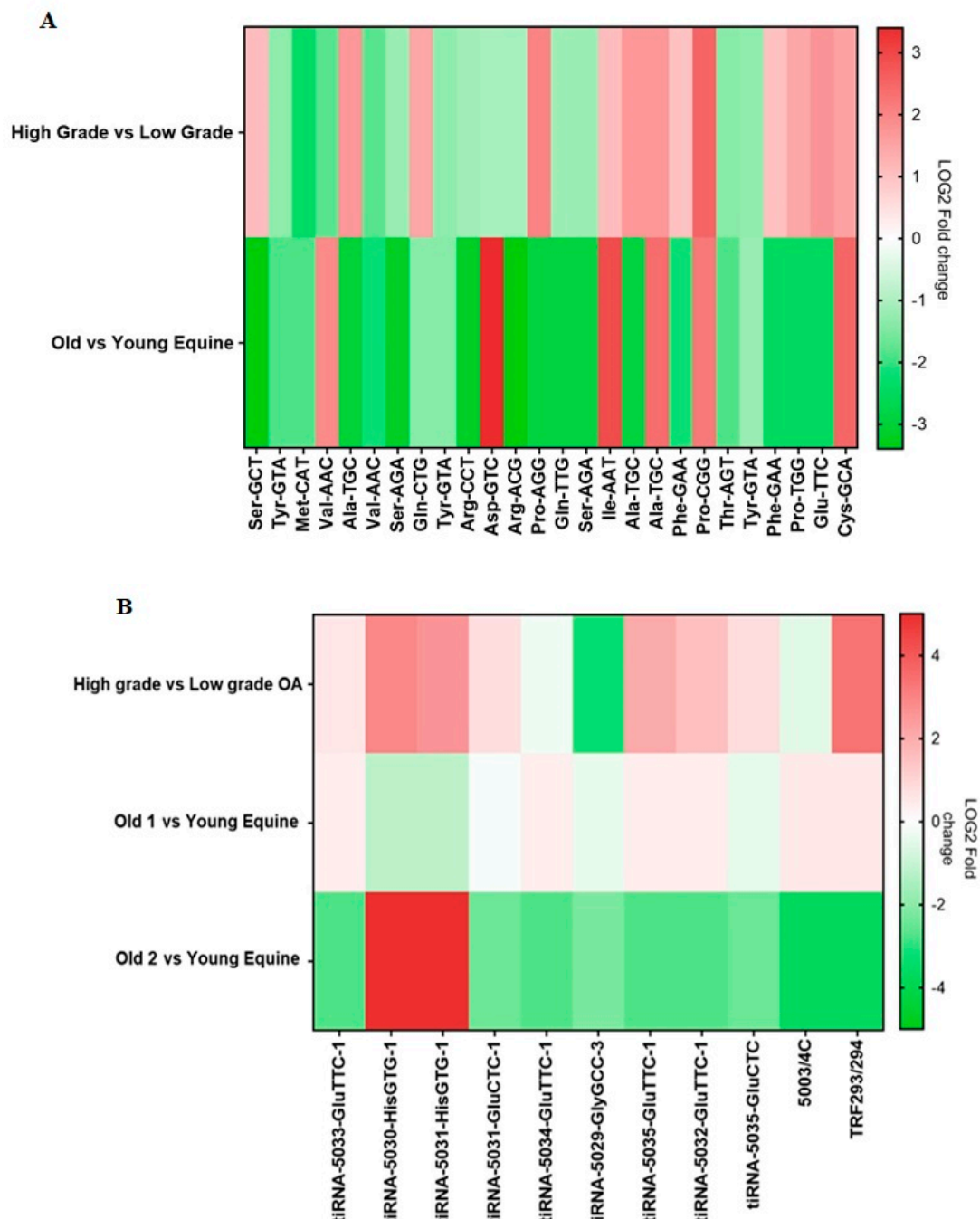


**Figure 6.** tRNA analysis of human osteoarthritic cartilage. (A) High grade versus low grade OA human cartilage and old versus young equine chondrocyte tRNA profiles. Heatmap of Log2 fold change expression of 26 tRNAs detected in both human and equine samples. Human cartilage tRNAs detected using a Human tRNA PCR Array. Red highlights induced tRNA expression in high grade OA human cartilage compared to low grade and in old equine chondrocytes compared to young. Green highlights reduced tRNA expression in high grade OA human cartilage compared to low grade and in old equine chondrocytes compared to young. (B) High grade OA versus low grade OA human cartilage and equine tRNA/tRF profiles. Heatmap of Log2 foldchange expression of 11 tRF/tiRNA fragments detected in both human and equine samples. Human cartilage tRF/tiRNA detected using a Human tRF&tiRNA PCR Array. Red highlights induced tRF/tiRNA expression in human high grade versus low grade OA samples and in old versus young equine samples. Green highlights reduced tRF/tiRNA expression in human high grade versus low grade OA samples and in old versus young equine samples.

In both human and equine samples, the tRF-5 fragment known as tRF293/294 and 10 tiRNAs were detected (Figure 6B). In high grade OA compared to low grade OA cartilage, seven tiRNAs and tRF293/294 were induced and three tiRNAs were reduced. In old 1 versus young equine, five tiRNAs and tRF293/294 were induced and five tiRNAs were reduced. In old 2 versus young equine, two tiRNAs were induced and eight tiRNAs and tRF293/294 were reduced. Of these tRNA fragments, three tiRNAs and tRF293/294 were induced and tiRNA-5029-GlyGCC-3 was reduced in high versus low grade OA cartilage and in old 1 versus young equine. Two tiRNAs were induced and three tiRNAs were reduced in high versus low grade OA cartilage and in old 2 versus young equine. In high versus low grade OA cartilage and old 1 versus young equine tiRNA-5029-GlyGCC was reduced.

#### 4. Discussion

Our study investigated the changing sncRNA landscape in ageing chondrocytes. Several risk factors exist that influence cartilage health and chondrocyte homeostasis. Among them, ageing is one of the leading risk factors contributing to cartilage-related diseases, such as OA [52]. Many studies have shown that ageing can affect cartilage in different ways, both at cellular and molecular level. Increased chondrocyte death, apoptosis, and a shift towards a catabolic profile have been observed in aged chondrocytes [53]. Additional age-related changes in articular cartilage include increased chondrocyte senescence [54], oxidative stress [55], and changes in the composition and structure of ECM [56]. Although the underlying molecular causes of these changes are not completely understood, it is hypothesised that aged chondrocytes respond differently to various stimuli, such as growth factors, [53,57] and demonstrate altered molecular signatures [6].

SncRNAs are a subset of epigenetic modifiers and their role in cartilage ageing has been studied increasingly in the last decade [6,31,58]. In the current study, we have used small RNA-seq to identify alterations in sncRNAs between young and old equine chondrocytes. The horse is a good model to study musculoskeletal ageing and disease as we could assess the whole joint for pathological perturbations during tissue collection. It is very challenging to source aged human cartilage that has no OA changes, whereas this is easily undertaken in equine samples. Moreover, the horse has been used as a model of OA and there has been significant research on equine joint anatomy and pathophysiology [59,60].

Within our set of differentially expressed sncRNAs, miRNAs are the best studied in musculoskeletal ageing and cartilage. In old chondrocytes, we identified two miRNAs with higher expression; miR-122 and miR-148a, and three miRNAs with lower expression; miR-143, miR-145, and miR-181b. Of these five miRNAs, all except miR-148a were validated in an extended cohort of young and old equine chondrocytes with qRT-PCR. MiR-122 has been researched extensively in liver [61,62], but its role in musculoskeletal ageing is less clear. MiR-122 was decreased in the serum and plasma of patients with osteoporosis, the most common age-related bone disease [63], but was significantly upregulated in senescent human fibroblasts [64] and was shown to upregulate p53 which is induced in senescence [65]. MiR-143 was downregulated in muscle satellite cells from old mice and primary myoblasts from old humans and mice [66]. In addition, circulating miR-143 was upregulated in young individuals following resistant exercise, but was downregulated in older individuals after resistant exercise [67]. MiR-145 was downregulated in old OA patients [68] as well as in experimental OA rat chondrocytes treated with tumour necrosis factor (TNF) [69] and, finally, miR-181b was downregulated in skeletal muscle of old rhesus monkeys [70].

To further investigate the potential role of the differentially expressed miRNAs identified in this study, we used IPA to combine them with the differentially expressed mRNAs from our previous equine cartilage study [31]. IPA miRNA ‘Target Filter and Expression Pairing’ identified 31 potential target genes. IPA core analysis of these genes revealed canonical pathways associated with cartilage physiology, such as role of chondrocytes in rheumatoid arthritis, OA-related pathways and bone morphogenic protein (BMP) signalling, all of which have been reported to change with ageing [56,71,72]. Moreover, top diseases and disorders linked to these genes, as identified by IPA, included skeletal and

muscular disorders and connective tissue disorders. Of note, follistatin (FST) which was upregulated in old equine cartilage and was predicted by IPA as a target of the downregulated miR-143, was overexpressed in human OA chondrocytes [73] and canine OA cartilage [74] and was induced by telomere shortening [75], a process associated with ageing. Moreover, *TNF ligand superfamily member 11* (*TNFSF11*), also known as *receptor activator of nuclear factor kappa-B ligand* (*RANKL*) was upregulated in old equine cartilage and was identified as a predicted target of the downregulated miR-181b. Higher expression of *TNFSF11/RANKL*, which correlated with bone loss, was reported in old C57BL/6 mice [76], rabbits with chronic antigen-induced arthritis [77], and in human high grade OA cartilage [78]. These results demonstrate the adverse effect of ageing on miRNA levels and their potential use as biomarkers or therapeutic targets for age-related musculoskeletal diseases.

Six snoRNAs were identified as differentially expressed due to ageing in chondrocytes. This conserved class of non-coding RNAs are principally characterised as guiding site-specific post-transcriptional modifications in ribosomal RNA [79] (canonical snoRNAs), but can also modify additional classes of RNAs including other snoRNAs, tRNAs and mRNAs; so called non-canonical snoRNAs [80,81]. Examples of age-related snoRNAs in equine ageing chondrocytes with canonical functions include snora71 and snord29. Novel non-canonical functions reported for snoRNAs including the modulation of alternative splicing [82], an essential involvement in stress response pathways [83] and the modulation of mRNA 3' end processing [84]. Similar to miRNAs, snoRNAs are emerging as important regulators of cellular function and disease development [15], related to their ability to fine-tune ribosomes accommodating changing requirements for protein production during development, normal function, and disease [85]. We have previously identified a role for snoRNAs in cartilage ageing and OA [16] and their potential use as biomarkers for OA [9]. Interestingly there was a reduction in snord113/114 in ageing chondrocytes which agrees with our previous findings in equine cartilage ageing [31]. We have also previously demonstrated that SNORD113 was reduced in ageing human knee cartilage but increased in OA [16] and increased in human anterior cruciate ligament [17]. SNORD113/114 are located in imprinted loci and may play a role in the evolution and/or mechanism of epigenetic imprinting. Although belonging to the C/D box class of snoRNAs which direct site-specific 2'-O-ribose methylation of substrate RNAs, they differ from other C/D box snoRNAs in their tissue specific expression profiles (including fibroblast, chondrocytes and osteoblasts) and the lack of known substrate RNA complementarity. This currently classifies them as orphan snoRNAs as they are not predicted to guide the 2'-O-ribose methylation but have novel, unknown roles [86]. Additionally, SNORD113 functions as a tumour suppressor in hepatic cell carcinoma by reducing cell growth, and it inactivates the phosphorylation of extracellular signal-regulated kinase (ERK) 1/2 and mothers against decapentaplegic homolog (SMAD) 2/3 in mitogen-activated protein kinase (MAPK)/ERK and transforming growth factor beta (TGF- $\beta$ ) pathways [87]. Together, our snoRNA findings indicate that age-related changes in chondrocyte snoRNAs could have important implications through both canonical and non-canonical snoRNA routes.

This is the first study to detect tRNA and tRNA fragments in equine chondrocytes and to compare these findings with tRNA and tRNA fragments detected in human OA cartilage. For our tRNA data, old donors clustered into two groups and further analysis was undertaken with these subgroups. There were no apparent differences in these subgroups with regards to age or sex and scores were all zero. The parent tRNA Cys-GCA was found to be increased in both aged equine chondrocytes and high grade OA human cartilage samples. tRNA Cys-GCA levels have previously been reported to be increased in human chondrocytes induced with the cytokine interleukin (IL) 1 beta resulting in the production of the tRNA fragment tRF-3003a, a type 3-tRF produced by the cleavage of Cys-GCA. tRF-3003a has been shown to post-transcriptionally regulate the Janus Kinase 3 (JAK3) expression through sequence complementarity via the Argonaute (AGO) / RNA-induced silencing complex (RISC) in human chondrocytes [27].

The Janus Kinase and Signal Transducer and Activator of Transcription (JAK-STAT) pathway is the target of several cytokines such as interferon- $\gamma$ , IL-2, IL-4, IL-6, IL-7, IL-10, IL-12, and IL-15.

Many of these cytokines are known to play important roles in synovial inflammation during OA pathogenesis [88,89].

The tRNA fragments detected in equine samples that matched with human samples consisted of 5' tiRNA and tRF-5 fragments. Many of the equine fragments detected did not fall into the classical tRF-3, tRF-5, or tiRNA size ranges and instead may likely be i-tRFs, which are internal to the respective tRNA and can straddle the anticodon loop. 5' tiRNA, 3' tiRNA, tRF-3, and tRF-5 fragments were detected in the low-grade OA cartilage and in the high grade OA cartilage. In our human studies, base modifications found on tRNAs and tRF/tiRNA fragments that would normally block reverse transcription were removed and this may account for some of the differences found between the equine and human tRNA/tRF profiles.

The importance of modulation of tRNA levels and tRNA fragments in articular cartilage homeostasis remains an unexplored area. This is the first evidence that aged equine samples have changes in the expression of specific tRNAs and tRFs when compared to young equine samples. We report for the first time several 5' tiRNAs, such as tiRNA Glu-TTC and tiRNA His-GTG, were induced in old compared to young equine chondrocytes and in high grade compared to low grade human OA cartilage. Previous reports have shown that 5' tiRNAs can be produced by cell stress in mammalian cells and these 5' tiRNA half fragments may have a role in inhibiting cell translation and could be involved in stress granule formation [90]. Further studies are required to find the mechanism by which these fragments are produced and whether the changes in the profile of fragments found in old compared to young equine chondrocytes or high compared to low grade OA cartilage potentially contribute to the development of OA.

We are aware our study has a number of limitations. The effect of ageing between young and old equine chondrocytes was small on the differential expression of sncRNAs. However, it is likely that we are therefore interrogating highly specific changes that are age dependent. Furthermore, we cannot rule out changes related to the use of chondrocytes instead of cartilage tissue. Even though chondrocytes of low passage were used, collagenase digestion and plating of cells could have affected their phenotype and gene expression. The choice of chondrocytes over cartilage tissue was made based on RNA from cartilage tissue is of low quality (in our hands) and heavily contaminated with proteoglycans [91], usually making it challenging for sequencing. In our previous study interrogating snoRNAs in human knee cartilage ageing and OA [16] we utilized cartilage tissue as opposed to chondrocytes. The old non-OA cartilage was derived from the grossly normal condyle of OA joints. In the study we found a number of age and OA specific snoRNAs, but we could not define the cartilage as truly normal as it was derived from an OA joint. Nevertheless, we identified two age related, no species specific snoRNAs that were DE in both our studies, snord113 and snord29. The use of the Illumina MiSeq platform would have contributed to the low number of differentially expressed sncRNAs as it offers less depth coverage compared to other platforms, such as the HiSeq platform. Finally, we have used a relatively small number of samples per group. Given the use of primary cells and the degree of variability observed, especially for the old group, the inclusion of five samples pre group may have contributed to the small number of differentially expressed sncRNAs in ageing equine chondrocytes on our study.

## 5. Conclusions

For the first time we have described, using unbiased methods, the effect of ageing on the expression of sncRNAs in equine chondrocytes. We detected variable classes of sncRNAs (the small non-coding RNAome) in young and old chondrocytes, which are differentially abundant, indicating that there are multiple levels of epigenetic control in cartilage and chondrocyte ageing. Among them, there were miRNAs, which are predicted to play a role in the development of the musculoskeletal system and in skeletal disorders. In addition, the current study is one of the few studies that have investigated tRNAs and tRNA fragments, in an attempt to uncover novel molecular signatures in aged and diseased

chondrocytes/cartilage that could be useful in the future as therapeutic targets. Further research is needed to elucidate the role and function of these molecules and their potential link to disease.

**Supplementary Materials:** Supplementary materials can be found at <http://www.mdpi.com/1422-0067/21/16/5675/s1>. File S1. .xls, Small RNA assay details; File S2. .xls, MiSeq read mapping details; File S3. .xls, Types of small non-coding RNAs identified in MiSeq data; File S4. .xls, miRNA-mRNA pairings in the correct direction; File S5. .xls, IPA analysis summary; File S6. .xls, differentially expressed tRNA halves/tRFs

**Author Contributions:** M.J.P., P.B., T.J.M.W., J.A.G. and T.M.H. conceived the study and designed the work; P.B., P.D., J.A.G., M.J.P., Y.A.K. acquired and analysed the data, Y.F., X.L., interpreted the data; all authors have drafted the work. All authors have approved the submitted version. All authors have agreed both to be personally accountable for the author's own contributions and to ensure that questions related to the accuracy or integrity of any part of the work, even ones in which the author was not personally involved, are appropriately investigated, resolved, and the resolution documented in the literature. All authors have read and agreed to the published version of the manuscript.

**Funding:** Mandy Peffers is funded through a Wellcome Trust Intermediate Clinical Fellowship (107471/Z/15/Z). Panagiotis Balaskas is funded through an MRC-DTP studentship supported by the Medical Research Council (MRC). Both are supported through Versus Arthritis as part of the MRC Versus Arthritis Centre for Integrated research into Musculoskeletal Ageing (CIMA). This work was also supported in part by the National Institute of Arthritis and Musculoskeletal and Skin Diseases (NIAMS) and the National Centre for Complementary and Integrative Health (NCCIH) of the National Institutes of Health (NIH) under award numbers R01-AR067056, and R01-AT007373 respectively and funds from NEOMED to TMH.

**Acknowledgments:** We would like to thank Catarina Castanheira for her assistance with the laboratory work.

**Conflicts of Interest:** T.J.M Welting is listed as inventors on patents WO2017178251 and WO2017178253. T.J.M Welting has shares in Chondropeptix. The remaining authors declare that they have no competing interests.

## Abbreviations

ECM	extracellular matrix
OA	osteoarthritis
sncRNAs	small non-coding RNAs
miRNAs or miRs	microRNAs
snRNAs	small nuclear RNAs
snoRNAs	small nucleolar RNAs
tRNAs	transfer RNAs
mRNA	messenger RNA
tiRNAs	tRNA halves
ANG	angiogenin
tRFs	tRNA-derived small RNA fragments
PCA	principle component analysis
logFC	log2 fold change
FDR	False Discovery Rate
IPA	Ingenuity Pathway Analysis
RNA-seq	RNA sequencing
qRT-PCR	real-time quantitative Polymerase Chain Reaction
lncRNAs	long non-coding RNAs
PCs	Principle components
GP6	glycoprotein 6
BMP	bone morphogenic protein
FST	follistatin
TNF	tumour necrosis factor
TNFSF11	TNF ligand superfamily member 11
RANKL	receptor activator of nuclear factor kappa-B ligand
ERK	extracellular signal-regulated kinase
SMAD	mothers against decapentaplegic homolog
MAPK	mitogen-activated protein kinase
TGF-β	transforming growth factor beta
IL	interleukin

JAK3	Janus Kinase 3
AGO	Argonaute
RISC	RNA-induced silencing complex
JAK-STAT	Janus Kinase and Signal Transducer and Activator of Transcription

## References

- Messina, O.D.; Wilman, M.V.; Neira, L.F.V. Nutrition, osteoarthritis and cartilage metabolism. *Aging Clin. Exp. Res.* **2019**, *31*, 807–813. [[CrossRef](#)] [[PubMed](#)]
- Decker, R.S. Articular cartilage and joint development from embryogenesis to adulthood. *Semin. Cell Dev. Biol.* **2016**, *62*, 50–56. [[CrossRef](#)] [[PubMed](#)]
- Sacitharan, P.K.; Vincent, T.L. Cellular ageing mechanisms in osteoarthritis. *Mamm. Genome* **2016**, *27*, 421–429. [[CrossRef](#)]
- Philipot, D.; Guérin, D.; Platano, D.; Chuchana, P.; Olivotto, E.; Espinoza, F.; Dorandeu, A.; Pers, Y.M.; Piette, J.; Borzi, R.; et al. p16INK4a and its regulator miR-24 link senescence and chondrocyte terminal differentiation-associated matrix remodeling in osteoarthritis. *Arthritis Res. Ther.* **2014**, *16*, R58. [[CrossRef](#)] [[PubMed](#)]
- Verzijl, N.; DeGroot, J.; Ben Zaken, C.; Braun-Benjamin, O.; Maroudas, A.; Bank, R.A.; Mizrahi, J.; Schalkwijk, C.G.; Thorpe, S.R.; Baynes, J.W.; et al. Crosslinking by advanced glycation end products increases the stiffness of the collagen network in human articular cartilage: A possible mechanism through which age is a risk factor for osteoarthritis. *Arthritis Rheum.* **2002**, *46*, 114–123. [[CrossRef](#)]
- Zhang, M.; Theleman, J.L.; Lygrisse, K.A.; Wang, J. Epigenetic Mechanisms Underlying the Aging of Articular Cartilage and Osteoarthritis. *Gerontology* **2019**, *65*, 387–396. [[CrossRef](#)]
- Greene, M.A.; Loeser, R.F. Aging-related inflammation in osteoarthritis. *Osteoarthr. Cartil.* **2015**, *23*, 1966–1971. [[CrossRef](#)]
- Sondag, G.R.; Haqqi, T.M. The Role of MicroRNAs and Their Targets in Osteoarthritis. *Curr. Rheumatol. Rep.* **2016**, *18*, 56. [[CrossRef](#)]
- Steinbusch, M.M.F.; Fang, Y.; Milner, P.I.; Clegg, P.D.; Young, D.A.; Welting, T.J.M.; Peffers, M.J. Serum snoRNAs as biomarkers for joint ageing and post traumatic osteoarthritis. *Sci. Rep.* **2017**, *7*, 43558. [[CrossRef](#)]
- Zhang, L.; Yang, M.; Marks, P.; White, L.; Hurtig, M.; Mi, Q.-S.; Divine, G.; Gibson, G. Serum non-coding RNAs as biomarkers for osteoarthritis progression after ACL injury. *Osteoarthr. Cartil.* **2012**, *20*, 1631–1637. [[CrossRef](#)]
- Kamaruzaman, H.; Kinghorn, P.; Oppong, R. Cost-effectiveness of surgical interventions for the management of osteoarthritis: A systematic review of the literature. *BMC Musculoskelet. Disord.* **2017**, *18*, 183. [[CrossRef](#)] [[PubMed](#)]
- Miyaki, S.; Sato, T.; Inoue, A.; Otsuki, S.; Ito, Y.; Yokoyama, S.; Kato, Y.; Takemoto, F.; Nakasa, T.; Yamashita, S.; et al. MicroRNA-140 plays dual roles in both cartilage development and homeostasis. *Genes Dev.* **2010**, *24*, 1173–1185. [[CrossRef](#)] [[PubMed](#)]
- Peffers, M.; Caron, M.; Cremers, A.; Surtel, D.; Fang, Y.; Dyer, P.; Balaskas, P.; Welting, T. snoRNA signatures in cartilage ageing and osteoarthritis. *Osteoarthr. Cartil.* **2018**, *26*, S164. [[CrossRef](#)]
- Brameier, M.; Herwig, A.; Reinhardt, R.; Walter, L.; Gruber, J. Human box C/D snoRNAs with miRNA like functions: Expanding the range of regulatory RNAs. *Nucleic Acids Res.* **2011**, *39*, 675–686. [[CrossRef](#)]
- Stepanov, G.A.; Filippova, J.A.; Komissarov, A.B.; Kulagina, E.V.; Richter, V.A.; Semenov, D.V. Regulatory Role of Small Nucleolar RNAs in Human Diseases. *BioMed Res. Int.* **2015**, *2015*, 1–10. [[CrossRef](#)] [[PubMed](#)]
- Peffers, M.J.; Chabronova, A.; Balaskas, P.; Fang, Y.; Dyer, P.; Cremers, A.; Emans, P.J.; Feczkó, P.Z.; Caron, M.M.; Welting, T.J.M. SnoRNA signatures in cartilage ageing and osteoarthritis. *Sci. Rep.* **2020**, *10*, 1–10. [[CrossRef](#)]
- Kharaz, Y.A.; Fang, Y.; Welting, T.; Peffers, M.; Comerford, E. Small RNA signatures of the anterior cruciate ligament from patients with knee 1 joint osteoarthritis. *medRxiv* **2020**. [[CrossRef](#)]
- Raina, M.; Ibba, M. tRNAs as regulators of biological processes. *Front. Genet.* **2014**, *5*, 171. [[CrossRef](#)]
- Yamasaki, S.; Ivanov, P.; Hu, G.-F.; Anderson, P. Angiogenin cleaves tRNA and promotes stress-induced translational repression. *J. Cell Biol.* **2009**, *185*, 35–42. [[CrossRef](#)]

20. Lee, Y.S.; Shibata, Y.; Malhotra, A.; Dutta, A. A novel class of small RNAs: tRNA-derived RNA fragments (tRFs). *Genes Dev.* **2009**, *23*, 2639–2649. [CrossRef]
21. Takaku, H.; Minagawa, A.; Takagi, M.; Nashimoto, M. A candidate prostate cancer susceptibility gene encodes tRNA 3' processing endoribonuclease. *Nucleic Acids Res.* **2003**, *31*, 2272–2278. [CrossRef] [PubMed]
22. Goodarzi, H.; Liu, X.; Nguyen, H.C.; Zhang, S.; Fish, L.; Tavazoie, S.F. Endogenous tRNA-Derived Fragments Suppress Breast Cancer Progression via YBX1 Displacement. *Cell* **2015**, *161*, 790–802. [CrossRef] [PubMed]
23. Cole, C.; Sobala, A.; Lu, C.; Thatcher, S.R.; Bowman, A.; Brown, J.W.; Green, P.J.; Barton, G.J.; Hutvagner, G. Filtering of deep sequencing data reveals the existence of abundant Dicer-dependent small RNAs derived from tRNAs. *RNA* **2009**, *15*, 2147–2160. [CrossRef] [PubMed]
24. Li, Z.; Ender, C.; Meister, G.; Moore, P.S.; Chang, Y.; John, B. Extensive terminal and asymmetric processing of small RNAs from rRNAs, snoRNAs, snRNAs, and tRNAs. *Nucleic Acids Res.* **2012**, *40*, 6787–6799. [CrossRef] [PubMed]
25. Telonis, A.G.; Loher, P.; Honda, S.; Jing, Y.; Palazzo, J.; Kirino, Y.; Rigoutsos, I. Dissecting tRNA-derived fragment complexities using personalized transcriptomes reveals novel fragment classes and unexpected dependencies. *Oncotarget* **2015**, *6*, 24797–24822. [CrossRef]
26. Jiang, P.; Yan, F. tRNAs & tRFs Biogenesis and Regulation of Diseases: A Review. *Curr. Med. Chem.* **2019**, *26*, 5849–5861. [CrossRef]
27. Green, J.; Ansari, M.; Ball, H.; Haqqi, T.M. tRNA-derived fragments (tRFs) regulate post-transcriptional gene expression via AGO-dependent mechanism in IL-1 $\beta$  stimulated chondrocytes. *Osteoarthr. Cartil.* **2020**, *28*, 1102–1110. [CrossRef]
28. Ormseth, M.J.; Solus, J.F.; Sheng, Q.; Ye, F.; Song, H.; Wu, Q.; Guo, Y.; Oeser, A.M.; Allen, R.M.; Vickers, K.C.; et al. The Endogenous Plasma Small RNAome of Rheumatoid Arthritis. *ACR Open Rheumatol.* **2020**, *2*, 97–105. [CrossRef]
29. Kawcak, C.; Frisbie, D.; Werpy, N.; Park, R.; McIlwraith, C. Effects of exercise vs experimental osteoarthritis on imaging outcomes. *Osteoarthr. Cartil.* **2008**, *16*, 1519–1525. [CrossRef]
30. Peffers, M.J.; Milner, P.; Tew, S.; Clegg, P.D. Regulation of SOX9 in normal and osteoarthritic equine articular chondrocytes by hyperosmotic loading. *Osteoarthr. Cartil.* **2010**, *18*, 1502–1508. [CrossRef]
31. Peffers, M.; Liu, X.; Clegg, P. Transcriptomic signatures in cartilage ageing. *Arthritis Res. Ther.* **2013**, *15*, R98. [CrossRef] [PubMed]
32. User Guide. 2011. Available online: [https://emea.support.illumina.com/sequencing/sequencing\\_software/casava2/questions.html](https://emea.support.illumina.com/sequencing/sequencing_software/casava2/questions.html) (accessed on 5 August 2020).
33. Martin, M. Cutadapt removes adapter sequences from high-throughput sequencing reads. *EMBnet J.* **2011**, *17*, 10. [CrossRef]
34. Kim, D.; Pertea, G.; Trapnell, C.; Pimentel, H.; Kelley, R.; Salzberg, S. TopHat2: Accurate alignment of transcriptomes in the presence of insertions, deletions and gene fusions. *Genome Biol.* **2013**, *14*, R36. [CrossRef] [PubMed]
35. Love, M.I.; Huber, W.; Anders, S. Moderated estimation of fold change and dispersion for RNA-seq data with DESeq2. *Genome Biol.* **2014**, *15*, 002832. [CrossRef] [PubMed]
36. Benjamini, Y.; Hochberg, Y. Controlling the False Discovery Rate: A Practical and Powerful Approach to Multiple Testing. *J. R. Stat. Soc. Ser. B* **1995**, *57*, 289–300. [CrossRef]
37. Livak, K.J.; Schmittgen, T.D. Analysis of relative gene expression data using real-time quantitative PCR and the 2(-Delta Delta C(T)) Method. *Methods* **2001**, *25*, 402–408. [CrossRef]
38. Langmead, B.; Salzberg, S.L. Fast gapped-read alignment with Bowtie 2. *Nat. Methods* **2012**, *9*, 357–359. [CrossRef]
39. Zhang, J.; Kobert, K.; Flouri, T.; Stamatakis, A. PEAR: A fast and accurate Illumina Paired-End reAd mergeR. *Bioinformatics* **2014**, *30*, 614–620. [CrossRef]
40. Johnson, N.; Yeoh, J.M.; Coruh, C.; Axtell, M.J. Improved Placement of Multi-mapping Small RNAs. *Genes Genomes Genetics* **2016**, *6*, 2103–2111. [CrossRef]
41. Oliveira, J.V.D.A.; Costa, F.; Backofen, R.; Stadler, P.F.; Walter, M.E.M.T.; Hertel, J. SnoReport 2.0: New features and a refined Support Vector Machine to improve snoRNA identification. *BMC Bioinform.* **2016**, *17*, 464–486. [CrossRef]
42. Pang, Z.; Chong, J.; Li, S.; Xia, J. MetaboAnalystR 3.0: Toward an Optimized Workflow for Global Metabolomics. *Metabolites* **2020**, *10*, 186. [CrossRef] [PubMed]

43. Xia, J.; Wishart, D.S. Using MetaboAnalyst 3.0 for Comprehensive Metabolomics Data Analysis. *Curr. Protoc. Bioinform.* **2016**, *55*, 14.10.1–14.10.91. [CrossRef] [PubMed]
44. Kumar, P.; Anaya, J.; Mudunuri, S.B.; Dutta, A. Meta-analysis of tRNA derived RNA fragments reveals that they are evolutionarily conserved and associate with AGO proteins to recognize specific RNA targets. *BMC Biol.* **2014**, *12*, 78. [CrossRef] [PubMed]
45. Kumar, P.; Mudunuri, S.B.; Anaya, J.; Dutta, A. tRFdb: A database for transfer RNA fragments. *Nucleic Acids Res.* **2014**, *43*, D141–D145. [CrossRef] [PubMed]
46. Olvedy, M.; Scaravilli, M.; Hoogstrate, Y.; Visakorpi, T.; Jenster, G.; Martens-Uzunova, E. A comprehensive repertoire of tRNA-derived fragments in prostate cancer. *Oncotarget* **2016**, *7*, 24766–24777. [CrossRef] [PubMed]
47. Selitsky, S.R.; Baran-Gale, J.; Honda, M.; Yamane, D.; Masaki, T.; Fannin, E.E.; Guerra, B.; Shirasaki, T.; Shimakami, T.; Kaneko, S.; et al. Small tRNA-derived RNAs are increased and more abundant than microRNAs in chronic hepatitis B and C. *Sci. Rep.* **2015**, *5*, 7675. [CrossRef]
48. Wang, Q.; Lee, I.; Ren, J.; Ajay, S.S.; Lee, Y.S.; Bao, X. Identification and Functional Characterization of tRNA-derived RNA Fragments (tRFs) in Respiratory Syncytial Virus Infection. *Mol. Ther.* **2013**, *21*, 368–379. [CrossRef]
49. Chan, P.P.; Lowe, T.M. GtRNAdb: A database of transfer RNA genes detected in genomic sequence. *Nucleic Acids Res.* **2009**, *37*, D93–D97. [CrossRef]
50. Chan, P.P.; Lowe, T.M. GtRNAdb 2.0: An expanded database of transfer RNA genes identified in complete and draft genomes. *Nucleic Acids Res.* **2016**, *44*, D184–D189. [CrossRef]
51. Jühling, F.; Mörl, M.; Hartmann, R.K.; Sprinzl, M.; Stadler, P.F.; Pütz, J. tRNAdb 2009: Compilation of tRNA sequences and tRNA genes. *Nucleic Acids Res.* **2009**, *37*, D159–D162. [CrossRef]
52. Lotz, M.K.; Loeser, R.F. Effects of aging on articular cartilage homeostasis. *Bone* **2012**, *51*, 241–248. [CrossRef] [PubMed]
53. Li, Y.; Wei, X.; Zhou, J.; Wei, L. The Age-Related Changes in Cartilage and Osteoarthritis. *BioMed Res. Int.* **2013**, *2013*, 1–12. [CrossRef] [PubMed]
54. Martin, J.A.; Buckwalter, J.A. Telomere erosion and senescence in human articular cartilage chondrocytes. *J. Gerontol. Ser. A Biol. Sci. Med Sci.* **2001**, *56*, B172–B179. [CrossRef] [PubMed]
55. Jallali, N.; Ridha, H.; Thrasivoulou, C.; Underwood, C.; Butler, P.E.; Cowen, T. Vulnerability to ROS-induced cell death in ageing articular cartilage: The role of antioxidant enzyme activity. *Osteoarthr. Cartil.* **2005**, *13*, 614–622. [CrossRef]
56. Rahmati, M.; Nalesto, G.; Mobasher, A.; Mozafari, M. Aging and osteoarthritis: Central role of the extracellular matrix. *Ageing Res. Rev.* **2017**, *40*, 20–30. [CrossRef]
57. Hodgson, D.; Rowan, A.D.; Falciani, F.; Proctor, C.J. Systems biology reveals how altered TGFbeta signalling with age reduces protection against pro-inflammatory stimuli. *PLoS Comput. Biol.* **2019**, *15*, e1006685. [CrossRef]
58. Weilner, S.; Grillari-Voglauer, R.; Redl, H.; Grillari, J.; Nau, T. The role of microRNAs in cellular senescence and age-related conditions of cartilage and bone. *Acta Orthop.* **2015**, *86*, 92–99. [CrossRef]
59. Goodrich, L.R.; Nixon, A.J. Medical treatment of osteoarthritis in the horse—A review. *Veter. J.* **2006**, *171*, 51–69. [CrossRef]
60. McIlwraith, C.; Frisbie, D.D.; Kawcak, C.E. The horse as a model of naturally occurring osteoarthritis. *Bone Jt. Res.* **2012**, *1*, 297–309. [CrossRef]
61. Liu, Y.; Li, P.; Liu, L.; Zhang, Y. The diagnostic role of miR-122 in drug-induced liver injury. *Medicine* **2018**, *97*, e13478. [CrossRef]
62. Thakral, S.; Ghoshal, K. miR-122 is a unique molecule with great potential in diagnosis, prognosis of liver disease, and therapy both as miRNA mimic and antimir. *Curr. Gene Ther.* **2015**, *15*, 142–150. [CrossRef] [PubMed]
63. Mandourah, A.Y.; Ranganath, L.; Barraclough, R.; Vinjamuri, S.; Hof, R.V.; Hamill, S.; Czanner, G.; Dera, A.A.; Wang, D.; Barraclough, D.L. Circulating microRNAs as potential diagnostic biomarkers for osteoporosis. *Sci. Rep.* **2018**, *8*, 8421. [CrossRef] [PubMed]

64. Markopoulos, G.S.; Roupakia, E.; Tokamani, M.; Vartholomatos, G.; Tzavaras, T.; Hatziapostolou, M.; Fackelmayer, F.O.; Sandaltzopoulos, R.; Polytarchou, C.; Kolettas, E. Senescence-associated microRNAs target cell cycle regulatory genes in normal human lung fibroblasts. *Exp. Gerontol.* **2017**, *96*, 110–122. [CrossRef] [PubMed]
65. Burns, D.M.; D’Ambrogio, A.; Nottrott, S.; Richter, J.D. CPEB and two poly(A) polymerases control miR-122 stability and p53 mRNA translation. *Nature* **2011**, *473*, 105–108. [CrossRef] [PubMed]
66. Soriano-Arroquia, A.; McCormick, R.; Molloy, A.P.; McArdle, A.; Goljanek-Whysall, K. Age-related changes in miR-143-3p:Igfbp5 interactions affect muscle regeneration. *Aging Cell* **2016**, *15*, 361–369. [CrossRef]
67. Margolis, L.; Lessard, S.J.; Ezzyat, Y.; Fielding, R.A.; Rivas, D. Circulating MicroRNA Are Predictive of Aging and Acute Adaptive Response to Resistance Exercise in Men. *J. Gerontol. Ser. A Biol. Sci. Med. Sci.* **2017**, *72*, 1319–1326. [CrossRef]
68. Liu, C.; Ren, S.; Zhao, S. Wang. LncRNA MALAT1/MiR-145 Adjusts IL-1beta-Induced Chondrocytes Viability and Cartilage Matrix Degradation by Regulating ADAMTS5 in Human Osteoarthritis. *Yonsei Med. J.* **2019**, *60*, 1081–1092. [CrossRef]
69. Hu, G.; Zhao, X.; Wang, C.; Geng, Y.; Zhao, J.; Xu, J.; Zuo, B.; Zhao, C.; Wang, C.; Zhang, X.-L. MicroRNA-145 attenuates TNF- $\alpha$ -driven cartilage matrix degradation in osteoarthritis via direct suppression of MKK4. *Cell Death Dis.* **2017**, *8*, e3140. [CrossRef]
70. Mercken, E.M.; Majounie, E.; Ding, J.; Guo, R.; Kim, J.; Bernier, M.; Mattison, J.; Cookson, M.R.; Gorospe, M.; Decabo, R.; et al. Age-associated miRNA Alterations in Skeletal Muscle from Rhesus Monkeys reversed by caloric restriction. *Aging* **2013**, *5*, 692–703. [CrossRef]
71. Collins, J.A.; Diekman, B.O.; Loeser, R. Targeting aging for disease modification in osteoarthritis. *Curr. Opin. Rheumatol.* **2018**, *30*, 101–107. [CrossRef]
72. Thielen, N.G.M.; van der Kraan, P.M.; van Caam, A.P.M. TGFbeta/BMP Signaling Pathway in Cartilage Homeostasis. *Cells* **2019**, *8*, 969. [CrossRef] [PubMed]
73. Tardif, G.; Hum, D.; Pelletier, J.-P.; Boileau, C.; Ranger, P.; Martel-Pelletier, J. Differential gene expression and regulation of the bone morphogenetic protein antagonists follistatin and gremlin in normal and osteoarthritic human chondrocytes and synovial fibroblasts. *Arthritis Rheum.* **2004**, *50*, 2521–2530. [CrossRef] [PubMed]
74. Tardif, G.; Pelletier, J.-P.; Boileau, C.; Martel-Pelletier, J. The BMP antagonists follistatin and gremlin in normal and early osteoarthritic cartilage: An immunohistochemical study. *Osteoarthr. Cartil.* **2009**, *17*, 263–270. [CrossRef] [PubMed]
75. Liu, N.; Yin, Y.; Wang, H.; Zhou, Z.; Sheng, X.; Fu, H.; Guo, R.; Wang, H.; Yang, J.; Gong, P.; et al. Telomere dysfunction impairs epidermal stem cell specification and differentiation by disrupting BMP/pSmad/P63 signaling. *PLoS Genet.* **2019**, *15*, e1008368. [CrossRef] [PubMed]
76. Cao, J.; Venton, L.; Sakata, T.; Halloran, B.P. Expression of RANKL and OPG Correlates With Age-Related Bone Loss in Male C57BL/6 Mice. *J. Bone Miner. Res.* **2003**, *18*, 270–277. [CrossRef]
77. Martinez-Calatrava, M.J.; Prieto-Potín, I.; Roman-Blas, J.A.; Tardío, L.; Largo, R.; Herrero-Beaumont, G. RANKL synthesized by articular chondrocytes contributes to juxta-articular bone loss in chronic arthritis. *Arthritis Res. Ther.* **2012**, *14*, R149. [CrossRef]
78. Upton, A.R.; Holding, C.A.; Dharmapatni, A.A.S.S.K.; Haynes, D. The expression of RANKL and OPG in the various grades of osteoarthritic cartilage. *Rheumatol. Int.* **2012**, *32*, 535–540. [CrossRef]
79. Dieci, G.; Preti, M.; Montanini, B. Eukaryotic snoRNAs: A paradigm for gene expression flexibility. *Genomics* **2009**, *94*, 83–88. [CrossRef]
80. Dupuis-Sandoval, F.; Poirier, M.; Scott, M.S. The emerging landscape of small nucleolar RNAs in cell biology. *Wiley Interdiscip. Rev. RNA* **2015**, *6*, 381–397. [CrossRef]
81. Kishore, S.; Gruber, A.R.; Jedlinski, D.J.; Syed, A.P.; Jorjani, H.; Zavolan, M. Insights into snoRNA biogenesis and processing from PAR-CLIP of snoRNA core proteins and small RNA sequencing. *Genome Biol.* **2013**, *14*, R45. [CrossRef]
82. Khanna, A.; Stamm, S. Regulation of alternative splicing by short non-coding nuclear RNAs. *RNA Biol.* **2010**, *7*, 480–485. [CrossRef] [PubMed]
83. Michel, C.I.; Holley, C.L.; Scruggs, B.S.; Sidhu, R.; Brookheart, R.T.; Listenberger, L.L.; A Behlke, M.; Ory, D.S.; Schaffer, J.E. Small Nucleolar RNAs U32a, U33, and U35a Are Critical Mediators of Metabolic Stress. *Cell Metab.* **2011**, *14*, 33–44. [CrossRef] [PubMed]

84. Huang, C.; Shi, J.; Guo, Y.; Huang, W.; Huang, S.; Ming, S.; Wu, X.; Zhang, R.; Ding, J.; Zhao, W.; et al. A snoRNA modulates mRNA 3' end processing and regulates the expression of a subset of mRNAs. *Nucleic Acids Res.* **2017**, *45*, 8647–8660. [[CrossRef](#)] [[PubMed](#)]
85. Montanaro, L.; Treré, D.; Derenzini, M. Nucleolus, Ribosomes, and Cancer. *Am. J. Pathol.* **2008**, *173*, 301–310. [[CrossRef](#)] [[PubMed](#)]
86. Jorjani, H.; Kehr, S.; Jedlinski, D.J.; Gumienny, R.; Hertel, J.; Stadler, P.F.; Zavolan, M.; Gruber, A.R. An updated human snoRNAome. *Nucleic Acids Res.* **2016**, *44*, 5068–5082. [[CrossRef](#)]
87. Xu, G.; Yang, F.; Ding, C.-L.; Zhao, L.-J.; Ren, H.; Zhao, P.; Wang, W.; Qi, Z. Small nucleolar RNA 113–1 suppresses tumorigenesis in hepatocellular carcinoma. *Mol. Cancer* **2014**, *13*, 216. [[CrossRef](#)]
88. Goldring, M.B. The role of cytokines as inflammatory mediators in osteoarthritis: Lessons from animal models. *Connect. Tissue Res.* **1999**, *40*, 1–11. [[CrossRef](#)]
89. Kapoor, M.; Martel-Pelletier, J.; Lajeunesse, D.; Pelletier, J.-P.; Fahmi, H. Role of proinflammatory cytokines in the pathophysiology of osteoarthritis. *Nat. Rev. Rheumatol.* **2011**, *7*, 33–42. [[CrossRef](#)]
90. Emara, M.M.; Ivanov, P.; Hickman, T.; Dawra, N.; Tisdale, S.; Kedersha, N.; Hu, G.-F.; Anderson, P. Angiogenin-induced tRNA-derived Stress-induced RNAs Promote Stress-induced Stress Granule Assembly. *J. Biol. Chem.* **2010**, *285*, 10959–10968. [[CrossRef](#)]
91. Ali, S.A.; Alman, B. RNA extraction from human articular cartilage by chondrocyte isolation. *Anal. Biochem.* **2012**, *429*, 39–41. [[CrossRef](#)]



© 2020 by the authors. Licensee MDPI, Basel, Switzerland. This article is an open access article distributed under the terms and conditions of the Creative Commons Attribution (CC BY) license (<http://creativecommons.org/licenses/by/4.0/>).

## List of Publications

This is the list of publications the author of this thesis was included in during his PhD:

<b>Title</b>	<b>Citation</b>
1. Small Non-Coding RNAome of Ageing Chondrocytes	(Balaskas et al., 2020)
2. MicroRNA Profiling in Cartilage Ageing	(Balaskas et al., 2017)
3. Osteoarthritis year in review 2017: genetics and epigenetics	(Peffers, Balaskas, & Smagul, 2018)
4. SnoRNA signatures in cartilage ageing and osteoarthritis	(Peffers et al., 2020)
5. Equine synovial fluid small non-coding RNA signatures in early osteoarthritis	(Castanheira et al., 2021)
6. Impaired chondrocyte U3 snoRNA expression in osteoarthritis impacts the chondrocyte protein translation apparatus	(Ripmeester et al., 2020)

**Balaskas, P.**, Goljanek-Whysall, K., Clegg, P., Fang, Y., Cremers, A., Emans, P., . . . Peffers, M. (2017). MicroRNA Profiling in Cartilage Ageing. *Int J Genomics*, 2017, 2713725. doi:10.1155/2017/2713725

**Balaskas, P.**, Green, J. A., Haqqi, T. M., Dyer, P., Kharaz, Y. A., Fang, Y., . . . Peffers, M. J. (2020). Small Non-Coding RNAome of Ageing Chondrocytes. *Int J Mol Sci*, 21(16). doi:10.3390/ijms21165675

Castanheira, C., **Balaskas, P.**, Falls, C., Ashraf-Kharaz, Y., Clegg, P., Burke, K., . . . Peffers, M. J. (2021). Equine synovial fluid small non-coding RNA signatures in early osteoarthritis. *BMC Vet Res*, 17(1), 26. doi:10.1186/s12917-020-02707-7

Peffers, M. J., **Balaskas, P.**, & Smagul, A. (2018). Osteoarthritis year in review 2017: genetics and epigenetics. *Osteoarthritis Cartilage*, 26(3), 304-311. doi:10.1016/j.joca.2017.09.009

Peffers, M. J., Chabronova, A., **Balaskas, P.**, Fang, Y., Dyer, P., Cremers, A., . . . Welting, T. J. M. (2020). SnoRNA signatures in cartilage ageing and osteoarthritis. *Sci Rep*, 10(1), 10641. doi:10.1038/s41598-020-67446-z

Ripmeester, E. G. J., Caron, M. M. J., van den Akker, G. G. H., Surtel, D. A. M., Cremers, A., **Balaskas, P.**, . . . Welting, T. J. M. (2020). Impaired chondrocyte U3 snoRNA expression in osteoarthritis impacts the chondrocyte protein translation apparatus. *Sci Rep*, 10(1), 13426. doi:10.1038/s41598-020-70453-9